Novel Translational Endpoints of Neuropathic Pain and Pain Relief

Michael Thomas Lanigan

Supervisory team: Dr Lisa Lione, Dr Sandor Kantor, Dr Sara Pritchard

Submitted to the University of Hertfordshire in partial fulfilment of the requirements of the degree of Doctor of Philosophy with industry experience

August 2024

Acknowledgements

To my supervisors; Dr Lisa Lione, Dr Sandor Kantor, Dr Sara Pritchard and Dr Amy Fisher you have supported me the whole way through and provided me with your expert knowledge and guidance without which none of this would have been possible. I will always be grateful for helping me to achieve my ambitions.

To the wonderful staff at the University of Hertfordshire, particularly in the Biological Services Unit; David Clarke, Chloe Phillips and Amanda Hewett. Thank you for sharing with me and teaching me your passion for animal care. It has made me a better researcher.

To the fantastic staff at Transpharmation LTD thank you for your sharing with me your expert knowledge in preclinical research and for supporting my studies. Without you the scope, impact and quality of my research would not have been the same.

To my wonderful family; Mum, Dad, Kieran, and my soon to be new family; Sophie, Warren and Dan thank you for keeping me motivated, keeping me fed and with a roof over my head. You always supported me and never let me lose sight of my goals.

Most importantly to my amazing partner Ellen. Your unending patience (though I think I pushed it pretty close) and support is what got me through the most difficult times. Thank you for always being by my side and making me smile.

And finally, to my Nan you have always been my biggest source of inspiration and I wish you could be here today to see this as I know you would be so proud.

List of Publications

Peer reviewed publications

Preclinical Neuropathic Pain Assessment; the Importance of Translatability and Bidirectional Research. Fisher, A. S., Lanigan, M. T., Upton, N., & Lione, L. A. (2021). *Frontiers in Pharmacology*, *11*, 614990. https://doi.org/10.3389/fphar.2020.614990

Ketamine supresses REM sleep and markedly increases EEG gamma oscillations in the Wistar Kyoto rat model of treatment-resistant depression. Kantor, S., Lanigan, M., Giggins, L., Lione, L., Magomedova, L., de Lannoy, I., Upton, N., & Duxon, M. (2023). *Behavioural Brain Research*, *449*, 114473. https://doi.org/10.1016/J.BBR.2023.114473

Published book chapter

Lione, L. A., Lanigan, M., & Fisher, A. (2023). Animal Models: Practical Use and Considerations. In S. E. Ward & A. Davis (Eds.), *The Handbook of Medicinal Chemistry 2nd edition* (p. 437 - 484). The Royal Society of Chemistry. https://doi.org/10.1039/9781837671076

Conference poster presentations

The effect of a reduced streptozocin dose and social housing on well-being, mechanical hypersensitivity and burrowing behaviour in type 1 diabetes rodents. Lanigan, M. T., Burnett, M., Kennard, P., Upton, N., Prichard, S., Fisher, A., & Lione, L. A. (2020). Poster and oral presentation at International Association for the Study of Pain conference 2020 (Virtual).

Oxaliplatin-induced neuropathic pain is associated with poor sleep quality and reduced EEG alpha power in the rat. Lanigan, M. T., Giggins, L., Lione, L. A., Duxon, M., & Kantor, S. (2023). Poster presentation at Society for Neuroscience conference 2023 (Washington DC, USA).

Development of type-1 diabetes changes in evoked and non-evoked neuropathic pain endpoints and reversal with pregabalin in the rat streptozotocin model. Lanigan, M. T., Kantor, S., Prichard, S. M., & Lione, L. A. (2024). British Pain Society conference 2024 (Nottingham, UK).

Internal presentations

Animals can't say "OW!" Neuropathic pain research fails to treat patients effectively. Three Minute Thesis (3MT®) competition 1st place (2022).

Translational non-evoked endpoints of neuropathic pain. Oral presentation at the annual School of LMS research conference (2022).

The 'Power' of in vivo experiments: Good experimental design. Lanigan, M.T., Pritchard, S.M. & Lione, L.A. Poster presentation at the annual School of LMS research conference (2022).

Refining drug discovery approaches to modelling neuropathic pain: Translatability and animal welfare. Lione, L.A., Lanigan, M.T. & Pritchard, S.M. Poster presentation at the annual School of LMS research conference (2022).

Social housing effects on pain measurements and facial grimace scoring in diabetic rodents. Lanigan, M.T., Pickard, J., Pritchard, S.M. & Lione, L.A. Poster presentation at the annual School of LMS research conference (2023). (Part of a submission that received the Understanding Animal Research Openness Award 2023).

Development of type-1 diabetes changes in evoked and non-evoked neuropathic pain endpoints. Lanigan, M.T., Pritchard, S.M. & Lione, L.A. Poster presentation at the annual School of LMS research conference (2024).

Abstract

This thesis examined novel neuropathic pain endpoints for their reproducibility, reversibility and translatability to identify if they could improve how we measure neuropathic pain preclinically. Burrowing, an ethological behaviour that can be objectively measured in rodents was impaired in the streptozotocin (STZ) type-1 diabetic rat model of neuropathic pain. Burrowing deficits developed slower (from day 18) than measures of neuropathic pain using the classical evoked technique of von Frey paw withdrawal thresholds (from day 9). Only home caging an STZ diabetic rat with a control rat improved the STZ diabetic rat's individual burrowing level. Whilst the first line neuropathic pain treatment pregabalin did not rescue burrowing deficits in STZ diabetic rats at 3, 10 or 30mg/kg doses. This was despite all three doses of pregabalin reversing paw withdrawal thresholds measurements of neuropathic pain. The burrowing deficits in the STZ diabetic rats up to day 18 were also not caused by changes in locomotor activity or gait. Ultimately this indicated that burrowing is a likely measure of the animal's overall wellbeing that may prove useful as a secondary endpoint in neuropathic pain studies.

The welfare of the STZ diabetic rats used in these and future studies was refined through the characterisation of a lower single 55mg/kg dose of anomer-equilibrated STZ. This lower single dose of STZ successfully produced mechanical allodynia that was reversed by pregabalin (10-30mg/kg) and a diabetic phenotype of hyperglycaemia (>16mmol/L), polydipsia and polyphagia. At the same time the STZ dose reduced the bodyweight loss and toxicity side effects of STZ administration, improving the welfare of these animals across three separate studies. It was identified that increased blood glucose levels correlated with increased weight loss as well as kidney and liver hypertrophy in these STZ diabetic rats. This is an important step to encourage researchers in this field to use insulin as a rescue measure to minimise excessive bodyweight loss and hyperglycaemic complications. Furthermore, whilst classical evoked measures of paw withdrawal threshold have limited translatability potential, a refinement to the current technique by omitting social isolation during preclinical testing was identified.

Locomotor activity is another ethological behaviour that can be measured objectively in animals. In rats that developed neuropathic pain after chronic constrictive injury (CCI) surgery to the sciatic nerve of the hind paw, locomotor activity levels were decreased. Decreased locomotor activity was identified as early as 3 days after CCI surgery but was not identified in STZ diabetic rats within the first 3 weeks. The reduced amount of locomotor activity in CCI rats is reminiscent of the decrease in neuropathic pain patient's activity levels. Locomotor activity levels and mechanical allodynia in CCI rats were rescued by 10mg/kg ketamine, a novel analgesic that is potentially more efficacious than currently available treatments such as pregabalin (10mg/kg) which reversed mechanical allodynia but not locomotor activity levels. Therefore, measuring home cage locomotor activity levels in CCI rats (but not STZ diabetic rats) could provide an objective and translatable neuropathic pain endpoint.

Sleep disruption is a common comorbidity experienced by neuropathic pain patients that can lead to worse pain outcomes. Sleep fragmentation was identified in CCI rats through electroencephalogram (EEG) recordings by measuring the average length and number of sleep/wake bouts and particularly short periods of wakefulness. The development of sleep fragmentation in CCI rats was fully reversed by 10mg/kg ketamine and partially reversed by 10mg/kg pregabalin. These results were obtained whilst using an automated sleep/wake scoring algorithm that can greatly increase the efficiency and reduce the cost of preclinical EEG screening studies. However, in the oxaliplatin single dose model of

transient chemotherapy induced peripheral neuropathy (CIPN), sleep fragmentation was not identified. This demonstrates that sleep disruption endpoints in CCI rats (but not CIPN rats) are sensitive to analgesic treatments, can be measured objectively and are translatable to human patients.

Sleep/wake amounts and EEG power spectral measurements of pain were also assessed as potential neuropathic pain endpoints. CCI rats spent more time asleep and similar results were identified in the CIPN rats. The increased time CCI rats spent asleep was corrected by ketamine treatment but not by pregabalin. However, increased sleep is not seen in most preclinical neuropathic pain models or in human patients limiting the translatability of these findings. Similarly, EEG power changes were not consistent with other preclinical or clinical reports and were not reversible with analgesic treatments, limiting their potential use as preclinical neuropathic pain screening endpoints.

The results of these studies can be used to further the research into the use of burrowing, locomotor activity and sleep/wake behaviours as preclinical neuropathic pain endpoints.

Table of Contents

List of Figures

Chapter 1

Chapter 2

Chapter 3

Chapter 4

Chapter 5

Chapter 6

Chapter 6 Supplementary figures

List of Tables

Chapter 3

Chapter 6

Chapter 1: Introduction

1.1 Neuropathic pain

Neuropathic pain is defined as “pain caused by a lesion or disease of the somatosensory system” whilst pain itself has recently had its definition revised to “an unpleasant sensory and emotional experience associated with, or resembling that associated with, actual or potential tissue damage’’ by the International Association for the Study of Pain (IASP) (Jensen et al., 2011; Loeser, 2011). These definitions provide an indication of the challenges faced when investigating neuropathic pain, as most preclinical research in this area requires an intact somatosensory system. Therefore, this leads to most of the preclinical research being conducted in vivo, on small animals such as rats and mice (Deuis et al., 2017). However, preclinical research has focussed on the nociception part of pain with limited interpretation of the emotional and brain processing aspect of pain in animals (Sandkühler et al., 2009).

Neuropathic pain affects 8.2-8.9% of people in England, whilst chronic pain affects 35-50% of the UK population (Fayaz et al., 2016). It is therefore concerning that the current treatments for neuropathic pain are effective for <50% of patients (Colloca et al., 2017). The current recommended first line drug treatments for neuropathic pain include gabapentin, pregabalin, tricyclic antidepressants and serotonin-noradrenaline reuptake inhibitors (SNRIs) (Finnerup et al., 2015). These drugs, although beneficial to patients, have large numbers needed to treat (NNT) for 50% pain relief of between 4 and 10 patients. Additionally, other than pregabalin, all of these first line treatments were originally licensed for other conditions but have since been back translated and licenced for use in treating neuropathic pain. This has led to a large unmet need for novel analgesics to treat neuropathic pain. Little success has been found in forward translating preclinical analgesics into successful clinical trials with only ziconotide, pregabalin and capsaicin 8% patches reaching the clinic. Out of ziconotide, pregabalin and capsaicin only pregabalin is considered a first line therapy for neuropathic pain and the extent to which it is an example of forward translation is debatable (Percie Du Sert & Rice, 2014). Ziconotide derived from a ω-conotoxin peptide has shown excellent results but is limited by then need for intrathecal administration (Malmberg & Yaksh, 1995). Whilst capsaicin 8% patches are one of the most recently approved analgesic for neuropathic pain in 2009, compliance is often hindered by the burning sensation that occurs via topical application (Vinik et al., 2016).

Diabetes is the most commonly reported cause of neuropathic pain (van Hecke et al., 2014). The prevalence of diabetic neuropathy is approximately 50% in patients (Feldman et al., 2019), with painful diabetic neuropathy occurring in 20-50% of these patients (Rosenberger et al., 2020). As such, investigations into treatments for diabetic neuropathic pain is a crucial area of research. The general underlying causes of neuropathic pain are still being investigated (Rosenberger et al., 2020). However, some of the commonly referenced mechanisms of neuropathic pain include sensitisation of nociceptors, ectopic action potential generation and spinal sensitisation (Campbell & Meyer, 2006; Hains & Waxman, 2007; Haroutounian et al., 2014). The development of neuropathic pain often leads to impaired quality of life, including disrupted sleep, increased stress and anxiety (Colloca et al., 2017). It is important to consider these factors of underlying mechanisms and impaired quality of life when selecting and designing animal model studies of neuropathic pain to ensure they accurately reflect the patient experience.

A key focus of improving research into neuropathic pain is the biomarkers and endpoints used to assess it (Deuis et al., 2017). Current neuropathic pain endpoints have been largely unsuccessful in forward translating drugs that show promising preclinical results, into clinical successes. Therefore, a focus has been placed on developing measurements of pain that have improved translatability over classical measures. Historically measurements of neuropathic pain have focused on quantifying mechanical and thermal allodynia or hyperalgesia in animal models, to assess the analgesic effects of novel compounds (Tappe-Theodor et al., 2019). These measurements such as von Frey and hot/cold plates are evoked, non-ethological behavioural measures that rely on human interpretation of an animal's pain, meaning they are subjective. Evoked endpoints also ignore the emotional aspect of pain and rather rely on interpreting animal's nociception of pain (Deuis et al., 2017; Tappe-Theodor et al., 2019). Most pain endpoints used clinically consider the whole impact of pain including the emotional processing and affective features of pain through using self-reporting (Jensen et al., 2015). Whilst these measures in humans are also subjective, they consider the emotional aspect of pain and provide a more accurate measure of an individual's pain, compared with subjective measures in animals. A first step in improving the translatability between species will be to produce objective measures of animal nociception, to remove the subjectivity introduced by human interpretation of evoked behaviours. The ideal translatable endpoint would be a directly translatable method that can be objectively measured in both animals and humans.

1.1.1 Abbreviations.

IASP – International Association for the Study of Pain, STZ – streptozotocin, CCI – chronic constrictive injury, NNT – numbers needed to treat, CNS – central nervous system, AMPA – α-amino-3-hydroxy-5-methyl-4-isoxazolepropionic acid, NMDA – N-methyl-D-aspartate, PAG – periaqueductal gray, ACC – anterior cingulate cortex, PFC – prefrontal cortex, S1 – primary somatosensory cortex, S2 – secondary somatosensory cortex, IC – insula cortex, SNRIs – serotonin noradrenaline reuptake inhibitors, GABA – gamma-aminobutyric acid, CFA – complete Freund's adjuvant, ZDF – Zucker diabetic fatty, ZL – Zucker lean, NFB – neurofeedback modulation, SNI – spared nerve injury, EEG – electroencephalogram, REM – rapid eye movement, NREM – non-rapid eye movement, HCN – hyperpolarization-activated cyclic nucleotide-gated, SubP – substance P, TRPV1 – transient receptor potential cation channel subfamily V member 1, CIPN – chemotherapy induced peripheral neuropathy.

1.2 The patient experience

It is important to distinguish neuropathic pain and the underlying cause of the neuropathy. Whilst neuropathic pain is currently defined by IASP as "pain caused by a lesion or disease of the somatosensory system" neuropathy is defined as a "disturbance of function or pathological change in a nerve" (Loeser, 2011). Therefore, whilst all neuropathic pain patients have a neuropathy that affects their somatosensory system, not all neuropathy patients will develop neuropathic pain. If a neuropathy affects the sensory neurons it often causes a disruption in sensory signals and presents as a loss of sensation and numbness (Calcutt, 2020). For a subset of these patients the neuropathy will also cause an increase in pain which is termed neuropathic pain (Loeser, 2011). This can lead to patients having a paradoxical combination whereby they experience both pain and sensory loss caused by this lesion or disease (Finnerup et al., 2016). The pain experienced by neuropathic pain

patients is often ongoing or intermittent, typically described as burning, prickling, pins and needles, shooting, squeezing or freezing pain (Finnerup et al., 2021).

Neuropathic pain is experienced as either evoked or spontaneous pain. Evoked pain is typically caused by thermal (hot or cold) or mechanical stimuli and often categorised as either allodynia (pain from a normally non painful stimuli) or hyperalgesia (increased pain from a normally painful stimuli) (Colloca et al., 2017). Spontaneous pain occurs without any provocation or stimulus and may be described by the patient in many ways including tingling, burning, prickling, pins and needles, or electric shooting pain (Marchettini et al., 2006). Additionally, spontaneous pain is often experienced without evoked pain however, evoked pain rarely occurs without spontaneous pain indicating there are distinct or overlapping mechanisms triggering these painful events (Finnerup et al., 2021).

Some of the common comorbidities of neuropathic pain include anxiety, depression, sleep disturbances as well as decreased physical activity and impacts on patient's social life or relationships (Attal et al., 2011). Patients often report that these types of chronic pain can limit and interfere with their daily activities such as exercise, work, daily chores and their social life or relationships (Widerstrom-Noga et al., 2001). This can lead to the development of anxiety and depression from the limitations and worries of experiencing pain during these activities and the inability to conduct them (Nicholson & Verma, 2004). Development of anxiety and depression as well as the pain itself can all be worsened by disrupted sleep, which has been associated with decreased pain thresholds and is closely linked with depression and anxiety (Kundermann et al., 2004; Nutt et al., 2008). These types of comorbidities can compound with the primary cause of the neuropathy and neuropathic pain leading to a negatively reinforcing pathology with all of these factors contributing to the overall effects on the patient's quality of life (Nicholson & Verma, 2004). It has even been considered that this may be part of the effectiveness of antidepressant drugs in treating neuropathic pain, in that they may initially provide direct pain relief alongside a secondary mood stabilisation aspect leading to better patient outcomes (Torta et al., 2017). This highlights that the impact of neuropathic pain on the patient's quality of life is not just the pain itself but also the effect it has on mental health and wellbeing.

These comorbidities and the neuropathic pain also occur alongside any symptoms of the root cause of the neuropathy including diabetes, chemotherapy treatment, neuronal damage (surgical or physical), stroke or an infectious disease (Didier Bouhassira et al., 2021). Neuropathic pain is often stratified by the underlying disease or mechanism of its development which are usually split into either peripheral or central causes based on the location. Trigeminal neuralgia is a type of orofacial pain usually triggered by chewing, brushing teeth or washing the face that trigger the trigeminal nerve and is a type of peripheral neuropathic pain (Cruccu et al., 2016). Nerve injury as a cause of neuropathic pain can occur through different mechanisms in both the periphery such as during a surgical procedure or in the central nervous system following an event such as a stroke or spinal cord injury (Finnerup et al., 2021). Viral infections that can cause neuropathic pain include human immunodeficiency virus (HIV), and postherpetic neuralgia that may occur following herpes zoster infection (Dworkin et al., 2008; Schütz & Robinson-Papp, 2013). Further mechanisms of neuropathic pain onset include metabolic conditions such as diabetes, particularly when the patient has poor glycaemic control (Tesfaye et al., 2013). A partially reversable neuropathic pain can occur following treatment with chemotherapeutic agents such as oxaliplatin which can be neurotoxic and even dose limiting side effects of cancer treatment (Staff et al., 2017). A key challenge in understanding and treating neuropathic pain is that there are clear differences in the underlying disease or cause of the neuropathy. Combined with the development of neuropathic pain being heterogeneous within the

same underlying pathology, further complicating the research into neuropathic pain (Finnerup et al., 2021).

1.3 Mechanisms and pathophysiology of neuropathic pain

The underlying neuropathies associated with the development of neuropathic pain are most often cause by metabolic conditions (e.g. diabetes), chemotherapeutic agent treatment (e.g. oxaliplatin), viral infectious disease (e.g. HIV, post herpetic neuralgia, leprosy), traumatic or surgical injury (e.g spinal cord injury or amputation), immune disorders and inherited neuropathies and channelopathies (e.g. erythromelalgia) (Cavalli et al., 2019; Colloca et al., 2017). Depending on the location of the lesion or disease that causes neuropathic pain, it can lead to central neuropathic pain affecting the spinal cord and/or brain, or it can lead to peripheral neuropathic pain which predominately occurs when the affected sensory nerves are afferents including Aβ, Aδ or C fibres (Figure 1.1) (Colloca et al., 2017). The pathophysiological changes that occur following neuronal damage are highly variable between patients. Even those with similar symptoms are often caused by various underlying mechanisms (von Hehn et al., 2012). This highlights the heterogeneity of the pathophysiology in both different underlying conditions and within them, as there is no set pathway from neuropathy onset to neuropathic pain development. The pathophysiological changes that lead to neuropathic pain development include; ectopic activity, central and peripheral sensitisation that results in an imbalance between excitatory and inhibitory somatosensory signalling (Figure 1.1) (Colloca et al., 2017).

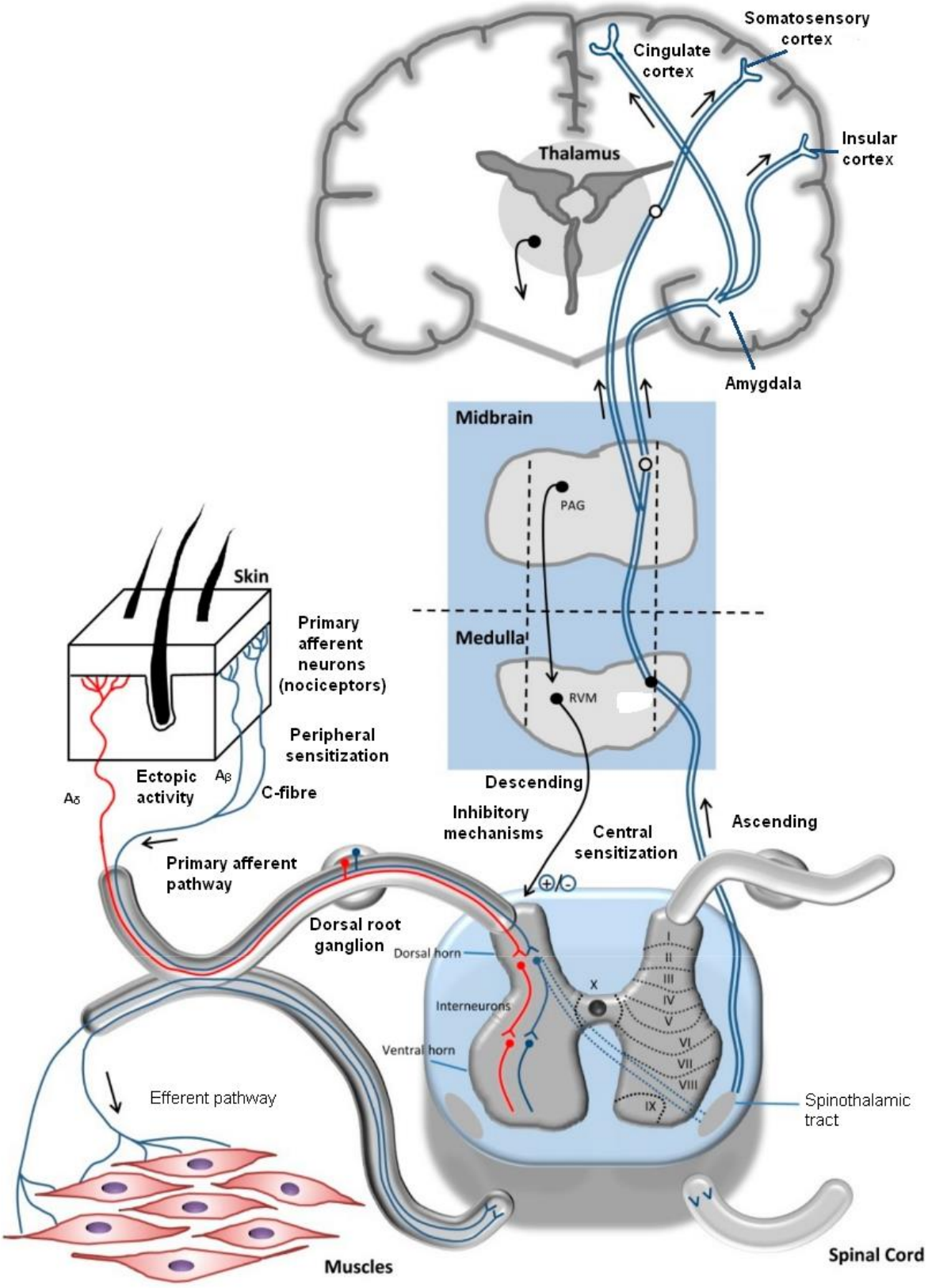

Figure 1.1) Schematic representation of the central and peripheral changes caused by peripheral neuropathy. These changes include effects on both the ascending pain pathway and descending inhibitory control pathways. RVM – rostral ventromedial medulla, PAG – periaqueductal gray. Adapted from (Yam et al., 2018).

1.3.1 Ectopic activity.

Current findings indicate that ectopic action potentials are a primary factor in the generation of spontaneous pain (Gilron et al., 2015). This ectopic activity is commonly identified in primary afferent neurons (Figure 1.1) where alterations in ion channel expression, distribution or changes in their function leads to rhythmic burst firing without a stimulus present (von Hehn et al., 2012). The two main types of ion channels involved in the generation of ectopic action potentials are voltage gated sodium (Na_v) channels and hyperpolarization-activated cyclic nucleotide-gated (HCN) channels. Na_v channels are important in transduction, action potential generation and neurotransmitter release in the somatosensory system. $Na_v1.3$ is a voltage gated sodium channel that is not normally expressed at detectable levels in adults, however its expression is greatly upregulated in dorsal root ganglion neurons after sensory nerve injury (Bennett et al., 2019). Activating the channels produces rapid fast firing currents that can lead to hyperexcitability of peripheral sensory neurons. Additionally, $Na_v1.6$ channels are involved in mediating repetitive high frequency firing of sensory neurons and their expression is increased in models of type-2 diabetes. Their knockdown in animal neuropathic pain models have been shown to reduce spontaneous action potentials and pain behaviours (Xie et al., 2015). HCN channels are important in facilitating and controlling neuron excitability. In particular HCN1 and HCN2 are highly expressed on dorsal root ganglion neurons. Increases in their expression or gain-of-function genetic mutations have both been demonstrated in neuropathic pain (Dini et al., 2018). These channels in neuropathic pain have been linked to spontaneous neuronal activity that leads to ectopic action potentials and spontaneous neuropathic pain (Chaplan et al., 2003). Altogether this leads to the conclusion that alterations in ion channels activity and the subsequent ectopic action potentials without a stimulus is one of the primary causes of spontaneous neuropathic pain.

1.3.2 Peripheral sensitisation.

Peripheral sensitisation similar to ectopic action potentials is often caused by changes to expression, distribution or function of ion channels. Although it relies on reducing the threshold or increasing the response to a stimulus rather than spontaneous activation (Jensen & Finnerup, 2014). This is termed allodynia: when a non-noxious stimulus such as light touch is perceived as painful, or hyperalgesia: when a painful stimulus is perceived as more painful than normal. One of the best characterised ion channels involved in peripheral sensitisation is transient receptor potential cation channel subfamily V member 1 (TRPV1) which is a ligand gated ion channel found predominately on peripheral nociceptive neurons. Its primary ligands include noxious heat (>43°C), capsaicin and membrane derived lipids (Labuz et al., 2015). TRPV1 is upregulated in neuropathic pain conditions including paclitaxel and diabetes induced neuropathic pain (Kamata et al., 2020; Pabbidi & Premkumar, 2017). Phosphorylation of TRPV1 through the protein kinase C (PKC) pathway mediated by proinflammatory molecules such as ATP, nerve growth factor (NGF), bradykinin and chemokines increases the sensitivity of these receptors (Gouin et al., 2017). This increase in expression or phosphorylation, can lead to a reduction in threshold or increase in excitability of sensory afferent neurons and thus peripheral sensitisation (von Hehn et al., 2012).

1.3.3 Central sensitisation.

Central sensitisation is defined by IASP as an “increased responsiveness of nociceptive neurons in the central nervous system to their normal or subthreshold afferent input” (Loeser, 2011). This

differs from peripheral sensitisation due to the location of the changes taking place in the central nervous system (CNS) rather than primary afferent neurons. Central sensitisation leads to enhanced neuronal activity in the CNS via increasing excitability and/or decreasing inhibition (Figure 1.1) and therefore contributing to neuropathic pain development (Latremoliere & Woolf, 2009). Some of the key initiators of this are increased intracellular Ca^{2+} levels through voltage gated Ca^{2+} channels and α-amino-3-hydroxy-5-methyl-4-isoxazolepropionic acid (AMPA) or N-methyl-D-aspartate (NMDA) receptors changes. This causes increased neurotransmission through receptor trafficking to the plasma membrane, phosphorylation of glutamate receptors and increased receptor transcription (Liu et al., 2018). Voltage gated calcium channels are involved in the release of neurotransmitters including glutamate at synaptic terminals such as the dorsal horn, where sensory afferent neurons enter the spinal cord (Park & Luo, 2010). Therefore, increased intracellular Ca^{2+} can lead to a lower activation threshold for neurotransmitter release and central sensitisation by lowering the amount of afferent input needed to activate second order somatosensory neurons (Perret & Luo, 2009). Some of the key evidence for this is the finding that there is an upregulation of the $\alpha_2\delta_1$ subunit of voltage gated Ca^{2+} channels in the dorsal horn of the spinal cord following oxaliplatin induced neuropathic pain (Yamamoto, Shimoshige, et al., 2016). Additional evidence has found that the primary method of pregabalin and gabapentin as analgesics is through inhibiting voltage gated calcium channels by binding to the $\alpha_2\delta_1$ subunit of voltage gated Ca^{2+} channels (Field et al., 2006).

The release of glutamate and other neurotransmitters such as substance P (SubP) into the dorsal horn leads to activation of glutamate receptors including NMDA and AMPA receptors. These receptors are found across the CNS including on postsynaptic membranes of second order somatosensory neurons in the dorsal horn and are important in normal pain signal transduction (Bardoni, 2013). Additionally, both receptors play a role in central sensitisation with NMDA receptors identified as playing a key role in this process. This has been demonstrated by blocking these receptors with the non-competitive inhibitor MK801 which reversed and prevented hyperexcitability (Woolf & Thompson, 1991). Furthermore, it has been shown that activation of NMDA receptors in the dorsal horn neurons increased intracellular calcium in second order somatosensory neurons (Li, Ge, et al., 2019). This increased intracellular calcium led to phosphorylation of various targets on NMDA and AMPA receptors increasing their response to glutamate, trafficking to the synapse and removing Mg^{2+} blocking (Latremoliere & Woolf, 2009). This ultimately leads to postsynaptic hyperexcitability and long-term potentiation of somatosensory neurons. However, unlike long-term potentiation in learning and memory, during neuropathic pain development the activation of NMDA receptors leads to long lasting heterosynaptic facilitation of low threshold inputs from Aβ (touch) and C (slow pain) fibres (von Hehn et al., 2012). Ending with long-lasting potentiation of surrounding neurons, strengthened synaptic activity and decreased activation thresholds leading to central sensitisation.

1.3.4 Inhibitory mechanisms.

One of the main ways that the body can modulate pain is through inhibitory mechanisms. In neuropathic pain these inhibitory controls are often lost or diminished. In the dorsal horn interneurons can release inhibitory neurotransmitters such as gamma-aminobutyric acid (GABA) and glycine that produce pre and post synaptic inhibition (Malcangio & Bowery, 1996). After peripheral nerve injury these inhibitory interneurons may be degraded by apoptosis leading to a disinhibition and thus neuropathic pain (Scholz et al., 2005). Additionally, descending pathways (Figure 1.1) from the midbrain and brainstem utilising monoaminergic neurotransmitters including noradrenaline and serotonin (5-HT), can profoundly modulate ascending pain pathways (Bannister & Dickenson, 2016).

The periaqueductal gray (PAG) is the primary control centre of descending pain modulation and receives inputs from areas such as the amygdala and hypothalamus. These inputs are coordinated through the rostral ventromedial medulla (RVM) which has direct neuronal projections to the dorsal horn (De Felice et al., 2011). The descending serotonergic pathway has dual function in that depending on the receptor activated it can either decrease ascending pain transmission (descending inhibition) or increase ascending pain transmission (descending facilitation). This occurs through activation of 5-HT_1 receptors in descending inhibition or 5-$HT_{2/3}$ receptors in descending facilitation (Ossipov et al., 2014). Noradrenergic pathways have only been shown to be involved in descending inhibition and act through α_2 receptors on postsynaptic secondary somatosensory neurons in the dorsal horn leading to decreased neurotransmitter release (Kwon et al., 2014). During neuropathic pain and central sensitisation a loss of control or function of these descending modulatory pathways, such as a loss of noradrenergic descending inhibition, can lead to an increase in primary pathway hyperexcitability.

1.4 Pain matrix

Whilst the nociceptive part of pain is important the brain processing, emotional impact and past experiences are equally if not more important in our induvial experience of pain. A key aspect of this includes the areas of the brain involved in processing and influencing pain which are still being elucidated. Using techniques such as functional magnetic resonance imaging (fMRI), positron emission tomography (PET) and electroencephalogram (EEG) source localisation, brain regions that are activated under painful conditions have been identified and termed the “pain matrix” (Prichep et al., 2011). These areas most often include the somatosensory cortex (primary (S1) and secondary (S2)), insula cortex (IC), anterior cingulate cortex (ACC), amygdala and thalamus (Apkarian et al., 2005; Melzack & Wall, 1965). However, many other brain regions have also been implicated in shaping our experience of pain including the prefrontal cortex (PFC) and PAG (Figure 1.2) (Reddan & Wager, 2018).

The thalamus acts as a relay system of the brain and in pain directs nerve transmission from the ascending pathway to either the somatosensory cortices S1&2 (lateral pathway) for processing the location and intensity of pain or to the ACC and IC (medial pathway) for the motivational component of pain (Kulkarni et al., 2005). Following the medial pathway the ACC is involved in the adaptation of pain to the emotional state of the patient including becoming activated by the anticipation or expectation of pain. This includes the placebo response whereby endogenous opioids are released in the ACC reducing the perception of pain and learned pain experiences which can increase pain perception (Iwata et al., 2005; Zubieta et al., 2005). The ACC has strong connections with other brain regions including the PFC and amygdala (Gao et al., 2004). Modulation of pain at the PFC is believed to work in tandem with the ACC anticipating pain responses and initiating the placebo response. This has been demonstrated by repetitive transcranial magnetic stimulation and Alzheimer’s degeneration that without the PFC the placebo response is not possible (Benedetti, 2010; Watson et al., 2012). The amygdala is involved in emotional processing in particular with fear conditioning and regulation and has connections to the PAG. Its role in pain processing is believed to involve attaching emotional significance to sensory inputs and modulates descending pain control accordingly (Simons et al., 2014). The connection between the amygdala and the PAG links with the previous discussion of its role as the primary control centre of descending pain control pathway. The influences of the

emotional processing of pain through areas such as the ACC, PFC and amygdala can influence whether the PAG produces descending inhibition or facilitation (Ossipov et al., 2014).

Following the lateral pathway from the thalamus leads to the primary somatosensory cortex (S1) which is involved in the localisation and conscious perception of somatosensory inputs including touch. It is the first level of conscious pain perception. However, it is not the "pain centre" of the brain as it works with other areas of the pain matrix to coordinate the overall pain perception (Backonja, 1996). The S1 region has direct connections to the secondary somatosensory cortex (S2) brain region which is thought to be involved in determining pain intensity (Timmermann et al., 2001). Together these areas work to establish the location and intensity of pain based on the inputs received from afferent neurons and the processing of this pain that occurs along the way in areas such as the dorsal horn. Finally, both pathways connect through the IC which plays an important role in integrating pain processing from the medial and lateral pain pathways (Brooks & Tracey, 2007). With the strong connections of the IC to the S2 region, ACC and amygdala it is believed that the primary role of the IC in the pain matrix is the integration of the localisation, intensity and emotional processing of pain (Starr et al., 2009). However, whilst important for pain processing the IC much like S1 region the IC is not the "pain centre" of the brain as pain perception requires a combined input of all of these different brain regions and others (Lu et al., 2016).

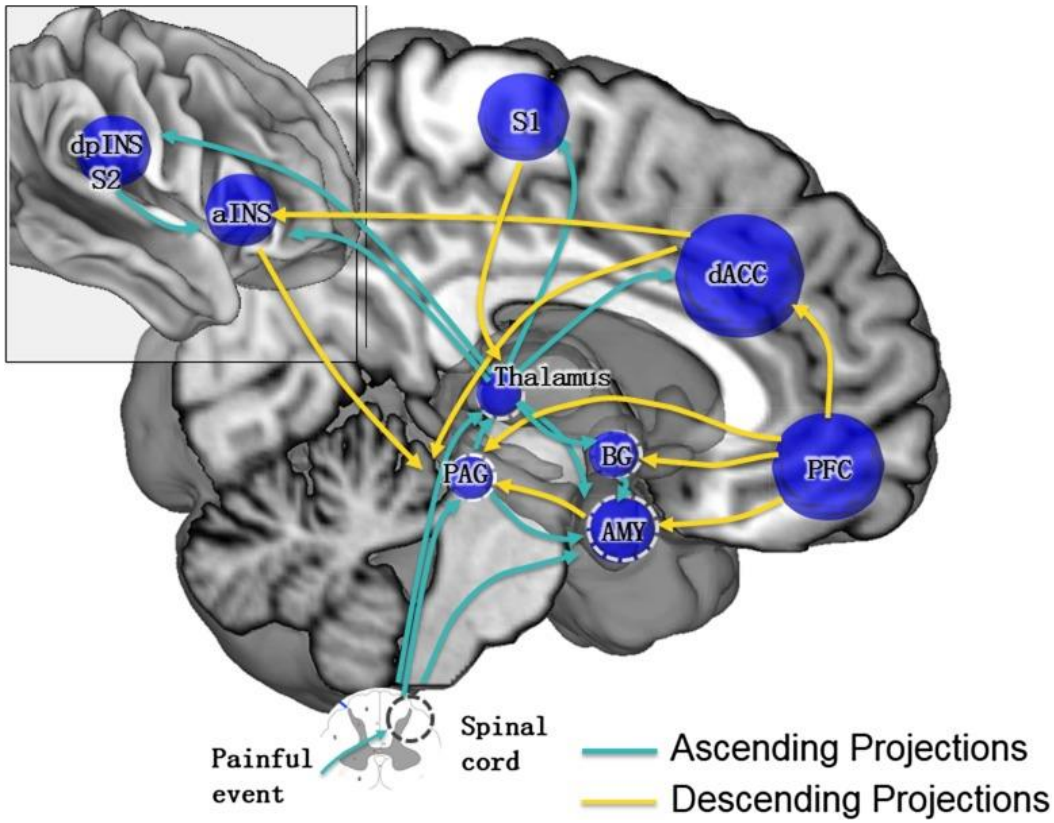

Figure 1.2) The pain matrix including the targets of the ascending (light blue) and descending (yellow) modulatory pathways for pain. ACC – anterior cingulate cortex, aINS – anterior posterior insula, dpINS – dorsal posterior insula, S1 – primary somatosensory cortex, S2 – secondary somatosensory cortex, PAG – periaqueductal gray, PFC – prefrontal cortices, BG – basal ganglia, AMY – amygdala. Taken from (Reddan & Wager, 2018).

1.5 Current recommended pharmacological treatments of neuropathic pain

The first line treatments of neuropathic pain are well established to include tricyclic antidepressants (amitriptyline), serotonin noradrenaline reuptake inhibitors (SNRIs; duloxetine, venlafaxine) and antiepileptics (gabapentin, pregabalin) (Cavalli et al., 2019; Colloca et al., 2017; Finnerup et al., 2015). Second line treatments include topical lidocaine and capsaicin 8% patches as well as botulinum toxin A. With opioids and ziconotide sometimes considered as third line treatments.

1.5.1 First line: Tricyclic antidepressants (Amitriptyline).

Tricyclic antidepressants such as amitriptyline can inhibit serotonin and noradrenaline reuptake in the dorsal horn leading to an increase in descending pain inhibition (Figure 1.1) through activation of 5-HT_1 and α_2 receptors respectively (Sindrup et al., 2005). Amitriptyline has one of the best NNT of all neuropathic pain treatments at 3.6 (CI 3.0-4.4) which is a measure of the number of patients needed to be treated with the pharmacological intervention for one patient to receive a >50% reduction in pain intensity (Finnerup et al., 2015). Amitriptyline was originally approved as an antidepressant. However empirical evidence in diabetic neuropathic pain patients taking amitriptyline displayed pain relief and the drug was subsequently approved for use to treat neuropathic pain (Davis et al., 1977). Tricyclic antidepressants cause side effects including anticholinergic effects, arrythmia, urinary retention and suicide risk whilst also being contraindicated in patients with cardiac disease, seizures and glaucoma (Cavalli et al., 2019; Colloca et al., 2017).

1.5.2 First line: SNRIs (Duloxetine, Venlafaxine).

Similar to tricyclic antidepressants, SNRIs such as duloxetine and venlafaxine act through inhibiting the reuptake of noradrenalin and serotonin in the dorsal horn to strengthen descending inhibition (Figure 1.1) (Sindrup et al., 2005). Venlafaxine and duloxetine are not as effective as amitriptyline at treating neuropathic pain with a NNT of 6.4 (CI 5.2 – 8.4). Though this is still adequate for them to be considered as first line treatments for neuropathic pain (Finnerup et al., 2015). Duloxetine, much like amitriptyline, was first approved for depression and urinary incontinence however evidence linking it to improvement of neuropathic pain led to its approval for this in 2005 (Raskin et al., 2005). SNRIs have several limiting side effects including lethargy, nausea, hypertension and are contraindicated in patients with hypertension, hepatic or cardiac diseases and those using tramadol (Cavalli et al., 2019; Colloca et al., 2017). The exact mechanism of action for both SNRIs and tricyclic antidepressants in treating neuropathic pain remains unclear. Though recent evidence points towards an importance of noradrenaline mediated inhibition of ascending pain pathway neurotransmitter release as a potential mechanism (Obata, 2017).

1.5.3 First line: C$\alpha_2\delta$ (Gabapentin / pregabalin).

Gabapentin was originally developed as a GABA analogue for the treatment of epilepsy and despite it not acting as a GABA analogue it still had antiepileptic activity and so was approved in 1993 (Taylor et al., 1993). Research subsequently demonstrated that gabapentin and 3-isobutyl GABA (pregabalin) both showed anticonvulsant activity through binding to the same site. Following

findings from clinical cases that gabapentin was a useful adjuvant medication for neuropathic pain, trials began to investigate both drugs analgesic properties (Field, McCleary, et al., 1999; Rosner et al., 1996). The current understanding of how pregabalin and gabapentin exhibit their analgesic properties is as non-selective ligands of the $\alpha_2\delta_1$ and $\alpha_2\delta_2$ subunit of voltage gated Ca^{2+} channels (Field et al., 2006). Though it appears their analgesic properties primarily occur through the $\alpha_2\delta_1$ subunit (Field et al., 2006). Thus, reducing excitatory ascending pain pathway transmission through a reduction in neurotransmitter release (Figure 1.1) and potentially decreasing central sensitisation (Kremer et al., 2016). Pregabalin and gabapentin have similar NNTs of 7.7 (CI 6.5 – 9.4) and 7.2 (CI 5.9 – 9.1) putting them in line with SNRIs (Finnerup et al., 2015). The main side effects of these ligands are dizziness, sedation, weight gain and peripheral oedema (Dworkin et al., 2007) which are understood to occur through their activity on the Ca^{2+} channels $\alpha_2\delta_2$ subunit (Kim et al., 2021). However, pregabalin achieves better responses at lower doses than those needed for the same outcome in gabapentin so has become the preferred gabapentinoid (Kremer et al., 2016). Both pregabalin and gabapentin have recently been reclassified to a class C drug in the UK due to concerns of abuse and potentially fatal interactions with alcohol and other CNS depressants (BNF | NICE, n.d.).

1.5.4 Second line: Lidocaine topical.

Topical application of 5% Lidocaine patches was first approved for use in neuropathic pain in 1999 (Gammaitoni et al., 2003). It is proposed that Lidocaine acts as a non-selective sodium channel blocker leading to a reduction in ectopic action potentials (Figure 1.1) with potential anti-inflammatory effects (Sawynok, 2014). Unfortunately, whilst it is an effective local anaesthetic, its non-selective inhibition of sodium channels also prevents its systemic use. The NNT for lidocaine as an adjuvant has been shown to be 4.4 (CI 2.5 – 17.5) although the large confidence interval does indicate greater variability (de León-Casasola & Mayoral, 2016). The side effects of topical lidocaine are relatively mild usually occurring as local rash, itching and erythema however its modest efficacy compared to placebo and limitation to topical use have left it as a second line or adjuvant treatment (Colloca et al., 2017).

1.5.5 Second line: Capsaicin 8% topical.

Similar to Lidocaine, capsaicin derived from chilli peppers at 8% can be applied through topical patches to treat neuropathic pain since its approval in 2009. The pharmacological effect of capsaicin in treating neuropathic pain is understood to be through activation followed by desensitisation of TRPV1 receptors (Anand & Bley, 2011). As TRPV1 receptors are mainly responsible for detection of noxious heat (>43°C) and capsaicin, they are the main reason for the burning sensation when consuming or coming into contact with capsaicin (Tominaga & Tominaga, 2005). Currently the NNT for topical capsaicin patches is around 10.6 (CI 7.4 – 18.8) which is relatively high (Finnerup et al., 2015). This comes along with the side effects of local pain, itching and erythema and the need for repeated application every 6 weeks and topical application has led to capsaicin 8% patches only being considered as a second line or adjuvant treatment (Colloca et al., 2017). The local pain caused by the activation of TRPV1 receptors can be someone ameliorated by pre-treatment with a low dose analgesic as well as cooling the area of the capsaicin patch (Baranidharan et al., 2013).

1.5.6 Second line: Botulinum toxin A.

One of the most toxic known substances is botulinum toxin which is a neurotoxin produced by *Clostridium botulinum* that blocks acetylcholine release in nerve fibres (Nigam & Nigam, 2010). These toxins, in particular botulinum toxin A, have multiple medical uses in humans including treating strabismus, facial spasms, cervical dystonia, chronic migraine and more recently neuropathic pain (Chen, 2012). Botulinum toxin A was first approved for use against strabismus by the FDA in 1989 and has since been found to be effective in many conditions including cosmetic use which was approved in 2002. The current understanding of the analgesic effects of botulinum toxin A in the treatment of neuropathic pain is through the inhibition of neurotransmitter release such as SubP and glutamate along with inhibiting TRPV1 receptors (Egeo et al., 2020). Although botulinum toxin A has the lowest NNT of all recommended treatments at 1.9 (CI 1.5 – 2.4), there is much less data currently available supporting its use along with it being limited to peripheral neuropathies has left it as a second line recommended treatment (Finnerup et al., 2015).

1.5.7 Third line: Opioids (Morphine, Oxycodone).

Opioids such as morphine are one of the strongest analgesics available to the clinician for treating moderate to severe acute pain. However, they have extensive and harmful side effects that range from constipation and nausea to addiction and respiratory depression (Boom et al., 2012; Furlan et al., 2006). It is understood that opioids analgesic efficacy is through activating μ-opioid receptors which can block the release of excitatory neurotransmitters such as SubP (Wan et al., 2017). This is particularly important in the dorsal horn where μ-opioid receptors are expressed on presynaptic afferent neurons and postsynaptic second order somatosensory neurons (Figure 1.1) (Kline IV & Wiley, 2008). Endogenous opioids are also particularly important in both the innate pain relieving systems and in the placebo response (Holden et al., 2005; Zubieta et al., 2005). Strong opioids demonstrate relatively good efficacy in neuropathic pain with an NNT of 4.3 (CI 3.4 – 5.8) which is in line with many first line treatments. However, they are currently only recommended as third line treatments for neuropathic pain due to their extensive side effects and risk of abuse (Finnerup et al., 2015).

1.5.8 Refractory pain: Ziconotide.

Ziconotide is one of the few recent examples of a novel non-opioid analgesic that has been approved for use in neuropathic pain. Originally discovered as a venom of the marine snail *Conus magnus*, ziconotide is a synthetic version of the ω-conotoxin MVIIA and was approved for use in 2005 (McGivern, 2007). The drug acts as a selective N-type voltage gated calcium channel blocker in the dorsal horn (Figure 1.1) stopping the release of excitatory neurotransmitters such as SubP and glutamate (Pope et al., 2017). It shows good efficacy with a NNT of 2.77 (CI 1.37 – 5.59) however it is severally hampered by the need for intrathecal administration (Brookes et al., 2017). The need for intrathecal administration of ziconotide is due to its low blood brain barrier pentation which limits its use due to the need for specialist administration of the drug (McGivern, 2007). Additionally, ziconotide does show concerning side effects linked with an increased risk of suicidal ideation and psychosis although patients do not appear to develop a tolerance to ziconotide unlike other analgesics such as strong opioids and gabapentin (Brookes et al., 2017). Overall, this has led to ziconotide being considered a treatment option primarily for cases of refractory neuropathic pain at

best or as a final treatment option for patients when alternatives have failed (Viswanath et al., 2019).

1.6 Failure to develop new treatments

Whilst research into analgesic treatments for neuropathic pain has been ongoing for many decades few effective treatments have been found and even those have limited efficacy and extensive side effects. As discussed, the majority of first line treatments were originally developed for other conditions such as depression and epilepsy and not originally designed as analgesics. In 2014 Gilron and Dickenson conducted an extensive review and identified 25 different compounds in phase II and III trials for neuropathic pain (Gilron & Dickenson, 2014). In the 10 years since this only mirogabalin has been approved in Japan and none have become first or second line treatments in the US or UK. Even mirogabalin is only an improved version of already available pregabalin and gabapentin which were originally developed to treat epilepsy (Kim et al., 2021). Mirogabalin preferentially binds to the $\alpha_2\delta_1$ subunit of voltage gated Ca^{2+} channels, with reduced affinity for the $\alpha_2\delta_2$ subunit that is involved in the unwanted side effects of pregabalin and gabapentin (Kim et al., 2021). One of the promising findings of this review by Gilron and Dickenson was that a wide range of different mechanisms and pathways were under investigation including; calcium, sodium and potassium channels, vanilloid, opioid or cannabinoid receptors and more novel targets including the angiotensin and orexin systems (Gilron & Dickenson, 2014). This highlights that there are a wide range of different targets being examined for the treatment of neuropathic pain many of which are progressing to human clinical trials. However, the evidence that novel analgesics are reaching phase II and III trials but not to the clinic suggests that there is a breakdown in the translation of promising preclinical evidence into successful human clinical trials (Becker et al., 2023). Becker et al. (2023) recently reviewed three different drug targets (nerve growth factors / NaV1.7 channel blockers / tachykinin receptor 1 antagonists) that made it to phase II/III clinical trials but failed due to off target side effects and poor efficacy in treating neuropathic pain (Becker et al., 2023).

1.6.1 Poor forward translation.

Despite the extensive search for neuropathic pain treatments, there is a failure is to translate promising preclinical data into clinical trial success (Attal & Bouhassira, 2019). Whilst many different studies have presented clear evidence of analgesic properties in animal models, these effects are not reproduced in humans demonstrating that there is drastic need for an improvement in this process. Several different ways to bridge this gap have been suggested, including using a multidimensional approach to patient selection, the improvement of the preclinical animal models and changing the way we quantify pain (D. Bouhassira & Attal, 2016; Percie Du Sert & Rice, 2014; Taneja et al., 2017). One of the most important areas is in how we measure and quantify pain as there is a mismatch between preclinical and clinical studies (Fisher et al., 2021; Tappe-Theodor et al., 2019). In preclinical studies the classical way to measure pain has been through measuring reflex-based assessments of stimulated pain that are interpreted by a trained human observer (Negus, 2019). In clinical trials the most common way to assess neuropathic pain is through the self reporting of the pain level by the patient using questionnaires and visual rating scales (Sachau et al., 2023). Clearly, it is not possible to ask an animal to self report their pain so steps must be taken to align how we measure pain

preclinically and clinically with the aim of improving the translation of preclinical results into clinical trials success.

In summary, Neuropathic pain has a large impact on society and the patients that suffer with it. Current treatments are largely ineffective and have dose limiting side effects. New treatments have been slow to develop, ineffective or have failed to reach market. There is still a large unmet clinical need leaving millions of patients without adequate treatment options and in pain. One of the main potential areas this failure occurs in the lack of translation from preclinical to clinical results. Therefore more translational ways of measuring preclinically are required to try and bridge this gap. To better understand why this failure is occurring it is important to understand how pain is currently measured both preclinically and clinically. Along with the new endpoints that are being developed to measure neuropathic pain including both the strengths and limitations of these new endpoints.

1.7 3R's and welfare

A core component of designing and conducting experiments involving animals is to ensure the welfare of all animals during the experiment. An agreed way of ensuring this are the 3R's principles of Replacement, Reduction and Refinement which were originally developed by William Russell and Rex Burch in 1959 to help researchers ensure their experimentation involving animals were conducted as humanely as possible (Russell & Burch, 1959). These three principles cover: Replacement - avoiding or replacing the use of animals in areas where they otherwise would have been used. Reduction - minimising the number of animals used consistent with scientific aims. Refinement - minimising the pain, suffering, distress or lasting harm that research animals might experience (NC3Rs, n.d.).

The 3R's core goal has not changed since its inception and it is globally employed today providing a clear set of goals for improving animal welfare in research (Hubrecht & Carter, 2019). The most important of the 3R's is replacement to ensure animals are not used where the same results can be achieved by other means (NC3Rs, n.d.). Neuropathic pain is a particularly difficult area to employ replacement as an intact somatosensory system is usually required for the assessment of analgesic compounds. However, the development and use of human and animal tissues assays is beginning to increase (Sadler et al., 2022). A key step in any experimental design is selecting the numbers used per group and is often the most important step for ensuring a reduction in the number of animals used is achieved without using too few animals such that false negative results are caused by a lack of statistical power. This can most often be ensured through conducting a thorough power analysis prior to conducting any animal research (Charan & Kantharia, 2013). By optimising study design researchers can minimise any distress, suffering, pain or lasting harm experienced by animals involved in research. Refinement can be achieved by understanding and improving the techniques, methodologies and environmental conditions used in preclinical experiments. This should be undertaken as a constant process employed over time as new techniques and understanding of animal welfare are discovered and should be shared (Lione et al., 2023; Musk, 2020).

1.8 Currently used clinical neuropathic pain endpoints

Selecting biomarkers or endpoints of neuropathic pain can be particularly challenging as there is no single marker that can identify neuropathic pain in all patients (Shaikh & Somani, 2010). Thus making the identification and detection of neuropathic pain in humans particularly challenging. Currently the primary endpoint used in clinical trials to measure the efficacy of analgesics is self-reported pain (Jensen et al., 2015). This primarily takes the form of questionnaires or rating scales such as visual analogue or a numeric rating scale (Figure 1.3) (Soliman et al., 2023). Techniques such as quantitative sensory testing, skin biopsy and laser-evoked potentials are all used to inform clinicians of neuropathic pain development but are not commonly used as endpoints in clinical trials (Colloca et al., 2017) (Figure 1.3).

Self-reported pain is often the primary endpoint in human clinical trials as it encompasses the entire pain experience of the patient which is an important factor in assessing analgesia. Although these endpoints are subjective, they encompass the emotional aspects of pain, as well as the nociception of it, and are more beneficial than evoked endpoints that are currently used preclinically. Pain rating scales for neuropathic pain such as “painDETECT” and “Neuropathic Pain Score” involve a range of questions with an accompanying scale with which the patient will rate their pain (Bendinger & Plunkett, 2016). These scales are either numeric, often on a 0-10 number line, or by marking a word that most closely equates to the pain such as none, slight, moderate, severe. The Leeds Assessment of Neuropathic Symptoms and Signs scale uses a combination of both interview questions and brief clinical assessments such as pain to light touch to gain a more accurate interpretation of neuropathic pain (Cruccu & Truini, 2009). Whilst the use of these endpoints is commonplace in clinical trials, selection of the correct reporting methods and the number of different types of reporting methods used are important because it has been identified that a minimum of two different methods are needed to create a valid assessment of the patient’s pain (Jensen et al., 2015).

Although the use of self-reported pain has been employed successfully to monitor and assess the analgesic properties of new compounds, their use as a clinical trial endpoint limits the translatability of preclinical findings. Additionally, they fail to provide the history of pain and are not suitable for use in patients who suffer from trigeminal neuralgia (Attal et al., 2018). The selection of the correct questionnaire is also important as they may not include the relevant descriptors for the type of neuropathic pain that the patient experiences. The way the self-reporting of pain is conducted is also important as diary recordings are prone to back filling, creating inaccuracies in the reports (Younger et al., 2009). The development of an objective marker that can be translated from preclinical to clinical trials would improve the success rate in developing novel analgesics.

Preclinical endpoints	Human RCT endpoints
***Stimulus evoked sensory endpoints** (thermal, mechanical, chemical withdrawal e.g. von Frey filaments)	Reflex Quantitative Sensory Threshold (QST) (thermal, mechanical, chemical withdrawal e.g. von Frey filaments)
X	***Reported pain intensity and Daily living (QoL)** (e.g. VAS numerical rating pain)
X	**Affective / Cognitive state** depression, anxiety, motivation, sleep anticipation of pain (preference/avoidance)
X	**Objective markers** EEG

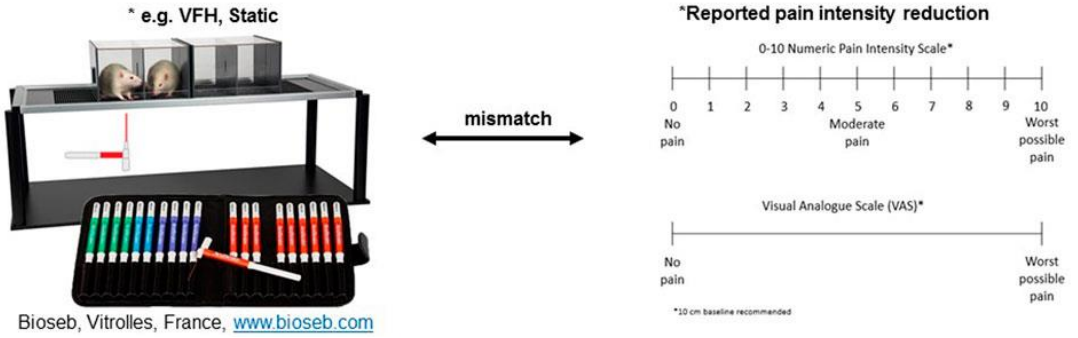

Bioseb, Vitrolles, France, www.bioseb.com

Figure 1.3) Representation of the mismatch in primary neuropathic pain assessment endpoints used between preclinical and clinical trials. *Indicates primary endpoint, EEG – electroencephalography, VFH – von Frey hair, RCT – randomised clinical trial, QoL – quality of life. Taken from (Fisher et al., 2021).

1.9 Classical preclinical neuropathic pain endpoints

The classically used endpoints for measuring nociception in rodent neuropathic pain models are stimulus evoked behaviours (Figure 1.3). These include those evoked by mechanical, heat and cold stimuli for which there are an array of different methods such as: von Frey filament application, Randall-Selitto and hot or cold plates (Tappe-Theodor et al., 2019). The key limitation of these endpoints is that they are evoked by the stimulus and thus usually measure allodynia or hyperalgesia which contrast human clinical trials where all types of spontaneous and stimulus evoked pains experienced by the patient are measured though self-reporting (Figure 1.3) (Jensen et al., 2015; Tappe-Theodor et al., 2019). Additionally, most preclinical stimulus evoked endpoints are measured by human interpretation of a reflex such as paw withdrawal (Deuis et al., 2017). This introduces subjectivity to these measurements as they are recorded by a human's interpretation of the behaviour. This is because a response to a stimulus does not definitely correspond to pain and ignores the emotional aspect of it (Sandkühler et al., 2009). A recent systematic review conducted by Bacalhau et al. (2023) identified that 97.1% of preclinical studies investigating paclitaxel induced neuropathic pain assessed mechanical allodynia using von Frey monofilaments, whilst only 1.4% assessed any kind of spontaneous pain testing (Bacalhau et al., 2023).

A key research finding involved in the preclinical research of neuropathic pain is that of Field et al. (1999), who identified that both pregabalin and gabapentin could successfully reverse static and dynamic mechanical allodynia in the streptozotocin (STZ) type-1 model of neuropathic pain (Field, McCleary, et al., 1999). This research was an early study where dynamic allodynia was assessed

using this model of neuropathic pain. Findings from this study showed that dynamic allodynia took twice as long as static allodynia to develop. The effects of pregabalin, gabapentin, morphine and amitriptyline were assessed on these endpoints and all four successfully reversed static allodynia. However, only pregabalin and gabapentin reversed dynamic allodynia and were therefore deemed by the authors to be superior to morphine and amitriptyline (Field, McCleary, et al., 1999). At present, morphine is not considered a first line treatment for neuropathic pain, primarily due to it side effect profile as its NNT is similar to antidepressants (Fornasari, 2017). Amitriptyline and pregabalin are believed to have equivalent efficacy in treating painful diabetic neuropathy with pregabalin only being deemed as the better choice based on an improved side effect profile (Bansal et al., 2009; Daniel et al., 2018). Whilst the evidence from the study by Field et al. (1999) was crucial in providing the preclinical data for two of the first line treatments for neuropathic pain, their use of dynamic mechanical allodynia data to deem them superior to amitriptyline and morphine has not replicated in a clinical setting (Field, McCleary, et al., 1999).

In summary, this evidence shows that although some success has been found in using these stimulus evoked markers of neuropathic pain, the translation of findings using these endpoints into clinical trials have been largely unsuccessful. Therefore, the development of novel markers of neuropathic pain is now largely focused on ethological behaviours and objective markers that are believed to improve the translatability of analgesics to treat neuropathic pain.

1.10 Current preclinical models of neuropathic pain

A wide array of neuropathic pain models exist that range from metabolic conditions such as diabetes, chemotherapeutic agents, genetic and surgically induced models (Jaggi et al., 2011; Lione et al., 2023). When selecting a model, the primary goal is choosing one that has: good face (replicates the disease model); construct (similar mechanism of neuropathic pain onset/causality); and predictive (likelihood to predict a similar outcome in humans) validity for the condition the research is investigating (Berge, 2011). As an example, differentiation between models that induce type-1 or type-2 diabetes must be made. Whilst type-1 diabetes may be easier to induce with chemicals or genetic models it represents only 10% of all human diabetic patients (Shaikh & Somani, 2010). It is important to assess the specific cause of neuropathic pain as well as the location and tissue type as this can affect the resulting pain and treatment profile (Gregory, 2013). Replicating both the mechanism and site of injury is important to better understand and produce treatments for human conditions (Gregory, 2013).

1.10.1 Diabetic models of neuropathic pain.

One of the most commonly used metabolic neuropathic pain models is the STZ type-1 model of diabetes. STZ is taken up by pancreatic β cells through the glucose transporter 2 (GLUT2) and causes alkylation and free radical damage of DNA, leading to cell death and thus decreased insulin secretion (King & Bowe, 2016; Shaikh & Somani, 2010). This lack of insulin secretion leads to a loss of glycaemic control and causes hyperglycaemia, polydipsia, polyurea and peripheral neuropathic pain (Wang-Fischer & Garyantes, 2018). Typically, STZ is used to induce type-1 diabetes with a single dose and has been widely used in preclinical neuropathic pain research since the discovery of the diabetogenic properties of this compound in 1963 (Rakieten et al., 1963). A key use of the single

dose STZ type-1 diabetic model was in the preclinical testing of pregabalin and gabapentin which resulted in the forward translation of pregabalin for clinical use in treating neuropathic pain. As discussed, gabapentin was shown to have efficacy in treating neuropathic pain and research showed that gabapentin and pregabalin both had anticonvulsant activity through binding to the same site (Taylor et al., 1993). Gabapentin and pregabalin were examined for their analgesic properties in models of inflammatory and post-operative pain in 1997 (Field, Holloman, et al., 1997; Field, Oles, et al., 1997) and subsequently in the STZ type-1 model of neuropathic pain in 1999 (Field, McCleary, et al., 1999). This resulted in their approval for use against neuropathic pain.

It can be considered that the STZ type-1 model of diabetes shows good face validity in the development of hyperglycaemia, polyurea, polydipsia and neuropathic pain. The model shows some construct validity in terms of damage to the pancreatic β cells being the reason for the development of hyperglycaemia. However, the exact cause of the β cell damage differs from autoimmune derived damage in humans (Gillespie, 2006). There is also evidence for the predictive validity of the model as it is one of the few that have been involved in the forward translation of a first line drug treatment (pregabalin), although the similarities to gabapentin which was back translated and pregabalin do limit this somewhat.

The STZ model is not perfect due to the limited range of STZ dosage able to achieve a hyperglycaemic state is usually >50mg/kg, whilst doses as low as 70mg/kg have been identified as causing high mortality rates (Gajdošík et al., 1999). This may also be related to the preparation and administration of STZ which is highly variable between publications and could lead to differences in results (Ghasemi & Jeddi, 2023). Additionally, mortality rate is very dependent on the age of the animals, with older animals being more susceptible to higher doses of STZ and the potential toxic effects on multiple organs (Wang-Fischer & Garyantes, 2018). There is cause for concern that in the Field et al. (1999) study, animals showed a relatively low BGL (of approximately 16mmol/L on average) which is lower than seen in other papers where typically the mean BGL is 25mmol/l or greater (Al Deeb et al., 2000; Field, McCleary, et al., 1999). Overall, it is important that the correct model of neuropathic pain is selected and that the face, construct and predictive validity of the model is assessed before its use.

Though the single dose STZ type-1 diabetes model is the most commonly used model and has demonstrated some forward translatability potential, it is not the only diabetic model. Others include multiple low doses of STZ being administered to induce a type-1 phenotype (Vieira et al., 2020), a low dose of STZ combined with a high fat diet to induce a type-2 model (Guo et al., 2018) and genetic models such as Zucker diabetic fatty (ZDF) type-2 diabetes rat model (Rutten et al., 2018). However, genetic models are limited by their much greater cost and slower development of neuropathic pain (Rutten et al., 2018). Similarly, the type-2 diabetes high fat diet models develop neuropathic pain only after 16 weeks (Castañeda-Corral et al., 2021). Compare to the single dose STZ type-1 diabetes model which can develop neuropathic pain withing the first two weeks (Field, McCleary, et al., 1999). Therefore, the single dose STZ type-1 diabetes model is still the most commonly used type-1 diabetes model used for preclinical screening of analgesic treatments.

1.10.2 Chemotherapy induced models of neuropathic pain.

There are several models of chemotherapy induced peripheral neuropathy (CIPN) using vinka alkaloid, taxanes or platinum based compounds (Authier et al., 2009). One such chemotherapeutic agent is oxaliplatin, a third-generation platinum analogue that is used in humans for a wide range of

anti-cancer treatments because of its reduced nephrotoxicity compared with second generation platinum based compounds (Yi et al., 2021). However, the key limiting factor in the use of oxaliplatin is the side effect of CIPN that is experienced by 85-90% of patients undergoing treatment, that initially lasts for up to a few days but with successive treatments can last for years after treatment (Branca et al., 2021; Takeshita et al., 2021). To improve research into this area, Ling et al. (2007) developed a rat model of oxaliplatin induced CIPN that develops cold and heat hypersensitivity consistent with the clinical presentation of oxaliplatin induced neuropathic pain in humans (Ling, Authier, et al., 2007). This model involves the administration of oxaliplatin either as a single bolus dose to cause a transient neuropathic pain phenotype (Ling, Coudoré-Civiale, et al., 2007) or repeated smaller doses that produce a chronic CIPN model (Ling, Authier, et al., 2007). These models induce cold allodynia through an oxalate metabolite and chronic development of mechanical allodynia through axonal degeneration (Egashira, 2021). Since its inception the oxaliplatin model of neuropathic pain has been refined and tested extensively with animals presenting with mechanical allodynia along with hypersensitivity to temperatures, however few drugs in clinical trials have shown much promise for improving the oxaliplatin induced peripheral neuropathy (Lv et al., 2023).

The oxaliplatin model of neuropathic pain shows good face and construct validity with animals developing a similar neuropathic pain phenotype to humans which is caused by the same treatment (oxaliplatin) that patients receive. The predictive validity is yet to be determined, as currently it has not translated any drugs into successful clinical application. Though it is a relatively newer model of neuropathic pain which may contribute to this (Velasco et al., 2021). One limiting factor of this model is the transient development of neuropathic pain after a single administration of oxaliplatin that could limit the time researchers have to investigate analgesics (Ling, Coudoré-Civiale, et al., 2007). Repeated administration of oxaliplatin does induce a longer, more sustained neuropathic pain phenotype, both of which appear to reflect the developments seen in humans (Ling, Authier, et al., 2007). Whilst other models of CIPN have been explored oxaliplatin induced CIPN is particularly important as the CIPN occurs in almost all patients (Branca et al., 2021; Takeshita et al., 2021). Alongside this very few drugs have been efficacious in clinical trials at treating oxaliplatin induced CIPN (Lv et al., 2023). Which is particularly concerning as CIPN is often the most dose limiting side effect of oxaliplatin as a chemotherapy treatment that can alter or reduce treatment plans (Mezzanotte et al., 2022; Miltenburg & Boogerd, 2014). Therefore, it is vital that the correct preclinical neuropathic pain endpoints are used in oxaliplatin CIPN models.

1.10.3 Surgically induced models of neuropathic pain.

Surgically induced neuropathic pain in rodents, models the effects of traumatic surgical or physical injuries in human patients (Bennett et al., 2003; Challa, 2015). These surgically induced models often focus on damaging the sciatic nerve and various models have been generated that involve ligating, transecting, or constricting this nerve at different locations (Challa, 2015). The chronic constrictive injury (CCI) model of peripheral neuropathic pain is the most commonly reported model used in preclinical neuropathic pain research (De Vry et al., 2004). It was originally developed by Bennett and Xie in 1988 to model nerve compression injuries such as nerve compression or entrapment (Bennett & Xie, 1988). This model involves applying loose ligatures (usually of suture material) around the sciatic nerve to occlude, but without stopping epineural blood flow to the area (Austin et al., 2012). Several other models following similar protocols of nerve injury usually to the sciatic have also been developed to target alternative causes of peripheral nerve injury such as nerve ligation or transection (Berge, 2011; Fonseca-Rodrigues et al., 2021). Animals undergoing CCI surgery develop both mechanical allodynia and thermal hyperalgesia that has been reversed with a wide range of

analgesic compounds including gabapentin and amitriptyline which are among the first line treatments in humans (De Vry et al., 2004).

The CCI model shows good construct validity in that it involves direct compression of the nerve however the underlying pathophysiology in humans is not yet fully understood meaning a proper understanding of the construct validity cannot be established (Berge, 2011). Neuropathic pain in humans caused by peripheral nerve injury presents as stimulus evoked (mechanical allodynia and thermal hyperalgesia) and spontaneous pain, both of which are present in the CCI model and supporting the face validity of its use (De Vry et al., 2004). The predictive validity of the CCI model does have some precedent with its involvement in the preclinical testing of pregabalin where it was identified to be better than morphine at relieving static and dynamic allodynia in the CCI model (Field, Bramwell, et al., 1999). Although it is considered an established model there are limitations to be considered which include animal self-mutilation and autotomy. This often occurs due to loss of sensation or pain as well as inter animal variability due to the tightness of ligature that is applied to the nerve. However, due to the relatively simplicity and reproducibility of this model that results in a sustained and stable level of pain it is a popular model of peripheral neuropathic pain and one of the only with evidence of predictive validity (Austin et al., 2012).

1.11 Novel preclinical neuropathic pain endpoints

A range of different endpoints and techniques have been developed with the aim of improving the translatability and accuracy of neuropathic pain measurements in rodents. Many of these focus on recording ethological behaviours that animals express such as burrowing, nesting or wheel running. These kinds of ethological markers focus on moving away from evoked endpoints such as von Frey to improve the accuracy of measuring neuropathic pain (Deuis et al., 2017). Additionally, objective measures that can be directly translated between humans and animals have also been developed such as EEG and gait analysis (Koyama, LeBlanc, et al., 2018; Vieira et al., 2020). Although historically hyperalgesia and allodynia are often used to determine the development of neuropathic pain in rodents, these conditions are only present in 15-50% of human neuropathic pain patients, meaning assessing neuropathic pain without measuring these directly could improve translatability (Jensen & Finnerup, 2014; LeBlanc, Bowary, et al., 2016).

1.11.1 Burrowing.

Burrowing is an ethological behaviour expressed in rodents that is currently being investigated as a novel neuropathic pain endpoint to improve upon the traditional reflex-based tests that are a mainstay of current analgesic research (Jirkof, 2014). As discussed, the current neuropathic pain endpoints have had little success in translating novel compounds for the treatment of neuropathic pain. Therefore, it is believed that ethological behavioural markers such as burrowing, rearing and grimacing may provide a more accurate representation of the global impact of pain rather than only assessing local sensitivity (Andrews et al., 2011). Burrowing is particularly relevant as it can be measured objectively without requiring a highly skilled or trained operator (Andrews et al., 2011, 2012; Deuis et al., 2017). An additional benefit of burrowing is that it can indicate sedative (100mg/kg) doses of gabapentin, demonstrated by reduced burrowing in naïve animals (Andrews et al., 2012). Burrowing is also considered an ethologically fundamental activity in rodents and

considered to be equivalent to activities undertaken by humans in their daily lives so would more likely reflect the overall impact of neuropathic pain (Zhang et al., 2022). This indicates that burrowing may become a sensitive marker of neuropathic pain with improved translatability and objectivity over currently used evoked measures of neuropathic pain.

1.11.1.1 Burrowing in neuropathic pain models.

Some of the key findings during the development of burrowing in pain research has been that of Andrews et al. (2012) and Lau et al. (2013) (Andrews et al., 2012; Lau et al., 2013). Andrews et al. (2012) demonstrated burrowing deficits in 3 models of peripheral nerve injury and the complete Freund's adjuvant (CFA) model in rats (Andrews et al., 2012). Tibial nerve transection induced burrowing deficits were reversed by 30mg/kg but not 100mg/kg gabapentin (Andrews et al., 2012). Lau et al. (2013) showed that rats following spared nerve injury (SNI) surgery presented a deficit in mechanical and cold allodynia as well as a deficit in burrowing all of which was reversed by 10mg/kg and 30mg/kg pregabalin (Lau et al., 2013). This study also demonstrated that carbamazepine had very modest efficacy in reversing mechanical allodynia and no effect on burrowing. This is consistent with findings in humans that pregabalin is superior to carbamazepine in treating neuropathic pain and demonstrates back translation of the effects of pregabalin on burrowing (Razazian et al., 2014).

The discussed studies in burrowing have been conducted on conditions that involve inducing inflammation or conducting surgery to a hind leg to generate this pain (Andrews et al., 2012; Lau et al., 2013). It is therefore unclear in these models if the reduction in burrowing in these models is a measure of the “global impact of pain” as suggested by the authors or is simply due to a lack of mobility or contact allodynia due to the surgical or inflammatory state. One study that investigated this limitation was conducted by Deseure and Hans (2018) and provided evidence that burrowing deficits are caused by changes induced by pain through monitoring burrowing in a model orbital nerve injury (Deseure & Hans, 2018). This study looked at a model of neuropathic pain that did not affect the hind limbs and found that orbital nerve pain caused a significant deficit in burrow compared with sham animals providing key validation to the theory that burrowing is a marker of “the global impact of pain” and animal wellbeing. However, the authors did not attempt to reverse this deficit with any analgesics limiting the validity of this claim (Deseure & Hans, 2018).

Some of the only published data regarding the effects of diabetes on burrowing has been presented by Rutten et al. (2018). This study analysed the effects of the Zucker diabetic fatty (ZDF) model, the STZ type-1 rat model of diabetes and the CCI model of surgically induced neuropathic pain on burrowing (Rutten et al., 2018). The ZDF model showed only moderate differences in burrowing compared with the Zucker lean (ZL) rats at 7 weeks, that increased further at 15 weeks. Though the difference in ZDF and ZL burrowing appears to be primarily driven by an increase in the total burrowing of the ZL animals as the ZDF group burrowing remains consistent at approximately 750g. Additionally pregabalin, gabapentin, morphine and tramadol were all unsuccessful in reversing this burrowing deficit in the ZDF model. STZ induced significant deficits in burrowing to negligible levels compared with control animals which remained at >1500g. Pregabalin at both 10 and 30mg/kg was unsuccessful at reversing this deficit. Promising results were identified in the CCI model however, where burrowing was reduced to approximately 600g compared with 1400g in sham animals. This was successfully reversed by a low dose of morphine and all doses of pregabalin and gabapentin tested (Rutten et al., 2018).

Whilst these results in the CCI model were excellent for the further development of burrowing as a marker of neuropathic pain, this study does have limitations. The authors claim that wellbeing alterations in the diabetic models may have led to the lack of efficacy of any of the standard analgesics in reversing deficits in either of the models tested (Rutten et al., 2018). This contributes to the findings that burrowing is a marker of overall wellbeing (Andrews et al., 2011; Deacon, 2006; Deseure & Hans, 2018; Jirkof, 2014). A comparatively large dose of STZ at 75mg/kg was used potentially increasing the effects of wellbeing on burrowing and reducing the likelihood these analgesics could reverse burrowing (Rutten et al., 2018). Additionally, this study summarised the results from experiments conducted across different facilities and it appears the protocol followed was not consistent. For example, some experiments used quartz sand as the substrate whereas others used pea shingle. Also, both the time allowed for burrowing to be conducted and the time after dosing the burrowing took place were inconsistent. This causes concern as a recent review found that rats tend to burrow sand and gravel differently with rats burrowing greater amounts of gravel (Zhang et al., 2022). More consistent research is needed to properly characterise burrowing in these models.

1.11.1.2 Limitations of burrowing as an endpoint.

The concept of differences in burrowing protocols are not limited to this study. Differences can be seen in most burrowing studies making it difficult to compare results. Various substrates have been used including quartz sand (Rutten et al., 2018), food pellets (Deseure & Hans, 2018; Rossato et al., 2018) and most commonly pea shingle (Andrews et al., 2012; Lau et al., 2013; Muralidharan et al., 2016; Rutten et al., 2018). Additionally, the point of the light dark cycle that burrowing has been conducted may be just before the dark period (Muralidharan et al., 2016), during the dark period (Deseure & Hans, 2018) or during the light period but the specific time is unreported (Andrews et al., 2012; Lau et al., 2013; Rossato et al., 2018; Rutten et al., 2018). Possibly most important is the length of time that burrowing is allowed to take place for such as 1 hour (Andrews et al., 2012; Lau et al., 2013; Muralidharan et al., 2016; Rossato et al., 2018; Rutten et al., 2018), 2 hours (Andrews et al., 2012; Rutten et al., 2018) or 4 hours (Deseure & Hans, 2018). This demonstrates the need for an in-depth analysis on the effects of these and other criteria such as the presence of a human observer in the room or the types of habituations used in burrowing. This would allow for a more accurate and robust protocol to be developed for measuring burrowing as an endpoint for pain studies.

It is also important to consider the variability of data that is generated by endpoints as understanding this allows for an assessment of the number of animals needed per group to ensure statistically significant differences are detected (Thomas & Juanes, 1996). If the numbers of animals needed per group are significantly higher than current endpoints, they may not be useable from an ethical standpoint as they do not conform to the 3R's (Fenwick et al., 2009). It is important to consider that burrowing has a much greater inter-animal variability compared with von Frey tests of mechanical allodynia and Randall-Selitto testing of mechanical hyperalgesia (Muralidharan et al., 2016). This study demonstrated that although burrowing in the CCI and CFA rat models was decreased, as it was for the evoked markers, the inter-animal variability was higher. This suggests the need for larger groups when using burrowing as an endpoint to ensure the reliability of the data. However, the authors technique for von Frey testing does not use the Dixon up-down method, as most studies in rats use today, and instead took the average of the filament the animal first responded to on 3 repeated tests. This method whilst appearing to generate valid data severely limits the variability achievable in the dataset. Thus the comparison of a normally distributed measures such as burrowing, with a von Frey testing protocol which generates very little variability,

is not particularly valid. Randall-Selitto data typically displays a normal distribution, so this comparison is likely more accurate (Muralidharan et al., 2016). However, the authors did not provide details of the equipment and technique used to measure this endpoint. The authors' findings that burrowing generates more variable data could well be correct but additional research is needed to compare this endpoint to others that generate truly normally distributed data (Muralidharan et al., 2016).

Overall, burrowing is a promising marker of neuropathic pain that provides an objective measure of an ethological behaviour that reflects animals' general wellbeing and not just pain. However, further development of the effects of various parts of the burrowing protocol are needed and an assessment of STZ deficits at a lower dose should be conducted.

1.11.2 Gait analysis.

Gait analysis is a technique that assesses different features of human and animal movement, speed, limb positioning and foot/paw pressure among other characteristics of movement (Lakes & Allen, 2016). Different types of gait analysis have been used for several years to analyse alterations in movement associated with different conditions, including pain (Lalli et al., 2013; Tappe-Theodor et al., 2019). Preclinically this has typically focussed on inflammatory pain occurring from arthritis (Clarke et al., 1997). Gait analysis has also been conducted in various models of neuropathic pain using a variety of techniques. Al Deeb et al. (2000) used a range of ink printing and inclined plane tests assessed in the STZ type-1 diabetes model and found no effect of STZ on these measures (Al Deeb et al., 2000). However, this study was limited by the human interpretation of the markers used. A key benefit of analysing changes in gait is that these measures can be easily and non-invasively assessed in both human and animal allowing for a direct translation of any results generated (Heinzel et al., 2020).

1.11.2.1 Gait analysis in neuropathic pain models.

A key improvement that has been made to gait analysis is the introduction of automated gait analysis such as the "CatWalk" system (Noldus, Netherlands system). This system was used by Vrinten and Hamers (2003) to show a reduction in stance phase and paw pressure which correlated to a reduction in von Frey paw withdrawal threshold in rats post CCI surgery (Vrinten & Hamers, 2003). Pitzer et al. (2016) demonstrated in two different automated gait analysis systems (CatWalk and Dynamic weight bearing (DWB) system (Bioseb)) that mice post SNI surgery showed significant deficits in different gait measures recorded by these systems such as paw contact intensity and stride length (Pitzer et al., 2016). However, manual methods using homemade apparatus are still employed successfully. For example, Karatan et al. (2019) found a decrease in measurements of paw imprint size in STZ diabetic rats using a homemade carboard tunnel and stamping ink (Karatan et al., 2019).

Recently Vieira et al. (2020) presented some of the first evidence of changes in gait caused by STZ induced type-1 diabetes recorded using an automated gait analysis system (CatWalk) (Vieira et al., 2020). This system allows for the automated and objective analysis of a naturalistic behaviour requiring no human interpretation of an evoked response. Over the course of 28 days post STZ both von Frey paw withdrawal and automated gait analysis were conducted, and a significant level of correlation was found between the two endpoints. This finding of altered gait in diabetic rodents

correlates with the human neuropathic pain condition which also shows changes in gait (Alam et al., 2017). This is particularly important as it can lead to falls in elderly diabetic patients.

1.11.2.2 Limitations of gait analysis.

Unfortunately, the gait data identified by Vieira et al. (2020) is limited as there was no attempt to reverse these markers with any standard or novel analgesics so it is not yet possible to understand if these changes in gait can be reversed (Vieira et al., 2020). Additionally, the authors only show the change from baseline of von Frey withdrawal threshold and not the absolute value, meaning the von Frey data cannot be compared with other studies. This study provides a good indication that gait analysis using an automated system can be successful in identifying gait changes in the STZ model and it may provide an excellent opportunity to develop a sensitive and objective marker that has translational links to human neuropathic pain (Vieira et al., 2020). However, extensive characterisation of this endpoint and its reversal with standard and novel analgesics is needed to develop a robust protocol for this in the STZ model. In other models automated gait analysis has been used extensively in models of both central and peripheral nerve injury with areas such as increased swing time, increased base of support and decreased toe spread being identified consistently across sciatic nerve injury models (Timotius et al., 2023).

1.11.3 Automated behavioural scoring.

Automated behavioural analysis is a useful tool for recording large amounts of behavioural data from free roaming animals in a home cage like environment (Deuis et al., 2017). These systems, whilst expensive, allow for the analysis of various ethological behaviours simultaneously without the need for human observations. They provide an excellent way to gather behavioural data in a range of animal models. Thus far in the pain field some success has been found in models such as arthritis and carrageenan induced inflammatory pain (Brodkin et al., 2014; Inglis et al., 2007, 2008; Miller et al., 2012). Inglis et al. (2008, 2007) identified that surgically induced osteoarthritis and collagen induced arthritis both resulted in decreased ethological behaviours such as locomotion and climbing in mice when recorded by the LABORAS system (Inglis et al., 2007, 2008). Similarly, Miller et al. (2012) found that the onset of mechanical allodynia measured by von Frey is followed by decreased movement, climbing and rearing in a mouse model of surgically induced arthritis (Miller et al., 2012). Comparisons have also been made between human video scoring and automated behavioural scoring in the carrageenan induced mouse model of inflammatory pain (Brodkin et al., 2014). This study showed a strong correlation between automated behavioural scoring and trained human operator scoring.

1.11.3.1 Automated behavioural scoring in neuropathic pain models.

The previously described positive result that changes in behaviour are caused by inflammatory pain, contrast the results found in a mouse model of post-surgical pain. Mouse grimace scale scoring was shown to correlate with manually scored behaviour, however automated behavioural scoring did not (Leach et al., 2012). Similarly Urban et al. (2011) found that although the CCI mouse neuropathic pain model showed some differences in automatically scored behaviours, post-surgery these returned to baseline by day 14 (Urban et al., 2011). They also found that mice undergoing SNI surgery failed to show any significant difference to baseline. Pitzer et al. (2016) showed similar

results with mice having a reduction in climbing but no other behavioural markers post SNI surgery, with only a trend towards a reduction in locomotion and distance moved (Pitzer et al., 2016).

1.11.3.2 Limitations of automated scoring studies.

The studies examining the effects of neuropathic pain on automated behavioural scoring thus far appear to have been conducted thoroughly and generated similar findings. The key limitation of these studies is that there is very little data reported on the effects of different types of neuropathic pain models and in different species. All the studies described were conducted in mouse models, likely due to the reduced cost of murine studies and the increased availability of transgenic models (Ellenbroek & Youn, 2016). It does not appear that any studies using automatic home cage behavioural analysis have been conducted in a diabetic or other metabolic models. Further categorisation of the changes in a range of neuropathic pain models and additional species are needed before this endpoint is completely ruled out of use as a neuropathic pain endpoint.

In summary, automated behavioural analysis research has demonstrated mixed success in pain models when measuring ethological behaviours. So far very little evidence supports the use of automated behavioural analysis in analysing neuropathic pain. However, there is a need for the assessment of automated behavioural scoring in future studies to see if the lack of change found so far is consistent across other neuropathic pain models. Particularly in a model that affects general wellbeing and induces a polyneuropathy such as the STZ type-1 rat model of diabetes rather than simple mononeuropathies that have been examined so far. This may help to bring out differences in home cage behaviour due to the greater changes in overall wellbeing compared with surgically induced mononeuropathies.

1.11.4 Electroencephalography.

Electroencephalography first conducted on human patients by Hans Berger in 1924, is a technique used to study electrical currents produced in the brain (Berger, 1929). It is recorded using electrodes: in humans commonly placed on the scalp (Sazgar & Young, 2019); in rodents usually placed in direct contact with the dura mater (Lundt et al., 2016), to produce an EEG recording. EEG recordings represent synchronised electrical activity from populations of neurons (Binnie & Prior, 1994). The two most prominent ways that recording EEG is applied is either to quantify the electrical activity of neuronal populations and/or as a method to quantify changes in sleep/wake behaviour (Campbell, 2009; Light et al., 2010). EEG electrical activity and sleep/wake behaviour may be useful as objective and translatable central markers of neuropathic pain. This is because EEG can be recorded objectively in both animals and humans without using evoked responses, that current neuropathic pain endpoints use (Bove, 2006; Leiser et al., 2011; Sullivan et al., 2015; Wilson et al., 2014).

1.11.4.1 Effects of neuropathic pain on spectral power changes in EEG recordings from human patients.

Early evidence of EEG electrical activity in neuropathic pain patients focused on changes in EEG power, a measure of the amount of activity in specific frequencies. EEG frequencies are typically divided into delta, theta, alpha, beta and gamma bands and the amount of activity in each band is

quantified as EEG power (Figure 1.4) (Xiao et al., 2018). In neuropathic pain patients this particularly focused on low frequencies such as an increase in theta (4-8Hz) power, decrease in alpha (8-12Hz) power and increased rhythmicity of theta oscillations that was termed thalamocortical dysrhythmia (Llinas et al., 1999). Evidence from animal models indicated that the ventral posterolateral nucleus of the thalamus (Figure 1.1) was the cause of thalamocortical dysrhythmia (Gerke et al., 2003). This population of neurons transmits spinal cord signals to the somatosensory cortex (Caylor et al., 2019). Thalamocortical dysrhythmia has continued to be a commonly referenced model for the changes in theta oscillations seen in neuropathic pain (LeBlanc, Lii, et al., 2016; Vanneste et al., 2018; Vučković, Gallardo, et al., 2018). In humans Stern et al. (2006) identified that whilst there were many similarities in EEG signal (such as increase theta power) differences in the extent of this increase in theta power were related to the neuropathic pain cause (Stern et al., 2006). Thus, developing our understanding of EEG signal patterns as markers of neuropathic pain, may produce individual patterns of EEG changes for different neuropathic pain causes.

The differences between neuropathic pain patients EEG frequency activity and that of healthy control patients has been routinely studied in different patient populations, with varying results (Mussigmann et al., 2022). An increase in theta power is one of the more consistently reported changes in studies investigating the EEG power spectral from neuropathic pain (Jensen et al., 2013; Krupina et al., 2020; Michels et al., 2011; Sarnthein et al., 2005; Sarnthein & Jeanmonod, 2008; Stern et al., 2006). Though changes in theta power are not reported in all studies (Zhou et al., 2018). Alterations in alpha power are often reported in these human neuropathic pain studies however the direction of these changes is less consistent with both increased (Michels et al., 2011; Stern et al., 2006) and decreased (Jensen et al., 2013; Simis et al., 2022) EEG alpha power reported. Changes in beta power are less commonly reported than both theta and alpha power changes, however similarly to theta power most research indicates that when beta power is identified, it is increased in neuropathic pain patients (Krupina et al., 2020; Stern et al., 2006). A recent review of resting state EEG in neuropathic pain patients found that increased theta (4-7Hz) power along with a shift of the dominant peak theta frequency towards a lower frequency were the most consistently reported finding. Overall, this provides supportive evidence that the increased theta power seen in many neuropathic pain studies may be a reproducible efficacy endpoint that can be used to screen drugs against. Though changes in other power bands should be investigated as they could indicate that different neuropathic pain causes have individual EEG power spectral profiles.

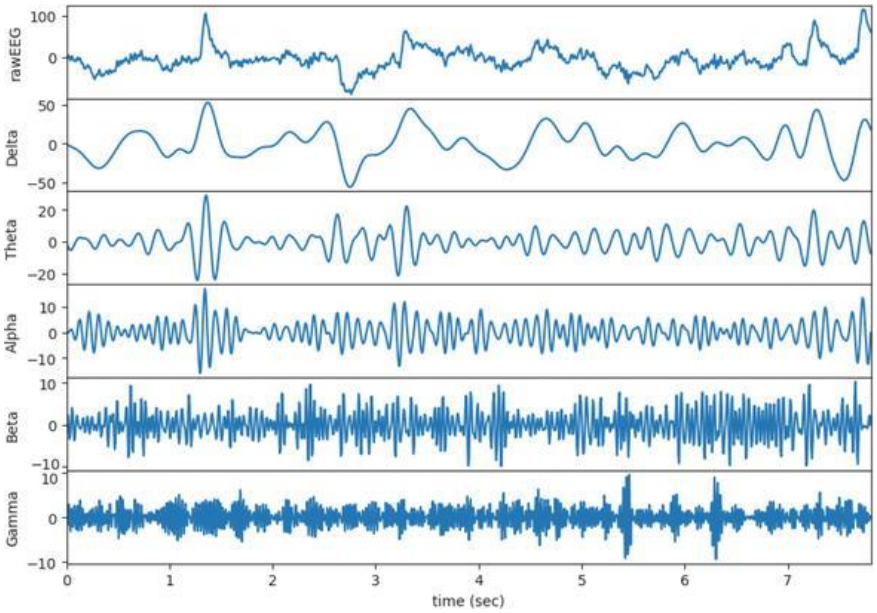

Figure 1.4) Representation of delta, theta, alpha, beta and gamma frequencies that together make up the raw EEG signal. Taken from (Bajaj & Bajaj, 2020).

1.11.4.2 Preclinical studies support theta power changes as a neuropathic pain endpoint.

Much of the published preclinical research investigating the impact of neuropathic pain of EEG power has been conducted by Carl Saab's researcher group. This group have extensively characterised that a CCI rat model of neuropathic pain demonstrates an increase in EEG theta power similar to that of human neuropathic pain patients (Koyama, LeBlanc, et al., 2018; Koyama, Xia, et al., 2018; Leblanc et al., 2014; LeBlanc, Bowary, et al., 2016; LeBlanc, Lii, et al., 2016). This group first demonstrated a decrease in thalamocortical coherence (2-30Hz) and increase in EEG theta power when recording above the S1 brain region (Leblanc et al., 2014). These changes in theta power and thalamocortical coherence provide further evidence of the link between thalamocortical dysrhythmia and theta power changes in the CCI rat model. This work further identified that EEG power was increased from 3-30Hz at the PFC, the ipsilateral and contralateral S1 regions and these changes were reversed by 10mg/kg pregabalin treatment (LeBlanc, Bowary, et al., 2016). In addition, they demonstrated evidence for the role of thalamocortical coherence in CCI induced neuropathic pain as inhibiting thalamic burst firing normalised theta power and evoked pain behaviours (LeBlanc, Lii, et al., 2016). This work culminated in the publication of a bioassay protocol using the increased theta power as a neuropathic pain endpoint for the CCI rat model (Koyama, LeBlanc, et al., 2018).

The characterisation of preclinical EEG recordings to generate a translatable preclinical neuropathic pain endpoint by Koyama et al. (2018) is one of the first to provide a detailed methodology that showed reversibility with clinically relevant analgesics (Koyama, LeBlanc, et al., 2018). Koyama et al. (2018) recorded short 3-5 minute sessions of EEG in CCI rats after 15 minutes of acclimatisation and only assessed periods of resting wakefulness. By doing so they detected an increase in resting state theta power at Day 7 and Day 14 after CCI surgery along with a corresponding decrease in paw withdrawal latency to heat. Using this methodology, the authors were able to differentiate between 3, 10 and 30mg/kg doses of pregabalin with 3mg/kg showing a lack of efficacy, 10mg/kg showing a significant reversal of the increased theta power and 30mg/kg showing a trend towards further increased theta power (Koyama, LeBlanc, et al., 2018). This dose dependent effect correlated with

their plasma concentration analysis that indicated 10mg/kg pregabalin falls within the equivalent therapeutic window in humans whilst 3mg/kg and 30mg/kg are sub and supra therapeutic doses, respectively. In contrast, the paw withdrawal latency to a heat source demonstrated efficacy at all three dose levels of pregabalin. A limitation of assessing neuropathic pain and analgesia through using increased theta power in this study was that only short periods of resting wakefulness were assessed which would not allow for the characterisation of any progressive effects of a treatment across an extended time period. Additionally, these changes have only been demonstrated up to 14 days after CCI surgery which could limit the ability for examining multiple doses of treatments in a cross over study or the assessment of treatments that require multiple doses to reach peak plasma concentrations. The back translation of the effect of pregabalin in this protocol is an important step in validating increased EEG theta power as a translatable neuropathic pain endpoint.

Whilst the development of preclinical screening protocol using increased theta power in the CCI model is invaluable, the results from other research groups are not completely consistent with these findings. Early research from Kontinen et al. (2003) identified no change in any power spectral frequency bands during either wakefulness or slow wave sleep across a 5-month long study in the CCI rat model (Kontinen et al., 2003). However, in a mouse sciatic nerve crush model Ho et al. (2024) identified an increase in theta and alpha power that correlated with mechanical withdrawal threshold measures of pain (Ho et al., 2024). They also tested the common peroneal nerve ligation model but did not find a correlation between theta and alpha power with mechanical withdrawal threshold measures of pain (Ho et al., 2024). In the mouse partial sciatic nerve ligation model it has been demonstrated that EEG delta power was increased and correlated with von Frey measurements of paw withdrawal threshold (Li, Ge, et al., 2019). Furthermore, treatments that promoted wakefulness and decreased delta power also attenuated paw withdrawal threshold measurements (Li, Ge, et al., 2019). Although these studies do not attempt to replicate the findings of Carl Saab's research group, they do highlight a lack of continuity in the results of measuring EEG power in preclinical neuropathic pain models similar to that of humans. These differences may be occurring due to; different pain models being used, different recording and analysis strategies being applied, different electrode placement or other factors. Together it highlights a need for further investigations of the impact of neuropathic pain on EEG power and reversibility with analgesics to determine if this is a reliable, reproducible and high throughput screening technique.

1.11.4.3 Sleep/wake changes induced by neuropathic pain.

Sleep is an important physiological process that can help aid in improving metabolism, immunity, recovering physical strength and is needed to allow humans to conduct their normal daily activities. Therefore, disruption to sleep can impact these processes including leading to reduced pain thresholds, interference with drug management of pain as well as psychological management of pain (Zhu & Huang, 2023). This is concerning as pain can lead to disrupted sleep itself and therefore form a cycle of disrupted sleep and increased pain levels (Almoznino et al., 2017). Sleep is generally separated into two distinct periods of non-rapid eye movement (NREM) and rapid eye movement (REM) sleep. NREM sleep is characterised by slow wave delta (0.5-4Hz) oscillations and REM sleep characterised by EEG theta (6-9Hz) oscillation along with skeletal muscle atonia and rapid eye movements (Vyazovskiy & Delogu, 2014). EEG often combined with other measures such as electromyography (EMG), eye movement and other physiological parameters can be employed in the measurement and quantification of sleep in both humans and animals enabling its potential as a translatable marker of neuropathic pain induced changes in sleep (Kourbanova et al., 2022).

1.11.4.4 Sleep/wake behavioural changes in the CCI model of neuropathic pain.

Differing results have been observed in the CCI model of neuropathic pain regarding what sleep changes occur following CCI surgery. Andersen et al. (2003) identified that rats post CCI surgery spent less total time asleep across the first 8-10 days. This was accompanied by an increase in short <15 seconds bouts of arousal particularly during the light period along with an increase in the latency to NREM sleep on days 2-7 and a decrease in latency to REM sleep on days 2-4 (Andersen & Tufik, 2003). However, these results have not been consistently identified across all CCI studies. Kontinen et al. (2003) studied the amount of time rats spent awake and in NREM and REM sleep across 146 days after CCI surgery and identified no differences in the amount of time spent in any sleep/wake state nor any changes in the number or average duration of sleep/wake episodes (Kontinen et al., 2003). The comparison between these studies is limited as the first timepoint that the Kontinen group measured changes in sleep/wake behaviour was at day 13 post surgery a timepoint where the changes identified by the Andersen et al. (2003) had already returned to baseline levels (Andersen & Tufik, 2003; Kontinen et al., 2003). This could mean that the changes in sleep/wake behaviour of CCI rats post-surgery are short lasting. This is further supported by the findings of Leys et al. (2013) in which although the total amount of slow wave sleep was not affected, the amplitude of slow wave oscillation (1-4Hz) was decreased across the first two weeks following CCI surgery (Leys et al., 2013). Tokunaga et al. (2007) highlighted that certain environmental conditions can play a role in sleep disturbances when they compared CCI rats using normal sawdust bedding versus sandpaper (Tokunaga et al., 2007). These results demonstrated that CCI rats on sawdust bedding had similar levels of sleep latency and sleep/wake amounts to sham animals. Though, when placed on a sandpaper flooring overnight to simulate an aversive condition the latency to sleep increased greatly along with the amount of time spent asleep decreasing (Tokunaga et al., 2007).

1.11.4.5 Current limitations of preclinical sleep/wake behavioural changes as neuropathic pain endpoints.

A recent study by Ho et al. (2024) further highlights the current limitations of sleep/wake changes in preclinical neuropathic pain models. To avoid the conflicting results in the CCI model they investigated the sciatic nerve crush injury and common peroneal nerve ligation mouse models (Ho et al., 2024). Both models demonstrated a significant decrease in paw withdrawal threshold across 15 days post-surgery. A decrease in the amount of time spent in NREM sleep was identified on day 1 and day 5 post surgery but returned to baseline levels from day 5 onwards. This was accompanied by sleep fragmentation at both of these time points with increased number and decreased length of NREM sleep bouts that again returned to baseline levels by day 10. The changes in REM sleep were more inconsistent with the sciatic nerve crush causing a decrease in REM sleep amounts across all timepoints measured whereas the common peroneal nerve ligation only caused a reduction in REM sleep amount from day 5 onwards. A development in this study was the correlation between paw withdrawal thresholds and the amount of time spent in NREM sleep in the sciatic nerve crush injury animals on day 1 along with positive correlations on between changes in alpha and theta EEG power and paw withdrawal thresholds on day 10 (Ho et al., 2024). These findings may indicate a paradigm of early sleep/wake changes followed by later development of EEG power spectral changes. Overall, this highlights the potentially transient nature of the changes to sleep/wake behaviour in these models and more investigation may be necessary to fully identify a reliable and robust marker of neuropathic pain using EEG measurements of sleep.

1.11.4.6 Potential in using NREM sleep fragmentation as a neuropathic pain endpoint.

A recent extensive study conducted by Alexandre et al. (2024) compared the SNI, CCI and spared nerve crush mice models for their effects on sleep/wake behaviour and particularity on NREM sleep fragmentation (Alexandre et al., 2024). In the SNI model the number of brief arousals and short bouts of wakefulness (<16 seconds) increased. This was accompanied by an increase in the number and decrease in the length of NREM sleep bouts. Though this did not affect the overall amount of NREM sleep as seen in other models (Andersen & Tufik, 2003; Ho et al., 2024). The development of NREM sleep fragmentation was maintained in the SNI model for at least 7 weeks and successfully reversed by the analgesic gabapentin (Alexandre et al., 2024). Similar results were achieved in the CCI model with increased short wakefulness bouts primarily during the light period of the recording that peaked at 5 weeks after surgery. CCI mice also spent more time in NREM sleep and less awake during the dark period up until 5 weeks unlike the SNI mice (Alexandre et al., 2024). Additionally this research group induced these brief arousals during NREM sleep with optogenetic activation of hind paw afferent fibres confirming that the brief arousals and sleep fragmentation measured were likely caused by spontaneous pain.

To further demonstrate the correlation between sleep fragmentation and neuropathic pain the sciatic nerve crush model was tested which develops a transient neuropathic pain phenotype (Alexandre et al., 2024). This model demonstrated NREM sleep fragmentation up to 4 weeks which returned to normal from week 5 onwards correlating with classical stimulus evoked measures of neuropathic pain. Interestingly models of surgical and inflammatory pain were examined and demonstrated no change in NREM sleep duration indicating that the development of NREM sleep fragmentation is restricted to neuropathic pain models.

This extensive characterisation of reproducible NREM sleep fragmentation in a variety of neuropathic pain models and its reversal with a standard analgesic indicate positive result for its potential use as an objective and translatable neuropathic pain endpoint. A key limitation is that identification of brief arousals required extensive manual scoring of the EEG recordings to produce these results. There are two main ways that preclinical rodent EEG recordings are processed to determine what periods of the recording the animals spent awake or asleep. These include manual scoring by a trained expert who visually assesses whether the EEG recording indicates that the animal was asleep or an automated sleep scoring algorithm that automatically determines the animals sleep state based on set criterion (Benington et al., 1994; Grieger et al., 2021). For sleep fragmentation to be applicable for use in a routine analgesic screening study it is likely that an automatic scoring system with minimal human intervention would need to be used to make this time and cost effective (Muto & Berthomier, 2023). Therefore, further investigations into the reproducibility and level of manual scoring intervention needed to consistently demonstrate these changes is required.

1.11.4.7 Other uses of EEG in neuropathic pain.

Other than the data generated through EEG recordings the technique also has uses in neuropathic pain treatment that avoids the use of animals by being applied directly to humans. One such method is neurofeedback modulation (NFB) which uses a real time EEG display, to allow patients to monitor and regulate their brain oscillations (Jensen et al., 2008). Following training, patients are given

targets such as to increase alpha (9-12Hz), whilst decreasing theta (4-8Hz) and high beta (20-30Hz) oscillations. This method of NFB has been found to significantly reduce pain for some patients (Hassan et al., 2015). Recently, patients have been able to practice NFB at home when it is most needed, improving the versatility of this treatment. In this study 12/15 patients achieved a statistically significant reduction in pain with upregulation of alpha (9-12Hz) oscillations (Vučković et al., 2019). Although placebo-controlled testing is difficult in NFB, pre-recorded EEG data has been examined during training session and patients reported no changes in pain scoring (Hassan et al., 2015). This data is from small sample sizes and needs further investigation to confirm these results in a much larger population as well as a variety of neuropathic pain conditions. However, it does provide additional evidence that modulating EEG oscillations can provide therapeutic benefit.

In spinal cord injury patients EEG signals have been used to classify (Wydenkeller et al., 2009) and predict patients that will develop neuropathic pain (Vučković, Gallardo, et al., 2018; Vučković, Jajrees, et al., 2018). Wydenkeller et al. (2009) found that a reduced peak EEG frequency between 6-12Hz could classify patients that were either neuropathic pain or non-neuropathic pain with 84% accuracy (Wydenkeller et al., 2009). Recently, EEG reactivity to eyes opening (Vučković, Jajrees, et al., 2018) and feature classification (Vučković, Gallardo, et al., 2018), have been used to predict neuropathic pain development in spinal cord injury patients. In 85% of cases these methods predicted non-neuropathic pain patients that would develop neuropathic pain. Interestingly this study found that the oscillations involved in the most accurate predictions included alpha (8-12Hz) and beta (13-30Hz) (Vučković, Gallardo, et al., 2018). If this area continues to develop and the accuracy of this potential neuropathic pain biomarker is further improved, it will open an opportunity for clinicians to characterise patients that are likely to develop neuropathic pain before they do so. This could allow for future studies to accurately test drugs to prevent the development of neuropathic pain.

1.11.4.8 Limitations of EEG as a neuropathic pain endpoint.

The analysis of EEG data as a neuropathic pain endpoint has solid potential; however, it does come with limitations. An example of this is the different methods of EEG electrode placement in humans and rodents (Lundt et al., 2016; Sazgar & Young, 2019). Differences in conductivity of the skull and skin can cause changes in the EEG recordings and affect translatability between species (Drinkenburg et al., 2016; Vorwerk et al., 2019). One way to improve this is using epicranial screws in rodents that are placed into but not through the skull and are therefore closer to the placement of electrodes in humans (Koyama, LeBlanc, et al., 2018; Koyama, Xia, et al., 2018; LeBlanc, Bowary, et al., 2016). Additionally, differences between rodent and human EEG signals may occur due to physiological differences in brain size and pathways, or procedural differences in EEG recordings (Leiser et al., 2011; Wilson et al., 2014). For example, coherence in the theta (4-9Hz) band was increased in human neuropathic pain patients but decreased in rats (Leblanc et al., 2014; Llinas et al., 1999; Sarnthein & Jeanmonod, 2008). EEG is a technique that provides a promising way of producing data that can be used as a neuropathic pain endpoint that is both translatable and unbiased. Further development is needed to fully characterise the changes produced by individual neuropathic pain causes and identify specific EEG patterns that translate between animals and humans.

1.11.4.9 Summary of EEG as a neuropathic pain endpoint.

The application of EEG recordings primarily falls into either assessing changes in EEG electrical activity such as EEG power or through its use to determine sleep/wake states and measure changes in sleep/wake behaviour. Both approaches have valid uses in preclinical and clinical settings for developing our understanding of neuropathic pain. In humans there is repeated evidence that an increase in theta power may be associated with neuropathic pain and this has been reproduced in rodent models. However, increased beta power and variable changes in alpha power have also been reported in human neuropathic pain patients. Likewise, the use of increased theta power as a preclinical neuropathic pain endpoint has mainly been investigated by a single research group, whilst others have reported more variable changes. Impaired sleep is often reported by neuropathic pain patients but has not been extensively investigated in humans. Preclinically, the amount of time neuropathic pain animals spend asleep appears variable. However, sleep fragmentation may provide a more consistent measure of neuropathic pain induced changes in preclinical animal models. EEG represents a translatable non-evoked and novel neuropathic pain endpoint that requires further characterisation to ensure it is reproducible and robust enough to be used for preclinical screening.

1.12 Summary and conclusions

Current endpoints used to evaluate neuropathic pain in both humans and animals need improvements to allow for successful forward translation of analgesics from preclinical into clinical studies. The ideal way for this to occur is through an objective endpoint such as EEG that can be measured in both humans and animals. An improvement would be to find endpoints in animals that better reflect the generalised effects of pain including on wellbeing and are therefore equivalent to those used in human clinical trials. Ideally all these preclinical endpoints would be objective to avoid any potential bias that may be introduced by human observers.

Some of these potential preclinical endpoints that have shown promise include: burrowing, gait analysis, automated behavioural scoring and EEG. Burrowing shows promise through its objective measurement of an ethological behaviour. To progress this, a robust reproducible protocol needs to be developed and further investigation into the effects of models that change general wellbeing need to be conducted. Investigations into the effects of neuropathic pain on gait analysis have been assessed but reversal of these changes with analgesics needs to be established. Automated behavioural scoring is yet to show any reliable changes that can be used to screen analgesics in neuropathic pain models. Though this may change when models of polyneuropathy such as the type-1 STZ diabetic model are examined. EEG is currently the endpoint with the best translational potential due to the ability to record it in both animals and humans. A protocol has been developed by Koyama et al. (2018) that needs further validation to characterise if the changes seen are reproducible and sensitive enough for preclinical screening.

Overall, progression is being made towards improving the translatability of neuropathic pain endpoints. However, several gaps in the research remain to be investigated before this can be successful. Once these gaps have been addressed, novel neuropathic pain endpoints will lead to the development of new analgesics to treat the large unmet need of patient who suffer with neuropathic pain.

1.13 Aims for this thesis

The aim for this thesis is to investigate novel, objective endpoints for neuropathic pain that will improve the translatability of preclinical neuropathic pain research. Additionally, this thesis looks to identify any animal welfare refinements that can be implemented to improve the reliability and ethical impacts of preclinical neuropathic pain research. To achieve this Chapter 2 will validate the STZ model of diabetic neuropathic pain and how social housing of diabetic animals can affect their responses. Chapter 3 will investigate the suitability of burrowing as an objective measure of neuropathic pain in the STZ diabetic model over an extended time course and identify if a clinical analgesic can reverse burrowing changes. Gait and locomotor activity will be measured in the STZ diabetic rats in Chapter 4 to understand if these can be used as neuropathic pain endpoints at early timepoints. Chapters 5 and 6 will look to examine how oxaliplatin and CCI neuropathic pain models affect measures of EEG and sleep/wake behaviour as potential neuropathic pain endpoints. Including examining if clinical and potential analgesics can normalise these objective EEG endpoints in Chapter 6.

Chapter 2: Validation of the 55mg/kg STZ type-1 diabetes rat model and burrowing changes

2.1 Introduction

There is a prevalent need for analgesics that can treat patients suffering from neuropathic pain as current treatments lack efficacy and have extensive side effects (Brooks & Kessler, 2017). Diabetes is a leading cause of neuropathic pain and with incidences of diabetes expected to rise, so too will the need for treatments (Dieleman et al., 2008). To determine the efficacy of novel analgesic compounds against diabetic peripheral neuropathy, the streptozotocin (STZ) type-1 diabetes model of neuropathic pain is routinely used for preclinical studies (Al Deeb et al., 2000; Burnett et al., 2014; Field, McCleary, et al., 1999; Furman, 2021; Rutten et al., 2018; Shamsaldeen et al., 2020; Wang-Fischer & Garyantes, 2018; Zafar & Naeem-ul-Hassan Naqvi, 2010). This model is induced by administering STZ to rodents and causes damage to pancreatic β cells and ultimately β cell death (Lenzen, 2008). Pancreatic β cell death represents good construct validity for this model, though it does not occur through autoimmune activity, the leading cause of type-1 diabetes in humans (Atkinson et al., 2014). The STZ model of type-1 diabetes demonstrates good face validity as animals develop hyperglycaemia, polyurea, polydipsia and neuropathic pain (Wang-Fischer & Garyantes, 2018). The STZ diabetic rat model was a decision-making screening step in the preclinical development and approval of pregabalin, a first line treatment for neuropathic pain (Finnerup et al., 2015). This is one of the only examples of forward translation in neuropathic pain research and provides evidence of predictive validity for the STZ diabetic rat model (Field, McCleary, et al., 1999). Therefore, it is a suitable model for assessing the effects of diabetic neuropathic pain in this study.

The current endpoints used preclinically to quantify neuropathic pain lack objectivity, primarily assess evoked behaviours and do not account for the cortical and emotional processing aspects of pain (Urban et al., 2011). In contrast clinical trial endpoints focus on patient reported pain, whilst subjective, do account for the emotional and cortical processing aspects of neuropathic pain (Figure 1.3) (Attal et al., 2018). A primary preclinical neuropathic pain endpoint is von Frey paw withdrawal threshold (Deuis et al., 2017; Fisher et al., 2021; Tappe-Theodor et al., 2019). This technique typically involves the use of a range of calibrated monofilaments applied to a rodent's hind paws to elicit a response that is interpreted by a trained human observer (Figure 2.2) (Deuis et al., 2017; Fisher et al., 2021; Tappe-Theodor et al., 2019). Von Frey paw withdrawal threshold has been used extensively in several preclinical neuropathic pain models including the chronic constrictive injury (CCI) (Austin et al., 2012; Rutten et al., 2018; Vrinten & Hamers, 2003), oxaliplatin (Kim et al., 2017), spinal cord injury (Gerke et al., 2003) and the STZ rat model of type-1 diabetes (Ali et al., 2015; Field, McCleary, et al., 1999; Vieira et al., 2020; Wang-Fischer & Garyantes, 2018; Yamamoto et al., 2009).

STZ diabetic rats typically develop a reduction in paw withdrawal threshold during the first 2 weeks after STZ administration and this can be maintained for up to 50 weeks (Field, McCleary, et al., 1999; Wang-Fischer & Garyantes, 2018). A decrease in von Frey paw withdrawal threshold is considered to represent a development of mechanical allodynia, a feature of neuropathic pain (Deuis et al., 2017). This has led to von Frey paw withdrawal threshold being used extensively in the STZ diabetic model to quantify neuropathic pain (Ali et al., 2015; Field, McCleary, et al., 1999; Vieira et al., 2020; Wang-Fischer & Garyantes, 2018; Yamamoto et al., 2009). The reversal of mechanical allodynia in STZ

diabetic rats is often achieved with the first line clinical treatment pregabalin at doses of 10mg/kg and 30mg/kg (Field, McCleary, et al., 1999; Finnerup et al., 2015; Yamamoto et al., 2009). However, as with many other preclinical neuropathic pain endpoints, von Frey paw withdrawal threshold is hindered by it being a subjective measure that may only capture spinal cord reflex activation and provide false positive results to sedative and motor altering compounds (Fisher et al., 2021; Tappe-Theodor et al., 2019). These limitations are considered to be contributory reasons for the lack of forward translation of novel analgesic treatments for neuropathic pain (Deuis et al., 2017; Fisher et al., 2021; Tappe-Theodor et al., 2019).

The mismatch between preclinical and clinical endpoints has led to the investigation of novel endpoints, such as burrowing, which is an ethological behaviour that can be measured objectively in rodents (Andrews et al., 2012; Fisher et al., 2021). Burrowing was originally conceived as a method to monitor prion diseases preclinically (Deacon, 2006). Since then the use has expanded to measure behavioural changes in a wide range of preclinical models including inflammation (Jirkof et al., 2013), brain lesions (Jirkof, 2014) and neuropathic pain (Rutten et al., 2018). It is simple to measure as it is quantified as the amount of a substrate (usually, gravel, sand or food pellets) displaced from a tube in a set period of time making it an objective measure that does not require any technical prowess to perform (Zhang et al., 2022). Burrowing is also considered an ethologically fundamental activity in rodents that reflects the activities undertaken by humans in their daily lives so may reflect the overall impact of neuropathic pain better than the current evoked endpoints (Zhang et al., 2022). Burrowing deficits have been identified in inflammatory models of pain and reversed with non-steroidal anti-inflammatory drug treatments but not anxiolytic or motor impairing drugs (Andrews et al., 2011, 2012; Gould et al., 2016). In the CCI model burrowing deficits have been shown to develop from as early as 3 days after CCI surgery (Muralidharan et al., 2016) which can be reversed by 3, 10 and 30mg/kg pregabalin administration (Rutten et al., 2018). Similarly in the rat spared nerve injury model 10mg/kg pregabalin reversed both the burrowing deficits of these rats (Lau et al., 2013).

However, in models of diabetes the results are less conclusive. In a model of a single high dose of 75mg/kg STZ Rutten et al. (2018) demonstrated that these STZ rats at Day 21 burrowed <250g on average and that neither 10mg/kg or 30mg/kg pregabalin could reverse these changes (Rutten et al., 2018). Additionally, this study also assessed burrowing in the Zucker diabetic fatty (ZDF) type-2 diabetes rat model which exhibited a less severe burrowing deficit (Rutten et al., 2018). ZDF rats burrowing was also not restored by pregabalin, gabapentin, morphine or tramadol administration (Rutten et al., 2018). The authors claim that the lack of burrowing deficit reversal in diabetic models may be related to general diabetes-associated alteration of animal well-being (Rutten et al., 2018). This could include sickness related motivational change that may be severe enough to mask the neuropathic pain changes (Rutten et al., 2018). This finding does contribute to the understanding that burrowing may be a measure of overall animal “wellbeing” and that normal expression of this ethological behaviour can indicate overall wellbeing in the animals being tested (Andrews et al., 2011; Deacon, 2006; Deseure & Hans, 2018; Jirkof, 2014). This can be viewed as an improvement over classical methods of measuring evoked pain such as von Frey measurements as it captures the global impact of pain on the animal and not just a reflexive reaction (Gould et al., 2016).

Previous research at University of Hertfordshire has identified that in a single dose 65mg/kg STZ model, home caging an STZ diabetic rat and control rat together (mixed) and allowing them to burrow together (paired burrowing) led to an increased amount of burrowing compared with two STZ rats burrowing together (STZ/STZ) (Burnett et al., 2014). A possible explanation for the increase in STZ diabetic rat burrowing either when paired burrowing with a control rat (Burnett et al., 2014) could be through social facilitation. Social facilitation in humans is often considered in the form of

social support of a loved one or family member and has been identified to improve wellbeing and pain scores (Mogil, 2015). In rodents this phenomenon is referred to as “social buffering” and can reduce the effects of aversive experiences and improve welfare in laboratory rodent (Denommé & Mason, 2022). However, this study did not assess if this effect was maintained when rats burrowed on their own (individual burrowing).

Recently the protocol used to induce a diabetic phenotype in rats at University of Hertfordshire has been refined to use a single, lower 55mg/kg dose of STZ and two hours of anomer equilibration to improve animal welfare. STZ occurs as an α and β anomer, of which α is the more toxic. Over the first two hours after being dissolved the usual >85% α anomer content decreases to an equivalent level of the β anomer (De La Garza-Rodea et al., 2010). Despite this, protocols for STZ administration still routinely describe administering STZ immediately after being dissolved and suggest using higher ≥65mg/kg doses in rats (Furman, 2021). Burrowing is yet to be examined in a type-1 diabetes model using a less than 65mg/kg dose of STZ model which reduces the limitation of any wellbeing or diabetes-associated alteration in burrowing and improves the accuracy of these results (Rutten et al., 2018).

2.1.1 Aims and hypotheses.

The primary aim of this study was to establish that a single low 55mg/kg dose of STZ in rats could induce a preclinical disease model of diabetic hyperglycaemia, polydipsia, polyphagia and mechanical allodynia equivalent to that seen at single, high >65mg/kg doses.

This study also looked to assess if rats administered 55mg/kg STZ could develop a similar decrease in burrowing to previous findings in higher >65mg/kg dose models.

The clinical analgesic pregabalin (30mg/kg) was also used in this study to establish if mechanical allodynia and decreased burrowing in the 55mg/kg STZ model could be reversed.

As previous studies at the University of Hertfordshire have indicated the potential of social facilitation through mixed home caging STZ diabetic and control rats can improve paired burrowing levels this effect was examined on individual burrowing levels when using a single lower dose 55mg/kg STZ model.

2.1.2 Abbreviations.

STZ – streptozotocin, CCI – chronic constrictive injury, SNI – spared nerve injury, SEM – standard error of the mean, BGL – blood glucose level, i.p. – intraperitoneal, p.o. – oral, ZDF – Zucker diabetic fatty.

2.2 Methods

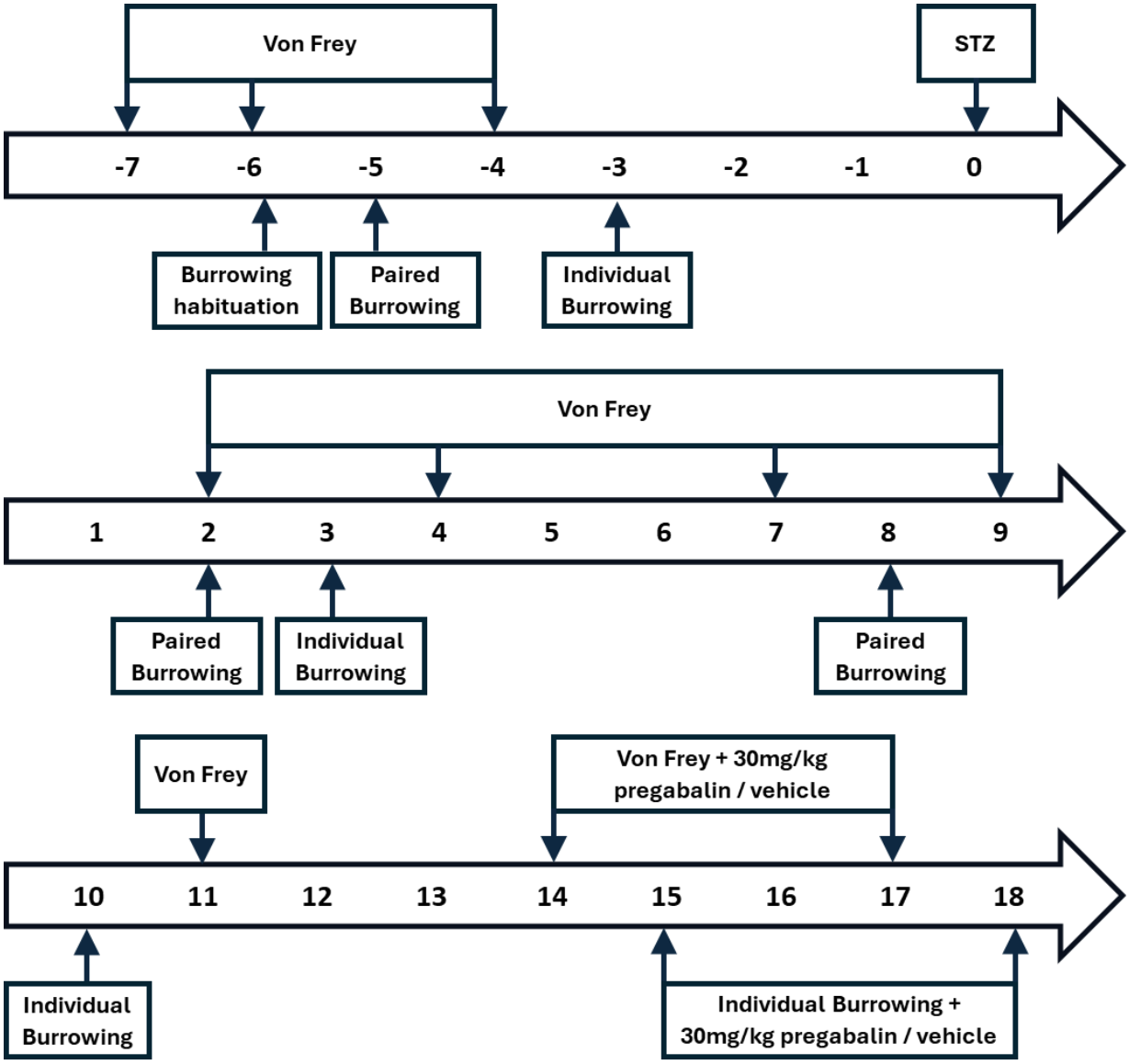

Figure 2.1) Timeline of the study depicting the days before and after 55mg/kg STZ intraperitoneal (i.p.) administration on Day 0. The days on which von Frey paw withdrawal threshold and individual or paired burrowing measurements were taken are displayed. The timepoints that vehicle and 30mg/kg pregabalin were administered are also denoted.

2.2.1 Ethics statement.

All research procedures/experiments were performed in accordance with Animals Scientific Procedures Act 1986 & European Directive 2010/63/EU. All studies performed were approved by the University of Hertfordshire Animal Welfare and Ethics Review Body and comply with the home office guidelines and codes of conduct. All work was authorised under University of Hertfordshire home office establishment licence and project licence titled: Diabetes mechanisms and treatments.

2.2.2 Animals used and induction of STZ.

34 Male Wistar Han IGS rats (300-450g at time of STZ administration) supplied by Charles River, UK were housed in pairs from arrival. At Day 0 (Figure 2.1) rats were administered either 55mg/kg streptozotocin (n=17 STZ) or 20mM citrate buffer (n=17 Control) intraperitoneal (i.p.) administration at a dose volume of 10ml/kg. STZ (Sigma-Aldrich, S0130) was protected from light and allowed to stand for at least 120 minutes on wet ice after weighing for anomer equalisation before dissolution. Citrate buffer 20mM was adjusted to pH 4-4.5 and stored on ice. After 120 minutes STZ was dissolved in fresh citrate buffer at 5.5mg/ml and stored in the at 4-8°C for 30 minutes to allow for further anomer equilibration before administration. Either STZ at 55mg/kg or citrate buffer (control) were administered once to rats via single i.p. injection using a new 23G needle. Rats were placed back in their home cage and monitored closely for 1 hour for signs of distress or discomfort. Additionally, banana porridge (Cow&Gate) and 2% sucrose solution were also provided for 48 hours post STZ administration to encourage feeding and maintain blood glucose levels.

2.2.3 Environmental conditions.

Rats were pair housed in Tecniplast 2000P cages and a 12:12 hr light-dark cycle (lights on at 07:00) was maintained throughout the study. Housing temperature was maintained at 21±2°C and 55±15% relative humidity. Food (5LF2 10% protein LabDiet, changed to 5LF5 22% protein LabDiet on day of STZ administration) and drinking water were provided ad libitum except during von Frey behavioural testing. Water was provided in two 1L bottles per cage. For 48 hours after STZ administration (Day 0,1), 2% sucrose solution was provided in one of the 1L bottles to avoid hypoglycaemia caused by STZ administration (Ghasemi & Jeddi, 2023). Water intake measurements were recorded from 1 week before STZ administration and as required until the end of the study. Food and water intake was calculated per cage as the change in weight (g) of the food hopper and both water bottle recorded at approximately 9am each day.

2.2.4 Animal welfare.

Blood glucose level (BGL) was recorded immediately prior to (Day 0) and at 7 days after STZ/control administration (Day 7) to confirm onset of hyperglycaemia. Following this BGLs were also measured at the end of the study (Day 18) to ensure maintenance of hyperglycaemia. Microsamples of blood were taken through tail tip vein puncture using a lancet (Valuemed, UK) and BGL was measured using Aviva Aucu-Chek. An inclusion criterion of >16mmol/dL BGL at all post administration timepoints for STZ diabetic rats was used to exclude rats that did not develop hyperglycaemia.

Daily bodyweight measurements were taken at regular intervals from Day -7 to Day 0 to monitor animal weight gain and progression. After STZ/control administration on Day 0, daily bodyweight measurements were taken to monitor animal welfare. Rats reaching 15% bodyweight loss compared with the Day 0 baseline weight were monitored closely. This included weighing twice daily, provision of additional nourishment in the form of seed, grains and banana porridge where appropriate and assessment by animal care staff and or veterinarians if needed. Any rats not stabilising or gaining weight within 48 hours were humanly euthanised. All rats were also checked daily by trained animal care staff to monitor welfare.

2.2.5 Burrowing.

Burrowing was assessed as the amount 2.5kg of pea shingle (0.5-2cm diameter, Wickes, UK) removed from a hollow plastic tube (320mm long x 100mm diameter) in 2 hours following a protocol adapted from Andrews et al. (2012) and Rutten et al. (2018) (Figure 2.2A,B). Burrowing testing was conducted in a separate cage to the home cage with minimal bedding (shredded paper wool) and free access to food and water. Rats were first habituated in pairs to empty burrowing tubes (Day -6) before paired burrowing was measured (Day -5). One baseline measurement of individual burrowing was also taken prior to STZ administration (Day -3). After STZ administration, paired burrowing recordings on Day 2 and Day 8 and whilst individual burrowing measurements were taken on Day 3 and Day 10 (Figure 2.1).

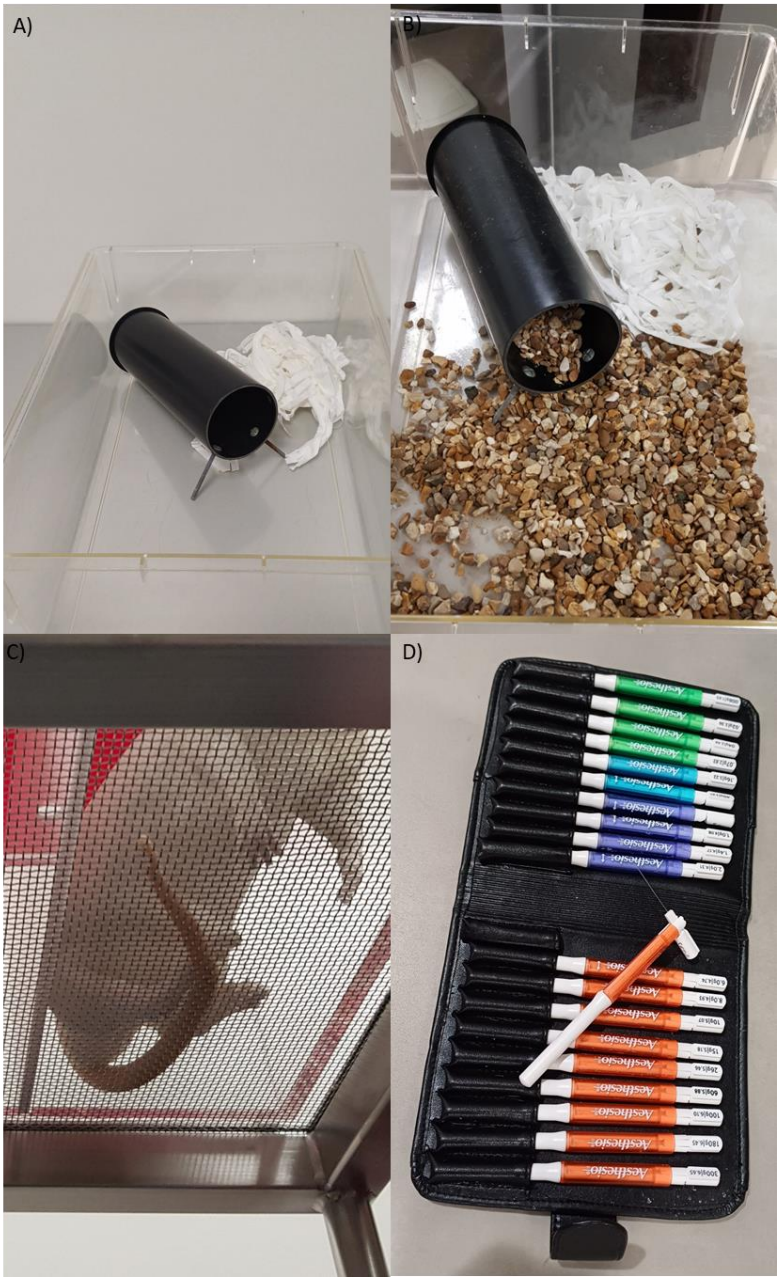

Figure 2.2) A) Burrowing cage setup prior to burrowing being conducted (with cage lid, food and water removed). B) Burrowing cage after burrowing has been conducted (with cage lid, food and water removed). C) Von Frey cage setup view from below through which von Frey monofilaments are applied. C) Von Frey monofilaments used for mechanical allodynia assessment (Bioseb, USA).

2.2.6 Mechanical allodynia.

Von Frey monofilaments (0.4, 0.6, 1, 1.4, 2, 4, 6, 8, 10, 15, 26; g) (Bioseb, USA) were applied to the plantar surface of the hind paw (Figure 2.2C,D). The up-down method was used to establish the paw withdrawal threshold by applying filaments of increasing or decreasing force depending on the previous response (Chaplan et al., 1994; Dixon, 1965). Beginning with the 4g filament a withdrawal response led to the next lowest filament in the series being applied (2g) whilst a lack of response led to the next highest filament being applied (6g). The monofilaments were held at the position for up to 8s with enough force to cause a slight bend of the filament. Only immediate sharp withdrawal responses from the stimulus (or flinching) or paw licking were considered to represent a positive response. Rats were elevated on a 0.5cm^2 grid mesh to allow access to the plantar surface of the hind paw and an inverted plexiglass container was placed on top of each rat. Testing was performed after an initial 15-20 minute acclimatisation period. Three baseline von Frey measurements were taken prior to STZ administration on Days -7, -6 and -4, the average of the last two were averaged as the baseline response. Mechanical allodynia development was assessed after STZ administration on Days 2, 4, 7, 9 and 11.

2.2.7 Pregabalin.

Pregabalin 30mg/kg p.o. (oral) (Ochem, USA) or 2ml/kg p.o. drinking water (vehicle) were administered in a crossover design on Day 14 and Day 17 for von Frey paw withdrawal threshold testing and on Day 15 and Day 18 for burrowing testing. The crossover design was such that if a rat was administered vehicle on Day 14 for von Frey testing, they would also be administered vehicle on Day 15 for burrowing testing. The same rat would then be administered 30mg/kg pregabalin on Day 17 for von Frey testing and 30mg/kg pregabalin again on Day 18 for burrowing. Von Frey testing was conducted at 1 and 2 hours after pregabalin/vehicle administration with individual burrowing assessments at 1-3 hours after pregabalin/vehicle administration. Crossover grouping was assigned by Latin square randomisation of animal identification numbers to randomise if pregabalin or vehicle were administered first.

2.2.8 Grouping, randomisation, blinding and exclusion or inclusion criteria.

The STZ and control grouping was randomised using the Latin square technique based on von Frey baseline data as the primary source of sorting to ensure an equal spread of baseline paw withdrawal thresholds. Following this consideration of baseline burrowing, bodyweight and caging were considered to ensure they were not significantly different. Five rats weighing <350g at day of STZ administration (Day 0) were deemed to have not reached a sufficient bodyweight and were swapped with a rat with an equivalent von Frey baseline. Rats were housed as either two control rats control/control (n=5 cages), two STZ diabetic rats STZ/STZ (n=5 cages) or as a mixed pair with one control rat and one STZ diabetic rat (mixed) (n=7 cages). All rats remained with their original cage partner from beginning of the study to avoid distress or aggressive behaviour from rehousing.

Exclusion criteria included >50% change from baseline for von Frey paw withdrawal threshold measurements of mechanical allodynia and at least 500g baseline burrowing amount were set. Additionally, a BGL of at least 16mmol/L was set as the threshold for development of hyperglycaemia and to be considered as representative of a diabetic phenotype. One rat developed an initial BGL >16mmol/L but was identified as dropping below this level at Day 18 and was excluded

from all other analysis (leaving n=16 STZ, n=6 mixed cages). One control rat and two STZ diabetic rats burrowed <500g at baseline and were excluded from all individual burrowing analysis (leaving n=9 control rats from control/control cages, n=6 STZ from mixed cage, n=8 STZ from STZ/STZ cage). Two STZ diabetic rats did not develop a >50% reduction in baseline paw withdrawal threshold and were excluded from von Frey paw withdrawal threshold analysis along with one control rat being excluded due to a baseline von Frey paw withdrawal threshold that was <10g (leaving n=9 control rats from control/control cages, n=5 STZ from mixed cage, n=9 STZ from STZ/STZ cage). All behavioural testing was conducted blinded to the test compound received or animal status. A maximum limit of 20% bodyweight loss was in place to exclude any rats that developed excessive weight loss.

2.2.9 Statistics.

To compare the results at each timepoints (Days) between control and STZ diabetic rats two-way mixed model analysis of variance (ANOVA) was used with Šídák's post hoc test to compare between control and STZ diabetic rats (BGL, von Frey, burrowing, bodyweight, daily food and water intake). For measures with additional comparisons within each group comparing between Days Dunnett's post hoc test was used (BGL, von Frey, burrowing) (Prism 10.2; GraphPad, San Diego, CA USA). A p value of <0.05 was considered statistically significant for all data. Data is reported as mean ± standard error of the mean (SEM).

2.3 Results

2.3.1 STZ (55mg/kg) administration caused hyperglycaemia and a diabetic phenotype.

Administration of a single dose of 55mg/kg STZ i.p. successfully raised BGLs above the 16mmol/L threshold in all but one rat [Time: $F(2,63) = 212.1$, $p<0.001$], [Treatment: $F(1,32) = 401.4$, $p<0.001$], [Interaction: $F(2,63) = 214.2$, $p<0.001$]. All STZ rats had BGLs above the hyperglycaemic threshold at Day 7 with one rats BGL decreasing from 18.2mmol/L at Day 7 to 9.4mmol/L at Day 18 (Figure 2.3). This rat was excluded from all other analysis due to not developing sustained hyperglycaemia. Both STZ and control rat's had equivalent BGLs at the pre STZ/control baseline with an average BGL of 6.2mmol/L and 6.3mmol/L respectively. Control rats BGLs remained stable at an average of 6-6.3mmol/L across the study. STZ rats BGL increased to an average of 29.6mmol/L at Day 7 and remained stable at 28.9mmol/L at Day 18 with both timepoints being over four times higher than the baseline timepoint and control rats at the same timepoint. This increase in STZ rats BGL above the hyperglycaemic threshold means that they can be deemed as developing a diabetic phenotype and referred to as STZ diabetic rats.

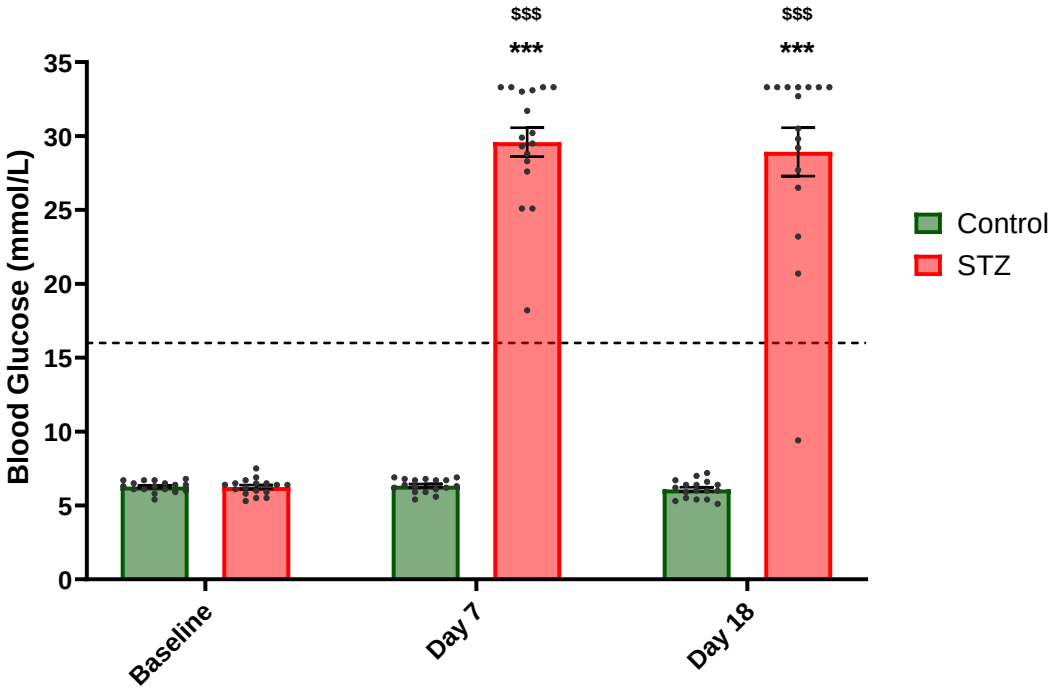

Figure 2.3) STZ administration caused an increase in blood glucose levels at both Day 7 and Day 18. Blood glucose level at baseline, Day 7 and Day 18 after STZ/control administration. Dashed line indicates 16mmol/L cutoff level for conformation of hyperglycaemia. ***p<0.001 vs baseline, $$$$p$<0.001 vs control. All data is reported as mean ± SEM, n=17 control, n=17 STZ.

2.3.2 STZ diabetic rats gained less bodyweight than control rats.

To monitor the health and welfare of rats after STZ/control administration bodyweight measurements were taken daily and demonstrated that STZ diabetic rats initially lost bodyweight before stabilising. The average bodyweight of the STZ diabetic rat group was slightly (but not significantly) higher at 417g compared to 383g in the control rat group on Day 0 (Figure 2.4A). STZ diabetic rats initially lost approximately 10g (4%) bodyweight across the first two days after STZ administration (Figure 2.4A,B). This loss of ~10g stabilised and STZ diabetic rats remained at an average bodyweight of 406g by Day 18 which was significantly lower than control rats at 427g [Time: $F(20,255) = 153.2$, $p<0.001$], [Treatment: $F(2,13) = 284.6$, $p<0.001$], [Interaction: $F(40,255) = 60.45$, $p<0.001$] (Figure 2.4A). When compared as the percentage change from Day 0 bodyweight, STZ diabetic rats bodyweight decreased at Day 1 before stabilising at ~4% by Day 2, significantly lower than control rats and remained at this level for the rest of the study (Day 18) [Time: $F(23,711) = 115.2$, $p<0.001$], [Treatment: $F(1,31) = 205.4$, $p<0.001$], [Interaction: $F(23,711) = 86.00$, $p<0.001$] (Figure 2.4B). Control rats continued to gain weight across the study and gained an average of 67g (16.85%) across the 18 days after administration. Any rats developing a bodyweight loss that exceeded 15% led to an increase in animal welfare monitoring and ultimately euthanasia if bodyweight loss approached 20%. This was required for one rat in this study on Day 17 but was not excluded from analysis. This demonstrates that STZ diabetic rats initially lost 4% bodyweight which remained stable for the rest of the 18 day study.

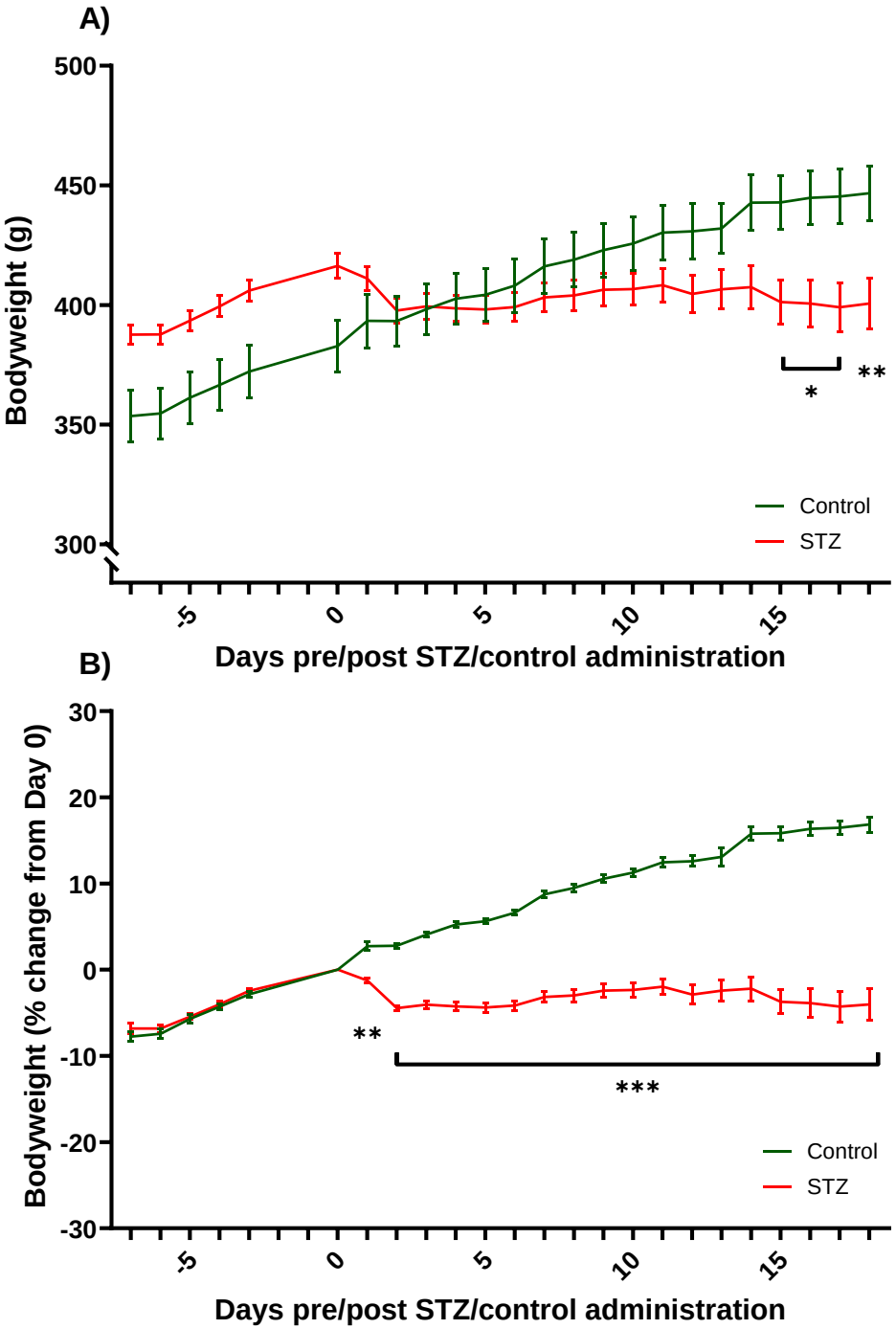

Figure 2.4) Control rats bodyweight continued to increase across the study whilst STZ diabetic rats bodyweight plateaued. The average bodyweight of STZ diabetic and control rats across the study expressed as the raw bodyweight (g) (A) and the percentage change in bodyweight from the pre STZ/control administration weight on Day 0 (B). *p<0.05, **p<0.01, ***p<0.001 vs control. All data is reported as mean ± SEM, n=17 control, n=16 STZ.

2.3.3 STZ diabetic rats developed polyphagia and polydipsia.

Another phenotype of diabetes and the STZ diabetic model is the development of polydipsia and polyphagia which was demonstrated in this study by increased daily food and water intake from cages with STZ diabetic rats. The amount of food consumed by STZ/STZ cages and mixed cages

progressively increased after Day 0, reaching a peak at Day 6 and then remained relatively stable until Day 18 (Figure 2.5A). By Day 6 mixed cages were consuming more food than control/control cages whilst STZ/STZ cages were consuming more than both other cage types [Time: $F(20,256) = 56.51$, $p<0.001$], [Treatment: $F(2,13) = 60.61$, $p<0.001$], [Interaction: $F(40,256) = 18.35$, $p<0.001$] (Figure 2.5A). For STZ/STZ cages the increased food consumption was over three times as high by Day 6 than the food consumption on Day 0. Similarly, mixed cage food consumption doubled by Day 6 whilst control/control cage food intake remained relatively stable across the study (Figure 2.5A). Water drinking levels followed the same trend as food intake and progressively increased until Day 6 in STZ/STZ and mixed cages before plateauing (Figure 2.5B). As early as Day 2 mixed cages were consuming more water than control/control cages whilst STZ/STZ cages were consuming more water than both other cage types [Time: $F(20,256) = 153.2$, $p<0.001$], [Treatment: $F(2,13) = 284.6$, $p<0.001$], [Interaction: $F(40,255) = 60.45$, $p<0.001$] (Figure 2.5B). At Day 6 mixed cages water intake had increased by 2.5 times whilst STZ/STZ cages water intake increased by over 5 times (Figure 2.5B). An excessive increase in food intake, such as that demonstrated by STZ diabetic rats in this study, is termed polyphagia whilst an excessive increase in water intake is termed polydipsia. Both polydipsia and polyphagia are symptoms of diabetes and have been demonstrated in this 55mg/kg STZ model.

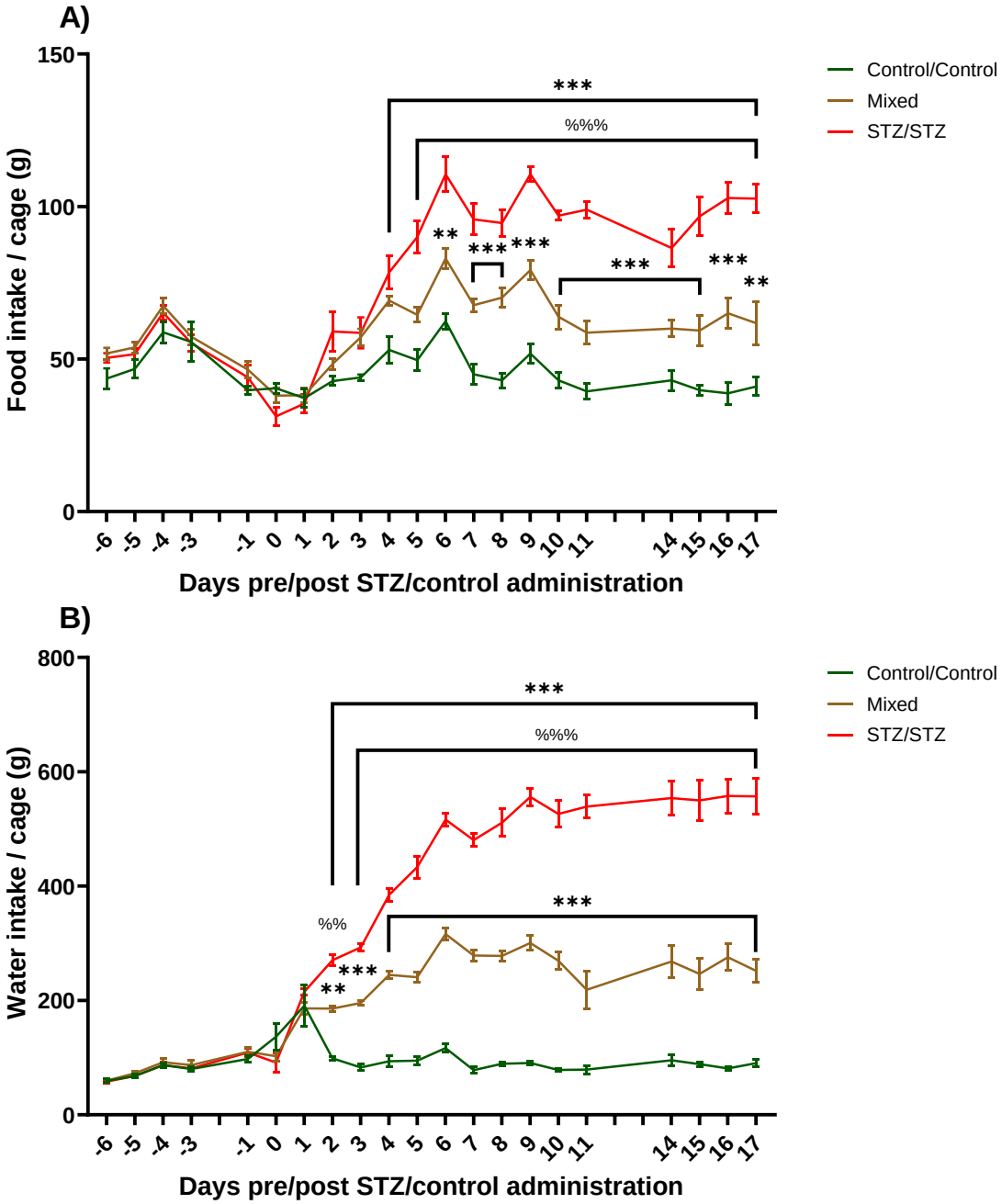

Figure 2.5) STZ diabetic rats developed polyphagia and polydipsia that stabilised after 6 days. The food (A) and water (B) intake per day from each home cage of paired rats. Home cage pairs were either two control rats (control/control), a control and STZ diabetic rat (mixed) or two STZ diabetic rats (STZ/STZ). **p<0.01, ***p<0.001 vs control/control, %%p<0.01, %%%p<0.001 vs mixed. All data is reported as mean ± SEM, n=5 control/control cages, n=6 mixed cages, n=5 STZ/STZ cages.

2.3.4 STZ diabetic rats developed mechanical allodynia on Day 9 and Day 11 regardless of home caging.

To establish if STZ or control administration caused mechanical allodynia development, paw withdrawal thresholds were measured from Day 2 to Day 11 (Figure 2.6A). Mechanical allodynia was induced in STZ diabetic rats irrespective of home caging at Day 9 and Day 11 after STZ administration as demonstrated by a reduction in von Frey paw withdrawal threshold [Time: $F(5,145) = 22.17$,

p<0.001], [Treatment: F(3,29) = 4.65, *p*=0.009], [Interaction: F(15,145) = 3.124, *p*<0.001] (Figure 2.6A). Paw withdrawal thresholds were also reduced in control rats in mixed cages compared to baseline at Day 11. At Day 9 STZ diabetic rats housed in a mixed cage paw withdrawal threshold reduced from 22.4g (baseline) to 9.9g, a >50% reduction which further decreased at Day 11 to 6.4g, a >70% reduction (Figure 2.6A). STZ diabetic rats caged with another STZ diabetic rat (STZ/STZ) showed a similar decrease from 24.4g (baseline) to 6.6g at Day 9, a >70% reduction which remained stable at Day 11 at 6.8g. Both STZ groups had much lower paw withdrawal thresholds at Day 9 than at baseline and control/control rats at the same Day 9 timepoint. Additionally, STZ/STZ diabetic rats paw withdrawal threshold was also significantly lower than control rats from a mixed cage. Some control rats also had decreased paw withdrawal thresholds particularly for control rats in a mixed cage at Day 11 which was lower than the baseline timepoint (Figure 2.6A). It was also identified that one control rats paw withdrawal threshold was <10g at baseline and was excluded from further von Frey analysis. This demonstrates that STZ diabetic rats developed mechanical allodynia at Day 9 and Day 11 in this study.

As with the baseline timepoint which was generated from the average response on Days -6&-4, timepoints after STZ/control administration were averaged to generate a more precise value for the selection of an appropriate timepoint to compare test compounds to assess their analgesic properties. At Days 4&7 STZ/STZ rats had already started to develop mechanical allodynia as paw withdrawal threshold decreased compared to baseline levels to 17.9g from 24.0g [Time: F(2,52) = 40.67, *p*<0.001], [Treatment: F(3,26) = 7.16, *p*=0.001], [Interaction: F(6,52) = 5.072, *p*<0.001] (Figure 2.6B). This further decreased to an average paw withdrawal threshold of 5.2g at Days 9&11 for STZ/STZ rats. At the Day 9&11 timepoint STZ diabetic rats in a mixed cage paw withdrawal threshold also decreased from 21.3g to 6.5g (Figure 2.6B). Additionally, the decreased STZ diabetic rats paw withdrawal threshold was significantly decreased compared to control/control rats for both STZ groups. However, only STZ/STZ rats paw withdrawal thresholds were decreased compared to control rats in a mixed cage. A slight decrease was also identified in control rats in a mixed cage at the Day 9&11 timepoint when compared to baseline though there was no change in control/control rats response. Two STZ diabetic rats did not develop a >50% change in paw withdrawal threshold at the Day 9&11 timepoint compared to baseline and were excluded from this von Frey analysis. Using these results the Day 9&11 timepoint was selected as the timepoint for the comparisons of analgesic test compounds to determine if they could reverse mechanical allodynia.

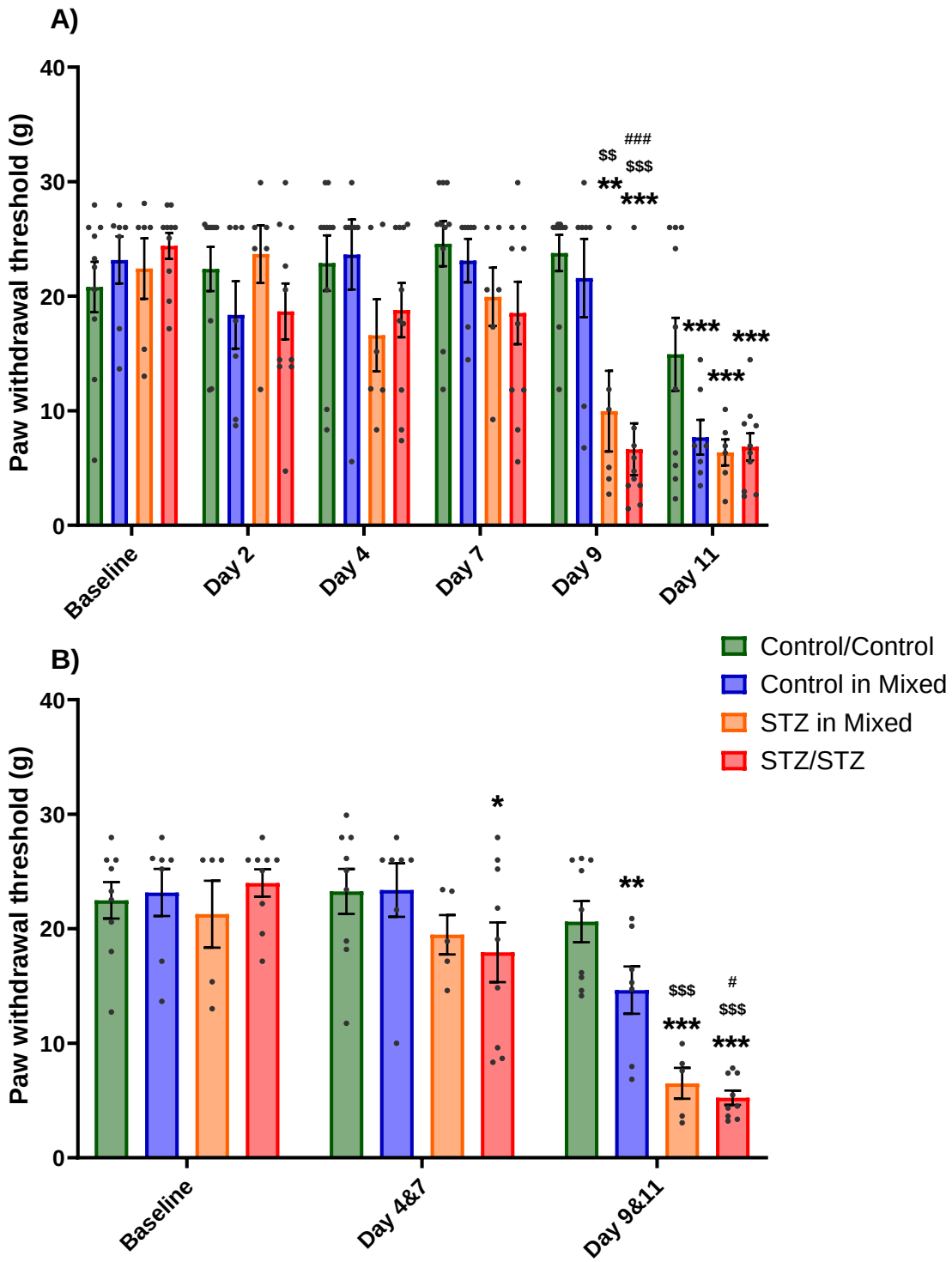

Figure 2.6) STZ diabetic rats developed a significant level of mechanical allodynia on Day 9 and Day 11 (Day 9&11). Von Frey paw withdrawal threshold was measured to monitor the development of mechanical allodynia at Days 2, 4, 7, 9 and 11 compared to a baseline (Day -6&-4) (A). Paw withdrawal thresholds were also averaged at Day 4 and Day 7 (Day 4&7) as well as Day 9 and Day 11 (Day 9&11) (B). Data is reported according to the animal's home caging of either two control rats (control/control), a control rat with an STZ diabetic rat (control in mixed), an STZ diabetic rat with a control rat (STZ in mixed) or two STZ diabetic rats (STZ/STZ). *p<0.05, **p<0.01, ***p<0.001 vs baseline, $$$p$<0.01, $$$$p$<0.001 vs control/control, #p<0.05, ###p<0.001 vs control in mixed. All data is reported as mean ± SEM, (A) n=10 control/control, n=7 control in mixed, n=6 STZ in mixed, n=10 STZ/STZ, (B) n=9 control/control, n=7 control in mixed, n=5 STZ in mixed, n=9 STZ/STZ.

2.3.5 Pregabalin (30mg/kg) reversed mechanical allodynia in STZ diabetic rats regardless of home caging.

Pregabalin, the first line clinical treatment for neuropathic pain reversed mechanical allodynia in STZ diabetic rats. Administration of 30mg/kg pregabalin increased the von Frey paw withdrawal threshold of STZ diabetic rats at both 1 and 2 hours after administration above the Day 9&11 timepoint level [Time: $F(5,130) = 37.07$, $p<0.001$], [Treatment: $F(1,28) = 37.42$, $p<0.001$], [Interaction: $F(5,130) = 6.91$, $p<0.001$]. (Figure 2.7A). At 1 hour after pregabalin administration STZ diabetic rats paw withdrawal threshold had increased from 5.7g at Day 9&11 to 17.7g a threefold increase though still lower than control rats at this timepoint (Figure 2.7A). STZ diabetic rats paw withdrawal threshold further increased to 22.2g by hour two an equivalent response to control rats. Vehicle administration had no effect on the STZ diabetic rats paw withdrawal threshold at either hour remaining significantly lower than the control rat response (Figure 2.7A). Control rats paw withdrawal threshold also increased after 30mg/kg pregabalin administration from 18.0g at Day 9&11 to ~25.6g (Figure 2.7A). This demonstrated that 30mg/kg administration of pregabalin can successfully reverse mechanical allodynia in STZ diabetic rats.

The effects of pregabalin administration to reverse paw withdrawal threshold in STZ diabetic rats was further evaluated to understand if home caging had any impact on the response to pregabalin. There was no difference in the response of STZ diabetic rats due to their home caging however, the effects of pregabalin on control rat paw withdrawal threshold occurred primarily in control rats from a mixed cage. Pregabalin (30mg/kg) administration successfully reversed the STZ induced mechanical allodynia in both STZ diabetic rat groups at 1 and 2 hours after pregabalin administration when compared to Day 9&11, no longer significantly different from control rats [Time: $F(5,120) = 36.01$, $p<0.001$], [Treatment: $F(3,26) = 11.97$, $p<0.001$], [Interaction: $F(15,120) = 3.048$, $p<0.001$] (Figure 2.7B). After 30mg/kg pregabalin administration STZ diabetic rats paw withdrawal threshold increased threefold from 6.5g (STZ in mixed) and 5.2g (STZ/STZ) to 18.2g and 17.3g respectively at 1 hour. This increase in paw withdrawal threshold continued at hour two with STZ diabetic rats in a mixed cage average response reaching 25.6g and 19.8g for STZ/STZ rats. Vehicle administration had no effect on STZ diabetic rats paw withdrawal threshold from either a mixed cage or STZ/STZ cage with average responses remaining <6g at both timepoints. This confirmed that the increase in STZ diabetic rat paw withdrawal threshold was caused by pregabalin (Figure 2.7B). Whilst the STZ groups were similar at all timepoints measured, control rats from a mixed cage paw withdrawal threshold were lower at Day 9&11 than baseline. This decrease in paw withdrawal threshold was not seen in control/control rat. Additionally, 30mg/kg pregabalin significantly increased the paw withdrawal threshold of control rats from mixed cages above the Day 9&11 level but had no effect on control/control rats (Figure 2.7B). This confirmed that mechanical allodynia in STZ diabetic rats is reversed by pregabalin irrespective of home caging. However, control rats home caged with and STZ diabetic rats have reduced paw withdrawal threshold that is increased by pregabalin administration.

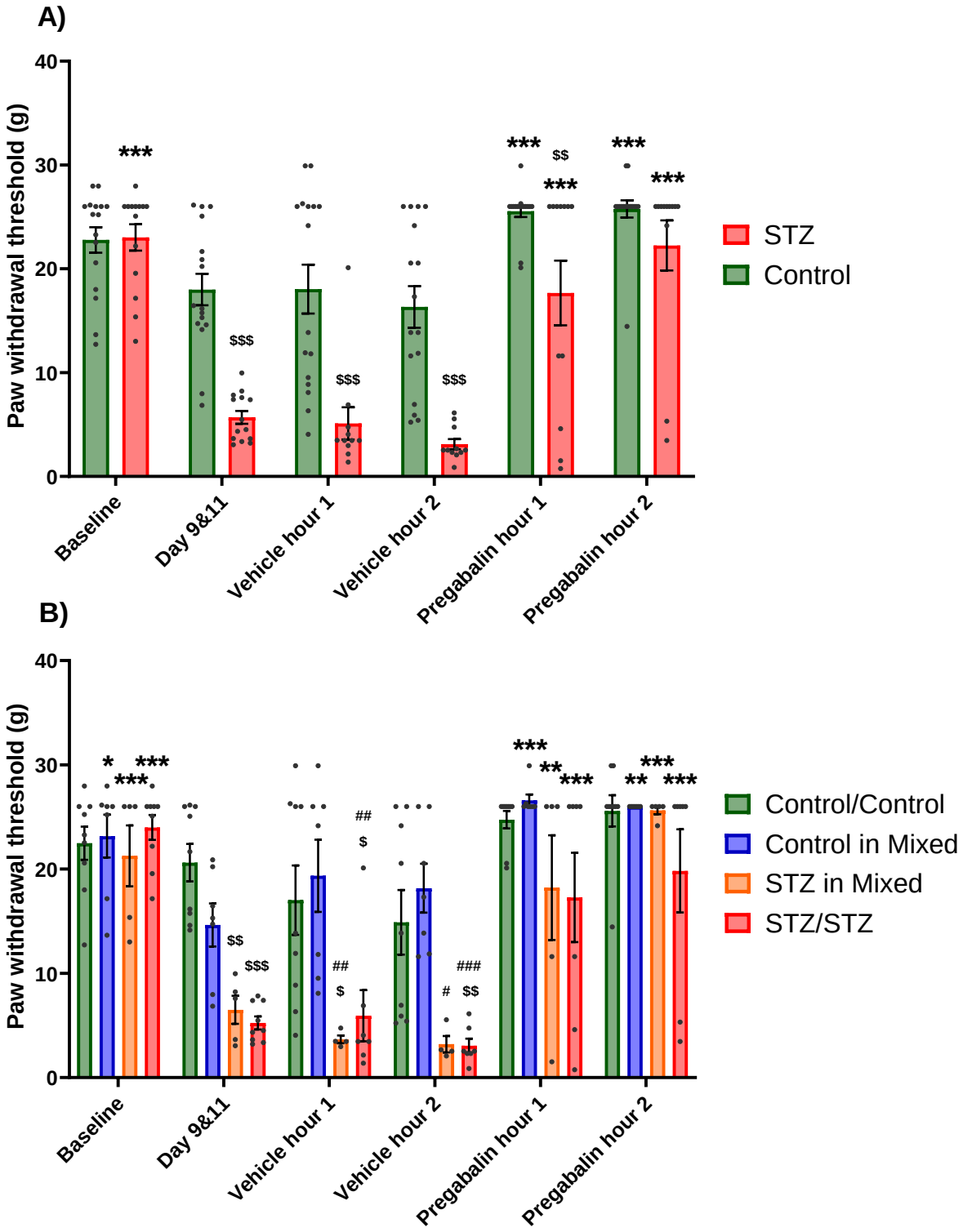

Figure 2.7) Pregabalin (30mg/kg) successfully reversed mechanical allodynia in STZ diabetic rats at 1 and 2 hours after administration. The effect of 30mg/kg pregabalin and vehicle administration (Days 14, 17) on von Frey paw withdrawal threshold was assess in STZ diabetic and control rats at 1 and 2 hours after administration. Paw withdrawal threshold was compared as both the overall effects on all STZ diabetic and control rats (A) or as the effect of home caging (control/control, mixed, STZ/STZ) (B). (A) ***p<0.001 vs Day 9&11, $$$p$<0.01, $$$$p$<0.001 vs control, (B) *$p$<0.05, **$p$<0.01, ***$p$<0.001 vs Day 9&11, $$p$<0.05, $$$p$<0.01, $$$$p$<0.001 vs control/control, #p<0.05, ##p<0.01, ###p<0.01 vs control in mixed. All data is reported as mean ± SEM, (A) n=16 control, n=14 STZ (B) n=9 control/control, n=7 control in mixed, n=5 STZ in mixed, n=9 STZ/STZ.

2.3.6 Home caging an STZ diabetic rat with a control rat improved their individual burrowing deficit but 30mg/kg pregabalin did not.

Paired burrowing was assessed to identify any social facilitation of allowing home cage partners to burrow together. Mixed cage paired burrowing initially decreased at Day 2 but returned to baseline levels at Day 8 whilst STZ/STZ burrowing progressively decreased (Figure 2.8). At baseline all cage types demonstrated similar levels of burrowing at ~1800g. By Day 2 this had decreased to 1080g for mixed cage pairs whilst control/control and STZ/STZ burrowing remained similar to baseline paired burrowing levels [Time: $F(2,26) = 3.170$, $p=0.06$], [Treatment: $F(2,13) = 3.868$, $p<0.05$], [Interaction: $F(4,26) = 4.793$, $p=0.005$] (Figure 2.8). However, this burrowing deficit for mixed cage pairs was not present at Day 8 as paired burrowing levels returned to baseline levels. STZ/STZ cage paired burrowing levels steadily decreased from 1716g at baseline to 1380g at Day 2 (though not a significant decrease) and finally 750g at Day 8 which was a significant reduction compared with baseline, control/control and mixed cages. This represented that pairing a control and STZ diabetic rat together in a mixed cage can avoid burrowing deficits compared to housing two STZ diabetic rats together.

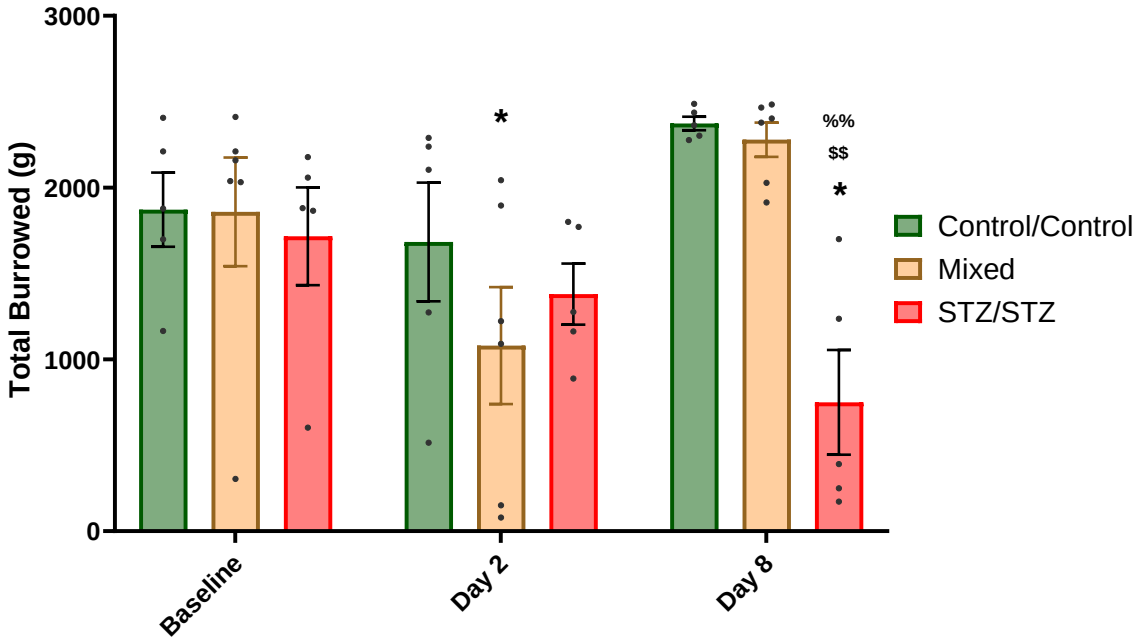

Figure 2.8) Paired burrowing was an initially decreased in mixed pairs at Day 2 but reversed by Day 8 whilst STZ/STZ paired burrowing progressive declined. Paired burrowing was measured with both rats from the home cage pair allowed to burrow at the same time and recorded at baseline, 2 and 8 days after STZ/control administration. *$p<0.05$ vs baseline, $$$p<0.01$ vs control/control, %%$p<0.01$ vs mixed. All data is reported as mean ± SEM, n=5 control/control cages, n=6 mixed cages, n=5 STZ/STZ cages.

Whilst the identification of improved burrowing levels by pairing an STZ diabetic rat with a control rat and allowing them to burrow together (paired burrowing) is interesting, it is not possible to separate out which rats were participating in the burrowing. Therefore, the effects of home cage pairing were assessed on individual burrowing amounts and demonstrated a similar effect that home cage pairing an STZ diabetic and control rat positively impacted individual burrowing levels. At

Day 3 STZ diabetic rats were only burrowing an average of 405g compared with 1713g at baseline a nearly fourfold decrease [Time: $F(4,110) = 4.848$, $p<0.001$], [Treatment: $F(1,28) = 4.848$, $p=0.04$], [Interaction: $F(4,110) = 3.615$, $p=0.008$] (Figure 2.9A). This was also much lower than control rat at Day 3 as control rats individual burrowing remained relatively stable at ~1300-1800g at all timepoints measured. However, the initial reduction in STZ diabetic rat burrowing levels at Day 3 reverted to levels equivalent to both control rats and baseline by Day 10 of 1313g (Figure 2.9A). Despite 30mg/kg pregabalin reversing mechanical allodynia (Figure 2.7), it had no effect on individual burrowing levels in STZ diabetic rats (Figure 2.9A). STZ diabetic rats burrowing levels remained at ~1200g after both pregabalin and vehicle administration. Additionally, burrowing levels in STZ diabetic rats remained significantly lower than at baseline after pregabalin and vehicle administration (Figure 2.9A). This demonstrated that 30mg/kg pregabalin did not reverse individual burrowing deficits in STZ diabetic rats.

The effects of home caging on individual burrowing also highlighted that home caging an STZ diabetic rat with a control rat improved burrowing whilst pregabalin administration did not. At Day 3 both STZ diabetic rats in a mixed cage and in an STZ/STZ cage individual burrowing levels greatly decreased to <500g (Figure 2.9B). This decrease in both STZ groups was significantly lower than baseline but not either control group at this timepoint [Time: $F(4,102) = 10.44$, $p<0.001$], [Treatment: $F(3,26) = 2.537$, $p=0.08$], [Interaction: $F(12,102) = 2.328$, $p=0.01$] (Figure 2.9B). By Day 10, STZ diabetic rats from a mixed home cage individual burrowing had returned to levels equivalent to baseline at 1850g. In comparison STZ diabetic rats from an STZ/STZ cage only burrowed half as much at 905g which was still significantly lower than at baseline (Figure 2.9B). This effect was maintained after vehicle administration with STZ diabetic rats from a mixed home cage individually burrowed 1825g whilst STZ rats from an STZ/STZ home cage only burrowed 800g. Neither the amount of time after control administration nor the effects of pregabalin or vehicle had any impact on either control groups burrowing level (Figure 2.9B). Pregabalin (30mg/kg) treatment had an opposing effect on each STZ group, with STZ diabetic rats in a mixed cage burrowed less than after vehicle administration at ~1250g (though not significantly different) (Figure 2.9B). STZ diabetic rats from an STZ/STZ home cage burrowed slightly more after pregabalin administration at 1090g which was not significantly different from baseline (1614g). However, this increased STZ diabetic rats from an STZ/STZ home cage burrowing was only marginally increased by <300g from vehicle administration levels when compared with the 1000g difference between STZ diabetic rat groups after vehicle administration (Figure 2.9B). This suggests that the slight increase in burrowing for STZ diabetic rats from an STZ/STZ cage after pregabalin administration is not a meaningful reversal of the burrowing deficit. Overall, it appears that home caging and STZ diabetic rat with a control rat reversed individual burrowing deficits whilst pregabalin had little to no efficacy in altering individual burrowing levels.

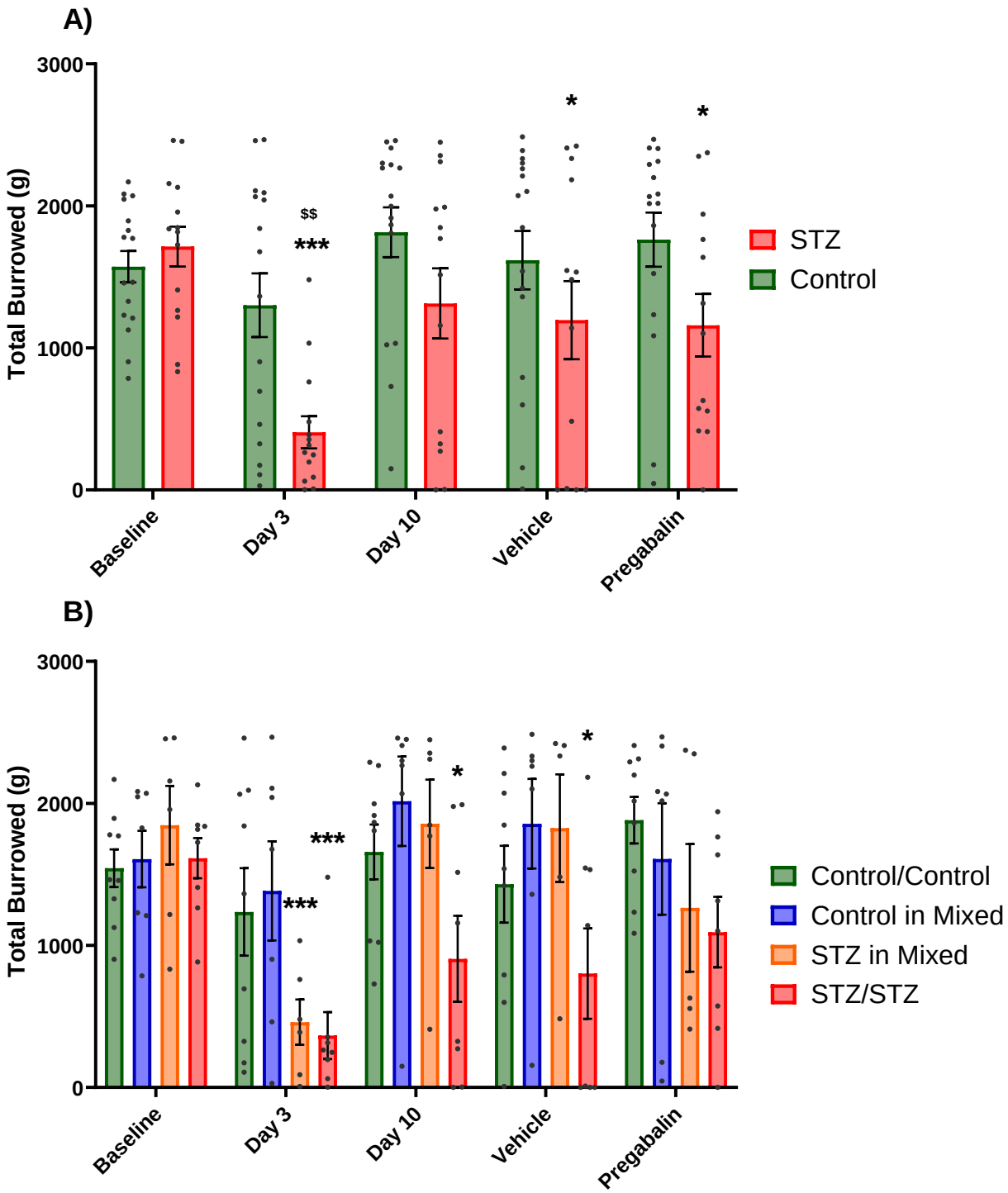

Figure 2.9) Home caging an STZ diabetic rat with a control rat increased individual burrowing levels but 30mg/kg pregabalin did not. Individual burrowing was measured at baseline, Day 3 and Day 10 to identify any change in STZ diabetic or control rats individual burrowing levels and if pregabalin (30mg/kg) or vehicle administration (Days 15, 18) had any effects. Both the development of individual burrowing changes and attempted reversal with 30mg/kg pregabalin were compared as the overall effects on all STZ diabetic and control rats (A) or as the effect of home caging (control/control, mixed, STZ/STZ) (B). (A) *p<0.05, ***p<0.001 vs baseline, $$$p$<0.01 vs control, (B) *$p$<0.05, ***$p$<0.001 vs baseline, p>0.05 between groups. All data is reported as mean ± SEM, (A) n=16 control, n=14 STZ (B) n=9 control/control, n=7 control in mixed, n=6 STZ in mixed, n=8 STZ/STZ.

2.4 Discussion

2.4.1 STZ (55mg/kg) administration caused sufficient hyperglycaemia to develop a diabetic phenotype.

The primary aim of this study was to assess the ability of a lower (55mg/kg) STZ dose to induce hyperglycaemia and a diabetic phenotype in rats which was confirmed by the increased BGL, food and water intake in the STZ rats. Various STZ doses from 45-75mg/kg have been used under different protocols to induce a type-1 diabetes phenotype in rats (Ali et al., 2015; Rutten et al., 2018; Wang-Fischer & Garyantes, 2018). Previous research at University of Hertfordshire has used an STZ model of diabetes induced at a higher 65mg/kg dose in Wistar Han rats (Burnett et al., 2014; Fisher et al., 2015). As part of a continued development of the STZ diabetic model and a refinement of animal welfare under the 3R's initiative a lower 55mg/kg STZ dose was trialled in this study. STZ administration at this lower dose was successful in inducing hyperglycaemia as measured by a change in BGLs above 16mmol/L in 94% of rats (Figure 2.3). The findings of this study were compared to previous results achieved at University of Hertfordshire using a similar experimental design at the higher (65mg/kg) dose of STZ (Lanigan et al., 2020). This comparison identified no difference in the development of hyperglycaemia when using the lower dose of STZ and thus confirming that 55mg/kg STZ can successfully induce hyperglycaemia in this model (Lanigan et al., 2020). In the present study one STZ administered rat initially developed hyperglycaemia above the threshold value of 16mmol/L at Day 7 but by Day 18 had decreased below the threshold. This may have occurred due to the animal not receiving a complete dose during administration, misposition of the needle during i.p. dosing or through regeneration of pancreatic β cells that has been reported in some STZ diabetic rats (Wang-Fischer & Garyantes, 2018). Measuring STZ rats BGLs confirmed the onset of hyperglycaemia and a diabetic phenotype in 16/17 rats.

2.4.2 STZ diabetic rats gained less bodyweight than control rats. developed polyphagia and polydipsia.

As expected, daily bodyweight, food and water intake measurements revealed the development and maintenance of polyphagia, polydipsia (Figure 2.5) and an initial bodyweight loss (Figure 2.4) in the STZ diabetic rats. Reduced bodyweight and the development of polydipsia and polyphagia have been consistently reported across research groups in the STZ type-1 diabetes model (Ali et al., 2015; Rutten et al., 2018; Vieira et al., 2020; Wang-Fischer & Garyantes, 2018; Yamamoto et al., 2009). Additionally, human type-1 diabetic patients also experience hyperglycaemia, polyphagia and polydipsia that can usually be managed through administration of insulin to reduce BGLs to a normal level through proper glycaemic management (Pasi & Ravi, 2022; Roche et al., 2005). This provided clear evidence that 55mg/kg STZ is sufficient to induce a diabetic phenotype and can be used as a preclinical model of type-1 diabetes induced changes. A key benefit of a reduced (55mg/kg) STZ dose, as used in this study, is the finding that lowering the STZ dose to 55mg/kg reduced the amount of bodyweight lost by ~50% when compared with previous results seen in the same model at 65mg/kg (Burnett et al., 2014; Fisher et al., 2015; Lanigan et al., 2020). During this study none of the 17 rats dosed with STZ suffered any acute toxicity from this lower 55mg/kg dose of STZ. This presented an improvement over the previously used 65mg/kg dose where in a similarly sized study one rat did suffer acute toxicity and was terminated shortly after dosing (Fisher et al., 2015; Lanigan et al., 2020). The establishment of a diabetic phenotype with improved animal welfare using

55mg/kg STZ provides important context in the finding of improvement animal welfare related burrowing levels in rats administered a lower 55mg/kg dose compared with 65 and 75mg/kg.

2.4.3 STZ diabetic rats developed mechanical allodynia on Day 9 and Day 11 regardless of home caging.

Measuring von Frey paw withdrawal thresholds demonstrated a clear development of mechanical allodynia in STZ diabetic rats at Day 9 and Day 11. This finding was important as a common use of the STZ type-1 diabetic model is to measure the development of mechanical allodynia. Mechanical allodynia is a feature of neuropathic pain and therefore treatments that reverse it are proposed as having analgesic properties (Ali et al., 2015; Field, McCleary, et al., 1999; Rutten et al., 2018; Wang-Fischer & Garyantes, 2018; Yamamoto et al., 2009). In this study a single administration of 55mg/kg STZ successfully induced mechanical allodynia at Day 9 as measured by von Frey paw withdrawal threshold with a >70% decrease in paw withdrawal threshold compared to baseline levels allowing for a substantial window for potential treatments to be examined (Figure 2.6). This level of mechanical allodynia has been demonstrated in other research including Ali et al. (2015) who showed a paw withdrawal threshold of ~5g in Sprague Dawley rats within 15 days after 50mg/kg STZ administration (Ali et al., 2015). Another important consideration with all preclinical neuropathic pain models is the time course of neuropathic pain development which in this study occurred at Day 9 and 11 after STZ administration. Others have identified mechanical allodynia beginning to develop as early as Day 3 with most rats having developed mechanical allodynia by Day 10 in a 50mg/kg STZ diabetic rat model (Field, McCleary, et al., 1999). However, the development timeline is not consistent with all studies as when using lower (45mg/kg STZ) (Yamamoto et al., 2009) or repeated administrations (25mg/kg STZ for 5 days) (Vieira et al., 2020) of STZ it can take up to 3 weeks to develop. The level of mechanical allodynia developed in this study was compared to previous results at University of Hertfordshire using the higher 65mg/kg STZ dose model with no differences identified (Lanigan et al., 2020). The development of mechanical allodynia in this study demonstrated that a 55mg/kg dose of STZ can be used to successfully produce a diabetic model of neuropathic pain.

2.4.4 Pregabalin (30mg/kg) reversed mechanical allodynia in STZ diabetic rats regardless of home caging.

Reversal of the mechanical allodynia that developed in STZ diabetic rats was achieved using 30mg/kg pregabalin administration. Pregabalin is a first line treatment in diabetic neuropathic pain (Finnerup et al., 2015) that is currently understood to exhibit analgesic properties as a ligand of the $\alpha_2\delta_1$ subunit of voltage gated Ca^{2+} channels leading to attenuation of calcium influx (Kumar et al., 2010). This causes a reduction of excitatory ascending pain pathway transmission through reduced neurotransmitter release and potentially decreasing central sensitisation (Kremer et al., 2016). Clinical studies have demonstrated the effectiveness of pregabalin in human diabetic peripheral neuropathy patients (Freeman et al., 2008; Razazian et al., 2014; Rosenstock et al., 2004). Pregabalin was selected as a test compound in this study due to its extensive characterisation in preclinical neuropathic pain models where it has demonstrated consistent and reproducible reversal of mechanical allodynia and thermal hyperalgesia in a range of different neuropathic pain models including spinal nerve ligation (Gustafsson & Sandin, 2009; Nozawa et al., 2022), STZ (Field, McCleary, et al., 1999), spared nerve injury (Gustafsson & Sandin, 2009; Lau et al., 2013), CCI (Field

et al., 2006) and oxaliplatin (Ling et al., 2008). Additionally, the STZ model was also involved in the development and approval of pregabalin following the evidence of its superior efficacy in reversing static and dynamic mechanical allodynia compared with morphine and amitriptyline (Field, McCleary, et al., 1999).

In this study 30mg/kg pregabalin achieved a complete reversal of mechanical allodynia demonstrated by increased von Frey paw withdrawal thresholds back to levels equivalent to the baseline timepoint (Figure 2.7). This highly significant reversal of mechanical allodynia using 30mg/kg pregabalin has also been demonstrated by others (Yamamoto et al., 2009). Interestingly, pregabalin also increased control rats paw withdrawal threshold which was primarily driven by an increase in control rats from mixed cages. This increased control rats paw withdrawal threshold may have been caused by a few different factors including somnolence induced by pregabalin and/or social transfer of pain. Somnolence is usually described as a state of drowsiness and a strong desire for sleep that is a common side effect of pregabalin, alongside dizziness and can lead to treatment being discontinued in humans (Kato et al., 2015). This side effect has also been identified in rodents including by Wang-Fischer et al. (2018) who found that 30mg/kg pregabalin caused an increase in "sleepiness" and reduced coordination resulting in them decreasing the dose of pregabalin used in a long-term STZ diabetes rat study (Wang-Fischer & Garyantes, 2018). Wang-Fischer et al. (2018) demonstrated a similar development of mechanical allodynia to this study with von Frey paw withdrawal threshold reaching a stable level at <4g that was almost completely rescued by 30mg/kg pregabalin (Wang-Fischer & Garyantes, 2018). However, their finding that pregabalin caused behavioural changes in the rats at this 30mg/kg dose matches the observations from the present study that rats were more immobile and drowsier compared with vehicle administered rats. The side effect of somnolence may be a reason for the increase in control rats paw withdrawal threshold following 30mg/kg pregabalin.

In addition to the increased paw withdrawal threshold after pregabalin administration, control rats paw withdrawal thresholds were decreased at Day 11 especially in control rats from a mixed home cage. Control rats from a mixed cage paw withdrawal threshold at this timepoint were similar to STZ diabetic rats whilst control/control housed rats and the overall control rats paw withdrawal threshold remained consistent with baseline levels. A potential explanation for this is the social transfer of pain that has been identified in rodents as a process by which animals not subjected to a painful condition can exhibit hyperalgesia (Langford et al., 2006; Smith et al., 2016). This transfer of pain is believed to be through audio communication, empathy recognition and even through olfactory cues (Smith et al., 2016). Previous research has demonstrated that naïve rats home caged with an animal experiencing spared nerve injury (SNI) induced neuropathic pain develop a significant decrease in paw withdrawal threshold as seen here that was termed "empathic mechanical pain hypersensitivity" (Li et al., 2018). This social transfer of pain may explain the decreased paw withdrawal threshold in control rats in a mixed cage as they spent increased time with their STZ diabetic cage mate who was experiencing increased levels of pain. Social transfer of pain may have also contributed to the effect of pregabalin by creating a window for this reversal to occur. Future low-dose STZ studies will look at decreasing the dose of pregabalin (Chapter 3) as it has been shown that 10mg/kg is still sufficient to reverse mechanical allodynia in this model (Yamamoto et al., 2009).

Overall, this was another key step in validating the lower (55mg/kg) STZ dose and demonstrated that both BGL and mechanical allodynia are present to similar degrees and the mechanical allodynia is reversible with analgesics. Additionally, this lower STZ dose model may be beneficial to animal welfare by decreasing weight loss compared to higher (65mg/kg) dose models. However, whilst von Frey testing of mechanical allodynia has been used extensively for characterising mechanical

allodynia in a range of preclinical neuropathic pain models it does have limitations (Field, McCleary, et al., 1999; Kim et al., 2017; Tilley et al., 2015; Vrinten & Hamers, 2003). Primarily these limitations stem from the subjective nature of a human interpreting an animal's reflexive reaction to an applied stimulus (Deuis et al., 2017). Whilst some criticism has focused on inter-operator variability and attempts have been made to improve and standardise testing protocols, the translatability of reflexive measures is still poor (Bonin et al., 2014). Therefore, development of behavioural measurements of pain that encompass the global impact or pain including cortical processing and require no subjective human interpretation would offer a potential replacement or adjunctive measure for classical evoked measurements with increased translational likelihood (Fisher et al., 2021).

2.4.5 Home caging an STZ diabetic rat with a control rat improved individual burrowing levels but 30mg/kg pregabalin did not.

The limitations of von Frey testing help to explain why many research groups are looking for alternative endpoints to measure neuropathic pain that may provide increased translatability between preclinical and clinical research. One such endpoint is burrowing an ethological behaviour of both wild and laboratory rodents that can be measured objectively using simple apparatus and is believed to measure overall animal wellbeing (Jirkof, 2014). Whilst there has been some success in using burrowing as an objective neuropathic pain endpoint this has primarily been in mononeuropathy rodent models (Andrews et al., 2012; Lau et al., 2013; Muralidharan et al., 2016; Rutten et al., 2018) and limited research has been published on the effects of STZ induced diabetes on burrowing (Rutten et al., 2018). The main study to date is by Rutten et al. (2018) who used a high dose 75mg/kg STZ diabetic rat model (Rutten et al., 2018). In the present study mixed results were found when assessing burrowing with the low-dose STZ (55mg/kg) rats presenting with deficits at Day 3 but not at Day 10 which was highly dependent on the home caging of the STZ diabetic rats, a stark contrast to von Frey measurements.

Although many burrowing protocols involve social facilitation of burrowing via placing pairs of animals to burrow together in the initial baseline phase, it is not routinely monitored after the baseline period or reported (Gould et al., 2016; Leung et al., 2019; Muralidharan et al., 2016; Rutten et al., 2018). The present study identified a small but significant reduction in mixed cage paired burrowing at Day 2 after STZ/control administration that returned to baseline levels by Day 10 (Figure 2.8). Additionally, STZ/STZ cages paired burrowing decreased progressively with a large reduction in burrowing levels seen at Day 10. This may indicate that housing an STZ diabetic rats with a control rats can lead to social facilitation of burrowing indicated by higher amounts of burrowing conducted by mixed cage pairs and was similar to previous research findings in the 65mg/kg STZ dose model (Burnett et al., 2014). Making this claim using paired burrowing data alone is challenging as there is no distinction between which rat conducted the burrowing meaning the level of burrowing in mixed cages could occur solely from control rats. Therefore, it was necessary to assess the level of burrowing conducted by STZ diabetic and control rats individually, as it is routinely measured.

Individual animal burrowing when assessed irrespective of home caging and demonstrated a clear reduction in STZ diabetic rats burrowing at Day 3 after STZ administration. However, by Day 10 this deficit had returned to baseline levels. This differs from previous data by Rutten et al. (2018) who demonstrated an almost complete suppression of burrowing activity in STZ rats at the single 3 week timepoint measured (Rutten et al., 2018). A key difference between the present study and that of

Rutten et al. (2018) that may contribute to this is the dose of STZ used to induce type-1 diabetes. Rutten et al. (2018) using a much higher 75mg/kg STZ dose and determined that burrowing deficits in these rats may have occurred due to sickness-associated changes in motivation and have been masked by diabetes-associated alteration in wellbeing (Rutten et al., 2018). The present study used a lower (55mg/kg) dose STZ model which has been demonstrated to have improved welfare based on weight loss compared to a higher (65mg/kg) dose STZ model (Lanigan et al., 2020). Therefore, the results in this study of using a lower (55mg/kg) dose STZ model provided a better indication of the changes associated with neuropathic pain development rather than diabetes related wellbeing. However, the effect of pregabalin in both the present study and that of Rutten et al. (2018) are consistent with pregabalin having had little to no impact on STZ diabetic rats burrowing levels in either study (Figure 2.9) (Rutten et al., 2018).

The lack of efficacy of pregabalin in rescuing burrowing deficits in the STZ model across different research groups is particularly interesting as pregabalin has been efficacious against burrowing deficits in a number of other neuropathic pain models including the CCI (Rutten et al., 2018) and SNI (Lau et al., 2013) models. Whilst the similar analgesic drug gabapentin reversed burrowing deficits in the tibial nerve transection model (Andrews et al., 2012). Importantly, the CCI, SNI and tibial nerve transection neuropathic pain models are mononeuropathy models induced by surgical techniques with pain being the predominant phenotype of the animals. In comparison metabolic neuropathic pain models such as the single dose STZ type-1 diabetes model displays other phenotypes of diabetes such as hyperglycaemia, polydipsia, polyphagia and polyneuropathy (Bennett & Xie, 1988; Rakieten et al., 1963). Furthermore, Rutten et al. (2018) identified that the Zucker diabetic fatty model of type-2 diabetes also developed a deficit in burrowing amounts that were not rescued by analgesic treatments including 30mg/kg pregabalin, gabapentin and morphine (Rutten et al., 2018). This further supports the evidence that burrowing is a good measure of overall animal wellbeing and potentially the global impact of pain because although standard analgesics can reverse burrowing in models with pain as the only phenotype, they do not affect more complex multimodal models (Rutten et al., 2018).

Whilst the first line analgesic treatment pregabalin did not improve diabetes induced burrowing deficits in this study, home caging an STZ diabetic rat with a control rat improved their individual burrowing. This finding contributes to the evidence that burrowing is a measure of overall animal wellbeing. A potential mechanism that may be behind this is the social support of a healthy animal that is paired with an animal in pain. In humans mixed reports have been shown for the effect of social interaction on pain intensity with patients who perceive a higher level of social support reporting less severe pain. However, attention from a spouse or close partner can lead to heightened pain severity linked with over pain behavioural displays (López-Martínez et al., 2008). This has been considered as a dual sided phenomenon whereby social support can improve wellbeing, and pain scores however if it reaches a point of solicitousness this can lead to the opposite effect with increased pain (Mogil, 2015). In rodents this is termed “social buffering” and has most often been explored in stress related scenarios with the presence of or home caging with a companion animal leading to a reduction in reaction and perception of aversive experiences and is being considered to improve welfare in laboratory rodent experiments (Denommé & Mason, 2022). Some evidence has also been identified in pain models with D’Amato (1997) reporting a decrease in pain thresholds when female mice encountered a familiar partner during pain testing (D’Amato, 1997). This evidence may indicate that home caging an STZ diabetic rat with a control rat can lead to social facilitation and buffering of the pain, improving the rat’s wellbeing, leading to more burrowing. This data supports the theory that burrowing may be a marker of wellbeing (Andrews et al., 2011; Deacon, 2006; Deseure & Hans, 2018; Jirkof, 2014) and not a simple measure of

nociception that evoked measures of von Frey paw withdrawal threshold are. This also contributes to the understanding that burrowing is an ethologically fundamental activity in rodents and considered to be equivalent to activities undertaken by humans in their daily lives (Zhang et al., 2022). This demonstrates that it is possible to reverse burrowing deficit in diabetic rodents meaning it may be possible to reverse these deficits with treatments that improve overall animal wellbeing including the global impact of pain.

2.4.6 Limitations of this study and improvements for future studies.

Whilst this study established that mechanical allodynia was present at Day 9 and Day 11, the time course and development of this has not yet been established at this lower 55mg/kg STZ dose. By measuring the development of mechanical allodynia over a longer period the timepoint at which the animals reach peak sensitivity could be identified. Also, the length of time this sensitivity is maintained and the variability that occurs in control rats, could be monitored to assess how long after STZ administration reversal of mechanical allodynia can be tested with analgesics (Chapter 3). In some models such as the oxaliplatin model it is possible to induce a transient neuropathic pain phenotype meaning it will be important to ensure that STZ at this 55mg/kg dose can maintain a consistent neuropathic baseline (Ling et al., 2008). The health and welfare of the animals over this time will also provide a better understanding of how long STZ diabetic rats can be kept safely without incurring adverse effects of prolonged hyperglycaemia.

Although this study identified some of the first evidence of improved burrowing in STZ diabetic rats the protocol for burrowing training was not consistent with published literature. This included reduced amount of baseline burrowing habituation and exposure compared with published literature that should be matched in future testing to allow for a more accurate comparison to published data (Andrews et al., 2012; Rutten et al., 2018). Additionally, a key limitation of burrowing data that may reduce its effectiveness as a neuropathic pain endpoint is increased inter-animal variability in comparison to von Frey measurements in this study. This phenomenon has also been reported by others researching burrowing in alternate neuropathic pain models highlighting that this is conserved across research groups and animal models (Andrews et al., 2012; Muralidharan et al., 2016). This could limit future research into burrowing due to the 3R's implications of increasing the number of animals used in research, however if it provides more translatable data compared with reflexive tests this may be justifiable (NC3Rs, n.d.). Also, the dose of pregabalin used should be closely considered as development of somnolence may have limited the ability of 30mg/kg pregabalin to reverse burrowing deficits (Wang-Fischer & Garyantes, 2018). Future studies will look to assess a dose response to pregabalin or alternative first line neuropathic pain treatments for their ability to reverse burrowing deficits in STZ diabetic rats (Chapter 3).

Another limitation of the paired data gained in this study is that the number of animals in each group were relatively low once organised by home cage pairing. This may have led to increased variability in the data gathered as well as caused potential type II errors due to low statistical power in this study. Future studies should look to conduct a power analysis using the paired data generated in this preliminary study to ensure that this work is sufficiently powered. Although the effects of mixed caging of STZ diabetic and control rats provided interesting results and important data in the reversibility of STZ burrowing deficits, the use in future studies must be considered closely. If studies aim to further elucidate the impact of mixed caging on these and other behavioural endpoints then they must use a larger number of animals if needed to ensure an appropriate level of statistical power is still achieved. Alternatively, studies looking to explore reversal of burrowing deficits with

analgesic treatments may choose to not use mixed cages to allow for increased numbers per group without increasing the total number of animals included in the study. This is also because STZ diabetic rats in a mixed cage showed a reversal of burrowing to levels equivalent to control which would not provide a window of deficit for analgesic reversal.

2.5 Conclusions

In conclusion, a lower single dose of STZ (55mg/kg) successfully induced mechanical allodynia combined with a diabetic phenotype, including hyperglycaemia, polydipsia and polyphagia. This model was superior to the 65mg/kg STZ model due to improved animal welfare through reduced bodyweight loss and increased survivability without affecting the rate of hyperglycaemic or mechanical allodynia development. Burrowing, an objective measure of wellbeing was reduced in STZ diabetic rats reflecting the effects of diabetes and neuropathic pain on patient's daily activities. The first line treatment pregabalin (30mg/kg) was unable to rescue burrowing deficits in these STZ diabetic rats. However, this study has provided some of the first evidence that burrowing in STZ rats can be reversed through home caging STZ rats with a control partner which aided in individual burrowing levels potentially through social facilitation. More work is needed to establish the extended time course for the development of mechanical allodynia and burrowing changes that occur following low-dose STZ administration in rats. Additionally, further research into alternative methods or analgesics to reverse these changes in burrowing at the lower dose of STZ will help in identifying methods that improve the overall well-being of STZ diabetic rats. Overall, burrowing shows promise as a marker of overall animal wellbeing however, increased inter-animal variability may limit future use because of increased animal numbers needed that could cause ethical implications.

Chapter 3: Time course of the 55mg/kg STZ type-1 diabetes rat model development of a diabetic phenotype, mechanical allodynia and burrowing changes

3.1 Introduction

Neuropathic pain affects 8.2-8.9% of the population and can lead to anxiety, depression and sleep disturbances that all together leads to a severe impact on the patient's quality of life (Colloca et al., 2017). The effects of neuropathic pain on quality of life are exacerbated by the limited efficacy and extensive side effects of current neuropathic pain treatments (Finnerup et al., 2015). A likely reason that new treatments have failed to be developed is the mismatch between evoked subjective preclinical neuropathic pain endpoints compared with the questionnaire and rating scale based endpoints used in clinical trials (Figure 1.3) (Deuis et al., 2017; Fisher et al., 2021; Tappe-Theodor et al., 2019). Therefore, the development of novel objective, non-evoked endpoints are likely to improve the translatability for preclinical neuropathic pain research (Fisher et al., 2021). As discussed in Chapter 2 one such endpoint is burrowing that has shown reproducibility and reversibility in surgically induced models of neuropathic pain (Lau et al., 2013; Muralidharan et al., 2016; Rutten et al., 2018). However, the results in diabetic models of neuropathic pain have only shown the development of a burrowing deficit and have not been reversed by analgesic treatments (Rutten et al., 2018).

It was identified in Chapter 2 that the burrowing deficit in streptozotocin (STZ) diabetic rats could be improved through social facilitation, but not through analgesic drug treatment with 30mg/kg pregabalin. This demonstrated some of the first evidence that decreased burrowing in STZ diabetic rats can be reversed. There is currently no evidence that this can be achieved with analgesic test compounds. The finding of Chapter 2 that the clinical analgesic pregabalin at 30mg/kg could not reverse the burrowing deficits in STZ rats is consistent with previous findings in a higher 75mg/kg STZ rat model (Rutten et al., 2018). However, 30mg/kg pregabalin caused a level of somnolence in the diabetic rats that may have limited its ability to reverse burrowing levels as demonstrated by increased control rat paw withdrawal thresholds (Chapter 2) and identified by others testing 30mg/kg pregabalin (Wang-Fischer & Garyantes, 2018). Burrowing as a behavioural endpoint has typically displayed negative results for test compounds that impair motor function, unlike the classical evoked pain endpoints such as von Frey paw withdrawal threshold which may display false positive results (Andrews et al., 2012; Fisher et al., 2021; Gould et al., 2016; Tappe-Theodor et al., 2019). Further clarification of the effects of lower doses of pregabalin against burrowing in this lower dose 55mg/kg STZ model is required.

Another area of burrowing research that has not been fully explored in diabetic models is a timeline of burrowing deficit development. In the chronic constrictive injury (CCI) model different studies have demonstrated burrowing deficits from Day 4 to Day 25 (Rutten et al., 2018) and from Day 3 to Day 14 (Muralidharan et al., 2016). However, in the spared nerve injury (SNI) model burrowing deficits only developed from Day 10 to Day 20 but not at Day 5 (Lau et al., 2013). This information would be vital for preclinical screening studies to understand the time course of when burrowing changes develop and for how long a stable baseline response can be achieved. By understanding the development and maintenance of burrowing changes in the STZ model, preclinical screening studies

can be designed to incorporate burrowing as an endpoint at the timepoints when a stable response is achieved.

Although identifying that social facilitation reverses burrowing deficits in Chapter 2 is a valuable step, applying this to all studies would limit the window for test compound induced reversal of burrowing deficits. Furthermore, to improve the reliability of burrowing data from Chapter 2, an increased number of burrowing habituation and baseline sessions needs to be conducted to more closely follow published protocols (Andrews et al., 2012; Muralidharan et al., 2016; Rutten et al., 2018). Alongside this, a key limitation of the results from Chapter 2 was the low number of animals used in each group which could be increased to improve the reliability of the data based on an updated power analysis (Table 3.3).

3.1.1 Aims and hypotheses.

The primary aim of this study was to establish a time course for the development and maintenance of burrowing deficits and reduced von Frey paw withdrawal thresholds across 49 days in a 55mg/kg STZ diabetic rat model.

This study explored how a range of 3, 10 and 30mg/kg pregabalin doses could reverse the established burrowing deficits and mechanical allodynia measured by von Frey paw withdrawal thresholds.

As with the previous Chapter 2 study, the development of phenotypical diabetes changes of hyperglycaemia, polydipsia, bodyweight along with any longer-term effects of diabetes on the health of STZ rats was monitored throughout the study to further validate the lower 55mg/kg STZ model.

3.1.2 Abbreviations.

STZ – streptozotocin, CCI – chronic constrictive injury, SNI – spared nerve injury, SEM – standard error of the mean, BGL – blood glucose level, i.p. – intraperitoneal, p.o. – oral, LC – Langerhans cells, IENF – intra-epidermal nerve fibres, IHC – immunohistochemical, ZDF – Zucker diabetic fatty, SD – standard deviation.

3.2 Methods

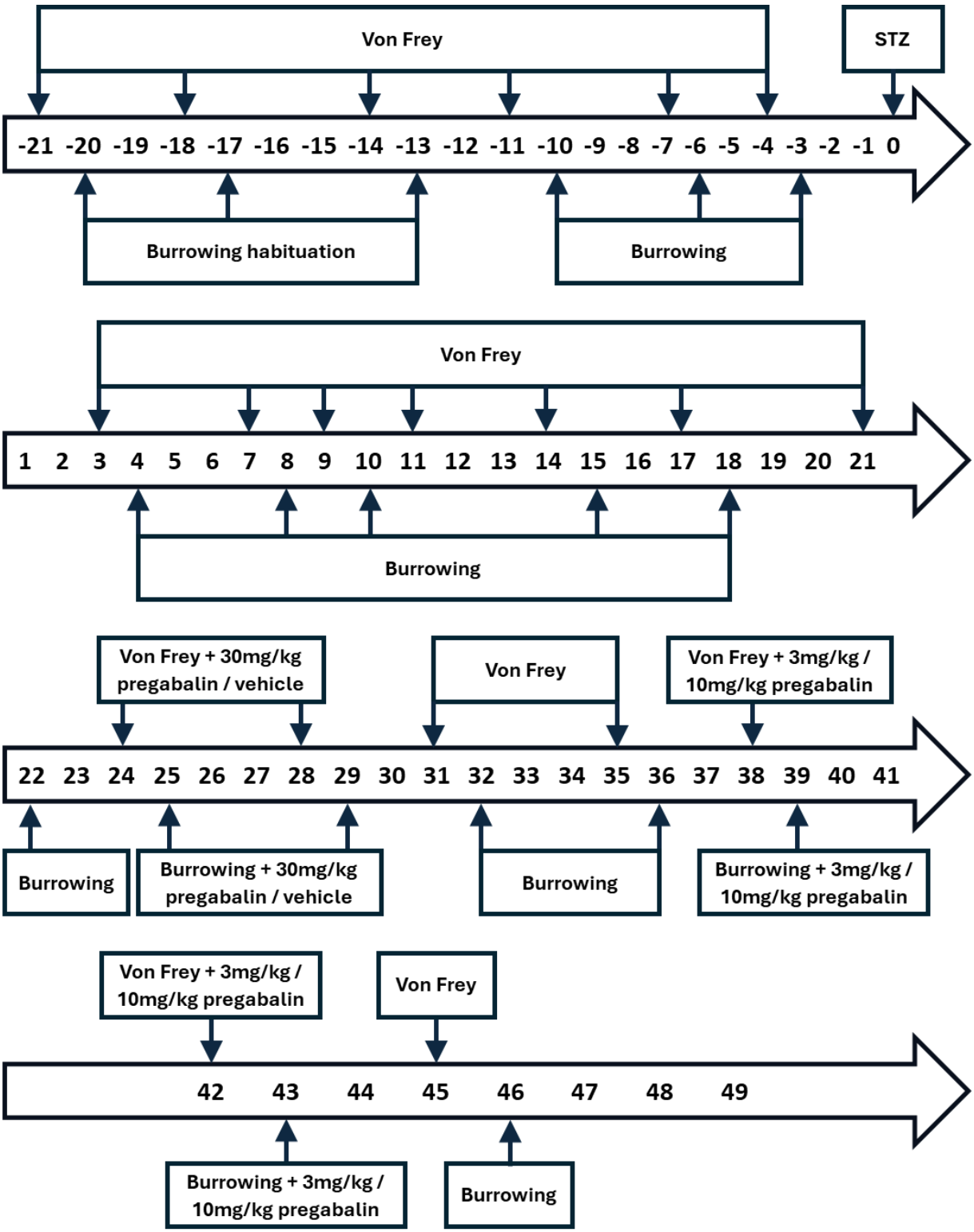

Figure 3.1) Timeline of the study depicting the days before and after 55mg/kg STZ intraperitoneal (i.p.) administration on Day 0. The days on which von Frey paw withdrawal threshold and burrowing measurements were taken are displayed. The timepoints that vehicle, 3, 10 and 30mg/kg pregabalin were administered are also denoted.

3.2.1 Power analysis and group sizes.

Before commencing with the study, a power analysis was conducted on previous STZ diabetic rats von Frey data collected from Chapter 2 and other studies conducted at University of Hertfordshire to calculate the optimal group sizes for the current study design. This was carried out to conform with the 3R's ensure that the study was not underpowered and that excess animals were not used. The von Frey data formed the basis of this power analysis as the primary neuropathic pain endpoint of the study. Both within and between group comparisons were calculated to ensure both were adequately powered using the Gpower 3.1 software (Faul et al., 2007).

The maximum effect size for within and between groups were calculated and displayed in table 3.1 comparing the control rats and STZ diabetic rats data (Between group) or baseline vs Day 9&11 (average of Day 9 and Day 11 responses after STZ/control administration) (Within group). This demonstrated that the maximum achievable effect size for these comparisons is 3.05 for within groups and 2.42 for between groups. Following this the minimum effect size that will be statistically significant using the previous study design data of an alpha of 0.05, a power of 0.8 and an n=10 was calculated in table 3.2. This was identified as 1.00 for within group and 1.32 for between groups which correlates to a percentage reversal of 32.8% for within group and 54.6% for between groups. In clinical studies an improvement of >50% is often used as a threshold value to demonstrate reversal of neuropathic pain (Azmi et al., 2019; Rice et al., 2021). Therefore, the between groups comparison were slightly underpowered to be able to detect changes of at least this amount because the minimum percentage for neuropathic pain reversal to become statistically significant was 54.6%. Thus, increasing the n number is justifiable. Due to caging requirements of the animals, the n number must be increased in groups of 2 to satisfy 2 animals per cage. Using Gpower software the power analysis was recalculated with an n=12 per group and displayed in table 3.3. This demonstrated that the increase of 2 animals per group brings the percentage of neuropathic pain reversal under the 50% threshold for the between group comparison.

Table 3.1) Calculation of the maximum possible effect size that can be achieved from previous data when comparing control and vehicle STZ data or Baseline vs Neuropathic baseline.

Comparison type	Mean difference between groups	Standard deviation (SD)	Maximum effect size achieved ((Mean 1 – Mean 2) / SD)	N
Within group	22.5g - 4.2g = 18.3g Baseline vs Day 9&11	6	3.05	10
Between groups	19.0g – 4.5g = 14.5g Control vs STZ at Day 9&11	6	2.42	10 per group (20 total)

Table 3.2) Calculation of the minimum statistical effect size that will be statistically significant with and alpha of 0.05, a power of 0.8 and n=**10**.

Comparison type	Effect size calculated in Gpower	Equivalent increase in mean value (mean increase = effect size x SD)	Percentage of pain reversal for statistical significance (Equivalent increase in mean value / Mean difference between groups *100)	Minimum paw withdrawal threshold for statistical significance (Day9&11 + equivalent increase in mean value)
Within group	1.00	6.00g	32.8%	10.2g
Between groups	1.32	7.92g	54.6%	12.42g

Table 3.3) Calculation of the minimum statistical effect size that will be statistically significant with and alpha of 0.05, a power of 0.8 and an increased n=**12**.

Comparison type	Effect size calculated in Gpower	Equivalent increase in mean value (mean increase = effect size x SD)	Percentage of pain reversal for statistical significance (Equivalent increase in mean value / Mean difference between groups *100)	Minimum paw withdrawal threshold for statistical significance (Day9&11 + equivalent increase in mean value)
Within group	0.89	5.34g	32.8%	10.2g
Between groups	1.20	7.20g	49.7%	11.70g

An additional consideration for the STZ diabetic rat model is exclusion of animals per STZ group due to non-development of diabetes (<16mmol/L blood glucose level), deviation from normal health (e.g. piloerection, inactivity, paw inflammation), bodyweight loss (>15% approaching 20% with no stabilisation within 48 hours) or lack of neuropathic pain development (<50% change from baseline at Day 9&11). From historical data collection approximately 10-15% of STZ diabetic rats will be excluded due to non-development of diabetes, deviation from normal health or >15% bodyweight loss etc. Additionally, approximately 15%-20% of STZ diabetic rats do not develop mechanical allodynia (Fisher et al., 2015). Therefore, an additional n=3 rats (30%) will be included in each study per STZ group to ensure that the n=12 rats remain at the end of the study. However, this study more than doubled the time course from 18 days (Chapter 2) to 45 days after STZ administration. Thus, an additional n=3 rats per group will be included to accommodate for animals excluded across this extended time course of diabetes development.

3.2.2 Ethics statement.

All research procedures/experiments were performed in accordance with Animals Scientific Procedures Act 1986 & European Directive 2010/63/EU. All studies performed were approved by the University of Hertfordshire Animal Welfare and Ethics Review Body and comply with the home office guidelines and codes of conduct. All work was authorised under University of Hertfordshire home office establishment licence and project licence titled: Diabetes mechanisms and treatments.

3.2.3 Animals and induction of STZ.

30 Male Wistar Han IGS rats (250-275g at arrival, 375-475g at time of STZ administration) supplied by Charles River, UK were housed in pairs from arrival. At Day 0 (Figure 3.1) rats were administered either 55mg/kg streptozotocin (n=18) or 20mM citrate buffer (n=12) intraperitoneal (i.p.) administration at a dose volume of 10ml/kg. STZ (Sigma- Aldrich, S0130) was prepared as described in Chapter 2. Either STZ at 55mg/kg or citrate buffer (control) were administered once to rats via single i.p. injection using a new 23G needle. Animals were placed back in their home cage and monitored closely for 1 hour for signs of distress or discomfort. Additionally, banana porridge (Cow&Gate) and 2% sucrose solution were provided for 48 hours after STZ administration to encourage feeding and maintain blood glucose levels.

3.2.4 Environmental conditions.

Rats were pair housed in Tecniplast 2000P cages and a 12:12 hr light-dark cycle (lights on at 07:00) was maintained throughout the study. Housing temperature was maintained at 21±2°C and 55±15% relative humidity. Food (5LF2 10% protein LabDiet, changed to 5LF5 22% protein LabDiet on day of STZ administration) and drinking water were provided ad libitum except during von Frey behavioural testing. Water was provided in two 1L bottles per cage. For 48 hours after STZ administration (Day 0,1), 2% sucrose solution was provided in one of the 1L bottles to avoid hypoglycaemia caused by STZ administration (Ghasemi & Jeddi, 2023). Water intake measurements were recorded from 1 week before STZ administration and as required until the end of the study. Water intake was calculated per cage as the change in weight (g) of the food hopper and both water bottle recorded at approximately 9am each day.

3.2.5 Animal welfare.

Blood glucose level (BGL) was recorded 1 day prior to (Day -1) and 7 days after (Day 7) STZ/control administration to confirm onset of hyperglycaemia. Following this BGLs were also measured on Day 21, Day 35 and at the end of the study (Day 49) to monitor progression and maintenance of hyperglycaemia. Microsamples of blood were taken through tail tip vein puncture using a lancet (Valuemed, UK) and BGL was measured using either Aviva Aucu-Chek (Day -1 to 7) or GlucoRx Nexus blood glucose meter (Day 7 to 45) calibrated before use. Both glucose meters were found to take equivalent measurements at Day 7. An inclusion criterion of >16mmol/dL BGL at all post administration timepoints for STZ diabetic rats was used to exclude animals that did not develop hyperglycaemia.

Daily bodyweight measurements were taken at regular intervals from Day -21 to Day 0 to monitor rats weight gain and progression. After STZ/control administration on Day 0, daily bodyweight

measurements were taken to monitor animal welfare. Rats reaching 15% bodyweight loss compared with the Day 0 baseline weight were monitored closely. This included weighing twice daily, provision of additional nourishment in the form of seed, grains and banana porridge where appropriate and assessment by animal care staff and or veterinarians if needed. Any rats not stabilising or gaining weight within 48 hours were humanly euthanised. All rats were also checked daily by trained animal care staff to monitor welfare.

3.2.6 Mechanical allodynia.

Von Frey paw withdrawal threshold was measured using the same protocol detailed in Chapter 2 with the exception that the range of monofilaments used for von Frey testing included 0.16, 0.4, 0.6, 1, 1.4, 2, 4, 6, 8, 10, 15, 26, 60; g (This is an increased range from the 0.4-26g used in Chapter 2). Paw withdrawal threshold was evaluated twice per week, for 3 weeks before STZ administration (Day -21,-18,-14,-12,-7,-4). From 3 days after STZ administration onwards von Frey paw withdrawal threshold was assessed up to 2 times per week up until the end of the study to monitor development of mechanical allodynia (Days 3,7,9,11,14,17,21,31,35,45). The effect of pregabalin or vehicle administration on mechanical allodynia were assessed from week 4 onwards (Days 24,28,38,42). At these analgesic assessment timepoints von Frey testing was conducted at 2 and 4 hours after pregabalin/vehicle administration.

3.2.7 Burrowing.

Burrowing measurements were taken using the same protocol as Chapter 2 with the only differences being the timepoints measured and amount of testing sessions. Burrowing habituation prior to STZ administration was conducted as: one paired habituation session with an empty tube session (Day -20), one paired habituation session with a filled tube (Day -17), one paired crossover burrowing session (Day -13), three individual filled tube burrowing session (Day -10&-6&-3) (Figure 3.1). After STZ administration burrowing was measured up to twice per week until the end of the study to assess changes in burrowing behaviour (Days 4,8,10,15,18,22,32,36,46). The effect of 3, 10 and 30mg/kg pregabalin or vehicle (drinking water) oral (p.o.) administration on burrowing deficits was assessed from week 4 onwards (Days 25,29,39,43). During the assessment of analgesics rats were placed into burrowing cages from 1 hour after pregabalin or vehicle administration.

3.2.8 Pregabalin.

Pregabalin (Carbosynth, 148553-50-8) at 3, 10 and 30mg/kg was dissolved in drinking water (vehicle) administered p.o. at 2ml/kg. The original design for the assessment of pregabalin/vehicle effect on von Frey and burrowing was through a full four arm crossover study where all rats would randomly receive either pregabalin at 3, 10, 30mg/kg or vehicle at four different timepoints. Due to cautionary concerns over the numbers of STZ rats remaining at the end of the study the design was adjusted to be run sequentially as two arm crossovers so that at Day 24 and Day 29 all rats received 30mg/kg pregabalin and vehicle and a second crossover at Day 38 and Day 43 where all rats received both 3mg/kg and 10mg/kg pregabalin to avoid exclusion of STZ rats impacting the powering of the treatment groups.

Pregabalin at 30mg/kg or vehicle were administered to half of each group (STZ/Control) on Day 24 (von Frey) and Day 25 (Burrowing) followed by a 72 hour washout period and crossover administration with the alternate test compound on Day 28 (von Frey) and Day 29 (Burrowing). Likewise, half of each group received either pregabalin at 3mg/kg or 10mg/kg on Day 38 (von Frey) and Day 39 (Burrowing) and the crossover occurred again after 72 hours on Day 42 (von Frey) and Day 43 (Burrowing). Von Frey testing was conducted 2 and 4 hours after administration whilst burrowing was commenced at 1 hour after administration so that hours 1-3 after test compound administration were captured during the burrowing.

3.2.9 Grouping, randomisation, blinding and exclusion or inclusion criteria.

The STZ and Control grouping were randomised using the Latin square technique based on von Frey baseline data as the primary source of sorting to ensure an equal spread of baseline paw withdrawal thresholds. Following this consideration of baseline burrowing, bodyweight and caging were considered to ensure they were not significantly different. All rats were assigned in pairs with their cage partner to the same group to ensure all cages were either STZ/STZ or control/control cages. All rats remained with their original cage partner from beginning of the study to avoid distress or aggressive behaviour from rehousing.

Exclusion criteria included >50% change from baseline at Day 9&11 for von Frey paw withdrawal threshold measurements of mechanical allodynia and at least 500g baseline burrowing (-10&-6&-3) amounts were set. Additionally, a BGL of at least 16mmol/L was set as the threshold for development of hyperglycaemia and to be considered as representative of a diabetic phenotype. A maximum limit of 20% bodyweight loss was in place to exclude any rats that developed excessive weight loss. Three STZ diabetic rats developed health complications throughout the study including bodyweight loss and paw inflammation at Days 6, 14 and 21 and were excluded from analysis other than bodyweight and BGL measurement. One control rat experienced health complications during Day 0 vehicle administration and was humanely euthanised and excluded from analysis other than bodyweight and BGL (leaving n=15 STZ and n=11 control). One rat's BGL after STZ administration did not reach the >16mmol/L BGL criteria and was excluded from further analysis, but remained with their home cage partner (leaving n=14 STZ). One STZ diabetic rat burrowed <500g at baseline (-10&-6&-3) and was excluded from analysis of drug reversal on burrowing (leaving n=13 STZ). One STZ diabetic rat did not develop a >50% reduction in von Frey paw withdrawal threshold at Day 9&11 compared to baseline and was excluded from further analysis of drug reversal of von Frey paw withdrawal thresholds (leaving n=13 STZ).

Administration of pregabalin or vehicle during the analgesic reversal testing was conducted blind to the treatment condition. The administration of pregabalin and vehicle was conducted blind using a coding system. The assignment of which rats received each test compound during the pregabalin crossovers was done using an unadjusted Latin square method.

3.2.10 Statistics.

To compare the results at each timepoints (Days) between control and STZ diabetic rats two-way mixed model analysis of variance (ANOVA) was used with Šídák's post hoc test to compare between control and STZ diabetic rats (BGL, von Frey, burrowing, bodyweight, daily water intake). For measures with additional comparisons within each group comparing between Days Dunnett's post

hoc test was used (BGL, average von Frey, average burrowing, pregabalin effects on von Frey and burrowing). Organ weight comparisons were conducted using an unpaired two tailed t test. Correlation analysis was conducted using Spearman's correlation coefficient (r_s) (Prism 10.2; GraphPad, San Diego, CA USA). A p value of <0.05 was considered statistically significant for all data. All data is reported as mean ± standard error of the mean (SEM) except for correlation data.

3.3 Results

3.3.1 STZ (55mg/kg) caused hyperglycaemia to develop from Day 7 until Day 49.

Administration of 55mg/kg STZ i.p. successfully increased BGLs above the 16mmol/L threshold in 17/18 (94%) rats across the full 49 day study length. At baseline (Day -1) there was no difference in BGL between STZ and control groups average BGL with both groups at 6.3mmol/L (Figure 3.2). Control rats BGL remained stable until Day 49 measured at <6mmol/L. By Day 7 after STZ administration all but one STZ rat had a BGL greater than the 16mmol/L threshold value with BGL increase over fourfold to 25.4mmol/L [Time: F(4,102) = 60.38, p<0.001], [Treatment: F(1,28) = 129.6, p<0.001], [Interaction: F(4,102) = 77.52, p<0.001] (Figure 3.2). This increased BGL in STZ rats was maintained across the study including the Day 49 timepoint. One STZ administered rats BGL remained at <6mmol/L in line with control rats across all timepoints leading to their exclusion from further analysis. The increased BGL in the remaining 17 rats administered STZ was sufficient to be deemed as hyperglycaemic and therefore a phenotypical model of type-1 diabetes.

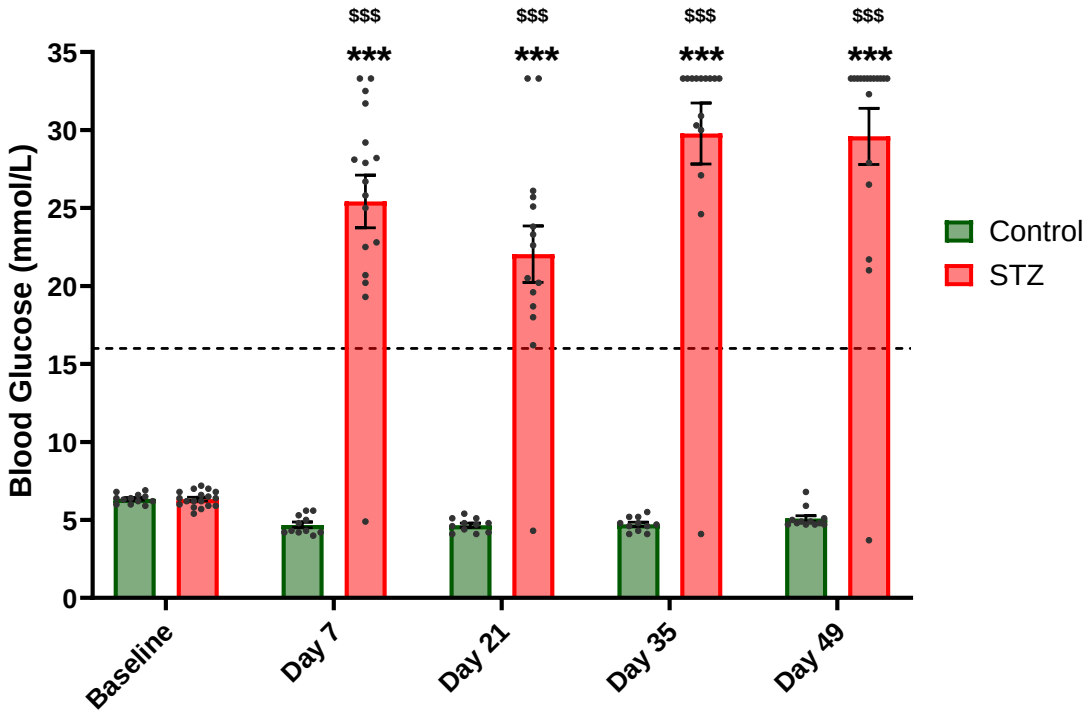

Figure 3.2) Blood glucose level increased and maintained a steady level of hyperglycaemia between Day 7 and Day 49 in rats after STZ administration but not control. Blood glucose levels were measured in control and STZ administered rats at baseline (Day -1), Day 7, 21, 35 and 49. Dashed line indicates 16mmol/L cutoff level for confirmation of hyperglycaemia. ***p<0.001 vs baseline, $$$$p$<0.001 vs control. All data is reported as mean ± SEM, n=11-12 control, n=15-18 STZ.

3.3.2 Mechanical allodynia developed in STZ diabetic rats by Day 7 and remained stable from Day 9 to Day 45.

To understand the development and maintenance of mechanical allodynia, von Frey paw withdrawal thresholds in STZ diabetic rats were measured over 45 days after STZ administration. From Day 7 onwards STZ diabetic rats paw withdrawal threshold was significantly lower than control rats and remained lower until Day 45 when assessed using the standard von Frey monofilament range (0.4-26g) [Time: $F(15,345) = 24.68$, $p<0.001$], [Treatment: $F(1,23) = 15.49$, $p<0.001$], [Interaction: $F(15,345) = 8.083$, $p<0.001$] (Figure 3.3A). A stable level of mechanical allodynia was achieved from Day 9 onwards with STZ diabetic rats paw withdrawal threshold reaching 6.4g compared to 18g in control rats at this timepoint. This level of reduced paw withdrawal threshold continued throughout the remainder of the study with STZ diabetic rats paw withdrawal threshold remaining between 3.8-6.9g and control rat thresholds >15g (Figure 3.3A). Prior to STZ/control administration both groups maintained a similar level of paw withdrawal threshold of ~20-25g.

To identify if the correct neuropathic timepoint to use as a comparator for drug treatment reversal was still the Day 9&11 timepoint as used in Chapter 2 and previous studies at University of Hertfordshire, two timepoint were averaged across the study were compared (Figure 3.3B). This identified that although there was already a decrease in paw withdrawal threshold in STZ diabetic rats as early as the Day 3&7 timepoint the first stable timepoint of paw withdrawal threshold was Day 9&11 as had been previously used [Time: $F(7,161) = 43.06$, $p<0.001$], [Treatment: $F(1,23) = 15.49$, $p<0.001$], [Interaction: $F(7,161) = 14.40$, $p<0.001$] (Figure 3.3B). The maintenance of a reduced paw withdrawal threshold until Day 45 also confirmed that mechanical allodynia remained throughout the study in STZ diabetic rats. Additionally, there was an at least threefold window for potential analgesic reversal between both pre STZ administration timepoints (baseline) and control rats at each timepoint. Mechanical allodynia developed in 17/18 rats (94%) administered STZ as defined by a >50% change in paw withdrawal threshold when comparing Day -7&-4 to Day 9&11. One STZ diabetic rat did not develop mechanical allodynia as their paw withdrawal threshold decreased by <50% so was excluded from further analysis of analgesic reversal with pregabalin. Control rats assessed across these timepoints also began to develop a reduced level of paw withdrawal threshold from the Day 14&17 timepoint (Figure 3.3). Control rat responses decreased from 22.7g at Day -7&-4 to 17.3g at Day 14&17 and 16.2g by Day 35&45 a 28% decrease by the end of the study. Measuring von Frey paw withdrawal thresholds over 45 days after STZ administration revealed a sustained levels of mechanical allodynia from Day 9&11 onwards in STZ diabetic rats.

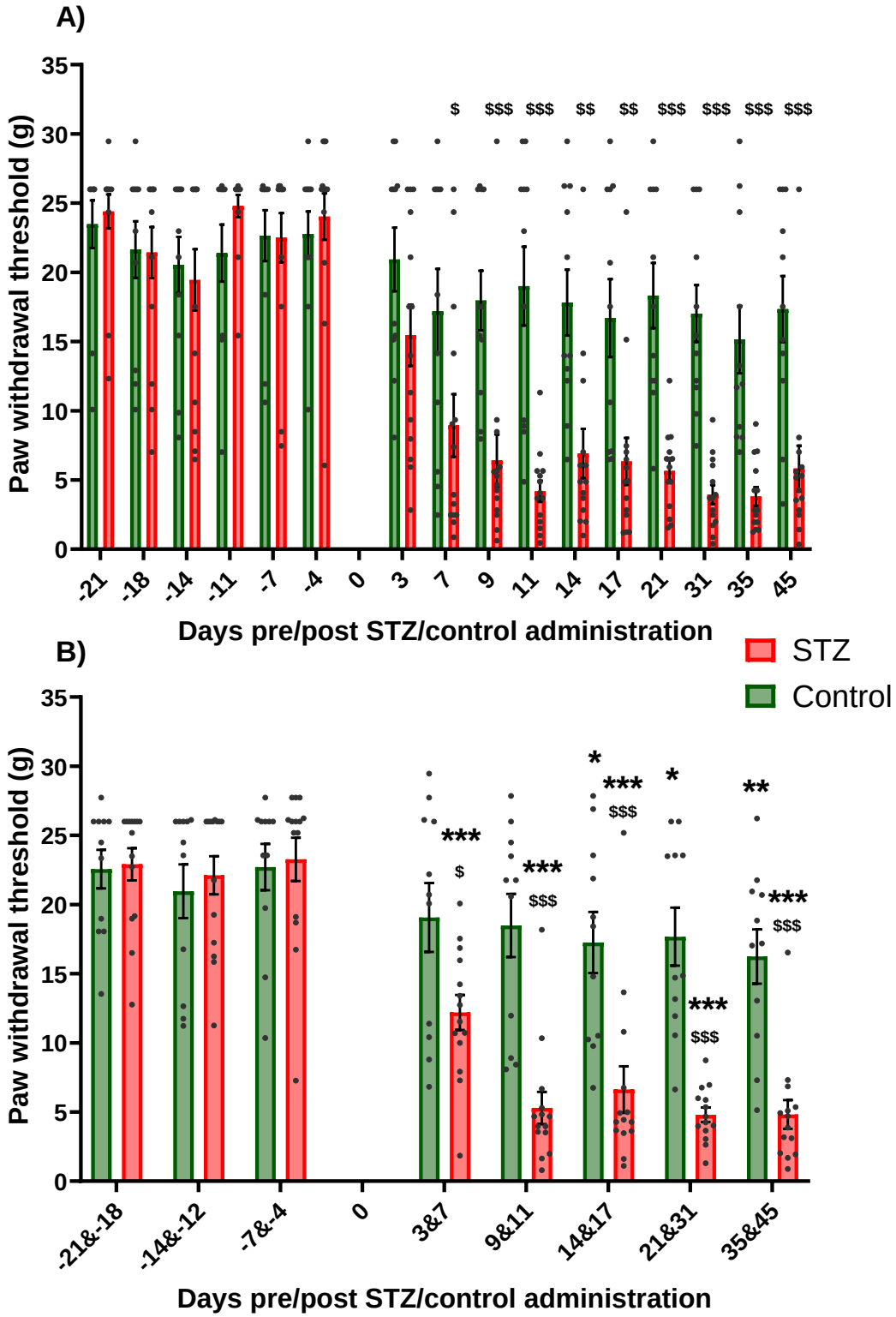

Figure 3.3) Mechanical allodynia developed from Day 7 onwards in STZ diabetic rats stabilising at Day 9&11. Von Frey paw withdrawal threshold was measured with von Frey monofilament using a 0.4-26g monofilament range across the study before and after STZ/control administration. Responses were assessed as either the paw withdrawal threshold at each timepoint measured (A) or the response at pairs of averaged timepoints (B) to identify a suitable comparator timepoint for test compound reversal. (A) $$p<0.05$, $$$p<0.01$, $$$$p<0.001$ vs control (B) *$p<0.05$ **$p<0.01$ ***$p<0.001$ vs baseline day -7&-4, $$p<0.05$, $$$p<0.001$ vs control. All data is reported as mean ± SEM, n=11 control, n=14 STZ.

3.3.3 Mechanical allodynia in STZ diabetic rats was progressively reversed by 3, 10 and 30mg/kg pregabalin.

Previous results discussed in Chapter 2 and published literature indicated that 30mg/kg pregabalin may lead to side effects including somnolence and drowsiness that could affect paw withdrawal behaviour. To elucidate this further, a dose response to 3, 10 and 30mg/kg pregabalin was conducted on von Frey paw withdrawal threshold and revealed that 10mg/kg pregabalin can successfully reverse mechanical allodynia in STZ diabetic rats (Figure 3.4). This was identified when being assessed with the standard von Frey monofilament range (0.4-26g). Even 3mg/kg pregabalin at 4 hours after administration increased STZ diabetic rats paw withdrawal threshold to double the Day 9&11 timepoint (9.6 vs 4.3g) [Time: $F(9,198) = 18.47$, $p<0.001$], [Treatment: $F(1,22) = 10.57$, $p=0.004$], [Interaction: $F(9,198) = 6.52$, $p<0.001$] (Figure 3.4). However, STZ diabetic rats paw withdrawal threshold were still significantly lower than control rats after 3mg/kg pregabalin administration. Pregabalin continued to show a positive dose response as 10mg/kg pregabalin at both 2 and 4 hours reversed mechanical allodynia in STZ diabetic rats to >17g which was equivalent to control rats. This trend continued with 30mg/kg pregabalin increasing the paw withdrawal threshold above 23g again in line with control rats. Control rats paw withdrawal thresholds were not altered after 3, 10 or 30mg/kg pregabalin administration when assessed using the standard 0.4-26g monofilament range. This demonstrates that 10 and 30mg/kg pregabalin fully reversed mechanical allodynia in STZ diabetic rats whilst 3mg/kg pregabalin partially reversed it.

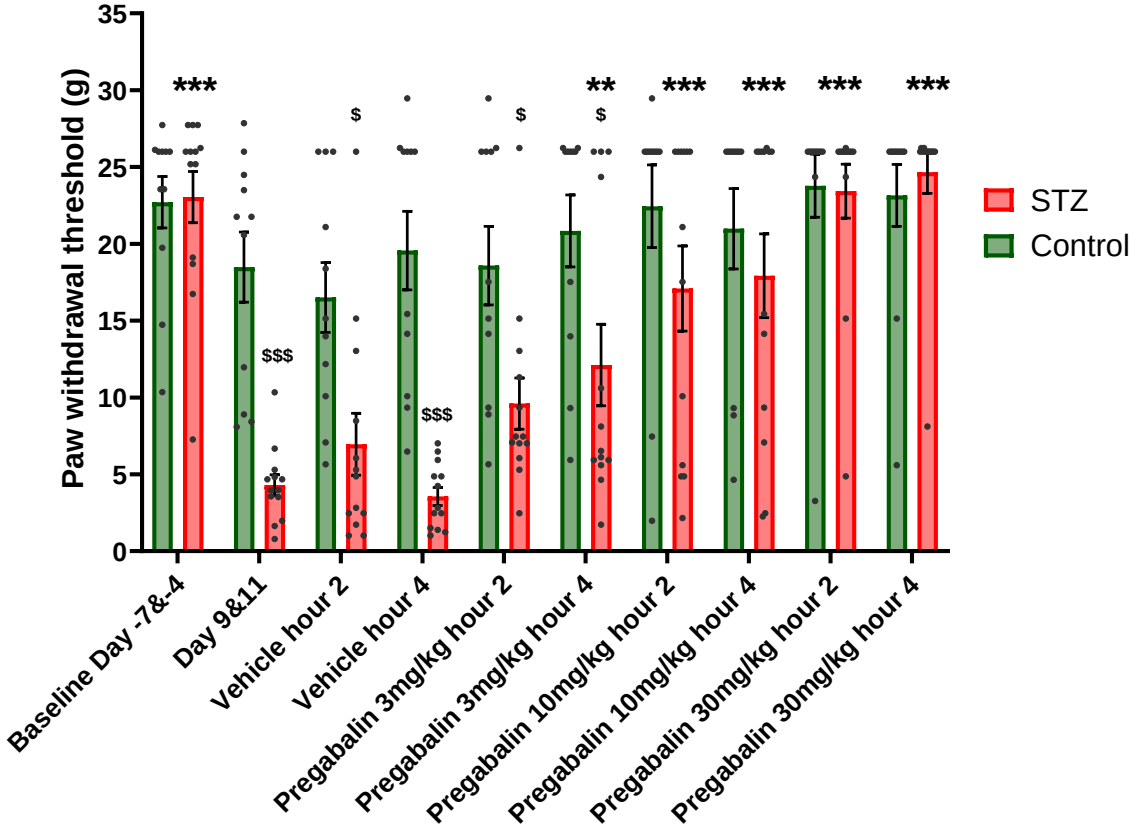

Figure 3.4) Pregabalin at 10 and 30mg/kg successfully reversed mechanical allodynia in STZ diabetic rats using the 0.4-26g monofilament range. Von Frey paw withdrawal thresholds were measured using a 0.4-26g monofilament range at 2 and 4 hours after 3, 10, 30mg/kg pregabalin or vehicle administration to both control and STZ diabetic rats. Pregabalin or vehicle were administered between Day 24 to Day 43 and compared with baseline (Day -7&-4) and Day 9&11 timepoints. **p<0.01 ***p<0.001 vs Day 9&11, $$p$<0.05, $$$$p$<0.001 vs control. All data is reported as mean ± SEM, n=11 control, n=13 STZ.

3.3.4 Measuring mechanical allodynia using an increased range of von Frey monofilaments increased variability and demonstrated potential side effects of 30mg/kg pregabalin.

In addition to the standard (0.4-26g) monofilament range for von Frey measurements, additional measurements were also taken with a wider range (0.16-60g) of monofilaments. Using this wider range had little impact on measuring decreased paw withdrawal thresholds in STZ diabetic rats after Day 0 (Figure 3.5A). However, the wider range produced greater variability in baseline (pre Day 0) and control rats measurements leading to reduced statistical significance when comparing control and STZ diabetic rats. Using the wider range of monofilaments, pre Day 0 paw withdrawal thresholds were increased at ~36g compared to ~22g using the standard range (Figure 3.3, 3.5). After STZ/control administration on Day 0 control rats paw withdrawal threshold stabilised at ~22g for the remainder of the study (Figure 3.5A). STZ diabetic rats paw withdrawal thresholds were similar to control in the pre Day 0 period at ~39g and decreased similarly to when using the standard range following STZ administration (Figure 3.3). Although both monofilament ranges followed the same general trend, STZ diabetic rats paw withdrawal thresholds were only significantly lower than control rats at two timepoints (Day 11, Day 21) when using the wider range [Time: $F(15,345) = 19.86$, p<0.001], [Treatment: $F(1,23) = 4.313$, p<0.05], [Interaction: $F(15,345) = 2.975$, p<0.001] (Figure 3.5A). In comparison all nine timepoints between Day 7-45 were significantly lower in STZ diabetic

rats compared to control rats when using the standard monofilament range (Figure 3.3). A key difference between the two monofilament ranges was the increased variability in data when using the wider range of monofilaments. Across all pre Day 0 timepoints the average SEM for both groups was 5.81 using the wider range versus 1.7 using the standard range highlighting the increased variability when using the wider von Frey monofilament range.

Pregabalin particularly at 30mg/kg increased paw withdrawal thresholds above baseline demonstrating the potential somnolence side effects of pregabalin. Using the wider monofilament range STZ still induced a clear level of mechanical allodynia at the Day 9&11 timepoint compared to baseline (Day -7&-4) [Time: $F(9,198) = 21.68$, $p<0.001$], [Treatment: $F(1,22) = 7.61$, $p=0.01$], [Interaction: $F(9,198) = 1.229$, $p=0.28$] (Figure 3.5B). Mechanical allodynia in STZ diabetic rats was successfully reversed by both 10 and 30mg/kg pregabalin above the Day 9&11 level. However, using the wider monofilament range also identified increased control rat paw withdrawal threshold at 4 hours after 10mg/kg pregabalin (42.1g vs 22.1g Day 9&11) and significant increase following 30mg/kg pregabalin to ~50g, over double the Day 9&11 level (Figure 3.5B). Additionally, this increased paw withdrawal threshold in control rats after 30mg/kg pregabalin was ~15g above the 35g baseline (Day -7&-4) timepoint (Figure 3.5B). Using a wider range (0.16-60g) of von Frey monofilaments increased the variability of paw withdrawal threshold data but also identified that 30mg/kg pregabalin increased control rats paw withdrawal threshold above baseline and Day 9&11 levels.

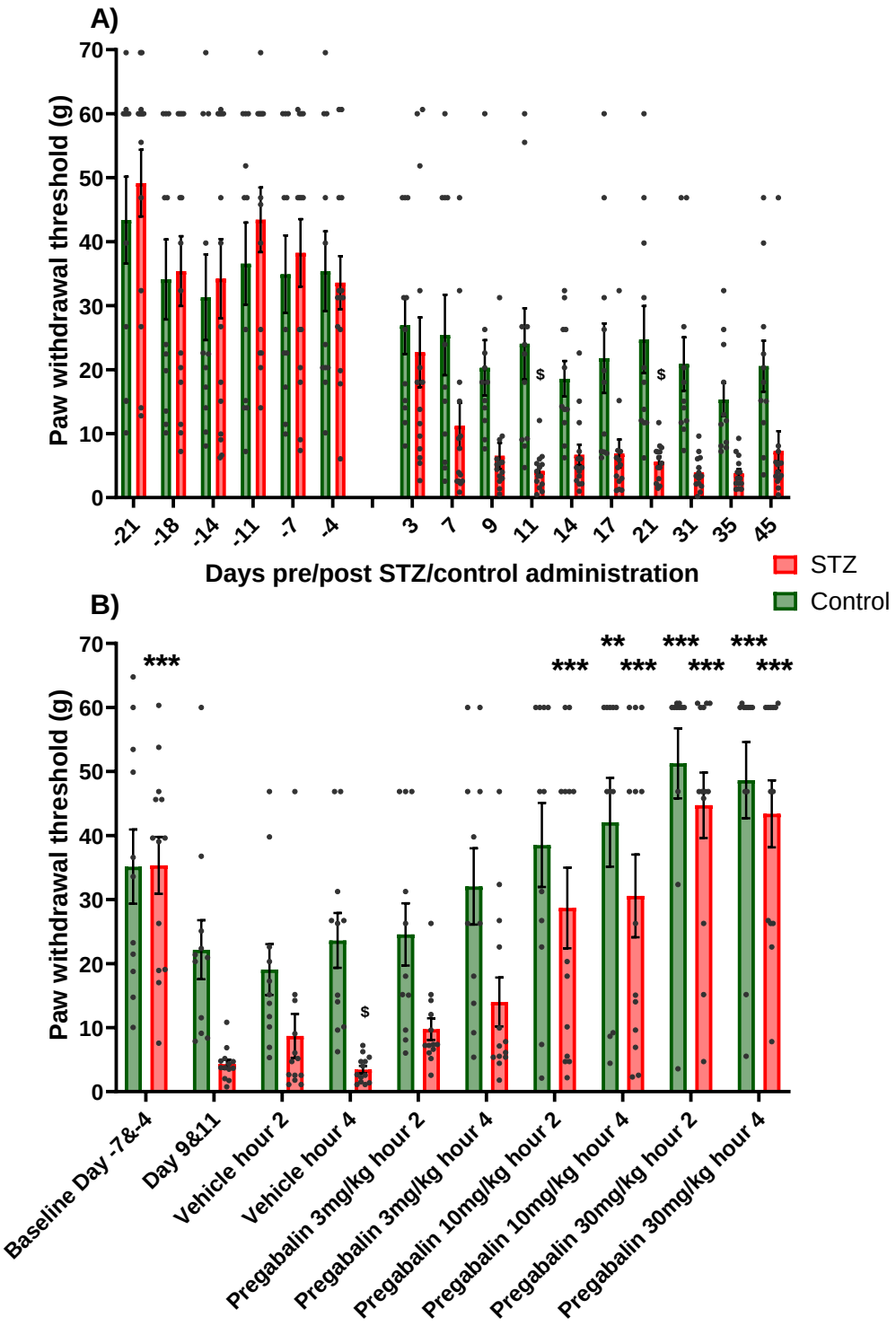

Figure 3.5) Paw withdrawal thresholds were variable when using an expanded range of von Frey monofilaments and highlighted that 30mg/kg pregabalin increases paw withdrawal thresholds above baseline levels. Von Frey Paw withdrawal thresholds were measured with von Frey monofilament using a 0.16-60g monofilament range through the study before and after STZ/control administration (A). Paw withdrawal thresholds were also measured using a 0.16-60g monofilament range at 2 and 4 hours after 3, 10, 30mg/kg pregabalin or vehicle administration to both control and STZ diabetic rats (B). Pregabalin or vehicle were administered between Day 24 to Day 43 and compared with baseline (Day -7&-4) and Day 9&11 timepoints. (A) $$p<0.05$ vs control, (B) **$p<0.01$, ***$p<0.001$ vs Day 9&11, $$p<0.05$ vs control. All data is reported as mean ± SEM, (A) n=11 control, n=14 STZ (B) n=11 control, n=13 STZ.

3.3.5 Burrowing deficits developed slower than mechanical allodynia in STZ diabetic rats.

Monitoring the development of STZ diabetic rats burrowing over the full study period highlighted a slower onset of burrowing deficits compared with von Frey measurements of mechanical allodynia. Pre Day 0 individual burrowing measurements in STZ diabetic and control rats were equivalent in both groups at ~1600g (Figure 3.6A). After STZ/control administration (Day 0) burrowing decreased in STZ diabetic rats at Day 18 and Day 22 compared with control rats to ~575g, a nearly threefold decrease [Time: $F(11,253) = 11.15$, $p<0.001$], [Treatment: $F(1,23) = 8.958$, $p=0.006$], [Interaction: $F(11,253) = 1.946$, $p=0.03$] (Figure 3.6A). This also reflected an apparent slower development in burrowing changes compared with von Frey measurements which were present as early as Day 7 in STZ diabetic rats and reached stable levels by Day 9 (Figure 3.3). In the remainder of the study STZ diabetic rats burrowing levels decreased slightly further reaching an average of 185g on Day 46 (Figure 3.6A). The lack of a significant difference between STZ diabetic and control rats from Day 32 onwards may have occurred due to a gradual decline in control rats burrowing levels that also decreased to <1200g (Figure 3.6A). At these timepoints, although STZ diabetic rat burrowing levels remained low, control rats burrowing levels had also decreased. Measuring burrowing levels over 46 Days indicated that STZ diabetic rats burrowing decreases slower than the development of mechanical allodynia.

To identify the correct timepoint to use as a comparator for drug treatment reversal two timepoint averages across the study were compared. This further confirmed that Day 18&22 as the first timepoint where burrowing levels in STZ diabetic rats are significantly lower than both baseline (575g vs 1530g) and control rats (575g vs 1610g) [Time: $F(4,92) = 11.28$, $p<0.001$], [Treatment: $F(1,23) = 9.081$, $p=0.006$], [Interaction: $F(4,92) = 2.782$, $p=0.03$] (Figure 3.6B). STZ diabetic rats burrowing remained low at 369g for the Day 32&36 timepoint. However control rats burrowing also decreased to 1161g a 30% decrease from baseline (Day -10&-6&-3) although not significantly different from baseline ($p=0.06$) but still significantly higher than STZ diabetic rats at this timepoint. Using the averaged timepoints one STZ diabetic rat was identified as having burrowed on average <500g at the baseline timepoint so was excluded from further analysis of analgesic reversal with pregabalin. Assessing averaged burrowing timepoints demonstrated that Day 18&22 was the first suitable timepoint for comparing the efficacy of analgesic compounds.

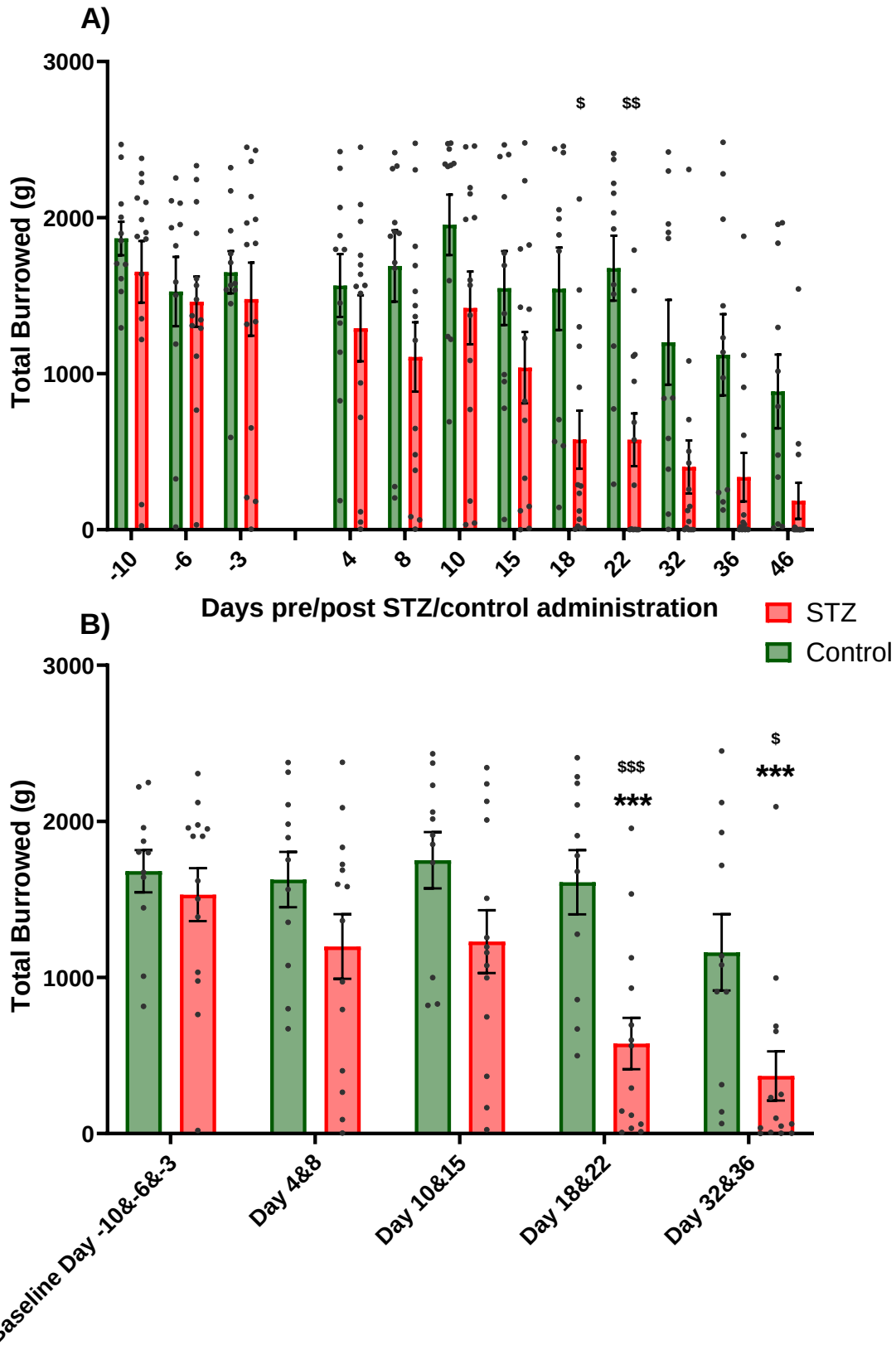

Figure 3.6) Burrowing deficits developed at Day 18 and Day 22 in STZ diabetic rats. Individual burrowing was measured across the duration of the study before and after STZ/control administration. Burrowing was assessed as either at each timepoint measured (A) or the burrowing amount at pairs of averaged timepoints (B) to understand a suitable comparator timepoint for test compound reversal. (A) $$p$<0.05, $$$p$<0.01 vs control. (B) ***p<0.001 vs baseline Day -10&-6&-3, $$p$<0.05, $$$$p$<0.001 vs control. All data is reported as mean ± SEM, n=11 control, n=14 STZ.

3.3.6 Burrowing deficits in STZ diabetic rats were not reversed by 3, 10 or 30mg/kg pregabalin.

Previous burrowing research identified that analgesics such as pregabalin can reverse burrowing deficits in surgical neuropathic pain models but not in STZ diabetic neuropathic pain models (Rutten et al., 2018). Assessing 3, 10 and 30mg/kg pregabalin showed no efficacy in reversing burrowing deficits in STZ diabetic rats in this study in clear contrast to the ability pregabalin in reversing mechanical allodynia (Figure 3.4, 3.7). STZ diabetic rats at Day 18&22 burrowed significantly less than control rats at the same timepoint and compared to the baseline timepoint (Day -10&-6&-3) [Time: $F(5,110) = 12.49$, $p<0.001$], [Treatment: $F(1,22) = 11.86$, $p=0.002$], [Interaction: $F(5,110) = 2.444$, $p=0.04$] (Figure 3.7). Administration of pregabalin at 3, 10 and 30mg/kg along with vehicle (drinking water) all had no effect in STZ diabetic rats burrowing with the amounts remaining <550g at an equivalent level with the Day 18&22 timepoint. Control rats burrowing were also largely unaffected by pregabalin or vehicle administration with the only change being decreased burrowing after 3mg/kg pregabalin administration compared with the Day 18&22 timepoint (Figure 3.7). Overall assessing the amount of burrowing revealed a slower development of burrowing deficits in STZ diabetic rats compared with von Frey paw withdrawal threshold changes that were not rescued by pregabalin.

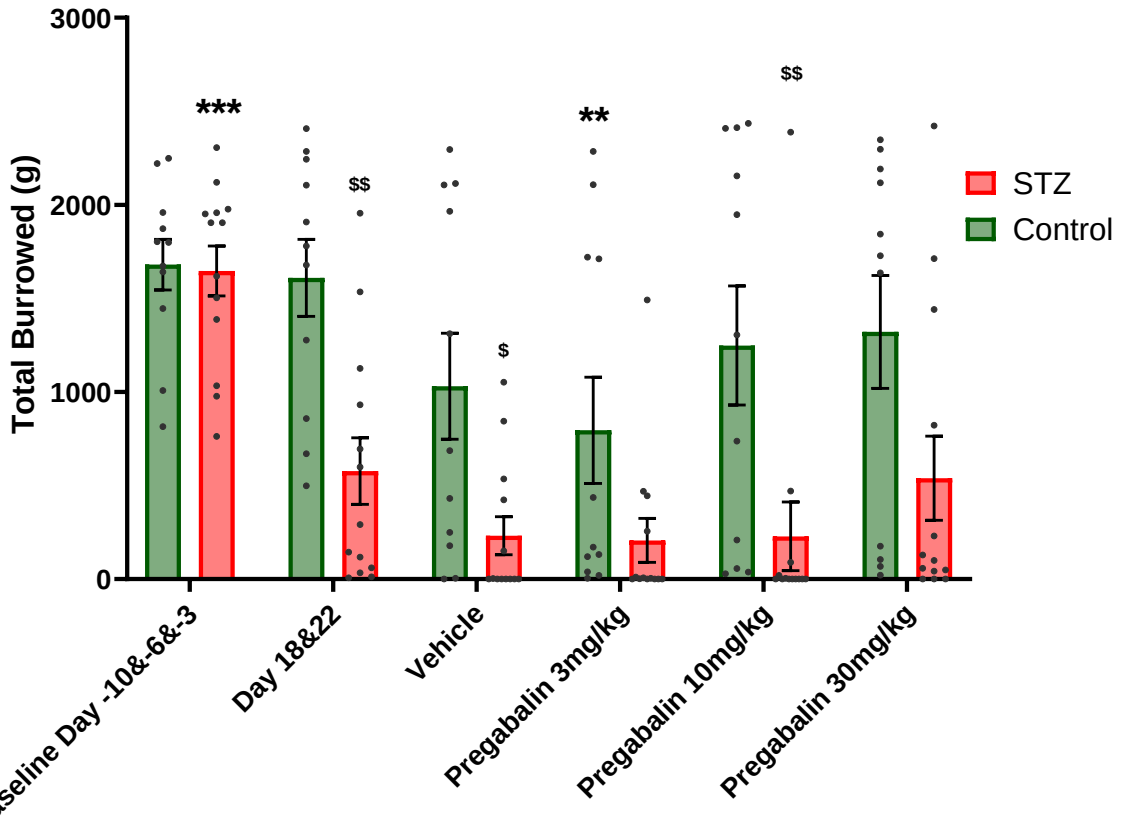

Figure 3.7) Burrowing deficits induced by Day 18&22 in STZ diabetic rats were not reversed by 3, 10 or 30mg/kg pregabalin administration. Individual burrowing was measured at baseline (Day -10&-6&-3), Day 18&22 along with attempted reversal in burrowing deficits through administration of 3, 10 and 30mg/kg pregabalin p.o. and its vehicle (drinking water) to control and STZ diabetic rats (Day 24 to Day 43).**$p<0.01$, ***$p<0.001$ vs Day 18&22, \$$p<0.05$, \$\$$p<0.01$ vs control. All data is reported as mean ± SEM, n=11 control, n=13 STZ.

3.3.7 Von Frey paw withdrawal thresholds and burrowing deficits did not correlate in STZ diabetic rats.

To better understand if burrowing and von Frey paw withdrawal threshold endpoints measure similar changes in STZ diabetic rats behaviour, correlational analysis was conducted between the two endpoints at timepoints after STZ administration. Across the study at Days 7, 21, 35 and 45 there was no correlation between von Frey paw withdrawal threshold and burrowing measurements in STZ diabetic rats (Figure 3.8).

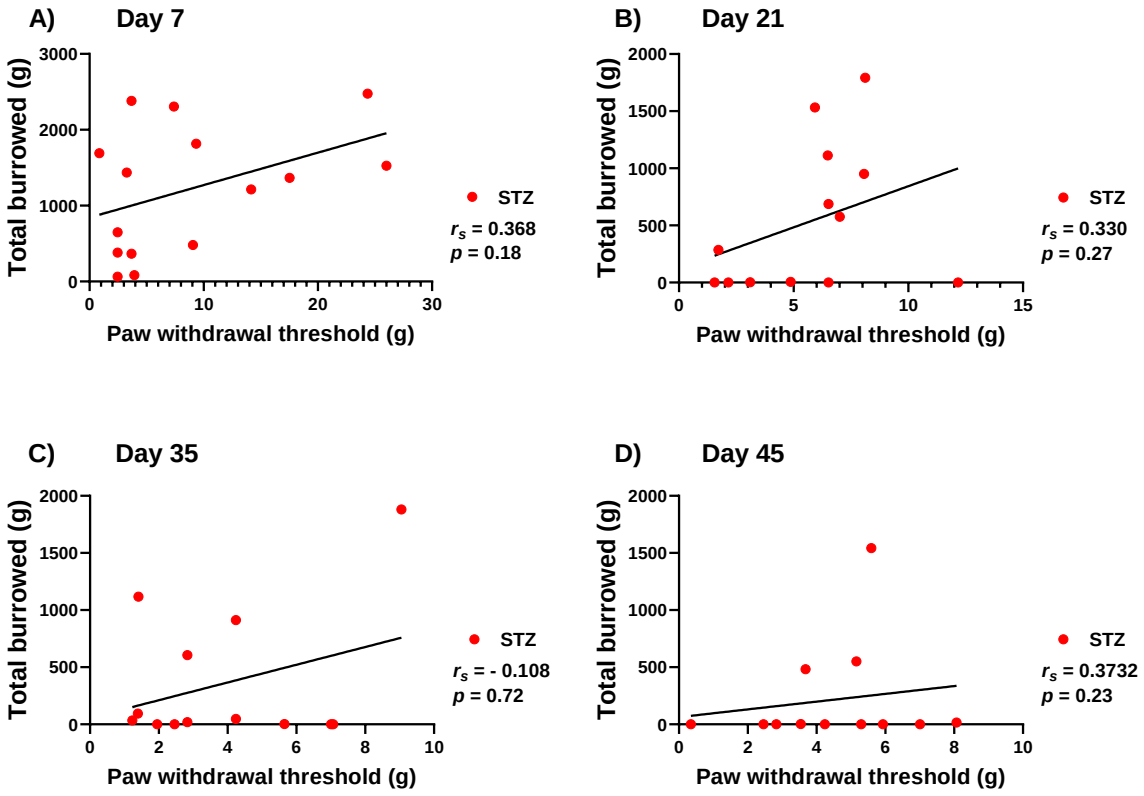

Figure 3.8) Correlation of STZ diabetic rats burrowing levels and von Frey paw withdrawal threshold revealed no correlation between the two measures at any timepoint. STZ diabetic rats von Frey measurements and burrowing amounts at the Day 7(A), Day 21(B), Day 35(C) and Day 45(D) timepoints assessed by Spearman's correlation (r_s). (A) n=15, (B,C) n=13, (D) n=12.

2.3.8 STZ diabetic rats developed polydipsia and gained less bodyweight than control rats, which correlated with blood glucose levels.

The health of STZ diabetic and control rats was monitored throughout the study in part by bodyweight measurements. STZ diabetic rats initially lost bodyweight compared with their weight on the day of STZ administration (Day 0) before plateauing throughout the remainder of the study, whilst control rats continued to gain weight across the full study. STZ diabetic rats initially lost an average of 31g across the first 5 days after STZ administration before stabilising at between ~5-15g from Day 15 onwards (Figure 3.9.A). Control rats consistently gained weight throughout the study reaching a level significantly higher than STZ diabetic rats by Day 5 and remained higher across the full 49 day time course of the study [Time: $F(60,1487) = 273.0$, $p<0.001$], [Treatment: $F(1,27) = 33.45$,

p<0.001], [Interaction: F(61,1487) = 61.70, *p*<0.001] (Figure 3.9.A). When expressed as a percentage change from the Day 0 bodyweight these changes become even more evident with STZ diabetic rats losing an average of -4.5% bodyweight on Day 1 which peaked at -7.35% bodyweight at Day 5. From Day 3 onwards this difference in STZ diabetic rats percentage bodyweight loss was significantly different from control rats [Time: F(49,1163) = 85.65, *p*<0.001], [Treatment: F(1,26) = 136.0, *p*<0.001], [Interaction: F(49,1163) = 49.32, *p*<0.001] (Figure 3.9B). STZ diabetic rats bodyweight progressed back towards their weight on Day 0 and stabilised at ~0-2% loss from Day 20 onwards. Control rats initially gained 4.5% bodyweight per week across the first 2 weeks which progressively slowed to ~1% bodyweight gain per week for the final 2 weeks of the study (Figure 3.9B). Three rats were excluded from the study on Days 6, 14 and 21 due to excess bodyweight loss (>15% approaching 20% threshold) that could not be stabilised by providing additional nourishment in the form of seed, grains and banana porridge. Assessing the bodyweight change of STZ diabetic and control rats was used as one of the health monitors and demonstrated an initial loss of bodyweight for STZ diabetic rats that stabilised after the first week.

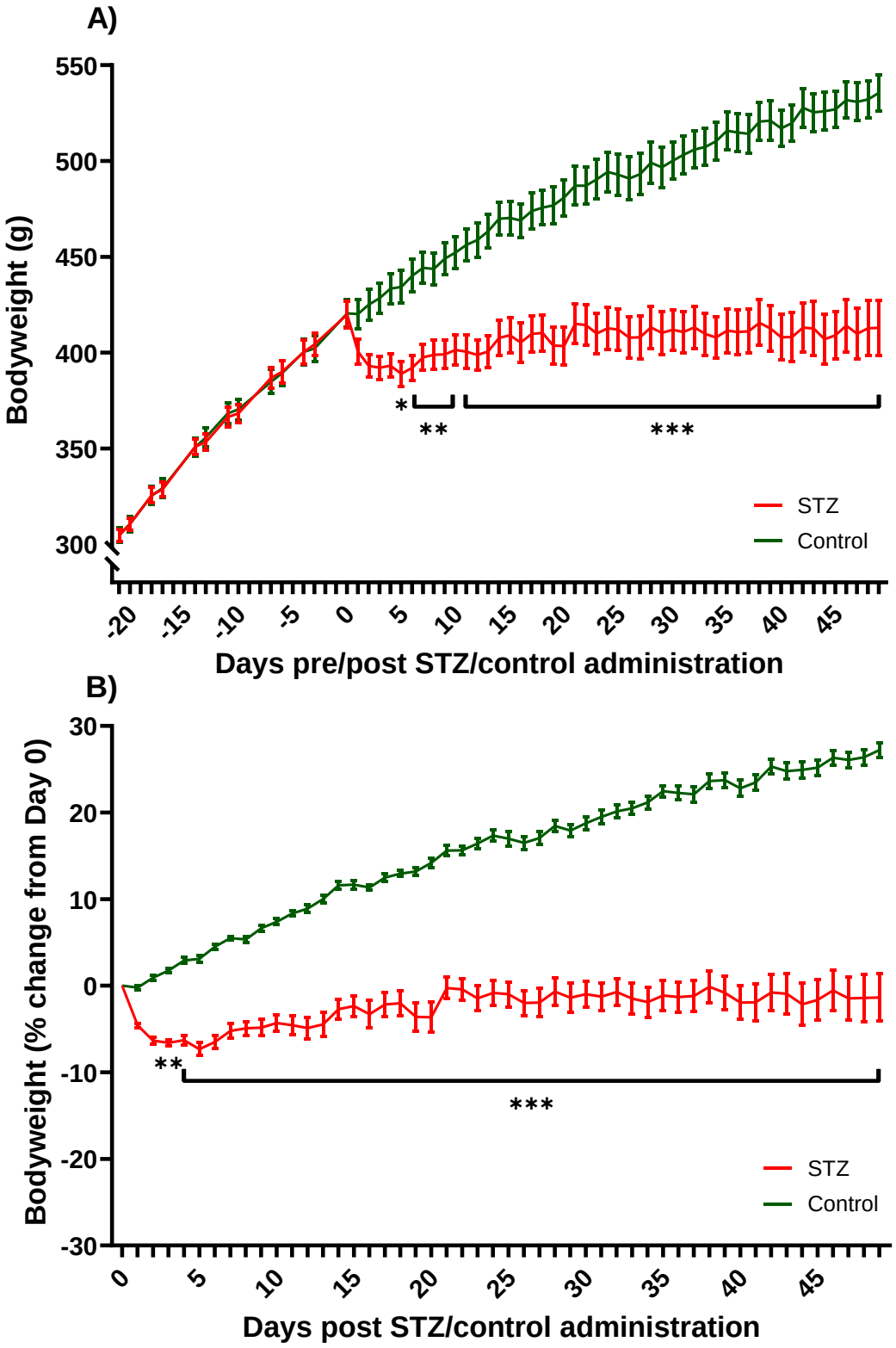

Figure 3.9) STZ diabetic rats gained less bodyweight after STZ administration than control rats. The bodyweight of STZ diabetic and control rats was measured repeatedly before STZ/control administration on Day 0 and daily after administration. Bodyweights were assessed as both raw bodyweight in grams (g) (A) and the percentage from Day 0 (B). *p<0.05, **p<0.01 ***p<0.001 vs control. All data is reported as mean ± SEM, n=11-12 control, n=14-17 STZ.

Correlational comparison of STZ diabetic rats BGL and bodyweight loss demonstrated a correlation between increased BGL and higher bodyweight loss. By Day 7 there was already a non-significant trend (p=0.08) towards a correlation between higher blood glucose levels and increased bodyweight loss in STZ diabetic rats (Figure 3.10A). From Day 21 onwards there was a significant correlation between BGL and bodyweight loss in STZ diabetic rats indicating that rats with higher BGLs also had higher bodyweight loss (Figure 3.10B,C,D).

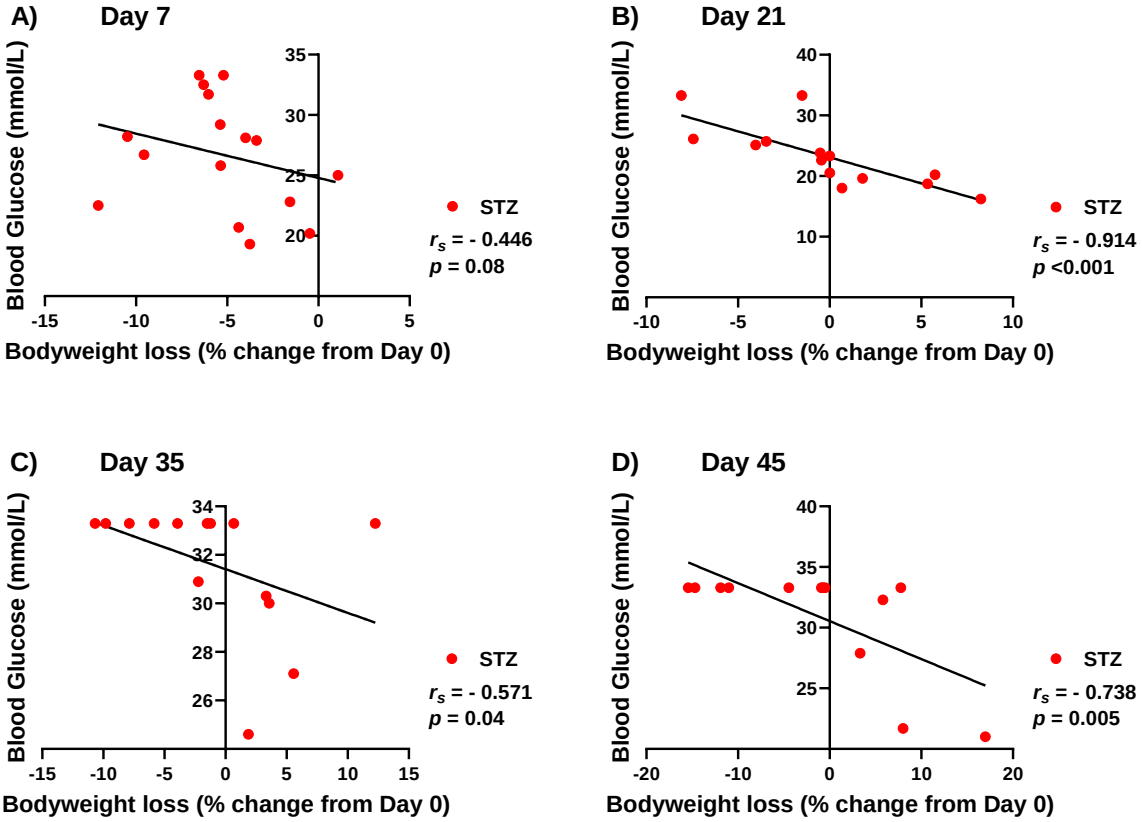

Figure 3.10) Higher STZ diabetic rats blood glucose levels correlated with increased bodyweight loss from Day 21 onwards. Correlational analysis of STZ diabetic rats BGL measurements and percentage bodyweight loss from Day 0 was compared at the Day 7(A), Day 21(B), Day 35(C) and Day 45(D) timepoints assessed by Spearman's correlation (r_s). (A) n=16, (B,C) n=14, (D) n=13.

STZ diabetic rats water intake is a representative measure of polydipsia development and reflected the diabetic phenotype of increased water intake throughout the study. STZ diabetic rats water intake increased rapidly after STZ administration on Day 0 reaching a stable level ~500g/cage/day by Day 11 (Figure 3.11). As early as Day 5 this increased STZ diabetic rats water intake significantly increased compared with control rats who maintained a steady intake of ~85g/cage/day across the full study period apart from days when sucrose was present (Day 0&1) [Time: $F(35,402) = 25.65$, $p<0.001$], [Treatment: $F(1,12) = 39.24$, $p<0.001$], [Interaction: $F(35,402) = 26.38$, $p<0.001$] (Figure 3.11). This increase in water intake represented the development of polydipsia a characteristic phenotype of STZ diabetic rats.

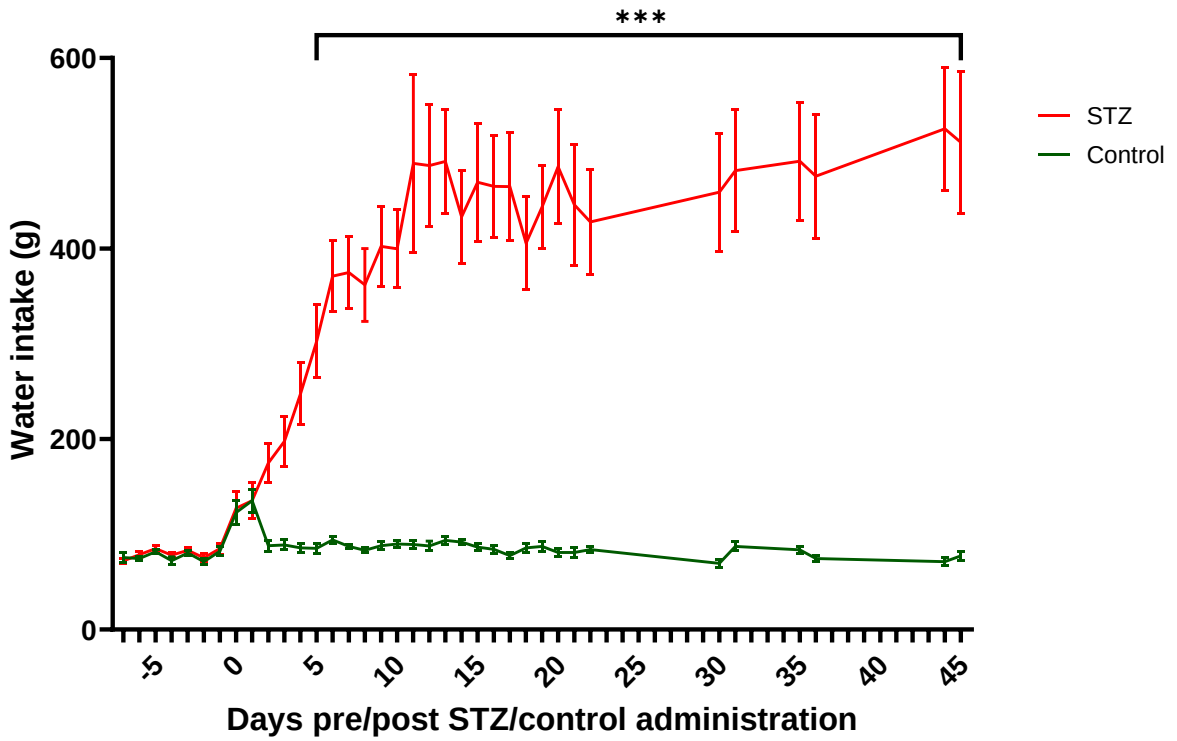

Figure 3.11) STZ diabetic rats caged together water intake sharply increased whilst control rat only cages water intake remained consistent across the study. Total water intake (g) per cage per day was measured across the study. ***p<0.001 vs control. All data is reported as mean ± SEM, n=5-6 control cages, n=7-8 STZ cages.

2.3.9 STZ diabetic rats had increased kidney and liver weight which correlated with increased blood glucose levels.

At the end of the study several tissue samples were taken for bio banking for other masters, PhD and undergraduate research projects to ensure the maximum amount of data could be gathered from each animal, in line with 3R's. Liver and kidneys were collected from 13 STZ and 6 control rats and tissues weighed. STZ diabetic rat's livers weighed on average 17% more than control rats at this Day 49 despite the average weight of control rats being 30% higher than STZ diabetic rats [$t(17) = 3.261$, $p< 0.0046$] (Figure 3.12A). Similarly, when kidney wet tissue weights were measured STZ diabetic rat's kidneys weighed on average 44% more than control rats [$t(17) = 6.378$, $p< 0.0001$] (Figure 3.12B). To also account for the difference in animal bodyweight the wet tissue weights were also calculated as the relative weight of the entire animals bodyweight on Day 49. This highlighted STZ diabetic rats relative liver weights were 50% greater than control rats [$t(17) = 5.204$, $p< 0.0001$] (Figure 3.12C). Whilst relative kidney weights in STZ diabetic rats were almost double control rats at 84% higher [$t(17) = 8.070$, $p< 0.0001$] (Figure 3.12D).

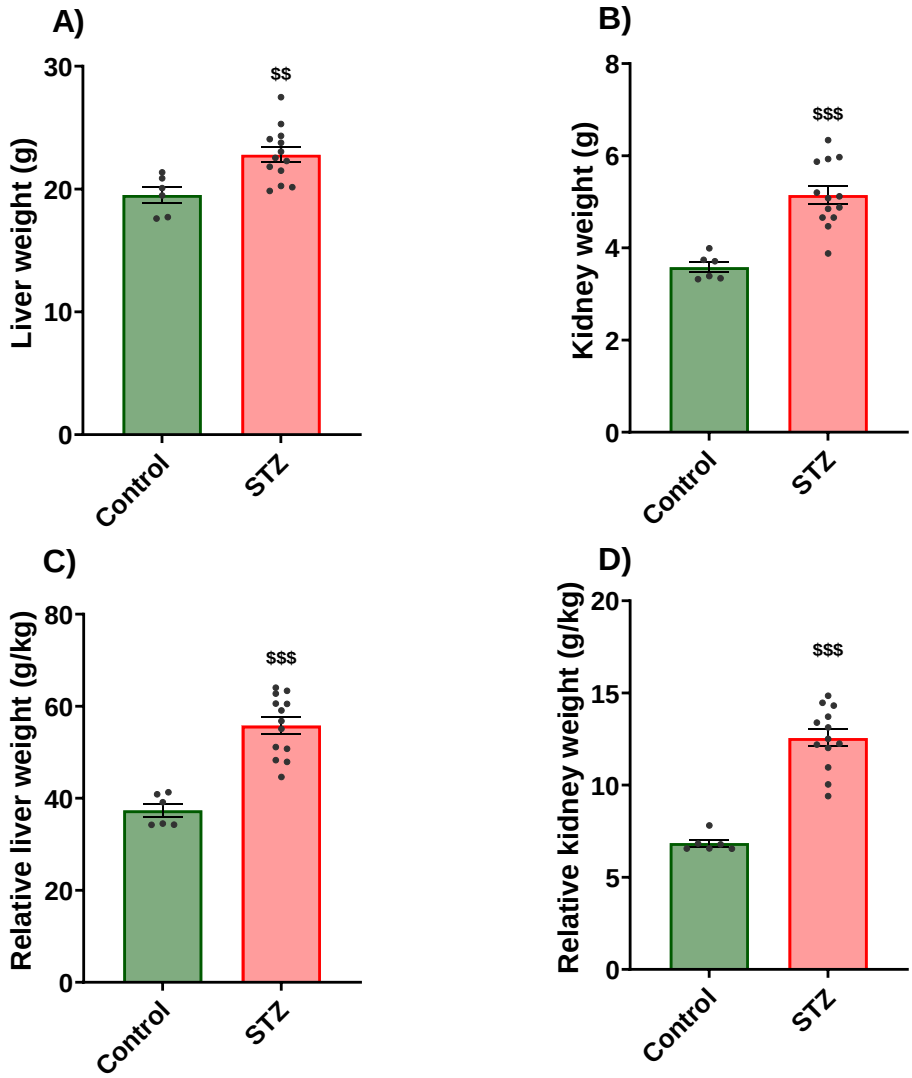

Figure 3.12) STZ diabetic rat's liver and kidneys weighed more than control rats. STZ diabetic and control rats liver (A) and kidney (B) weights at Day 49 expressed as wet tissue weights (g) immediately after dissection. Liver (C) and kidney (D)weights at Day 49 were also expressed as a proportion of the organs weight per overall animal bodyweight (g/kg) at Day 49. $$$p$<0.01, $$$$p$<0.001 vs control. All data is reported as mean ± SEM, n=6 control, n=13 STZ.

As it was identified that higher BGLs were correlated with greater bodyweight loss, the change in organ weights were also correlated to BGL to identify any correlation between these changes seen in STZ rats. No correlation was found between BGL and the wet tissue weights for either liver (Figure 3.13A) or kidneys (Figure 3.13B) in STZ diabetic rats. However, when BGLs were correlated with the relative weight of the liver and kidneys of STZ diabetic rats there was a strong positive correlation such that an increase in BGLs was correlated with an increase in relative liver (Figure 3.13C) and relative kidney weights (Figure 3.13D).

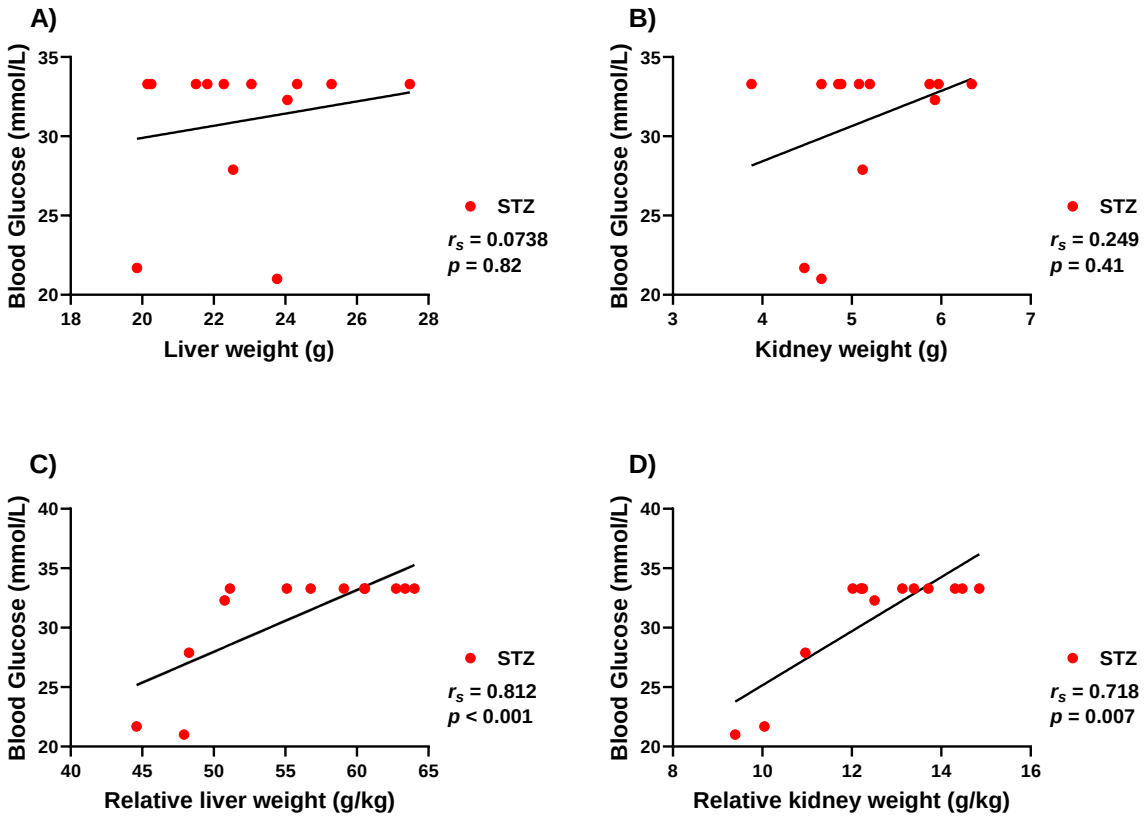

Figure 3.13) Correlation analysis of STZ diabetic rats blood glucose levels and tissue weights highlighted that higher blood glucose levels are correlated with increased relative liver and kidney weights. STZ diabetic rats BGL measurements at Day 49 were compared by correlational analysis with the wet tissue liver (A) and kidney (B) weight along with the relative liver (C) and relative kidney (D) weights as a proportion of overall bodyweight at Day 49 assessed by Spearman's correlation (r_s). (A-D) n=13 STZ.

3.4 Discussion

3.4.1 STZ (55mg/kg) caused hyperglycaemia to develop from Day 7 until Day 49.

The development of hyperglycaemia is the main feature of the single dose STZ diabetic model that is widely used to validate it as representative of a type-1 diabetic phenotype (King & Bowe, 2016). Chapter 2 demonstrated that at the lower single 55mg/kg dose of anomer-equilibrated STZ, successfully induced and maintained hyperglycaemia over 18 days (Figure 2.3). The present study evaluated the same STZ diabetic phenotype over an extended period of 49 days. Monitoring BGLs throughout the study confirmed that administration of 55mg/kg STZ successfully induced hyperglycaemia above the 16mmol/L threshold in 94% of rats at all timepoints measured (Day 7 to Day 49) (Figure 3.2). Likewise to Chapter 2, one STZ administered rat did not develop a stable hyperglycaemic level, with BGL remaining at <7mmol/L at all timepoints assessed in this study. This may have been caused by the rat not receiving a complete dose during administration or misposition of the needle during i.p. dosing affecting the bioavailability of STZ. The development and maintenance of hyperglycaemia in STZ diabetic rats is in line with findings by others that a hyperglycaemic level can be maintained for at least between 8-40 weeks (Furman, 2021; Kambiz et

al., 2015; Wang-Fischer & Garyantes, 2018; Zafar & Naeem-ul-Hassan Naqvi, 2010). Interestingly Wang-Fischer et al. (2018) characterised the STZ diabetic rat model over an extensive period of over 1 year and identified that after 40 weeks after STZ administration BGLs began to trend towards normal glycaemic levels and reached this point by 60 weeks (Wang-Fischer & Garyantes, 2018). It was discussed that a potential cause of this may be due to natural regeneration of pancreatic β cells at this timepoint. The confirmation that STZ administered rats maintained a BGL >16mmol/L until Day 49 in this study confirms that this 55mg/kg STZ model can be considered representative of type-1 diabetes until at least this timepoint.

An animal welfare improvement identified for baseline BGL measurements by taking the microsamples at least one day prior (Day -1) to STZ/control administration on Day 0). Standard operating procedure at University of Hertfordshire has previously microsampled baseline BGL measurements immediately prior to STZ/control administration on Day 0. However, whilst the testing of BGL requires only a small microsample of blood, the additional handling and unfamiliar procedure for animals can lead to increased levels of handling stress during the STZ/control administration on the same day. Hence, taking BGL measurements at least 24 hours prior to STZ/control administration minimised the animals stress by allowing for adequate recovery time in between each procedural event.

3.4.2 Mechanical allodynia developed in STZ diabetic rats by Day 7 and remained stable from Day 9 to Day 45.

A primary aim of this study was to monitor the changes in von Frey paw withdrawal thresholds in STZ diabetic and control rats across an extended time course. This demonstrated that a stable level of mechanical allodynia was induced from Day 9 onwards in STZ diabetic rats. This confirmed that the Day 9&11 timepoint identified in Chapter 2 was still suitable as a reference timepoint for the reversal of mechanical allodynia with analgesic treatments (Figure 3.3). Mechanical allodynia developed at a similar rate in this study compared to in Chapter 2 with mechanical allodynia already present by Day 7 and a stable baseline achieved from Day 9 onwards. The maintenance of a stable level of mechanical allodynia between Day 9 and Day 45 confirmed the time period during which attempts to reverse mechanical allodynia with analgesic treatments can be conducted in this low dose 55mg/kg STZ model. The finding of a stable neuropathic baseline for an extended period of time in the STZ model is in line with current research findings that mechanical allodynia in STZ rats can be maintained for at least 8 weeks (Wang-Fischer & Garyantes, 2018; Yamamoto et al., 2009). Measuring von Frey paw withdrawal thresholds confirmed that mechanical allodynia developed by Day 9&11, as seen previously in Chapter 2, and was maintained throughout the study.

3.4.2.1 Confirmation of diabetic neuropathy development.

The development of diabetic neuropathy in these STZ diabetic rats at day 49 was confirmed on skin tissue samples from the plantar skin of the left hind paw and correlated with the von Frey paw withdrawal thresholds taken at Day 46. Immunohistochemical (IHC) analysis of PGP9.5 and Langerhans cells (LC) density were undertaken as part of an MSc research project to confirm the development of diabetic neuropathy in these STZ diabetic rats (Blackstone Whines, 2022). PGP9.5 is a ubiquitin hydrolase that is highly expressed by intra-epidermal nerve fibres (IENF) and LC are a type of dendritic antigen presenting cells closely associated with IENF (Hamzeh et al., 2000). Following PGP9.5 IHC staining of plantar paw skin paraffin embedded sections from STZ diabetic

rats, decreased IENF density and an increased LC density was observed compared with control rat skin sections (Blackstone Whines, 2022). IHC assessment of IENF and LC density in human diabetic patients has previously identified a decrease in IENF density and increase in LC present in skin samples taken (Casanova-Molla et al., 2012). Both of these changes in IENF and LC density have also been demonstrated in the STZ diabetic rat model by multiple groups along with correlations to other measurements of neurophysiology (Kambiz et al., 2015; Lauria et al., 2005). These results confirm that the STZ diabetic rats in this study exhibit diabetic neuropathy in plantar skin at Day 49 which corresponds with the findings both in human diabetic patients and in the other STZ diabetic rat models.

3.4.3 Measuring mechanical allodynia using an increased range of von Frey monofilaments increased variability.

An observation made in Chapter 2 was that many rats when measured using the standard 0.4-26g von Frey monofilament range reached the upper threshold and therefore an increased range of 0.16-60g was explored in this study. This demonstrated much greater variability in paw withdrawal thresholds for both STZ diabetic and control rats particularly at the pre Day 0 timepoints when using higher 0.16-60g range (Figure 3.5). The assessment of von Frey paw withdrawal threshold using von Frey monofilaments can be conducted in a number of ways including manually using a range of monofilaments, as used in this study, or using an electronic system that applies increasing pressure until the animal reacts (Austin et al., 2012). Manual von Frey can also be assessed in different ways including the up-down method (used in these studies), percentage response (repeated application of all monofilaments even after response) or ascending stimulus (increasing monofilaments until response) (Deuis et al., 2017). The range of monofilaments used also differs between studies and can include 0.4-15g (Lindner et al., 2006), 1.08-21.09g (Vrinten & Hamers, 2003), 0.6-26g (Hu et al., 2020), 0.7-29g (Field, McCleary, et al., 1999) in rats.

To understand the impact of increasing the range of monofilaments used in this study an additional low and high monofilament was introduced in the von Frey testing for this study (**0.16**, 0.4, 0.6, 1, 1.4, 2, 4, 6, 8, 10, 15, 26, **60**; g). Introducing this monofilament range caused an increase in the variability of the data generated by von Frey measurements, likely due to the logarithmic nature of the difference in von Frey filaments that do not increase in pressure applied in a linear fashion. This is also one of the key limitations of the manual von Frey method of measuring mechanical allodynia and affects both the sensitivity of detecting changes at higher paw withdrawal thresholds and the algorithms used to generate the average paw withdrawal threshold (Christensen et al., 2020). Recording von Frey measurements using the higher 0.16-60g range did not change the overall development of mechanical allodynia in STZ diabetic rats. However, it did reduce the level of statistical significance and statistical power particularly in comparisons between STZ diabetic and control rats. Continuing to introduce this in future experiments would require a greater number of animals to be used in each group to achieve the same level of significance as using the original 0.4-26g range. Despite this manual von Frey is still the favoured way to measure paw withdrawal thresholds and is routinely employed (Deuis et al., 2017). Measuring von Frey paw withdrawal thresholds using an increased (0.16-60g) monofilament range highlights the need for novel objective neuropathic pain endpoints due to large variability and low sensitivity.

3.4.4 Mechanical allodynia in STZ diabetic rats was progressively reversed by 3, 10 and 30mg/kg pregabalin.

Upon establishing the time course of mechanical allodynia development using von Frey paw withdrawal threshold at the standard (0.4-26g) monofilament range, attempts to reverse mechanical allodynia with the first line treatment pregabalin were made. To overcome the previous limitation that 30mg/kg pregabalin caused potentially confounding side effects of somnolence, this study examined a dose response to pregabalin using 3, 10 and 30mg/kg (Figure 3.4). Testing lower doses of pregabalin demonstrated that even at 3mg/kg pregabalin partially reversed the von Frey paw withdrawal threshold measurements of mechanical allodynia in STZ diabetic rats compared with Day 9&11, although did not reverse paw withdrawal thresholds in line with control rats. Pregabalin at 10mg/kg did however successfully reverse mechanical allodynia in STZ diabetic rats to levels equivalent to control rats as did 30mg/kg pregabalin. Pregabalin has previously been demonstrated to be efficacious using a 10mg/kg dose in the STZ model against von Frey measurements (Yamamoto et al., 2009). It has also been identified that 10mg/kg pregabalin more closely represents a standard human pregabalin dose of between 300 and 600mg/day (Koyama, LeBlanc, et al., 2018). Therefore, using a lower 10mg/kg dose of pregabalin that has similar efficacy to the higher 30mg/kg dose and is closer to the human equivalent dose of pregabalin is likely to provide more accurate results. Additionally, using 10mg/kg pregabalin with reduced side effects of somnolence that may impact the animal's ability to react to von Frey monofilaments, would improve the use of pregabalin as a reference analgesic in this model (Wang-Fischer & Garyantes, 2018). Overall in this study, a lower 10mg/kg pregabalin successfully reversed mechanical allodynia to baseline levels in STZ diabetic rats.

Further evidence for the side effects of 30mg/kg pregabalin were demonstrated when using the increased (0.16-60g) monofilament range that 30mg/kg pregabalin significantly increased control rats paw withdrawal threshold. 30mg/kg pregabalin and to some extent 10mg/kg pregabalin increased the paw withdrawal thresholds in control rats above the Day 9&11 level (Figure 3.5). Particularly at 30mg/kg this increase was ~15g above the baseline timepoint paw withdrawal threshold and therefore is likely representative of some level of somnolence in these rats as has previously been identified (Wang-Fischer & Garyantes, 2018). Together, these findings provided a clear indication that pregabalin affects not only STZ animals paw withdrawal threshold but also control rats, something not previously identified when using the standard 0.4-26g monofilament range (Figure 3.4). A potential cause for this is the somnolence side effect of pregabalin that has been noted at 30mg/kg by others and in both this and the Chapter 2 study (Wang-Fischer & Garyantes, 2018). An alternative or additional mechanism for this could be reduced sensitivity of the control rats as pregabalin is proposed to reduce the release of neurotransmitters on ascending pain pathways by inhibiting calcium channels (Alles et al., 2020). As discussed in Chapter 2 the possible social transfer of pain may be contributing to this increase in control rats paw withdrawal threshold, particularly compared with the Day 9&11 timepoint where control rats are tested in the presence of STZ diabetic rats experiencing mechanical allodynia (Langford et al., 2006; Smith et al., 2016). The identification of increased control rat paw withdrawal thresholds above baseline levels further supports the use of a lower 10mg/kg dose of pregabalin for future studies to reverse neuropathic pain preclinically, particularly in the STZ diabetic rat model.

3.4.5 Burrowing deficits developed slower than mechanical allodynia in STZ diabetic rats.

Burrowing deficits in STZ diabetic rats developed only by Day 18 and 22 in this study, much slower than the von Frey paw withdrawal thresholds that had already stabilised by Day 9. As discussed in

Chapter 2, whilst the development, maintenance and reversal of burrowing deficits in several different neuropathic pain models have been characterised, the changes in the STZ type-1 diabetes rat model are less understood (Andrews et al., 2012; Lau et al., 2013; Rutten et al., 2018). Therefore, this study set out to characterise the time course of changes in burrowing in the STZ rat model and attempt to reverse those changes with 3, 10 and 30mg/kg pregabalin. These results provided the first evidence that a stable level of burrowing deficit can be induced and maintained across 18-46 days in a low (55mg/kg) dose STZ model (Figure 3.6). Previous research into STZ burrowing by Rutten et al. (2018) focused on assessing a single timepoint of burrowing at Day 21 after a high (75mg/kg) dose of STZ in which burrowing was almost completely abolished (<100g) (Rutten et al., 2018).

The present study found that burrowing was significantly suppressed by STZ administration at an equivalent timepoint (Figure 3.6) and extended this finding by demonstrating that burrowing deficits could be identified as early as Day 18 and maintained to the end of the study at Day 46. Although the development and maintenance of burrowing deficits has not previously been explored in the STZ diabetic rat model it has been assessed in other neuropathic pain models. This includes by Rutten et al. (2018) who demonstrated that the CCI rat model exhibits burrowing deficits as soon as 4 days after surgery that are maintained for 25 days (Rutten et al., 2018). A similar finding in another groups CCI rat model demonstrated that burrowing deficits were present at 3 days after CCI surgery and maintained for at least two weeks (Muralidharan et al., 2016). Interestingly Lau et al. (2013) demonstrated a slower onset of burrowing deficits in the SNI rat model with burrowing deficits evident at Day 10 after surgery and maintained until at least Day 30 (Lau et al., 2013). Lau et al. (2013) also identified that the onset of burrowing deficits was delayed compared to von Frey measurements of mechanical allodynia a finding consistent with this study in the STZ model (Figure 3.3) (Lau et al., 2013). Whilst von Frey measurements of mechanical allodynia emerged as early as Day 7 (Figure 3.3), burrowing deficits in the STZ diabetic rat model did not appear until Day 18 (Figure 3.6). This delay in burrowing deficit observed here (and by others) indicates that von Frey and burrowing measure distinct changes in the neuropathic pain condition and may contribute further to the evidence that burrowing is a measure of the overall animal's wellbeing (Andrews et al., 2011; Deacon, 2006; Deseure & Hans, 2018; Jirkof, 2014).

3.4.6 Burrowing deficits in STZ diabetic rats were not reversed by 3, 10 or 30mg/kg pregabalin.

Even using a low 55mg/kg dose of STZ diabetic rats burrowing was not reversed by 3, 10 or 30mg/kg pregabalin (Figure 3.7). Whilst in most neuropathic pain models pregabalin or other similar analgesics are effective at reversing neuropathic pain induced burrowing deficits (Andrews et al., 2012; Lau et al., 2013; Rutten et al., 2018), the same is not true for diabetic models (Rutten et al., 2018). Previous research by Rutten et al. (2018) used a high 75mg/kg dose of STZ to induce type-1 diabetes and identified large deficits in burrowing (Rutten et al., 2018). Rutten et al. (2018) also found similar deficits in the Zucker diabetic fatty (ZDF) model of type-2 diabetes neither of which were reversable with pregabalin at 10 or 30mg/kg. One of the main theories behind the burrowing deficits in both the ZDF type-2 and STZ type-1 rat models of diabetes not being reversable with pregabalin administration is due to them being "masked" by changes in the animal's overall wellbeing related to diabetes (Rutten et al., 2018). Therefore, this study assessed if these burrowing deficits were also present in a lower dose (55mg/kg) model of STZ induced type-1 diabetes with improved animal wellbeing (Chapter 2). Even at this lower dose of STZ pregabalin at 3, 10 and 30mg/kg had no effect on the amount of burrowing conducted by STZ type-1 diabetic rats (Figure 3.7). In contrast, pregabalin at these same three doses rescued burrowing deficits in the CCI model

and at 10mg/kg in the SNI model (Lau et al., 2013; Rutten et al., 2018). Additionally, pregabalin at 3, 10 and 30mg/kg improved von Frey measurements of paw withdrawal threshold in this study in contrast to the lack of changes with any dose of pregabalin on burrowing deficits (Figure 3.4). This provided further evidence that burrowing in the STZ model is measuring changes other than reflexive mechanical allodynia and instead provided some measure of overall animal wellbeing that pregabalin treatment alone cannot rescue. As the findings in Chapter 2 demonstrated that housing STZ diabetic rats with a control rat home cage partner rescues burrowing levels it would appear that this can be achieved just not by pregabalin (Figure 2.9). Therefore, further research is needed to examine additional ways to rescue burrowing levels in diabetic models of neuropathic pain such as treatment with insulin to determine if normalising hyperglycaemia can rescue changes in burrowing. Alternatively other first line treatments such as amitriptyline or duloxetine should also be assessed (Finnerup et al., 2015). This is particularly important for future neuropathic pain research as although pregabalin is effective in almost all studies using von Frey measurements, its NNT in humans is estimated to be ~7.2, much lower than its efficacy preclinically (Finnerup et al., 2015). Further evaluating burrowing as a robust measure of wellbeing may offer a secondary screening endpoint for novel analgesics that can reverse both von Frey paw withdrawal thresholds and wellbeing leading to the identification of treatments with lower NNT.

Whilst there is increasing evidence supporting burrowing as a wellbeing endpoint it is not without limitations (Deseure & Hans, 2018; Rutten et al., 2018). One limitation of burrowing is the variability of the data gathered (as discussed in Chapter 2) and the variability in responses between studies as indicated by the difference in early burrowing levels in Chapter 2 compared to this study. Chapter 2 demonstrated a burrowing deficit occurring as early as Day 3 in STZ diabetic rats (Figure 2.9). However, during the current study STZ diabetic rats burrowing deficits did not develop until Day 18 (Figure 3.6). This difference in the timeframe of burrowing deficit development may have been caused by the early measurement of burrowing in Chapter 2 that was too close to STZ administration and therefore STZ diabetic rats were still recovering from the initial effects of STZ induced pancreatic β cell damage (Luippold et al., 2016). The first 48-72 hours after STZ administration are often considered the most critical due to the initial hypoglycaemia caused by insulin release from damaged pancreatic β cells and then followed by rapid hyperglycaemia (Ghasemi & Jeddi, 2023). An alternative reason for the difference between this study and Chapter 2 is the more extensive baseline period of social burrowing facilitation, and greater number of individual burrowing sessions used in this study which is more in line with other published protocols (Andrews et al., 2012; Lau et al., 2013; Rutten et al., 2018). This could have improved the reliability of the data achieved in this current study compared with Chapter 2.

Another limitation of burrowing measurements was the apparent development of a non-significant decrease in control rats burrowing from Day 32 onwards (Figure 3.6). Although not significantly decreased, control rats did appear to begin burrowing less substrate at around Day 32. The cause of this is unknown but could reflect an overstimulation of rats to the burrowing activity across the course of the study leading to a reduction in burrowing levels. Alternatively, this could be a delayed onset of the possible social transfer of pain discussed in Chapter 2 with control rats exhibiting a decrease in overall wellbeing due to being housed and tested in close proximity to STZ diabetic rats experiencing neuropathic pain (Langford et al., 2006; Smith et al., 2016). To attempt to overcome this, once the timeline for burrowing development has been established in a specific neuropathic pain model, the number of timepoints that burrowing is measured could be reduced to ensure the activity remains a novel enrichment and still reflects the ethological behaviour. The increased variability in burrowing measurements compared with the von Frey measurements (when using the standard 0.4-26g monofilament range) may also be a limitation of this endpoint as has been

reported by others (Andrews et al., 2012; Muralidharan et al., 2016) and in Chapter 2. Preclinical screening assays that aim to use burrowing as a neuropathic pain endpoint would have to increase the number of rats used in each group to achieve the same statistical power. This would require ethical justification and could be considered as going against the 3R's of reduction (NC3Rs, n.d.). However, burrowing may still provide a useful secondary endpoint measurement of wellbeing as evidenced by its improvement in Chapter 2 by pairing STZ diabetic and control rat together (Figure 2.9).

3.4.7 Von Frey paw withdrawal thresholds and burrowing deficits did not correlate in STZ diabetic rats.

Based on the finding that STZ induced burrowing deficits developed slower than mechanical allodynia these changes were correlated across different timepoints throughout the study to identify if changes in burrowing were in any way associated with changes in von Frey measurements. Even when assessed at timepoints when both burrowing deficits and mechanical allodynia occurred, changes in burrowing did not correlate with mechanical allodynia (Figure 3.8). This finding of a lack of correlation between burrowing deficits and evoked neuropathic pain endpoints (Figure 3.8) have been replicated across a range of different neuropathic pain models including the SNI, tibial nerve transection, spinal nerve transection, CCI, STZ and partial sciatic nerve ligation models (Andrews et al., 2012; Lau et al., 2013; Muralidharan et al., 2016; Rutten et al., 2018). In the SNI rat model burrowing deficits were not correlated with von Frey paw withdrawal measurements (Lau et al., 2013). In the CCI rat model two independent studies have demonstrated a lack of correlation between burrowing deficits and cold allodynia (Rutten et al., 2018) or von Frey paw withdrawal (Muralidharan et al., 2016). This trend continues with findings in the tibial nerve transection, spinal nerve transection and partial sciatic nerve ligation models rat models that reduced von Frey paw withdrawal thresholds did not correlate to deficits in burrowing (Andrews et al., 2012). Specifically in the STZ diabetic rat model, burrowing deficits were not correlated to the Randall-Selitto test of mechanical sensitivity (Rutten et al., 2018).

This finding that evoked mechanical allodynia did not correlate with burrowing changes in STZ diabetic rats (Rutten et al., 2018) was replicated in the present study where STZ burrowing deficits did not correlate with von Frey measurements of mechanical allodynia (Figure 3.8). However, whilst the aforementioned studies were all conducted in rats a study in an SNI mouse model demonstrated a strong correlation between burrowing deficits and von Frey measurements potentially reflecting a species difference in this endpoint (Shepherd et al., 2018). This is also reflected in findings that rats and mice burrow substrates differently, in particular mice tend to prefer to burrow food pellets whilst rats burrow very little food pellets and instead prefer to burrow gravel or sand (Deacon, 2009). Though burrowing changes appear to generally not correlate with evoked neuropathic pain endpoints, particularly in rats, these evoked endpoints have been demonstrated to correlate with other non-evoked endpoints in the STZ model previously. Vieira et al. (2020) demonstrated that von Frey paw withdrawal thresholds in the STZ model were correlated with changes in stride length, paw print area and maximum contact area measured using an automated gait analysis system (Vieira et al., 2020). The overall finding that burrowing and traditional evoked endpoints changes do not correlate, further supports burrowing as an alternative endpoint in neuropathic pain models that reflects the overall wellbeing of the animal and is not a simple measure of reflexive pain.

3.4.8 STZ diabetic rats developed polydipsia and gained less bodyweight than control rats which correlated with blood glucose level.

Polydipsia, assessed through the increased consumption of water by STZ diabetic rats in this study is a common phenotype of both STZ diabetic rats (Ali et al., 2015; Rutten et al., 2018; Vieira et al., 2020; Wang-Fischer & Garyantes, 2018; Yamamoto et al., 2009) and human diabetic patients (Pasi & Ravi, 2022; Roche et al., 2005). The development of polydipsia was similar in this study to that of Chapter 2 in which STZ diabetic rats water intake increased across the first few days before plateauing around Day 10 and remained at ~500g/cage/day across the remainder of both studies (Figure 3.11). This increased water intake is a further confirmation that a single 55mg/kg STZ dose can induce and maintain a diabetic phenotype for 49 days.

An important measure that is used to monitor STZ diabetic rats is their bodyweight which is often used as a measure of their health and welfare to ensure animals do not experience excessive suffering in line with good animal practices (Gajdošík et al., 1999). In this study the STZ model was extended to 49 days compared with previous studies conducted at University of Hertfordshire that lasted ~21 days after STZ administration (Burnett et al., 2014; Fisher et al., 2015; Lanigan et al., 2020). Changes in the rats bodyweight were monitored closely across the study. The changes in STZ diabetic rats bodyweight followed a similar trend to that seen in Chapter 2 with an initial loss of bodyweight that stabilised after the first week and even began to normalise back to baseline towards the end of the study (Figure 3.9). Though the bodyweight loss was slightly higher in the present study at 5.2% on Day 7 versus 3.2% in the Chapter 2 study (Figure 2.4). In the majority of STZ diabetic rats, bodyweight and animal health remained stable throughout the study. However, three STZ diabetic rats were euthanised within the first 3 weeks after STZ administration due to health complications. The first of these animals developed a paw inflammation/swelling along with bodyweight loss by Day 6 whilst the other two rats primarily developed continuous gradual bodyweight loss that could not be stabilised by Day 14 and Day 21. This development of health complication in ~15% of STZ diabetic rats was an unexpected increase compared with Chapter 2 in which only one STZ diabetic rat (6%) presented with excessive weight loss at Day 17. A possible cause of these health complication is the weight of animals at the time of STZ administration which occurred due to an increase in the amount of baseline testing conducted to improve the burrowing measurements. The previous belief at University of Hertfordshire was that administering rats with STZ at a higher bodyweight was preferential for the rats wellbeing and weight stabilisation. However, findings from other research groups indicates that younger, lighter weight rats have improved survivability particularly those at <400g (Wang-Fischer & Garyantes, 2018). Therefore, administering STZ to rats at an average weight of ~430g in the present study may have contributed to this increased bodyweight loss and future studies should aim to use younger and therefore lighter animals to improve animal welfare.

An additional finding in this study was the STZ diabetic rats BGLs were correlated with their bodyweight loss, such that higher BGLs were associated with increased weight loss (Figure 3.10). Whilst bodyweight changes are used to monitor the health and welfare of STZ diabetic rats, BGL is used to confirm hyperglycaemia and the diabetic phenotype. Both developments are regularly reported together in STZ diabetic rat studies and are often considered to be associated (Furman, 2021; Lee et al., 2008; Mitani et al., 2008; Wang-Fischer & Garyantes, 2018). However, correlational analysis of BGLs and bodyweight loss is not usually conducted. This study therefore provided the first evidence of a correlation between BGL changes and bodyweight loss in STZ type-1 diabetic rats (Figure 3.10). This negative correlation indicated that an increase in BGL is correlated with greater bodyweight loss. Although correlation does not signify causation, this finding could be used as an

indication that slightly reducing the BGL of STZ diabetic rats that have excessive weight loss could provide a possible solution to limiting their bodyweight loss and improving their welfare. This technique is currently applied by some research groups using the STZ diabetic rat model by administering a slow-release insulin tablet to STZ diabetic rats (Ghasemi & Jeddi, 2023). Rescue insulin for STZ mice that exhibit >10% bodyweight loss has been successfully used and the same principle can be applied to STZ rats used in future studies to improve their welfare and reduce animal loss (Nørgaard et al., 2018). Using BGLs and bodyweight measurements to apply a treatment of rescue insulin when needed would stop excess animal exclusions from these studies and improve the welfare of these animals.

3.4.9 STZ diabetic rats had increased kidneys and liver mass which correlated with increased blood glucose levels.

An often-reported comorbidity in both humans with diabetes and animal models of diabetes is nephropathy (Luippold et al., 2016). In humans an early structural change that occurs during diabetic nephropathy is renal hypertrophy particularly in the glomerular and tubular cells (Habib, 2018). More recently another comorbidity of type-1 diabetes that is gradually being explored is alteration in liver function including haptic steatosis, a build-up of fat in liver cells that may contribute to the development of non-alcoholic fatty liver disease (Regnell & Lernmark, 2011). The presence of this non-alcoholic fatty liver disease is believed to be larger in type-1 diabetes than previously thought and is also associated with chronic kidney disease in these patients (de Vries et al., 2022; Targher et al., 2014). Based on this research, the weight of kidney and livers tissue were taken at the end of the study to understand if these changes were present in this STZ type-1 diabetes rat model. The wet tissue weights of both kidneys and livers were increased in STZ diabetic rats compared with control rats despite STZ diabetic rats weighing significantly less than control rats (Figure 3.12). Additionally, the difference became even greater when these weights were expressed as the relative weight of the whole animal. This finding has been demonstrated previously that STZ rat kidney and liver weights are increased including that proportionally this increase is higher in kidneys compared to the liver (Lee et al., 2008; Zafar & Naeem-ul-Hassan Naqvi, 2010). The present study also provides some of the first evidence that these changes, when expressed as a relative organ weight, are correlated with BLGs (Figure 3.13) supporting the evidence that there is a link between hyperglycaemia and organ hypertrophy in the STZ type-1 model (Zafar & Naeem-ul-Hassan Naqvi, 2010).

3.4.10 Limitations of this study and improvements for future studies.

One of the main findings from this study is that burrowing deficits were induced and maintained across an extended period (Day 18-46) in STZ diabetic rats. Although during this period, the amount of control rats burrowing also trended towards being decreased. A potential cause for this could be that the repeated assessment of burrowing which although an ethological behaviour could lose its novelty and therefore future burrowing studies could look to reduce the frequency of burrowing testing to mitigate this problem. Additionally, this study found that burrowing deficits in the STZ diabetic rat models were not rescued by analgesic treatment with pregabalin. However, alternative first line neuropathic pain treatment such as tricyclic antidepressant have not been examined and could potentially demonstrate different results to pregabalin which should be explored (Finnerup et al., 2015). Alongside these alternative ways to improve STZ diabetic rat's wellbeing should be explored for its impact on burrowing deficits. In particular insulin administration to regulate

hyperglycaemia would determine if hyperglycaemia a predominant factor in STZ induced burrowing deficits. Together with this, burrowing should be assessed in other non-surgical models of neuropathic pain that include other comorbidities such as the oxaliplatin induced model of chemotherapy induced peripheral neuropathy (Ling et al., 2008). This would help determine if the lack of pregabalin efficacy on burrowing in diabetic disease models is caused by alterations in wellbeing outside of neuropathic pain or if there is another reason that the results are inconsistent with surgically induced mononeuropathy pain models burrowing deficits. Future studies should also look at assessing the locomotor activity of STZ diabetic rats to ensure the changes in burrowing are not caused by limitations to their movement (Chapter 4) (Andrews et al., 2011, 2012; Gould et al., 2016).

Measuring von Frey paw withdrawal thresholds is not an ideal method for determining neuropathic pain preclinically as evidenced by its general failure to translate any recent successful analgesics (Fisher et al., 2021). However, until a completely objective and translation endpoint for neuropathic pain is developed, its utility could be improved particularly by moving away from manual von Frey measurements which is limited by both subjectivity of the observer and the logarithmic nature of the start von Frey monofilaments used. This limitation was particularly evident in this study when using an expanded range of monofilaments.

A further improvement of the STZ diabetic rat model used in this study that should be implemented in future STZ research is the identification of a correlation between bodyweight loss and BGL measurements. As STZ diabetic rat's bodyweight are checked on a regular basis for health and welfare monitoring, animals approaching 10% bodyweight loss could be administered a low dose of insulin to attempt to mitigate the bodyweight loss whilst still maintaining a type-1 diabetic phenotype. Doing so would both improve the welfare of the individual animal by limiting cases of extreme and chronic hyperglycaemia and reduce the loss of animals to health changes, improving the statistical power of the results. Additionally, STZ diabetic rats should be dosed at an early age and therefore lighter bodyweight in the hope that this will reduce bodyweight loss and increase animal survivability. This would be a further improvement in the welfare of the model when combined with the reduced STZ dose introduced in Chapter 2.

3.5 Conclusions

In conclusion, this study identified that STZ diabetic rats develop an extended burrowing deficit beginning from Day 18 onwards. These burrowing deficits occurred much later than the development of mechanical allodynia measured through the classical evoked measurements of von Frey paw withdrawal threshold which occurred as early as Day 7. Decreased burrowing levels and paw withdrawal thresholds in STZ diabetic rats were not correlated at any timepoint during the study. Additionally, whilst the first line analgesic pregabalin at 10 and 30mg/kg fully reversed the changes in von Frey paw withdrawal threshold, burrowing deficits were not reversed by any dose of pregabalin. This provides clear evidence that burrowing deficits and decreased paw withdrawal thresholds measure different changes in STZ diabetic rat's behaviour, with burrowing a likely measure of overall animal wellbeing. Nevertheless, burrowing may be a useful objective secondary endpoint in preclinical neuropathic pain studies as a measure of the animal's wellbeing that reflects the impacts on patient's daily activities. This study also demonstrated that a high dose of 30mg/kg pregabalin increased von Frey paw withdrawal thresholds in control rats above baseline levels. This

is likely through its somnolent effects and therefore 10mg/kg pregabalin should be used in future studies as an analgesic reference positive control. Welfare of STZ diabetic rats should be improved by administering STZ to rats with a lower bodyweight while rats that lose excessive bodyweight (approaching 15%) could be rescued using insulin administration to reduce hyperglycaemia. In conclusion, using burrowing as a secondary endpoint in neuropathic pain studies to measure overall wellbeing would help to identify analgesics with improved efficacy over current analgesic treatments.

Chapter 4: Locomotor activity and gait assessment in the 55mg/kg STZ type-1 diabetes rat model

4.1 Introduction

For patients suffering with neuropathic pain, treatment options are often limited, with extensive side effects, limited efficacy and high numbers needed to treat (NNT) (Colloca et al., 2017; Finnerup et al., 2015). Despite extensive research into novel analgesic treatments very few have been approved within the last 20 years (Gammaitoni et al., 2003; McGivern, 2007; Raskin et al., 2005; Vinik et al., 2016). First line treatments remain primarily as drugs that were originally approved as antiepileptics (pregabalin, gabapentin) and antidepressants (amitriptyline, duloxetine) (Finnerup et al., 2015). One area that is believed to be contributing to a lack of new drug development is a mismatch between clinical and preclinical neuropathic pain endpoints (Deuis et al., 2017; Fisher et al., 2021; Tappe-Theodor et al., 2019). Neuropathic pain endpoints used in preclinical screening studies have focused on evoked subjective endpoints, whilst clinical trials mainly use questionnaire and verbal rating scale based endpoints (Figure 1.3) (Deuis et al., 2017; Fisher et al., 2021; Tappe-Theodor et al., 2019). Therefore, a focus has been placed on developing novel preclinical screening endpoints that are less subjective, non-evoked and consider the emotional and cortical processing components of neuropathic pain (Fisher et al., 2021). Changes in gait and locomotor activity are two such endpoints that are being examined in preclinical screening studies to identify if measuring these may better reflect the impact of neuropathic pain development (Fisher et al., 2021; Fonseca-Rodrigues et al., 2021; Vieira et al., 2020).

Locomotor activity and gait are similar preclinical endpoints as they both assess an animal's ability to ambulate or walk (Fisher et al., 2021; Fonseca-Rodrigues et al., 2021; Vieira et al., 2020). Locomotor activity typically focusses on the amount of time spent moving, the speed of that movement and how long animal spends moving (Fonseca-Rodrigues et al., 2021; Medeiros et al., 2021; Mogil et al., 2010; Urban et al., 2011). Assessing an animal's gait usually involves looking at changes in the animal's stride such as swing speed, limb positioning and foot/paw pressure among other characteristics of their movement (Lakes & Allen, 2016). The assessment of locomotor activity has demonstrated mixed results, often depending on the type of neuropathic pain model and the way that locomotor activity is quantified. In the chronic constructive injury (CCI) model locomotor changes are often assessed using open field testing (OFT) rather than through monitoring home cage locomotion (Fonseca-Rodrigues et al., 2021). These studies often report limited changes in locomotor activity in CCI models, suggesting that locomotor activity is not a useful measure of neuropathic pain (Medeiros et al., 2021; Mogil et al., 2010). Although, studies of CCI mice in a home cage type environment, have suggested that these animals spend less time moving and more time stationary (Urban et al., 2011). Locomotor activity has also been used as an objective measure of pain in osteoarthritic models of pain (Alsalem et al., 2020).

In streptozotocin (STZ) diabetic rat studies, locomotor activity assessments have also primarily been through using OFT systems or similar apparatus. These studies have demonstrated a reduction in measures of locomotor activity in STZ diabetic rats, though typically these changes are demonstrated at >4 weeks after STZ administration (Bădescu et al., 2016; Doria et al., 2016; Kou et al., 2014). One study has assessed locomotor activity before this point and identified a reduction in

paw withdrawal thresholds at Day 14 after STZ administration, whilst a reduction in locomotor activity only developed at Day 28 (Kou et al., 2014). This may suggest once again that changes in non-evoked neuropathic pain endpoints develop later than evoked measures of neuropathic pain as was identified in Chapter 3. Additionally, if changes in locomotor activity only develop after 4 weeks in STZ diabetic rats it would support that the deficits in burrowing at Day 18 and Day 22 in Chapter 3 (Figure 3.6) were not caused by impaired locomotor activity. Therefore, this study will assess how changes in locomotor activity develop across the first 3 weeks after STZ administration as there is currently limited evidence to characterise these changes (Kou et al., 2014).

Changes in gait are a common occurrence in as many as half of diabetic neuropathic pain patients (Alam et al., 2017; Alle et al., 2008). Changes in these patient's gait can lead to an increased risk of falls and subsequent injuries (Alam et al., 2017; Alle et al., 2008). Therefore, assessing changes in gait as a neuropathic pain endpoint in preclinical diabetic models would identify treatments that improve not only neuropathic pain but also reduce the risk of further injury to human patients. In rodent models of neuropathic pain, gait is considered as a potential objective translational non-evoked endpoint (Fisher et al., 2021). STZ diabetic rats gait has been assessed previously using both manual ink or paint based methods as well as using automated gait analysis systems (Al Deeb et al., 2000; Karatan et al., 2019; Vieira et al., 2020). Some of the first investigations in STZ diabetic rats gait identified no changes in gait parameters when using manual ink staining at 3 weeks after STZ administration compared to control rats (Al Deeb et al., 2000). However, others have identified changes in STZ diabetic rats gait including Karatan et al. (2019) who demonstrated increased footprint length and sciatic nerve function tests using a manual paw printing technique (Karatan et al., 2019). More recently Vieira et al. (2020) used the automated 'CatWalk' gait analysis system and demonstrated changes in stride length of STZ diabetic rats at Day 28 (Vieira et al., 2020). In a human study of gait in diabetic neuropathy patients with pain, a wearable gait measuring device identified a greater variance in step length and velocity that was associated with an increase in falls (Lalli et al., 2013). This highlights that there is potential for changes in preclinical measures of gait to translate into human studies assessing similar endpoints.

Though identifying novel endpoints to measure neuropathic pain preclinically is an important step, in the short term any improvements that can be made to how classical evoked endpoints are assessment will offer an immediate 3Rs benefits for animal welfare. This may include steps such as using electronic von Frey devices (as suggested in Chapter 3) or through improving the welfare and environment whilst conducting these von Frey tests (NC3Rs, n.d.). The current practice used in preclinical pain studies to assess evoked paw withdrawal thresholds is conducted with animals separated from their home cage partners for the duration of the test. Research has shown that even short-term social isolation can lead to an increase in depressive-like behaviours in rodents, that could be avoided by keeping animals in their home cage pairs during von Frey testing (Takatsu-Coleman et al., 2013). Consequently, von Frey testing rodents in their home cage pairs would avoid the short-term isolation and improve the accuracy of the primary evoked endpoint assessment measurements.

4.1.1 Aims and hypotheses.

The primary aim of this study was to establish if locomotor activity and/or walking gait are altered in a 55mg/kg STZ diabetic rat model over 18 days and whether one or both of these measures might present an early objective neuropathic pain endpoint.

A secondary aim of this student was to determine whether pair housing ('pair') versus single housing ('solo' current practice) of rodents during von Frey testing could achieve the same primary evoked endpoint assessment whilst improving animal welfare by avoiding short term isolation.

The development of phenotypical diabetes changes in hyperglycaemia, polydipsia, polyphagia, bodyweight of the STZ rats was monitored throughout the study to further validate the lower 55mg/kg STZ model.

4.1.2 Abbreviations.

STZ – streptozotocin, CCI – chronic constrictive injury, SEM – standard error of the mean, BGL – blood glucose level, i.p. – intraperitoneal, OFT – open field testing.

4.2 Methods

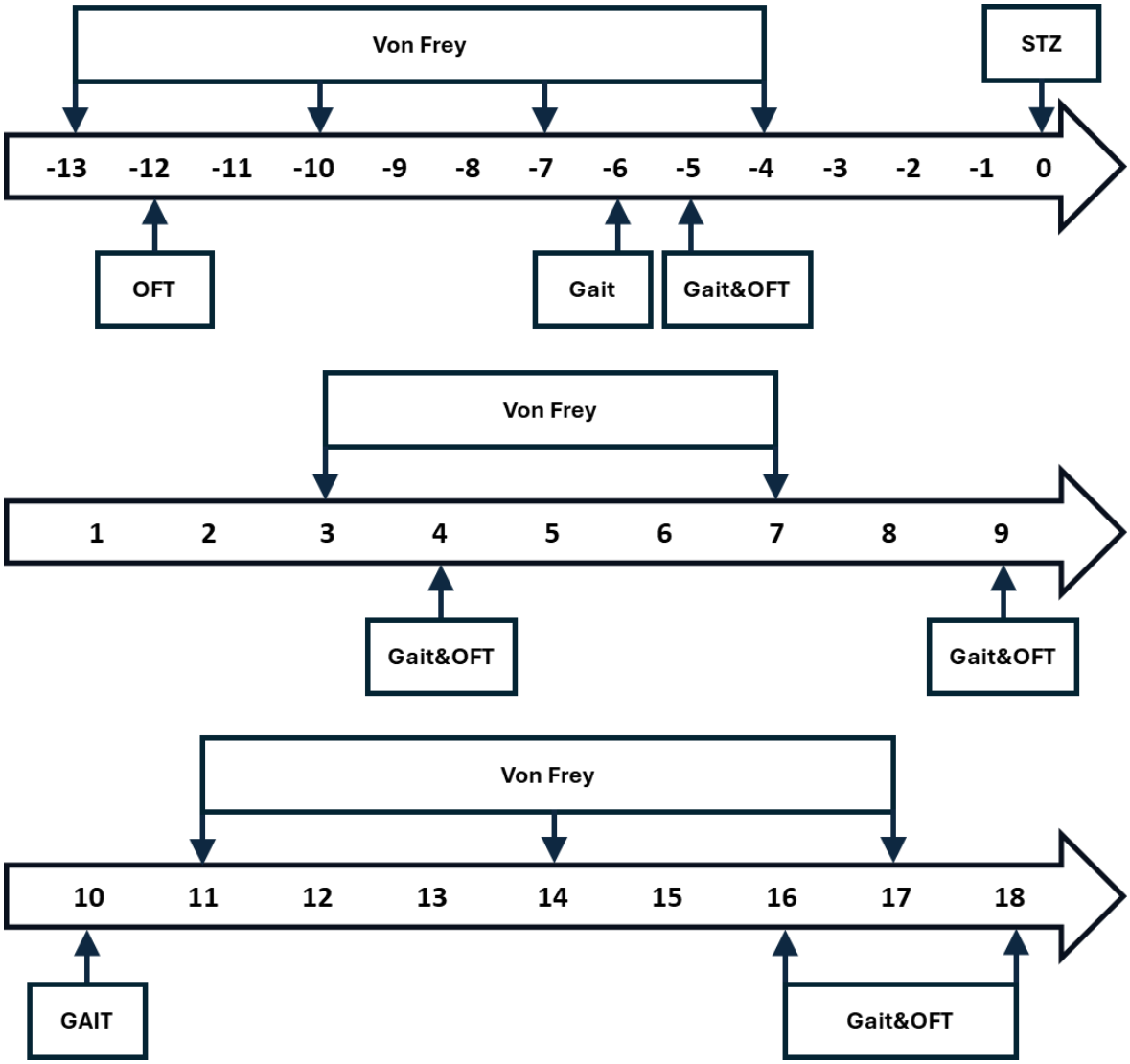

Figure 4.1) Timeline of the study depicting the days before and after 55mg/kg STZ intraperitoneal (i.p.) administration on Day 0. The days on which von Frey paw withdrawal threshold, gait and locomotor activity (OFT) measurements were taken are also denoted.

4.2.1 Ethics statement.

All research procedures/experiments were performed in accordance with Animals Scientific Procedures Act 1986 & European Directive 2010/63/EU. All studies performed were approved by the University of Hertfordshire Animal Welfare and Ethics Review Body and comply with the home office guidelines and codes of conduct. All work was authorised under University of Hertfordshire home office establishment licence and project licence titled: Diabetes mechanisms and treatments.

4.2.2 Animals and induction of STZ.

14 Male Wistar Han rats (300-325g at arrival, 325-390g at time of STZ administration) supplied by Envigo, UK were housed in pairs from arrival. At Day 0 (Figure 4.1) rats were administered either 55mg/kg streptozotocin (n=10) or 20mM citrate buffer (n=4) intraperitoneal (i.p.) administration at a dose volume of 10ml/kg. STZ (Sigma- Aldrich, S0130) was prepared as described in Chapter 2. Either STZ at 55mg/kg or citrate buffer (control) were administered once to rats via single i.p. injection using a new 23G needle. Rats were placed back in their home cage and monitored closely for 1 hour for signs of distress or discomfort. Additionally, banana porridge (Cow&Gate) and 2% sucrose solution were provided for 48 hours post STZ/control administration to encourage feeding and maintain blood glucose levels.

4.2.3 Environmental conditions.

Rats were pair-housed in Tecniplast 2000P cages and a 12:12 hr light-dark cycle (lights on at 07:00) was maintained throughout the study. Housing temperature was maintained at 21±2°C and 55±15% relative humidity. Food (5LF2 10% protein LabDiet) and drinking water were provided ad libitum except during von Frey, locomotor activity and gait behavioural testing. Water was provided in two 1L bottles per cage. For 48 hours after STZ/control administration (Day 0,1), 2% sucrose solution was provided in one of the 1L bottles to avoid hypoglycaemia caused by STZ administration (Ghasemi & Jeddi, 2023). Water intake measurements were recorded from 1 week before STZ/control administration and as required until the end of the study. Food and water intake was calculated per cage as the change in weight (g) of the food hopper and both water bottles recorded at approximately 9am each day.

4.2.4 Animal welfare.

Blood glucose level (BGL) was recorded 1 day prior to (Day -1) at 7 days after (Day 7) STZ/control administration to confirm onset of hyperglycaemia and at euthanasia (Day 21-32 due to provision of tissue for other projects) to monitor progression and maintenance of hyperglycaemia. Microsamples of blood were taken through tail tip vein puncture using a lancet (Valuemed, UK) and BGL was measured using a GlucoRx Nexus blood glucose meter calibrated before use. An inclusion criterion of >16mmol/dL BGL at all timepoints after STZ administration was used to exclude rats that did not develop hyperglycaemia.

Daily bodyweight measurements were taken at regular intervals from Day -13 to Day 0 to monitor rats weight gain and progression. After STZ/control administration on Day 0, daily bodyweight measurements were taken to monitor animal welfare. Rats reaching 15% bodyweight loss compared with the Day 0 baseline weight were monitored closely. This included weighing twice daily, provision of additional nourishment in the form of seed, grains and banana porridge where appropriate and assessment by animal care staff and or veterinarians if needed. Any rats not stabilising or gaining weight within 48 hours were humanly euthanised. All rats were checked daily by trained animal care staff to monitor welfare.

4.2.5 Mechanical allodynia (paired and solo von Frey assessment).

Von Frey paw withdrawal threshold was measured using the same protocol detailed in Chapter 2 which included using the same 0.4, 0.6, 1, 1.4, 2, 4, 6, 8, 10, 15, 26; g monofilament range (not the increased 0.16-60g range using in Chapter 3). Paw withdrawal threshold was evaluated twice per week for 2 weeks before STZ/control administration (Day -13,-10,-7,-4). Day 3, after STZ/control administration, paw withdrawal thresholds were assessed up to twice per week until the end of the study to monitor development of mechanical allodynia (Days 3,7,11,14,17). At all timepoints von Frey paw withdrawal threshold measurements were taken with rats housed either on their own with an opaque divider separating all rats (solo) or together with their home cage partner (paired) (Figure 4.2). Both solo and paired von Frey measurements were taken on the same day with rats being returned to their home cage for at least 30 minutes before being tested again. The order that solo and paired von Frey measurements were taken at each timepoint alternated to ensure that there was no bias from repeated testing affecting the results.

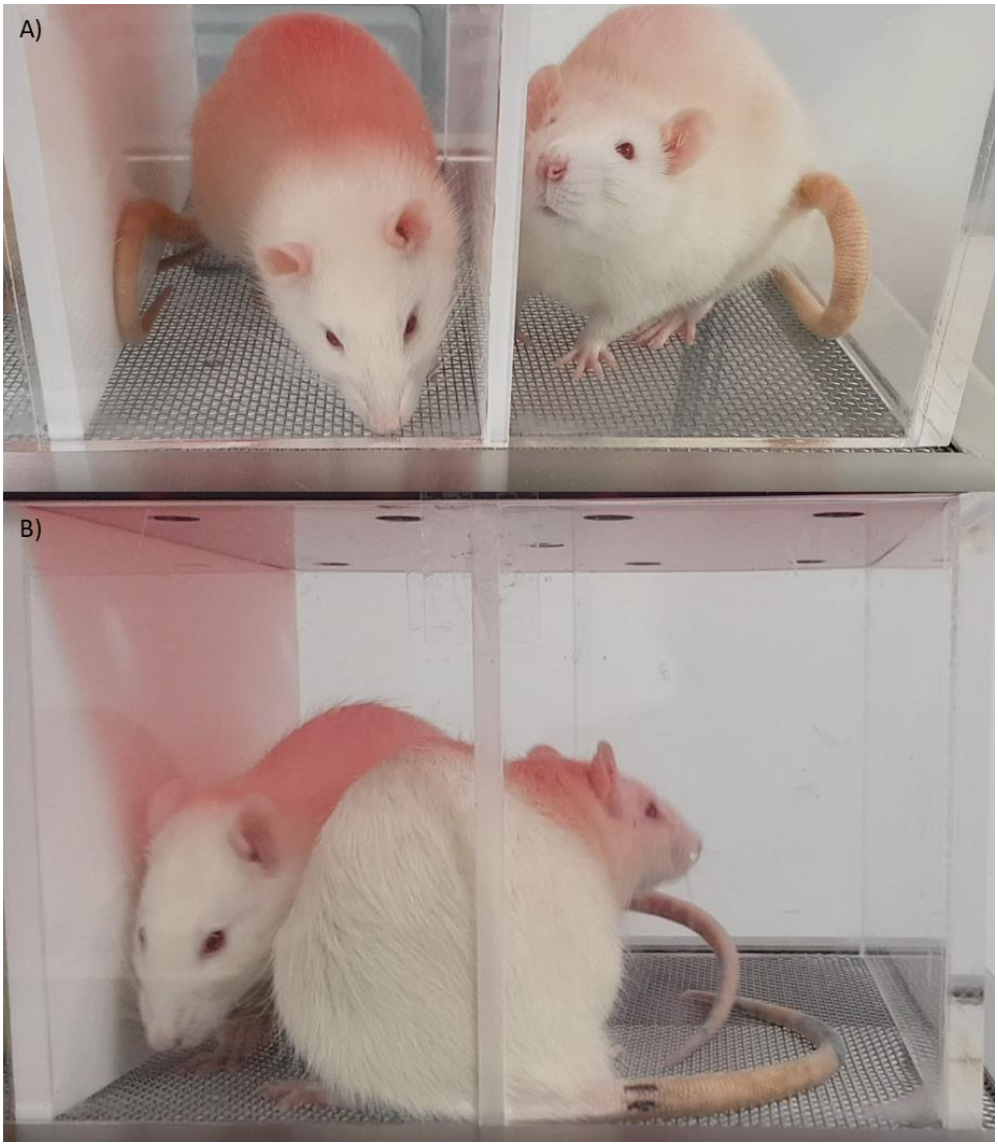

Figure 4.2) A) Single rat von Frey assessment method conducted in the standard fashion with rats separated by an opaque divider (solo). B) Paired von Frey assessment of home caged pairs of rats allowed to remain together through assessment of von Frey paw withdrawal thresholds on both rats with the divider removed and free socialisation allowed (paired).

4.2.6 Gait.

Changes in STZ diabetic and control rats stride length and stride width were assessed by application of a non-toxic paint to the hind paws of rats and allowing them to freely walk along an enclosed walkway (420mm x 100mm) (Figure 4.3). Rats were lightly restrained and paint applied to the hind paws using a soft paintbrush. Rats were then placed at the start of the walkway and allowed to walk freely into a dark enclosed area. Each session included two repeats of the rats walking along the apparatus and the results from each successful run were averaged to give a final value. Measurements were taken of the left and right side stride length as well as the width between the strides to measure changes in the rats gait (Figure 4.3B). Rats were first trained to walk along the apparatus without paint being applied on Day -12 and encouraged with seeds placed in the box at the end of the walkway. Two baseline measurements of gait were taken on Day -6 and Day -5 with paint applied on both occasions. Following STZ/control administration gait measurements were taken up to twice a week on Days 4, 9, 10, 16 and 18 to monitor development of any changes in gait measurements.

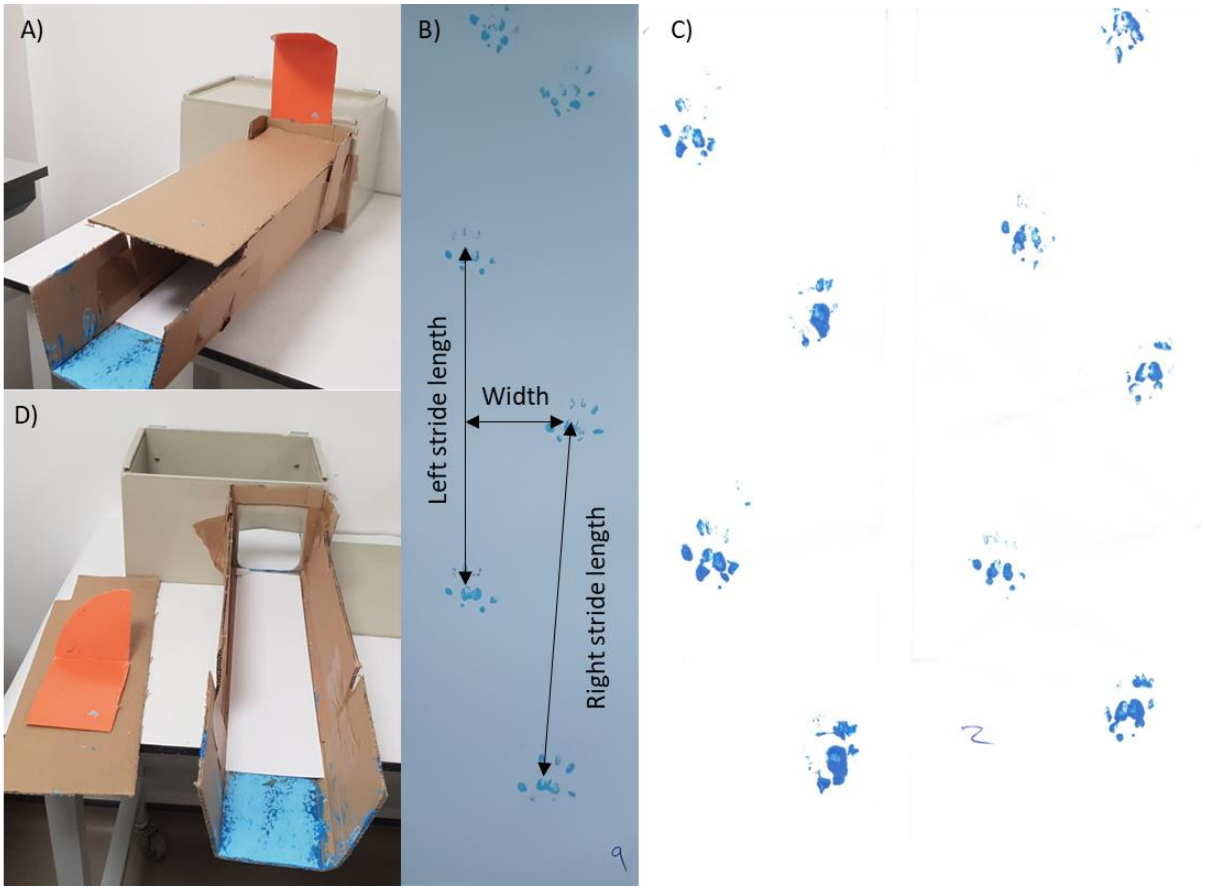

Figure 4.3) A) Gait assessment apparatus demonstrating the covered walkway as it was used during testing. Rats were placed into the tunnel opening (bottom left) and allowed to freely walk into a dark chamber along a walkway lined with white paper. B) Representative paw print pattern left behind by a rat freely walking along the walkway and the width, left and right stride length measurements taken. C) Representative smudged or incomplete paw print pattern. D) Gait assessment apparatus with the tunnel and chamber lids removed to demonstrate the path along which rats freely walked. The end of the tunnel was covered once a rat had entered the final chamber to stop rats from returning along the walkway.

4.2.7 Locomotor activity.

Locomotor activity was measured using an open field testing (OFT) apparatus to assess STZ diabetic and control rat movement during the study. Rats were placed in a 400mm x 400mm opaque underlit box with a high-quality camera placed overhead and recorded for 30 minutes at each timepoint (Figure 4.4). Total distance (cm), average velocity (cm/s) and percentage time spent moving were all measured automatically using EthoVision XT software (v15.0 Noldus, NL). EthoVision software tracked the rat's movement across the 30 minutes session using a centre point tracking on the rat's body. Two baseline recording sessions were taken on Day -12 and Day -5. After STZ/control administration locomotor activity measurements were taken up to twice a week on Days 4, 9, 10, 16 and 18 to monitor the development of any changes in locomotor activity measurements.

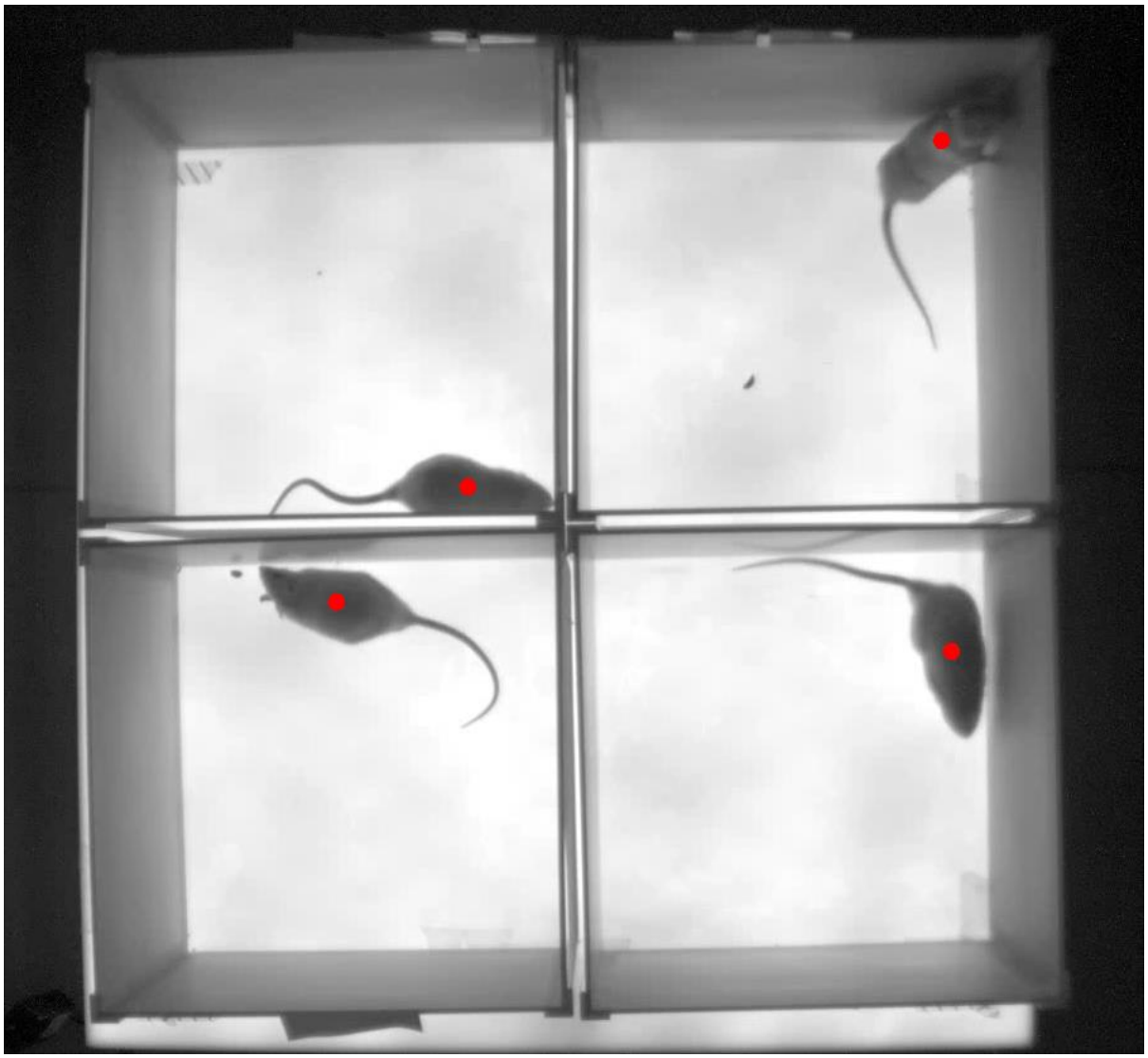

Figure 4.4) Locomotor activity measurements taken in a 400mm x 400mm chamber with EthoVision XT automatic measurements of locomotor activity.

4.2.8 Grouping, randomisation, blinding and exclusion or inclusion criteria.

The STZ and Control grouping was randomised using the Latin square technique based on von Frey baseline data and bodyweight, to ensure an equal spread of baseline paw withdrawal thresholds and bodyweights. All rats were assigned in pairs with their cage partner to the same group to ensure all cages were either STZ/STZ or control/control cages. All rats remained with their original cage partner from beginning of the study to avoid distress or aggressive behaviour from rehousing.

Exclusion criteria were a >50% change from baseline for von Frey measurements of mechanical allodynia. Also a BGL of at least 16mmol/L was set as the threshold for development of hyperglycaemia and diabetic phenotype. All rats BGLs increased after STZ administration reaching the >16mmol/L BGL criteria (100%). No STZ diabetic rats encountered health issues during the study. All STZ diabetic rats developed a >50% reduction in paw withdrawal threshold. One STZ diabetic rat was removed prematurely from the first baseline timepoint (Day -12) of locomotor activity testing due to jumping out of the recording apparatus. Their second baseline timepoint (Day -5) was included in the data analysis as a plexiglass lid was fashioned that safely contained the rats without impacting camera performance. All behavioural testing was conducted blind to the animal status. A maximum limit of 20% bodyweight loss was in place to exclude any rats that developed excessive weight loss.

4.2.9 Statistics.

To compare the results at each timepoints (Days) between control and STZ rats two-way mixed model analysis of variance (ANOVA) was used with Šídák's post hoc test to compare between control and STZ diabetic rats (BGL, von Frey, bodyweight, daily food intake, daily water intake, gait, locomotor activity). For measures with additional comparisons within each group comparing between Days Dunnett's post hoc test was used (BGL, average von Frey, gait, locomotor activity, total liquid consumption) (Prism 10.2; GraphPad, San Diego, CA USA). A p value of <0.05 was considered statistically significant for all data. All data is reported as mean ± standard error of the mean (SEM) except for correlation data.

4.3 Results

4.3.1 STZ (55mg/kg) administration caused hyperglycaemia and a diabetic phenotype.

Administration of 55mg/kg STZ increased the blood glucose level (BGL) of the rats above the 16mmol/L threshold in all rats at all timepoints measured during the study. At baseline there was no difference in BGLs between STZ and control rats with both groups average BGL at 5.1mmol/L [Time: $F(2,36) = 88.34$, $p<0.001$], [Treatment: $F(1,36) = 341.1$, $p<0.001$], [Interaction: $F(2,36) = 85.69$, $p<0.001$] (Figure 4.5). For control rats BGLs remained stable across the entire study remaining at <6mmol/L. By Day 7 after administration all STZ rats had a BGL greater than the 16mmol/L threshold value with BGL increase over fivefold to 29.8mmol/L (Figure 4.5). This increased BGL in STZ rats was maintained across the study including the Day 21-32 timepoint (30.4mmol/L). All rats administered STZ developed increased BGL above the 16mmol/L hyperglycaemia cutoff threshold. Therefore this demonstrates that all STZ rats had developed a diabetic phenotype.

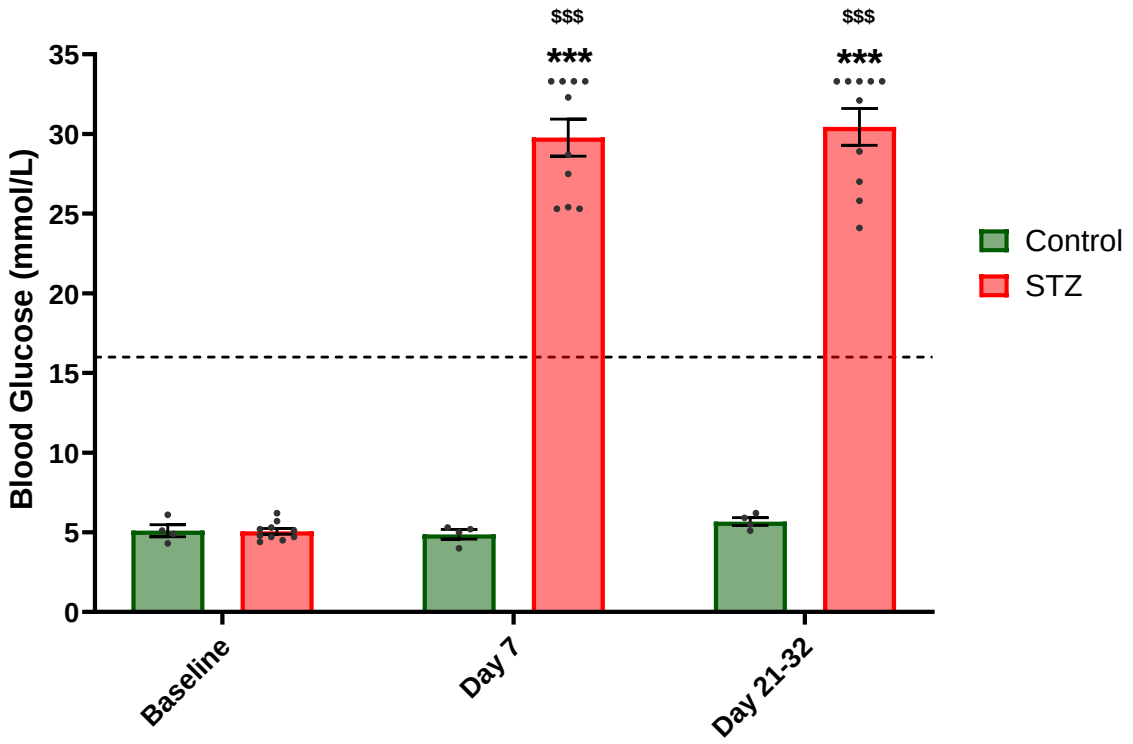

Figure 4.5) Blood glucose levels increased and maintained a steady level of hyperglycaemia between Day 7 and Day 21-32 in rats after STZ administration but not control. Blood glucose levels were measured at baseline (Day -1), Day 7 (7 days after STZ/control administration) and Day 21-32 (taken at euthanasia). Dashed line indicates 16mmol/L cutoff level for confirmation of hyperglycaemia. ***p<0.001 vs baseline, $$$$p$<0.001 vs control. All data is reported as mean ± SEM, n=4 control, n=10 STZ.

4.3.2 STZ diabetic rats gained less bodyweight than control rats.

The health and welfare of STZ diabetic and control rats were monitored throughout the study in several ways, including bodyweight measurements. Due to the small number of control rats, randomisation of control and STZ diabetic rat assignment caused a slight but not significant difference in the control and STZ diabetic rat bodyweights prior to STZ/control administration (Figure 4.6A). At Day -13 control rats weighed an average of 315.8g compared with 324.3g for STZ diabetic rats with this slight difference remaining at Day 0 when control rats weighed 346.1g whilst STZ diabetic rats weighed 363.1g [Time: $F(29,348) = 33.93$, $p<0.001$], [Treatment: $F(1,12) = 2.140$, $p=0.17$], [Interaction: $F(29,348) = 22.49$, $p<0.001$] (Figure 4.6A). STZ diabetic rats initially lost ~20g across the first 3 days after STZ administration reaching 341.3g. STZ diabetic rats bodyweight plateaued at this level for the remainder of the study staying between 340-350g. Control rats continually gained bodyweight across the study gaining 10g in the first 3 days whilst STZ diabetic rats lost 20g. Control rats proceeded to gain ~15g per week across the remainder of the study. Likely due to the differences in starting weight, control rats bodyweight only became significantly higher than STZ diabetic rats from Day 17 onwards (Figure 4.6A). The differences between STZ diabetic and control rats bodyweights became more obvious when expressed as the percentage change from Day 0 bodyweight. When assessed as percentage change, STZ diabetic rats bodyweight was significantly lower than control rats from as early as Day 2 onwards [Time: $F(21,252) = 9.383$, $p<0.001$], [Treatment: $F(1,12) = 57.58$, $p<0.001$], [Interaction: $F(21,252) = 25.04$, $p<0.001$] (Figure 4.6B). STZ diabetic rats lost on average -6% bodyweight by Day 3, which remained at between -5.7% and -3.7%

until Day 17. At Day 17 STZ diabetic rats bodyweight declined slightly further reaching -6.4% by Day 21. Control rats by comparison gained 4.4% bodyweight across the first week and a total of 11.5% increase to bodyweight by Day 21. This demonstrates that STZ diabetic rats initially lost 6% bodyweight which remained relatively stable for the rest of the 21 days after STZ administration.

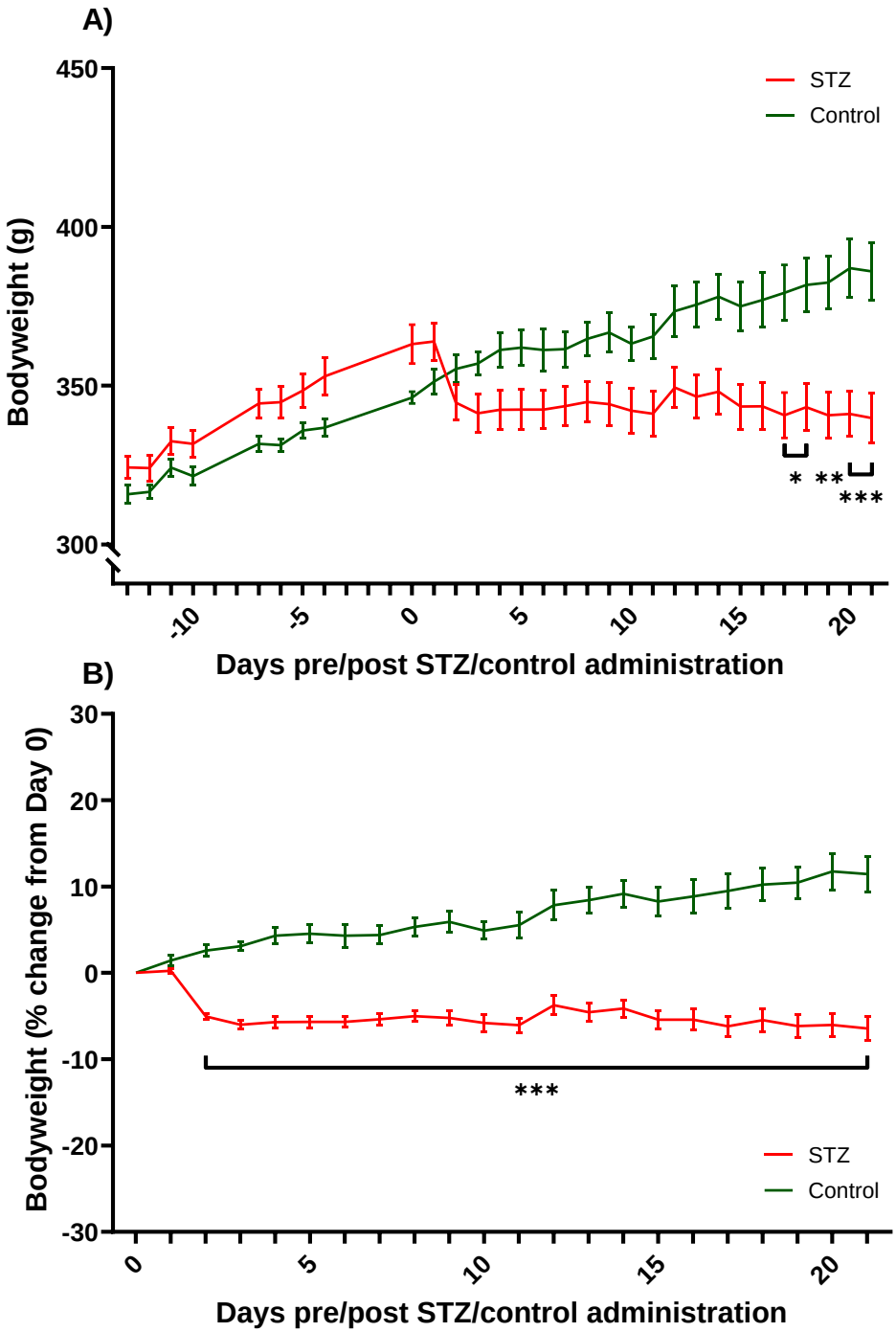

Figure 4.6) STZ diabetic rats bodyweight initial decreased followed by a plateau whilst control treated rats continued to gain bodyweight throughout the study. The average bodyweight of STZ diabetic and control rats across the study expressed as the raw bodyweight (g) (A) and the percentage change in bodyweight from the pre STZ/control administration weight on Day 0 (B). *p<0.05, **p<0.01, ***p<0.001 vs control. All data is reported as mean ± SEM, n=4 control, n=10 STZ.

4.3.3 STZ diabetic rats developed polyphagia and polydipsia.

As well as hyperglycaemia, other diabetic phenotypes include polyphagia and polydipsia both of which developed in the STZ diabetic rats. In this STZ type-1 model of diabetes, STZ diabetic rats food intake gradually increased across the study from ~40g/cage/day to over double this at 86g/cage/day by Day 21 [Time: $F(33,165) = 19.41$, $p<0.001$], [Treatment: $F(1,5) = 112.2$, $p<0.001$], [Interaction: $F(33,165) = 8.137$, $p<0.001$] (Figure 4.7A). This increased STZ food consumption became significantly greater than control rats from Day 3 onwards (apart from Day 4 and Day 7). Control rats food intake remained consistent across the study at an average of ~36g/cage/day with small fluctuations. These fluctuations were likely caused by differences in the time of food intake measurements for logistical reasons or due to behavioural testing being conducted. STZ diabetic rats also developed polydipsia demonstrated by a large increase in water intake from Day 1 onwards. Both control and STZ cage water intake remained at ~55g/cage/day across the baseline time period before STZ/control administration [Time: $F(33,165) = 58.15$, $p<0.001$], [Treatment: $F(1,5) = 210.3$, $p<0.001$], [Interaction: $F(33,165) = 59.39$, $p<0.001$] (Figure 4.7B). On Day 0 after STZ/control administration when sucrose was present to avoid hypoglycaemia control animal drinking levels increased rapidly above STZ animals (Figure 4.7B). However, by Day 1 this had reversed and STZ animals consumed more liquid than control animals, which remained this way for the rest of the study. Whilst control animal water consumption returned and remained at ~55g/cage/day after sucrose was removed, STZ animals drinking continued to increase and plateaued at ~400g/cage/day on Day 7. Both polydipsia and polyphagia are symptoms of diabetes and have been demonstrated in this 55mg/kg STZ model. This is further evidence that the STZ rats in this study had developed diabetes.

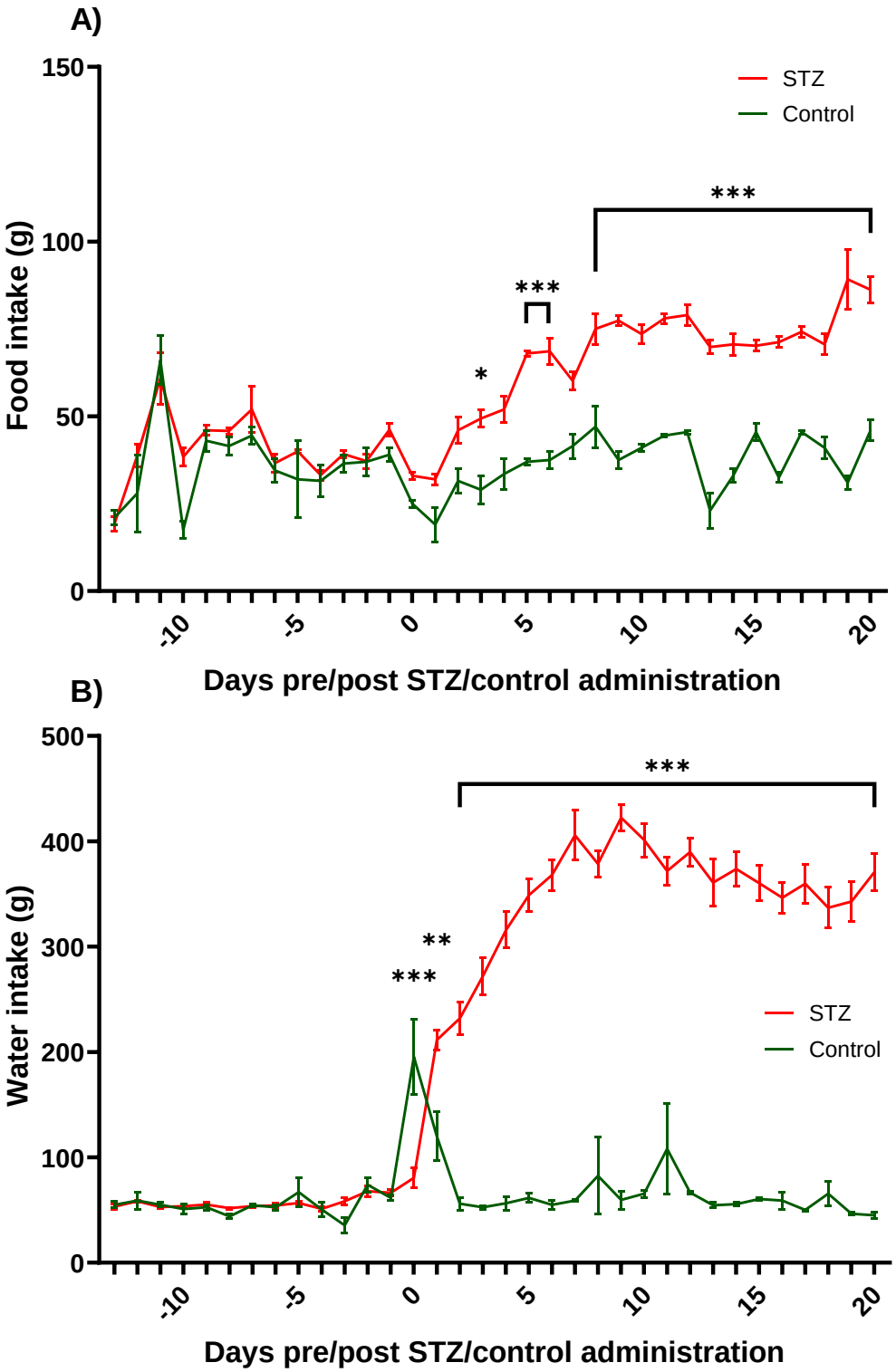

Figure 4.7) STZ diabetic rats developed polyphagia and polydipsia that stabilised after 6 days. The food (A) and water (B) intake per day from each home cage of paired rats. Home cage pairs were either two control rats (control) or two STZ diabetic rats (STZ). *p<0.05, **p<0.01, ***p<0.001 vs control. All data is reported as mean ± SEM, n=2 control cages, n=5 STZ cages.

4.3.4 Mechanical allodynia developed in STZ diabetic rats by Day 3 and was not affected by having a home cage partner present.

To compare the onset of mechanical allodynia in this study and previous ones, rats von Frey paw withdrawal threshold measurements were taken with rats on their own before and after STZ/control administration. STZ diabetic rats paw withdrawal thresholds rapidly decreased dropping below control rats paw withdrawal thresholds by Day 3 reaching 6.5g compared with 18.4g in control rats [Time: $F(8,96) = 13.83$, $p<0.001$], [Treatment: $F(1,12) = 24.13$, $p<0.001$], [Interaction: $F(8,96) = 11.28$, $p<0.001$] (Figure 4.8A). This development of a reduced paw withdrawal threshold in STZ diabetic rats was maintained throughout the study and even decreased further reaching its lowest point at Day 14 of 2g. Control rats generally maintained a stable level of paw withdrawal thresholds at 18-23g. Though at Day 7 this dropped slightly to 12.6g (Figure 4.8A). As has been conducted previously, STZ diabetic and control rats paw withdrawal thresholds were averaged across two timepoints. This demonstrated that compared with baseline (Day -7&-4) and control rats both the Day 3&7 and Day 11&14 timepoints were significantly decreased in STZ diabetic rats [Time: $F(3,36) = 26.7$, $p<0.001$], [Treatment: $F(1,12) = 13.89$, $p=0.003$], [Interaction: $F(3,36) = 19.46$, $p<0.001$] (Figure 4.8B). Assessing the average timepoints also demonstrated no change in control rats paw withdrawal thresholds compared with baseline (Day -7&-4) (Figure 4.8B). Von Frey paw withdrawal thresholds were reduced in STZ diabetic rats by Day 3, a clear sign that mechanical allodynia had developed.

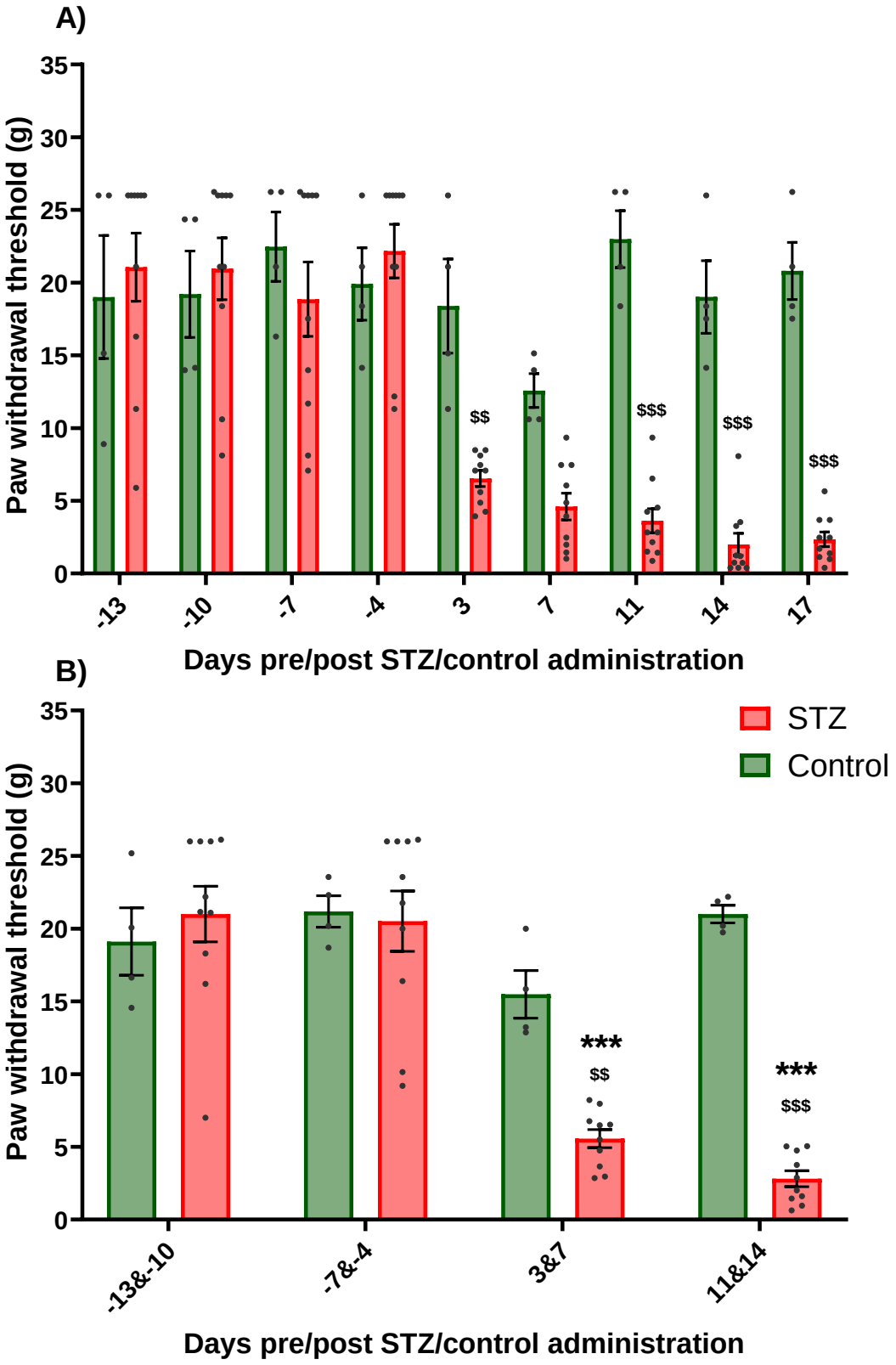

Figure 4.8) Mechanical allodynia developed from Day 3 onwards in STZ diabetic rats on their own. Von Frey paw withdrawal threshold was measured before and after STZ/control administration with rats without their home cage partner present (Figure 4.2A). Responses were assessed as either the von Frey paw withdrawal threshold at each timepoint measured (A) or the response at pairs of averaged timepoints (B). (A) $$$p$<0.01, $$$$p$<0.001 vs control (B) ***p<0.001 vs baseline Day -7&-4, $$$p$<0.01, $$$$p$<0.001 vs control. All data is reported as mean ± SEM, n=4 control, n=10 STZ.

As part of an effort to improve animal welfare and evoked endpoint accuracy, control and STZ diabetic rats von Frey paw withdrawal thresholds were measured with the rats together (paired) with their home cage partner (Figure 4.2). Conducting von Frey testing with paired rats produced no change in either control or STZ diabetic rats when compared between their solo versus paired measurements (Figure 4.9). At Day 3, 11, 14 and 17 both STZ solo and STZ paired measurements were significantly reduced compared with solo control rats [Time: $F(8,192) = 31.60$, $p<0.001$], [Treatment: $F(3,24) = 16.68$, $p<0.001$], [Interaction: $F(24,192) = 7.992$, $p<0.001$] (Figure 4.9). However, at Day 7 there was a slight reduction in solo control rats paw withdrawal thresholds to 12.6g which was no longer significantly higher than either solo or STZ diabetic rats measurements (solo 4.6g, paired 5.5g at this timepoint). However, testing paw withdrawal thresholds in these same control rats when paired with their home cage partnered remained significantly higher than STZ diabetic rats at all timepoints. This indicated a potential improvement over the classical solo von Frey testing method by pairing rats together with their home cage partner. Mechanical allodynia developed in STZ diabetic rats by Day 3 and was not affected by having a home cage partner present, however control rats paw withdrawal thresholds were slightly improved by paired testing.

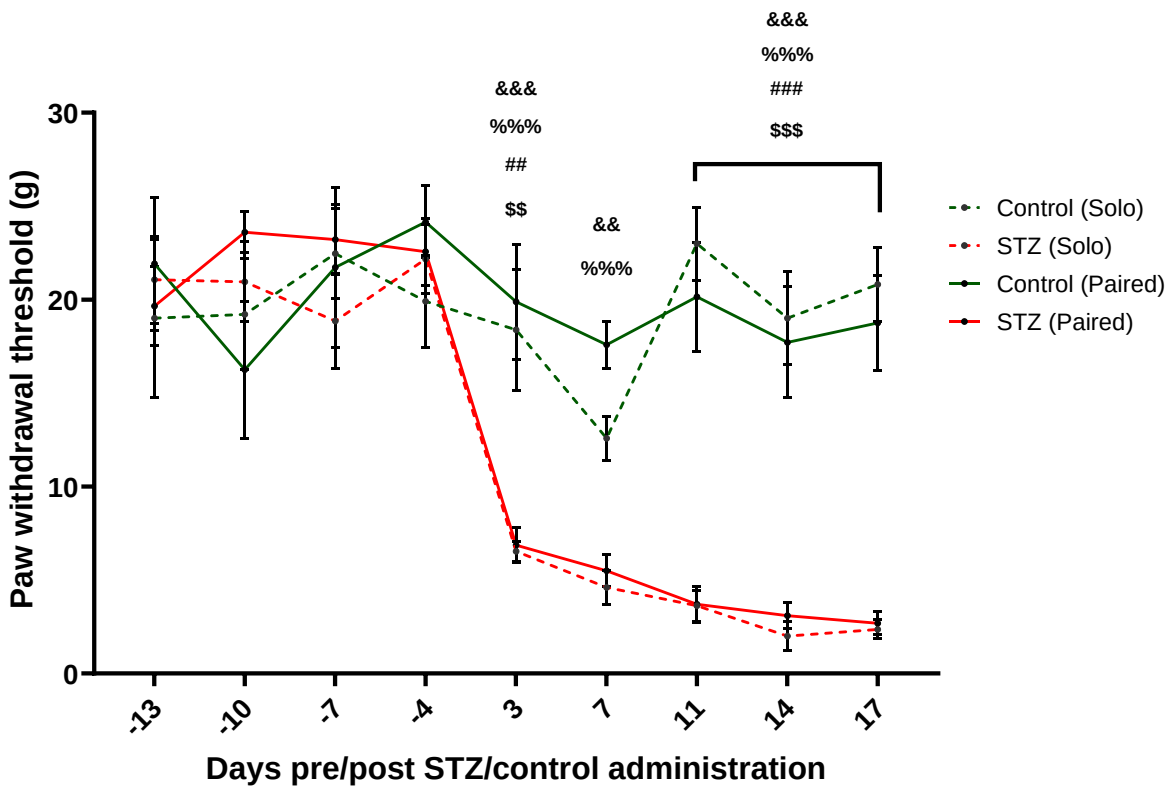

Figure 4.9) Home cage pairs of rats tested together for paw withdrawal thresholds had no effect on STZ diabetic rats but slightly improved control rat responses. Von Frey paw withdrawal thresholds in control and STZ diabetic rats with von Frey testing conducted either with the rat alone (solo) (Figure 4.2A) or with their home cage partner (paired) (Figure 4.2B) during testing. $$$p<0.01$, $$$p<0.001$ control solo vs STZ solo, ##$p<0.01$, ###$p<0.001$ control solo vs STZ paired, %%%$p<0.001$ control paired vs STZ solo, &&$p<0.01$, &&&$p<0.001$ control paired vs STZ paired. $p>0.05$ STZ solo vs STZ paired. $p>0.05$ control solo vs control paired. All data is reported as mean ± SEM, n=4 control, n=10 STZ.

4.3.5 Locomotor activity in STZ diabetic rats remained comparable to control rats.

STZ diabetic and control rat's locomotor activity levels remained equivalent during the first 18 days after STZ/control administration. To monitor the development of any locomotor activity changes in STZ diabetic or control rats, regular measurements were taken using an automatic recording and analysis setup designed for OFT. This identified very few changes in the STZ diabetic rats' locomotion across the full 18 day study. During the 18 days after STZ/control administration there were no significant changes in STZ diabetic or control rats total distance moved. At baseline control rats moved a total distance 2350cm whilst STZ diabetic rats moved 2550cm during the 30-minute measurement period (Figure 4.10A). This increased slightly but not significantly at Day 4 when control rats moved 3080cm and STZ diabetic rats moved 2850cm. From Day 4 onward both STZ diabetic and control rats total distance moved decreased marginally to 2400cm at Day 18 for control rats and 2045cm for STZ diabetic rats (Figure 4.10A). However, at all timepoints measured there were no significant differences between STZ diabetic and control rats or between either group and baseline (Day -12&-5) [Time: $F(4,48) = 3.382$, $p=0.02$], [Treatment: $F(1,12) = 0.925$, $p=0.36$], [Interaction: $F(4,48) = 1.158$, $p=0.34$] (Figure 4.10A).

As well as the total distance moved the average speed or velocity of the rats were recorded to assess if, although the total movement stayed the same, the speed that the rats moved had changed. STZ diabetic rats did move slower than baseline (Day -12&-5) at Day 18 (1.42cm/s versus 1.07cm/s) (Figure 4.10B). However, this was in line with control rats movement speed at 1.25cm/s [Time: $F(4,48) = 5.029$, $p=0.002$], [Treatment: $F(1,12) = 0.910$, $p=0.36$], [Interaction: $F(4,48) = 1.192$, $p=0.33$] (Figure 4.10B). During the full course of the study average velocity followed a similar trend to the total distance moved with Day 4 movement speed being marginally higher (though not significantly) and trended back down by Day 18 (Figure 4.10B).

To confirm if the amount of time spent moving was altered in the STZ diabetic or control rats this was also assessed. Again a similar trend in the time spent moving for both distance moved and velocity showed a marginal non-significant increase at Day 4 but not significant alterations in either STZ diabetic or control rats. At baseline control rats spent 26.7% of the time moving whereas STZ diabetic rats spent 31.1% of the time moving (Figure 4.10C). This was not a significant increase, reaching ~35% by Day 4 and started to trend back down to ~25% by Day 18 [Time: $F(4,48) = 4.374$, $p=0.004$], [Treatment: $F(1,12) = 0.013$, $p=0.91$], [Interaction: $F(4,48) = 0.915$, $p=0.46$] (Figure 4.10C). There was a decrease in STZ diabetic rat's average velocity at Day 18 compared to baseline, although there was no difference between the STZ diabetic and control rats locomotor activity.

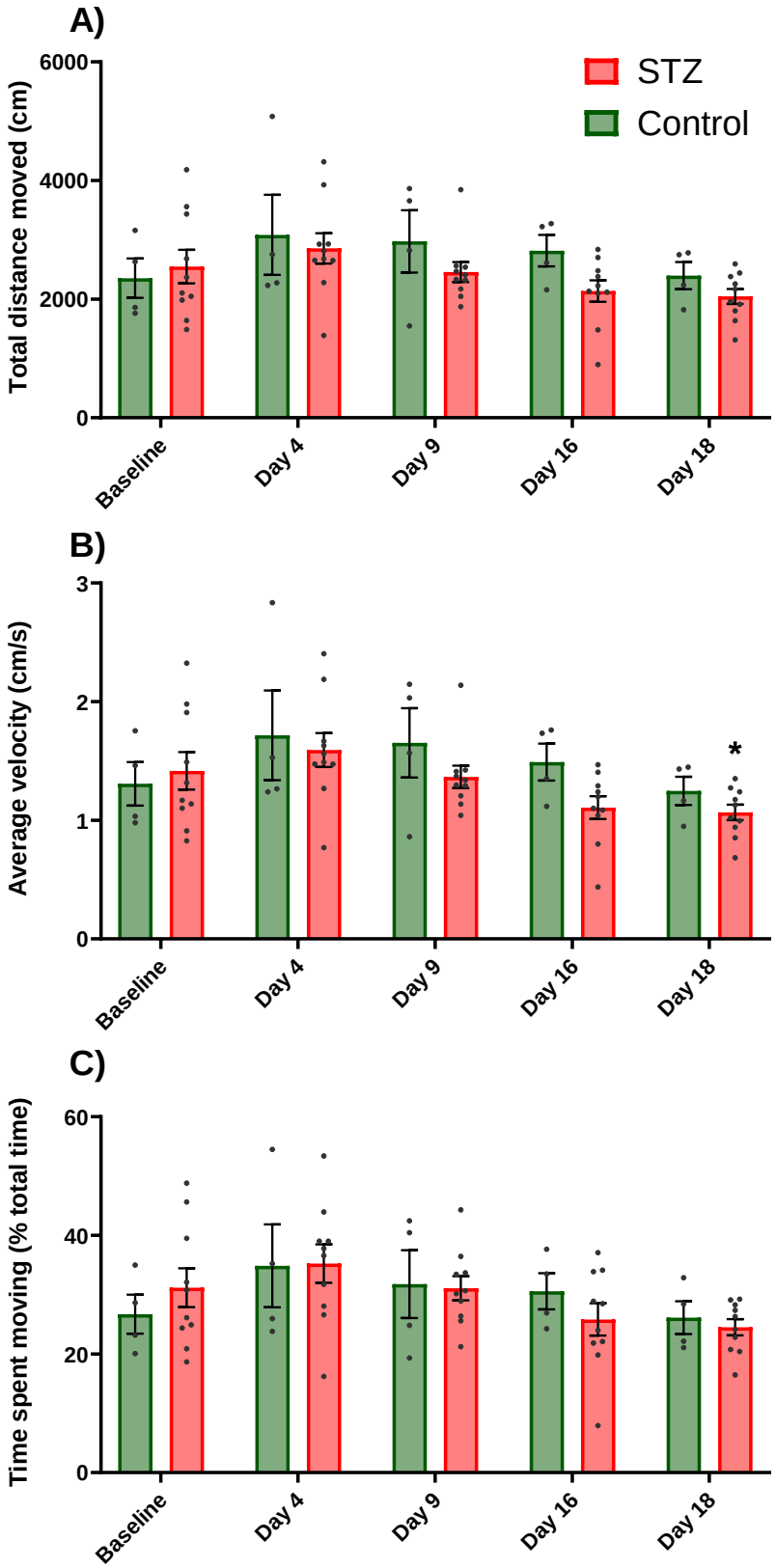

Figure 4.10) Locomotor activity in STZ diabetic and control rats was mostly unchanged during the first 18 days after STZ/control administration. Measurements of the total distance moved (A), average velocity (B) and amount of time spent moving (C) of STZ diabetic and control rats in 30 minutes at baseline (Day -12&-5) and across the study after STZ/control administration. *p<0.05 vs baseline Day -12&-5. p>0.05 STZ vs control. All data is reported as mean ± SEM, n=4 control, n=10 STZ.

4.3.6 Gait measurements in STZ diabetic rats remained comparable to control rats.

Similar to locomotor activity, measurements of STZ diabetic rats gait were not different from control rats at any point during this study. In both STZ diabetic and control rats the left side stride length increased compared to baseline after STZ/control administration however, there were no differences between the groups. At baseline (Day -6&-5) both STZ diabetic and control rats had almost identical left side stride length at 130.6mm [Time: $F(5,60) = 5.714$, $p<0.001$], [Treatment: $F(1,12) = 0.188$, $p=0.67$], [Interaction: $F(5,60) = 2.244$, $p=0.06$] (Figure 4.11A). This left stride length increased significantly compared to baseline in control rats at Day 9 (155.9mm) and at Day 10 (147.8mm) after control administration (Figure 4.11A). Similarly in STZ diabetic rats at Day 10 their average stride length increased to 142.0mm and further increased to 145.7mm at Day 16 compared to baseline (Figure 4.11A).

Likewise, the right side stride length increased over time in both STZ diabetic and control rats. At baseline (Day -6&-5) control rats right side stride length was 128.0mm which was not different from STZ diabetic rats at 133.0mm [Time: $F(5,60) = 8.420$, $p<0.001$], [Treatment: $F(1,12) = 0.044$, $p=0.84$], [Interaction: $F(5,60) = 0.871$, $p=0.51$] (Figure 4.11B). In control rats their right side stride length continued to increase to 150.8mm by Day 9, significantly higher than baseline, and maintained at ~150mm for the remainder of the study (Figure 4.11B). In STZ diabetic rats this change was evident slightly earlier and increased above baseline (Day -6&-5) at Day 4 to 144.2mm and plateaued by Day 9 at ~147mm. At no timepoint were STZ diabetic or control rats right side stride length significantly different from each other (Figure 4.11B).

Alongside the changes in stride length, the width between the strides was also measured. Unlike the increase in stride length in both STZ diabetic and control rats after STZ/control administration there were no changes in stride width in either group. At baseline (Day -6&-5) control and STZ diabetic rats both had an equivalent stride width at 34.6mm [Time: $F(5,60) = 2.118$, $p=0.08$], [Treatment: $F(1,12) = 0.011$, $p=0.92$], [Interaction: $F(5,60) = 0.592$, $p=0.71$] (Figure 4.11C). This remained consistent throughout the study with only minor fluctuations but remining within 30-35mm for both groups (Figure 4.11C). There were no differences in STZ diabetic and control rat's measurements of walking gait at any timepoint during the study despite increased stride length developing after STZ/control administration in both groups.

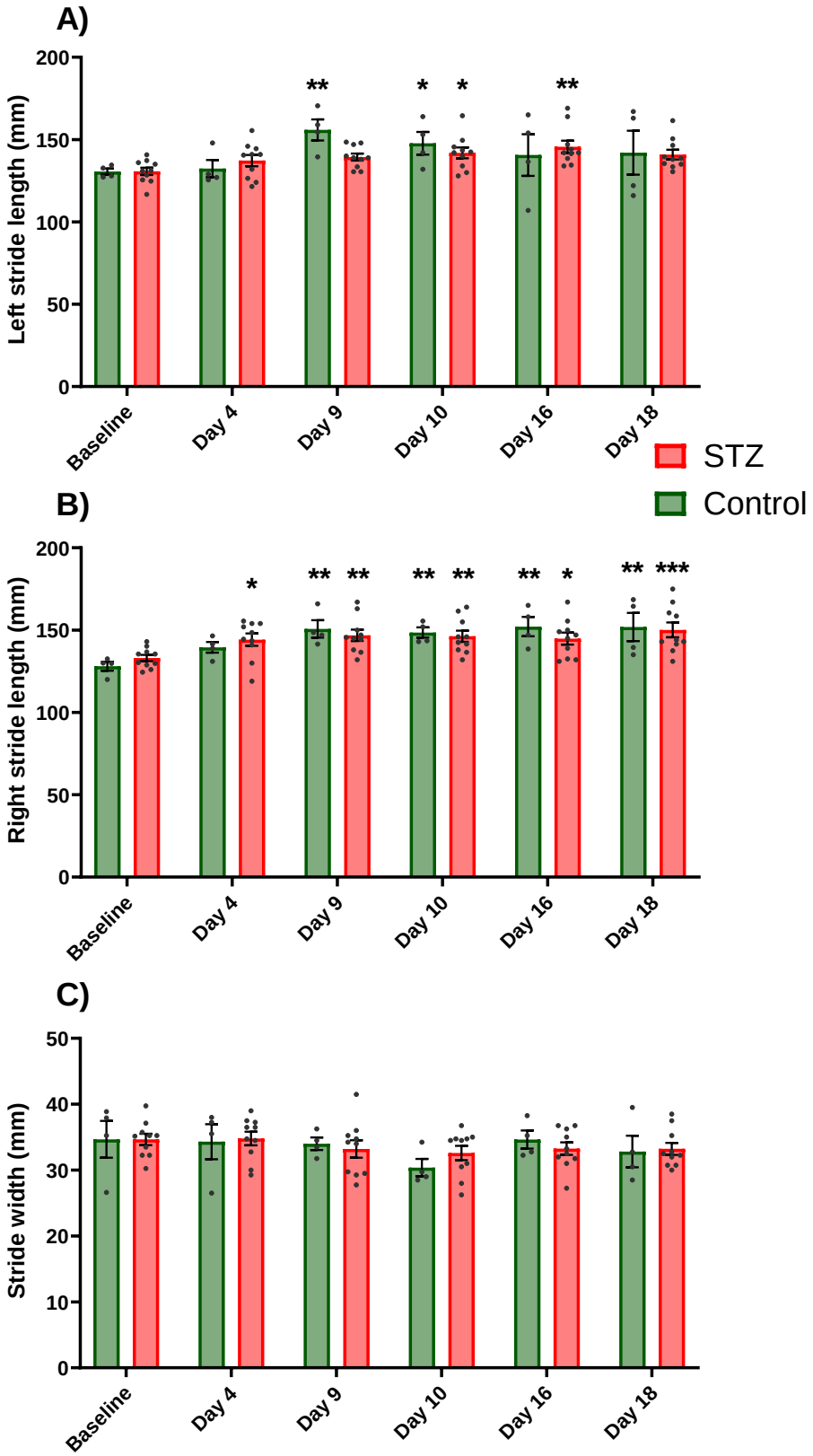

Figure 4.11) Left and right stride length increased equally in STZ diabetic and control rats during the first 18 days following STZ/control administration. Measurements of the left side stride length (A), right side stride length (B) and the width between strides (C) of STZ diabetic and control rats at baseline (Day -6&-5) and across the study after STZ/control administration. *p<0.05, **p<0.01, ***p<0.001 vs baseline Day (-6&-5). p>0.05 STZ vs control. All data is reported as mean ± SEM, n=4 control, n=10 STZ.

4.4 Discussion

4.4.1 STZ (55mg/kg) administration caused sufficient hyperglycaemia to develop a diabetic phenotype in all rats.

STZ (55mg/kg) administered to Wistar Han rats produced a stable level of hyperglycaemia to develop in this study (Figure 4.5). Although a timeline of hyperglycaemia and mechanical allodynia development was demonstrated in Chapter 2 and Chapter 3, this study used an alternative animal supplier (Envigo Wistar Han versus Charles River Wistar Han IGS used previously). Therefore hyperglycaemia and von Frey development were re-assessed for their consistency with previous results. Both suppliers provided the same strain of male Wistar Han rats however, as they have been maintained at different facilities there may have been previous environmental differences before starting this study. Hyperglycaemia development was consistent with previous findings that by Day 7 STZ administered rats BGLs increased above the 16mmol/L threshold, and this was maintained across the study (Figure 4.5). All Envigo Wistar Han STZ rats did developed hyperglycaemia, slightly more than the 94% in the Charles River cohorts in both Chapters 2 and 3 (Figure 2.3, 3.2). However, it is not possible to rule out whether this occurred due to random variability or even improved administration technique so a much larger sample size would be needed to confirm this. Overall, 55mg/kg STZ induced a stable level of hyperglycaemia in all rats administered STZ and therefore all STZ rats in this study can be considered as developing a diabetic phenotype.

4.4.2 STZ diabetic rats gained less bodyweight than control rats.

In this study STZ diabetic rats initially lost a small amount of bodyweight that stabilised by Day 3, as seen previously in Chapter 2 and Chapter 3. The Envigo Wistar Han rats used in this study were administered 55mg/kg STZ at a slightly lower average bodyweight of 363g compared with ~420g previously. This was decided based on a learning in Chapter 3, that lower bodyweight rats may experience reduced bodyweight loss and have improved survivability following STZ administration (Wang-Fischer & Garyantes, 2018). In this study Envigo STZ rats had improved survivability as no rats were excluded due to bodyweight loss or health complications. In comparison both Chapter 2 and Chapter 3 studies did have STZ diabetic rats excluded based on excessive weight loss and/or health complications that developed. Administering STZ to lighter weight and younger rats was expected to cause reduced bodyweight loss compared to previous studies (Wang-Fischer & Garyantes, 2018). STZ diabetic rats in the present study lost 5.68% across the first five days (Figure 4.6) which was in between the bodyweight loss of Chapter 2 study at 4.38% (Figure 2.4) and Chapter 3 study at 7.32% (Figure 3.9), both of which STZ rats were ~420g at the time of administration. This seeming lack of improvement in STZ diabetic rat's bodyweight when using lighter rats at Day 0 STZ administration may reflect a difference in the Envigo and Charles River Wistar Han strains growth and metabolism curves. During their first week of baseline testing Envigo Wistar Han rats gained an average of 19g bodyweight per week (Figure 4.6) whilst Charles River Wistar Han IGS rats in Chapter 3 gained 40g (Figure 3.9) despite starting bodyweights being similar at 322g for Envigo and 311g for Charles River animals (Figure 3.9, 4.6). Although there was a difference in bodyweight gain even in rats before STZ/control dosing, once STZ was administered Envigo rats in this study initially lost a small amount of bodyweight before maintaining a stable bodyweight across the study consistent with previous findings in Chapter 2, Chapter 3 and published research (Furman, 2021; Mitani et al., 2008; Wang-Fischer & Garyantes, 2018).

4.4.3 STZ diabetic rats developed polyphagia and polydipsia.

The development of polyphagia and polydipsia are also phenotypical developments of a type-1 diabetes model and were evident in STZ diabetic rats in this study (Ali et al., 2015; Vieira et al., 2020; Wang-Fischer & Garyantes, 2018). STZ diabetic rats developed polyphagia at Day 3 after STZ administration and polydipsia occurred at Day 1. Both polydipsia and polyphagia reached a peak at around Day 7-10 and were maintained at this level for the remainder of the study (Figure 4.7). The development of polydipsia and polyphagia were similar to that of STZ diabetic rats in Chapter 2 and 3, although the peak food and water intake was slightly lower in the present study. By Day 10 the average daily water intake of STZ cages in Chapter 2 reached ~550g (Figure 2.5), slightly higher than the ~500g in Chapter 3 (Figure 3.11) and higher than the ~400g in this study (Figure 4.7). Likewise food intake in STZ diabetic rats in this study reached a peak of ~75g (Figure 4.7) whilst STZ diabetic rats in Chapter 2 consumed ~110g (Figure 2.5). This could be considered as indicative of a slightly reduced type-1 diabetic phenotype although this is unlikely as the BGLs were similar across all studies. Despite the slight differences in food and water intake between Envigo and Charles River animals, STZ diabetic rats developed polyphagia and polydipsia, both of which are phenotypical of a type-1 diabetes model.

4.4.4 Mechanical allodynia developed in STZ diabetic rats by Day 3 and was not affected by having a home cage partner present.

Mechanical allodynia developed in all STZ diabetic rats by Day 3. Measuring von Frey paw withdrawal thresholds highlighted that Envigo STZ rats developed mechanical allodynia earlier than the STZ diabetic rats in Chapter 2 and Chapter 3. In this study, paw withdrawal thresholds reached 6.5g by Day 3 after STZ administration whilst Charles River rats remained at 15.5g in Chapter 3 (Figure 3.3). Envigo STZ diabetic rats also developed a slightly lower stable level of mechanical allodynia at ~2g paw withdrawal threshold by Day 14 (Figure 4.8) whilst Charles River rats in Chapter 3 maintained a neuropathic baseline level of ~5g (Figure 3.3). Both Envigo and Charles River Wistar Han rats developed mechanical allodynia and a diabetic phenotype after STZ administration.

Using a novel pairing approach to measuring von Frey paw withdrawal thresholds in this study did not alter the development of mechanical allodynia in STZ diabetic rats. As part of the continual support of the 3R's initiative it is important to evaluate and refine in vivo protocols to minimise pain, suffering or distress in each study (NC3Rs, n.d.). Though a primary aim of this research is to identify alternative endpoints for neuropathic pain, improving the classical evoked measures, at least in the short term, is beneficial. One aspect of von Frey testing that is not often considered is that animals are separated from their home cage partners for the duration of testing, albeit as short as reasonably practical. Research has shown that even short-term social isolation can lead to an increase in depressive like behaviours in rodent that could be overcome by allowing animals to remain with their home cage partner during von Frey testing (Takatsu-Coleman et al., 2013). To assess the impact of this short-term isolation, von Frey paw withdrawal thresholds were repeated with home cage STZ/STZ or control/control pairs together (paired).

Conducting von Frey measurements on paired rats had no impact on STZ diabetic rats compared with when tested on their own. Paired control rats had a more stable paw withdrawal threshold compared to when the same control rats were tested on their own (Figure 4.9). At Day 7 solo control rats paw withdrawal thresholds decreased slightly in a similar fashion to that seen in Chapter 2

which was attributed to social transfer of pain in mixed STZ/control pairs (Langford et al., 2006; Smith et al., 2016). Pairing control rats during von Frey testing appeared to eliminate this effect at Day 7, maintaining von Frey paw withdrawal thresholds significantly higher than STZ diabetic rats at all timepoint measured. One potential limitation of conducting von Frey testing in paired groups of animals exhibiting pain, is the social transfer of pain discussed in Chapter 2 and Chapter 3 that could lead to increased sensitivity in the partner animal (Langford et al., 2006; Smith et al., 2016). Assessing mixed STZ diabetic and control rats together to demonstrate if social transfer of pain may lead to reduced control rats paw withdrawal thresholds should be explored in the future. This study demonstrates that allowing rats to remain with their home cage partner during von Frey testing improves animal welfare by avoiding short term isolation whilst still achieving the same scientific result as with solo rats.

4.4.5 Locomotor activity in STZ diabetic rats remained comparable to control rats.

The development of a diabetic phenotype and mechanical allodynia in STZ diabetic rats had no effect on locomotor activity. In the present study although there were non-significant trends towards increased and then decreased locomotor activity, these occurred in both STZ diabetic and control rats equally (Figure 4.10). These changes are therefore more likely indicative of environmental changes such as the rats increasing or decreasing their exploratory behaviour as they become used to their environment (Brown & Nemes, 2008). Only on Day 18 was there a significant decrease in STZ diabetic rat's average velocity, although this was not different from control rats average velocity (Figure 4.10). Therefore, it is unlikely that any of the changes in locomotor activity in this study occurred due the type-1 diabetic phenotype or mechanical allodynia. As such locomotor activity in the STZ type-1 diabetic model is not a useful endpoint for neuropathic pain or diabetes related changes at least until Day 18.

Locomotor activity has previously been studied in STZ diabetic rats and typically does demonstrate a reduction in measures of locomotor activity, which on face value presents conflicting results to the present study (Bădescu et al., 2016; Doria et al., 2016; Haider et al., 2013; Kou et al., 2014; Sevak et al., 2008). However, these studies report changes in locomotor activity at timepoints >4 weeks after STZ administration (Bădescu et al., 2016; Doria et al., 2016; Kou et al., 2014) or do not report the timepoint at which locomotor activity was measured (Haider et al., 2013; Sevak et al., 2008). Interestingly, Kou et al. (2014) identified a reduction in paw withdrawal threshold at Day 14 after STZ administration but no changes in locomotor activity at this timepoint (Kou et al., 2014). Kou et al. (2014) did identify decreased total distance and average velocity in STZ diabetic rats compared with control rats developed at Day 28 (Kou et al., 2014). These results are not unlike the present study in that up to Day 18 there were no differences in locomotor activity between STZ diabetic rats and control rats (Figure 4.10). This supports that if changes in locomotor activity do develop in STZ diabetic rat models, this is likely to develop much later than both mechanical allodynia and burrowing deficits (Chapter 3).

Whilst Chapter 3 demonstrated a clear and maintained burrowing deficit (Figure 3.6) a potential confounding factor of these results was that changes in burrowing levels could have been caused by reduced locomotor activity in STZ type-1 diabetic rats (Shepherd et al., 2018). As discussed, there were no differences between STZ diabetic rats and control rats across the study indicating that at least up to Day 18 locomotor activity is not altered in STZ diabetic rats (Figure 4.10). This suggested that the deficits in STZ diabetic rat burrowing that developed in Chapter 3 at Day 18 was unlikely to have been caused by changes in locomotor activity (Figure 3.6). It is more likely that the

development of burrowing changes in STZ diabetic rats is caused by alterations to animal wellbeing, that does not affect their locomotion (Rutten et al., 2018; Shepherd et al., 2018). Overall, the lack of changes in locomotor activity observed in this study supports the burrowing deficits identified in Chapter 3 were not caused by reduced locomotor activity deficits and that locomotor activity is not a useful neuropathic pain endpoint (at least until Day 18) in STZ diabetic rats.

4.4.6 Gait measurements in STZ diabetic rats remained comparable to control rats.

Although changes in STZ diabetic rat's gait have previously been considered as a neuropathic pain endpoint, there were no alterations in the STZ diabetic rat's gait in this study compared to control rats (Figure 4.11). In human diabetic neuropathy patients, gait may be affected in as many as 50% of patients and can lead to an increased risk of falls causing further injury (Alam et al., 2017; Alle et al., 2008). Hence, changes in gait have been considered a possible translational objective endpoint as they can be measured in both human and rodents without using a stimulus to evoke any changes (Fisher et al., 2021). However, this study identified no such in gait at least during the 18 days assessed as there was no difference between STZ diabetic and control rat's gait (Figure 4.11). Though there was an increase in gait length for both groups equally suggesting that it is likely that this occurred due to environmental factors, such as the animals learning to walk along the gait measuring equipment (Figure 4.3).

Changes in STZ diabetic rats gait have been assessed previously using both manual methods, as used in this study, as well as using automated gait analysis systems (Al Deeb et al., 2000; Karatan et al., 2019; Vieira et al., 2020). Some of the first investigations into alteration in STZ rat gait parameters identified no change in print length, landing foot splay inclined plane or hind limb functional tests using manual ink staining at 3 weeks in STZ diabetic rats compared to control rats (Al Deeb et al., 2000). This lack of change in STZ diabetic rats compared with control rats is consistent with the findings of the present study that no changes in paw stride length or width occurred across 18 days after STZ administration (Figure 4.11). However, others have identified changes in gait after STZ administration, such as Karatan et al. (2019), who demonstrated an increase in footprint length and sciatic nerve function testing using a manual paw printing technique (Karatan et al., 2019). One limiting factor in the comparison of these studies is that the changes identified in footprint length and sciatic nerve function by Karatan et al. (2019) occurred at 8 and 12 weeks after STZ, a much later timepoint than measured either in this study (Figure 4.11) or the up to 3 weeks by Al Deeb et al. (2000) (Al Deeb et al., 2000; Karatan et al., 2019). Thus indicating that changes in STZ diabetic rats gait may occur between 3 and 8 weeks after STZ administration. This is further confirmed by the findings of Vieira et al. (2020) using the 'CatWalk' gait analysis system. Vieira et al. (2020) demonstrated a development of von Frey paw withdrawal threshold and gait changes in paw placement as early as Day 14 however, changes in stride length of STZ diabetic rats only occurred at Day 28 (Vieira et al., 2020). This supports the present study that changes in stride length were not altered in STZ rats within the first 3 weeks after STZ administration but did indicate that this may develop at a later timepoint (Figure 4.11).

Interestingly the development of paw placement changes at Day 14 in the study by Vieira et al. (2020) only occurred at this specific timepoint not at Day 7, 21 or 28 indicating a variable nature of the changes in STZ diabetic rats, that may limit the use of these types of measures. Some of the only evidence of reversal of gait changes in STZ diabetic rats can be seen in Vieira et al. (2022) where they demonstrated that photomodulation of the mitogen-activated protein kinases pathway could relieve some of these gait changes (Vieira et al., 2022). The development of paw withdrawal threshold

changes before gait changes by Vieira et al. (2020) match the finding in this study that mechanical allodynia developed at Day 3 whilst there were no changes in gait even at Day 18 (Figure 4.11) (Vieira et al., 2020). This also highlighted that similarly to burrowing, changes in gait are likely not assessing the same behavioural changes in the STZ diabetic rats as von Frey paw withdrawal thresholds are. Therefore, the development of changes in STZ diabetic rats gait should be further characterised across a longer time period and across multiple research groups and assessed for the efficacy of analgesics to reverse any changes.

4.4.7 Limitations, improvements and future work

A limitation of this study was the shorter three-week timeline experimental design. The animals procured in this study were designated for multiple research projects. Firstly for the objectives set out and later to provide multiple control and STZ diabetic tissues or cells for in vitro biochemical, cell and molecular biological undergraduate and postgraduate student projects at University of Hertfordshire, in line with 3Rs of reduction (NC3Rs, n.d.). Future studies investigating gait and locomotor activity changes in STZ diabetic rats should assess a longer timeline of their development and reversibly with analgesics to fully identify if they could be a translatable neuropathic pain endpoint. This does pose a challenge for their easy replacement of current preclinical neuropathic pain endpoints as the mechanical allodynia measured by von Frey paw withdrawal threshold occurs much earlier than this. This would lead to increased costs associated with running STZ diabetic studies for longer periods of time. Although this would still add value to the research field if gait and locomotor activity provide translatable measurements of neuropathic pain.

An improvement to this study would have been the use of an automated gait scoring system. The manual method of applying paint/ink to measure changes in gait was achieved successfully in this study and by others (Al Deeb et al., 2000; Karatan et al., 2019). However, the thickness of paint application and the restraining of the animals required to apply them led to smudged or incomplete paw print patterns (Figure 4.3C). The use of an automated gait analysis system would reduce the need for additional animal restraining. These automated systems can also measure additional gait parameters such as swing speed or animal movement speed which are not possible with manual print/ink methods but require substantial investment in the equipment required.

4.5 Conclusions

This study identified that there was no development of locomotor or gait changes in STZ type-1 diabetic rats for 3 weeks following STZ administration. Despite hyperglycaemia and mechanical allodynia developing during this time along with other phenotypical developments of polydipsia, polyphagia and bodyweight loss in these diabetic rats. This indicated that changes in burrowing levels at these early timepoints were not caused by changes in locomotor activity but instead by some affective component of diabetes reducing the drive or motivation for burrowing, such as wellbeing. Further studies should monitor the development of gait and locomotor activity changes in STZ diabetic rats across a longer period to identify if any changes occur at a delayed timepoint and whether they correlate to deficits in burrowing or mechanical allodynia.

Chapter 5: Sleep/wake behaviour and EEG changes in the single dose oxaliplatin model of chemotherapy induced peripheral neuropathy

5.1 Introduction

Neuropathic pain is often experienced by cancer patients whilst undergoing chemotherapy treatment. Particularly when the treatment involves platinum or taxanes based compounds such as oxaliplatin, cisplatin or paclitaxel (Quintão et al., 2019). This phenomenon is referred to as chemotherapy induced peripheral neuropathy (CIPN) and occurs in as many as 70-100% of patients undergoing platinum-based chemotherapy (Banach et al., 2017). The neuropathy caused by platinum-based compounds is believed to occur through similar mechanisms to the chemotherapy antineoplastic changes. These antineoplastic changes include binding to DNA, damaging mitochondria and activating immune system responses (Zajączkowska et al., 2019). For many of these chemotherapeutic drugs, CIPN is becoming the most dose limiting side effect (Mezzanotte et al., 2022; Miltenburg & Boogerd, 2014). There are currently no preventative strategies to stop CIPN development, and duloxetine is one of the only drugs licenced for the treatment of CIPN (Mezzanotte et al., 2022). Thus, the neurotoxic effects of chemotherapy treatment and the lack of analgesia can limit cancer treatment leading to altered or reduced treatment plans (Miltenburg & Boogerd, 2014). Therefore, development of better and more effective treatments for CIPN is essential.

The single dose oxaliplatin induced model of CIPN has been developed and used to represent the human treatment regime of metastatic colorectal cancer patients where painful CIPN is experienced by >90% of patients (Cersosimo, 2005). This model has excellent construct validity as the same chemotherapeutic agent is used as in the human condition. Additionally, rats administered with a single dose of oxaliplatin develop a transient CIPN phenotype for up to 8 days based on previous reports (Ling, Coudoré-Civiale, et al., 2007). The single administration model captures the transient neuropathic pain that is experienced by a greater proportion of patients (>90%) (Cersosimo, 2005) than chronic CIPN experience by ~30% of patients (Colvin, 2019). Alternative models of oxaliplatin induced CIPN involve the repeated administration of oxaliplatin, known as the multiple dose model, to produce a chronic CIPN model with allodynic phenotypes lasting over 6 weeks after oxaliplatin administration (Ling, Authier, et al., 2007; Xiao et al., 2012). An additional difference between the single and multiple dose oxaliplatin models is that the single dose oxaliplatin model typically causes no effect on the rat's bodyweight after administration (Ling, Coudoré-Civiale, et al., 2007; Ling et al., 2008). Whereas the multiple dose oxaliplatin model causes progressive bodyweight loss (Ling, Authier, et al., 2007; Xiao et al., 2012). Oxaliplatin is not routinely administered to rats of the age used in the study (~8 months) compared with the age of the rats typically used in preclinical studies (~2 months) (Jackson et al., 2017; Kim et al., 2017; Wang-Fischer & Garyantes, 2018). Therefore to limit the possibility of health complications and excessive weight loss from repeated administration of oxaliplatin the single dose model was selected for this study.

Currently, the primary endpoints used to quantify neuropathic pain in chemotherapy induced preclinical models involve measuring thermal or mechanical allodynia (Flatters et al., 2017; Warren et al., 2024). To determine thermal allodynia, a temperature of 15°C is used as naïve rats only react

to temperatures of <5°C, thus a reaction to 15°C would indicate cold allodynia (Allchorne et al., 2005). Whilst these types of hypersensitivities do reflect how patients experience CIPN, they have poor predictive validity as indicated by the largely unsuccessful drug development efforts so far (Zajączkowska et al., 2019). A possible reason for this lack of translatability is that thermal and mechanical allodynia are assessed using evoked endpoints that do not capture the brain and emotional processing of pain (Fisher et al., 2021; Tappe-Theodor et al., 2019).

Changes in sleep/wake behaviour and EEG have been demonstrated in rodent models of surgically induced neuropathic pain such as the chronic constrictive injury (CCI) model. These changes include increased EEG theta power (Koyama, LeBlanc, et al., 2018), decreased time spent asleep (Andersen & Tufik, 2003; Ho et al., 2024) and frequent sleep disturbances (Alexandre et al., 2024). These results have established sleep and EEG measures as potential preclinical endpoints for neuropathic pain. Sleep and EEG measures of pain also possess a strong translational potential since they are objective, non-evoked and directly measurable endpoints in both humans and animals (Fisher et al., 2021). However, the available preclinical and clinical data on the effects of oxaliplatin treatment on EEG is very limited. Some of the available clinical data involving EEG and CIPN comes from Prinsloo et al. (2017,2018) who have used EEG neurofeedback (NFB), a technique that provides a rewarding stimulus to the patient when they achieve designated changes in their EEG power spectra. These NFB studies have described positive, short-term impacts of NFB on patient reported pain scores (Prinsloo et al., 2017). As well as long term improvement in pain severity, numbness, general health and fatigue (Prinsloo et al., 2018). Prinsloo et al. (2017) demonstrated that the use of NFB led to increased alpha activity and decreased beta activity, and this change in beta activity correlated with an improvement in reported pain scores (Prinsloo et al., 2017). This indicated that reduced alpha activity and increased beta activity during wakefulness could be associated with CIPN. Therefore, the present study assessed whether more objectively measured changes in sleep/wake behaviour and electroencephalogram (EEG) in a rat model of oxaliplatin induced CIPN can be used as alternative neuropathic pain endpoints with better translational potential. To assess potential CIPN-induced changes in sleep/wake behaviour and brain EEG activity, rats previously implanted for EEG and electromyogram (EMG) recordings were used. These rats were used in sleep/wake behaviour and/or evoked potential studies at Transpharmation LTD previously in line with the 3Rs of reduction (NC3Rs, n.d.).

5.1.1 Aims and hypotheses.

The primary aim of this study was to identify sleep/wake and EEG changes in oxaliplatin treated rats that develop CIPN.

This study assessed the effect of oxaliplatin treatment on the development of cold allodynia and animal welfare indicated by bodyweight measurements.

Also, this study assessed if CIPN development decreased the time oxaliplatin treated rats spent asleep, as has been demonstrated in other neuropathic pain models.

This study also assessed the development of any sleep fragmentation in rats that experienced CIPN.

EEG power was also assessed in the rats that developed CIPN to understand if any of the changes associated with neuropathic pain, such as increased theta power, reduced alpha power or increased beta power during wakefulness, occurred in these animals.

5.1.2 Abbreviations.

CCI – chronic constrictive injury, EEG – electroencephalogram, EMG – electromyogram, ZT – Zeitgeber time, REM – rapid eye movement, NREM – non-rapid eye movement, CIPN – chemotherapy induced peripheral neuropathy, SNI – spared nerve injury, FFT – fast Fourier transformation, i.p. – intraperitoneal, s.c. – subcutaneously, CFA – complete Freund's adjuvant, NFB – neurofeedback modulation, SEM – standard error of the mean.

5.2 Methods

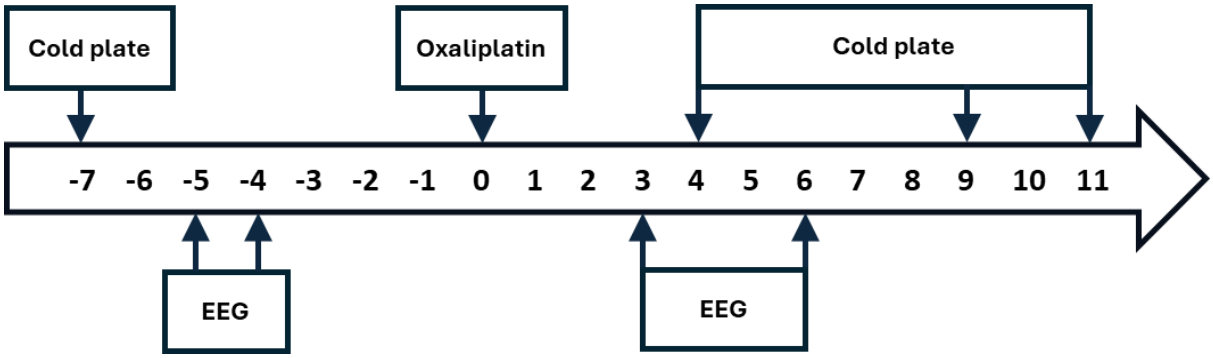

Figure 5.1) Timeline of the study depicting the days before and after 10mg/kg oxaliplatin intraperitoneal (i.p.) administration on Day 0. The days on which cold plate withdrawal latency measurements were taken and EEG recordings were started.

5.2.1 Ethics statement.

All research procedures/experiments were performed in accordance with Animals Scientific Procedures Act 1986 & European Directive 2010/63/EU. All studies performed were approved by the Discovery Park Animal Welfare and Ethics Review Body and comply with the home office guidelines and codes of conduct. All work was authorised under Discovery Park home office establishment licence and project licence titled: Translational pharmacology for drug discovery.

5.2.2 Animals and oxaliplatin administration.

9 male Sprague Dawley rats (Charles River, UK) had been previously surgically implanted under general anaesthesia with telemetry devices (HD-S02; Data Sciences International, USA) to measure frontoparietal EEG and EMG from neck extensor muscles. All Sprague Dawley rats (625-875g on day of oxaliplatin administration) were administered 10mg/kg oxaliplatin intraperitoneal (i.p.) (Tocris, UK 61825-94-3) dissolved in 5% dextrose solution on Day 0 (Figure 5.1) (Ling, Coudoré-Civiale, et al., 2007; Yamamoto, Ono, et al., 2016). All rats were monitored closely across the first 5 days after oxaliplatin administration for signs of distress or discomfort, and daily bodyweight measurements were taken. Periodic bodyweight measurements were taken throughout the rest of the study for a continual monitor of animal health and welfare. One rat was terminated before the end of the study on Day 8 due to health complications unrelated to the oxaliplatin treatment.

5.2.3 Environmental conditions.

Rats were housed in groups of 2 or 3 with environmental enrichment provided and regularly replaced. Home caging area lighting was maintained on a 12:12 h light-dark cycle [lights on: 08:00 / Zeitgeber time 0 (ZT0), lights off at 20:00 (ZT12)] throughout the study. A constant temperature (21 ± 1°C) and relative humidity (55±15%) was maintained in the housing environment with food and water available ad libitum.

5.2.4 Cold allodynia.

Cold allodynia was measured using a 15°C cold plate prior to and after oxaliplatin administration, to confirm the development of CIPN using a traditional evoked neuropathic pain endpoint. The development of cold allodynia was assessed by measuring paw withdrawal latency (s) to a 15°C cold plate. Rats were placed with all four paws on the cold plate and monitored for lifting, flinching or licking of either hind paw. Rats were removed and returned to their home cages after observing a behavioural reaction to the normally non-noxious 15°C cold plate or after reaching the maximum time limit in the test that was set to 150s. Any rats that did not react by this maximum time cutoff point were removed and 150s was recorded as their latency. Baseline measurements of cold plate paw withdrawal latency were taken seven days (Day -7) before oxaliplatin administration (Day 0). After oxaliplatin administration, the cold plate measurements were retaken on Day 4 to determine the level of CIPN development. Additionally, cold plate measurements were taken on Day 9 and Day 11 to confirm the transient reversal of CIPN development (Figure 5.1). Thank you to the technical staff at Transpharmation LTD for conducting the oxaliplatin administration and cold plate measurements.

5.2.5 EEG surgery.

Since surgical implantation of wireless EEG and EMG transmitters is considered a major intervention, the rats used for this study had been previously used in sleep/wake behaviour and/or evoked potential studies at Transpharmation LTD. This reduced the welfare impact of this study and promoted the 3Rs initiative of reduction by ensuring that no additional rats underwent an extensive surgery unnecessarily (NC3Rs, n.d.). Nine Sprague Dawley rats were implanted with telemetry transmitters (HD-S02; Data Sciences International, USA), with the transmitter body placed into the peritoneal cavity. Rats were anaesthetised with 5% isoflurane and maintained at ~2% isoflurane during surgery. To maintain fluid levels during surgery, saline (5ml) was administered subcutaneously (s.c.) in the hind flank. Rimadyl (Carprofen, Zoetis) 1ml/kg was diluted in saline 0.9% NaCl (Baxter) and administered s.c. pre- and post-surgically for pain management. Clippers were used to remove excess hair from the scalp, neck and all areas were cleaned with HibiScrub. Rats were placed on a 37°C warming blanket to maintain body temperature during surgery and the head was fixed in a stereotaxic frame. An incision was made in the abdomen and blunt dissection was used to reach the abdominal cavity. The HDS02 transmitter body was inserted into the abdomen and sutured to the abdominal wall using a non-dissolvable suture material (Figure 5.2). The EEG and EMG leads were passed from the abdominal wall at a site separate from the incision using a 19-gauge needle so that the body of the transmitter was secured inside of the abdomen with the wires travelling through the abdominal wall under the skin. The muscle layer of the abdomen was sutured closed with a non-dissolvable suture material.

A second incision was made along the top of the skull and down the neck to expose the skull and neck extensor muscles. The cables were passed from the site of the abdominal incision under the skin to the neck incision using a trocar. The top of the skull was cleared of any membranes and the area was cleaned with saline. Then using a rotary dental drill, two holes were drilled over the frontal (2 mm anterior / 1 mm lateral to Bregma) and parietal cortices (0 mm anterior / 1.5 mm lateral to Lambda) above the left hemisphere for frontoparietal EEG recordings. EEG recording wires were placed gently into each hole in the skull to be in contact with the dura but without applying pressure. Each EEG wire was secured in place with quick setting dental glue. In case of EMG wires, a 1cm section of the wire was exposed and passed through the neck muscle perpendicular to the spine and travelling in opposite directions. Non dissolvable suture material was used to secure the wires in place in the neck muscles. Once all wires were in place the incision along the abdomen, skull and neck were sutured closed using intradermal absorbable sutures. Rats were placed in a recovery warming box and monitored for breathing rate and any indications of pain until they were recovered their righting reflex in the warming box at which point they were placed back into a clean home cage. Post surgery, rats were kept singly housed for 24 hours to avoid cage mate disturbance of the surgical sites before returning to groups of 2-3 rats for the remainder of the seven day post-surgical recovery. Post operative monitoring included carprofen 5mg/kg administration for at least 3 days with wet mash and regular diet provided along with chew sticks, enrichment and nesting materials. Rats were checked twice daily for surgical wound health, pain levels, bodyweight and a single attempt at reclosing any incision or reattaching an EEG lead was allowed if there was damage to these. Thank you to the technical staff at Transpharmation LTD for conducting the EEG surgery and recordings.

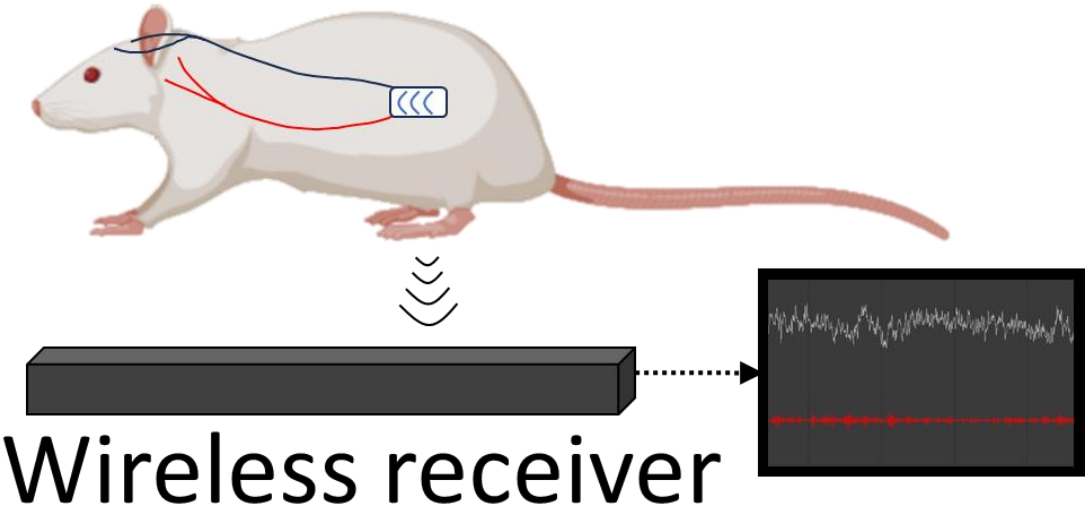

Figure 5.2) Example of the wireless EEG recording setup used with transmitter placed in the abdominal cavity and sending signals wirelessly to a recording baseplate underneath the rat's home cage.

5.2.6 EEG recordings.

Rats were placed in individual recording chambers in a sound-attenuated room with a 12:12h light-dark cycle [lights on at 08:00 (ZT0), lights off at 20:00 (ZT12)], constant temperature (21 ± 1°C) and relative humidity (55±15%), with food and water available ad libitum. EEG, EMG and locomotor activity were recorded for up to 48 hours starting at 5 days before oxaliplatin administration (Day -5, Day -4) and up to 24 hours starting at 3 and 6 days after oxaliplatin administration (Day 3, Day 6) (Figure 5.1). Recordings began at approximately ZT0 (8:00). EEG, EMG and locomotor activity signals were detected by an antenna (RPC-1, Data Sciences International, USA) placed below the recording cages.

5.2.7 EEG processing and manual scoring.

EEG/EMG signals were amplified, analogue filtered (0.5–100Hz), digitised at 500Hz, and recorded alongside locomotor activity for offline analysis (Spike2; CED, UK). EEG and EMG signals were resampled at 256Hz, digitally filtered (EEG: 0.5–100Hz; EMG: 5–100Hz), and automatically scored as wake, rapid eye movement (REM) sleep or non-REM (NREM) sleep, in 10s epochs (Figure 5.3) using SleepSign (Kissei Comtec, Japan). After automatic scoring of vigilance states, two 3 hour-long segments [3 to 6 hours after light onset (ZT3-ZT6) and 3 to 6 h after dark onset (ZT15-ZT18)] were visually checked and corrections were made where it was necessary. These 3 hour periods were selected for visual correction and analysis to identify any changes during an equivalent portion of the light and dark periods that did not include initial animal exploration or human disturbances. Epochs with missing data and/or movement-related artifacts were marked and excluded from power spectral analysis. A 48 hour-long baseline EEG recordings was made on Day -5 and Day -4, and the data recorded on these days was averaged and used as the baseline.

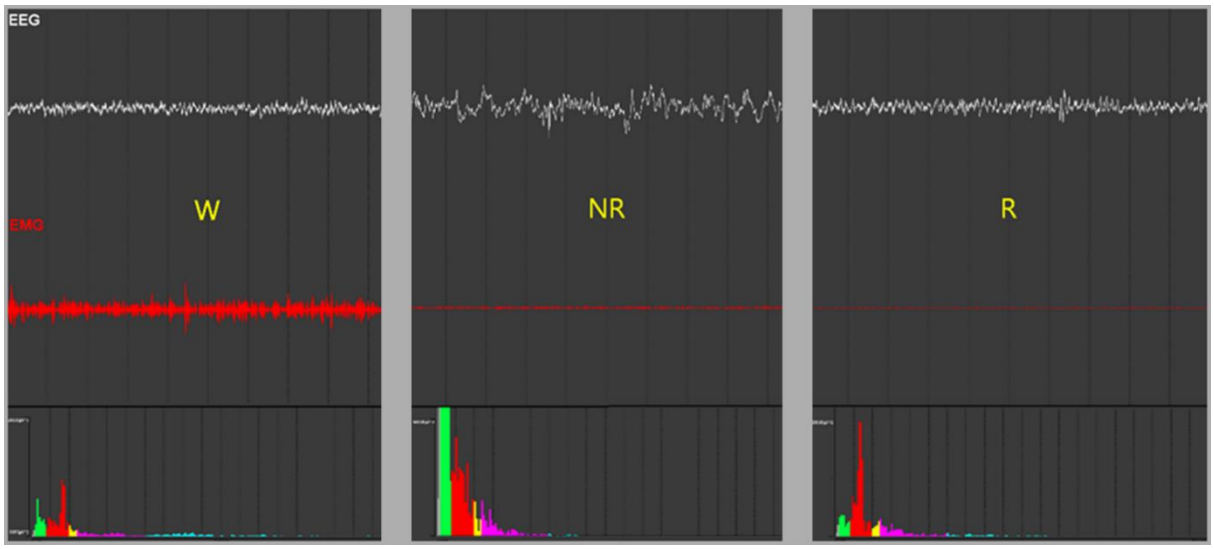

Figure 5.3) Examples of separate 10s EEG and EMG epochs that were manually scored as either wakefulness (W), NREM sleep (NR) or REM sleep (R) using EEG signal (white), EMG signal (red) and fast Fourier transformation (FFT) (bottom graph).

5.2.8 EEG analysis.

To quantify if oxaliplatin treatment and subsequent neuropathic pain development altered sleep/wake behaviour, the percentage of time that the rats spent in each behavioural state of wakefulness, NREM and REM sleep were assessed. Changes in sleep/wake behaviour were further assessed by measuring the average duration and total number of wakefulness, NREM and REM sleep bouts. In addition, the distribution of sleep/wake bout lengths were further assessed by calculating the total number of short (≤10 s) and medium (10-50 s) bout lengths that occurred.

To understand if there were any changes in the frequency content of the recorded signal, power spectral analysis of the EEG was conducted. EEG power spectra was computed for artifact-free 2-s epochs in the 0.5–100Hz frequency range by fast Fourier transformation (FFT) with a frequency resolution of 0.5Hz. Before FFT, a window weighting function (Hanning) was applied. The values of consecutive 2-s EEG epochs per vigilance states were averaged over the visually scored sections during ZT3-ZT6 in the light period and ZT15-ZT18 in the dark period. To determine any changes in specific frequency bands, the area under the curve (AUC) of the EEG power spectrum in the delta (0.5–4Hz), theta (4–8Hz), sigma (8–13Hz), beta (13–30Hz) and gamma (30–100Hz) were calculated during wakefulness, NREM and REM sleep. All EEG and sleep/wake measurements were analysed during the visually scored ZT3-ZT6 in the light period and ZT15-ZT18 in the dark period.

5.2.9 Blinding and exclusion or inclusion criteria.

All EEG scoring was conducted blind to the animal's treatment condition. The response to cold plate induced thermal allodynia was assessed blind. A cutoff threshold of at least 50% reduced paw withdrawal latency at Day 4 compared to Day -7 was used to exclude rats that did not develop CIPN. A maximum limit of 20% bodyweight loss was in place to exclude any rats that developed excessive weight loss.

5.2.10 Statistics.

To compare the results at each timepoint, one-way mixed model analysis of variance (ANOVA) was used followed by Dunnet's post hoc test. Post hoc analysis was conducted to compare pre-oxaliplatin baseline timepoints to timepoints after oxaliplatin treatments (sleep/wake behaviour and EEG) (Prism 10.2; GraphPad, San Diego, CA USA). A p value of <0.05 was considered statistically significant for all data. All data is reported as mean ± SEM.

5.3 Results

5.3.1 Oxaliplatin administration caused CIPN development and bodyweight loss.

The onset of CIPN in oxaliplatin treated rats was confirmed at Day 4 using paw withdrawal latency to a non-noxious 15°C cold plate. When assessed including all of the oxaliplatin treated rats there was a 36.5% reduction in paw withdrawal latency from 126s at baseline to 80s at Day 4 after oxaliplatin administration [$F(2,15) = 5.02$, $p<0.05$] (Figure 5.4A). By Day 9&11 paw withdrawal latency returned to baseline levels of 121s confirming the transient development of CIPN. To identify if the reduced

paw withdrawal latency developed in all rats, the percentage change in cold plate paw withdrawal threshold was assessed by reviewing the percentage change from baseline. At Day 4, only 4 out of 9 rats had a >50% decrease in paw withdrawal threshold at Day 4 compared to baseline. This reduction in paw withdrawal latency can be considered as cold allodynia a phenotype of chemotherapy induced peripheral neuropathy (CIPN). These 4 rats were therefore termed as having developed CIPN, whilst the remaining 5 rats did not develop cold allodynia were termed as non-CIPN (nonCIPN) (Figure 5.4B). The CIPN and nonCIPN rats paw withdrawal latencies were also separated. In CIPN rats paw withdrawal latency was significantly decreased by 68% from baseline (146s) to 46s at Day 4 further confirming CIPN onset in these rats [$F(2,9) = 32.70$, $p<0.001$] (Figure 5.4C). CIPN rats paw withdrawal latency returned to baseline equivalent levels by Day 9&11 demonstrating the transient development of CIPN [$F(2,9) = 32.70$, $p<0.001$] (Figure 5.4C). In nonCIPN rats there was no change in paw withdrawal latency at any timepoint with paw withdrawal latency changing by <5s from baseline (110s) at Day 4 (108s) or Day 9&11 (105s) [$F(2,7) = 0.185$, $p=0.835$] (Figure 5.4D). This demonstrated that CIPN developed transiently in 4 out of 9 rats by Day 4, but it was no longer present on Day 9&11.

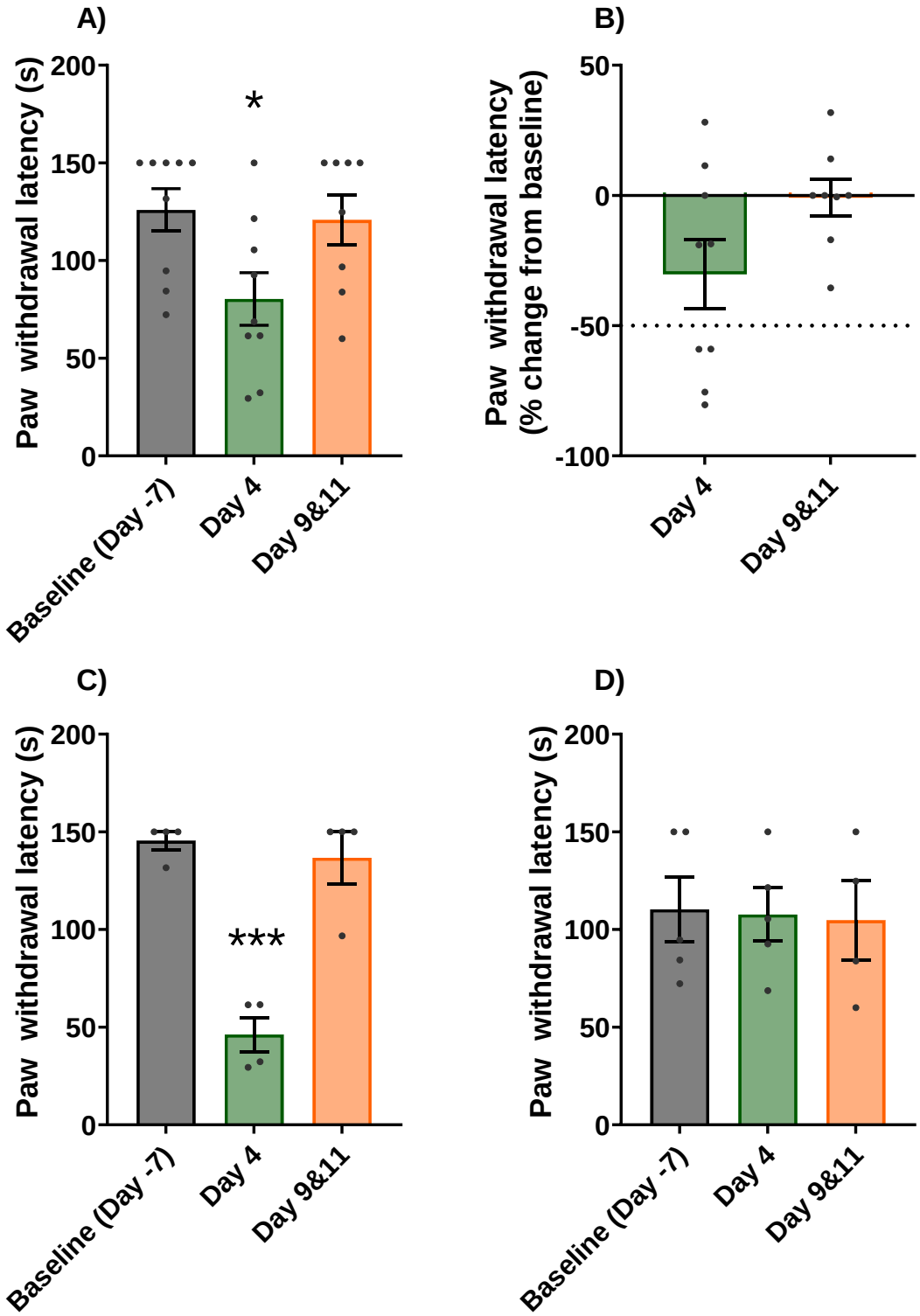

Figure 5.4) Oxaliplatin administration decreased the paw withdrawal latency to non-noxious 15°C cold plate in 4 out of 9 rats. Paw withdrawal latency to 15°C cold plate were measured at baseline (Day -7), Day 4 after oxaliplatin treatment to confirm CIPN onset and at Day 9 and Day 11 (Day 9&11) to confirm reversal of transient CIPN (A). The percentage change in paw withdrawal latency from baseline (Day -7) to Day 4 and Day9&11 were used to confirm CIPN onset by a >50% decrease in paw withdrawal latency (B). Paw withdrawal latency presented separately in rats that developed cold allodynia (CIPN) (C), and in rats that did not develop cold allodynia (nonCIPN) (D). (A,C,D) *p<0.05, ***p<0.001 vs baseline. (B) No statistical comparisons conducted. All data is reported as mean ± SEM, n=8-9 (A,B) n=4 (C), n=4-5 (D).

Oxaliplatin administration caused bodyweight loss from Day 1 onwards [F(10,76) = 22.34, p<0.001] (Figure 5.5). The average bodyweight of rats on Day 0 was 729g which decreased to 716g by Day 1 and remained relatively stable across the first 5 days after oxaliplatin administration (Figure 5.5A). The rats lost more bodyweight after Day 5 reaching 674g by Day 14 with a downwards trend for the remainder of the study. The loss of bodyweight was also reflected when assessed as a percentage change from Day 0 which demonstrated that rats initially lost ~2% bodyweight across the first 5 days after oxaliplatin administration. The rats continued to lose bodyweight reaching -5.3% by Day 14. [F(10,76) = 23.69, p<0.001] (Figure 5.5B).

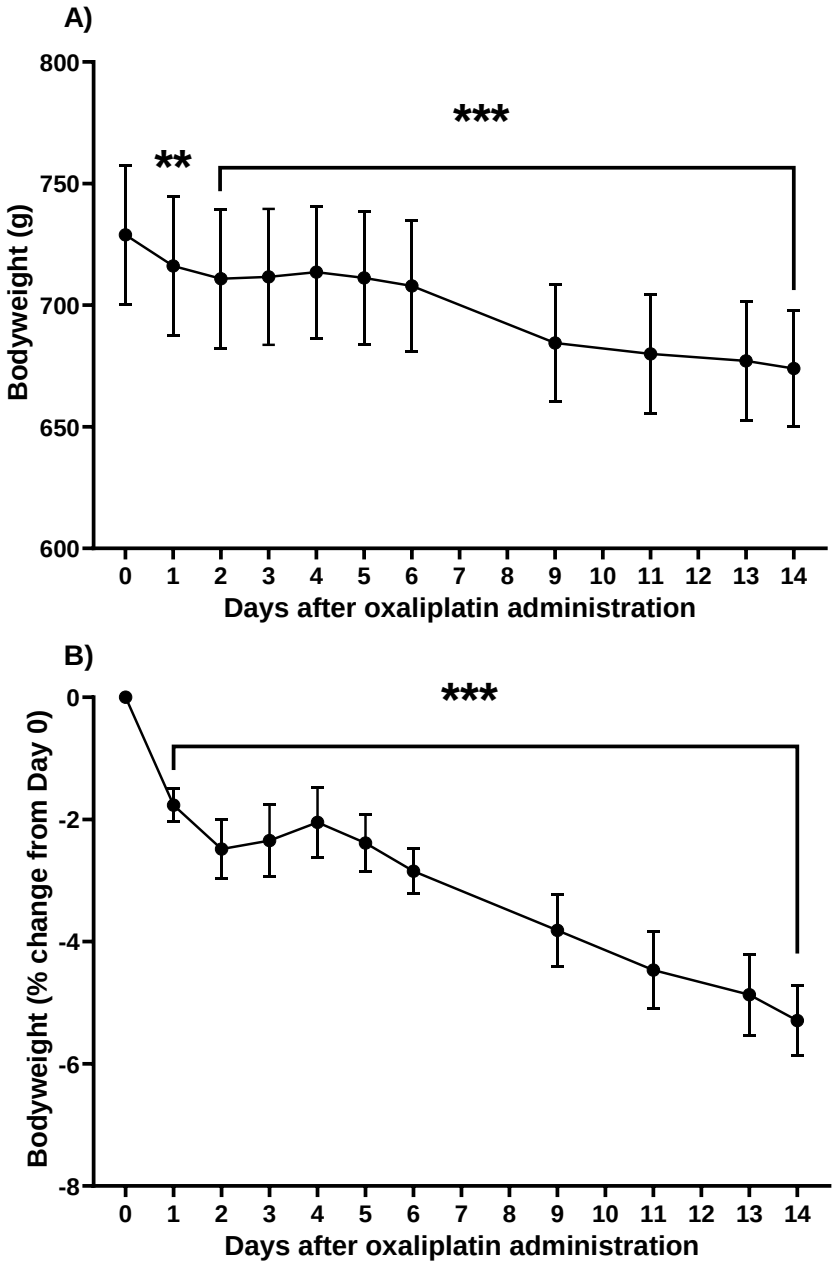

Figure 5.5) Rats treated with oxaliplatin lost bodyweight during the first two weeks after drug administration. A) The changes in bodyweight in oxaliplatin treated rats from their baseline bodyweight on Day 0 until Day 14 after oxaliplatin treatment. B) The percentage change in bodyweight from Day 0 baseline bodyweights in oxaliplatin treated rats. **p<0.01 vs Day 0, ***p<0.001 vs Day 0. All data is reported as mean ± SEM, n=8-9.

5.3.2 Limited effects of CIPN development on sleep/wake amounts.

To understand the impact of oxaliplatin treatment and subsequent CIPN development on sleep/wake behaviour, the changes in wake (Figure 5.6A,B), NREM (Figure 5.6C,D) and REM sleep (Figure 5.6E,F) amounts were measured. This assessment of sleep/wake amounts found trends towards increased sleep and decreased wakefulness in the CIPN rats but none of these reached the (p<0.05) significance level. Specifically, rats spent ~28% of the time awake throughout ZT3-ZT6 in the light period during the baseline recordings which progressively decreased to 22% by Day 3 and to 17% by Day 6 after oxaliplatin administration. This decrease in wakefulness however, was not significant [$F(2,6) = 3.83$, p=0.085] (Figure 5.6A). The decrease in wakefulness was accompanied by a corresponding (but not significant) increase in NREM sleep during ZT3-ZT6 (Figure 5.6C). CIPN rats spent 5% more time in NREM sleep by Day 3 and 8% more by Day 6 compared with 57% time in NREM sleep during baseline recordings. However, this increase in NREM sleep was also not significant, though at Day 6 the post hoc comparison was (p=0.04) [$F(2,6) = 4.73$, p=0.059] (Figure 5.6C). Although the trends towards increased NREM sleep and decreased wakefulness were not significant, possibly due to the low number of CIPN rats, these changes may still represent disrupted sleep/wake behaviour in CIPN rats. Time spent in REM sleep was not affected in CIPN rats during ZT3-ZT6 [$F(2,6) = 1.51$, p=0.30] (Figure 5.6E). These trends towards increased wakefulness and decreased NREM sleep were not maintained during ZT15-ZT18 in the dark period. There was no difference in the amount of time CIPN rats spent awake [$F(2,6) = 1.75$, p=0.25] (Figure 5.6B), in NREM sleep [$F(2,6) = 1.77$, p=0.25] (Figure 5.6D) or REM sleep [$F(2,6) = 1.21$, p=0.36] (Figure 5.6F) during ZT15-ZT18. Though not significantly affected CIPN rats tended to spend more time in NREM sleep and less time awake during ZT3-ZT6 in the light period.

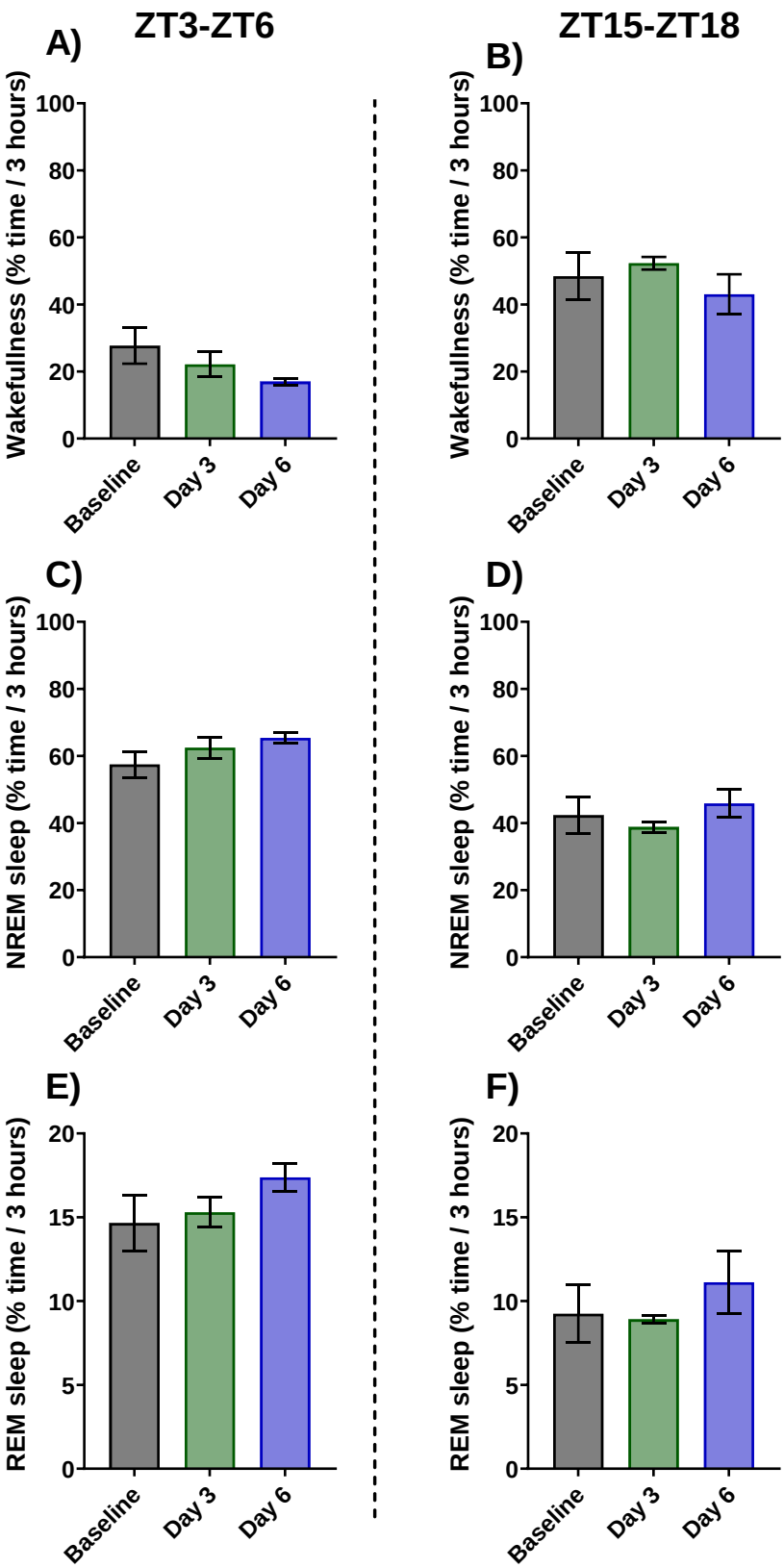

Figure 5.6) There were no changes in the sleep/wake amounts of CIPN rats. The percentage of time the CIPN rats spent awake (A,B), in NREM sleep (C,D) and in REM sleep (E,F) on Day 3 and Day 6 after oxaliplatin treatment were compared to the baseline recording (Day -5&-4). The amount of time rats spent awake or asleep were assessed during ZT3-ZT6 in the light period (A,C,E) and ZT15-ZT18 in the dark period (B,D,F). p>0.05 Day 3 vs baseline, p>0.05 Day 6 vs baseline (A-F). All data is reported as mean ± SEM, n=4 (A-F).

5.3.3 Limited effects of CIPN development on sleep and wakefulness bouts.

After the finding of a trend towards increased sleep and decreased wakefulness, the impact of CIPN development on sleep fragmentation was assessed through the average length and total number of wakefulness and sleep bouts. The main effects of CIPN development on sleep/wake bouts was a trend towards the length of wakefulness bouts decreasing but otherwise there was no effect of CIPN on sleep/wake bouts. During ZT3-ZT6 in the light period the average length of wakefulness bouts was reduced by 42% at Day 3 and by over 50% at Day 6. Despite the average length of wakefulness bouts decreasing by half this did not reach statistical significance in neither in the overall ANOVA (p=0.09) or in post hoc analysis (p=0.07) [$F(2,6) = 3.63$, p=0.09] (Figure 5.7A). The reduction in wake bout length is still a robust change and therefore could indicate that wakefulness was less consolidated in CIPN rats. The decreased average wake bout length was not accompanied by an increased number of wake bouts during the same period (ZT3-ZT6) [$F(2,6) = 2.28$, p=0.18] (Figure 5.7B). Additionally, during ZT15-ZT18 in the dark period there was no change in the average wake bout length in CIPN rats at Day 3 or Day 6 [$F(2,6) = 1.31$, p=0.34] (Figure 5.7C). The total number of wakefulness bouts during ZT15-ZT18 was also unaltered after CIPN development [$F(2,6) = 0.22$, p=0.81] (Figure 5.7D). Both NREM and REM sleep average bout lengths were not altered in CIPN rats at either Day 3 or Day 6 (Figure 5.7E,G,I,K). Similarly, the average length of both NREM and REM sleep bouts were not affected by CIPN development (Figure 5.7F,H,J,L). The average length of wakefulness bouts was reduced by half in CIPN rats at Day 6 after oxaliplatin administration. Though this did not reach significance it may still indicate that periods of wakefulness were less consolidated in CIPN rats at Day 3 and Day 6 after oxaliplatin treatment.

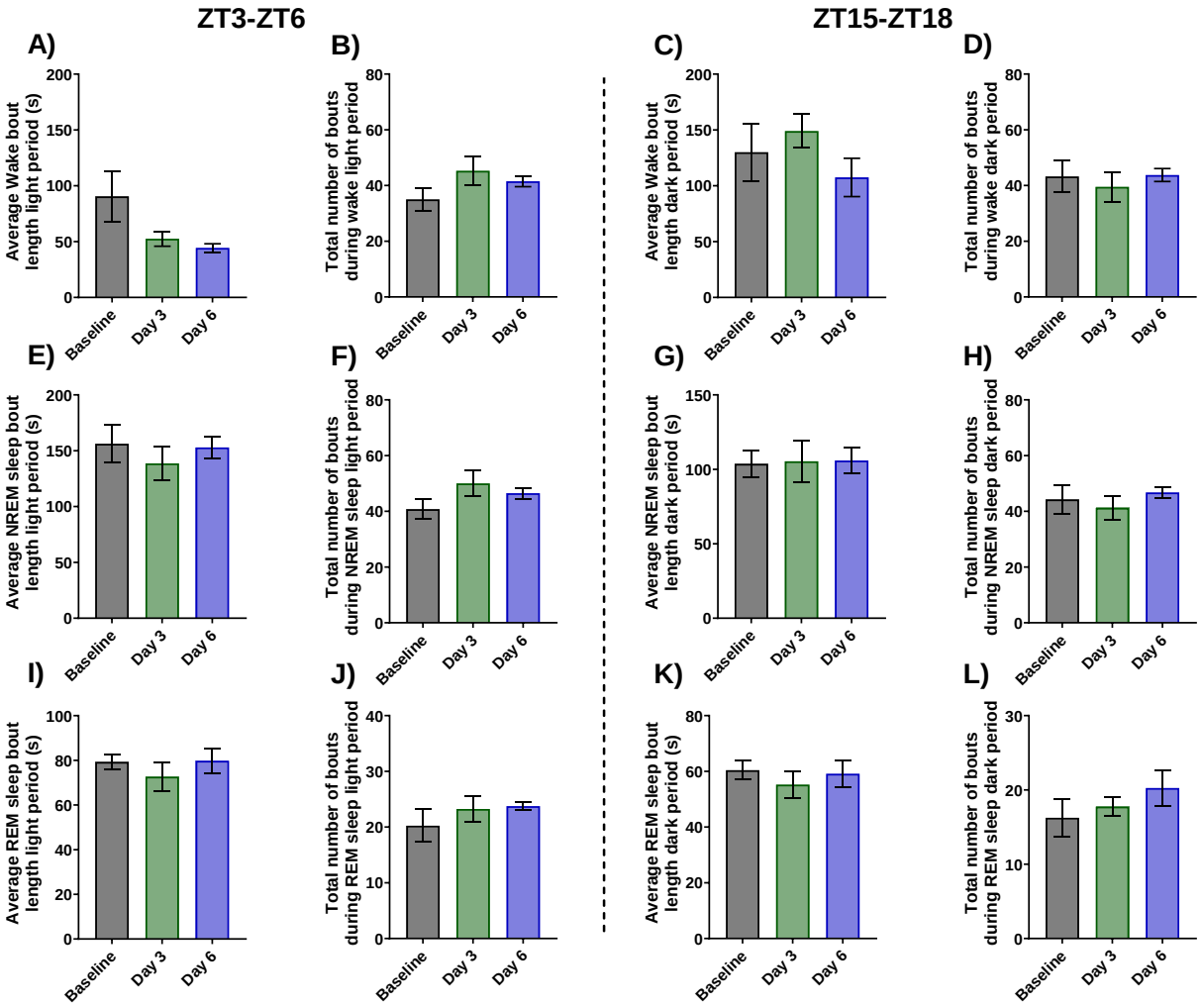

Figure 5.7) The length and number of sleep and wakefulness bouts were not affected in CIPN rats. The average length of each bout of wakefulness (A,C), NREM sleep (E,G) and REM sleep (I,K) at Day 3 and 6 after oxaliplatin treatment were compared to the baseline timepoint (Day -5&-4). The total number of bouts of wakefulness (B,D), NREM sleep (F,H) and REM sleep (J,L) at Day 3 and 6 after oxaliplatin treatment were also compared to the baseline recording (Day -5&-4). Both the average length of sleep/wake bouts and the total number of bouts were assessed during ZT3-ZT6 in the light period (A,B,E,F,I,J) and ZT15-ZT18 in the dark period (C,D,G,H,K,L) in CIPN rats. p>0.05 Day 3 vs baseline, p>0.05 Day 6 vs baseline (A-L). All data is reported as mean ± SEM, n=4 (A-L).

Although sleep fragmentation was not clearly identified through analysing the sleep/wake bout lengths another common report from patients and preclinical models is increased brief awakenings. Based on this the effects of CIPN development on the number of short (≤10s) and medium (10-50s) length sleep/wake bouts was assessed. Interestingly, the main finding from this was an increase in short (≤10s) length NREM sleep bouts during ZT15-ZT18 in the dark period (Figure 5.8). Neither short (≤10s) [$F(2,6) = 1.84$, p=0.24] (Figure 5.8A) or medium [$F(2,6) = 1.66$, p=0.27] (10-50s) length wakefulness bouts (Figure 5.8B) were increased significantly when CIPN rats were assessed during ZT3-ZT6. This was despite the average length of wakefulness bouts decreasing by half (Figure 5.7A). Likewise when assessed during ZT15-ZT18 there was no change in the number of short [$F(2,6) = 0.54$, p=0.61] (Figure 5.8C) or medium length wakefulness bouts [$F(2,6) = 0.48$, p=0.64] (Figure 5.8D) in the CIPN rats. There were also no changes in the number of short [$F(2,6) = 0.67$, p=0.55] (Figure 5.8E) or

medium[F(2,6) = 0.74, *p*=0.52] (Figure 5.8F) length NREM sleep bouts during ZT3-ZT6 for the CIPN rats. Though during ZT15-ZT18 in the dark period the number of short (≤10s) NREM sleep bouts was significantly increased at Day 6 after oxaliplatin treatment in CIPN rats [F(2,6) = 5.15, *p*<0.05] (Figure 5.8G). This could indicate increased sleep disruption through sleep fragmentation in the CIPN rats during this ZT15-ZT18 period of the recording on Day 6. REM sleep short and medium length bouts were not affected by CIPN development at either of the ZT3-ZT6 or ZT15-ZT18 periods assessed (Figure 5.8I,J,K,L). The number of short and medium length bouts were assessed to identify if the decreased average wake bout length was associated with an increase in short awakenings, but this was not the case for the CIPN rats in this study. However, the number of short (≤10s) length NREM sleep bouts were increased at Day 6 during ZT15-ZT18 in the dark period when assessed in CIPN rats, a possible indicator of sleep in these rats being disturbed.

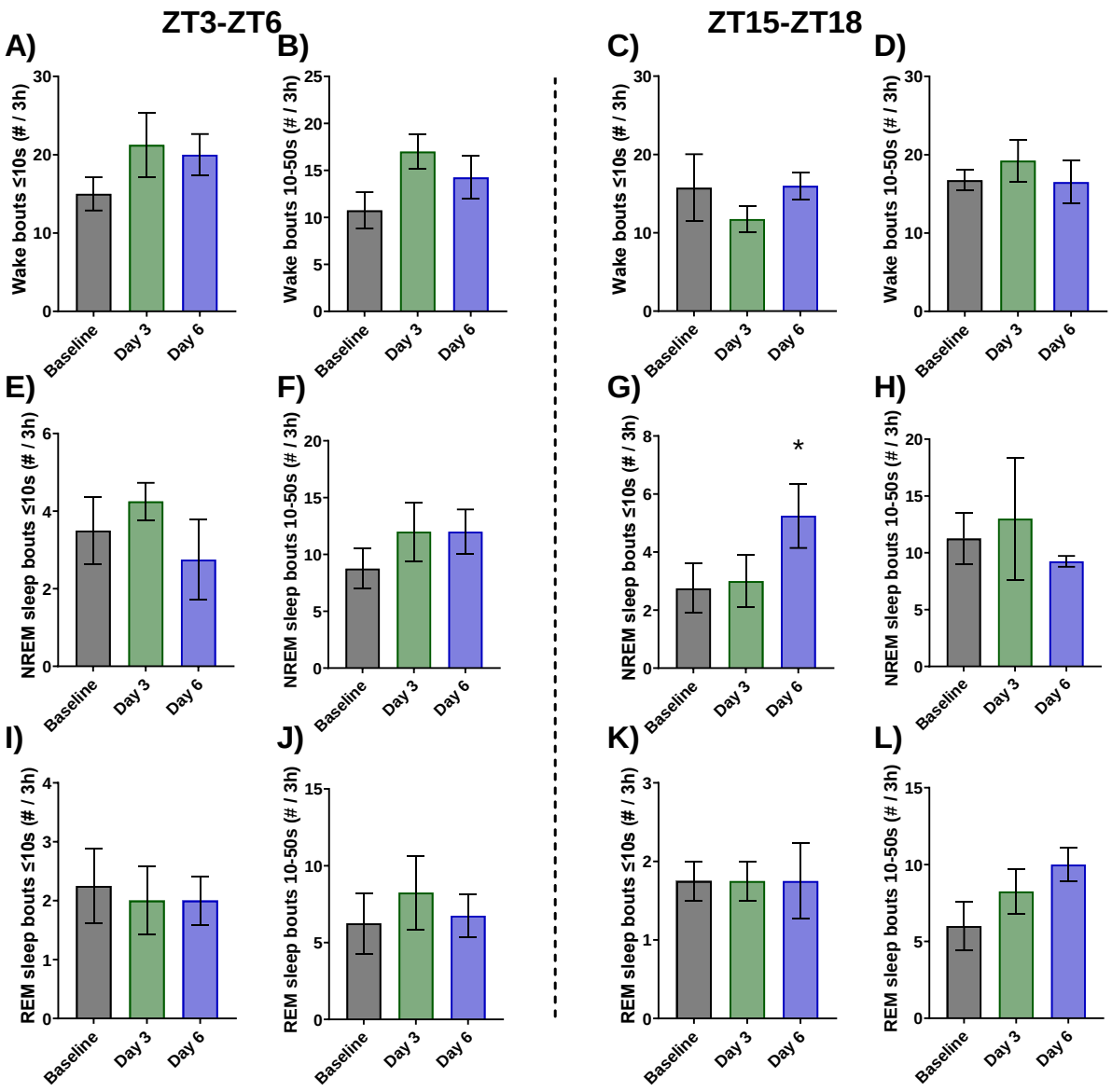

Figure 5.8) CIPN rats short (≤10s) bouts of NREM were increased at Day 6 during ZT15-ZT18 in the dark period. The total amount of short (≤10s) bouts of wakefulness (A,C), NREM sleep (E,G) and REM sleep (I,K) at Day 3 and Day 6 after oxaliplatin treatment were compared to the baseline timepoint(Day -5&-4). The total amount of 10-50s bouts of wakefulness (B,D), NREM sleep (F,H) and REM sleep (J,L) at Day 3 and 6 after oxaliplatin treatment were also compared to the baseline timepoint (Day -5&-4). For all bout lengths the total amounts were assessed during ZT3-ZT6 in the light period (A,B,E,F,I,J) and ZT15-ZT18 in the dark period (C,D,G,H,K,L). *p<0.05 vs baseline. All data is reported as mean ± SEM, n=4 (A-L).

5.3.4 CIPN development decreased EEG power particularly theta power (NREM sleep/wakefulness), sigma power (NREM/REM sleep) and gamma power (NREM sleep).

After establishing that CIPN development caused limited sleep/wake behavioural changes in the rats, the changes in EEG power spectra were assessed with the goal to better understand any functional differences in brain activity before and after CIPN development in the rats. The EEG power spectral data suggested general trends such as decreased low frequency EEG power particularly during wakefulness and NREM sleep (Figure 5.9). The data also suggested that NREM sleep EEG gamma power decreased during ZT15-ZT18 in the dark period (Figure 5.10).

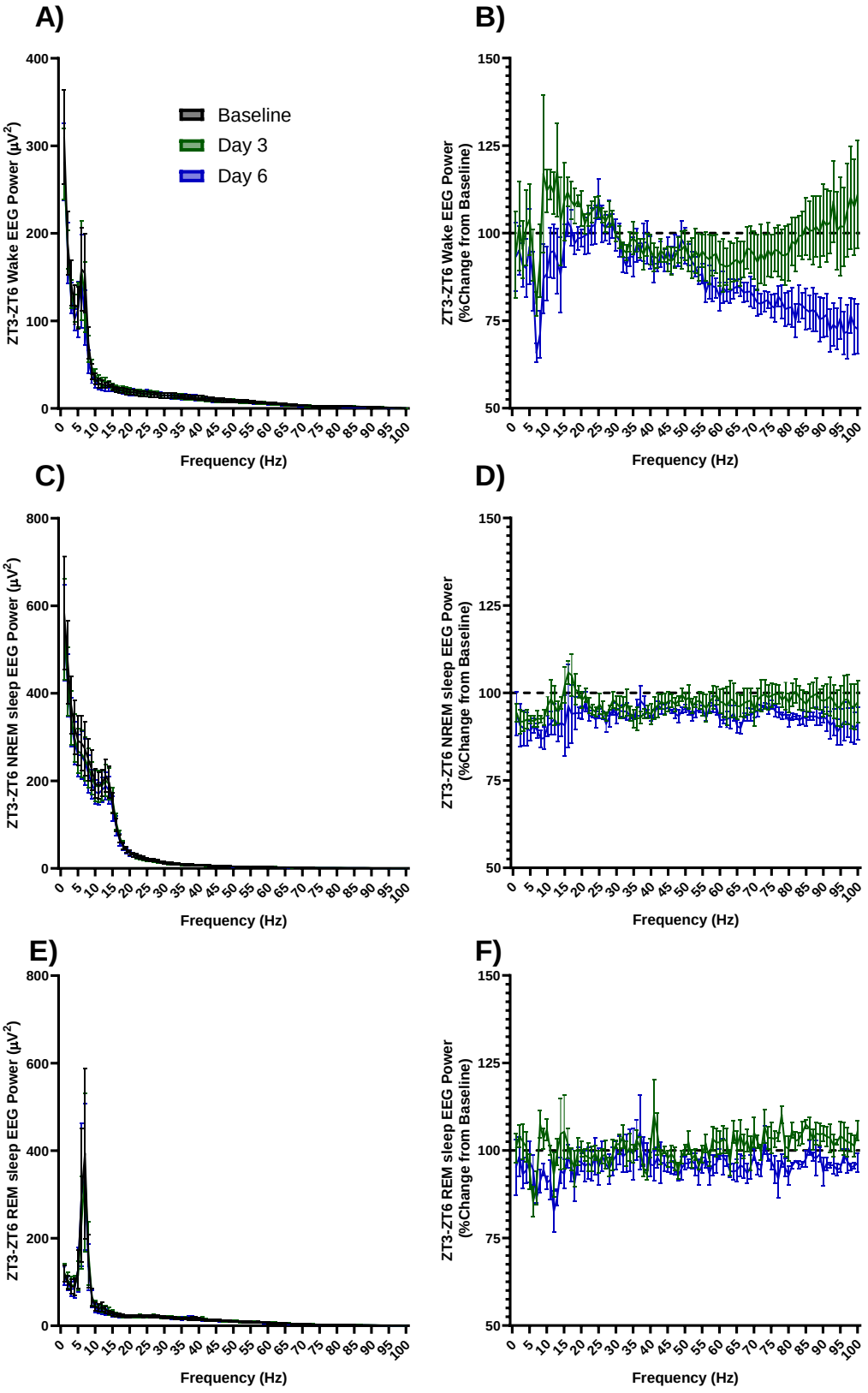

Figure 5.9) Changes in the EEG power spectra of CIPN rats during ZT3-ZT6 in the light period. EEG power spectrum during wakefulness (A), NREM sleep (C) and REM sleep (E) on baseline recording days (Day -5&-4), Day 3 and 6 after oxaliplatin treatment in CIPN rats. The percentage changes from baseline (Day -5&-4) in EEG power spectra at Day 3 and 6 after oxaliplatin treatment during wakefulness (B), in NREM sleep (D) and REM sleep (F). All data is reported as mean ± SEM, n=4 (A-F). No statistical comparisons conducted.

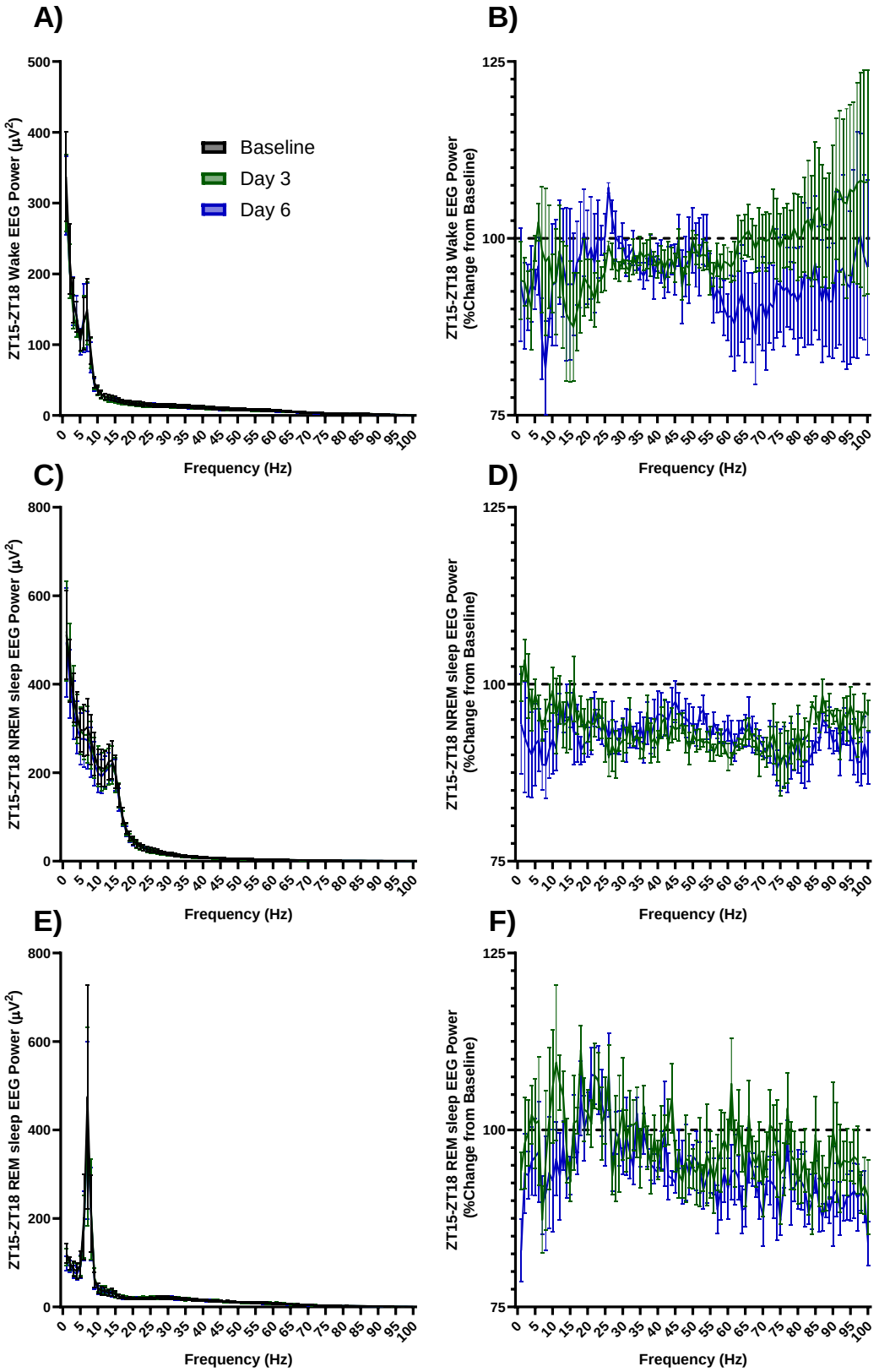

Figure 5.10) Changes in the EEG power spectra of CIPN rats during ZT15-ZT18 in the dark period. EEG power spectrum during wakefulness (A), NREM sleep (C) and REM sleep (E) on baseline recording days (Day -5&-4), Day 3 and 6 after oxaliplatin treatment in CIPN rats. The percentage changes from baseline (Day -5&-4) in EEG power spectra at Day 3 and 6 after oxaliplatin treatment during wakefulness (B), in NREM sleep (D) and REM sleep (F). All data is reported as mean ± SEM, n=4 (A-F). No statistical comparisons conducted.

Based on previous reports from preclinical neuropathic pain studies and human CIPN NFB interventions, EEG theta and beta power were expected to increase whilst alpha power was expected to decrease in the CIPN rats during wakefulness. However, when the impact of CIPN development on EEG power bands was assessed during ZT3-ZT6 in the light period it found that power theta (4-8Hz) decreased during wakefulness and alpha and beta power were not altered. Specifically during ZT3-ZT6 in the light period whilst CIPN rats were awake EEG theta power at Day 6 decreased by 17.5% compared with baseline in the CIPN rats [$F(2,6) = 15.79$, p=0.004] (Figure 5.11D). All other EEG power bands during wakefulness including delta (Figure 5.11A), alpha (Figure 5.11G), beta (Figure 5.11J) and gamma (Figure 5.11M) were not altered after CIPN development in rats at either Day 3 or Day 6. As such none of the anticipated increase in theta and beta power or the decrease in alpha power occurred in CIPN rats during wakefulness.

The EEG power spectra of CIPN rats was also assessed during NREM and REM sleep to identify any changes that may relate to sleep quality. During NREM sleep EEG theta power was reduced as well as sigma (8-12Hz) power decreased during NREM and REM sleep in CIPN rats. In particular whilst CIPN rats were in NREM sleep during ZT3-ZT6 delta power trended non-significantly (p=0.10) towards a decrease at Day 6 which was 10% lower than during the baseline recordings [$F(2,6) = 2.67$, p=0.15] (Figure 5.11B). NREM sleep theta power significantly decreased at both Day 3 and Day 6 after oxaliplatin treatment by ~10% in CIPN rats during ZT3-ZT6 [$F(2,6) = 9.88$, p=0.01] (Figure 5.11E). Furthermore EEG sigma power decreased at Day 6 compared to baseline by >10% during NREM sleep [$F(2,6) = 5.45$, p=0.04] (Figure 5.11H). Together these changes along with a lack of any change in NREM sleep beta (Figure 5.11K) or gamma (Figure 5.11N) EEG power, indicated a general reduction in NREM sleep low frequency EEG power after CIPN development during ZT3-ZT6 in the light period. REM sleep EEG power in CIPN rats was largely unaffected during the ZT3-ZT6 in the light period with only sigma power at Day 6 reduced by 9% [$F(2,6) = 7.56$, p=0.02] (Figure 5.11I). All other REM sleep EEG power including delta (Figure 5.11C), theta (Figure 5.11F), beta (Figure 5.11L) and gamma (Figure 5.11O) bands were not altered at Day 3 or Day 6 in the CIPN rats during ZT3-ZT6. Overall, during NREM sleep low frequency EEG power was reduced, whilst during REM sleep this was limited to sigma power reducing in the CIPN rats.

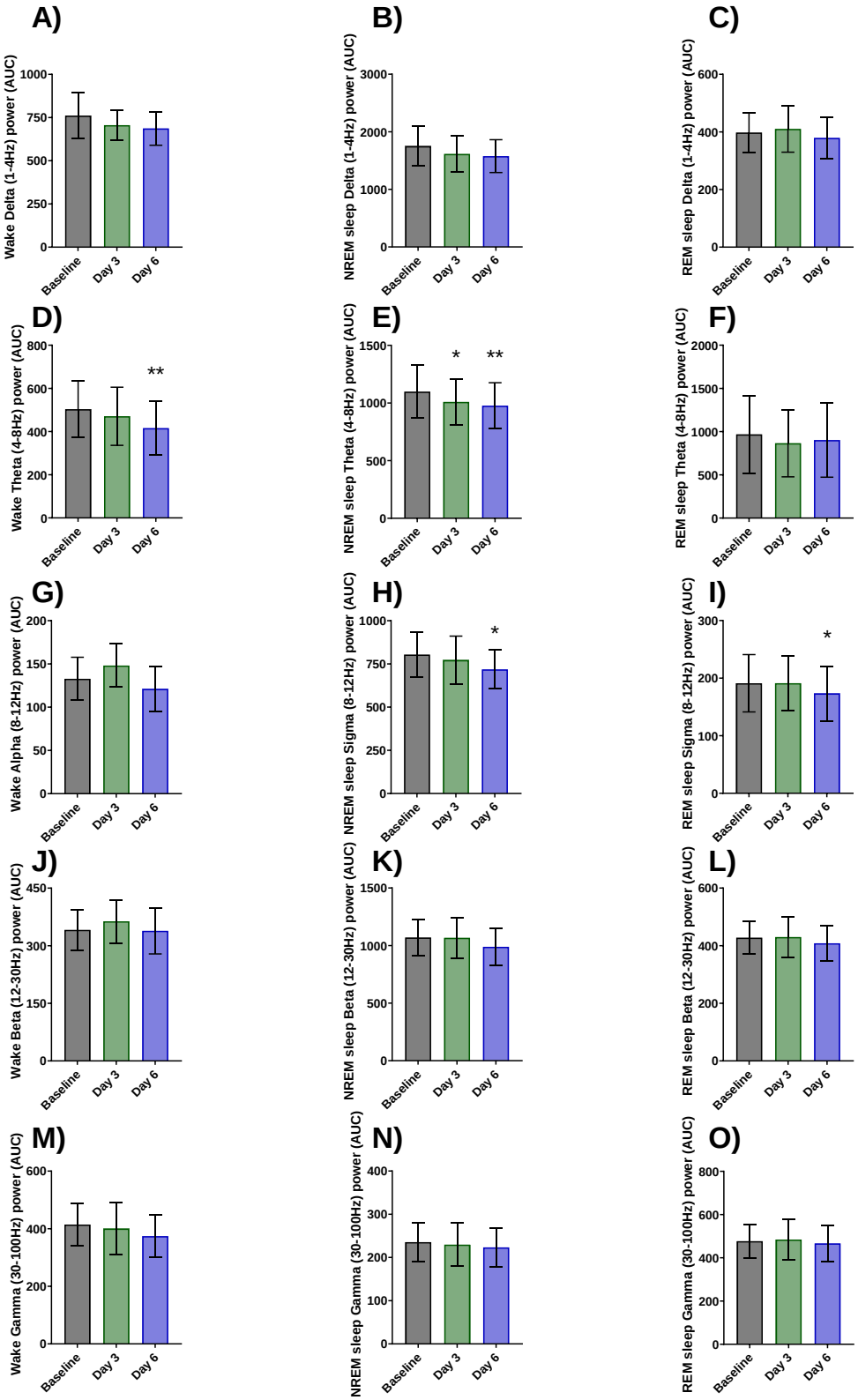

Figure 5.11) Wake and NREM sleep theta power as well as NREM and REM sleep sigma power were decreased in CIPN rats during the ZT3-ZT6 in the light period. The total area under the curve (AUC) of the EEG power spectra in the delta (1-4Hz) (A,B,C), theta (4-8Hz) (D,E,F), alpha/sigma (8-12Hz) (G,H,I), beta (13-30Hz) (J,K,L) and gamma (30-100Hz) frequency bands were assessed in CIPN rats. The change in each frequency band were calculated during either wakefulness (A,D,G,J,M), NREM sleep (B,E,H,K,N) or REM sleep (C,F,I,L,O) throughout ZT3-ZT6 in the light period. *p<0.05, **p<0.01 vs baseline. All data is reported as mean ± SEM, n=4 (A-L).

The effects of CIPN development on EEG power were assessed during ZT15-ZT18 in the dark period. None of the changes identified during ZT3-ZT6 in the light period or the anticipated changes in wake EEG power occurred during ZT15-ZT18 during the dark period, only NREM sleep gamma power decreased after CIPN development. Specifically, during wakefulness there was no effect of CIPN development on any of the EEG frequency bands analysed (Figure 5.12A,D,G,J,M). Whilst CIPN rats were in NREM sleep only gamma power significantly decreased compared to baseline with both Day 3 and 6 decreased by 7% [$F(2,6) = 7.28$, p=0.02] (Figure 5.12N). None of the other EEG power bands were affected by CIPN development in the rats during ZT15-ZT18 in the dark period (Figure 5.12B,E,H,K). This was very different from during ZT3-ZT6 in the light period where delta, theta and sigma power reduced during NREM sleep in the CIPN rats (Figure 5.11). Much like during wakefulness there was no effect of CIPN development on any of the EEG frequency bands analysed whilst CIPN rats were in REM sleep throughout ZT15-ZT18 in the dark period (Figure 5.12C,F,I,L,O). Overall, this demonstrated that the none of the changes seen in EEG power during ZT3-ZT6 were conserved during ZT15-ZT18 in the dark period with only NREM sleep gamma power decreased during this period in CIPN rats.

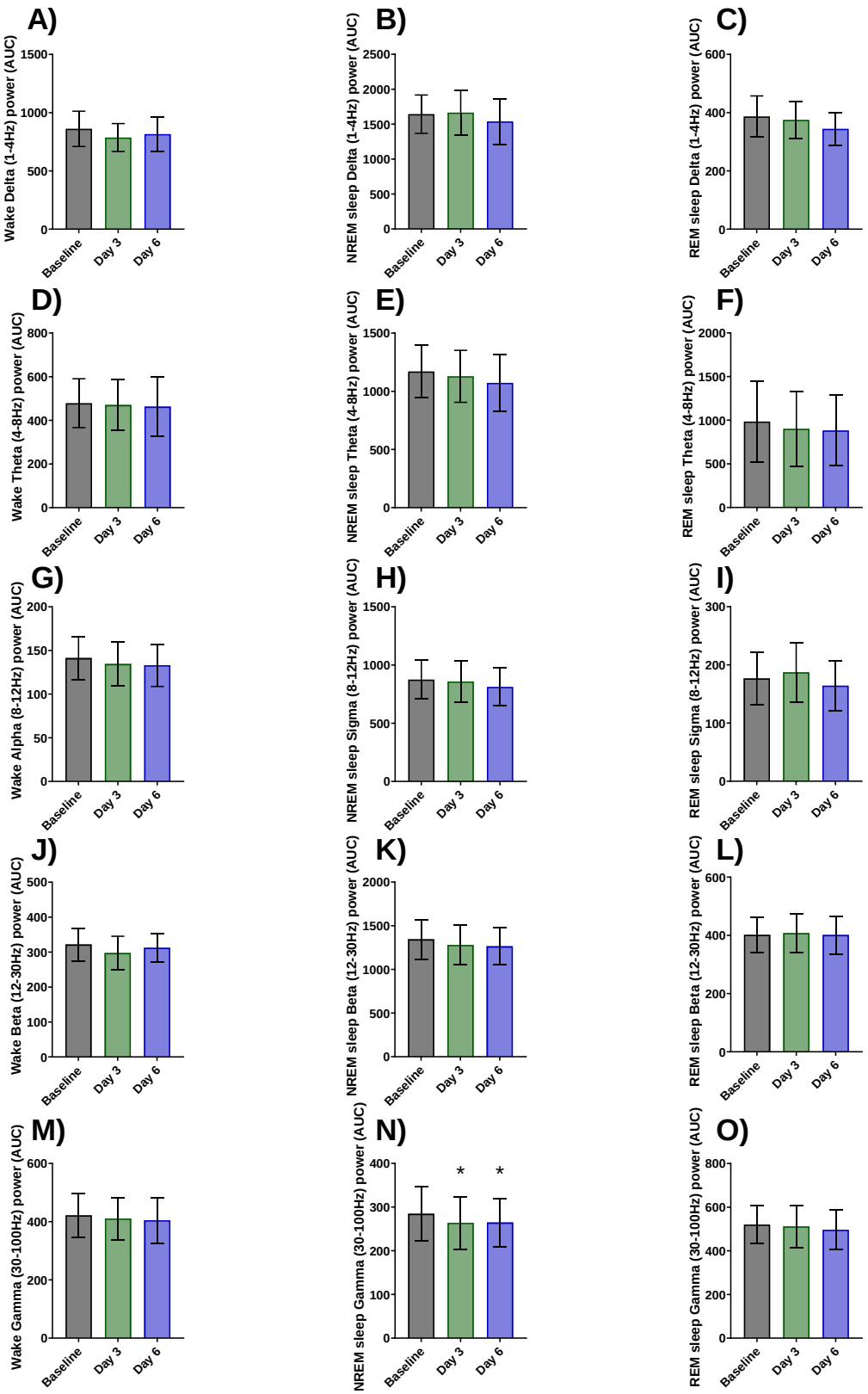

Figure 5.12) NREM sleep gamma power decreased in the CIPN rats during ZT15-ZT18 in the dark period. The total area under the curve (AUC) of EEG power spectra in the delta (1-4Hz) (A,B,C), theta (4-8Hz) (D,E,F), alpha/sigma (8-12Hz) (G,H,I), beta (13-30Hz) (J,K,L) and gamma (30-100Hz) frequency bands was assessed in CIPN rats. The change in each frequency band was calculated during either wakefulness (A,D,G,J,M), NREM sleep (B,E,H,K,N) or REM sleep (C,F,I,L,O) throughout ZT15-ZT18 in the dark period. *p<0.05 vs baseline. All data is reported as mean ± SEM, n=4 (A-L).

5.4 Discussion

Many patients undergoing platinum or taxanes-based chemotherapy treatment experience CIPN, a painful condition and dose limiting side effect that can alter anti-cancer treatment plans. Current analgesic strategies to reduce this CIPN, and maintain the prescribed chemotherapy treatment are limited, often with extensive side effect profiles (Cersosimo, 2005). Therefore, new treatments for CIPN are needed. One possible cause for the lack of new analgesic development has been the limited translatability from rodent models of CIPN that are used for screening novel analgesics into human clinical trials (Fisher et al., 2021; Tappe-Theodor et al., 2019). These studies use thermal or mechanically based evoked endpoints that measure reflexes and are subjectively assessed by a human observer. Thus, identifying an objective non-evoked endpoints such as changes in sleep/wake behaviour and EEG recordings would improve the translatability of current preclinical endpoints for CIPN.

5.4.1 Oxaliplatin administration caused transient chemotherapy induced neuropathy (CINP) and bodyweight loss development.

A primary use of the single dose oxaliplatin model is to understand the development of transient CIPN and attempt to reverse this CIPN with novel treatments. Of the 9 rats administered a single 10mg/kg oxaliplatin dose in this study, only 4 rats developed cold allodynia at Day 4 (Figure 5.4B). This was much lower than the 100% successful development of mechanical and thermal allodynia that has been previously reported when using the single dose oxaliplatin model (Ling, Coudoré-Civiale, et al., 2007; Ling et al., 2008). A key reason for the limited success with inducing cold allodynia in this study is likely the advanced age of the rats used in this study (~8 months) compared with the age of the rats typically used in preclinical studies (~2 months) (Jackson et al., 2017; Kim et al., 2017; Wang-Fischer & Garyantes, 2018). Despite the lower than anticipated development of cold allodynia, the rats that did develop cold allodynia had a paw withdrawal latency 67% lower than at baseline. This was very similar to the 69% maximal development of cold allodynia identified by Ling et al. (2007) when using a single dose oxaliplatin rat model (Ling, Coudoré-Civiale, et al., 2007). The development of cold allodynia was also consistent with reports from the spared nerve injury (SNI) and spinal nerve ligation rat models that also developed a ~60-70% reduction in paw withdrawal latency when using the 15°C cold plate test (Allchorne et al., 2005). Therefore, the 4 rats that reached a >50% reduction in paw withdrawal latency at Day 4 were termed as having developed cold allodynia and could be used as a model of CIPN development in this study.

A key feature of the single dose oxaliplatin model is the CIPN that develops is transient in nature (Ling, Coudoré-Civiale, et al., 2007; Ling et al., 2008), when compared with the multiple dose oxaliplatin model where animals develop a chronic form of neuropathic pain (Ling, Authier, et al., 2007; Xiao et al., 2012). In this study the paw withdrawal latencies for the 4 rats that developed CIPN at Day 4 returned to baseline levels by Day 9&11 (Figure 5.4C). This is similar to previous reports in the single dose oxaliplatin rat model that CIPN is maintained for 8 days after oxaliplatin treatment (Ling, Coudoré-Civiale, et al., 2007). The transient nature of the CIPN in this study is also similar to that experienced by patients undergoing oxaliplatin treatment (Cersosimo, 2005). This confirmed the successful development of a transient CIPN model in 4 of the 9 rats administered 10mg/kg oxaliplatin. These rats were referred to as CIPN rats and further assessed for the development of EEG and sleep/wake behavioural changes.

In this study, oxaliplatin treated rats progressively lost ~5% bodyweight throughout the 14 days after oxaliplatin (10mg/kg, s.c.) administration (Figure 5.5). One of the primary reasons for selecting the transient single dose oxaliplatin model over the chronic multiple dose oxaliplatin model was due to reduced chance of bodyweight loss (Ling, Authier, et al., 2007; Ling, Coudoré-Civiale, et al., 2007; Ling et al., 2008; Xiao et al., 2012). Previous reports suggested that rats administered a single dose of 3-12mg/kg oxaliplatin should not lose bodyweight compared to control rats (Ling, Coudoré-Civiale, et al., 2007; Ling et al., 2008) whilst the multiple dose oxaliplatin model would be expected to (Ling, Authier, et al., 2007; Xiao et al., 2012). Therefore, to limit the possibility of health complications and excessive weight loss from repeated administration of oxaliplatin the single dose model was selected. In this study it was found that across two weeks oxaliplatin treated rats lost 5% bodyweight compared to Day 0 and were on a downwards trajectory. Thus confirming the correct selection of the transient model as this bodyweight loss likely would have been amplified by using the multiple dose model. The starting bodyweight of the rats in this study (625-875g) was much higher than those used by others (150-175g) (Ling, Coudoré-Civiale, et al., 2007; Ling et al., 2008) and was likely the cause of the difference in the tolerability of the single oxaliplatin dose. Older rats were used in this study as they had previously been implanted for other sleep/wake behaviour and/or evoked potential studies. This reduced the number of rats undergoing extensive EEG/EMG wireless transmitter implantation and conformed with the 3R's of reduction (NC3Rs, n.d.). Therefore, future studies using oxaliplatin induced models of CIPN could avoid using older animals to ensure CIPN development and limit bodyweight loss.

5.4.2 Limited effects of CIPN development on sleep/wake amounts.

Sleep disruption is frequently reported by neuropathic pain patients including those experiencing CIPN during chemotherapy treatment (Guntel et al., 2021; Tofthagen et al., 2013). For CIPN patients this includes increased sleep latency (time to fall asleep), decreased sleep duration (total amount of time spent asleep), increased sleep disturbances (frequent awakenings) and reduced sleep efficiency (proportion of time in bed spent sleeping) (Mahfouz et al., 2024). For patients with CIPN induced sleep disruption they often report greater levels of impact on their social lives, reduced physical function and greater impacts on their mental health such as depression when compared to patients experiencing CIPN without sleep disruptions (Mahfouz et al., 2024). Therefore, quantifying the development of sleep/wake changes in a rodent CIPN model could be useful for identifying treatments to improve sleep disturbances in CIPN patients.

Oxaliplatin treated rats that developed CIPN in this study did not show any significant changes in sleep or wakefulness amounts across either of the ZT3-ZT6 or ZT15-ZT18 periods assessed. However, there were trends towards decreased amounts of wakefulness and increased amounts of NREM sleep during ZT3-Z6 in the light period (Figure 5.6). Rodents are active during both the day and night with greater amounts of time spent awake during the night. Their sleep is also polyphasic meaning they spend more than two periods of time per 24 hours sleeping, as such they spend time during both the light and dark periods asleep and awake (Rayan et al., 2022). Thus the trend towards decreased wakefulness and increased NREM sleep during ZT3-ZT6 in the light period occurred when the CIPN rats would typically spend more time asleep. This trend towards increased NREM sleep at the expense of wakefulness does not conform to the human phenotype of CIPN patients spending less time asleep (Mahfouz et al., 2024). Therefore, the trends towards increased NREM sleep and decreased wakefulness were unexpected in this study and have highlighted a reduced translatability for sleep/wake changes in CIPN rat studies.

Although these are the first results from a preclinical CIPN model on sleep/wake behaviour there is extensive research in surgically induced models of neuropathic pain. The results from surgical pain models typically report either no change in sleep/wake amounts (Alexandre et al., 2024; Kontinen et al., 2003; Leys et al., 2013) or increased wakefulness at the expense of sleep (Andersen & Tufik, 2003; Ho et al., 2024). One study has identified that during the dark period CCI mice spent more time in NREM sleep at expense of wakefulness (Alexandre et al., 2024). One cause of these differences could be discrepancies in environmental conditions, such as the type of bedding can impact sleep/wake amounts in preclinical neuropathic pain models (Tokunaga et al., 2007). Therefore, it is possible that the increased time spent in NREM sleep is a feature of the CIPN rat model. Though, more extensive and repeated characterisation is needed to understand if this is repeatable or if it is heavily influenced by the environmental factors that differ between research facilities.

5.4.3 Limited effects of CIPN development on sleep and wakefulness bouts.

Sleep disruption including more frequent awakenings is a common complaint from neuropathic pain and CIPN patients (Guntel et al., 2021; Mahfouz et al., 2024; Tofthagen et al., 2013). Additionally, sleep disruption in the form of changes to sleep and wakefulness bouts is consistently reported in preclinical neuropathic pain models. The length of each sleep/wake bout, the total number of bouts that occur and the number of short bouts of each sleep state are all often used as a measure of sleep fragmentation and hence sleep disruption in rodents (Alexandre et al., 2024; Andersen & Tufik, 2003; Ho et al., 2024; Kantor et al., 2023). Therefore, it was unexpected that in this study there were limited indications of sleep fragmentation. Assessing the average length and number of sleep/wake bouts only identified a trend towards wakefulness bouts being less consolidated in the CIPN rats. As the decreased average wake bout length was not accompanied by any changes in NREM or REM sleep bouts it does not appear that the CIPN rats sleep was fragmented (Summa et al., 2024). There was a 50% decrease in the average length of wakefulness bouts during ZT3-ZT6 in the light period that was close to being significant (p=0.07) (Figure 5.7). This indicated that wakefulness bouts were on average shorter in length and therefore less consolidated (Frank et al., 2017). Nevertheless, this decrease in the average length of wakefulness bouts did not come with an increase in short bouts of wakefulness, that could have indicated an increase in brief arousals (Figure 5.8). Increased brief arousals of <15s have previously been reported in rats after CCI surgery for at least 3 weeks (Andersen & Tufik, 2003). Additionally, increased brief arousals and NREM sleep fragmentation have been reported in the SNI and CCI mouse models (Alexandre et al., 2024). Therefore, it is unlikely that the less consolidated wakefulness bouts in the CIPN rats would provide a useful endpoint for CIPN induced sleep disruption as this did not occur primarily through brief arousals in this study.

Despite there being no changes in the overall NREM or REM sleep bouts in CIPN rats that would indicate sleep fragmentation the number of short NREM sleep bouts increased during ZT15-ZT18 in the dark period in this study (Figure 5.8). This increased short NREM sleep bouts could indicate the development of sleep fragmentation occurring at Day 6 after oxaliplatin treatment in the CIPN rats. However, as there was no change in the overall average length or number of NREM sleep bouts the generalisability of this increased number of short (≤10s) bouts only at Day 6 during ZT15-ZT18 is limited. There has been previous reported data of an increased number of overall NREM sleep bouts in the sciatic nerve crush injury and common peroneal nerve ligation mouse models (Ho et al., 2024). Additionally, in these sciatic nerve crush injury and common peroneal nerve ligation mouse models the length of NREM sleep bouts had a corresponding decrease (Ho et al., 2024). Further evidence from Alexandre et al. (2024) indicated that the development of sleep fragmentation through

increased number and decreased length of NREM sleep bouts occurred in three surgical models of neuropathic pain, but not in the CFA model of inflammatory pain or the capsaicin model of acute pain (Alexandre et al., 2024). Therefore, the lack of definitive sleep fragmentation in this CIPN rat model indicated that the development of sleep fragmentation and sleep disruption might be limited to surgically induced models of neuropathic pain. Though further research into a multiple dose oxaliplatin model of chronic CIPN would help to identify if the lack of sleep fragmentation is limited to the transient single dose model of CIPN.

5.4.4 CIPN development decreased EEG power particularly theta power (NREM sleep/wakefulness), sigma power (NREM/REM sleep) and gamma power (NREM sleep).

Various changes in EEG power during wakefulness have been reported to be associated with neuropathic pain. Specifically, CIPN has been linked with a decrease in alpha and increase in beta EEG power. This was demonstrated when CIPN patients increasing alpha and decreasing beta power using NFB were able to reduce their pain (Prinsloo et al., 2017, 2018). In this study alpha and beta power were not altered by CIPN development in rats during wakefulness at either ZT3-ZT6 or ZT15-ZT18 (Figure 5.11, 5.12). Additionally theta power has been reported to increase in neuropathic pain patients and in surgically induced preclinical neuropathic pain models (Koyama, LeBlanc, et al., 2018; Mussigmann et al., 2022; Stern et al., 2006; Vučković, Gallardo, et al., 2018). Increased theta power was not found in CIPN rats in this study and theta power was paradoxically decreased at Day 6 during ZT3-ZT6 (Figure 5.11). This was an unexpected result as increased theta power is one of the more consistently reported changes in EEG power for neuropathic pain. Therefore, it appears that alterations in EEG power during wakefulness in the CIPN rat model do not reflect the development of neuropathic pain.

Whilst EEG power does not appear to be a useful neuropathic pain endpoint in CIPN rats, it is also regularly used to assess sleep, particularly low frequencies during NREM sleep. In this study low frequency EEG power was decreased in CIPN rats during NREM sleep. Specifically, delta power decreased (though not significantly p=0.10) and theta power significantly decreased (Figure 5.11). Though both changes were of a similar magnitude (10% decrease). Increased delta power during NREM sleep has been associated with increased sleep quality (Long et al., 2021). Therefore, the decreased low frequency EEG power during NREM sleep in the CIPN rats may indicate decreased sleep quality. This reduced low frequency power in combination with the indication that CIPN rats spent more time asleep and less time awake (Figure 5.6) suggests that the CIPN rats slept more but that this sleep was of lower quality.

A possible cause of some of the EEG power changes in this study included the decreased theta power during wakefulness, gamma power during NREM sleep and sigma power during NREM and REM sleep was alterations in cognition. Chemotherapy treatment itself can be associated with cognitive impairment termed chemo-brain (Liu et al., 2022). Part of this cognitive impairment includes a disruption of learning, attention and working memory which often leads to subtle but impactful changes on quality of life (Ahles & Saykin, 2007). Chemotherapy treatment has been associated with decreased theta power in the hippocampus that is thought to be associated with impaired learning and may have led to these changes in theta power during wakefulness in this study (Nokia et al., 2012). Gamma oscillations during sleep are considered to relate to memory consolidation, potentially through coupling with sleep spindles (usually sigma band) (Dalal et al., 2010; Weber et al., 2021). This could mean that the decreased NREM sleep gamma power, along with decreased NREM and REM sleep sigma power, may be related to chemotherapy induced

alteration in memory and cognitive impairment (Dalal et al., 2010; Weber et al., 2021). These types of cognitive impairments have previously been demonstrated in single dose oxaliplatin induced models of CIPN where rats administered 6mg/kg oxaliplatin displayed cognitive impairment in novel object recognition and conditioned fear response tasks (Johnston et al., 2017). This demonstrates that some of the EEG power changes particularly decreased wake (theta), NREM sleep (sigma, gamma) and REM sleep (sigma, gamma) power may have occurred due to oxaliplatin induced cognitive impairment rather than through CIPN related changes.

Overall, EEG power changes did not appear to be a useful neuropathic pain endpoint in the transient single dose CIPN model. Though decreased low frequency NREM sleep power may have indicated reduced sleep quality in CIPN rats. Additionally, chemotherapy related changes in cognition could have caused confounding alterations in EEG power particularly during NREM and REM sleep.

5.4.5 Limitations, improvements and future work.

Whilst this study provides some of the first results for the effects of CIPN on sleep/wake and EEG recording changes in a preclinical model, it does have limitations that impact the generalisability of results. A primary limitation of this study is the low number of animals (only 4 out of 9 rats) that developed CIPN which may have increased the chance of both false positive and false negative results (Faber & Fonseca, 2014). This likely would have left the study underpowered to detect changes in sleep/wake and EEG power that otherwise could have been detected with a larger sample size, especially those that showed trends towards significance. Using a cohort of rats at a lighter bodyweight that aligns more closely with previously published CIPN studies may achieve the expected >90% development rate of CIPN following oxaliplatin administration. Additionally, a multi-dose regimen of oxaliplatin administration could be explored to compare the effects in a chronic CIPN phenotype. However, as the rats in this study showed significant weight loss after a single dose, this experimental design would again require the use of lighter weight/younger rats to better tolerate the oxaliplatin administration and associated weight loss.

In this study only two 3 hour-long segments [3 to 6 hours after light onset (ZT3-ZT6) and 3 to 6 h after dark onset (ZT15-ZT18)] were visually scored and assessed. A preliminary analysis of the automatic scoring using a SleepSign scoring algorithm was used to select ZT3-ZT6 and ZT15-ZT18 as the time periods with the potential for the greatest differences between the pre and post oxaliplatin recordings. However, as these areas identified only minor differences in sleep/wake behaviour and EEG changes further manual scoring and analysis was determined to be unlikely to provide greater insight into the sleep/wake changes of the CIPN rats. To better understand the potential effect of homeostatic and circadian processes on CIPN induced changes in EEG and sleep/wake behaviour, future studies should assess the entire 24 hour periods in the rat (Borbély et al., 2016). Particularly as rodents are typically more active during the first period of the dark period (Steel et al., 2024) there may be differences in their experience of evoked pain as they explore their environment (Tokunaga et al., 2007). However, towards the end of the dark period when the homeostatic drive for sleep increases and locomotion decreases, changes in sleep/wake and EEG may be more likely to be driven by spontaneous pain (Borbély et al., 2016). As such future work should consider assessing both the early and late stages of the light and dark period to identify the potential differences in EEG measures of sleep/wake homeostasis, EEG power spectra or sleep/wake amounts between these time periods. This that could help to identify sleep/wake and EEG endpoints of neuropathic pain in preclinical CIPN models.

The age/weight of the rats used in this study could be considered a limitation, particularly as this may have caused the lack of CIPN development in 5 of the 9 rats at Day 4. However, cancer patients are frequently diagnosed and treated later in life, which does not reflect the younger respective age of rodents used in preclinical studies (Siegel et al., 2017). Therefore, the increased age of the rats used in this study would better reflect the true situation of patients undergoing chemotherapy treatment.

One other limitation of CIPN EEG studies is the difficulty of separating any changes caused by oxaliplatin treatment from CIPN specifically. Oxaliplatin treatment has been associated with cognitive dysfunction termed chemo-brain that may have caused some of the EEG spectral power changes seen in this study (Liu et al., 2022). Future studies into the effect of neuropathic pain on sleep/wake and EEG changes could look to use a model with less potential impact on EEG power spectral analysis. However, this would continue to perpetuate the lack of understanding of the impacts of CIPN on sleep/wake and EEG power changes for which further research is needed. Thus, a better understanding of the impacts of oxaliplatin treatment, possibly at a lower non-CIPN dose would be useful to distinguish between oxaliplatin induced and CIPN induced changes. Additionally, a model that maintains a longer period of neuropathic pain development would allow for repeated testing to confirm the development and maintenance of the changes and trends seen in this study. This would also allow for the assessment of analgesic reversal of neuropathic pain induced changes in sleep/wake and EEG recordings.

5.5 Conclusions

In conclusion, oxaliplatin treatment and subsequent CIPN development caused limited changes to sleep/wake behaviour and EEG measures that are unlikely to prove useful as preclinical neuropathic pain endpoints. A single 10mg/kg i.p. dose of oxaliplatin caused transient chemotherapy induced peripheral neuropathy (CIPN) in less than half of the >600g rats used in this study, lower than the expected >90% CIPN development that occurs in lighter (<300g) weight rats. The rats veered towards spending more time asleep than awake after CIPN development. This sleep also appeared to be of lower quality due to CIPN rats NREM sleep delta power decreasing. Wakefulness bouts were less consolidated in the CIPN rats, though this was not accompanied by any changes in sleep bouts or brief awakenings that would have confirmed sleep fragmentation. EEG power during wakefulness did not demonstrate any of the anticipated changes of increased theta and beta power or decreased alpha power which have previously been demonstrated in human CIPN patients or other preclinical models. Though these changes in EEG power may have been overshadowed by EEG power changes that could have occurred due to oxaliplatin induced cognitive impairment, rather than through CIPN related changes. Overall, this study highlighted that changes in sleep/wake behaviour and EEG may not be suitable for use as chemotherapy induced neuropathic pain endpoints. Further investigations in a chronic model are required to confirm the preliminary findings of this study.

Chapter 6: Sleep/wake behaviour and EEG changes in the CCI rat model of neuropathic pain

6.1 Introduction

Alongside neuropathic pain models of specific metabolic disorders such as diabetes or the effects of chemotherapy, surgically induced models of neuropathic pain are some of the most routinely used (Rice et al., 2018). Surgically induced models of neuropathic pain provide some benefit over other models due to the specific physical/inflammatory damage to the nerve fibres (van der Wal et al., 2015). This can avoid the confounding factors of chemotherapy treatment and diabetes development, aiding in the isolation of the impacts of neuropathic pain development specifically. The specificity of surgical models comes about through the main pathophysiological change occurring via injury and damage to the nerve fibre, without the metabolic changes of chemotherapy or diabetes models of neuropathic pain (Berge, 2011). Surgically induced neuropathic pain in rodents often models the effects of traumatic surgical or physical injuries in human patients (Bennett et al., 2003; Challa, 2015). These surgically induced models typically focus on damaging the sciatic nerve and various models have been generated that involve ligating, transecting, or constricting this nerve at different locations (Challa, 2015).

6.1.1 Current research into sleep/wake behaviour and EEG changes in surgically induced preclinical models.

One of the oldest and most published models of surgically induced neuropathic pain is the chronic constrictive injury (CCI) model that was originally developed by Bennett and Xie (Bennett & Xie, 1988). Under anaesthesia loose ligatures of suture material are tied proximal to the trifurcation of the sciatic nerve with no transection or additional crushing injury applied to the nerve fibre (Austin et al., 2012). These ligatures cause an inflammatory immune response and oxidative stress induced injury to the sciatic nerve leading to neuropathic pain development (Tan et al., 2009). A useful utility of the CCI model is that animals present with both mechanical and thermal allodynia allowing it to be used for the screening of potential analgesic compounds (Austin et al., 2012). The development of neuropathic pain in the form of mechanical and thermal allodynia occurs as early as one day after CCI surgery and can last over four months (Chen et al., 2019; Kontinen et al., 2003). This mechanical and thermal allodynia typically only develops in the hind paw that surgery is conducted on (ipsilateral) allowing the contralateral hind paw to be used as control or reference measurement throughout the study. Animals also exhibit other behavioural characteristics after CCI surgery including guarding of the hind paw, altered posture of the affected paw and sometimes decreased locomotor activity (Austin et al., 2012; Bagriyanik et al., 2014). The CCI model has shown previous evidence of forward translation as, similarly to the STZ model, it was involved in the approval of pregabalin as a treatment for neuropathic pain (Field, Bramwell, et al., 1999).

The CCI model of peripheral neuropathic pain is easily reproducible, well characterised and frequently used for behavioural pharmacology studies (Challa, 2015). In addition to its typical use for modelling reflexive based thermal and mechanical allodynia, interests have increased around the effects of CCI surgery induced neuropathic pain on sleep/wake behaviour and electroencephalogram

(EEG) recordings. Differing results have been reported about the effects of CCI surgery on sleep/wake behaviour and EEG. For instance, some studies have found that the amount of time spent awake, in non-rapid eye movement (NREM) and rapid eye movement (REM) sleep can be affected in the CCI model, particularly with increased wakefulness during the first few weeks (Andersen & Tufik, 2003; Ho et al., 2024). However, others have reported no change in the amount of time spent asleep in the CCI model, including a long-term study by Kontinen et al. (2003) which identified no changes measuring up to 5 months after surgery (Alexandre et al., 2024; Kontinen et al., 2003; Leys et al., 2013). These changes may be influenced by environmental conditions, as Tokunaga et al. (2007) found no changes in CCI rats sleep/wake amounts until they were placed on sandpaper flooring which decreased the total time spent asleep (Tokunaga et al., 2007).

Sleep fragmentation has been explored as a measure of neuropathic pain demonstrating more consistent results. In particular, the number of arousals and disrupted NREM sleep bouts have been demonstrated in: CCI rats (Andersen & Tufik, 2003), in the sciatic nerve crush injury mouse model (Ho et al., 2024), in common peroneal nerve ligation models (Ho et al., 2024), in the spared nerve injury mouse model (Alexandre et al., 2024), CCI mouse model (Alexandre et al., 2024) and in the sciatic nerve crush mouse model (Alexandre et al., 2024). These results are consistent and the efficacy of analgesic treatment has been demonstrated on increased brief arousals in some of these models (Alexandre et al., 2024). However, it is yet to be seen if an automated scoring system is sensitive enough to detect these changes which would allow for the application in high throughput preclinical screening.

Besides changes in sleep/wake behaviour, neuropathic pain induced differences in EEG power spectra have also been characterised in the CCI rat model. Extensive work by Carl Saab's research group has described increased theta power in the CCI rat model that was reversible with 10mg/kg pregabalin analgesic treatment (Koyama, LeBlanc, et al., 2018). However, this protocol only utilises very short (<15 minute) periods of EEG recordings meaning that it should be established if increased theta power is present across extended time periods. The increased theta power identified in the CCI rat model is consistent with the findings in human neuropathic pain patients that may help to support the translatability of this measure as a neuropathic pain endpoint (Jensen et al., 2013; Krupina et al., 2020; Michels et al., 2011; Sarnthein et al., 2005; Sarnthein & Jeanmonod, 2008; Stern et al., 2006). However, increased theta power has not been identified in all preclinical neuropathic pain studies. In a similar CCI rat model, Kontinen et al. (2003) did not find any changes in the EEG power spectra frequency bands during either wakefulness or NREM sleep during a 5-month long study (Kontinen et al., 2003). Whilst increased theta power is the most commonly reported change in neuropathic pain patients, bidirectional changes in alpha power and increased beta power have also been reported (Mussigmann et al., 2022). In the partial sciatic nerve ligation mouse model, others have demonstrated increased EEG delta power that correlated with von Frey measurements of paw withdrawal threshold (Li, Ge, et al., 2019). Whilst more data has come to light about the effects of CCI surgery on sleep/wake behaviour and EEG, many of these results are conflicting, not assessed together and not reversed with analgesics. Therefore, further characterisation is needed into whether sleep fragmentation along with increased theta power (demonstrated in CCI rats and patients), increased delta power (demonstrated in partial sciatic nerve ligation mouse model), or increased beta power (demonstrated in patients) could be used as neuropathic pain endpoints in a high throughput preclinical screening application.

6.1.2 Novel analgesic test compounds with potential anti-depressive properties.

Correcting the comorbidities that come alongside neuropathic pain such as depression, anxiety and sleep disruption are just as important as treating the pain itself (Nicholson & Verma, 2004). Drugs that provide both analgesic efficacy and reduce comorbidities such as depression and sleep disruption, that worsen pain outcomes, will likely provide greater benefit to patients when compared to current treatments. Ketamine and psilocybin are two drugs that have previously shown evidence for the treatment of depression were examined further in these experiments for their impact on sleep/wake behaviour and EEG in the CCI model of neuropathic pain.

Ketamine is an N-methyl-D-aspartate (NMDA) receptor antagonist, that is approved for use as an anaesthetic agent, has shown evidence for other applications when used at a subanaesthetic dose including as an anti-depressant and analgesic (Kurdi et al., 2014). Recently, ketamine has demonstrated both clinical (Bratsos et al., 2019) and preclinical (Kantor et al., 2023) evidence for its use as a novel anti-depressant including use against preclinical models of treatment resistant depression (Kantor et al., 2023). Ketamine has also been extensively studied in a range of preclinical neuropathic pain models including the CCI model. A recent review by Velzen et al. (2021) captured the extent of this preclinical testing and highlighted the efficacy of a single administration of between 1-50mg/kg ketamine to effectively reverse neuropathic pain in the first 3 hours (Velzen et al., 2021). However, the analgesic effects of a single dose of ketamine do not last until the next day, although repeated administration can produce longer lasting analgesia in rodents (Velzen et al., 2021). In human randomised control trials ketamine has demonstrated efficacy in reducing neuropathic pain in patients, though this does come with adverse effects of discomfort and psychedelic effects (Guimarães Pereira et al., 2022). Ketamine is not yet officially licensed for use in neuropathic pain management. Although, it is still used both off label as well as at “ketamine clinics” in the USA and UK, where patients can pay for ketamine infusions (Voute et al., 2022). A key limitation for the use of ketamine is the abuse potential caused by its dissociative, hallucinogenic and reinforcing properties that have led to it become a controlled substance in most countries (Liu et al., 2016). Whilst the analgesic and antidepressant properties of ketamine appear clear, its impact on preclinical EEG based measurements of neuropathic pain have yet to be established and could provide additional supportive evidence for its clinical use.

Psilocybin has also proved to be effective as an anti-depressant treatment in recent human randomised controlled trials (Bornemann et al., 2021; Davis et al., 2021). Psilocybin (O-phosphoryl-4hydroxy-N, N-dimethyltryptamine) is a secondary metabolite isolated from over 200 different fungi with *Psilocybe Cubensis* being the most widespread (Lowe et al., 2021). It is rapidly metabolised into its active metabolite psilocin (4-hydroxy-N, N-dimethyltryptamine) which is an agonist for serotonergic 5-HT_{2A} receptors in the pre-frontal cortex (Vollenweider & Preller, 2020). A key benefit of psilocybin over other psychedelics is its safety profile which is considered to be one of the most favourable of the classic psychedelics particularly with reduced abuse potential (Hendricks et al., 2015; Ziff et al., 2022). Although both psilocybin and ketamine have anti-depressant properties, psilocybin may be superior to ketamine because of its smaller side effect profile. However, there is limited preclinical and clinical data available to support the efficacy of psilocybin in treating neuropathic pain. Some clinical results indicate that psilocybin self-medication may improve chronic pain (Bornemann et al., 2021) and that micro-dosing improved pain without the psychedelic experiences, according to a case study (Lyes et al., 2023). Preclinical data is sparse with some evidence that psilocybin improved mechanical allodynia in the formalin chronic inflammatory pain model (Kolbman et al., 2023). Whilst the only available evidence of psilocybin’s efficacy in a preclinical neuropathic pain model indicated that psilocybin reversed mechanical and thermal

sensitivity in a paclitaxel mouse model (Koseli et al., 2023). Though this report has currently only been presented in conference proceedings so should be considered as a preliminary finding. Whilst the evidence of psilocybin antidepressant properties is clear, there is limited evidence for its analgesic efficacy.

In summary, psilocybin and ketamine both show anti-depressant properties, psilocybin has a better side effect profile but there is more evidence that supports ketamine's analgesic property. Neither ketamine or psilocybin have been examined in a preclinical model of neuropathic pain using sleep/wake behaviour and EEG as endpoints. Therefore, this study aimed to identify if sleep/wake behaviour and EEG endpoints of neuropathic pain can be detected in CCI rats using an automated scoring and EEG analysis system that is suitable for high throughput preclinical screening. Additionally, this study aimed to identify if these endpoints are reversible by the first line human neuropathic pain treatment pregabalin along with the novel analgesic ketamine and potential analgesic psilocybin.

6.1.3 Aims and hypotheses.

The primary aim of this study was to identify sleep/wake and EEG changes that could be used as neuropathic pain endpoints and reversed with standard (pregabalin), novel (ketamine) and possible (psilocybin) analgesic compounds.

The classical evoked endpoint of von Frey paw withdrawal threshold was used to confirm mechanical allodynia, a standard measure of neuropathic pain onset and maintenance. This was anticipated to be reduced by CCI surgery and reversed by test compounds. The contralateral hind paw that did not have CCI surgery conducted was used an internal paired control measure.

Locomotor activity was measured to identify any reduction in CCI rat ambulation that could indicate neuropathic pain onset and could be reversed by test compounds.

Due to the conflicting results in the CCI model as to whether the amount of sleep is affected by neuropathic development, sleep/wake changes were monitored across the study. This study also assessed if this could be reversed by test compounds.

The development of sleep fragmentation was monitored as published results suggest it provides a more consistent measure of neuropathic pain induced changes in sleep/wake behaviour. The aim was to identify sleep fragmentation using an automated sleep scoring algorithm and reverse the possible changes in sleep fragmentation with the test compounds.

Since changes in EEG power spectra, particularly increased theta power have been used as a neuropathic pain endpoint in the CCI model previously, changes in EEG power spectra were monitored throughout the study and it was tested whether these changes could be reversed with the test compounds.

6.1.4 Abbreviations.

CCI – chronic constrictive injury, EEG – electroencephalogram, EMG – electromyogram, FFT – fast Fourier transformation, ZT – Zeitgeber time, REM – rapid eye movement, NREM – non-rapid eye movement, NMDA – N-methyl-D-aspartate SEM – standard error of the mean, i.p. – intraperitoneal, p.o. – oral, s.c. – subcutaneously, OFT – open field testing.

6.2 Methods

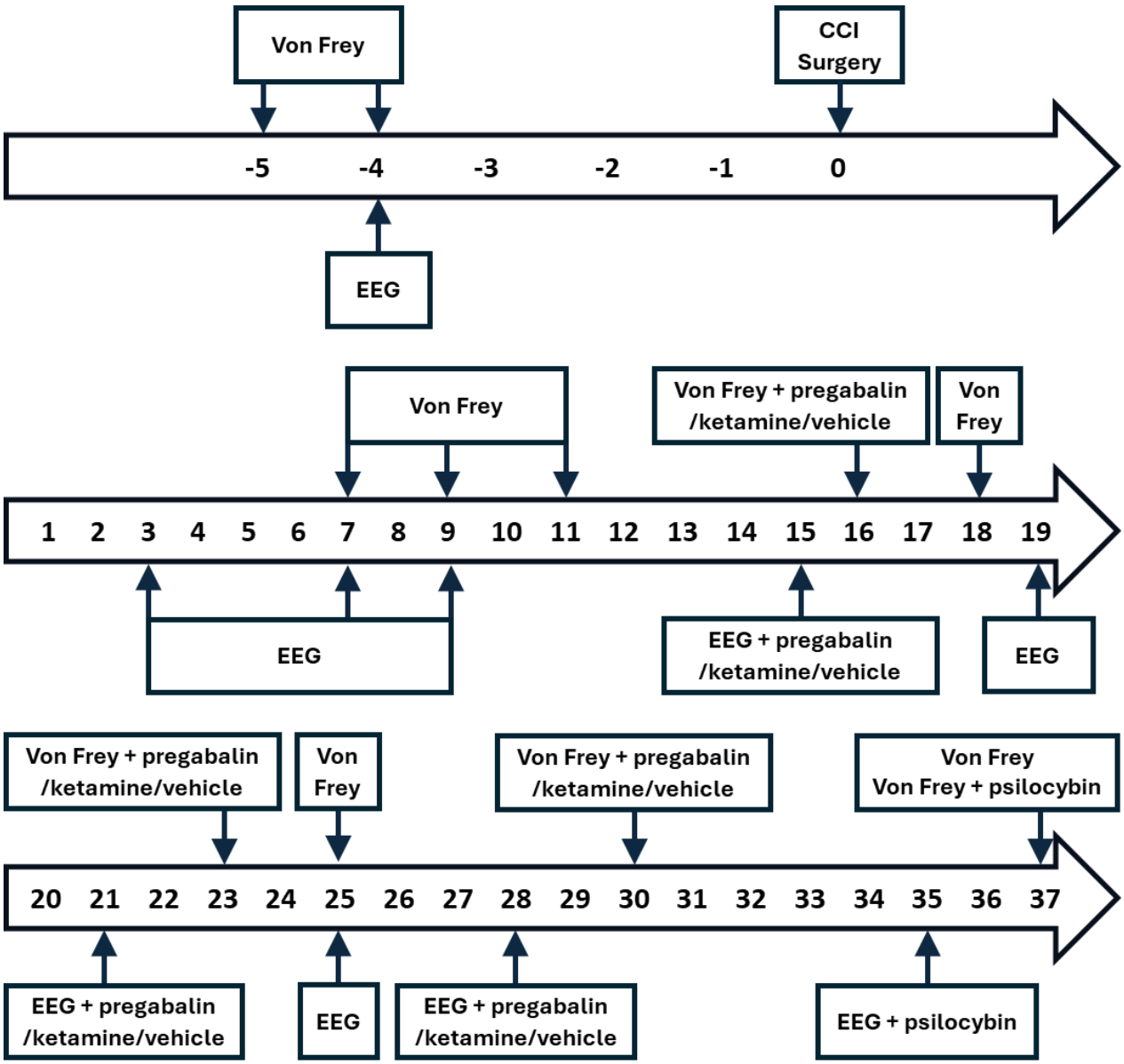

Figure 6.1) Timeline of the study depicting the days before and after CCI surgery on Day 0. The days on which von Frey paw withdrawal threshold measurements were taken, and EEG recordings were started. The timepoints that vehicle, 10mg/kg pregabalin, 10mg/kg ketamine and 3mg/kg psilocybin were administered are also denoted.

6.2.1 Ethics statement.

All research procedures/experiments were performed in accordance with Animals Scientific Procedures Act 1986 & European Directive 2010/63/EU. All studies performed were approved by the Discovery Park Animal Welfare and Ethics Review Body and comply with the home office guidelines and codes of conduct. All work was authorised under Discovery Park home office establishment licence and project licence titled: Translational pharmacology for drug discovery.

6.2.2 Animals and EEG surgery.

17 Adult male Sprague Dawley rats (180-200g) on arrival, Charles River, UK were previously surgically implanted under general anaesthesia with telemetry devices (HD-S02; Data Sciences International, USA) to measure frontoparietal EEG and electromyogram (EMG) from neck extensor muscles. EEG implantation surgery was conducted as described in Chapter 5 to implant EEG and EMG electrodes for recording biopotentials from Sprague Dawley rats. These rats were previously used in sleep/wake behaviour and/or evoked potential studies at Transpharmation LTD and 17 were approved for re-use in the present study by a veterinarian. Thank you to the technical staff at Transpharmation LTD for conducting the EEG surgery.

6.2.3 Environmental conditions.

Rats were housed in groups of 2 or 3 with environmental enrichment provided and regularly replaced and maintained on a 12:12 h light-dark cycle [lights on: 08:00 / Zeitgeber time 0 (ZT0)] throughout the study. A constant temperature (21 ± 1°C) and relative humidity (55±15%) was maintained in the housing environment with food and water available ad libitum. During EEG recordings, rats were placed in individual recording chambers in a sound-attenuated room with a 12:12 h light-dark cycle [lights on at 08:00 (ZT0), lights off at 20:00 (ZT12)], constant temperature (21 ± 1°C) and relative humidity (55±15%), with food and water available ad libitum.

6.2.4 CCI surgery.

All rats (600-860g at time of CCI surgery) were administered 5mg/kg carprofen (Zoetis, UK) subcutaneously (s.c.) 30-minutes prior to surgery conducted on Day 0 (Figure 6.1). Rats were inducted with ventilated isoflurane anaesthesia mixed with oxygen (3:1, 1L/min) and placed on a warming pad to maintain body temperature. The site of the incision in the upper thigh of the left hind leg was shaved clean of fur and sterilised with HibiScrub (Chlorhexidine gluconate 4.0%). A 1cm incision was made in the upper thigh and the biceps femoris muscle layer was dissected with a blunt pair of scissors to reveal the common sciatic nerve. Four loops of 4.0 Catgut Chrome (SMI, Belgium) suture material were tied loosely around the nerve fibre spaced evenly apart and excess from the knots were trimmed. The nerve fibre was replaced in the muscle ensuring there were no twists in the nerve fibres and the skin was sutured using a box stitch and absorbable Vicryl (Ethicon, USA) suture material. Rats were placed into a 27°C warming box to ensure body temperature was maintained and closely monitored during their recovery for breathing rate and signs of discomfort. An additional 5mg/kg dose of carprofen was administered if required to any rats demonstrating signs of distress. Once the rats were awake and regained their righting reflex in the warming box, they were replaced in a single level post-surgery cage with their original cage mates including soft bedding, additional enrichment wet mash food to aid with recovery. Rats were closely monitored for recovery in the 5 days following surgery for changes in vocalisation, bodyweight, grimacing, autophagy including the administration of 5mg/kg carprofen for 3 days following surgery. Thank you to the technical staff at Transpharmation LTD for conducting the CCI surgery.

6.2.5 Mechanical allodynia.

Von Frey paw withdrawal threshold was measured using the same protocol detailed in Chapter 2 included using the same monofilament range 0.4, 0.6, 1, 1.4, 2, 4, 6, 8, 10, 15, 26; g (not the increased 0.16-60g range used in Chapter 3). All von Frey testing was conducted on solo rats as undertaken in Chapter 2 and 3. The paired testing of von Frey as in Chapter 4 was not used due to the size of the rats (600-860g). In the present study all von Frey measurements were taken in both the ipsilateral (left) and contralateral (right) hind paw to allow for a measurement of the impact of CCI surgery and use of the contralateral paw as an additional time matched within animal control.

Paw withdrawal threshold was evaluated three times before CCI surgery (Days -6,-5,-4 before CCI surgery). The average of the last two pre CCI surgery von Frey timepoints was used as the baseline measurement (Day -5&-4). After CCI surgery the development and maintenance of mechanical allodynia was monitored repeatedly in CCI rats throughout the 6-week study (Days 7, 9, 18, 25, 37 after CCI surgery) (Figure 6.1). The effects of 10mg/kg pregabalin, 10mg/kg ketamine and vehicle administration on mechanical allodynia was assessed using a crossover study design at three timepoints (Day 16, 23, 30). The effects of 3m/kg psilocybin on von Frey paw withdrawal threshold were measured on Day 37 with all CCI rats receiving the same dose. Psilocybin was administered separately from pregabalin, ketamine and vehicle based on previous reports of long washout periods being required that could have impacted other test compounds in a crossover design (Shore et al., 2024). Paw withdrawal threshold measurements were repeatedly taken at 1, 2 and 4 hours after test compound administration.

6.2.6 EEG recordings.

Rats were placed in individual recording chamber and EEG, EMG and locomotor activity were recorded for up to 24 hours prior to CCI surgery on Day -4 (Baseline) and after CCI surgery on Day 3, 7, 9, 19 and 25 to monitor the development of changes in sleep/wake and EEG recordings. The effects of 10mg/kg pregabalin, 10mg/kg ketamine and vehicle administration on EEG, EMG and locomotor activity recordings were assessed using a crossover study design at three timepoints (Day 15, 21, 28). The effects of 3mg/kg psilocybin on EEG, EMG and locomotor activity recordings were tested on Day 35. EEG, EMG and locomotor activity signals were detected by an antenna (RPC-1, Data Sciences International, USA) placed below the recording cages. On days without test compound administration (Day 3, 7, 9, 19, 25) recordings began from the time the rats were placed in the recording chamber as close to ZT5 (5 hours after light onset) as possible. On drug treatment days (Day 15, 21, 28, 35), the recordings started at the time of compound administration that was as close to ZT5 as possible. Recordings stopped approximately 24 hours later at around ZT5, however, only 23 hours were analysed and presented as the 24th hour of the recordings were often incomplete.

6.2.7 EEG processing and automatic scoring.

All data was aligned to the time the rats were placed in the recording chamber (approximately ZT5) (Day -4, 3, 7, 9, 19 and 25) or the time when they were dosed with test compounds (pregabalin, ketamine, psilocybin and vehicle). Sleep/wake epochs were defined as “non-overlapping 10-second (s) time segments”. EEG was analysed using short-time fast Fourier transformation (FFT: amplitude/second, 1-second non-overlapping, unpadded Hann windows), producing 1-100Hz spectra with 1Hz frequency resolution. For each epoch, the resulting spectra were reduced to the

median value for each frequency, and the area under the curve was used to calculate quantitative EEG values for the following frequency bands: delta (1-4Hz), theta (4-7Hz), sigma/alpha (8-12Hz), beta (13-30Hz), gamma (30-100Hz). EMG data was digitally bandpass filtered (50-150 Hz), rectified, summed in 1-second bins and median values were calculated for each epoch. Locomotor activity was rectified and summed to generate the epoch values.

10s epochs were automatically scored as wakefulness (Wake), non-rapid-eye-movement (NREM) sleep or rapid eye movement (REM) sleep, using proprietary Transpharmation LTD software. Briefly, wakefulness was defined as active movement, or high EMG tone with high EEG gamma power. NREM sleep was defined as inactivity combined with lower muscle tone and low EEG gamma power. REM sleep was defined as inactivity combined with very-low muscle tone and high EEG gamma power. All scoring was quality-checked by confirming identification of data-clouds corresponding to each vigilance state. Signal loss (missing data) during acquisition was defined as two or more consecutive samples of value "0" (for both EEG and EMG). Fast, high-amplitude electrical spiking artefacts were detected and also treated as missing data. EEG spectral estimates for a 1-second window were invalidated if more than 10% of the samples in that window were missing.

6.2.8 Automatic scoring accuracy assessment.

To validate the automatic sleep scoring system, the results of previously manually scored and published EEG recordings were compared with the results generated by the automatic scoring system (Kantor et al., 2023). Each 10s epoch was compared for the accuracy of the automatic scoring system to correctly score each 10s as either wakefulness, NREM sleep or REM sleep. The automatic scoring system achieved a 93.9% match for wakefulness epochs, 92.6% match for NREM sleep epoch and an 82.7% match for REM sleep epochs. The overall accuracy when comparing all 10s epochs scored manually versus automatically was 91.8% and therefore deemed accurate enough to be used for this dataset.

6.2.9 EEG analysis.

To quantify if CCI surgery and/or drug treatment (pregabalin, ketamine, vehicle, psilocybin) altered sleep/wake behaviour, the percentage of time that the rats spent in each behavioural state of wakefulness, NREM and REM sleep was assessed. To measure the propensity for NREM and REM sleep the length of time (latency) between hour 0 and the first uninterrupted bout of 180s of NREM sleep was recorded as the latency to NREM sleep. Similarly, the length of time between hour 0 and the first uninterrupted 60s bout of REM sleep was recorded as the latency to REM sleep. Any changes to the rat's ambulation were assessed as the amount of locomotor activity the rats conducted measured by the HD-S02 devices implanted into the rats.

Changes in sleep/wake behaviour were further assessed for sleep fragmentation by measuring the duration and total number of wakefulness, NREM and REM sleep bouts to identify sleep fragmentation. In addition, the distribution of sleep/wake bout lengths was also assessed by calculating the total number of short (≤10s), medium (10-50s wake & REM sleep, 10-150s NREM sleep) and long (>50s wake & REM sleep, >150s NREM sleep) bout lengths.

To understand the changes in the frequency content of the recorded signal, power spectral analysis of the EEG recording was performed. To determine any changes in specific frequency bands, the area under the curve (AUC) of the EEG power spectrum in the delta (1-4Hz), theta (4-7Hz),

sigma/alpha (8-12Hz), beta (13-30Hz), gamma (30-100Hz) were calculated during wakefulness, NREM and REM sleep.

The locomotor activity along with the percentage of time rats spent asleep or awake were assessed at each hour of the 23 hour recordings that were analysed. These measurements along with all other sleep/wake and EEG measurements were analysed as the combined effects across two 6 hour sections of ZT5-ZT11 in the light period (hours 0-6 of the recording) and a corresponding 6 hour portion from ZT17-ZT23 in the dark period (hours 12-18 of the recording). These sections were selected for analysis as ZT5-ZT11 was the longest uninterrupted section of the light period after the drug treatments (pregabalin, ketamine, vehicle, psilocybin) that could be captured. Whilst ZT17-ZT23 was selected as the corresponding period during the dark period of equal length to identify any differences in sleep/wake and EEG measures that may have been differentially affected during these periods.

6.2.10 Test compounds.

Pregabalin 10mg/kg (Ochem, USA) p.o. dissolved in drinking water, Ketamine 10mg/kg (Tocris, USA) s.c. dissolved in saline 0.9% NaCl (Baxter), psilocybin 3mg/kg i.p. dissolved in saline 0.9% NaCl (Baxter) along with the vehicle of saline 0.9% NaCl (Baxter) s.c. were the selected test compounds in this study. Pregabalin at 10mg/kg was selected as a first line treatment reference compound based on the findings in Chapter 3 that this dose reversed mechanical allodynia without excessive somnolence. Ketamine at 10mg/kg was selected based on this dose being effective as an antidepressant (Kantor et al., 2023) and within the effective dose range reported to have analgesic efficacy in rat models of neuropathic pain (Velzen et al., 2021). Psilocybin at 3mg/kg was selected based on previous studies at Transpharmation LTD identifying that this dose appeared to be effective as an antidepressant (unpublished observations).

6.2.11 Blinding and exclusion or inclusion criteria.

All 17 Sprague Dawley rats underwent CCI surgery (Day 0) on the left hind paw which was successful in all rats. Four rats were excluded from further assessment within the first three weeks after CCI surgery, one due to autotomy injury to the left hind paw and three due to health complications unrelated to the CCI surgery. The EEG and von Frey data of these four rats were excluded from data analysis. One rat was terminated 32 days after the CCI surgery (Day 32), prior to the psilocybin treatment, due to health complications unrelated to the CCI surgery. Data from this rat was still included in the CCI and EEG analysis due to providing data at most timepoints. One rat's data was not collected on Day 9 due to technical complications but had data at all other timepoints and it was included in the study. One rat's EEG signal quality was not suitable for automated EEG analysis and was excluded from EEG data analysis. The von Frey data collection was conducted blind to the rats treatment condition. An exclusion criterion of a >50% change from baseline at the Day 7&9 timepoint was set for inclusion in the study to confirm the onset of mechanical allodynia development. All rats developed mechanical allodynia and were include in von Frey and EEG analysis. This resulted in an n=12-13 for von Frey testing and an n=11-12 for all other measures.

6.2.12 Statistics.

To compare the results from the development of neuropathic pain and test compound reversal one-way or two-way mixed model analysis of variance (ANOVA) was used followed by Dunnet's post hoc test. Two-way ANOVA was used to compare locomotor activity and sleep/wake amounts measured across the 23 hour recording period. One way ANOVA was used to compare all the other measurements (Prism 10.2; GraphPad, San Diego, CA USA). A p value of <0.05 was considered statistically significant for all data. All data is reported as mean ± SEM.

6.3 Results

6.3.1 CCI surgery caused mechanical allodynia that was reversed by pregabalin and ketamine.

Mechanical allodynia developed in all rats from Day 7 to Day 37 after CCI surgery in the ipsilateral paw with no change in the contralateral paw. Paw withdrawal threshold was measured through von Frey monofilament application using the up-down method in both the ipsilateral (Figure 6.2A) and contralateral hind paw (Figure 6.2B). In all 13 rats paw withdrawal threshold decreased by >50% in the ipsilateral paw at Day 7 compared with the baseline (Day -5&-4) timepoint demonstrating development of mechanical allodynia. Additionally, as all rats paw withdrawal threshold decreased by >50% they all reached the inclusion criteria and could all be included in all analysis. The decreased paw withdrawal threshold was maintained throughout the study in the ipsilateral paw at ≤4g after CCI surgery compared to the 20.8g at the baseline timepoint [$F(5,59) = 109.9$, $p<0.001$] (Figure 6.2A). In the contralateral hind paw that did not have CCI surgery conducted to it, there was no change in paw withdrawal threshold at any timepoint with all remaining >19g [$F(5,59) = 0.525$, $p=0.756$] (Figure 6.2B). This demonstrates that CCI surgery successfully induced mechanical allodynia in all rats which can be considered as the development of neuropathic pain.

Pregabalin and ketamine administration successfully reversed mechanical allodynia, but not psilocybin. Compared to the development of mechanical allodynia at Day 7&9, 10mg/kg pregabalin reversed the mechanical allodynia induced by CCI surgery at one, two and four hours after administration in the ipsilateral hind paw [$F(12,141) = 11.06$, $p<0.001$] (Figure 6.2C). Pregabalin increased paw withdrawal latency from 3.2g at Day 7&9 to over four times as much at 15g by hour one, which further increased to 18.9g by hour four. Ketamine (10mg/kg) administration also reversed mechanical allodynia at the first and fourth hour (Figure 6.2C). At the first hour after ketamine administration, the CCI rats paw withdrawal thresholds increased to 15g, similar to pregabalin at this hour. The increased paw withdrawal threshold was not maintained at hour two after ketamine administration with the average response at 8.5g (Figure 6.2C). Ketamine administration at hour four increased paw withdrawal thresholds compared to the Day 7&9 timepoint to 9.7g. Psilocybin (3mg/kg) administration did not significantly increase paw withdrawal threshold at either one, two or four hours after administration (Figure 6.2C). To ensure these effects were related the test compounds and not to the vehicle or any environmental conditions the effect of vehicle administration alone were examined. There was no effect of vehicle administration on paw withdrawal thresholds which did not increase above 5.3g compared to the 3.3g at the Day 7&9 timepoint. The effect of all three test compounds and vehicle administration was assessed on the contralateral paw. Pregabalin, ketamine and vehicle caused no effect on contralateral paw withdrawal threshold [$F(12,141) = 5.70$, $p<0.001$] (Figure 6.2D). Unusually, psilocybin administration

at hour two and four decreased the contralateral paw withdrawal threshold from 21.2g at Day 7&9 to 13.9g and 14.8g at hour two and four respectively (Figure 6.2D). Measuring paw withdrawal thresholds confirmed neuropathic pain onset after CCI surgery and that 10mg/kg pregabalin and 10mg/kg ketamine administration successfully reversed this neuropathic pain.

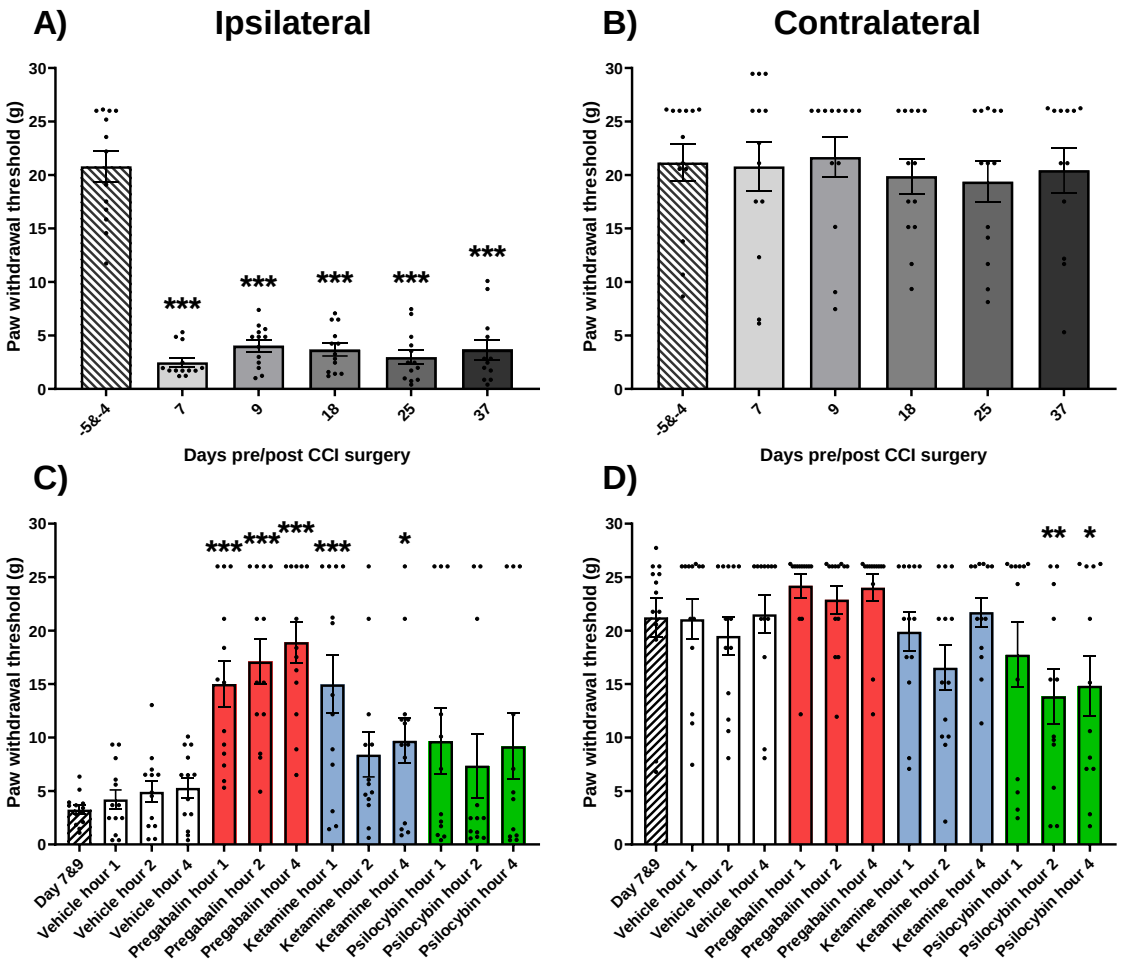

Figure 6.2) CCI surgery induced a sustained level of neuropathic pain that was reversed by 10mg/kg pregabalin and 10mg/kg ketamine treatment. The change in von Frey paw withdrawal threshold was measured at baseline (Day -5&-4) and at Days, 7, 9, 18, 25 and 37 after CCI surgery in the ipsilateral (A) and contralateral (B) hind paw. The reversal of any changes to paw withdrawal threshold was assessed with vehicle, 10mg/kg pregabalin, 10mg/kg ketamine (Days 16, 23, 30) and 3mg/kg psilocybin (Day 37) at 1, 2 and 4 hours after test compound administration in the ipsilateral (C) and contralateral (D) hind paw. (A,B) ***p<0.001 vs Day -5&4. (C,D) *p<0.05, **p<0.01, ***p<0.001 vs Day 7&9. All data is reported as mean ± SEM, n=12-13 (A-D).

6.3.2 Locomotor activity was reduced in CCI rats and normalised by ketamine.

To identify if there were any changes in the rat's ambulation and activity after CCI surgery, the amount of locomotor activity was assessed. In CCI rat's locomotor activity progressively decreased after CCI surgery from as early as Day 3 and was later reversed by ketamine. Across the full 23 hour time course of the recording, locomotor activity decreased at Days 7, 9, 19 and 25 during the first

two hour of the recording [Time: F(22,1430) = 42.90, p<0.001], [Treatment: F(5,65) = 9.23, p<0.001], [Interaction: F(110,1430) = 2.08, p<0.001] (Figure 6.3A). Additionally during the dark period (ZT12-ZT0) locomotor activity decreased at various points on all recording days, particularly during the final hour of the dark period (Figure 6.3A). When assessing the ability of test compounds to improve locomotor activity 10mg/kg ketamine increased locomotor activity during the first hour after administration back to similar levels of the baseline activity [Time: F(22,1188) = 26.34, p<0.001], [Treatment: F(4,54) = 10.44, p<0.001], [Interaction: F(88,1188) = 2.83, p<0.001] (Figure 6.3B). Additionally, 10mg/kg pregabalin increased locomotor activity during the final hour of the dark period (ZT23-ZT0). Whilst 3mg/kg psilocybin further decreased locomotor activity during the final hour of the recording (ZT3- ZT4).

These effects of decreased locomotion in CCI rats that and reversal by ketamine administration were further highlighted when assessing the first six hours of the recording after test compound administration (ZT5-ZT11 during the light period) and an equivalent portion of the dark period (ZT17-ZT23). During ZT5-ZT11, locomotor activity progressively declined at Day 7 reaching a level significantly (32%) lower than baseline (Day -4) [F(5,54) = 8.818, p<0.001] (Figure 6.3C). The amount of locomotor activity further declined by Day 9 with CCI rats spending half as much time active compared with baseline. This reduction in locomotor activity maintained at this level on Day 19 and Day 25 as well (Figure 6.3C). A similar effect of reduced locomotor activity was also identified during ZT17-ZT23 in the dark period, though the reduction began even earlier at Day 3 [F(5,54) = 12.93, p<0.001] (Figure 6.3D). This again reached a stable reduction in locomotor activity with Day 9, Day 19 and Day 25 being ~40% lower than baseline (Day -4) (Figure 6.3E). Ketamine (10mg/kg) returned locomotor activity back to baseline levels and increased locomotor activity by 66% above the vehicle treatment level during the first six hours after administration (ZT5-ZT11) [F(4,43) = 9.652, p<0.001] (Figure 6.3D). However, neither 10mg/kg pregabalin nor 3mg/kg psilocybin had any effect on locomotor activity during ZT5-ZT11 (Figure 6.3D). Though locomotor activity was reduced during ZT17-ZT23, the effects of ketamine did not remain as the reduction in locomotor activity in CCI rats was not reversed by any of the test compounds at this time period [F(4,43) = 18.91, p<0.001] (Figure 6.3F). Overall, locomotor activity decreased in CCI rats indicating impaired ambulation that was only reversed by ketamine not pregabalin or psilocybin during the first six hours after administration.

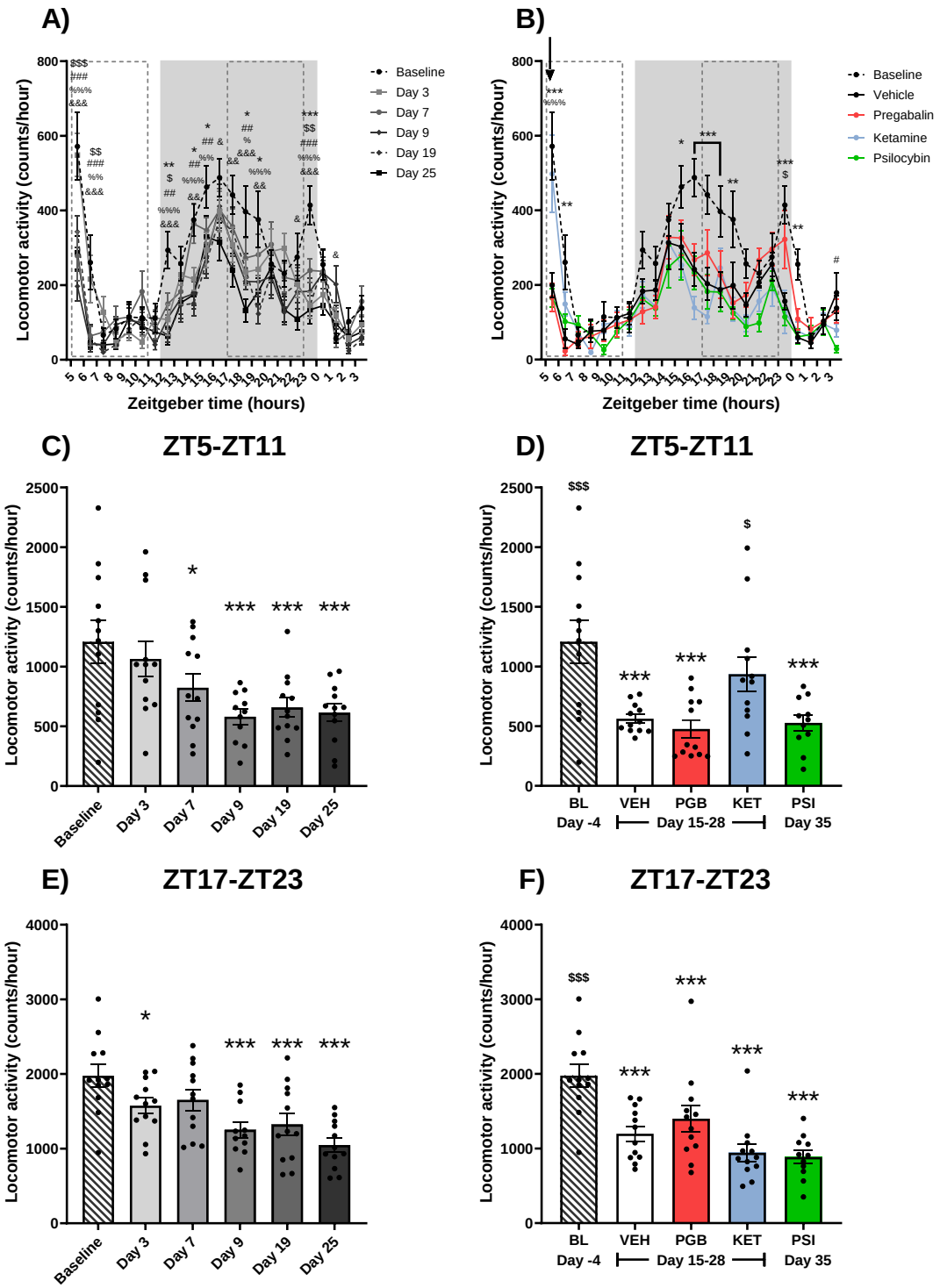

Figure 6.3) CCI rats Locomotor activity decreased from Day 3 after CCI surgery and which was reversed by ketamine. The average locomotor activity of the rats at baseline (Day -4) were compared to Days 3, 7, 9, 19 and 25 after CCI surgery at each hour (A), during ZT5-ZT11 (C) and ZT17-ZT23 (E). The effect of vehicle, 10mg/kg pregabalin, 10mg/kg ketamine (Days 15, 21, 28) and 3mg/kg psilocybin (Day 35) on locomotor activity were also assessed at each hour (B), during ZT5-ZT11 (D) and ZT17-ZT23 (F). (A) *p<0.05, **p<0.01, ***p<0.001 Day 3 vs baseline, $$p$<0.05, $$$p$<0.01, $$$$p$<0.001 Day 7 vs baseline, ##p<0.01, ###p<0.001 Day 9 vs baseline, %p<0.05, %%p<0.01, %%%p<0.001 Day 19 vs baseline, &p<0.05, &&p<0.01, &&&p<0.001 Day 25 vs baseline. (B) *p<0.05, **p<0.01, ***p<0.001 baseline vs vehicle, $$p$<0.05 pregabalin vs vehicle, #p<0.05 psilocybin vs vehicle, %%%p<0.001 ketamine vs vehicle. (C-F) *p<0.05, ***p<0.001 vs baseline. (D,F) $$p$<0.05, $$$$p$<0.001 vs vehicle. Grey shaded area denotes dark period. Dashed boxes indicate ZT5-ZT11 (left) and ZT17-ZT23 (right). Black arrow denotes time of test compound administration. All data is reported as mean ± SEM, n=11-12 (A-F).

6.3.3 CCI rats spent more time in NREM sleep at the expense of wakefulness which was corrected by ketamine.

Firstly, the CCI rat's sleep was analysed as how much time the rats spent awake, in NREM sleep or in REM sleep throughout the full 23 hour recording. The general trend was that the amount of NREM and REM sleep increased at the expense of wakefulness in the rats after CCI surgery, with ketamine demonstrating the most robust reversal of these effects. After CCI surgery the amount of time the rats spent awake decreased during the first two hours (ZT5-ZT7) of the recording and throughout much of the dark (ZT12-ZT0) period [Time: $F(22,1430) = 79.95$, $p<0.001$], [Treatment: $F(5,65) = 13.83$, $p<0.001$], [Interaction: $F(110,1430) = 2.29$, $p<0.001$] (Figure 6.4A). Whilst the main effect of the test compounds occurred during the first two hours as ketamine increased wakefulness at both hours and psilocybin increased wakefulness at the second hour [Time: $F(22,1188) = 49.55$, $p<0.001$], [Treatment: $F(4,54) = 12.08$, $p<0.001$], [Interaction: $F(88,1188) = 3.78$, $p<0.001$] (Figure 6.4B).

During NREM sleep the opposite effect occurred with CCI rats having an increased propensity for sleep, spending more time asleep during the first two hours (ZT5-ZT7) and throughout much of the dark (ZT12-ZT0) period [Time: $F(22,1430) = 84.45$, $p<0.001$], [Treatment: $F(5,65) = 11.38$, $p<0.001$], [Interaction: $F(110,1430) = 2.33$, $p<0.001$] (Figure 6.4C). Ketamine again effectively reversed the increased propensity for sleep in the first two hours (ZT5-ZT7) however, psilocybin produced mixed results [Time: $F(22,1188) = 59.29$, $p<0.001$], [Treatment: $F(4,54) = 9.34$, $p<0.001$], [Interaction: $F(88,1188) = 3.91$, $p<0.001$] (Figure 6.4D). Psilocybin initially decreased the excess NREM sleep at the second hour (ZT6-ZT7) but further increased the amount of time CCI rats spend in NREM sleep from ZT8-ZT10 (Figure 6.4D).

The amount of time spent in REM sleep marginally increased in the CCI rats primarily at the second hour (ZT6-ZT7) of the recording and the first hour of the dark period (ZT12-ZT3) [Time: $F(22,1430) = 39.11$, $p<0.001$], [Treatment: $F(5,65) = 5.07$, $p<0.001$], [Interaction: $F(110,1430) = 1.56$, $p<0.001$] (Figure 6.4E). All three test compounds decreased the amount of time CCI rats spent in REM sleep during the first few hours after administration [Time: $F(22,1188) = 17.58$, $p<0.001$], [Treatment: $F(4,54) = 1.52$, $p<0.001$], [Interaction: $F(88,1188) = 3.91$, $p<0.001$] (Figure 6.4F). However, psilocybin and ketamine decreased REM sleep below baseline levels with almost no REM sleep occurring during the first two hours of the recording. For ketamine the decreased REM sleep was maintained across the first 3 hours (ZT5-ZT8) and psilocybin supressed REM sleep for 5 hours after administration (ZT5-ZT10) (Figure 6.4F). These results highlighted that CCI rats spend more time asleep at the expense of wakefulness that was corrected by ketamine treatment.

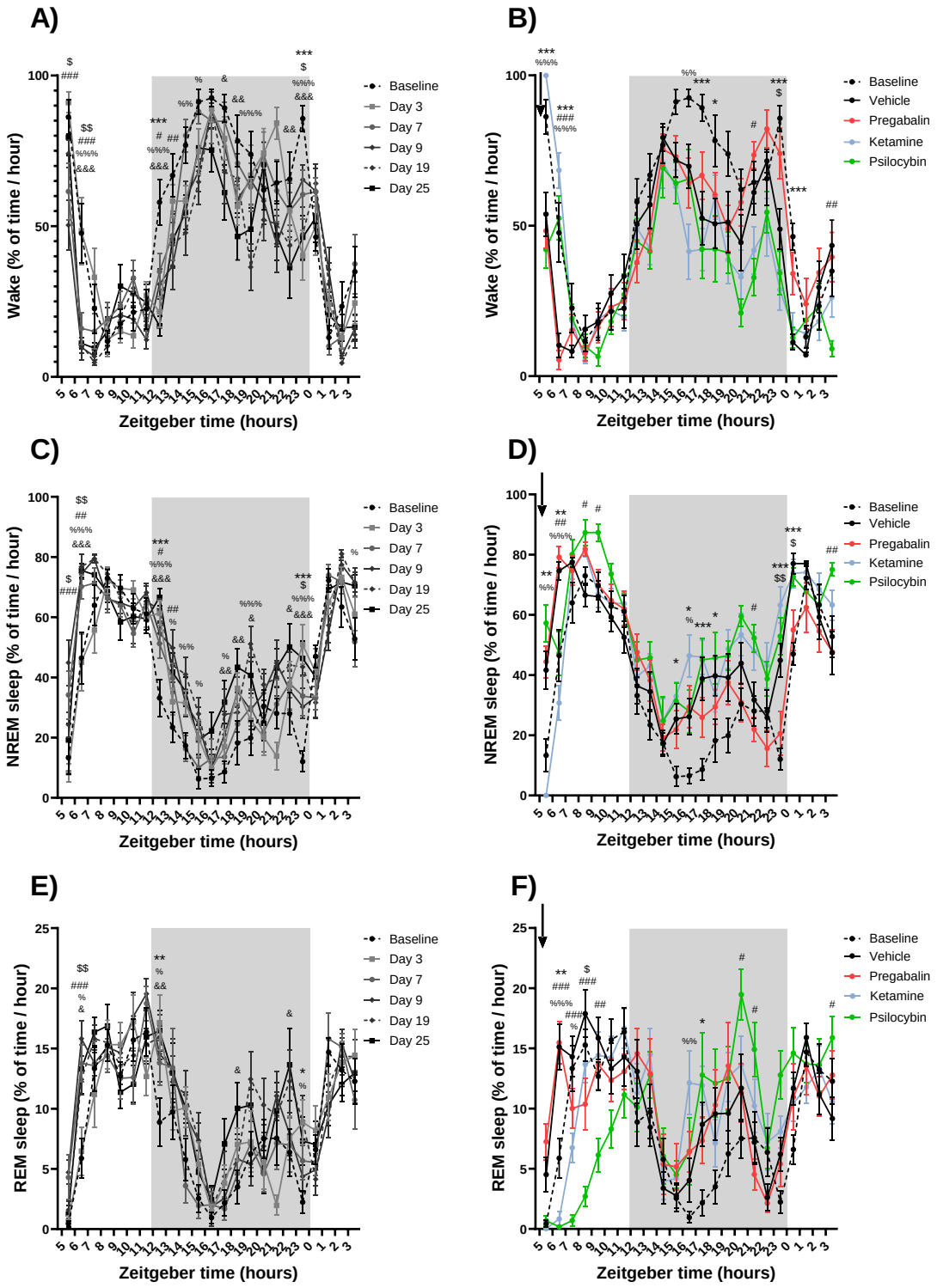

Figure 6.4) CCI rats spent more time awake and less time in NREM sleep which was reversed by ketamine. The effect of CCI surgery on the percentage of time spent awake (A), in NREM sleep (C) and REM sleep (E) at Days 3, 7, 9, 19 and 25. The effect of vehicle, 10mg/kg pregabalin, 10mg/kg ketamine (Days 15, 21, 28) and 3mg/kg psilocybin (Day 35) on the percentage of time spent awake (B), in NREM sleep (D) and REM sleep (F). (A,C,E) *p<0.05, **p<0.01, ***p<0.001 Day 3 vs baseline, \$$p$<0.05, \$\$$p$<0.01 Day 7 vs baseline, #p<0.05, ##p<0.01, ###p<0.001 Day 9 vs baseline, %p<0.05, %%p<0.01, %%%p<0.001 Day 19 vs baseline, &p<0.05, &&p<0.01, &&&p<0.001 Day 25 vs baseline. (B,D,F) *p<0.05, **p<0.01, ***p<0.001 baseline vs vehicle, \$$p$<0.05, \$\$$p$<0.01 pregabalin vs vehicle, #p<0.05, ##p<0.01, ###p<0.001 psilocybin vs vehicle, %p<0.05, %%p<0.01, %%%p<0.001 Ketamine vs vehicle. Grey shaded area denotes dark period and black arrow denotes time of test compound administration. All data is reported as mean ± SEM, n=11-12 (A-F).

To more specifically assess the effects of CCI surgery and the drug treatments on the amount of time the rats spend awake and sleep, the first six hours after drug administration (ZT5-ZT11 in the light period) along with a corresponding period of the dark period (ZT17-ZT23) were individually analysed. The overall effects of CCI surgery on the amount of time the CCI rats spend awake, in NREM sleep and REM sleep during ZT5-ZT11 in the light period indicated that CCI rats spent more time asleep and less time awake which reversed by Day 25. The amount of time rats spent awake during the first six hours of the recordings (ZT5-ZT11) progressively declined after CCI surgery by 15% reaching 20% at Day 9 compared with 35% at baseline (Day -4) [$F(5,54) = 7.56$, $p<0.001$] (Figure 6.5A). However, by Day 25 wakefulness had increased back to 29% (Figure 6.5A). NREM sleep in CCI rats increased by 10% at Day 9 and 8% at Day 19 before returned back to baseline (Day -4) levels at Day 25 [$F(5,54) = 6.93$, $p<0.001$] (Figure 6.5C). Whilst REM sleep was only increased on Day 9 from 10.5% to 13.5% compared to baseline during ZT5-ZT11 [$F(5,54) = 3.52$, $p=0.008$] (Figure 6.5E). This demonstrated that during ZT5-ZT11 in the light period CCI rats spent more time awake at the expense of sleep. Though this increased propensity for sleep did not remain throughout the 25 days studied when assessed during ZT5-ZT11 in the light period. The increased NREM and REM sleep amount at the expense of wakefulness was more robust during ZT17-ZT23 in the dark period (Supp figure 6.13). During this ZT17-ZT23 period, the amount of time CCI rats spent awake progressively declined [$F(5,54) = 16.81$, $p<0.001$] (Supp figure 6.13A), whilst the propensity for NREM [$F(5,54) = 15.54$, $p<0.001$] (Supp figure 6.13C) and REM sleep [$F(5,54) = 11.92$, $p<0.001$] (Supp figure 6.13E) increased throughout the study. This peaked at Day 25 with CCI rats spending ~20% less time awake and both NREM and REM sleep correspondingly increased during ZT17-ZT23. This demonstrated that CCI rats spent more time asleep at the expense of wakefulness particularly during ZT17-ZT23 in the dark period.

Ketamine was the only drug to fully reverse the altered sleep/wake amounts in the CCI rats. Ketamine (10mg/kg) increased the amount of time CCI rats spent awake to baseline levels during the first six hours after administration [$F(4,43) = 13.76$, $p<0.001$] (Figure 6.5B). Ketamine also decreased the amount of NREM sleep back to baseline levels [$F(4,43) = 15.47$, $p<0.001$] (Figure 6.5D). Neither 10mg/kg pregabalin or 3mg/kg psilocybin had any positive effects on the amount of wakefulness or NREM sleep during this ZT5-ZT11 period. Psilocybin further increased the amount of time CCI rats spent in NREM sleep above the amount of the vehicle level (Figure 6.5D). This increased the propensity for NREM sleep after psilocybin treatment came at the expensive of REM sleep which was much lower than during both the baseline and vehicle recordings [$F(4,43) = 21.93$, $p<0.001$] (Figure 6.5F). Ketamine also decreased REM sleep though this was only lower than after vehicle recordings and remained at an equivalent level to the baseline. The positive effects of ketamine did not remain through to ZT17-ZT23 in the dark period and slightly decreased wakefulness below the amount of the vehicle timepoint during this period of the recording [$F(4,43) = 22.17$, $p<0.001$] (Supp figure 6.13B). Psilocybin similarly further decreased wakefulness and increased NREM sleep [$F(4,43) = 15.77$, $p<0.001$] (Supp figure 6.13D) and REM sleep [$F(4,43) = 11.31$, $p<0.001$] (Supp figure 6.13F) during ZT17-ZT23 exacerbating the effects of CCI surgery. Interestingly, despite pregabalin not improving sleep/wake amounts immediately after dosing (ZT5-ZT11), it partially reversed the increased NREM sleep and decreased wakefulness during ZT17-ZT23 in the dark period. Assessing the effects of the test compounds on sleep/wake amounts revealed that ketamine reversed the abnormally increased propensity for sleep in CCI rats immediately after dosing, whilst pregabalin had a delayed effect leading to a partial reversal of these effects.

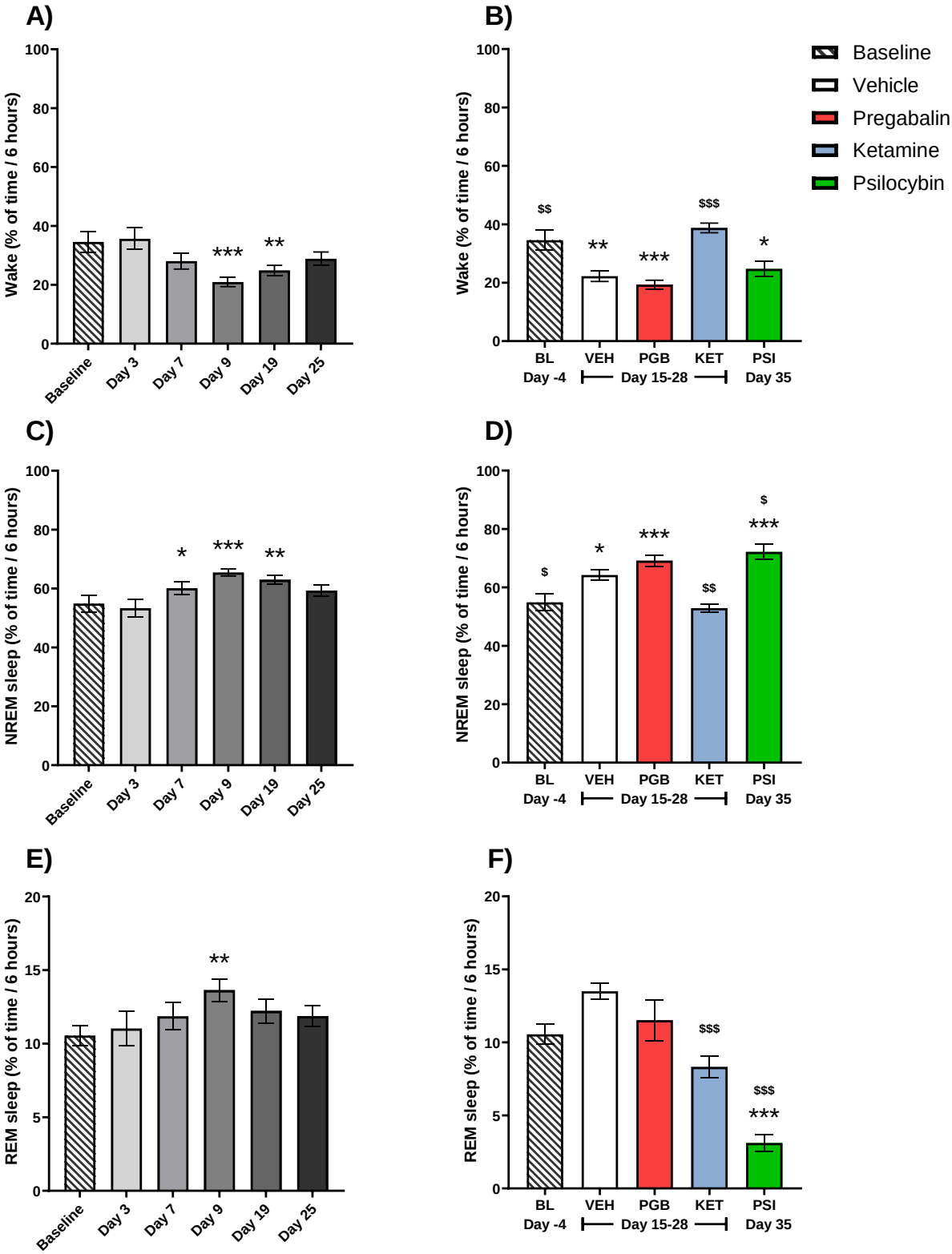

Figure 6.5) CCI rats spent less time awake and more time in NREM sleep which was corrected by ketamine during ZT5-ZT11. The effect of CCI surgery (Days 3, 7, 9, 19 and 25) along with vehicle, 10mg/kg pregabalin, 10mg/kg ketamine (Days 15, 21, 28) and 3mg/kg psilocybin (Day 35) test compounds on the percentage of time spent awake (A,B), in NREM sleep (C,D) and REM sleep (E,F) during ZT5-ZT11 in the light period. (A-F) *p<0.05, **p<0.01, ***p<0.001 vs baseline (Day-4). (B,D,F) $$p$<0.05, $$$p$<0.01, $$$$p$<0.001 vs vehicle. All data is reported as mean ± SEM, n=11-12 (A-F).

6.3.4 CCI surgery decreased the latency to NREM sleep which was corrected by ketamine and decreased the latency to REM sleep which was reversed by psilocybin and ketamine.

As it was identified that CCI rats spent more time asleep at the expense of wakefulness, next it was assessed if there was also an effect on how long it took these rats to fall asleep by measuring the latency to NREM and REM sleep. CCI rats had a reduced latency to entering NREM sleep which was corrected by ketamine and a reduced latency to REM sleep which was reversed by psilocybin and ketamine. At baseline (Day -4) the CCI rats took an average of 83 minutes until the first bout of NREM sleep which decreased by Day 7 and Day 9 to <50 minutes [$F(5,54) = 8.02$, $p<0.001$] (Figure 6.6A). This increased propensity to enter into NREM sleep was reversed by 10mg/kg ketamine administration back to 102 minutes, which was equivalent to the baseline [$F(4,43) = 13.21$, $p<0.001$] (Figure 6.6B). Neither 10mg/kg pregabalin and 3mg/kg psilocybin had any effect on NREM sleep latency (Figure 6.6B). Similarly, the latency to REM sleep was decreased from 112 minutes at baseline (Day -4) to <77 minutes at Days 7, 9, 19 and 25 [$F(5,54) = 13.23$, $p<0.001$] (Figure 6.6C). The maximum effect on REM sleep latency also occurred on Day 9 as with NREM sleep latency, with CCI rats entering REM sleep within 50 minutes on average (Figure 6.6C). Ketamine reversed the REM sleep latency in CCI rats, though this was overcorrected to longer than the baseline at 154 minutes [$F(4,43) = 98.57$, $p<0.001$] (Figure 6.6D). Whilst psilocybin did not alter the latency to NREM sleep it excessively increased the latency to REM sleep reaching over three times as long as at baseline (Figure 6.6D). This demonstrated that after CCI surgery the rats had a greater propensity to enter both NREM and REM sleep which was corrected by ketamine and overcorrected by psilocybin.

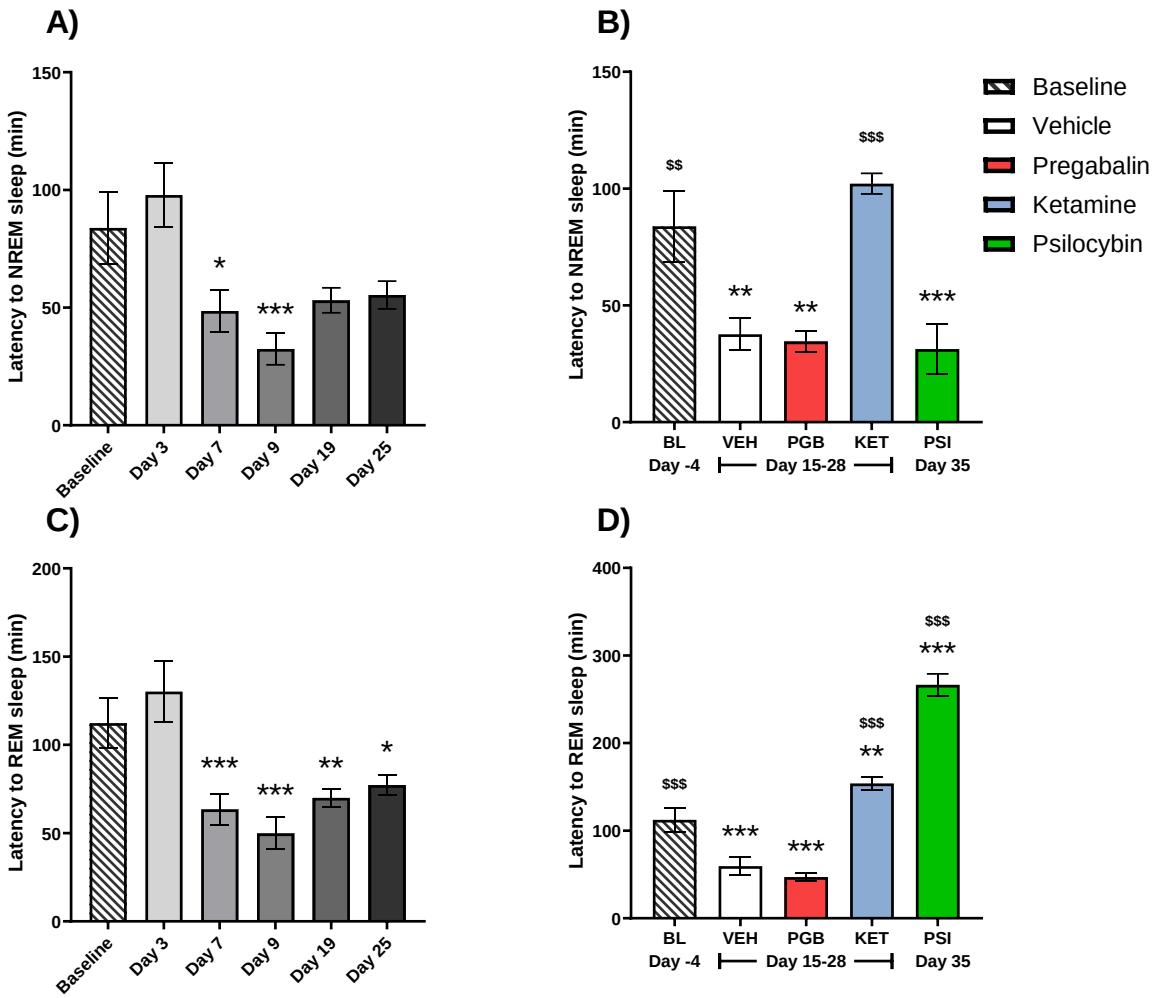

Figure 6.6) CCI rats latency to NREM sleep was reduced which was corrected by ketamine and a reduced latency to REM sleep that was increased by psilocybin and ketamine. The effect of CCI surgery (Days 3, 7, 9, 19 and 25) along with vehicle, 10mg/kg pregabalin, 10mg/kg ketamine (Days 15, 21, 28) and 3mg/kg psilocybin (Day 35) test compounds on the latency to NREM sleep (A,B) and REM sleep (C,D). (A-D) *p<0.05, **p<0.01, ***p<0.001 vs baseline (Day-4). (B,D). $$$p$<0.01, $$$$p$<0.001 vs vehicle. All data is reported as mean ± SEM, n=11-12 (A-F).

6.3.5 CCI rats sleep was fragmented which was corrected by ketamine and partially corrected by pregabalin.

Sleep fragmentation, a commonly reported comorbidity of neuropathic pain, was assessed in the CCI rats by measuring the number of continuous periods (bouts) of wakefulness, NREM sleep or REM sleep and subsequently how long each bout lasted. CCI rats sleep was fragmented as demonstrated by the increased number of wakefulness and NREM sleep bouts accompanied by their decreased length. During ZT5-ZT11 in the light period the total number of wakefulness bouts progressively increased after CCI surgery stabilising at 50% higher than baseline by Day 7 (Day -4) [$F(5,54) = 4.95$, p<0.001] (Figure 6.7A). This increased number of wakefulness bouts occurred despite the amount of time CCI rats spent awake decreasing during this period (Figure 6.5A). NREM sleep bouts followed the same trend as wakefulness bouts and increased after CCI surgery by Day 7 and remained increased until Day 25 [$F(5,54) = 6.68$, p<0.001] (Figure 6.7C). The number of REM sleep bouts was unaffected in CCI rats when assessed throughout the study at Days 3, 7, 9, 19 and 25 [$F(5,54) = 2.36$,

p=0.05] (Figure 6.7E). However, when comparing CCI rats after vehicle administration REM sleep bouts occurred more often than at baseline [F(4,43) = 18.41, *p*<0.001] (Figure 6.7F). An increased number of wake bouts [F(5,54) = 5.29, *p*<0.001] (Supp figure 6.14A), NREM sleep bouts [F(5,54) = 5.84, *p*<0.001] (Supp figure 6.14C) and REM sleep bouts [F(5,54) = 9.18, *p*<0.001] (Supp figure 6.14E) were also identified during ZT17-ZT23 in the CCI rats. This demonstrated that after CCI surgery the rats sleep became more fragmented as there were more sleep/wake bouts.

The increased number of wakefulness bouts was reversed by 10mg/kg ketamine and 10mg/kg pregabalin back to baseline (Day -4) levels during the first six hours after administration (ZT5-ZT11) [F(4,43) = 17.03, *p*<0.001] (Figure 6.7B). Conversely, 3mg/kg psilocybin caused the opposite effect and further increased the number of wakefulness bouts compared with after vehicle administration (Figure 6.7B). Only ketamine successfully reversed the increased number of NREM sleep bouts, whilst pregabalin and psilocybin had no effect on the number of NREM sleep bouts during ZT5-ZT11 [F(4,43) = 13.02, *p*<0.001] (Figure 6.7D). Both ketamine and psilocybin reduced the number of REM sleep bouts in the CCI rats during ZT5-ZT11 (Figure 6.7F). Though ketamine reduced the number of REM sleep bouts in line with the baseline amount, psilocybin decreased the number of REM sleep bouts below the baseline level (Figure 6.7F). The effects of these test compounds did not remain throughout ZT17-ZT23 in the dark period (Supp figure 6.14B,D,F). Though psilocybin did have the opposite effect of increasing the number of REM sleep bouts during this ZT17-ZT23 period [F(4,43) = 8.38, *p*<0.001] (Supp figure 6.14F). Overall, ketamine fully reversed the fragmented sleep of the CCI rats based on the number of sleep/wake bouts whilst pregabalin and psilocybin had partial efficacy in reversing these.

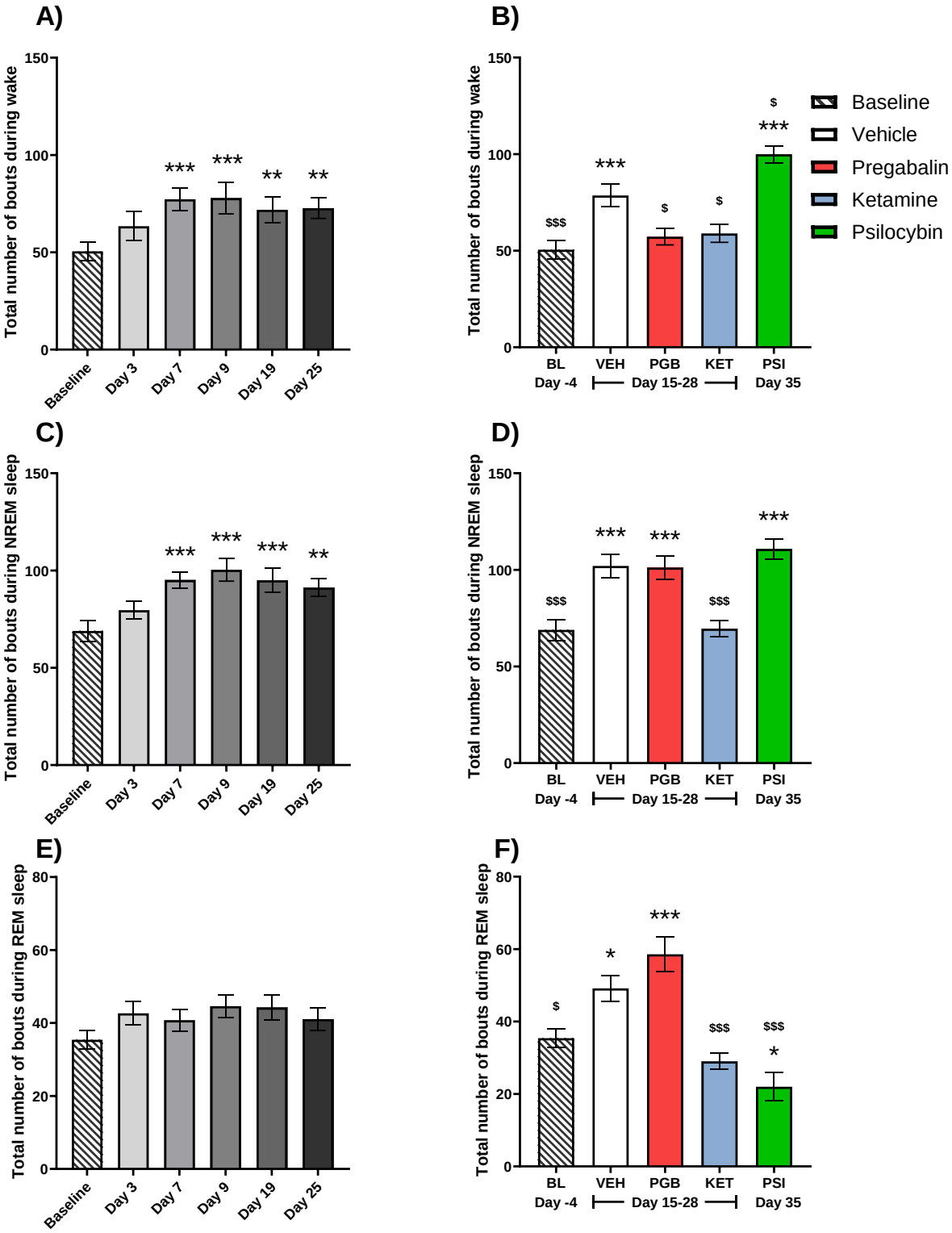

Figure 6.7) CCI rats sleep was fragmented by an increased number of wake and NREM sleep bouts which was corrected by pregabalin and ketamine administration during ZT5-ZT11The effect of CCI surgery (Days 3, 7, 9, 19 and 25) along with vehicle, 10mg/kg pregabalin, 10mg/kg ketamine (Days 15, 21, 28) and 3mg/kg psilocybin (Day 35) test compounds on the total number of wakefulness (A,B), NREM sleep (C,D) and REM sleep (E,F) bouts during ZT5-ZT11 in the light. (A-F) *p<0.05, **p<0.01, ***p<0.001 vs baseline (Day-4). (B,D,F) $$p$<0.05, $$$$p$<0.001 vs vehicle. All data is reported as mean ± SEM, n=11-12 (A-F).

Alongside the sleep fragmentation demonstrated through the increased number of wake and NREM sleep bouts, the average length of each bout also decreased in CCI rats. During ZT5-ZT11 in the light period the average length of wake bouts decreased by 50% in CCI rats at Day 7, which was maintained until at least Day 25 [$F(5,54) = 8.05$, $p<0.001$] (Figure 6.8A). NREM sleep average bout length followed a similar trend, though decreased even earlier after CCI surgery. The average length of NREM sleep bouts decreased by ~20% at Day 3 compared with baseline (Day -4) and remained relatively stable at this level until at least Day 25 [$F(5,54) = 5.22$, $p<0.001$] (Figure 6.8C). There was no effect of CCI surgery on the average length of REM sleep bouts during ZT5-ZT11 the light period [$F(5,54) = 2.25$, $p=0.06$] (Figure 6.8E). Only the decreased average length of wakefulness bouts was found during ZT17-ZT23 the dark period [$F(5,54) = 9.51$, $p<0.001$] (Supp figure 6.15A). Whilst NREM sleep [$F(5,54) = 2.07$, $p=0.08$] (Supp figure 6.15C) and REM sleep [$F(5,54) = 0.57$, $p=0.72$] (Supp figure 6.15E) average bout length remained unchanged in the rats after CCI surgery during this period. Thus, NREM sleep was highly fragmented during ZT5-ZT11 in the light period but was more consolidated during ZT17-ZT23 in the dark period.

Ketamine was again the most effective test compound at reversing sleep fragmentation. Ketamine (10mg/kg) successfully increased the average wake bout length back to 153s an equivalent level to the baseline (Day -4) recording of 169s [$F(4,43) = 10.49$, $p<0.001$] (Figure 6.8B). Neither 10mg/kg pregabalin or 3mg/kg psilocybin had any effect on the average length of wake bouts during the first six hours after administration (ZT5-ZT11) (Figure 6.8B). Both ketamine and pregabalin partially reversed the fragmented NREM sleep bout lengths, as they increased the average length of NREM sleep bouts in line with baseline, though did not reverse them completely [$F(4,43) = 2.96$, $p=0.03$] (Figure 6.8D). Despite there being no effect of the CCI surgery on the average length of REM sleep bouts, both pregabalin and psilocybin decreased the average length of REM sleep bouts during ZT5-ZT11 in the light period [$F(4,43) = 18.90$, $p<0.001$] (Figure 6.8F). The beneficial effects of ketamine and pregabalin on the average length of wakefulness bouts did not continue during ZT17-ZT23 in the dark period [$F(4,43) = 17.81$, $p<0.001$] (Supp figure 6.15B). Additionally, whilst there was no change in the CCI rats NREM sleep bout length, 10mg/kg pregabalin decreased the average length whilst 3mg/kg psilocybin increased the average length of NREM sleep bouts during the ZT17-ZT23 period [$F(4,43) = 7.84$, $p<0.001$] (Supp figure 6.15D). Assessing sleep fragmentation through the average length of sleep/wake bouts further highlighted ketamine as the most efficacious treatment in reversing sleep disruption in the CCI rats, whilst pregabalin was partially effective.

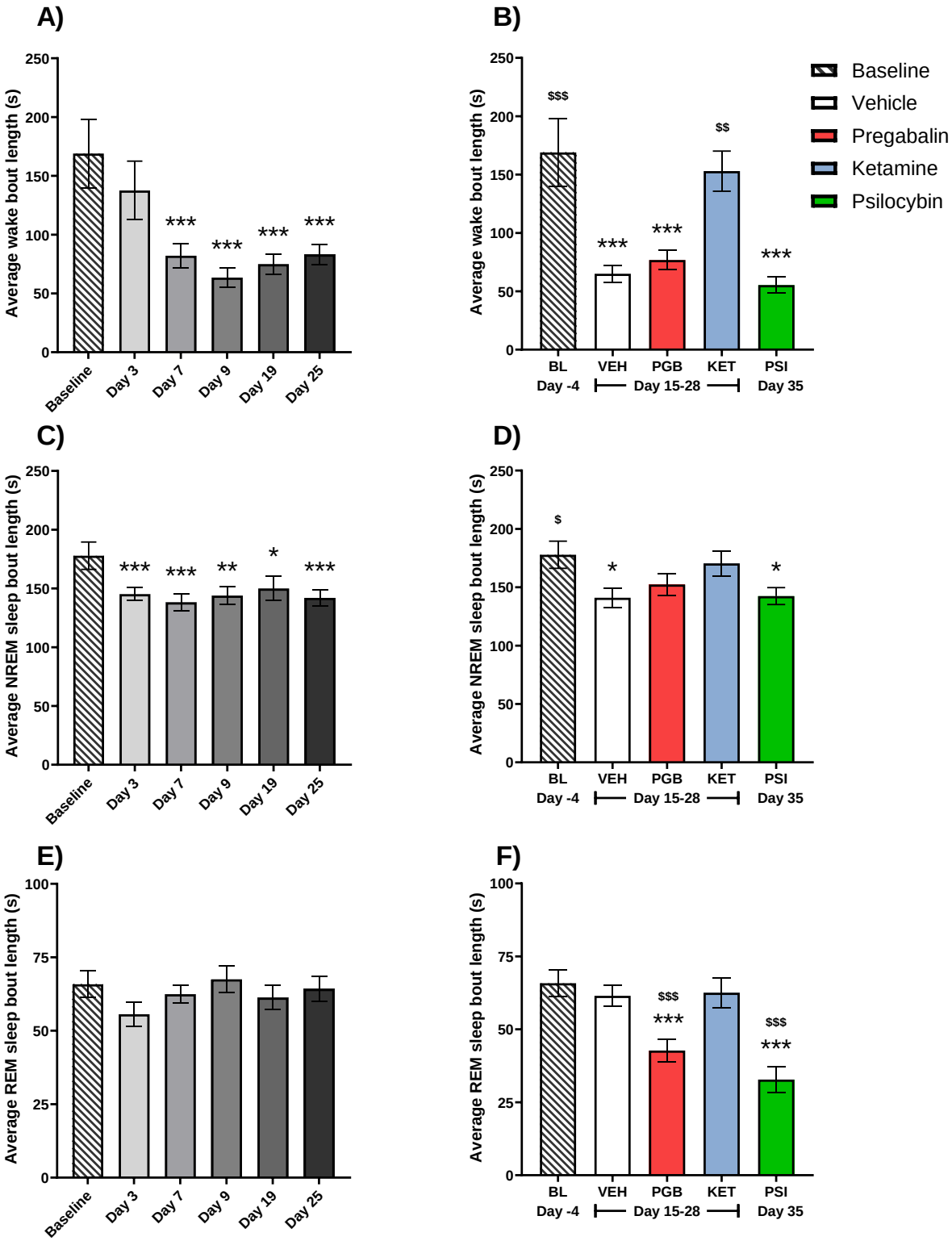

Figure 6.8) CCI rats sleep was fragmented by the decreased average length of wake and NREM sleep bouts which was corrected by ketamine administration during ZT5-ZT11. The effect of CCI surgery (Days 3, 7, 9, 19 and 25) along with vehicle, 10mg/kg pregabalin, 10mg/kg ketamine (Days 15, 21, 28) and 3mg/kg psilocybin (Day 35) test on the average length of wakefulness (A,B), NREM sleep (C,D) and REM sleep (E,F) bouts during ZT5-ZT11 in the light. (A-F) *p<0.05, **p<0.01, ***p<0.001 vs baseline (Day-4). (B,D,F) $$p$<0.05, $$$p$<0.01, $$$$p$<0.001 vs vehicle. All data is reported as mean ± SEM, n=11-12 (A-F).

6.3.6 Sleep fragmentation in CCI rats was primarily caused by increased short (≤10s) bouts of wakefulness and was corrected by pregabalin and ketamine.

Since sleep fragmentation was identified in these CCI rats, it was further assessed to understand if this fragmentation occurred through the animals waking more frequently for short periods of time, as reported by patients and in other neuropathic pain models. To quantify frequent awakenings, the number of short, medium and long bouts of each sleep state were totalled to understand the distribution of the sleep/wake bout lengths. There was a large and consistent increase in the amount of short (≤10s) bouts of wakefulness during both ZT5-ZT11 in the light period and ZT17-ZT23 in the dark period after CCI surgery in the rats. This confirmed that the CCI rats were waking more frequently for short periods of time. Specifically, during ZT5-ZT11 the amount of short (≤10s) bouts of wakefulness progressively increased reaching a 70% increase at Day 9 and remained increased until Day 25 [$F(5,54) = 6.06$, $p<0.001$] (Figure 6.9A). Medium (10-50s) length bouts of wakefulness also increased though only from Day 7 until Day 19 [$F(5,54) = 3.15$, $p=0.015$] (Supp figure 6.16B). The increased short bouts of wakefulness were accompanied by medium (10-150s) length bouts of NREM sleep which were also robustly increased to 70% by Day 7 and remained increased until Day 25 [$F(5,54) = 7.89$, $p<0.001$] (Figure 6.9C). As the average length of REM sleep bouts remained relatively consistent throughout ZT5-ZT11 this was also reflected by a lack of any consistent changes to the number of short (≤10s), medium (10-50s) or long (>50s) bouts of REM sleep in the CCI rats (Supp figure 6.16). The development of increased short bouts of wakefulness was also identified during ZT17-ZT23 in the dark period [$F(5,54) = 6.19$, $p<0.001$] (Figure 6.9E). However, the increased NREM sleep medium bouts were less consistent during this ZT17-ZT23 period [$F(5,54) = 3.31$, $p=0.011$] (Supp figure 6.17E). During ZT17-ZT23 the main effects on NREM and REM sleep bouts were an increased number of long bouts particularly at Day 19 and Day 25 (Supp figure 6.17). The identification of a consistent development of increased short bouts of wakefulness demonstrated that CCI rats were waking more frequently for short periods of time. Particularly during ZT5-ZT11 in the light period when increased short bouts of wakefulness were accompanied by increased medium length NREM sleep bouts further demonstrating the fragmentated nature of the CCI rats sleep.

Both pregabalin and ketamine reversed the increased short wakefulness bouts in the CCI rats. During the first six hours after administration (ZT5-ZT11) 10mg/kg pregabalin and 10mg/kg ketamine both reversed the amount of short (≤10s) bouts of wakefulness back to baseline levels [$F(4,54) = 12.60$, $p<0.001$] (Figure 6.9B). Additionally, both pregabalin and ketamine partially reversed the amount of medium bouts of wakefulness that were increased in the CCI rats [$F(4,54) = 8.78$, $p=0.006$] (Supp figure 6.18B). Though, only ketamine decreased the number of medium NREM sleep bouts back in line with baseline but pregabalin and psilocybin had no effect [$F(4,54) = 6.80$, $p<0.001$] (Figure 6.9D). The effects of pregabalin and ketamine to reverse the increased short bouts of wakefulness in CCI rats were not maintained during ZT17-ZT23 in the dark period [$F(4,43) = 4.70$, $p=0.003$] (Figure 6.9F). Psilocybin had no effect on the number of short bouts of wakefulness or medium bouts of NREM sleep. The main effect of psilocybin administration was that it greatly decreased long (>50s) bouts of REM sleep during the first six hours after administration (ZT5-ZT11) [$F(4,43) = 27.58$, $p<0.001$] (Supp figure 6.18I). Along with this psilocybin subsequently increased long bouts of NREM sleep [$F(4,43) = 17.84$, $p<0.001$] (Supp figure 6.19F) and REM sleep [$F(4,43) = 11.94$, $p<0.001$] (Supp figure 6.19I) during ZT17-ZT23 in the dark period. Pregabalin also caused a shift towards shorter bouts of REM sleep at the expense of longer REM sleep bouts during the first six hours after administration (ZT5-ZT11) (Supp figure 6.18). The overall effects of test compounds on short, medium and long sleep/wake bouts highlighted that both pregabalin and ketamine were efficacious in reducing the number of short bouts of wakefulness. Though ketamine also demonstrated efficacy in correcting the increased number of medium NREM sleep bouts during the first six hours after administration.

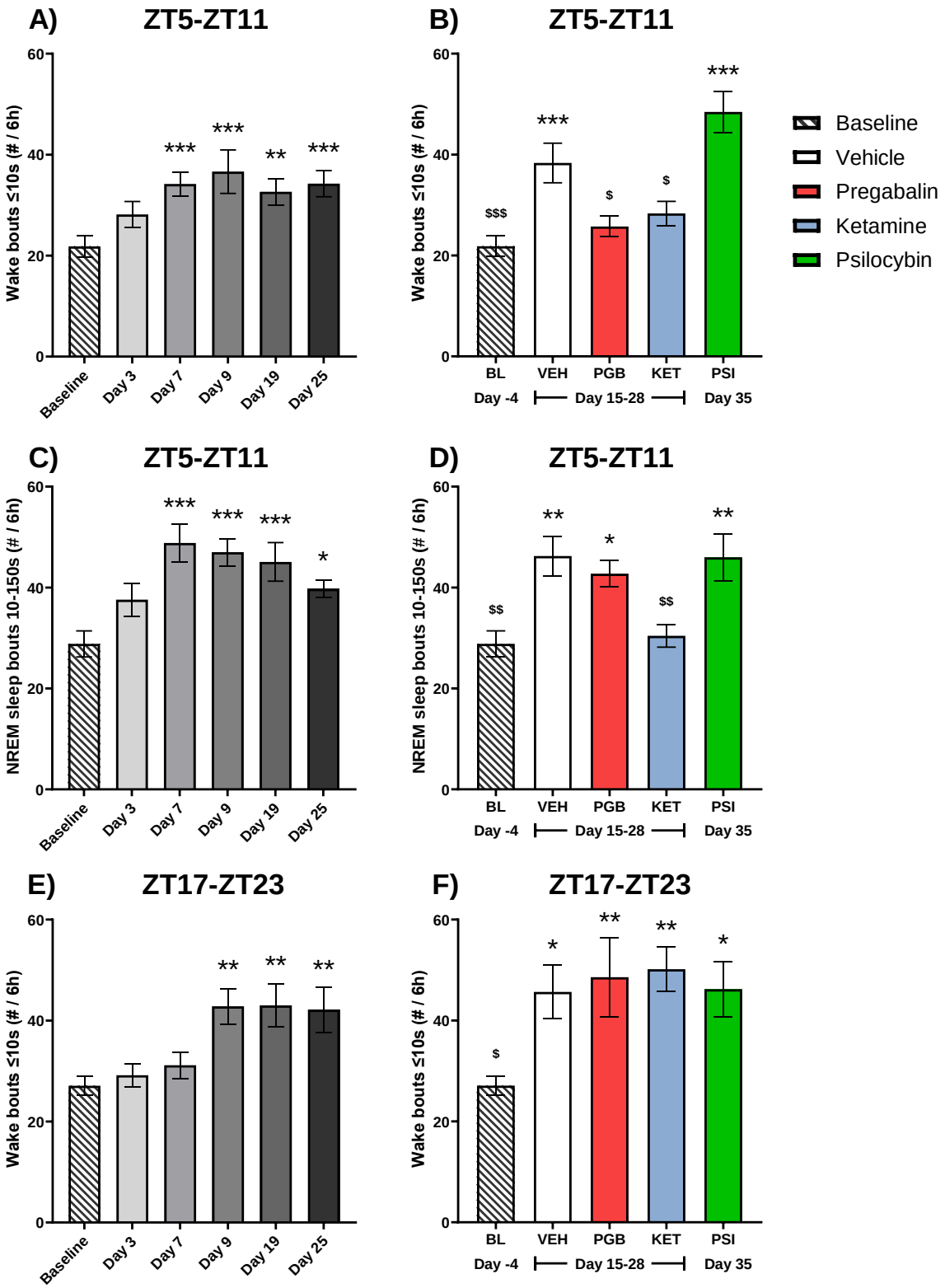

Figure 6.9) CCI rats sleep was fragmented by increased short (≤10s) wake bouts which were normalised by pregabalin and ketamine during ZT5-ZT11. The effect of CCI surgery (Days 3, 7, 9, 19 and 25) along with vehicle, 10mg/kg pregabalin, 10mg/kg ketamine (Days 15, 21, 28) and 3mg/kg psilocybin (Day 35) test compounds on short (≤10s) bouts of wakefulness during ZT5-ZT11 (A,B) and ZT17-ZT23 (E,F) along with medium (10-150s) NREM sleep bouts during ZT5-ZT11 (C,D). (A-F) *p<0.05, **p<0.01, ***p<0.001 vs baseline (Day-4). (B,D,F) $$p$<0.05, $$$p$<0.01,vs vehicle. All data is reported as mean ± SEM, n=11-12 (A-F).

6.3.7 Summary of the sleep/wake behavioural changes in CCI rats.

Table 6.1) Summary of sleep/wake behavioural data in CCI rats during ZT5-ZT11 in the light period and ZT17-ZT23 in the dark period.

	ZT5-ZT11 (light period)			ZT17-ZT23 (dark period)		
	Wake	NREM sleep	REM sleep	Wake	NREM sleep	REM sleep
% time spent	↓	↑	↑	↓	↑	↑
Latency	-	↓	↓	-	-	-
Total number bouts	↑	↑	↑	↑	↑	↑
Average bout length	↓	↓	=	↓	=	=
Short (≤10s) bouts	↑	=	=	↑	=	=
Medium (10-50) / (10-150s) bouts	↑	↑	=	=	↑	=
Long (>50) / (>150s) bouts	=	↑	↑	↑	↑	↑

Summary is based on the comparison between the vehicle (Days 15, 21, 28) and baseline (Day -4) recordings in the CCI rats. ↑ indicates measure was increased after CCI surgery at the vehicle timepoint. ↓ indicates measure was decreased after CCI surgery at the vehicle timepoint. = indicates there was no change after CCI surgery at the vehicle timepoint. – indicates a measurement not recorded.

The overall effects on sleep/wake behaviours in CCI rats indicated relatively consistent changes that occurred during both ZT5-ZT11 in the light period and ZT17-ZT23 in the dark period (Table 6.1). The amount of time the CCI rats spent awake decreased, whilst the number of wake bouts increased, and the average length of each wakefulness bout decreased. This highlights the development of increased fragmentation of the time the CCI rats spent awake. This disruption in wakefulness occurred primarily through increased short and medium length bouts during ZT5-ZT11. Whilst during the ZT17-ZT23 period this occurred through increased short and long bouts of wakefulness. Together these changes indicated that wakefulness became less consolidated with increased short (≤10s) bouts of wakefulness being consistently observed.

The changes in CCI rats NREM sleep were also consistent between the ZT5-ZT11 and ZT17-ZT23 periods, with the main difference being a lack of decreased average bout length during ZT17-ZT23 (Table 6.1). The amount of time the CCI rats spent in NREM sleep was consistently increased and corresponded with an increased number of bouts that occurred. During the ZT5-ZT11 period the increased time spent in NREM sleep and number of NREM sleep bouts were accompanied by the average length of these NREM sleep bouts decreasing which would indicate sleep fragmentation. However, during the ZT17-ZT23 period the average length of NREM sleep bouts was not altered in the CCI rats which could indicate more consolidated NREM sleep during this period. Though there was still a clear disruption to the number and length of wakefulness bouts during the ZT17-ZT23

period. The increased NREM sleep amount and bout number occurred primarily through increased medium and long bouts across the ZT5-ZT11 and ZT17-ZT23 periods. Assessing the development of changes from Day 3 to Day 25 suggested that this effect was predominantly through medium length bouts during the ZT5-ZT11 period and long bouts during the ZT17-ZT23 period.

The effects of CCI surgery on REM sleep were minimal demonstrating primarily increased time spent in REM sleep and an increased number of REM sleep bouts during both the ZT5-ZT11 and ZT17-ZT23 periods. These changes occurred mainly through an increased number of long bouts of REM sleep without many of the other indicators of a disruption to REM sleep homeostasis. The latency to both NREM sleep and REM sleep also decreased in CCI rats which further highlighted the increased propensity for sleep in the rats after CCI surgery. Overall, there was consistent fragmentation of the CCI rats sleep during both ZT5-ZT11 in the light period and ZT17-ZT23 in the dark period that is likely related to the development of neuropathic pain.

6.3.8 Summary of the sleep/wake behavioural changes of pregabalin, ketamine and psilocybin in CCI rats.

Table 6.2) Summary of the test compound effects on sleep/wake behavioural data in CCI rats during ZT5-ZT11 in the light period and ZT17-ZT23 in the dark period.

Sleep/wake behavioural measures	Test compound	ZT5-ZT11 (light period)			ZT17-ZT23 (dark period)		
		Wake	NREM sleep	REM sleep	Wake	NREM sleep	REM sleep
% time spent	10mg/kg Pregabalin	=	=	=	=	=	=
	10mg/kg Ketamine	↑	↓	↓	↓	=	↑
	3mg/kg Psilocybin	=	↑	↓	↓	↑	=
Latency	10mg/kg Pregabalin	-	=	=	-	-	-
	10mg/kg Ketamine	-	↑	↑	-	-	-
	3mg/kg Psilocybin	-	=	↑	-	-	-
Total number bouts	10mg/kg Pregabalin	↓	=	=	=	=	=
	10mg/kg Ketamine	↓	↓	↓	=	=	=
	3mg/kg Psilocybin	↑	=	↓	=	=	↑
Average bout length	10mg/kg Pregabalin	=	=	↓	=	↓	=
	10mg/kg Ketamine	↑	=	=	=	=	=
	3mg/kg Psilocybin	=	=	↓	=	↑	=
Short (≤10s) bouts	10mg/kg Pregabalin	↓	=	=	=	=	=
	10mg/kg Ketamine	↓	=	=	=	=	=
	3mg/kg Psilocybin	=	↑	=	=	=	=
Medium (10-50) / (10-150s) bouts	10mg/kg Pregabalin	=	=	↑	=	=	=
	10mg/kg Ketamine	=	↓	↓	=	=	=
	3mg/kg Psilocybin	=	=	↓	=	=	=
Long (>50) / (>150s) bouts	10mg/kg Pregabalin	=	=	↓	=	↓	=
	10mg/kg Ketamine	=	↓	↓	=	=	=
	3mg/kg Psilocybin	=	↓	↓	↓	↑	↑

Summary is based on the comparison between the 10mg/kg pregabalin, 10mg/kg ketamine (Days 15, 21, 28) and 3mg/kg psilocybin (Day 35) versus vehicle (Days 15, 21, 28) recordings in CCI rats. ↑ indicates measure was increased after test compound administration. ↓ indicates measure was decreased after test compound administration. = indicates there was no change in the measure after test compound administration. – indicates a measurement not recorded. Green boxes indicate a positive change in the direction of the baseline (Day -4) measurement. Red boxes indicate a negative change away from the baseline (Day -4) measurement. Yellow boxes indicate a change after test compound administration whilst there was no difference between baseline (Day -4) and vehicle timepoints.

Of the test compounds tested in this study ketamine was the most effective at correcting sleep/wake behaviours in the CCI rats (Table 6.2). Ketamine fully corrected the changes in CCI rats sleep/wake amounts including normalising the latency to NREM and REM sleep. This demonstrated that ketamine corrected the increased propensity for the CCI rats to enter and remain in NREM sleep during the first six hours after administration. Importantly ketamine also corrected the average length and total number of wakefulness bouts, particularly via reducing the number of short wake

bouts in the CCI rats. This decreased number of short wake bouts was also accompanied by decreased medium and long NREM and REM sleep bouts that had been increased in the CCI rats. Ketamine treatment reduced the fragmentation of sleep, consolidated wakefulness and decreased the abnormal amount of time that CCI rats spent asleep. One limitation of ketamine is that during ZT17-ZT23 in the dark period it caused the CCI rats to spend even more time in NREM sleep at the expense of wakefulness.

Pregabalin was the second most effective test compound at correcting sleep/wake behaviours in the CCI rats (Table 6.2). Although it did not alter the amount of time the CCI rats spent awake or asleep nor the latency to NREM and REM sleep, it decreased the amount of wake bouts. Critically this decreased number of wake bouts occurred primarily through decreasing short bouts of wakefulness. Thus indicating pregabalin may be able to consolidate wakefulness and improve the fragmentation of sleep in CCI rats. Pregabalin administration also had some effects on REM sleep leading to increased medium REM sleep bouts and decreased long REM sleep bouts. Though the positive effects of pregabalin were mainly limited to reducing short bouts of wakefulness it also had negligible negative effects on sleep/wake behaviour.

Psilocybin demonstrated limited positive effects on correcting sleep/wake behaviour, primarily altering measures of REM sleep which was the least affected sleep state in the CCI rats (Table 6.2). The lack of psilocybin efficacy on sleep and EEG measures may correlate with its lack of efficacy against the classical evoked measure of von Frey paw withdrawal thresholds. Psilocybin decreased the amount of time CCI rats spent in REM sleep through delaying the onset of REM sleep and decreasing the number of REM sleep bouts. The changes to REM sleep caused by psilocybin came at the expense of NREM sleep which was further increased in the CCI rats. Psilocybin also further increased the number of wakefulness bouts and increased the number of short bouts of NREM sleep. Though psilocybin did correct the number of medium length REM sleep bouts and the number of long NREM and REM sleep bouts. Psilocybin did not appear to correct the fragmentation of CCI rats sleep or consolidate wakefulness and did not demonstrate any efficacy in classical reflexive pain measures.

6.3.9 EEG power during wakefulness was inconsistent and not reversed by analgesic treatments.

Changes in EEG power have been considered as neuropathic pain endpoints, in particular increased theta power. To understand what changes in EEG power occurred after CCI surgery the full EEG power spectrum at Days 3, 7, 9, 19 and 25 (Figure 6.10) along with the effects of test compounds (Figure 6.11) on EEG power were assessed. The largest trends in EEG power occurred during NREM sleep and indicated a shift in EEG power from low to high frequencies (Figure 6.10C,D). Additionally, after test compound administration 10mg/kg ketamine appeared to have increased EEG power of high frequency oscillations during wakefulness (Figure 6.11A,B). Psilocybin (3mg/kg) decreased EEG power at low frequencies during NREM sleep (Figure 6.11C,D) and 10mg/kg pregabalin appeared to have increased EEG power at lower frequencies during REM sleep (Figure 6.11E,F).

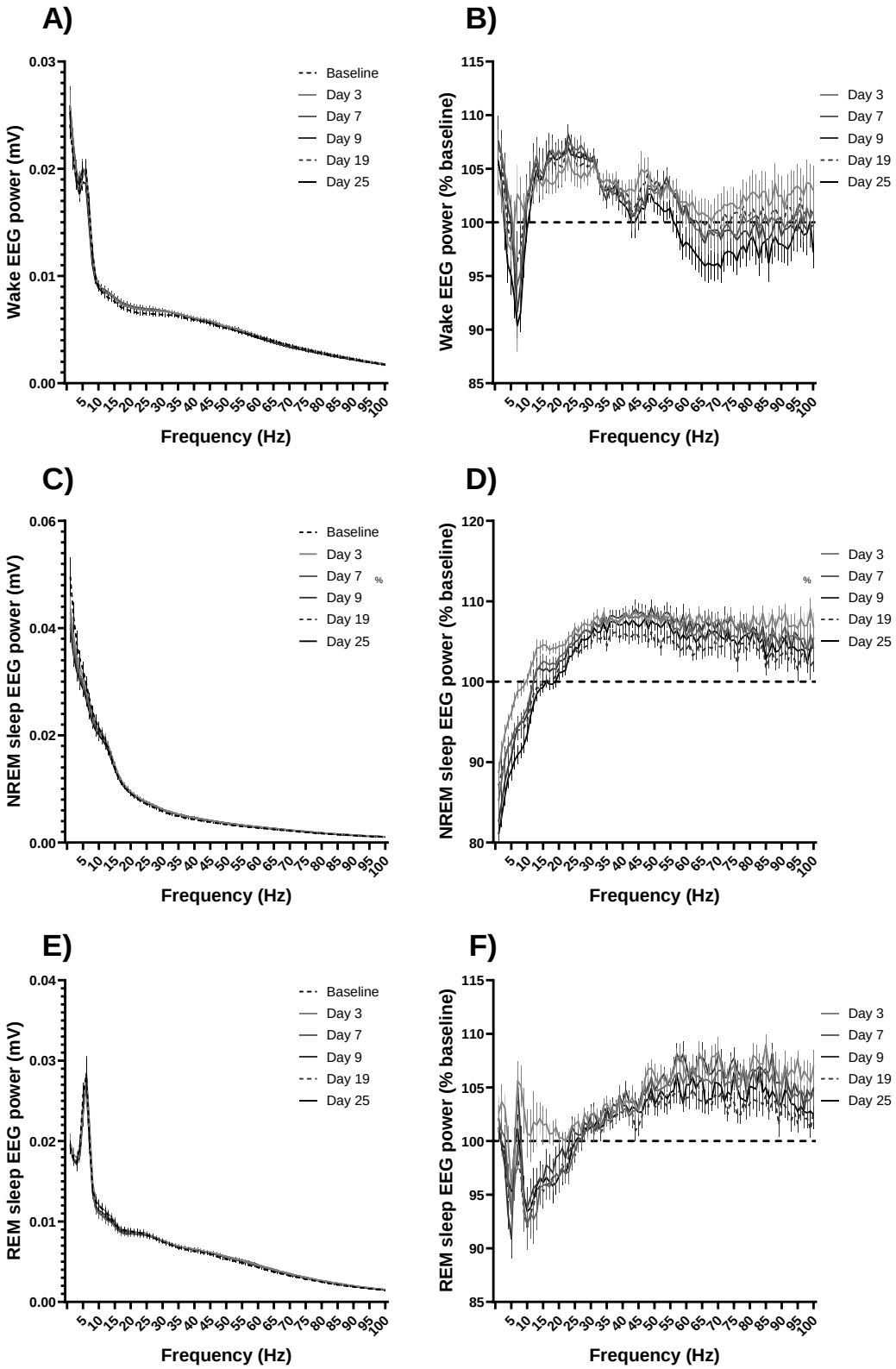

Figure 6.10) The full EEG power spectrum during ZT5-ZT11 in the light period indicated a shift towards higher frequencies during NREM sleep in CCI rats. The effects of CCI surgery (Days 3, 7, 9, 19 and 25) on the full EEG power spectrum during wakefulness (A), NREM sleep (C) and REM sleep (E) across ZT5-ZT11 in the light period. The effects of CCI surgery on the percentage change from baseline (Day -4) EEG power spectrum during wakefulness (B), NREM sleep (D) and REM sleep (F) across ZT5-ZT11 in the light period. No statistical comparisons conducted. All data is reported as mean ± SEM, n=11-12 (A-F).

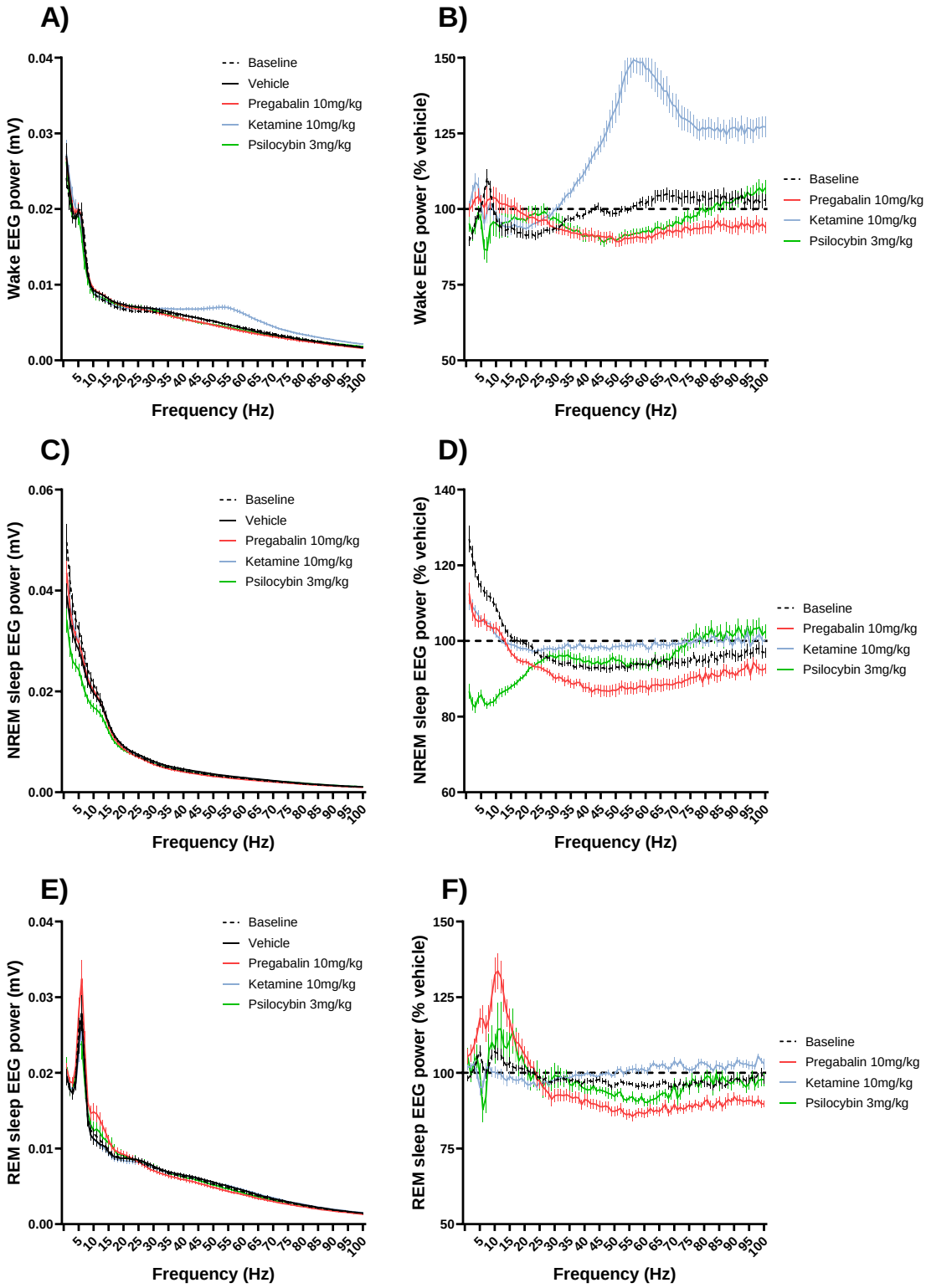

Figure 6.11) The full EEG power spectrum during ZT5-ZT11 in the light period demonstrates that ketamine increased gamma power during wakefulness and psilocybin further decreased low frequency NREM sleep power. The effects of vehicle, 10mg/kg pregabalin, 10mg/kg ketamine (Days 15, 21, 28) and 3mg/kg psilocybin (Day 35) test compounds on the full EEG power spectrum during wakefulness (A), NREM sleep (C) and REM sleep (E) across ZT5-ZT11 in the light period. The effects of test compound administration on the percentage change from vehicle EEG power spectrum during wakefulness (B), NREM sleep (D) and REM sleep (F) across ZT5-ZT11 in the light period. No statistical comparisons conducted. All data is reported as mean ± SEM, n=11-12 (A-F).

Since various changes in EEG power including increased theta power, increased delta power, altered alpha power (bidirectionally changed in patients) or increased beta power have been reported to be associated with neuropathic pain, these were assessed in awake CCI rats. During ZT5-ZT11 in the light period delta EEG power in awake CCI rats increased from Day 7 to Day 19 but not at Day 25 [$F(5,54) = 4.56$, $p=0.002$] (Figure 6.12A). Though increased theta power has previously been reported in CCI rats this was not identified in this study at any point. Theta power was even decreased in the CCI rats in this study at Day 25 [$F(5,54) = 4.82$, $p<0.001$] (Figure 6.12C). Similarly there were no robust changes in alpha power in awake CCI rats during ZT5-ZT11 [$F(5,54) = 5.18$, $p<0.001$] (Supp figure 6.20G). However, beta power in awake CCI rats was increased from as early as Day 3 after CCI surgery and remained increased until Day 25 [$F(5,54) = 6.95$, $p<0.001$] (Figure 6.12E). Though, when assessed during ZT17-ZT23 in the dark period neither increased delta nor beta power were identified and there were no consistent changes to the EEG power spectra of awake CCI rats during ZT17-ZT23 (Supp figure 6.21). This overall demonstrated that of the anticipated changes in delta, theta, alpha and beta EEG power in awake CCI rats, only increased delta and beta power were identified and not consistently during the ZT5-ZT11 and ZT17-ZT23 periods assessed.

To identify if the changes in EEG power of awake CCI rats were reversible with drug treatment the effects of 10mg/kg pregabalin, 10mg/kg ketamine and 3mg/kg psilocybin were tested but were not efficacious. Neither 10mg/kg pregabalin or 10mg/kg ketamine had any effect on delta power during the first six hours after administration (ZT5-ZT11), despite both demonstrating efficacy against classical evoked and sleep/wake measures of neuropathic pain [$F(4,43) = 7.09$, $p<0.001$] (Figure 6.12B). Psilocybin (3mg/kg) which had no effect on classical evoked neuropathic pain measures and minimal effect on sleep/wake behaviours did partially reverse the increased delta power in CCI rats. However, as delta power was not increased in the CCI rats at Day 25 (Figure 6.12A) and psilocybin was assessed at Day 35 this may represent a lack of increased delta power in the CCI rats rather than any efficacy of psilocybin. Additionally, neither pregabalin, ketamine or psilocybin had any effect on theta power or alpha power [$F(4,43) = 1.67$, $p=0.26$] (Supp figure 6.22G) in the awake CCI rats during the first six hours after administration (ZT5-ZT11) [$F(4,43) = 3.11$, $p=0.025$] (Figure 6.12D). Despite beta power being increased in the CCI rats from Day 3 to Day 25 (Figure 6.12E) this was not robust enough to reach significance in the overall ANOVA when comparing the effects of vehicle to the baseline, and none of the compounds tested had any effect on beta power [$F(4,43) = 2.52$, $p=0.055$] (Figure 6.12F). Whilst none of the test compounds had efficacy in altering delta, theta, alpha or beta power pregabalin, ketamine and psilocybin did alter gamma power in the awake CCI rats even though CCI surgery had no effect [$F(4,43) = 137.7$, $p<0.001$] (Supp figure 6.22M). Both pregabalin and psilocybin decreased gamma power in the awake CCI rats whilst ketamine increased gamma power (Supp figure 6.22M). Therefore, whilst increased delta and beta power were identified in the EEG power spectra of awake CCI rats, neither of these changes were corrected by pregabalin, ketamine or psilocybin treatment.

Despite the lack of positive results from EEG power spectra in awake CCI rats the EEG power spectra of CCI rats were also assessed during NREM and REM sleep to identify any changes that may relate to sleep quality. The most important change identified was decreased NREM sleep delta power in CCI rats, which was decreased from Day 3 to Day 25 during ZT5-ZT11 in the light period [$F(5,54) = 32.32$, $p<0.001$] (Figure 6.12G). This represented decreased NREM sleep quality that was partially reversed by both pregabalin and ketamine [$F(4,43) = 40.35$, $p<0.001$] (Figure 6.12H). Whilst psilocybin further decreased NREM sleep delta power in the CCI rats during this ZT5-ZT11 period (Figure 6.12H). Alongside the decreased NREM sleep delta power theta and sigma power decreased during both ZT5-ZT11 in the light period (Supp figure 6.20) and ZT17-ZT23 in the dark period (Supp figure 6.21). NREM sleep gamma power also correspondingly increased during both ZT5-ZT11 and

ZT17-ZT23 periods demonstrating a shift in EEG power towards higher frequencies in the CCI rats. REM sleep EEG power was largely unaltered in the CCI rats during either the ZT5-ZT11 (Supp figure 6.20) or ZT17-ZT23 (Supp figure 6.21) with only gamma power being increased after CCI surgery during ZT5-ZT11. Ketamine and psilocybin had little effect on REM sleep EEG power however pregabalin caused a shift towards increased lower frequency (delta, theta, sigma) power and decreased gamma power during both the ZT5-ZT11 (Supp figure 6.20) and ZT17-ZT23 (Supp figure 6.21) periods. CCI rats had decreased NREM sleep delta power, a measure of lower sleep intensity, which was partially corrected by pregabalin and ketamine.

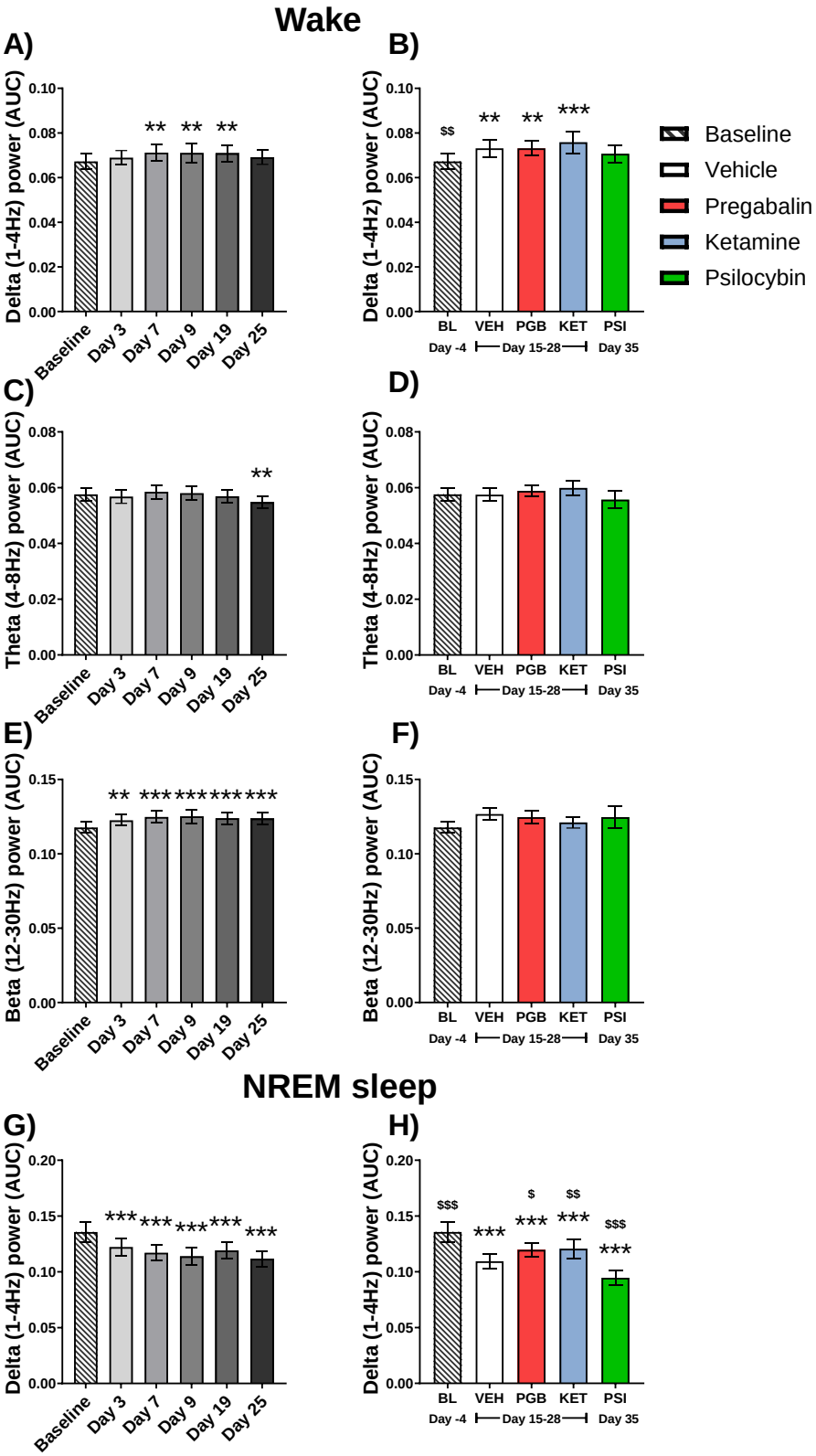

Figure 6.12) Increased delta and beta power during wakefulness in the CCI rats were not corrected by drug treatment. The effect of CCI surgery (Days 3, 7, 9, 19 and 25) along with vehicle, 10mg/kg pregabalin, 10mg/kg ketamine (Days 15, 21, 28) and 3mg/kg psilocybin (Day 35) test compounds on the EEG power in the delta (1-4Hz) (A,B,C), theta (4-8Hz) (D,E,F), and beta (13-30Hz) (J,K,L) frequency bands during wakefulness. Along with the effects on delta (1-4Hz) power during NREM sleep across ZT5-ZT11 in the light period. (A-H) $^{**}p<0.01$, $^{***}p<0.001$ vs baseline (Day-4). (B,D,F,H) $\$p<0.05$, $\$\$p<0.01$, $\$\$\$p<0.001$ vs vehicle. All data is reported as mean ± SEM, n=11-12 (A-H).

6.4 Discussion

Current treatments for neuropathic pain are limited and have extensive side effects leaving many patients without adequate treatment options. Despite many years of research forward translation of new treatments for neuropathic pain have often failed upon reaching clinical trials (Fisher et al., 2021). This lack of forward translation has led to questions over the validity of the animal models and neuropathic pain endpoints that are currently used preclinically. The classical ways that neuropathic pain has been measured preclinically involve the subjective analysis of evoked responses from animals using thermal or mechanical stimuli (Cobos & Portillo-Salido, 2013; Tappe-Theodor et al., 2019). Whilst these classical evoked neuropathic pain endpoints deliver reproducible results across studies and research groups, they have thus far have lacked forward translatability (Cobos & Portillo-Salido, 2013; Fisher et al., 2021; Tappe-Theodor et al., 2019). Therefore, novel objective and non-evoked endpoints of neuropathic pain are being investigated to try and improve the translatability of preclinical neuropathic pain research. However, these novel endpoints must be reliable, reproducible, cost efficient, time effective and most importantly predictive to encourage an improvement in the use of evoked preclinical screening techniques (Bouali-Benazzouz et al., 2021).

One tool that is being used to develop an objected non-evoked neuropathic pain endpoint is EEG (Koyama, LeBlanc, et al., 2018). Two main approaches are being applied to EEG recordings in neuropathic pain models, measuring sleep/wake behavioural changes and brain electrical activity in the form of EEG power (Alexandre et al., 2024; Koyama, LeBlanc, et al., 2018). Both sleep/wake behavioural changes and EEG power have shown mixed results in preclinical neuropathic pain models (Andersen & Tufik, 2003; Ho et al., 2024; Koyama, LeBlanc, et al., 2018; Li, Ge, et al., 2019; f). However, increased sleep fragmentation and increased theta power stand out as the most consistently reported changes in EEG recordings for measuring neuropathic pain (Alexandre et al., 2024; Ho et al., 2024; Koyama, LeBlanc, et al., 2018; LeBlanc, Bowary, et al., 2016). This study therefore aimed to identify sleep/wake behavioural and EEG changes that could be quantified using an automatic sleep/wake scoring algorithm as neuropathic pain endpoints in a rodent model of CCI. The suitability of these endpoints for preclinical screening studies was also assessed through their reversibility with standard (pregabalin), novel (ketamine) and potential (psilocybin) analgesic test compounds.

6.4.1 CCI surgery caused mechanical allodynia that was reversed by pregabalin and ketamine.

The effects of CCI surgery on the classical evoked neuropathic pain endpoint of von Frey paw withdrawal threshold was measured throughout the study. This demonstrated that all CCI rats paw withdrawal thresholds decreased in the ipsilateral hind paw at all timepoints measured from Day 7 to Day 37 (Figure 6.2A). Reduced paw withdrawal latency in CCI rats is a classical way to measure the development of mechanical allodynia, defined as an increased sensitivity to a normally non painful pressure being applied (Austin et al., 2012; Kumar et al., 2010; Medeiros et al., 2021; van der Wal et al., 2015). The onset of mechanical allodynia confirms that all rats developed neuropathic pain. This is consistent with previous findings that a robust level of neuropathic pain develops in rats shortly after CCI surgery (Austin et al., 2012; Kumar et al., 2010; Medeiros et al., 2021; van der Wal et al., 2015). The contralateral hind paw is often used a time matched control measure of paw withdrawal threshold in CCI rats (Austin et al., 2012; Medeiros et al., 2021). Unlike bilateral neuropathic pain

models such as the oxaliplatin and streptozotocin induced models, if CCI surgery is conducted on only a single hind paw the development of neuropathic pain should be unilateral (Gao et al., 2019; Ling et al., 2008). In this study there was no change in the contralateral paw withdrawal threshold in CCI rats which confirmed that the changes in the ipsilateral paw were due to the CCI surgery and not environmental factors.

The reversal of the von Frey paw withdrawal threshold is a standard method for assessing the efficacy of analgesic treatments against neuropathic pain (Bacalhau et al., 2023). Both pregabalin and ketamine successfully reversed the mechanical allodynia of CCI rats confirming their analgesic potential against the classical neuropathic pain endpoint of von Frey paw withdrawal threshold (Figure 6.2C). The reversal of neuropathic pain with pregabalin is consistent with previous research including the assessment of pregabalin's efficacy in the CCI model prior to its approval for neuropathic pain, one of the only examples of forward translation in a neuropathic pain model (Field, Bramwell, et al., 1999). Whilst pregabalin has consistently demonstrated its efficacy in preclinical models and is an approved treatment for neuropathic pain patients, ketamine is not yet approved for use against neuropathic pain. Ketamine does however consistently demonstrate efficacy in preclinical neuropathic pain models, including the CCI model (Velzen et al., 2021). Additionally, there is clinical evidence that ketamine effectively reversed pain in patients with various causes of neuropathic pain, though its use is limited by psychedelic side effects (Guimarães Pereira et al., 2022). Ketamine is also used off label at "ketamine clinics" to treat neuropathic pain patients (Voute et al., 2022). This suggests that the effects of ketamine and pregabalin see here are consistent with both human and animal data in reversing neuropathic pain.

The evidence of psilocybin's analgesic potential is more tenuous as it did not reverse the mechanical allodynia in the CCI rats in this study. In preclinical models there is limited evidence of psilocybin producing robust reversal of classical neuropathic pain models (Kolbman et al., 2023; Koseli et al., 2023). There is also limited clinical evidence of psilocybin's efficacy as an analgesic in neuropathic pain patients, despite some clinical reports of off label patient use (Bornemann et al., 2021; Lyes et al., 2023). The lack of both preclinical and clinical evidence of psilocybin analgesia supported the lack of analgesia experienced by the CCI rats in this study after psilocybin administration (Figure 6.2C). Notably, psilocybin decreased the paw withdrawal threshold in the contralateral control paw after psilocybin administration (Figure 6.2D). This may have occurred as the descending facilitatory pain pathway often involves 5-HT_2 receptor activation and as such psilocybin as a 5-HT_{2a} agonist may have caused hypersensitivity through this mechanism (Ossipov et al., 2014). Overall, assessing the classical evoked neuropathic pain endpoint of von Frey paw withdrawal threshold indicated that pregabalin and ketamine demonstrated analgesia in CCI rats, but psilocybin did not.

6.4.2 Locomotor activity was reduced in CCI rats and normalised by ketamine.

Locomotor activity was assessed in this study to understand if there were any effects of the CCI surgery on the rat's ambulation or movement levels as measurements of their ethological behaviours. Locomotor activity progressively decreased in the CCI rats during both ZT5-ZT11 in the light period and ZT17-ZT23 in the dark period (Figure 6.3). The development of locomotor activity also matched the development of mechanical allodynia as both were detected at Day 7 and maintained throughout the study. Changes in locomotor activity have previously been assessed in neuropathic pain models yielding mixed results. In CCI models locomotor changes have primarily been assessed through open field testing (OFT) or gait changes not typically through monitoring home cage behaviours over extended periods (Fonseca-Rodrigues et al., 2021). These types of

studies often report a lack of changes in locomotor activity in CCI models suggesting that locomotor activity is not a useful measure of neuropathic pain (Medeiros et al., 2021; Mogil et al., 2010; Foudah et al., 2022). Though some studies have reported decreased walking distance in CCI rats using OFT systems (Bagriyanik et al., 2014). Additionally, some evidence from monitoring CCI mice over long periods of time in a home cage type environment have suggested that these animals spend less time in locomotion and more time stationary (Urban et al., 2011). Locomotor activity is also used as an objective measure of pain in osteoarthritic models of pain suggesting changes in locomotor activity may be related to pain (Alsalem et al., 2020). Most importantly, decreased physical activity is often reported in patients with neuropathic pain (Attal et al., 2011). Therefore, as locomotor activity is an ethological behaviour expressed by rodents that is reduced after neuropathic pain onset and can be measured objectively, these changes may prove to be translatable to the effects of neuropathic pain on patients' daily activities (Attal et al., 2011). Overall, the development of locomotor activity changes in CCI rats in this study provide evidence towards the use of home cage locomotor activity recordings as an objective translatable preclinical neuropathic pain endpoint.

Ketamine was the only test compound that increased the locomotor activity of CCI rats back to baseline levels in the first six hours after administration. This increased locomotor activity could be considered to represent a stimulant-like effect such as that caused by amphetamine (Minassian et al., 2016). However previously published results indicated that 10mg/kg ketamine does not increase locomotor activity in naïve Sprague Dawley rats (Kantor et al., 2023). Therefore, the increased locomotor activity caused by ketamine in these CCI rats likely reflected a reversal of neuropathic pain induced deficits in locomotor activity and further supported its use as a measure of neuropathic pain. Though the effects of ketamine to improve locomotor activity did not remain throughout the ZT17-ZT23 periods this aligns with previous preclinical reports that the analgesic efficacy of ketamine is limited to the first few hours after administration (Velzen et al., 2021). The short-lasting efficacy of a single dose of ketamine may be expected due to its short half-life of only 25 minutes in rodents (Ganguly et al., 2018). Future work should assess if repeated ketamine doses, that have demonstrated mechanical allodynia reversal for over 72 hours (Velzen et al., 2021), are also effective at reversing locomotor activity across a similar time frame.

As both pregabalin and ketamine reversed the von Frey paw withdrawal threshold classical measure of neuropathic pain, it was expected that pregabalin would reverse the deficit in locomotor activity in CCI rats. However, the lack of pregabalin efficacy in reversing locomotor activity could be due to ketamine demonstrating superior efficacy as a neuropathic pain treatment above both pregabalin and psilocybin in this study. Alternatively, the lack of pregabalin efficacy could be due to the somnolence effects of pregabalin that have been demonstrated in Chapter 3 (Brooks & Kessler, 2017). Though this is unlikely as the 10mg/kg pregabalin dose was selected as it did not demonstrate somnolence in either Chapter 3 when assessing control rats or in this study when assessing the effects of pregabalin on the contralateral paw (Figure 6.2D). This is some of the first evidence that home cage locomotor activity measurements in CCI rats are progressively decreased and can be reversed by ketamine but not pregabalin or psilocybin. This may therefore indicate that measuring locomotor activity can preferentially select compounds that improve the affective aspects of neuropathic pain on ethological behaviours above simple reflex-based measurements of von Frey paw withdrawal thresholds.

6.4.3 CCI rats spent more time in NREM sleep at the expense of wakefulness which was corrected by ketamine.

Sleep disruption is frequently reported by neuropathic pain patients and is associated with worse pain outcomes meaning sleep/wake behavioural endpoints could provide important and translatable results (Guntel et al., 2021; Tofthagen et al., 2013). Sleep/wake behavioural assessments of neuropathic pain models have focused on two main areas: changes in the amount of sleep and/or fragmentation of sleep. In patients a decrease in the amount of time spent asleep is often reported (Guntel et al., 2021; Mahfouz et al., 2024; Widerstrom-Noga et al., 2001). However, the reports of neuropathic pain induced changes in sleep/wake amounts in preclinical models are more inconsistent, with some reporting a decrease in time spent asleep (Andersen & Tufik, 2003; Ho et al., 2024) whilst others have reported no change in sleep/wake amount (Alexandre et al., 2024; Kontinen et al., 2003; Leys et al., 2013). An increase in the amount of time neuropathic pain models spend asleep is rarely reported. However, one study has identified that CCI mice spend more time in NREM sleep at expense of wakefulness during the dark period (Alexandre et al., 2024). Sleep disruption through sleep fragmentation is also commonly reported in patients (Guntel et al., 2021; Mahfouz et al., 2024; Widerstrom-Noga et al., 2001) and is more consistently reported as an alteration in neuropathic pain animals sleep/wake behaviour. In particular the number of arousals or increased short bouts of wakefulness have been reported in a range of neuropathic pain models and may provide a useful objective neuropathic pain endpoint (Alexandre et al., 2024; Andersen & Tufik, 2003; Ho et al., 2024).

In this study, after CCI surgery the rats spent more time in NREM sleep at the expense of wakefulness, particularly during ZT17-ZT23 in the dark period. CCI rats progressively spent more time in NREM and REM sleep across the first 25 days of the study during ZT17-ZT23 (Supp figure 6.13). A similar effect was observed during ZT5-ZT11 in the light period however, this returned to baseline levels by Day 25 (Figure 6.5). During both the ZT5-ZT11 and ZT17-ZT23 periods this increased propensity for sleep was at the expense of less time spent awake. Further supporting this the CCI rats in this study had an increased propensity to enter into both NREM and REM sleep as demonstrated by the decreased latency to enter these sleep states (Figure 6.6). These changes of increased propensity for NREM sleep at the expense wakefulness were similar to the findings that CCI mice spent more time in NREM sleep at expense of wakefulness during the dark period (Alexandre et al., 2024). However, they also contrast previous findings in CCI rats that NREM sleep was decreased (Andersen & Tufik, 2003). Additionally, others have reported no change in CCI rats sleep/wake amount as far as 5 months after surgery (Kontinen et al., 2003). The differences in sleep/wake amount demonstrated across different studies in CCI rat models could be due to differences in environmental and housing conditions. For example Tokunaga et al. (2007) detected no change in CCI rats sleep/wake amount until they were placed on sandpaper flooring (Tokunaga et al., 2007). Importantly, the development of increased sleep at the expense of wakefulness in the present study is inconsistent with clinical findings that patients spend less time asleep (Guntel et al., 2021; Mahfouz et al., 2024; Widerstrom-Noga et al., 2001). The inconsistent findings in sleep/wake amounts across research groups and contradictory findings to the human condition may limit its usefulness as a preclinical neuropathic pain endpoint by hampering the translatability potential.

As with locomotor activity, ketamine was the most effective test compound at reversing the changes in sleep/wake amount and sleep latency. Ketamine was the only test compound that fully corrected the amount of time CCI rats spent awake and in NREM sleep back to baseline levels (Figure 6.5). Additionally, ketamine was the only test compound that reversed the latency to NREM and REM sleep, correcting the propensity for CCI rats to enter into sleep (Figure 6.6). The positive effects of

ketamine were again limited to the first six hours after administration. Interestingly, despite pregabalin having no effect on sleep/wake amounts or sleep latency in the first six hours after administration, it partially corrected NREM sleep and wakefulness amounts in the CCI rats during ZT17-ZT23 in the dark period (Supp figure 6.13). Psilocybin had no beneficial effects on wakefulness or NREM sleep in the CCI rats only causing a large decrease in REM sleep amount at the expense of further increased NREM sleep. This effect of psilocybin was also accompanied by a long delay in CCI rats entering REM sleep. The evidence that ketamine corrected the propensity for sleep along with the partial effects of pregabalin on sleep/wake amounts is the first report of drug treatments improving sleep/wake amounts in CCI rats.

Increased time spent in REM sleep and decreased REM sleep latency are both hallmarks of depression (Palagini et al., 2013; Wilson & Argyropoulos, 2005). In this study CCI rats had a decreased latency to REM sleep (Figure 6.6) and REM sleep marginally increased, though not when comparing the vehicle and baseline recordings (Figure 6.5). Additionally the changes in REM sleep in depressed patients are usually accompanied by decreased NREM sleep which was not identified in the CCI rats in this study (Figure 6.5) (Palagini et al., 2013; Wilson & Argyropoulos, 2005). The decreased REM sleep latency and increased REM sleep in this study are also not reported in all CCI rat studies (Andersen & Tufik, 2003; Kontinen et al., 2003). Though depressive characteristics have previously been identified in CCI rats when using the sucrose preference test and forced swimming tests (Xi et al., 2023). As such there is not enough evidence in this study to determine if the CCI rats were depressed, therefore future studies could include a more specific depression endpoint to assess this. Despite the inconclusive evidence of depression in the CCI rats in this study, the effects of psilocybin and ketamine on REM sleep are likely evidence of their anti-depressant properties. Ketamine (10mg/kg) has previously been demonstrated to increase REM sleep latency and decrease REM sleep amount in naïve Sprague Dawley rats and in a treatment resistant depression rat model (Wistar-Kyoto rats) (Kantor et al., 2023). The delayed REM sleep onset and reduction in REM sleep amount caused by psilocin, the active metabolite of psilocybin, has also previously been demonstrated in naïve C57BL/6 J mice (Thomas et al., 2022). Additionally, both the effects on REM sleep amount and latency by 3mg/kg psilocybin have been identified by Transpharmation LTD in naïve Sprague Dawley and Wistar-Kyoto rats (unpublished observation). Therefore, the effects of ketamine and psilocybin on the amount of REM sleep and REM sleep latency in the CCI rats in this study are likely evidence of their anti-depressant properties, despite the CCI rats not developing a clear depressive phenotype. Notably as ketamine also demonstrated a reversal of mechanical allodynia and abnormal sleep/wake amounts, this study suggests that ketamine may have analgesic, anti-depressive and sleep corrective properties in CCI rats.

6.4.4 CCI rats sleep was fragmented primarily through short (≤10s) bouts of wakefulness.

CCI rats sleep was fragmented in this study particularly during ZT5-ZT11 in the light period as demonstrated by the increased number (Figure 6.7) and decreased average length (Figure 6.8) of sleep/wake bouts over 25 days. This phenomenon of fragmented sleep in preclinical neuropathic pain models has been demonstrated previously in the sciatic nerve crush injury mouse model (Ho et al., 2024), common peroneal nerve ligation models (Ho et al., 2024), spared nerve injury mouse model (Alexandre et al., 2024), CCI mouse model (Alexandre et al., 2024) and CCI rat model (Andersen & Tufik, 2003). Additionally, sleep fragmentation is also commonly reported in patients (Guntel et al., 2021; Mahfouz et al., 2024; Widerstrom-Noga et al., 2001). In this study CCI rats were awake more frequently but for shorter periods during both the ZT5-ZT11 and ZT17-ZT23 periods. However, whilst NREM sleep was similarly affected during ZT5-ZT11 there was no change in the

length of NREM sleep bouts during ZT17-ZT23 in the CCI rats. Whilst this could reflect that the CCI rats sleep was more consolidated during the ZT17-ZT23 period, there were still significant changes to the number of sleep bouts and the periods of wakefulness in between were far less consolidated. Thus, it appears that measuring the disrupted sleep in CCI rats was most consistently measured through the changes to the length and number of wakefulness bouts.

As the fragmentation of sleep in the CCI rats in this study was consistent with other preclinical neuropathic pain models, it was assessed if this also occurred primarily through increased brief awakenings. In this study CCI rats demonstrated consistently increased short (≤10s) bouts of wakefulness during both ZT5-ZT11 in the light period and ZT17-ZT23 in the dark period (Figure 6.9). Many of the studies that identified sleep fragmentation in preclinical neuropathic pain models also assessed fragmentation of NREM sleep via the number of transitions from NREM sleep to wakefulness (Ho et al., 2024), the amount of >15s arousals followed by NREM sleep (Andersen & Tufik, 2003) or the quantity of brief <16s arousals that interrupt NREM sleep (Alexandre et al., 2024). These studies all demonstrated an increased number of arousals, particularly short bouts of wakefulness, that were considered to reflect neuropathic pain induced disruption of sleep and possibly even spontaneous neuropathic pain (Alexandre et al., 2024; Andersen & Tufik, 2003; Ho et al., 2024). Alexandre et al. (2024) demonstrated that brief <16s arousals were decreased by analgesic treatments and genetic silencing of peripheral sensory neurons in mice (Alexandre et al., 2024). Additionally, Alexandre et al. (2024) also found that models of inflammatory and postoperative pain did not develop sleep fragmentation or increased brief arousals suggesting these changes are restricted to neuropathic pain models (Alexandre et al., 2024). Therefore, the findings of the present study that short ≤10s bouts of wakefulness were highly elevated in CCI rats (Figure 6.9) is likely related to neuropathic pain induced changes in sleep fragmentation and is consistent with published findings. A key feature of these previous studies is that they used human visual scoring of the EEG data to determine which epochs were wakefulness, NREM sleep or REM sleep. Whilst this is typically the most accurate way to score EEG recordings it is time, labour and cost intensive making its application in high throughput preclinical screening studies limited (Muto & Berthomier, 2023). Therefore, the identification in this study that sleep fragmentation and increased short bouts of wakefulness can be detected through an automated sleep/wake scoring algorithm demonstrates great evidence for their use as preclinical neuropathic pain endpoints. Whilst the evidence that patient's sleep is also fragmentated further supports that the objective recording of sleep fragmentation has good translatability potential (Guntel et al., 2021; Mahfouz et al., 2024; Widerstrom-Noga et al., 2001).

Assessing short, medium and long bout of wakefulness and sleep also indicated that NREM sleep fragmentation during ZT5-ZT11 in the light period occurred primarily through increased medium (10-150s) length NREM sleep bouts (Figure 6.9). Whilst during ZT17-ZT23 in the dark period, when NREM sleep was more consolidated, long (>150s) bouts were the primary source of this change, likely due to the increased time CCI rats spent asleep. This effect is similar during REM sleep in the CCI rats for which increased long (>50s) bouts were the primary cause of the increased number of REM sleep bouts whilst the average length remained consistent. The increased long REM sleep bouts also supported the evidence that neuropathic pain has limited impact on REM sleep in CCI rats with the main effects occurring on NREM sleep and wakefulness. The limited effects on REM sleep in CCI rats is consistent with findings in the spared nerve injury and CCI mice models (Alexandre et al., 2024).

6.4.5 Sleep fragmentation and increased short (≤10s) bouts of wakefulness were corrected by pregabalin and ketamine.

Whilst the identification of sleep fragmentation and increased short bouts of wakefulness in CCI rats is interesting, these changes must be reversible by analgesic treatments to be a useful as neuropathic pain endpoints (Alexandre et al., 2024). In this study both pregabalin and ketamine demonstrated varying levels of efficacy to correct measures of sleep fragmentation whilst psilocybin affected almost exclusively REM sleep. Ketamine demonstrated the best efficacy to reverse measures of sleep fragmentation including normalising the number of wake, NREM and REM sleep bouts back to baseline levels (Figure 6.7). Additionally, ketamine improved the average length of wakefulness bouts reversing this measure to baseline levels (Figure 6.8). Ketamine also corrected the short bouts of wakefulness that have routinely been considered as a measure of neuropathic pain in these CCI rats (Figure 6.8). Furthermore, ketamine decreased the amount of medium and long bouts of both sleep states to levels equivalent of the baseline timepoint. Thus, it appears ketamine's correction of sleep/wake amounts focused on reversing the effects of CCI surgery on sleep and wakefulness bouts without causing additional fragmentation of sleep. These findings of corrected sleep/wake amount, latency to sleep and sleep fragmentation after ketamine treatment provided the first evidence of the efficacy of ketamine to reverse sleep/wake behavioural endpoints of neuropathic pain in a preclinical model.

In contrast to ketamine, psilocybin had no positive effects on the sleep fragmentation or short bouts of wakefulness detected in the CCI rats. Psilocybin decreased the number of long bouts of NREM sleep however this was at the expense of increasing the number of short bouts of NREM sleep (Supp figure 6.18). The main effects of psilocybin on sleep/wake fragmentation revolved around altering REM sleep and demonstrated little potential as an analgesic treatment by correcting sleep fragmentation or short bouts of wakefulness. Psilocybin instead almost eradicated long bouts of REM sleep and decreased medium bouts of REM sleep. This led to a reduction in both the number and average length of REM sleep bouts often far below baseline levels, changes that are likely associated with its anti-depressant properties (Palagini et al., 2013; Wilson & Argyropoulos, 2005).

Further research into the effects of analgesics on these sleep/wake behavioural endpoint is needed and has not yet been conducted (Andersen & Tufik, 2003; Ho et al., 2024). Some of the only evidence of reversing sleep fragmentation and increased short bouts of wakefulness have been demonstrated by Alexandre et al. (2024). They demonstrated that gabapentin and carbamazepine, two clinically used neuropathic pain treatments, reversed these sleep fragmentation and brief arousal endpoints of neuropathic pain (Alexandre et al., 2024). Therefore, it is promising that in the present study pregabalin, a compound with the same mechanism of action to gabapentin, corrected some of the sleep/wake behavioural endpoints. The main effect of pregabalin in reversing sleep/wake behavioural endpoints in this study was that it decreased the total number of wake bouts (Figure 6.7). This decrease in wake bouts occurred primarily through pregabalin reducing the number of short wake bouts to baseline levels. Therefore, both ketamine and pregabalin have demonstrated efficacy in reversing the increased number of short bouts of wakefulness caused by CCI surgery. Pregabalin, unlike ketamine, did induce a change in REM sleep medium bouts that appear to be unrelated to its analgesic effects. Namely pregabalin caused a shift in REM sleep bout lengths towards increased medium bouts at the expense of long REM sleep bouts despite not affecting the overall amount of time CCI rats spend in REM sleep. The comparative effects of ketamine and pregabalin on sleep/wake behavioural changes in this study suggests superior efficacy of ketamine at reversing CCI surgery induced changes. This is in contrast to the efficacy of these drugs against the traditional non-evoked endpoint of von Frey paw withdrawal threshold. Both

pregabalin and ketamine reversed mechanical allodynia in the CCI rats however, the effects were more robust with pregabalin (Figure 6.2). As such sleep/wake behavioural tests such as sleep fragmentation and increase short bouts of wakefulness may prove to be a useful preclinical neuropathic pain endpoint and offer insight into the analgesic efficacy of test compounds in preclinical neuropathic pain models.

Overall, as both pregabalin and ketamine reduced the number of overall wakefulness bouts, ketamine increased the average wake bout length and particularly both pregabalin and ketamine reduced the number of short bouts of wakefulness, it supports the use of sleep fragmentation and increased short wake bouts use as objective assessment endpoints of neuropathic pain. Moreover, ketamine may offer superior analgesic efficacy compared to pregabalin despite pregabalin demonstrating a more consistent and larger reversal of the classical von Frey evoked endpoint. This is supported by the clinical finding that in spinal cord injury patients with neuropathic pain, ketamine was ranked the second most effective analgesic treatment, behind botulinum toxin A whilst pregabalin was ranked fifth out of eleven analgesics tested (Ling et al., 2022). A direct comparative clinical study between ketamine and pregabalin is needed to validate these findings further and the translatability of them. Positively the effects of pregabalin and ketamine on reversing sleep fragmentation were able to be assessed using an automatic sleep/wake scoring algorithm that would be suitable for high throughput preclinical screening studies. This study demonstrated that measuring sleep fragmentation and particularly short bouts of wakefulness were sensitive to analgesic treatments and provided objective translatable endpoints of neuropathic pain with the potential for increased sensitivity over classical evoked subjective endpoints.

6.4.6 EEG power during wakefulness was inconsistent and not reversed by analgesic treatment.

As there has been various changes in EEG power including increased theta power (demonstrated in CCI rats and patients), increased delta power (demonstrated in partial sciatic nerve ligation mouse model), altered alpha power (bidirectionally changed in patients) or increased beta power (demonstrated in patients) reported to be associated with neuropathic pain these were assessed in awake CCI rats. Unexpectantly, only delta and beta power were increased in the CCI rats and neither were corrected by drug treatments (Figure 6.12). Due to the repeated identification of increased theta power in neuropathic pain patients (Jensen et al., 2013; Krupina et al., 2020; Michels et al., 2011; Sarnthein et al., 2005; Sarnthein & Jeanmonod, 2008; Stern et al., 2006) and in CCI rats during wakefulness (Koyama, LeBlanc, et al., 2018), it was anticipated that theta power would also be increased in this study. Though increased theta power is the most consistently reported change in EEG power associated with neuropathic pain (Mussigmann et al., 2022) it has not been detected in all preclinical neuropathic pain studies (Kontinen et al., 2003; Li, Ge, et al., 2019). Increased delta power has been associated with elevated neuropathic pain in the partial sciatic nerve ligation mouse model (Li, Ge, et al., 2019). Whilst in humans bidirectional changes in alpha power and increased beta power have also been reported (Mussigmann et al., 2022). This includes the use of changes in alpha and beta power to predict the development of neuropathic pain in spinal cord injury patients (Vučković, Gallardo, et al., 2018).

Increased theta power was not detected in CCI rats during wakefulness at any timepoint during this study either during ZT5-ZT11 in the light period (Figure 6.12) or ZT17-ZT23 in the dark period (Supp figure 6.21). This is in contrast to the effects of neuropathic pain in patients (Jensen et al., 2013; Krupina et al., 2020; Michels et al., 2011; Sarnthein et al., 2005; Sarnthein & Jeanmonod, 2008; Stern

et al., 2006) and in some of the previous studies assessing CCI rats (Koyama, LeBlanc, et al., 2018). However, other studies assessing the CCI rat model have detected no change in EEG power during wakefulness across an extended time course study (Kontinen et al., 2003). One main difference in the recording of EEG power changes between this study and that of Koyama et al. (2018) who identified increased theta power in CCI rats, is that they used very short 3–5-minute recordings of EEG after 15 minutes of acclimatisation (Koyama, LeBlanc, et al., 2018). The present study was more detailed as it continuously recorded EEG changes over 23 hours and focused on the first six hours after drug administration during the light period (ZT5-ZT11) and a corresponding six-hour segment of the dark (ZT17-ZT23) period. This decision was made to capture the full effects of the test compounds across a longer period and to correlate any changes in EEG power with changes in sleep/wake behaviour. Interestingly there were also differences in the detection of the effects of 10mg/kg pregabalin between this study and that of Koyama et al. (2018). In this study there was no effect of the 10mg/kg pregabalin, 10mg/kg ketamine or 3mg/kg psilocybin on EEG theta power in awake CCI rats (Figure 6.12). However, Koyama et al. (2018) demonstrated that 10mg/kg pregabalin decreased EEG theta power in awake CCI rats that was increased at Day 14 after CCI surgery (Koyama, LeBlanc, et al., 2018). The lack of an increase in theta power and even a decrease at Day 25 suggested that theta power may not be a reproducible endpoint in preclinical neuropathic pain models.

Assessing other EEG frequency band changes during wakefulness in the CCI rats in this study indicated that beta and delta power were increased during ZT5-ZT11 in the light period (Figure 6.12). Increased delta power has previously been associated with neuropathic pain (Li, Ge, et al., 2019). However, neither pregabalin or ketamine had any efficacy in reversing this increased delta power in the CCI rats (Figure 6.12). Delta power was partially reversed after psilocybin treatment, however as delta power began to decrease back to baseline levels by Day 25 the effects of psilocybin on Day 35 may have been due to a lack of increased delta power in the CCI rats at this timepoint. Additionally, the increased delta power during wakefulness was not detected during ZT17-ZT23 in the dark period which suggested that increased delta power is not a reproducible or reversible endpoint of neuropathic pain. Increased beta power was also identified in the CCI rats however, was not different from baseline after vehicle administration, meaning that there was no window for any of the test compounds to demonstrate efficacy (Figure 6.12). The increased beta power was also not maintained during the ZT17-ZT23 period. Whilst gamma power during wakefulness was not altered after CCI surgery assessing test compound induced changes in gamma power does provide an indication of their pharmacological activity. Both psilocybin and pregabalin decreased gamma power compared to control and baseline which has previously been seen been identified at Transpharmation LTD (unpublished observations) and in published reports for psilocybin (Thomas et al., 2022). Whereas ketamine increased gamma power during wakefulness which has also been identified in published reports (Gilbert & Zarate, 2020; Kantor et al., 2023). As such it appears that measuring EEG power during wakefulness in CCI rats over extended periods of time does not provide a consistent or reversible endpoint of neuropathic pain for screening analgesic test compounds.

Other than effects of CCI surgery and test compound administration on EEG power during wakefulness, the impact of these on NREM and REM sleep EEG power were also assessed. NREM sleep EEG power strongly shifted towards higher frequency oscillations whilst REM sleep EEG power was largely unaffected by CCI surgery. Specifically, delta, theta and sigma band power were decreased in CCI rats during NREM sleep in both the light and dark periods whilst gamma power increased. As delta waves predominate NREM sleep, they are often used to characterise its intensity (Leemburg et al., 2010; Vyazovskiy et al., 2007). Following sleep deprivation NREM sleep delta power is often increased, whilst throughout the night this delta power gradually decreases (Leemburg et

al., 2010; Long et al., 2021; Vyazovskiy et al., 2007). Therefore it has been considered that increased delta power is associated with increased sleep quality and intensity (Leemburg et al., 2010; Long et al., 2021; Vyazovskiy et al., 2007). As such the decrease in delta and low frequency EEG power in CCI rats likely reflected that these rats spent more time in NREM sleep but of a lower intensity and quality, possibly to compensate for the increase in frequent short awakenings (Figure 6.9) (Long et al., 2021). In support of this both pregabalin and ketamine partially reversed NREM sleep delta power whilst decreasing short bouts of wakefulness. Psilocybin on the other hand which demonstrated no efficacy against classical evoked neuropathic pain endpoints or against sleep fragmentation further decreased NREM sleep delta power (Figure 6.9). Overall EEG power during wakefulness appears not to provide a reliable objective endpoint of neuropathic pain, whilst NREM sleep EEG power indicates decreased sleep intensity in CCI rats that was partially corrected by pregabalin and ketamine.

6.4.7 Improvements, limitations and future work.

Whilst this study demonstrated the use of sleep fragmentation and short bouts of wakefulness as novel objective neuropathic pain endpoints that can be reversed by standard (pregabalin) and novel (ketamine) analgesics, there are limitations to this study. A key consideration of this study was the use of an automatic sleep/wake scoring algorithm to reflect the established practice in preclinical sleep EEG screening studies (Grieger et al., 2021). Whilst these algorithms have been routinely used for many years with reasonable levels of accuracy, they trade the finer level of detailed scoring of a human technician for vastly superior speed and efficiency (Benington et al., 1994; Muto & Berthomier, 2023). This is beneficial for preclinical screening studies as it reduces costs and increases throughput (Muto & Berthomier, 2023). However, it requires that the endpoints being used to determine test compound efficacy are robust enough to still be measurable. In the present study sleep fragmentation and increased short bout of wakefulness both appear to pass this criterion. However, the development of increased theta power that has been demonstrated by others in the CCI rat model was not identified in this study, possibly due to the use of automated scoring (Koyama, LeBlanc, et al., 2018).

The age of the rats used in this study is another consideration that must be made when continuing this research. The Sprague Dawley rats used in this study were previously implanted for sleep/wake behaviour and/or evoked potential studies at Transpharmation LTD leading to them being older (approximately 7-9 months) than the younger age rats that are typically tested preclinically (2-3 months) (Andersen & Tufik, 2003; Kontinen et al., 2003; Koyama, LeBlanc, et al., 2018). Whilst the age of the rats used in this study likely better represents that of the adult patient population, it may limit the translatability to other preclinical studies that have focused on younger animals (Almeida et al., 2018). Therefore, repeating this study in a younger cohort of rats that better reflects the general age used in other studies could improve the translatability whilst also providing an understanding of any age-related effects on these sleep/wake endpoints.

A consideration should be made in this study for the effects of the test compounds including pregabalin, ketamine and psilocybin as these were not assessed in any sham group. Sham animals can help to elucidate whether there is an effect of the surgical procedure irrespective of the nerve injury whilst also identifying the effects of the test compounds on naïve animals that may be masking rather than reversing any phenotypical changes (Johnson & Besselsen, 2002). Sham animals were not included in this study due to the limited development of oxaliplatin induced CIPN in Chapter 5 and the previously unknown effectiveness of the CCI surgery on aged animals, to ensure

the maximum number of animals with a successful neuropathic pain phenotype could be included. Additionally, the ethics of including a sham group were considered as this would have increased the number of animals included in the study and was instead replaced with comparisons to a vehicle control group to avoid the use of age matched sham animals (Knopp et al., 2015). Previous data from studies at Transpharmation LTD using 10mg/kg ketamine in naïve Sprague Dawley rats indicates similar effects of more consolidated wakefulness whilst reducing NREM and REM sleep amounts (Kantor et al., 2023). However, ketamine had no effect on locomotor activity or NREM sleep latency in naïve Sprague Dawley rats which may support these as a more selective endpoint for the effects of ketamine against neuropathic pain. The effects of ketamine have previously not been investigated on short bouts of wakefulness which should be explored in the future. Additionally, the effects of 3mg/kg psilocybin on sleep/wake behaviour were also similar in internal Transpharmation LTD studies of naïve Sprague Dawley rats with almost exclusively delaying the onset of REM sleep without altering wakefulness (unpublished observations). As such future work investigating EEG and sleep/wake changes in this model should consider including sham animals to ensure the effects of the nerve constriction and not the surgical procedure are identified alongside understanding the effects of treatments in non-painful animals.

In human EEG recordings the conventional approach uses the 10-20 system to determine the placement of electrodes on the scalp for EEG recordings (Sanei, S., & Chambers, 2007). However, in rodent EEG recordings the placement of electrodes varies and can depend on the type of apparatus being used and what is being measured (Ho et al., 2024; Kantor et al., 2023; Koyama, LeBlanc, et al., 2018). In the present study frontal (2 mm anterior / 1 mm lateral to Bregma) and parietal (0 mm anterior / 1.5 mm lateral to Lambda) electrodes were implanted above the left hemisphere for frontoparietal EEG recordings on the ipsilateral side of the CCI surgery. However, research from Carl Saab's research group has identified increased theta power in CCI rats placed an electrode corresponding to the contralateral primary somatosensory cortex or S1 region of the nerve injury (2mm posterior / 2 mm lateral to Bregma) (Koyama, LeBlanc, et al., 2018). As brain processing of information is conducted on the contralateral hemisphere (Jin et al., 2018) it may be a limitation of the present study that EEG recordings were conducted on the ipsilateral side. However, previous studies from Carl Saab's research group also identified increased theta power across both ipsilateral and contralateral EEG recording electrodes (LeBlanc, Bowary, et al., 2016). The demonstration of EEG power changes across both brain hemispheres indicates that if increased theta power was present in this study, it should have been detectible across either hemisphere. However, future studies should look to optimise the placement of EEG electrodes to allow for the maximum chance to detect EEG power changes, which was not possible in this study as the rats were pre-implanted with EEG electrodes.

The time periods selected for analysis during most of this study included two 6 hour sections of ZT5-ZT11 in the light period (hours 0-6 of the recording) and a corresponding 6 hour portion from ZT17-ZT23 in the dark period (hours 12-18 of the recording). Whilst ZT5-ZT11 was the longest uninterrupted section of the light period after the drug treatments, ZT17-ZT23 was selected as the corresponding period during the dark period of equal length. However, as rodents are typically more active during the first period of the dark period (Steel et al., 2024) there may be differences in their experience of evoked pain as they moved around more and experience allodynia or hyperalgesia from interacting with their environment (Tokunaga et al., 2007). However, the homeostatic drive for sleep increases towards the dark period (Borbély et al., 2016). Therefore, differences in the homeostatic drive for sleep in rodents experiencing sleep disturbance are most likely to occur at the end of the dark period, as assessed in this study. Future work should consider assessing both the early and later stages of the dark period to identify if there are any differences in EEG measures of

sleep/wake homeostasis, brief arousals or sleep/wake amounts between these time periods. This could help to better understand how sleep regulation is affected in preclinical neuropathic pain models.

Future studies should look to examine the effects of a dose response and possibly chronic dosing of pregabalin and ketamine. Due to the design of this study aiming to understand both the development of CCI surgery induced changes throughout the study and the reversal of these changes, each test compound was limited to a single dose (Figure 6.1). Using multiple doses of each test compound to demonstrate a dose response effect would have further support the findings of improved sleep fragmentation and reduced short bouts of wakefulness. Therefore, future research should aim to repeat the assessment of these test compound at a range of doses, ideally in a younger cohort of animals. Additionally, the assessment of sleep/wake behaviour in alternative neuropathic pain models, including other surgically induced models such as the spared nerve injury and metabolic models such as the streptozotocin model would provide improved validation of these neuropathic pain endpoints. Once established, validation of other test compounds such as amitriptyline and duloxetine that are currently approved for the treatment of neuropathic pain could aid in the validation of sleep fragmentation and increased short bouts of wakefulness as neuropathic pain endpoints (Finnerup et al., 2015).

6.5 Conclusions

In conclusion, this study demonstrated that sleep fragmentation and increased short bouts of wakefulness appear to be reliable neuropathic pain endpoints that are reversible by analgesic treatments. Examining these sleep/wake behavioural changes in CCI rats determined ketamine has superior analgesic efficacy over pregabalin despite a classical evoked neuropathic pain endpoint indicating the opposite. This study provided the first data supporting the use of an automatic sleep/wake scoring algorithm to detect sleep fragmentation and increased short bouts of wakefulness as objective measures of neuropathic pain and their reversal by ketamine and pregabalin. This will allow future high throughput preclinical screening studies to apply these neuropathic pain endpoints without the use of laborious human scoring of EEG recordings. Additionally, assessing sleep/wake behaviours in CCI rats provided a more detailed comparison of test compound efficacy and the affective aspects of pain compared with reflexive measurements. Sleep fragmentation is also reported by neuropathic pain patients and can be objectively measured in rodents supporting its translatability potential. Furthermore, measuring changes in home cage locomotor activity provided additional data that supported the determination of analgesic efficacy and is similar to the reports of decreased activity levels in patients. More work is needed to ensure that these sleep fragmentation endpoints are robust and reproducible across various neuropathic pain models and analgesic compounds.

6.6 Supplementary figures

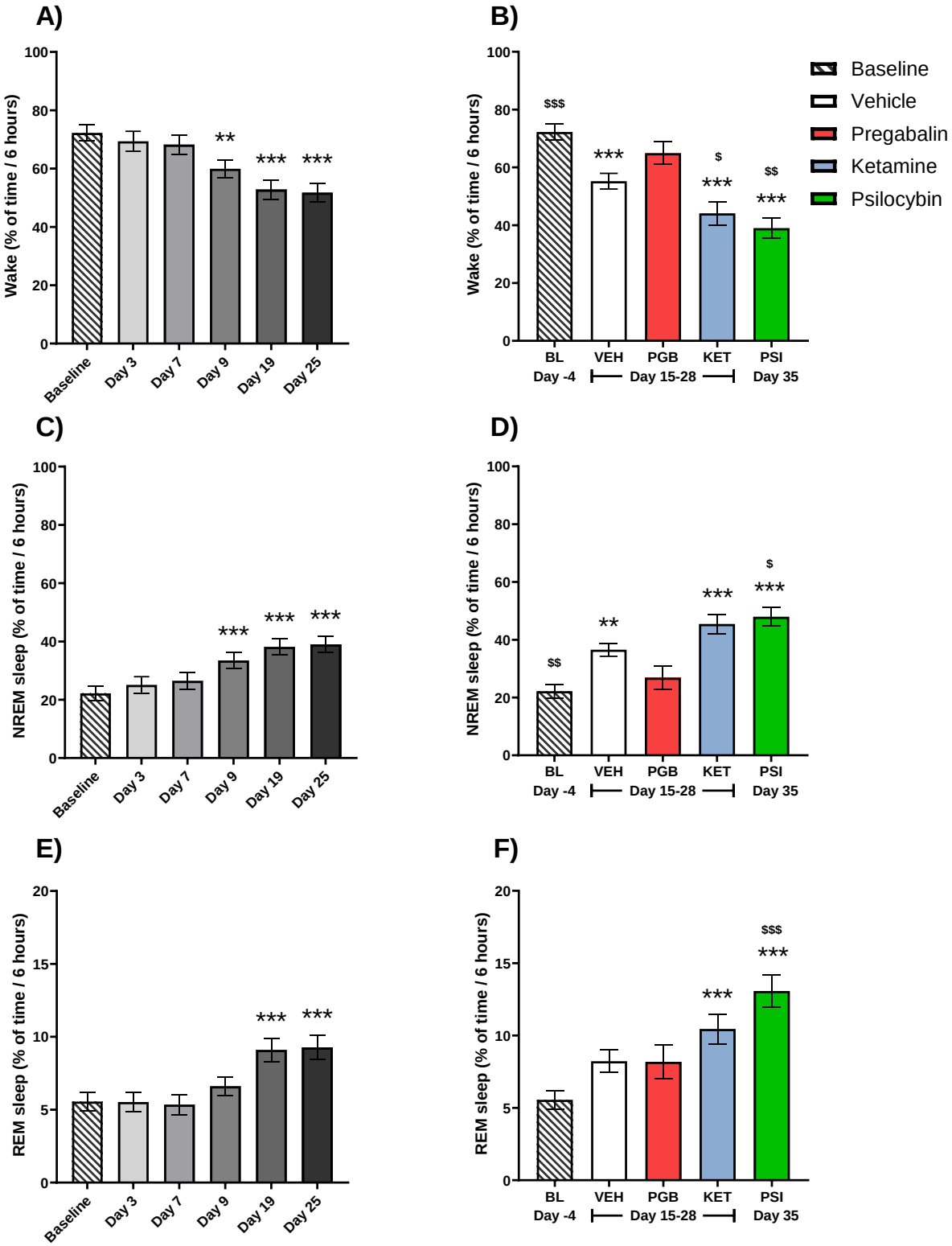

Supp figure 6.13) During ZT17-ZT23 in the dark period CCI rats spent less time awake and more time in NREM sleep and REM sleep. The effect of CCI surgery (Days 3, 7, 9, 19 and 25) along with vehicle, 10mg/kg pregabalin, 10mg/kg ketamine (Days 15, 21, 28) and 3mg/kg psilocybin (Day 35) test compounds on the percentage of time spent awake (A,B), in NREM sleep (C,D) and REM sleep (E,F) during ZT17-ZT23 in the dark period. (A-F) **p<0.01, ***p<0.001 vs baseline (Day-4). (B,D,F) \$$p$<0.05, \$\$$p$<0.01, \$\$\$$p$<0.001 vs vehicle. All data is reported as mean ± SEM, n=11-12 (A-F).

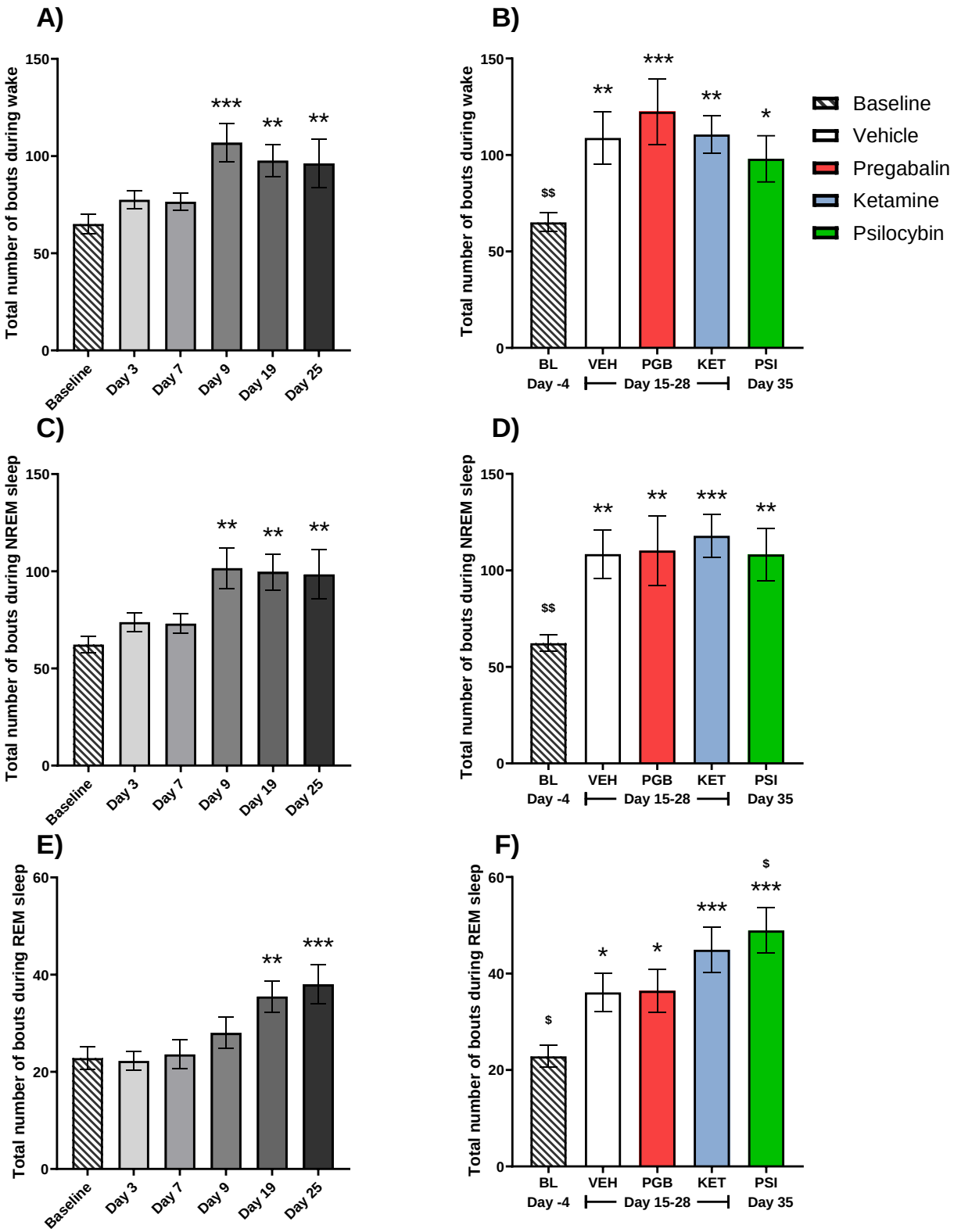

Supp figure 6.14) The total number of wake, NREM sleep and REM sleep bouts was increased in the CCI rats during ZT17-ZT23 in the dark period. The effect of CCI surgery (Days 3, 7, 9, 19 and 25) along with vehicle, 10mg/kg pregabalin, 10mg/kg ketamine (Days 15, 21, 28) and 3mg/kg psilocybin (Day 35) test compounds on the total number of wakefulness (A,B), NREM sleep (C,D) and REM sleep (E,F) bouts during ZT17-ZT23 in the dark period. (A-F) *p<0.05, **p<0.01, ***p<0.001 vs baseline (Day-4). (B,D,F) $$p$<0.05, $$$p$<0.01 vs vehicle. All data is reported as mean ± SEM, n=11-12 (A-F).

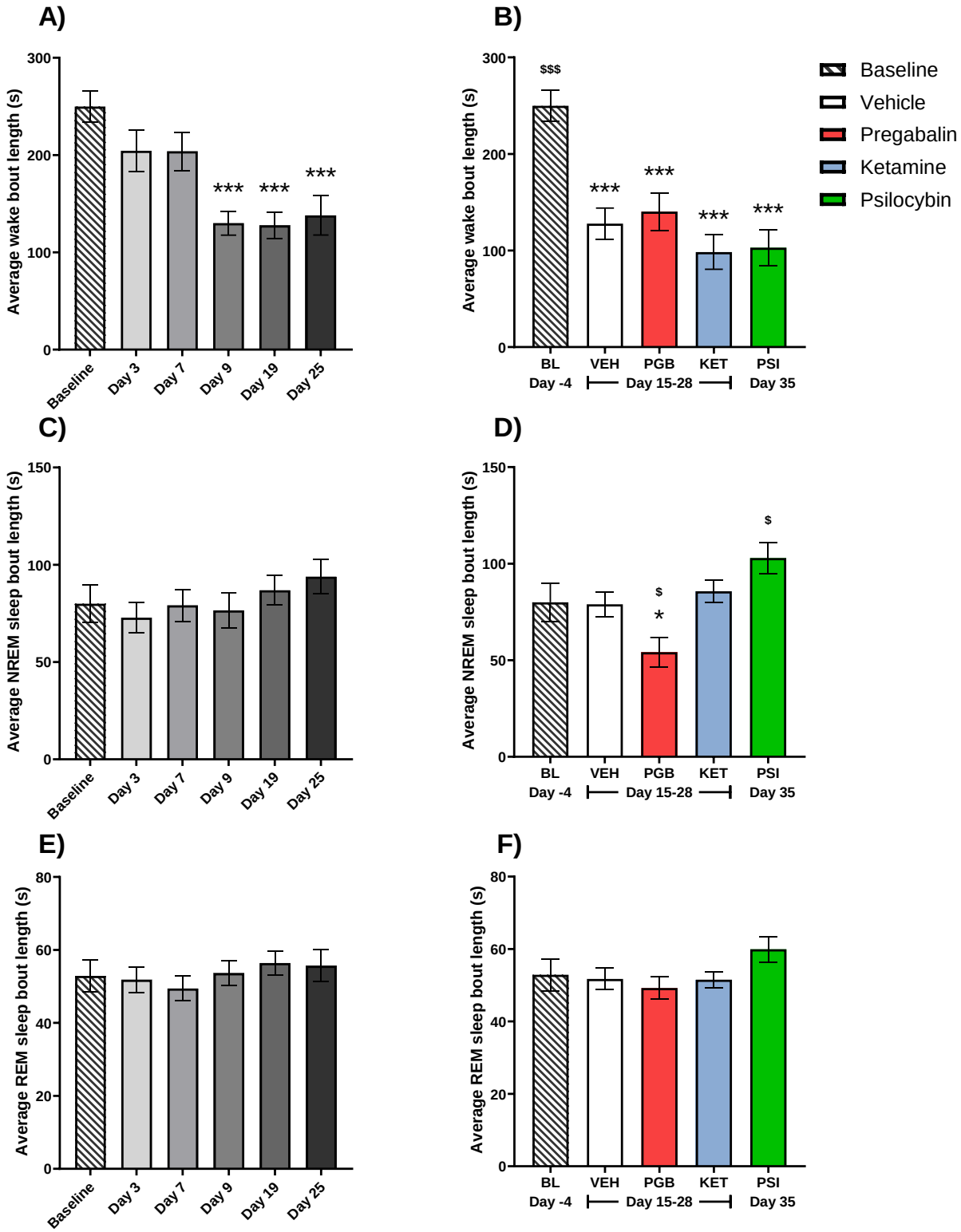

Supp figure 6.15) The average length of wake bouts was increased in CCI rats but was not corrected by test compound administration during ZT17-ZT23 in the dark period. The effect of CCI surgery (Days 3, 7, 9, 19 and 25) along with vehicle, 10mg/kg pregabalin, 10mg/kg ketamine (Days 15, 21, 28) and 3mg/kg psilocybin (Day 35) test compounds on the average length of wakefulness (A,B), NREM sleep (C,D) and REM sleep (E,F) bouts during ZT17-ZT23 in the dark period. (A-F) *p<0.05, ***p<0.001 vs baseline (Day-4). (B,D,F) $$p$<0.05 vs vehicle. All data is reported as mean ± SEM, n=11-12 (A-F).

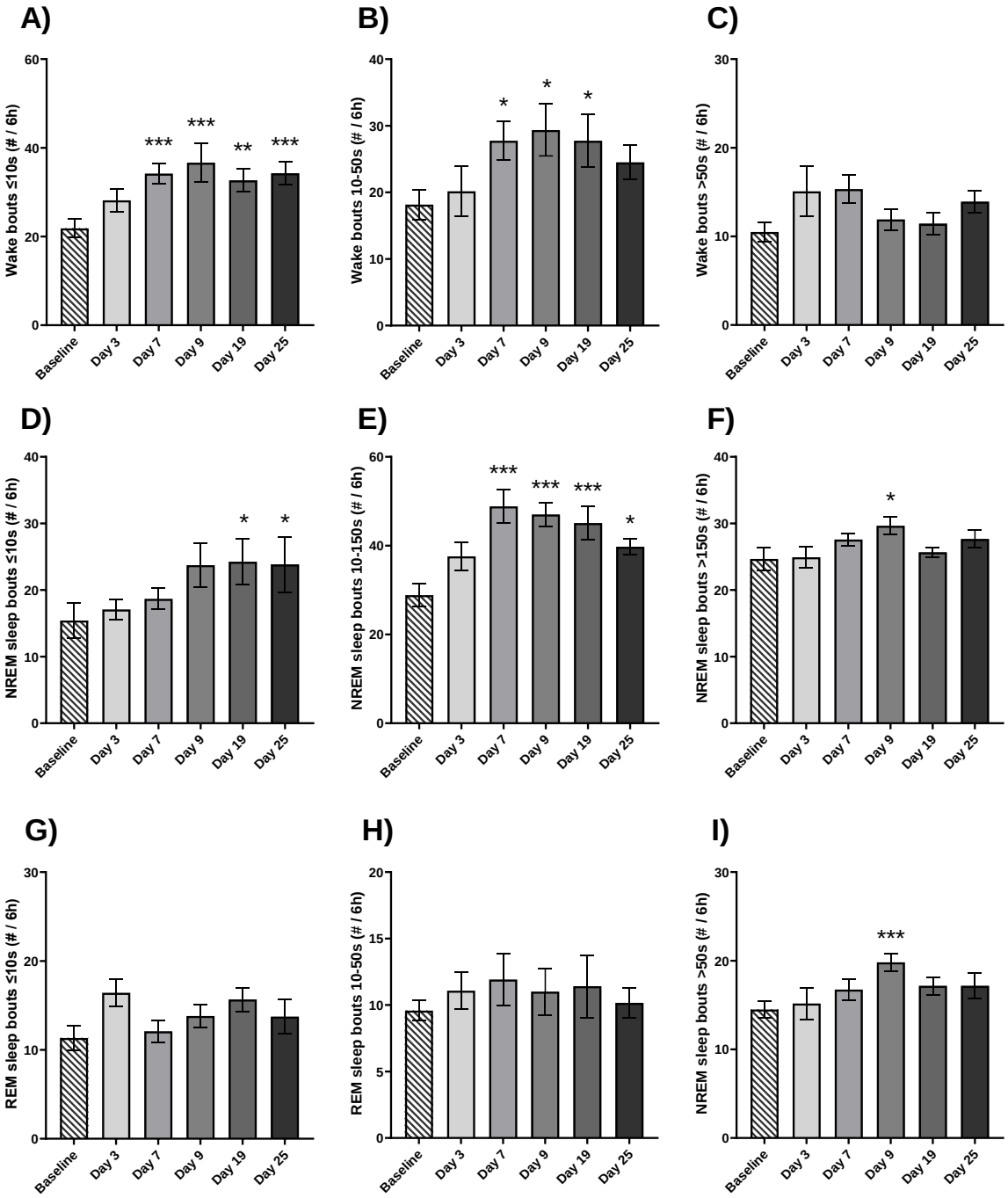

Supp figure 6.16) CCI rats had increased short (≤10s) wake bouts during ZT5-ZT11 in the light period. The effects of CCI surgery (Days 3, 7, 9, 19 and 25) on short (≤10s), medium (10-50s wake/REM sleep, 10-150s NREM sleep) and long (>50s wake/REM sleep, >150s NREM sleep) bouts of wakefulness (A,B,C), NREM sleep (D,E,F) and REM sleep (G,H,I) during ZT5-ZT11 in the light period. **p*<0.05, ***p*<0.01, ****p*<0.001 vs baseline (Day-4). All data is reported as mean ± SEM, n=11-12 (A-I).

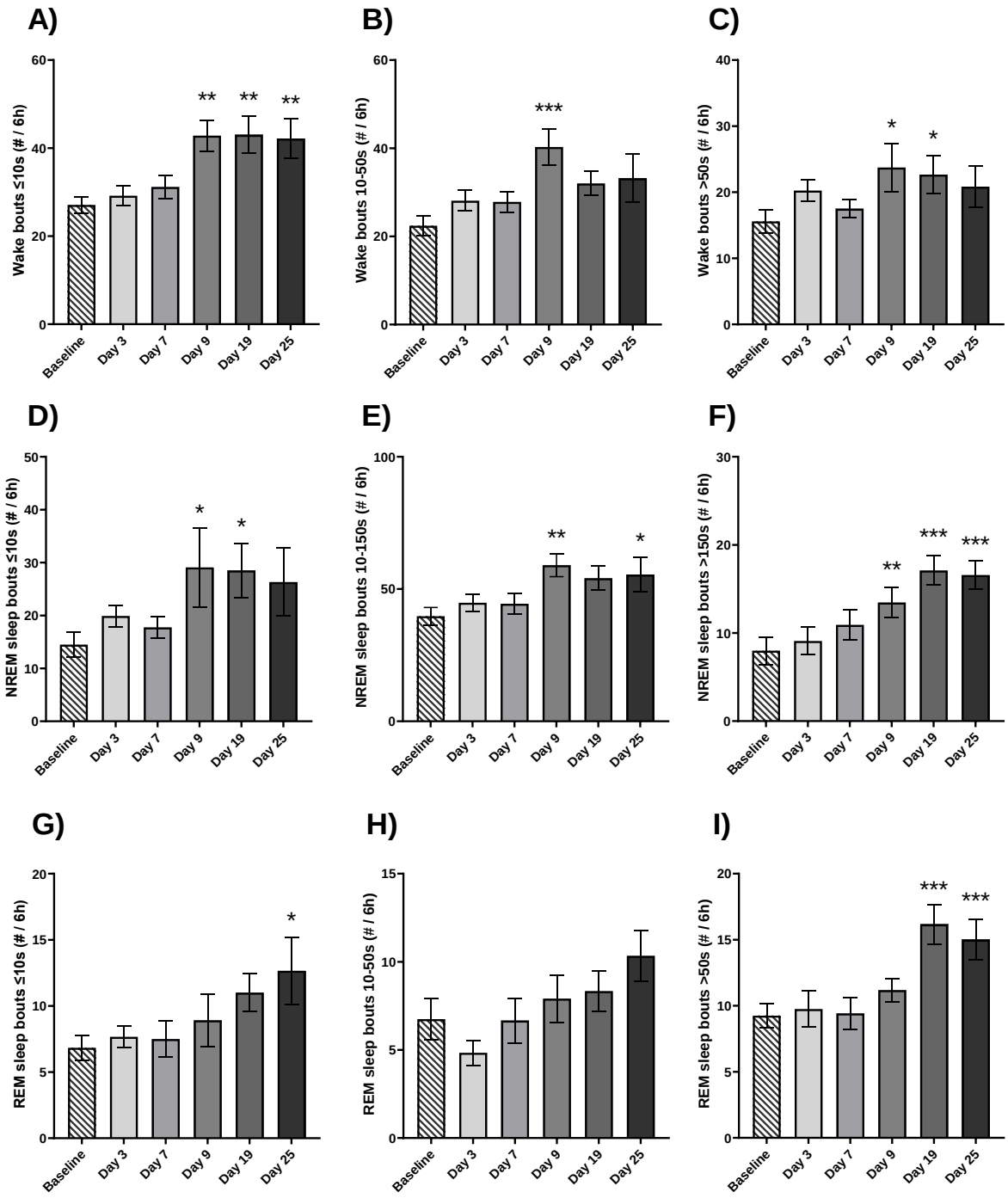

Supp figure 6.17) CCI rats also had increased short (≤10s) wake bouts during ZT17-ZT23 in the dark period. The effects of CCI surgery (Days 3, 7, 9, 19 and 25) on short (≤10s), medium (10-50s wake/REM sleep, 10-150s NREM sleep) and long (>50s wake/REM sleep, >150s NREM sleep) bouts of wakefulness (A,B,C), NREM sleep (D,E,F) and REM sleep (G,H,I) during ZT17-ZT23 in the dark period. **p*<0.05, ***p*<0.01, ****p*<0.001 vs baseline (Day-4). All data is reported as mean ± SEM, n=11-12 (A-I).

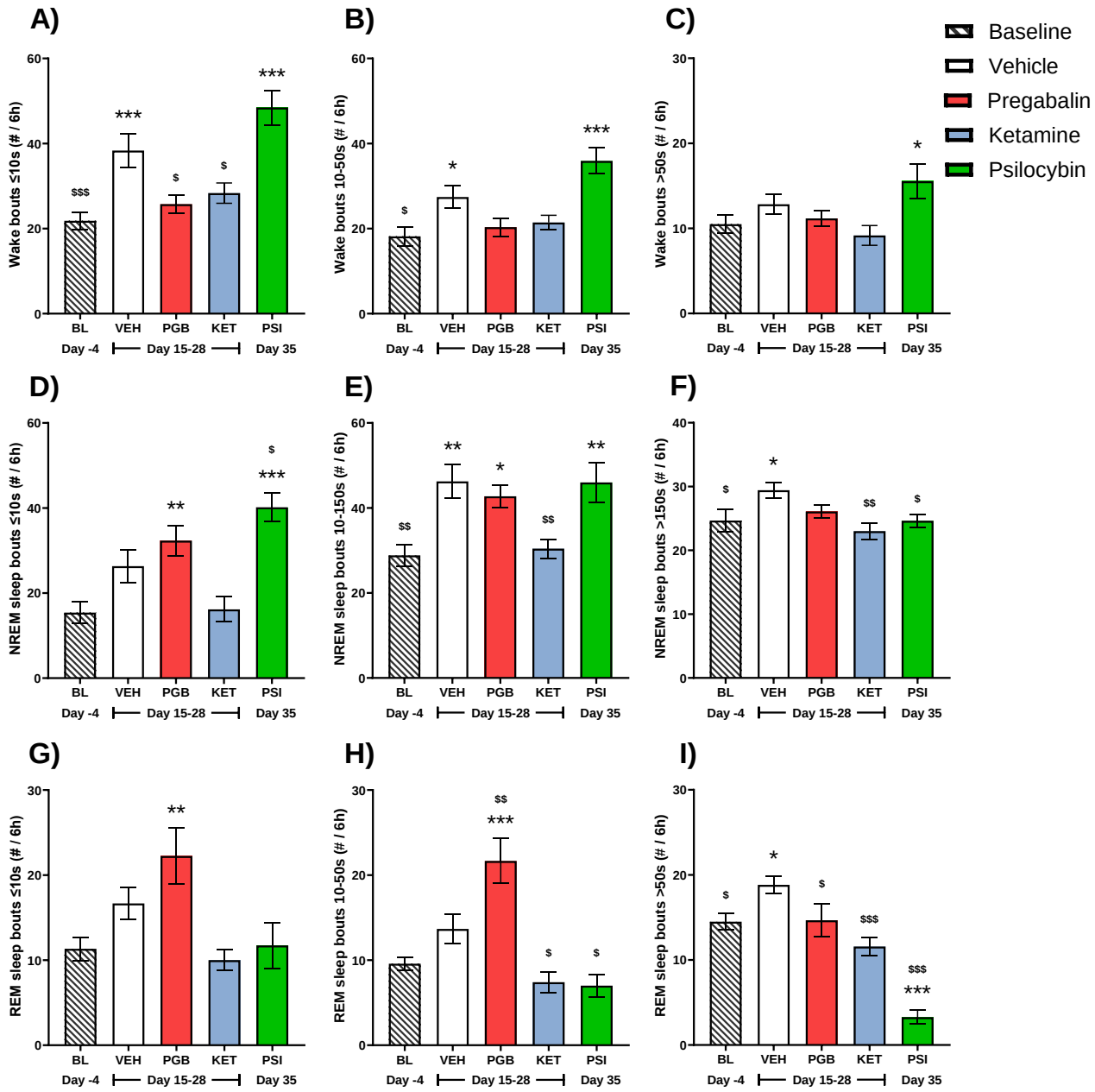

Supp figure 6.18) Pregabalin and ketamine normalised the number of short (≤10s) wake bouts during ZT5-ZT11 in the light period. The effects of vehicle, 10mg/kg pregabalin, 10mg/kg ketamine (Days 15, 21, 28) and 3mg/kg psilocybin (Day 35) test compounds on short (≤10s), medium (10-50s wake/REM sleep, 10-150s NREM sleep) and long (>50s wake/REM sleep, >150s NREM sleep) bouts of wakefulness (A,B,C), NREM sleep (D,E,F) and REM sleep (G,H,I) during ZT5-ZT11 in the light period. **p*<0.05, ***p*<0.01, ****p*<0.001 vs baseline (Day-4), $*p*<0.05, $$*p*<0.01, $$$*p*<0.001 vs vehicle. All data is reported as mean ± SEM, n=11-12 (A-I).

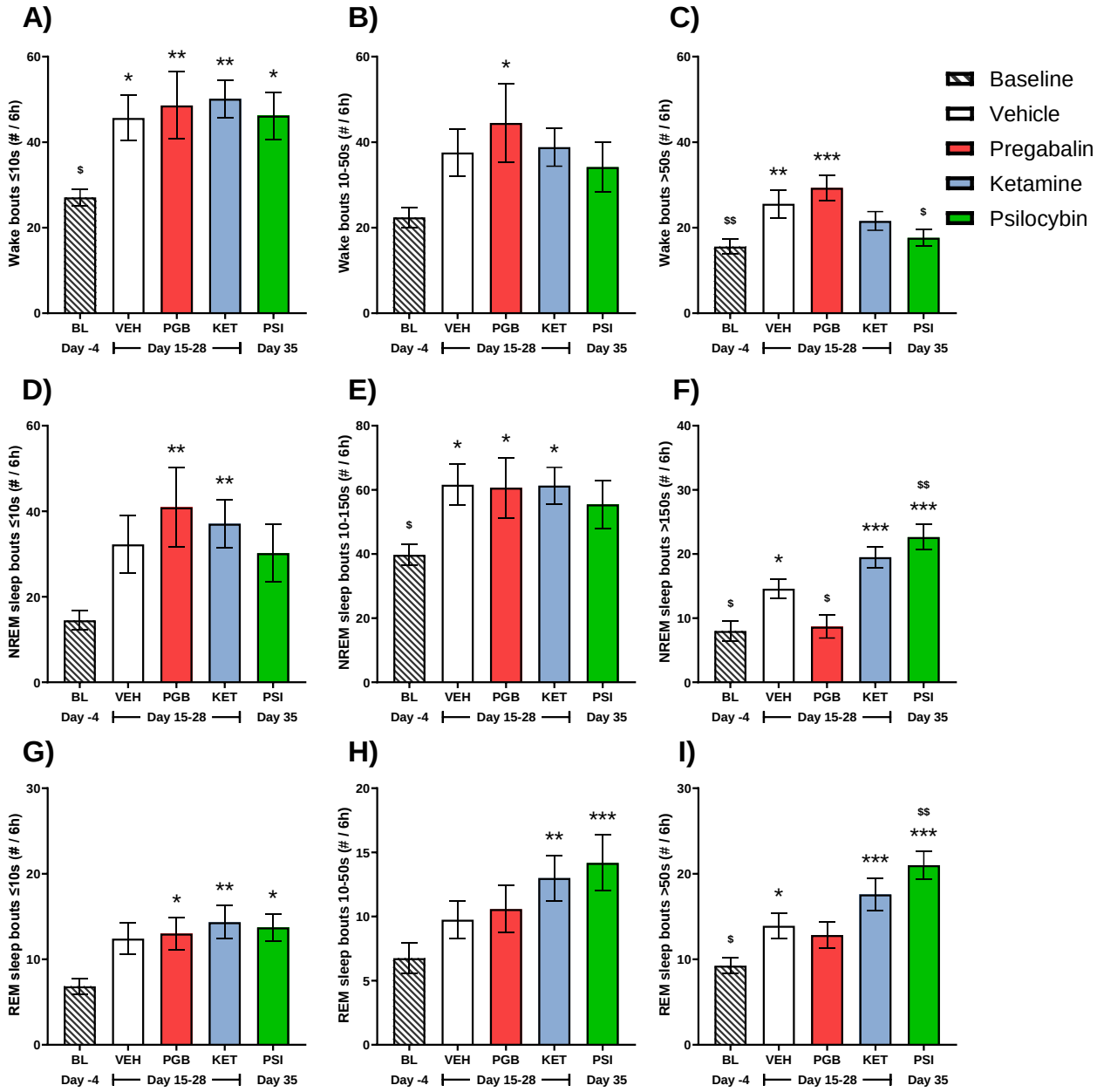

Supp figure 6.19) Psilocybin decreased long (>50s) bouts of wakefulness whilst long bouts of NREM and REM sleep were increased during ZT17-ZT23 in the dark period. The effects of vehicle, 10mg/kg pregabalin, 10mg/kg ketamine (Days 15, 21, 28) and 3mg/kg psilocybin (Day 35) test compounds on short (≤10s), medium (10-50s wake/REM sleep, 10-150s NREM sleep) and long (>50s wake/REM sleep, >150s NREM sleep) bouts of wakefulness (A,B,C), NREM sleep (D,E,F) and REM sleep (G,H,I) during ZT17-ZT23 in the dark period. *p<0.05, **p<0.01, ***p<0.001 vs baseline (Day-4), $$p$<0.05, $$$p$<0.01 vs vehicle. All data is reported as mean ± SEM, n=11-12 (A-I).

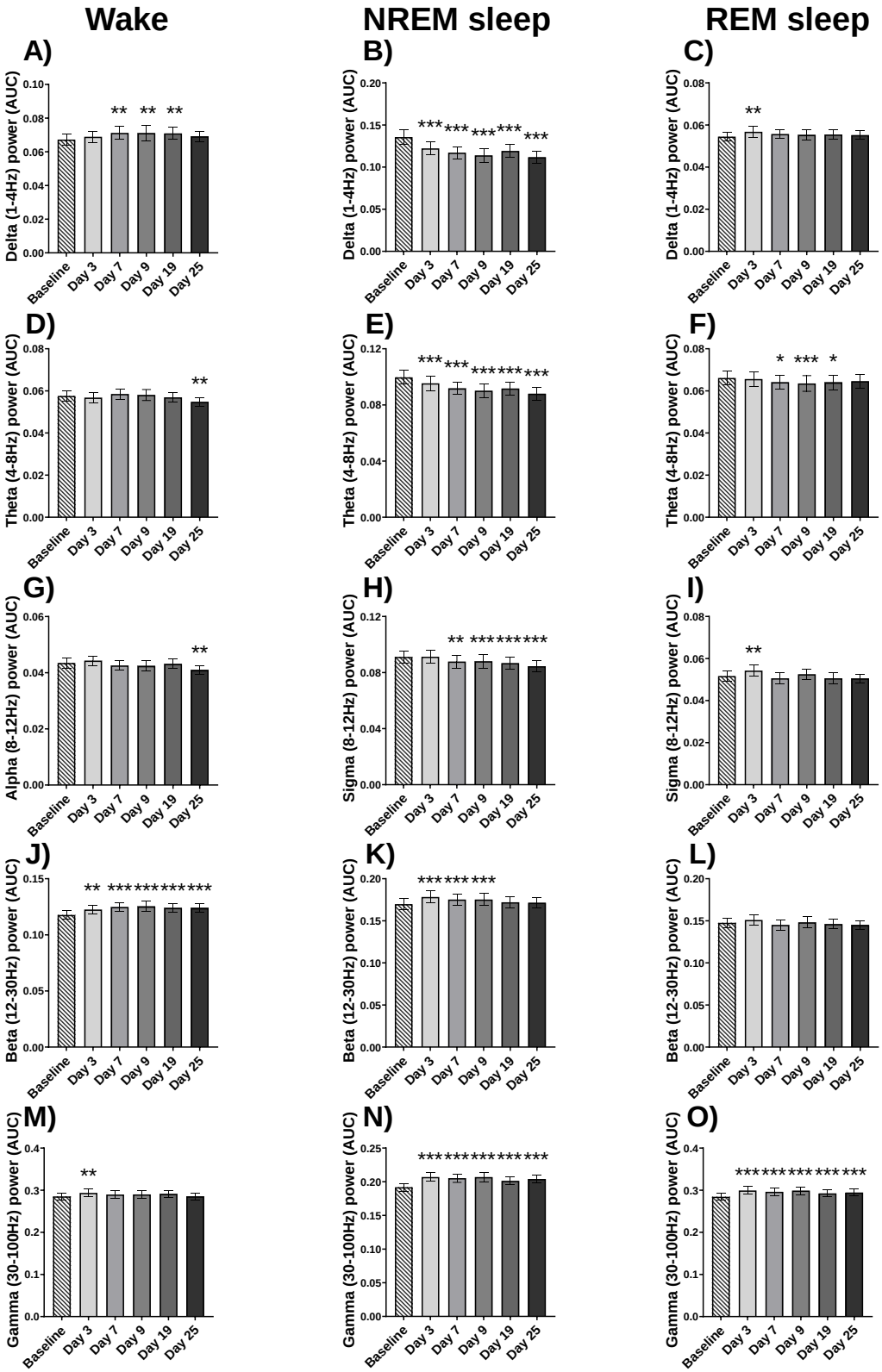

Supp figure 6.20) NREM sleep EEG power was increased at higher frequencies and decreased at lower frequencies in CCI rats. Whilst theta power during wakefulness was not increased during ZT5-ZT11 in the light period. The effects of CCI surgery (Days 3, 7, 9, 19 and 25) on the EEG power in the delta (1-4Hz) (A,B,C), theta (4-8Hz) (D,E,F), alpha/sigma (8-12Hz) (G,H,I), beta (13-30Hz) (J,K,L) and gamma (30-100Hz) (M,N,O) frequency bands during wakefulness, NREM sleep and REM sleep during ZT5-ZT11 in the light period. *p<0.05, **p<0.01, ***p<0.001 vs baseline (Day-4). All data is reported as mean ± SEM, n=11-12 (A-O).

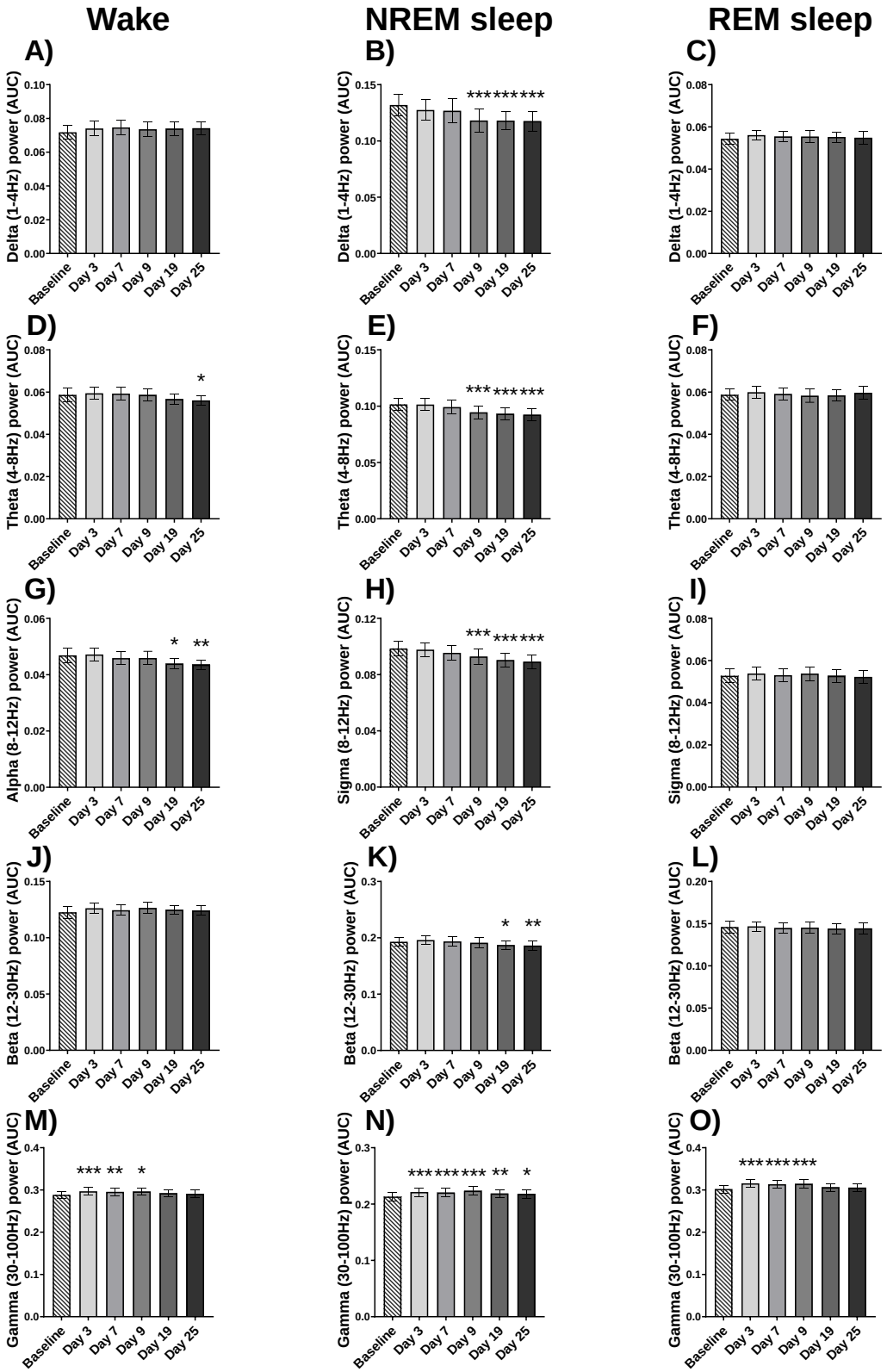

Supp figure 6.21) NREM sleep EEG power at lower frequencies was decreased, whilst gamma power was increased in CCI rats. Additionally, theta power during wakefulness was not increased during ZT17-ZT23 in the dark period. The effects of CCI surgery (Days 3, 7, 9, 19 and 25) on the EEG power in the delta (1-4Hz) (A,B,C), theta (4-8Hz) (D,E,F), alpha/sigma (8-12Hz) (G,H,I), beta (13-30Hz) (J,K,L) and gamma (30-100Hz) (M,N,O) frequency bands during wakefulness, NREM sleep and REM sleep during ZT17-ZT23 in the dark period. *p<0.05, **p<0.01, ***p<0.001 vs baseline (Day-4). All data is reported as mean ± SEM, n=11-12 (A-O).

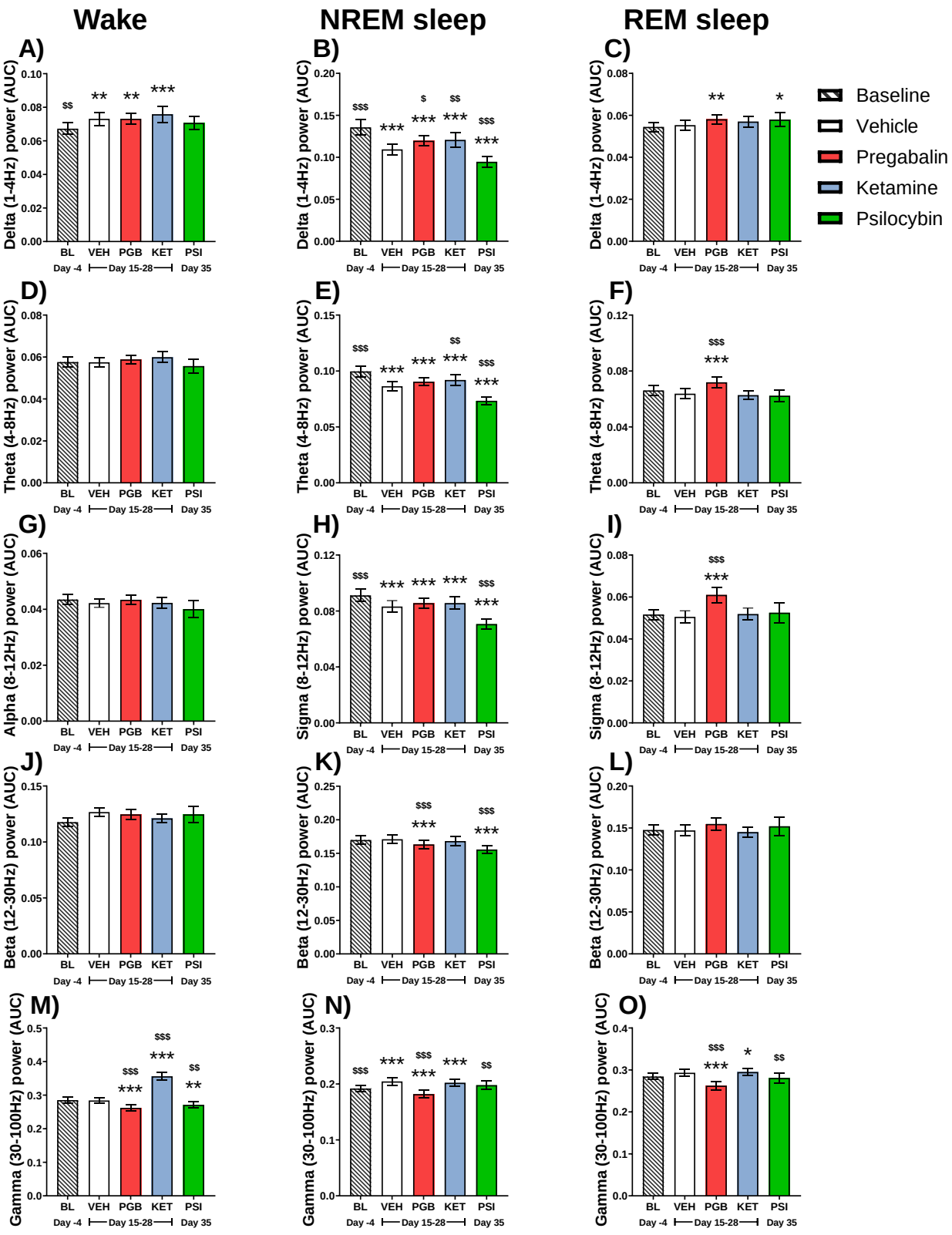

Supp figure 6.22) Pregabalin and ketamine increased delta power during NREM sleep during ZT5-ZT11 in the light period. The effects of vehicle, 10mg/kg pregabalin, 10mg/kg ketamine (Days 15, 21, 28) and 3mg/kg psilocybin (Day 35) test compounds on the EEG power in the delta (1-4Hz) (A,B,C), theta (4-8Hz) (D,E,F), alpha/sigma (8-12Hz) (G,H,I), beta (13-30Hz) (J,K,L) and gamma (30-100Hz) (M,N,O) frequency bands during wakefulness, NREM sleep and REM sleep during ZT5-ZT11 in the light period. *p<0.05, **p<0.01, ***p<0.001 vs baseline (Day-4). $$p$<0.05, $$$p$<0.01, $$$$p$<0.001 vs vehicle. All data is reported as mean ± SEM, n=11-12 (A-O).

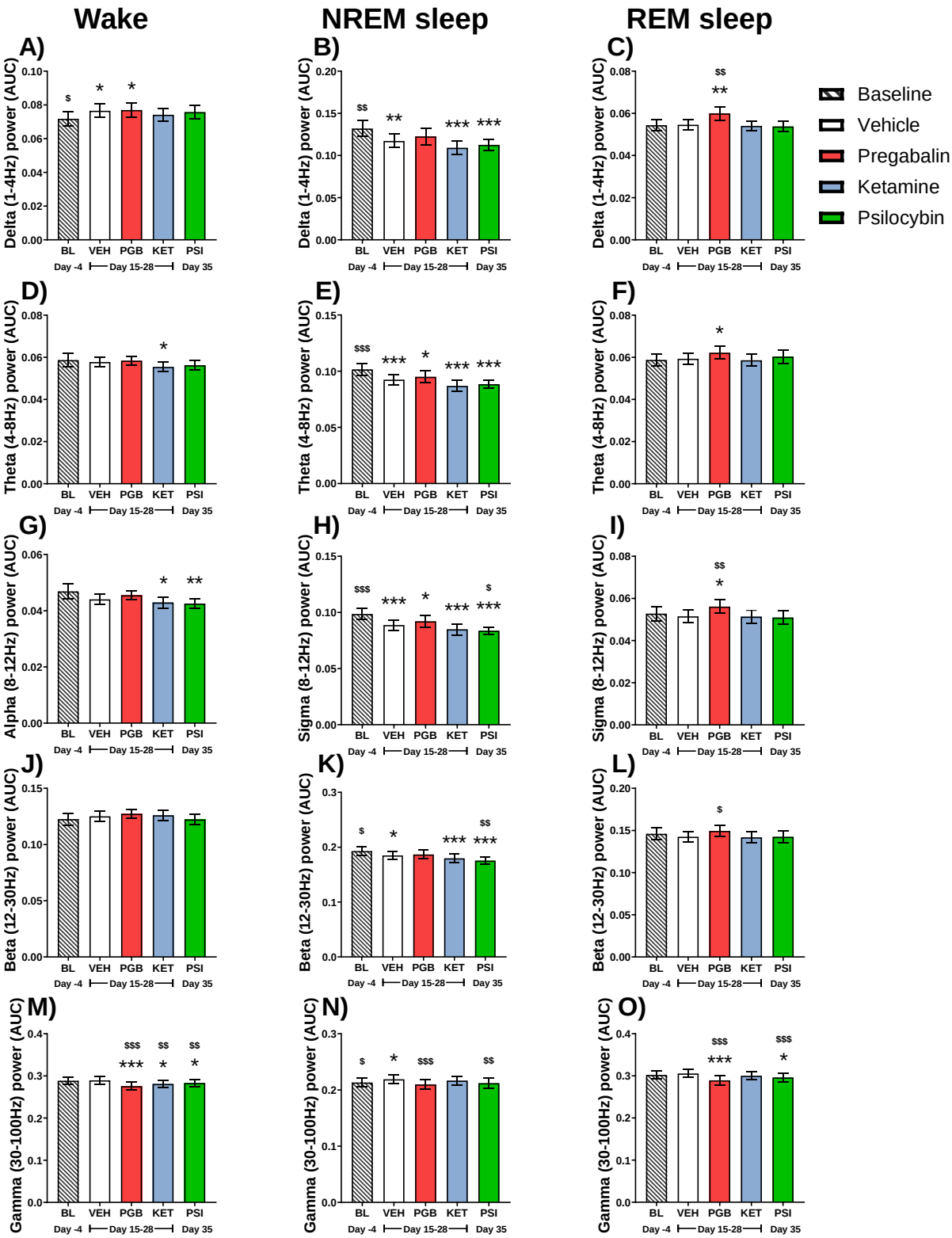

Supp figure 6.23) Test compounds had limited effects on EEG power during ZT17-ZT23 in the dark period. The effects of vehicle, 10mg/kg pregabalin, 10mg/kg ketamine (Days 15, 21, 28) and 3mg/kg psilocybin (Day 35) test compounds on the EEG power in the delta (1-4Hz) (A,B,C), theta (4-8Hz) (D,E,F), alpha/sigma (8-12Hz) (G,H,I), beta (13-30Hz) (J,K,L) and gamma (30-100Hz) (M,N,O) frequency bands during wakefulness, NREM sleep and REM sleep during ZT17-ZT23 in the dark period. *p<0.05, **p<0.01, ***p<0.001 vs baseline (Day-4). \$$p$<0.05, \$\$$p$<0.01, \$\$\$$p$<0.001 vs vehicle. All data is reported as mean ± SEM, n=11-12 (A-O).

Chapter 7: Overall discussion

Neuropathic pain affects 8.2-8.9% of people in England (Fayaz et al., 2016) which is concerning as current treatments of neuropathic pain are effective for less than half of them (Colloca et al., 2017). Little success has been found in forward translating preclinical analgesics into successful clinical trials. With pregabalin the only first line treatment for neuropathic pain that has successfully forward translated (Percie Du Sert & Rice, 2014). A key focus to improve neuropathic pain research is to review the endpoints that are used to assess it (Deuis et al., 2017; Fisher et al., 2021; Tappe-Theodor et al., 2019). There is currently a mismatch between the primary neuropathic pain endpoints used in clinical trials and preclinical studies. Clinical trials most often measure the efficacy of analgesics through verbal self-reported pain (Jensen et al., 2015). This captures the overall impact of pain including the affective components, emotional and brain processing, albeit subjectively (Jensen et al., 2015; Simons et al., 2014; Torta et al., 2017). In contrast the classical way to measure neuropathic pain preclinically has been through subjective measures of evoked reflexes interpreted by a human observer (Negus, 2019). These classical evoked endpoints measure simple reflexes that do not consider the central processing of neuropathic pain (Deuis et al., 2017; Fisher et al., 2021; Tappe-Theodor et al., 2019). Thus, it is important to identify and validate novel objective neuropathic pain endpoints that assess the overall impact of neuropathic pain and may improve forward translatability potential over current classical reflex-based endpoints (Fisher et al., 2021).

Therefore, this thesis set out to investigate novel objective endpoints of neuropathic pain that would improve the translatability of preclinical neuropathic pain research. Additionally, this thesis identified improvements and refinements to animal welfare that should be implemented to increase the reliability and reduce the ethical impacts of preclinical neuropathic pain research. Whilst most preclinical research focuses on understanding pathways, mechanisms and drug efficacy, this thesis instead aimed to look at how preclinical neuropathic pain medications are screened. This is particularly important as it is the final efficacy assessment step in the development of novel analgesic treatments before they enter human clinical trials. As such it is vital that the ways we measure pain preclinically are effective and translatable. Little has changed in the preclinical screening landscape for neuropathic pain over the past 30 years, and with it, few treatments have proceeded to clinical use due to both lack of efficacy and adverse effects. This has left neuropathic pain patients without adequate treatment and so a focus must be placed on how we determine analgesic efficacy.

7.1 Validation of the single dose 55mg/kg streptozotocin (STZ) type-1 diabetes rat model

The first few studies of this thesis validated that a single 55mg/kg STZ intraperitoneal (i.p.) administration successfully induced and maintained a type-1 diabetic phenotype in rats, even after allowing for anomer equilibration. STZ occurs as an α and β anomer, of which α is the more toxic. Over the first two hours after being dissolved the usually >85% α anomer content decreases to an equivalent level of the less toxic β anomer (De La Garza-Rodea et al., 2010). Despite this, protocols for STZ administration still routinely describe administering STZ immediately after being dissolved and suggest using higher ≥65mg/kg doses in rats (Furman, 2021). The characterisation that an

anomer-equilibrated 55mg/kg STZ dose can successfully induce and maintain a type-1 diabetic phenotype, supports the use of this refinement that can limit the adverse effects of STZ administration (Lanigan et al., 2020).

The development of a diabetic phenotype in rats after STZ administration was confirmed through measuring the rats blood glucose level (BGL) as a primary endpoint. In all three studies using the STZ type-1 diabetic model, increased BGL above the 16mmol/L hyperglycaemic threshold was achieved in 95% of the rats. The maintenance of hyperglycaemia was confirmed to last for at least 49 days, allowing for an adequate time window to conduct preclinical screening using this model. Importantly, the development and maintenance of this level of hyperglycaemia was consistent with higher dose 65mg/kg STZ models that do not allow for anomer equilibration (Lanigan et al., 2020; Wang-Fischer & Garyantes, 2018). The diabetic phenotype of the STZ rats was also confirmed here through assessing the development and maintenance of polydipsia, polyphagia and bodyweight loss in the 55mg/kg STZ diabetic. Bodyweight loss and the development of polydipsia and polyphagia are consistently reported across research groups in the STZ type-1 diabetes model (Ali et al., 2015; Rutten et al., 2018; Vieira et al., 2020; Wang-Fischer & Garyantes, 2018; Yamamoto et al., 2009) and in human type-1 diabetic patients with poor glycaemic management (Pasi & Ravi, 2022; Roche et al., 2005).

A common use of the STZ type-1 diabetic model is to measure the development of mechanical allodynia through the classical evoked endpoint of von Frey paw withdrawal thresholds. Mechanical allodynia is a feature of neuropathic pain and therefore treatments that reverse it are proposed as having analgesic properties (Ali et al., 2015; Field, McCleary, et al., 1999; Rutten et al., 2018; Wang-Fischer & Garyantes, 2018; Yamamoto et al., 2009). Mechanical allodynia development was demonstrated in all three STZ studies presented here by Day 9, with 93% of the STZ diabetic rats developing mechanical allodynia. The development of mechanical allodynia was maintained for at least 45 days after STZ administration which is consistent with published literature (Wang-Fischer & Garyantes, 2018; Yamamoto et al., 2009). Initially it was identified that pregabalin, a first line treatment for neuropathic pain (Finnerup et al., 2015), fully reversed mechanical allodynia in the STZ diabetic rats at a 30mg/kg dose. However, it was also found that 30mg/kg pregabalin caused somnolence as evidenced by increased control rats paw withdrawal thresholds above baseline levels. A dose response to pregabalin at 3, 10 and 30mg/kg was conducted and identified that 10mg/kg pregabalin successfully reversed mechanical allodynia in the STZ diabetic rats without any evidence of somnolence. The maintenance of mechanical allodynia and its successful reversal with a clinical analgesic allowed for an adequate time and reversal window to conduct preclinical screening using this lower dose 55mg/kg STZ diabetic model.

7.1.1 Abbreviations.

STZ – streptozotocin, CCI – chronic constrictive injury, EEG – electroencephalogram, NREM – non-rapid eye movement, i.p. – intraperitoneal, BGL – blood glucose level, OFT – open field testing, CIPN – chemotherapy induced peripheral neuropathy.

7.2 Welfare refinements in the STZ type-1 diabetes rat model

An important secondary aim of these studies, which should always be considered when conducting preclinical research, is the welfare of the animals and any improvements that can be made. A cornerstone of improving the welfare of animal research for many decades has been the 3R's principles of Replacement, Reduction and Refinement (Russell & Burch, 1959). As discussed, the first way that the welfare of the STZ diabetic rats used in these studies was improved was through a reduction in the STZ dose to 55mg/kg. This reduced the bodyweight loss by 50% and no acute toxicity side effects of STZ administration were identified compared with the previous 65mg/kg STZ model, thus improving the welfare of these rats (Burnett et al., 2014; Fisher et al., 2015; Lanigan et al., 2020). Additionally, a small refinement was made to the protocol for measuring BGLs prior to STZ administration by taking the baseline BGL measurement the day before STZ administration. This reduced the stress of the animals on the day of STZ administration by limiting the amount of handling and restraining these animals experienced on the same day. Another key finding in the STZ diabetic model that was demonstrated here and has not previously been reported was that increased BGLs correlated with increased weight loss. This is significant as bodyweight loss is an important welfare and humane endpoint with STZ diabetic rats being euthanised and removed from the study if their weight loss approached 20% without stabilising. Additionally, it was identified that increased BGLs correlated with increased organ hypertrophy. Therefore, the provision of a low dose of slow-release insulin should be used as a rescue measure to minimise this excessive bodyweight loss, as is currently employed by some research groups (Ghasemi & Jeddi, 2023). This correlation between BGL and weight loss will encourage researchers in future STZ studies to regularly correlate BGL and weight loss along with the provision of insulin (as needed) to maximise animal welfare and limit animal exclusion based on bodyweight loss.

Whilst the primary aim of these studies was to identify novel ways to measure neuropathic pain with improved translatability, refining the existing protocols maximises animal welfare and good practice. One improvement to the classical von Frey paw withdrawal threshold endpoint that was identified in these studies was testing rats paired with a home cage partner, which has not previously been reported. Conducting von Frey testing with paired rats had no impact on STZ diabetic rats von Frey measurements. Meaning that allowing STZ diabetic rats to remain in their home cage pair did not cause any detrimental changes in STZ diabetic rats paw withdrawal threshold. Additionally, assessing paired control rats paw withdrawal thresholds slightly improved von Frey measurements compared with when tested on their own, by maintaining a more stable paw withdrawal threshold level. Though one possible limitation of conducting von Frey testing in pairs is that social transfer of pain could lead to increased sensitivity in the partner animal (Langford et al., 2006; Smith et al., 2016). Further assessment of paired rat testing needs to be explored in the future particularly by assessing STZ diabetic and control rats together to demonstrate whether the social transfer of pain may occur, leading to a reduction in the control rats paw withdrawal threshold. This observation does demonstrate that allowing rats to remain with their home cage partner during von Frey testing does not alter paw withdrawal thresholds and avoids short term isolation. These simple yet impactful refinements can be implemented by researchers using the STZ diabetic rat model along with other preclinical models to reduce the welfare impacts of preclinical research maintaining the accuracy, rigour and robustness of the scientific data.

A final welfare consideration in the EEG chemotherapy induced peripheral neuropathy (CIPN) and chronic constrictive injury (CCI) studies was the re-use of animals that had already been part of other

research studies. This ensured that 26 rats did not undergo extensive EEG/EMG implantation surgery in support of reduction as part of the 3rs (NC3Rs, n.d.). Although this differs from most other published studies, it prioritised welfare. Additionally, using older animals potentially improved the translatability of the results to patients as neuropathic pain is often developed later in life.

7.3 Use of male versus female animals

The use of male rodents has historically predominated preclinical research most often with the reasoning pertaining to hormonal related increases in variability (Kaluve et al., 2022). This has led to 81% of preclinical investigations of non-evoked neuropathic pain endpoint studies assessing only males rodents (Huerta et al., 2024) despite strong evidence for there being no difference in variability between the male and female mice (Prendergast et al., 2014). It is therefore unfortunate that this thesis contributed to this lack of inclusion of female rodents in preclinical research. A primary reason for this is that female rodents are more resistant to the diabetogenic effects of STZ than male rodents leading to a less pronounced diabetic phenotype (Ghasemi & Jeddi, 2023; Kim et al., 2020). This phenomenon has been associated with the protective effects of oestrogens (Merlin et al., 2024) though, more recently this has been overcome by increasing the dose of STZ administered to female rodents achieving a successful diabetic model (Saadane et al., 2020). More detailed investigations of this are needed however, as increased STZ doses are associated with a greater risk of mortality (Mostafavinia et al., 2016).

The use of female rats was also not possible during the EEG investigations in these studies due to the animals being supplied from previous investigations at Transpharmation LTD in which only male rats were used, in line with the 3Rs of reduction. As such future work investigating EEG and sleep/wake changes associated with neuropathic pain should include female rodents to understand any sex related differences that may be present. This is particularly important as in clinical studies it has been identified that females are more susceptible to chronic neuropathic pain (Fayaz et al., 2016). Additionally, both clinical and preclinical evidence appears to indicate that females are more susceptible to acute and chronic pain than males (Mogil, 2020). Whilst sleep assessments indicate that women spend less time asleep, take longer to fall asleep but are more predisposed to REM sleep than men (Guidozzi, 2015). How sex related differences on both pain perception and sleep/wake changes interact will require detailed investigations to ensure that the preclinical results generated are as translatable as possible whilst reducing the historic and still ongoing bias towards male dominated preclinical pain research.

7.4 Burrowing in STZ diabetic rats is a measure of overall animal wellbeing

Burrowing is an ethological behaviour expressed by rodents that can be objectively measured (Andrews et al., 2012; Fisher et al., 2021). Changes in burrowing are also considered to be equivalent to the effects on activities undertaken by humans in their daily lives (Zhang et al., 2022). It has previously been demonstrated that burrowing deficits develop in models of surgically induced neuropathic pain from as early as 3 days after CCI surgery (Muralidharan et al., 2016). The deficits in CCI rat models can be reversed by 3, 10 and 30mg/kg pregabalin administration (Rutten et al., 2018).

Conversely whilst burrowing deficits develop in diabetic models of neuropathic pain, published results suggest that these deficits are not reversed by either 10mg/kg or 30mg/kg pregabalin (Rutten et al., 2018). The lack of reversibility was believed to occur due being "masked" by changes in overall wellbeing related to diabetes in a relatively high dose 75mg/kg STZ diabetic model (Rutten et al., 2018). This thesis outlined for the first time the development timeline of STZ diabetic rats burrowing deficits which first occurred at Day 18 and were maintained until Day 46. The development of burrowing deficits took twice as long compared to the development of mechanical allodynia, which had reached a stable baseline by Day 9. This alone indicates that burrowing deficits may measure different features of the STZ type-1 diabetes model than the classical evoked mechanical allodynia measures of neuropathic pain.

Further differences between classical evoked measures of mechanical allodynia and burrowing deficits were identified when assessing the effects of 3, 10 and 30mg/kg pregabalin. Similarly to the findings of Rutten et al. (2018), pregabalin had no effect on STZ diabetic rats burrowing at any dose, despite all three doses demonstrating efficacy in reversing mechanical allodynia (Rutten et al., 2018). Additionally, pregabalin was still ineffective regardless of the present studies using a much lower 55mg/kg STZ dose model with potentially improved animal welfare compared to the 75mg/kg STZ diabetic model (Lanigan et al., 2020; Rutten et al., 2018). This confirmed that the first line treatment for neuropathic pain pregabalin was ineffective at reversing burrowing deficits in STZ diabetic models of neuropathic pain. It was also verified that the locomotion and gait of STZ diabetic rats were not altered during the time when burrowing deficits occurred. Confirming that the burrowing deficits were caused by an affective component of the diabetic and neuropathic pain phenotype in the STZ diabetic rats. This contributed to the research that indicates burrowing is a measure of overall animal wellbeing as it was not improved by treating mechanical allodynia (Andrews et al., 2011; Deacon, 2006; Deseure & Hans, 2018; Jirkof, 2014).

This thesis provided an interesting addition to previous research, being the first to provide evidence of burrowing deficits being reversed in STZ diabetic rats, though not through analgesic treatment. Home caging an STZ diabetic rat with a control rat improved the STZ diabetic rats individual burrowing. This was the first example of STZ diabetic rats burrowing improving, demonstrating that it is possible to reverse the burrowing deficits in these animals. A potential mechanism that may explain this phenomenon is the social support of a healthy animal that is paired with an animal in pain. In rodents this is termed "social buffering" and has most often been explored in stress related scenarios with the presence of or home caging with a companion animal leading to a reduction in reaction and perception of aversive experiences (Denommé & Mason, 2022). Therefore, this thesis has provided evidence that it may be possible to reverse the burrowing deficits in STZ diabetic rats with treatments that improve overall animal wellbeing.

Though burrowing appears to be a useful measure of overall animal wellbeing, a key limitation that may reduce its effectiveness as a neuropathic pain endpoint is increased inter-animal variability in comparison to classical evoked endpoints. This phenomenon has been reported by others researching burrowing in alternate neuropathic pain models and highlights that this is a consistently reported challenge with burrowing (Andrews et al., 2012; Muralidharan et al., 2016). Preclinical screening assays that aim to use burrowing as a neuropathic pain endpoint would likely have to increase the number of animals used to achieve the same statistical power. This could limit future research into burrowing due to the 3R's implications of increasing the number of animals used in research. Additionally, as burrowing deficits developed later (Day 18) than mechanical allodynia (Day 9) this would require preclinical screening studies to be extended in length, increasing costs and decreasing throughout. However, if it provides more translatable data compared with evoked tests

this may be justifiable (NC3Rs, n.d.). Burrowing may still provide a useful objective secondary endpoint measuring the wellbeing of STZ diabetic rats that could identify novel analgesics with superior efficacy to current treatments like pregabalin which are ineffective at reversing burrowing deficits.

7.5 Locomotor activity is a translatable neuropathic pain endpoint in CCI rats but not in STZ diabetic rats

Locomotor activity and gait were first assessed in STZ diabetic rats, through measuring the amount of time spent moving and the distance travelled during half an hour spent in an open field testing (OFT) apparatus. The gait of STZ diabetic rats was assessed via the application of paint to the rat's hind paws and allowing them to freely walk along a covered walkway to manually measure any change in their stride and walking gait. Neither locomotor activity nor walking gait were altered in STZ diabetic rats up to Day 18 after STZ administration, whilst mechanical allodynia was already detectable by Day 3. Reduced locomotor activity has previously been identified in STZ diabetic rats though this typically only develops four weeks after STZ administration (Bădescu et al., 2016; Doria et al., 2016; Kou et al., 2014). Likewise changes in STZ diabetic rat's gait, particularly when measured as the stride length, appears to only occur after at least four weeks (Al Deeb et al., 2000; Karatan et al., 2019; Vieira et al., 2020). Therefore, this research provides evidence that changes in gait and locomotor activity in the STZ diabetic rat model are not useful preclinical neuropathic pain endpoints during the first three weeks after STZ administration. More research is needed to characterise if the development of these changes at later timepoints are consistent and reversible with analgesic treatments.

Conversely to the results seen in STZ diabetic rats, locomotor activity did provide a useful objective measure of neuropathic pain in CCI rats when assessed in a home cage environment. The CCI rat model was surgically induced by tying four loose ligatures of suture material around the sciatic nerve to develop a unilateral model of neuropathic pain (Bennett & Xie, 1988). Locomotor activity was recorded in CCI rats as part of a sleep/wake study and progressively decreased after CCI surgery from Day 7 to Day 25. This matched the development of mechanical allodynia which was also identified at Day 7 in these CCI rats, and maintained for 37 days. This demonstrated the reversal of decreased locomotor activity in CCI rats by ketamine treatment, a finding that has not previously been reported. Ketamine is a novel analgesic and antidepressant treatment (Bratsos et al., 2019; Kantor et al., 2023) that has shown promise in preclinical (Velzen et al., 2021) and clinical (Guimarães Pereira et al., 2022) studies of neuropathic pain. Critically, locomotor activity was not improved by pregabalin, a first line treatment for neuropathic pain (Finnerup et al., 2015) despite it demonstrating superior efficacy to ketamine in classical evoked measures of mechanical allodynia. This is supported by the finding that in spinal cord injury patients with neuropathic pain, ketamine was ranked the second most effective analgesic treatment behind botulinum toxin A, whilst pregabalin was ranked fifth out of eleven treatments (Ling et al., 2022). Locomotor activity was also not improved by psilocybin, another novel antidepressant (Bornemann et al., 2021; Davis et al., 2021), with limited analgesic evidence (Koseli et al., 2023; Lyes et al., 2023). Decreased physical activity is often reported in patients with neuropathic pain (Attal et al., 2011). Therefore, this thesis provides evidence that home cage locomotor activity measurements in CCI rats provides a translatable neuropathic pain endpoint with improved sensitivity for effective analgesic treatments.

7.6 Sleep/wake amount needs more development work to be considered a neuropathic pain endpoint

Sleep disruption is frequently reported by neuropathic pain patients and is associated with worse pain outcomes (Guntel et al., 2021; Tofthagen et al., 2013). One such change in patients sleep is a decrease in the amount of time spent asleep (Guntel et al., 2021; Mahfouz et al., 2024; Widerstrom-Noga et al., 2001). However, in preclinical models the reports of neuropathic pain induced changes in sleep/wake amount are inconsistent. Some report decreased time spent asleep (Andersen & Tufik, 2003; Ho et al., 2024) whilst others have reported no change in sleep/wake amount (Alexandre et al., 2024; Kontinen et al., 2003; Leys et al., 2013) and more rarely an increased amount of time spent asleep (Alexandre et al., 2024). Presented in this thesis was the first evidence that oxaliplatin treated rats that developed neuropathic pain, in the form of CIPN, did not show any significant changes in sleep/wake amount. However, there was a trend towards decreased wakefulness and increased non-rapid eye movement (NREM) sleep in the CIPN rats assessed. Interestingly, this trend in CIPN rats matched findings in CCI rats that spent more time asleep at the expense of wakefulness. Though the translatability of the CIPN rat findings may be limited by the low number of animals (4/9) that developed CIPN. Similarly to locomotor activity, ketamine reversed the development of sleep/wake amount changes in CCI rats back to baseline levels. Whereas pregabalin only had a delayed partial effect in reversing this endpoint. This is the first report to provide evidence of a drug treatment correcting sleep/wake amounts in CCI rats. Although the increased NREM sleep amount was consistent in two models of neuropathic pain and reversed with analgesic treatments, most published preclinical results and the pathophysiology of patients is for the time spent asleep to be decreased. This is likely to limit the translatability potential of increased NREM sleep as a neuropathic pain endpoint. Therefore, more work is needed to characterise the changes in sleep/wake amounts in various neuropathic pain models across different research groups before this can be conclusively considered as a neuropathic pain endpoint.

7.7 Sleep fragmentation and brief awakenings are translatable neuropathic pain endpoints

Sleep disruption through sleep fragmentation is also commonly reported in patients (Guntel et al., 2021; Mahfouz et al., 2024; Widerstrom-Noga et al., 2001) and is more consistently reported in preclinical neuropathic pain models (Alexandre et al., 2024; Andersen & Tufik, 2003; Ho et al., 2024). This thesis found that in CIPN rats there was no clear development of sleep fragmentation, however there was a trend towards decreased average length of wakefulness bouts and increased short bouts of NREM sleep. The development of sleep fragmentation in CCI rats was more definitive with wakefulness and NREM sleep bouts occurring more often and for shorter periods of time. These findings of sleep fragmentation are consistent with previously published results in CCI models (Alexandre et al., 2024; Andersen & Tufik, 2003). However this is the first report of sleep fragmentation being characterised through an automated sleep/wake scoring algorithm. The use of these algorithms vastly increases the efficiency of scoring sleep states in electroencephalogram

(EEG) recordings and reduces the costs associated with EEG data scoring and analysis when used as a preclinical screening technique (Muto & Berthomier, 2023).

Sleep fragmentation through increased brief awakenings or short periods of wakefulness are reported in neuropathic pain models (Alexandre et al., 2024; Andersen & Tufik, 2003; Ho et al., 2024). This was identified using an automated sleep/wake scoring algorithm, through an increase in the number of short bouts of wakefulness in CCI rats. Although, it was not identified in the CIPN rats. Additionally, ketamine reversed almost all measures of sleep fragmentation in the CCI rats. Pregabalin had some efficacy particularly in reversing the total number of wake bouts and short bouts of wakefulness, whilst psilocybin had very little effect on sleep fragmentation in the CCI rats. This demonstrated that sleep fragmentation may be able to provide a way to differentiate between analgesic compounds that classical evoked endpoints cannot. The lack of definitive sleep fragmentation in the CIPN rat model of neuropathic pain may indicated a difference between preclinical models of surgically induced (CCI) and chemotherapy induced (CIPN) neuropathic pain. As CCI rats developed sleep fragmentation but the CIPN rats did not, sleep fragmentation may be limited to surgically induced models of neuropathic pain which would impact the translatability to clinical trials. Though further research into a model of chronic CIPN could help to identify if the lack of sleep fragmentation is limited to the transient single dose model of CIPN used here. Overall, sleep fragmentation appears to be a reproducible, reversible and translatable neuropathic pain endpoint that is applicable to high throughput screening studies that use automated sleep/wake scoring.

7.8 EEG power spectra changes in neuropathic pain models do not appear to provide consistent or reversible results

An alternative way that EEG recordings have been employed as neuropathic pain endpoints is through assessing EEG power spectra changes. The most consistently reported change is increased theta power which has been identified in both human patients (Jensen et al., 2013; Krupina et al., 2020; Michels et al., 2011; Sarnthein et al., 2005; Sarnthein & Jeanmonod, 2008; Stern et al., 2006) and in CCI rats during wakefulness (Koyama, LeBlanc, et al., 2018). This thesis however, did not identify increased theta power in either CCI rats or CIPN rats. This aligns to other research that has not identified increased theta power in preclinical neuropathic pain models (Kontinen et al., 2003; Li, Ge, et al., 2019). Increased delta power has been reported in the partial sciatic nerve ligation mouse model (Li, Ge, et al., 2019) and was identified during these studies in CCI rats. However, increased delta power was only observed during the first part of the EEG recording, did not remain consistently increased and was not reversed by pregabalin or ketamine treatment. Increased beta power was also identified in the CCI rats which has previously been reported in some clinical studies (Mussigmann et al., 2022). This increase in beta power was only identified during the first part of the recording. Additionally, pregabalin and ketamine had no effect on beta power, though there was not a sufficient window to compare their efficacy as the baseline and vehicle timepoints. Therefore, measuring EEG power in CIPN and CCI neuropathic pain models did not appear to provide consistent or reversible results and is likely not a useful preclinical neuropathic pain endpoint.

7.9 Summary Statement

There is a dire need for new treatments for neuropathic pain and the current preclinical neuropathic pain endpoints are not providing the translatability required to identify novel efficacious analgesic treatments. Novel neuropathic endpoints were examined to identify those that are objective, measure ethological behaviours and can also be measured in humans. Burrowing is an ethological behaviour that can be objectively measured in rodents and reflects the changes in behaviour of a human's daily activities. In the STZ diabetic rat model burrowing appears to measure the overall wellbeing of the animals and provides a useful secondary endpoint in neuropathic pain studies. Locomotor activity is another ethological behaviour that can be measured objectively in the animal's normal home cage environment and is sensitive to analgesic efficacy. This provides a useful tool to translate the effects of neuropathic pain on patients' daily activities. EEG recordings of power spectra changes did not appear to provide a useful neuropathic pain endpoint. However, the development of sleep/wake changes and particularly sleep fragmentation is similar in CCI rats to those reported in humans. Additionally, sleep fragmentation was reversible with analgesic treatment and separated the effects of different analgesics. EEG recordings of sleep/wake behaviour can also be recorded, scored and assessed objectively in both humans and animals. The results of the studies outlined in this thesis can be used to further the research into the use of burrowing, locomotor activity and sleep/wake behaviours to improve the translatability of preclinical neuropathic pain endpoints.

References

Ahles, T. A., & Saykin, A. J. (2007). Candidate mechanisms for chemotherapy-induced cognitive changes. *Nature Reviews. Cancer*, *7*(3), 192. https://doi.org/10.1038/NRC2073

Al Deeb, S., Al Moutaery, K., Arshaduddin, M., Biary, N., & Tariq, M. (2000). Attenuation of acrylamide-induced neurotoxicity in diabetic rats. *Neurotoxicology and Teratology*, *22*(2), 247–253. https://doi.org/10.1016/S0892-0362(99)00060-4

Alam, U., Riley, D. R., Jugdey, R. S., Azmi, S., Rajbhandari, S., D'Août, K., & Malik, R. A. (2017). Diabetic Neuropathy and Gait: A Review. *Diabetes Therapy*, *8*(6), 1253–1264. https://doi.org/10.1007/s13300-017-0295-y

Alexandre, C., Miracca, G., Holanda, V. D., Sharma, A., Kourbanova, K., Ferreira, A., Bicca, M. A., Zeng, X., Nassar, V. A., Lee, S., Kaur, S., Sarma, S. V., Sacré, P., Scammell, T. E., Woolf, C. J., & Latremoliere, A. (2024). Nociceptor spontaneous activity is responsible for fragmenting non–rapid eye movement sleep in mouse models of neuropathic pain. *Science Translational Medicine*, *16*(743), 32. https://doi.org/10.1126/scitranslmed.adg3036

Ali, G., Subhan, F., Abbas, M., Zeb, J., Shahid, M., & Sewell, R. D. E. (2015). A streptozotocin-induced diabetic neuropathic pain model for static or dynamic mechanical allodynia and vulvodynia: validation using topical and systemic gabapentin. *Naunyn-Schmiedeberg's Archives of Pharmacology*, *388*(11), 1129–1140. https://doi.org/10.1007/s00210-015-1145-y

Allchorne, A. J., Broom, D. C., & Woolf, C. J. (2005). Detection of Cold Pain, Cold Allodynia and Cold Hyperalgesia in Freely Behaving Rats. *Molecular Pain*, *1*, 1744-8069-1–36. https://doi.org/10.1186/1744-8069-1-36

Alle, L., Armand, S., Golay, A., Monnin, D., de Bie, R. A., & de Bruin, E. D. (2008). Gait characteristics of diabetic patients: a systematic review. *Diabetes/Metabolism Research and Reviews*, *24*(3), 173–191. https://doi.org/10.1002/DMRR.809

Alles, S. R. A., Cain, S. M., & Snutch, T. P. (2020). Pregabalin as a Pain Therapeutic: Beyond Calcium Channels. *Frontiers in Cellular Neuroscience*, *14*(April), 1–9. https://doi.org/10.3389/fncel.2020.00083

Almeida, F. C., Castilho, A., Cesarino, C. B., Ribeiro, R. de C. H. M., & Martins, M. R. I. (2018). Correlation between neuropathic pain and quality of life. *Brazilian Journal Of Pain*, *1*(4), 349–353. https://doi.org/10.5935/2595-0118.20180066

Almoznino, G., Benoliel, R., Sharav, Y., & Haviv, Y. (2017). Sleep disorders and chronic craniofacial pain: Characteristics and management possibilities. *Sleep Medicine Reviews*, *33*, 39–50. https://doi.org/10.1016/J.SMRV.2016.04.005

Alsalem, M., Haddad, M., Altarifi, A., Aldossary, S., Kalbouneh, H., Abojaradeh, A., & El-Salem, K. (2020). Impairment in locomotor activity as an objective measure of pain and analgesia in a rat model of osteoarthritis. *Experimental and Therapeutic Medicine*, *20*(6), 1–1. https://doi.org/10.3892/etm.2020.9294

Anand, P., & Bley, K. (2011). Topical capsaicin for pain management: therapeutic potential and mechanisms of action of the new high-concentration capsaicin 8% patch. *BJA: British Journal of Anaesthesia*, *107*(4), 490. https://doi.org/10.1093/BJA/AER260

Andersen, M. L., & Tufik, S. (2003). Sleep patterns over 21-day period in rats with chronic

constriction of sciatic nerve. *Brain Research*, *984*(1–2), 84–92. https://doi.org/10.1016/S0006-8993(03)03095-6

Andrews, N., Harper, S., Issop, Y., & Rice, A. S. C. C. (2011). Novel, nonreflex tests detect analgesic action in rodents at clinically relevant concentrations. *Annals of the New York Academy of Sciences*, *1245*(1), 11–13. https://doi.org/10.1111/j.1749-6632.2011.06342.x

Andrews, N., Legg, E., Lisak, D., Issop, Y., Richardson, D., Harper, S., Pheby, T., Huang, W., Burgess, G., Machin, I., & Rice, A. S. C. S. (2012). Spontaneous burrowing behaviour in the rat is reduced by peripheral nerve injury or inflammation associated pain. *European Journal of Pain (London, England)*, *16*(4), 485–495. https://doi.org/10.1016/j.ejpain.2011.07.012

Apkarian, A. V., Bushnell, M. C., Treede, R. D., & Zubieta, J. K. (2005). Human brain mechanisms of pain perception and regulation in health and disease. *European Journal of Pain*, *9*(4), 463. https://doi.org/10.1016/j.ejpain.2004.11.001

Atkinson, M. A., Eisenbarth, G. S., & Michels, A. W. (2014). Type 1 diabetes. *The Lancet*, *383*(9911), 69–82. https://doi.org/10.1016/S0140-6736(13)60591-7

Attal, N., & Bouhassira, D. (2019). Translational neuropathic pain research. *Pain*, *160*(5), S23–S28. https://doi.org/10.1097/j.pain.0000000000001522

Attal, N., Bouhassira, D., & Baron, R. (2018). Diagnosis and assessment of neuropathic pain through questionnaires. *The Lancet Neurology*, *17*(5), 456–466. https://doi.org/10.1016/S1474-4422(18)30071-1

Attal, N., Lanteri-Minet, M., Laurent, B., Fermanian, J., & Bouhassira, D. (2011). The specific disease burden of neuropathic pain: Results of a French nationwide survey. *Pain*, *152*(12), 2836–2843. https://doi.org/10.1016/j.pain.2011.09.014

Austin, P. J., Wu, A., & Moalem-Taylor, G. (2012). Chronic Constriction of the Sciatic Nerve and Pain Hypersensitivity Testing in Rats. *Journal of Visualized Experiments : JoVE*, *61*, 3393. https://doi.org/10.3791/3393

Authier, N., Balayssac, D., Marchand, F., Ling, B., Zangarelli, A., Descoeur, J., Coudore, F., Bourinet, E., & Eschalier, A. (2009). Animal Models of Chemotherapy-Evoked Painful Peripheral Neuropathies. *Neurotherapeutics*, *6*(4), 620–629. https://doi.org/10.1016/J.NURT.2009.07.003

Azmi, S., ElHadd, K. T., Nelson, A., Chapman, A., Bowling, F. L., Perumbalath, A., Lim, J., Marshall, A., Malik, R. A., & Alam, U. (2019). Pregabalin in the Management of Painful Diabetic Neuropathy: A Narrative Review. *Diabetes Therapy*, *10*(1), 35. https://doi.org/10.1007/S13300-018-0550-X

Bacalhau, C., Costa-Pereira, J. T., & Tavares, I. (2023). Preclinical research in paclitaxel-induced neuropathic pain: a systematic review. *Frontiers in Veterinary Science*, *10*. https://doi.org/10.3389/FVETS.2023.1264668/FULL

Backonja, M. M. (1996). Primary somatosensory cortex and pain perception: Yes Sir, your pain is in your head (part I). *Pain Forum*, *5*(3), 174–180. https://doi.org/10.1016/S1082-3174(96)80026-2

Bădescu, S. V., Tătaru, C. P., Kobylinska, L., Georgescu, E. L., Zahiu, D. M., Zăgrean, A. M., & Zăgrean, L. (2016). Effects of caffeine on locomotor activity in streptozotocin-induced diabetic rats. *Journal of Medicine and Life*, *9*(3), 275.

Bagriyanik, H. A., Ersoy, N., Cetinkaya, C., Ikizoglu, E., Kutri, D., Ozcana, T., Kamanga, L. G., & Kiray, M. (2014). The effects of resveratrol on chronic constriction injury of sciatic nerve in rats. *Neuroscience Letters*, *561*, 123–127. https://doi.org/10.1016/J.NEULET.2013.12.056

Bajaj, N., & Bajaj, N. (2020). Wavelets for EEG Analysis. *Wavelet Theory*.

https://doi.org/10.5772/INTECHOPEN.94398

Banach, M., Juranek, J. K., & Zygulska, A. L. (2017). Chemotherapy-induced neuropathies—a growing problem for patients and health care providers. *Brain and Behavior*, *7*(1). https://doi.org/10.1002/BRB3.558

Bannister, K., & Dickenson, A. H. (2016). What do monoamines do in pain modulation? *Current Opinion in Supportive and Palliative Care*, *10*(2), 143. https://doi.org/10.1097/SPC.0000000000000207

Bansal, D., Bhansali, A., Hota, D., Chakrabarti, A., & Dutta, P. (2009). Amitriptyline vs. pregabalin in painful diabetic neuropathy: a randomized double blind clinical trial. *Diabetic Medicine*, *26*(10), 1019–1026. https://doi.org/10.1111/j.1464-5491.2009.02806.x

Baranidharan, G., Das, S., & Bhaskar, A. (2013). A review of the high-concentration capsaicin patch and experience in its use in the management of neuropathic pain. *Therapeutic Advances in Neurological Disorders*, *6*(5), 287–297. https://doi.org/10.1177/1756285613496862

Bardoni, R. (2013). Role of Presynaptic Glutamate Receptors in Pain Transmission at the Spinal Cord Level. *Current Neuropharmacology*, *11*(5), 477. https://doi.org/10.2174/1570159X11311050002

Becker, J., Effraim, P. R., Dib-Hajj, S., & Rittner, H. L. (2023). Lessons learned in translating pain knowledge into practice. *Pain Reports*, *8*(6), E1100. https://doi.org/10.1097/PR9.0000000000001100

Bendinger, T., & Plunkett, N. (2016). Measurement in pain medicine. *BJA Education*, *16*(9), 310–315. https://doi.org/10.1093/bjaed/mkw014

Benedetti, F. (2010). No prefrontal control, no placebo response. *Pain*, *148*(3), 357–358. https://doi.org/10.1016/j.pain.2009.10.009

Benington, J. H., Kodali, S. K., & Heller, H. C. (1994). Scoring transitions to REM sleep in rats based on the EEG phenomena of pre-REM sleep: an improved analysis of sleep structure. *Sleep*, *17*(1), 28–36. https://doi.org/10.1093/SLEEP/17.1.28

Bennett, D. L., Clark, X. A. J., Huang, J., Waxman, S. G., & Dib-Hajj, S. D. (2019). The role of voltage-gated sodium channels in pain signaling. *Physiological Reviews*, *99*(2), 1079–1151. https://doi.org/10.1152/PHYSREV.00052.2017/ASSET/IMAGES/LARGE/Z9J0011929010023.JPEG

Bennett, G. J., Chung, J. M., 5.32.2), M. H. (Table, & Seltzer, Z. (2003). Models of Neuropathic Pain in the Rat. *Current Protocols in Pharmacology*, *21*(1), 5.32.1-5.32.16. https://doi.org/10.1002/0471141755.PH0532S21

Bennett, G. J., & Xie, Y. K. (1988). A peripheral mononeuropathy in rat that produces disorders of pain sensation like those seen in man. *Pain*, *33*(1), 87–107. https://doi.org/10.1016/0304-3959(88)90209-6

Berge, O. G. (2011). Predictive validity of behavioural animal models for chronic pain. *British Journal of Pharmacology*, *164*(4), 1195–1206. https://doi.org/10.1111/j.1476-5381.2011.01300.x

Berger, H. (1929). Über das Elektrenkephalogramm des Menschen - Dritte Mitteilung. *Archiv Für Psychiatrie Und Nervenkrankheiten*, *94*(1), 16–60. https://doi.org/10.1007/BF01835097

Binnie, C. D., & Prior, P. F. (1994). Electroencephalography. *Journal of Neurology, Neurosurgery & Psychiatry*, *57*(11), 1308–1319. https://doi.org/10.1136/jnnp.57.11.1308

Blackstone Whines, W. (2022). *Characterisation of peripheral neuropathy and neuronal and endothelial markers of neuropathic pain: A comparative study across preclinical models of neuropathic pain* (September). University of Hertfordshire.

Bonin, R. P., Bories, C., & De Koninck, Y. (2014). A simplified up-down method (SUDO) for measuring mechanical nociception in rodents using von Frey filaments. *Molecular Pain*, *10*(1). https://doi.org/10.1186/1744-8069-10-26

Boom, M., Niesters, M., Sarton, E., Aarts, L., W. Smith, T., & Dahan, A. (2012). Non-analgesic effects of opioids: opioid-induced respiratory depression. *Current Pharmaceutical Design*, *18*(37), 5994–6004. https://doi.org/10.2174/138161212803582469

Borbély, A. A., Daan, S., Wirz-Justice, A., & Deboer, T. (2016). The two-process model of sleep regulation: A reappraisal. *Journal of Sleep Research, 25*(2), 131–143. https://doi.org/10.1111/jsr.12371

Bornemann, J., Close, J. B., Spriggs, M. J., Carhart-Harris, R., & Roseman, L. (2021). Self-Medication for Chronic Pain Using Classic Psychedelics: A Qualitative Investigation to Inform Future Research. *Frontiers in Psychiatry*, *12*, 735427. https://doi.org/10.3389/FPSYT.2021.735427/BIBTEX

Bouali-Benazzouz, R., Landry, M., Benazzouz, A., & Fossat, P. (2021). Neuropathic pain modeling: Focus on synaptic and ion channel mechanisms. *Progress in Neurobiology*, *201*, 102030. https://doi.org/10.1016/j.pneurobio.2021.102030

Bouhassira, D., & Attal, N. (2016). Translational neuropathic pain research: A clinical perspective. *Neuroscience*, *338*, 27–35. https://doi.org/10.1016/j.neuroscience.2016.03.029

Bouhassira, Didier, Branders, S., Attal, N., Fernandes, A. M., Demolle, D., Barbour, J., Ciampi de Andrade, D., & Pereira, A. (2021). Stratification of patients based on the Neuropathic Pain Symptom Inventory: development and validation of a new algorithm. *Pain*, *162*(4), 1038–1046. https://doi.org/10.1097/j.pain.0000000000002130

Bove, G. (2006). Mechanical sensory threshold testing using nylon monofilaments: The pain field's "Tin Standard." *Pain*, *124*(1), 13–17. https://doi.org/10.1016/j.pain.2006.06.020

Branca, J. J. V., Carrino, D., Gulisano, M., Ghelardini, C., Di Cesare Mannelli, L., & Pacini, A. (2021). Oxaliplatin-Induced Neuropathy: Genetic and Epigenetic Profile to Better Understand How to Ameliorate This Side Effect. *Frontiers in Molecular Biosciences*, *8*, 643824. https://doi.org/10.3389/FMOLB.2021.643824/BIBTEX

Bratsos, S., Saleh, S. N., Bratsos, S., & Saleh, S. N. (2019). Clinical Efficacy of Ketamine for Treatment-resistant Depression. *Cureus*, *11*(7). https://doi.org/10.7759/CUREUS.5189

Brodkin, J., Frank, D., Grippo, R., Hausfater, M., Gulinello, M., Achterholt, N., & Gutzen, C. (2014). Validation and implementation of a novel high-throughput behavioral phenotyping instrument for mice. *Journal of Neuroscience Methods*, *224*, 48–57. https://doi.org/10.1016/j.jneumeth.2013.12.010

Brookes, M. E., Eldabe, S., & Batterham, A. (2017). Ziconotide Monotherapy: A Systematic Review of Randomised ControlledTrials. *Current Neuropharmacology*, *15*(2), 217. https://doi.org/10.2174/1570159X14666160210142056

Brooks, J. C. W., & Tracey, I. (2007). The insula: A multidimensional integration site for pain. *Pain*, *128*(1–2), 1–2. https://doi.org/10.1016/j.pain.2006.12.025

Brooks, K. G., & Kessler, T. L. (2017). Treatments for neuropathic pain. *Clinical Pharmacist*, *9*(12), 1–

14. https://doi.org/10.1211/CP.2017.20203641

Brown, G. R., & Nemes, C. (2008). The exploratory behaviour of rats in the hole-board apparatus: Is head-dipping a valid measure of neophilia? *Behavioural Processes*, *78*(3), 442. https://doi.org/10.1016/J.BEPROC.2008.02.019

Burnett, M., Fisher, A., Pye, L., Upton, N., & Lione, L. A. (2014). *Impairment in burrowing in the rat streptozocin (STZ) diabetes model of neuropathic pain and the benefits of social housing*.

Calcutt, N. A. (2020). *Diabetic neuropathy and neuropathic pain: a (con) fusion of pathogenic mechanisms? 161*(9).

Campbell, I. G. (2009). EEG Recording and Analysis for Sleep Research. *Current Protocols in Neuroscience*, *49*(1), Unit10.2. https://doi.org/10.1002/0471142301.ns1002s49

Campbell, J. N., & Meyer, R. A. (2006). Mechanisms of Neuropathic Pain. *Neuron*, *52*(1), 77–92. https://doi.org/10.1016/j.neuron.2006.09.021

Casanova-Molla, J., Morales, M., Planas-Rigol, E., Bosch, A., Calvo, M., Grau-Junyent, J. M., & Valls-Solé, J. (2012). Epidermal Langerhans cells in small fiber neuropathies. *Pain*, *153*(5), 982–989. https://doi.org/10.1016/J.PAIN.2012.01.021

Castañeda-Corral, G., Velázquez-Salazar, N. B., Martínez-Martínez, A., Taboada-Serrano, J. N., Núñez-Aragón, P. N., González-Palomares, L., Acosta-González, R. I., Petricevich, V. L., Acevedo-Fernández, J. J., Montes, S., & Jiménez-Andrade, J. M. (2021). Characterization of Mechanical Allodynia and Skin Innervation in a Mouse Model of Type-2 Diabetes Induced by Cafeteria-Style Diet and Low-Doses of Streptozotocin. *Frontiers in Pharmacology*, *11*. https://doi.org/10.3389/FPHAR.2020.628438/FULL

Cavalli, E., Mammana, S., Nicoletti, F., Bramanti, P., & Mazzon, E. (2019). The neuropathic pain: An overview of the current treatment and future therapeutic approaches. *International Journal of Immunopathology and Pharmacology*, *33*. https://doi.org/10.1177/2058738419838383

Caylor, J., Reddy, R., Yin, S., Cui, C., Huang, M., Huang, C., Rao, R., Baker, D. G., Simmons, A., Souza, D., Narouze, S., Vallejo, R., & Lerman, I. (2019). Spinal cord stimulation in chronic pain: evidence and theory for mechanisms of action. *Bioelectronic Medicine*, *5*(1), 12. https://doi.org/10.1186/s42234-019-0023-1

Cersosimo, R. J. (2005). Oxaliplatin-associated neuropathy: A review. *Annals of Pharmacotherapy*, *39*(1), 128–135. https://doi.org/10.1345/aph.1E319

Challa, S. R. (2015). Surgical animal models of neuropathic pain: Pros and Cons. *International Journal of Neuroscience*, *125*(3), 170–174. https://doi.org/10.3109/00207454.2014.922559

Chaplan, S. R., Bach, F. W., Pogrel, J. W., Chung, J. M., & Yaksh, T. L. (1994). Quantitative assessment of tactile allodynia in the rat paw. *Journal of Neuroscience Methods*, *53*(1), 55–63. https://doi.org/10.1016/0165-0270(94)90144-9

Chaplan, Sandra R., Guo, H. Q., Lee, D. H., Luo, L., Liu, C., Kuei, C., Velumian, A. A., Butler, M. P., Brown, S. M., & Dubin, A. E. (2003). Neuronal Hyperpolarization-Activated Pacemaker Channels Drive Neuropathic Pain. *The Journal of Neuroscience*, *23*(4), 1169. https://doi.org/10.1523/JNEUROSCI.23-04-01169.2003

Charan, J., & Kantharia, N. (2013). How to calculate sample size in animal studies? *Journal of Pharmacology and Pharmacotherapeutics*, *4*(4), 303–306. https://doi.org/10.4103/0976-500X.119726

Chen, Q. Y., Tan, C. Y., Wang, Y., Ma, K. T., Li, L., & Si, J. Q. (2019). Mechanism of persistent

hyperalgesia in neuropathic pain caused by chronic constriction injury. *Neural Regeneration Research*, *14*(6), 1091. https://doi.org/10.4103/1673-5374.250631

Chen, S. (2012). Clinical Uses of Botulinum Neurotoxins: Current Indications, Limitations and Future Developments. *Toxins*, *4*(10), 913. https://doi.org/10.3390/TOXINS4100913

Christensen, S. L., Hansen, R. B., Storm, M. A., Olesen, J., Hansen, T. F., Ossipov, M., Izarzugaza, J. M. G., Porreca, F., & Kristensen, D. M. (2020). Von Frey testing revisited: Provision of an online algorithm for improved accuracy of 50% thresholds. *European Journal of Pain (United Kingdom)*, *24*(4), 783–790. https://doi.org/10.1002/ejp.1528

Clarke, K. A., Heitmeyer, S. A., Smith, A. G., & Taiwo, Y. O. (1997). Gait analysis in a rat model of osteoarthrosis. *Physiology and Behavior*, *62*(5), 951–954. https://doi.org/10.1016/S0031-9384(97)00022-X

Cobos, E., & Portillo-Salido, E. (2013). "Bedside-to-Bench" Behavioral Outcomes in Animal Models of Pain: Beyond the Evaluation of Reflexes. *Current Neuropharmacology*, *11*(6), 560–591. https://doi.org/10.2174/1570159x113119990041

Colloca, L., Ludman, T., Bouhassira, D., Baron, R., Dickenson, A. H., Yarnitsky, D., Freeman, R., Truini, A., Attal, N., Finnerup, N. B., Eccleston, C., Kalso, E., Bennett, D. L. H., Dworkin, R. H., & Raja, S. N. (2017). Neuropathic Pain. *Nat Rev Dis Primers*, *3*(doi:10.1038/nrdp.2017.2), 1–45. https://doi.org/10.1038/nrdp.2017.2.Neuropathic

Colvin, L. A. (2019). Chemotherapy-induced peripheral neuropathy (CIPN): where are we now? *Pain*, *160*(Suppl 1), S1. https://doi.org/10.1097/J.PAIN.0000000000001540

Cruccu, G., Finnerup, N. B., Jensen, T. S., Scholz, J., Sindou, M., Svensson, P., Treede, R. D., Zakrzewska, J. M., & Nurmikko, T. (2016). Trigeminal neuralgia: New classification and diagnostic grading for practice and research. *Neurology*, *87*(2), 220–228. https://doi.org/10.1212/WNL.0000000000002840/SUPPL_FILE/APPENDIX_E-3.PDF

Cruccu, G., & Truini, A. (2009). Tools for Assessing Neuropathic Pain. *PLoS Medicine*, *6*(4), e1000045. https://doi.org/10.1371/journal.pmed.1000045

D'Amato, F. R. (1997). Neurobiological and Behavioral Aspects of Recognition in Female Mice. *Physiology & Behavior*, *62*(6), 1311–1317. https://doi.org/10.1016/S0031-9384(97)00343-0

Dalal, S. S., Hamamé, C. M., Eichenlaub, J. B., & Jerbi, K. (2010). Intrinsic Coupling between Gamma Oscillations, Neuronal Discharges, and Slow Cortical Oscillations during Human Slow-Wave Sleep. *Journal of Neuroscience*, *30*(43), 14285–14287. https://doi.org/10.1523/JNEUROSCI.4275-10.2010

Daniel, S. R., Badyal, D. K., Jacob, J. J., & Kaur, J. (2018). Efficacy and safety of pregabalin versus amitriptyline in patients with painful diabetic neuropathy. *International Journal of Advances in Medicine*, *5*(3), 716. https://doi.org/10.18203/2349-3933.ijam20182129

Davis, A. K., Barrett, F. S., May, D. G., Cosimano, M. P., Sepeda, N. D., Johnson, M. W., Finan, P. H., & Griffiths, R. R. (2021). Effects of Psilocybin-Assisted Therapy on Major Depressive Disorder: A Randomized Clinical Trial. *JAMA Psychiatry*, *78*(5), 481–489. https://doi.org/10.1001/jamapsychiatry.2020.3285

Davis, J. L., Lewis, S. B., Kaplan, R. A., Schultz, T. A., Wallin, J. D., & Gerich, J. E. (1977). Peripheral Diabetic Neuropathy Treated With Amitriptyline and Fluphenazine. *JAMA*, *238*(21), 2291–2292. https://doi.org/10.1001/JAMA.1977.03280220059023

De Felice, M., Sanoja, R., Wang, R., Vera-Portocarrero, L., Oyarzo, J., King, T., Ossipov, M. H.,

Vanderah, T. W., Lai, J., Dussor, G. O., Fields, H. L., Price, T. J., & Porreca, F. (2011). Engagement of descending inhibition from the rostral ventromedial medulla protects against chronic neuropathic pain. *Pain*, *152*(12), 2701–2709. https://doi.org/10.1016/j.pain.2011.06.008

De La Garza-Rodea, A. S., Knaän-Shanzer, S., Den Hartigh, J. D., Verhaegen, A. P. L., & Van Bekkum, D. W. (2010). Anomer-equilibrated streptozotocin solution for the induction of experimental diabetes in mice (Mus musculus). *Journal of the American Association for Laboratory Animal Science*, *49*(1), 40–44.

de León-Casasola, O. A., & Mayoral, V. (2016). The topical 5% lidocaine medicated plaster in localized neuropathic pain: a reappraisal of the clinical evidence. *Journal of Pain Research*, *9*, 67. https://doi.org/10.2147/JPR.S99231

de Vries, M., Westerink, J., El-Morabit, F., Kaasjager, H. A. H. (Karin., & de Valk, H. W. (2022). Prevalence of non-alcoholic fatty liver disease (NAFLD) and its association with surrogate markers of insulin resistance in patients with type 1 diabetes. *Diabetes Research and Clinical Practice*, *186*(March), 109827. https://doi.org/10.1016/j.diabres.2022.109827

De Vry, J., Kuhl, E., Franken-Kunkel, P., & Eckel, G. (2004). Pharmacological characterization of the chronic constriction injury model of neuropathic pain. *European Journal of Pharmacology*, *491*(2–3), 137–148. https://doi.org/10.1016/j.ejphar.2004.03.051

Deacon, R. M. J. (2006). Burrowing in rodents: a sensitive method for detecting behavioral dysfunction. *Nature Protocols*, *1*(1), 118–122.

Deacon, R. M. J. (2009). Burrowing: A sensitive behavioural assay, tested in five species of laboratory rodents. *Behavioural Brain Research*, *200*(1), 128–133. https://doi.org/10.1016/j.bbr.2009.01.007

Denommé, M. R., & Mason, G. J. (2022). Social Buffering as a Tool for Improving Rodent Welfare. *Journal of the American Association for Laboratory Animal Science : JAALAS*, *61*(1), 5–14. https://doi.org/10.30802/AALAS-JAALAS-21-000006

Deseure, K., & Hans, G. (2018). Orofacial neuropathic pain reduces spontaneous burrowing behavior in rats. *Physiology and Behavior*, *191*(April), 91–94. https://doi.org/10.1016/j.physbeh.2018.04.020

Deuis, J. R., Dvorakova, L. S., & Vetter, I. (2017). Methods used to evaluate pain behaviors in rodents. *Frontiers in Molecular Neuroscience*, *10*(September), 284. https://doi.org/10.3389/fnmol.2017.00284

Dieleman, J. P., Kerklaan, J., Huygen, F. J. P. M., Bouma, P. A. D., & Sturkenboom, M. C. J. M. (2008). Incidence rates and treatment of neuropathic pain conditions in the general population. *PAIN®*, *137*(3), 681–688. https://doi.org/10.1016/J.PAIN.2008.03.002

Dini, L., Del Lungo, M., Resta, F., Melchiorre, M., Spinelli, V., Di Cesare Mannelli, L., Ghelardini, C., Laurino, A., Sartiani, L., Coppini, R., Mannaioni, G., Cerbai, E., & Romanelli, M. N. (2018). Selective blockade of HCN1/HCN2 channels as a potential pharmacological strategy against pain. *Frontiers in Pharmacology*, *9*(NOV), 1252. https://doi.org/10.3389/FPHAR.2018.01252/BIBTEX

Dixon, W. J. (1965). The Up-and-Down Method for Small Samples. *Journal of the American Statistical Association*, *60*(312), 967–978.

Doria, A. B., Nadia, B., & Abdelkrim, T. (2016). Hesperidin effects on behavior and locomotor activity of diabetic Wistar rat. *African Journal of Biotechnology*, *15*(45), 2572–2577. https://doi.org/10.5897/AJB2016.15715

Drinkenburg, W. H. I. M., Ruigt, G. S. F., & Ahnaou, A. (2016). Pharmaco-EEG Studies in Animals: An Overview of Contemporary Translational Applications. *Neuropsychobiology*, *72*(3–4), 151–164. https://doi.org/10.1159/000442210

Dworkin, R. H., Gnann, J. W., Oaklander, A. L., Raja, S. N., Schmader, K. E., & Whitley, R. J. (2008). Diagnosis and Assessment of Pain Associated With Herpes Zoster and Postherpetic Neuralgia. *Journal of Pain*, *9*(1 SUPPL.), 37–44. https://doi.org/10.1016/j.jpain.2007.10.008

Dworkin, R. H., O'Connor, A. B., Backonja, M., Farrar, J. T., Finnerup, N. B., Jensen, T. S., Kalso, E. A., Loeser, J. D., Miaskowski, C., Nurmikko, T. J., Portenoy, R. K., Rice, A. S. C., Stacey, B. R., Treede, R. D., Turk, D. C., & Wallace, M. S. (2007). Pharmacologic management of neuropathic pain: Evidence-based recommendations. *Pain*, *132*(3), 237–251. https://doi.org/10.1016/j.pain.2007.08.033

Egashira, N. (2021). Pathological Mechanisms and Preventive Strategies of Oxaliplatin-Induced Peripheral Neuropathy. *Frontiers in Pain Research*, *2*, 804260. https://doi.org/10.3389/FPAIN.2021.804260

Egeo, G., Fofi, L., & Barbanti, P. (2020). Botulinum Neurotoxin for the Treatment of Neuropathic Pain. *Frontiers in Neurology*, *11*(August), 1–15. https://doi.org/10.3389/fneur.2020.00716

Ellenbroek, B., & Youn, J. (2016). Rodent models in neuroscience research: Is it a rat race? *DMM Disease Models and Mechanisms*, *9*(10), 1079–1087. https://doi.org/10.1242/dmm.026120

Faber, J., & Fonseca, L. M. (2014). How sample size influences research outcomes. *Dental Press Journal of Orthodontics*, *19*(4), 27. https://doi.org/10.1590/2176-9451.19.4.027-029.EBO

Faul, F., Erdfelder, E., Lang, A. G., & Buchner, A. (2007). G*Power 3: A flexible statistical power analysis program for the social, behavioral, and biomedical sciences. *Behavior Research Methods*, *39*(2), 175–191. https://doi.org/10.3758/BF03193146

Fayaz, A., Croft, P., Langford, R. M., Donaldson, L. J., & Jones, G. T. (2016). Prevalence of chronic pain in the UK: A systematic review and meta-analysis of population studies. *BMJ Open*, *6*(6). https://doi.org/10.1136/bmjopen-2015-010364

Feldman, E. L., Callaghan, B. C., Pop-Busui, R., Zochodne, D. W., Wright, D. E., Bennett, D. L., Bril, V., Russell, J. W., & Viswanathan, V. (2019). Diabetic neuropathy. *Nature Reviews Disease Primers*, *5*(1). https://doi.org/10.1038/s41572-019-0092-1

Fenwick, N., Griffin, G., & Gauthier, C. (2009). The welfare of animals used in science: how the "Three Rs" ethic guides improvements. *The Canadian Veterinary Journal = La Revue Veterinaire Canadienne*, *50*(5), 523–530.

Field, M, J., Bramwell, S., Hughes, J., & Singh, L. (1999). Detection of static and dynamic components of mechanical allodynia in rat models of neuropathic pain: Are they signalled by distinct primary sensory neurones? *Pain*, *83*(2), 303–311. https://doi.org/10.1016/S0304-3959(99)00111-6

Field, M, J., Holloman, E. F., McCleary, S., Hughes, J., & Singh, L. (1997). Evaluation of gabapentin and S-(+)-3-isobutylgaba in a rat model of postoperative pain. *Journal of Pharmacology and Experimental Therapeutics*, *282*(3), 1242–1246.

Field, M. J., Cox, P. J., Stott, E., Melrose, H., Offord, J., Su, T., Bramwell, S., Corradini, L., England, S., Winks, J., Kinloch, R. A., Hendrich, J., Dolphin, A. C., Webb, T., & Williams, D. (2006). Identification of the alpha-2-delta-1 dependent calcium channels as a molecular target for pain mediating the analgesic actions of pregabalin. *Proceedings of the National Academy of Sciences of the United States of America*, *103*(46), 17537–17542.

Field, M. J., McCleary, S., Hughes, J., & Singh, L. (1999). Gabapentin and pregabalin, but not morphine and amitriptyline, block both static and dynamic components of mechanical allodynia induced by streptozocin in the rat. *Pain*, *80*(1–2), 391–398. https://doi.org/10.1016/S0304-3959(98)00239-5

Field, M. J., Oles, R. J., Lewis, A. S., McCleary, S., Hughes, J., & Singh, L. (1997). Gabapentin (neurontin) and S -(+)-3-isobutylgaba represent a novel class of selective antihyperalgesic agents. *British Journal of Pharmacology*, *121*(8), 1513–1522. https://doi.org/10.1038/sj.bjp.0701320

Finnerup, N. B., Attal, N., Haroutounian, S., McNicol, E., Baron, R., Dworkin, R. H., Gilron, I., Haanpää, M., Hansson, P., Jensen, T. S., Kamerman, P. R., Lund, K., Moore, A., Raja, S. N., Rice, A. S. C., Rowbotham, M., Sena, E., Siddall, P., Smith, B. H., & Wallace, M. (2015). Pharmacotherapy for neuropathic pain in adults: A systematic review and meta-analysis. *The Lancet Neurology*, *14*(2), 162–173. https://doi.org/10.1016/S1474-4422(14)70251-0

Finnerup, N. B., Haroutounian, S., Kamerman, P., Baron, R., Bennett, D. L. H., Bouhassira, D., Cruccu, G., Freeman, R., Hansson, P., Nurmikko, T., Raja, S. N., Rice, A. S. C., Serra, J., Smith, B. H., Treede, R.-D., & Jensen, T. S. (2016). Neuropathic pain: an updated grading system for research and clinical practice. *Pain*, *157*(8), 1599–1606. https://doi.org/10.1097/j.pain.0000000000000492

Finnerup, N. B., Kuner, R., & Jensen, T. S. (2021). Neuropathic pain: Frommechanisms to treatment. *Physiological Reviews*, *101*(1), 259–301. https://doi.org/10.1152/physrev.00045.2019

Fisher, A. S., Kennard, P., Upton, N., & Lione, L. (2015). The streptozocin model of diabetes induces neuropathic pain , anhedonia and impaired burrowing in rats. *PA2 Online*, *13*(3), 252P.

Fisher, A. S., Lanigan, M. T., Upton, N., & Lione, L. A. (2021). Preclinical Neuropathic Pain Assessment; the Importance of Translatability and Bidirectional Research. *Frontiers in Pharmacology*, *11*, 614990. https://doi.org/10.3389/fphar.2020.614990

Flatters, S. J. L., Dougherty, P. M., & Colvin, L. A. (2017). Clinical and preclinical perspectives on Chemotherapy-Induced Peripheral Neuropathy (CIPN): a narrative review. *British Journal of Anaesthesia*, *119*(4), 737–749. https://doi.org/10.1093/BJA/AEX229

Fonseca-Rodrigues, D., Amorim, D., Almeida, A., & Pinto-Ribeiro, F. (2021). Emotional and cognitive impairments in the peripheral nerve chronic constriction injury model (CCI) of neuropathic pain: A systematic review. *Behavioural Brain Research*, *399*, 113008. https://doi.org/10.1016/J.BBR.2020.113008

Fornasari, D. (2017). Pharmacotherapy for Neuropathic Pain: A Review. *Pain and Therapy*, *6*(S1), 25–33. https://doi.org/10.1007/s40122-017-0091-4

Foudah, A. I., Alqarni, M. H., Devi, S., Singh, A., Alam, A., Alam, P., & Singh, S. (2022). Analgesic Action of Catechin on Chronic Constriction Injury–Induced Neuropathic Pain in Sprague–Dawley Rats. *Frontiers in Pharmacology, 13*, 1–9. https://doi.org/10.3389/fphar.2022.895079

Frank, M. G., Ruby, N. F., Heller, H. C., & Franken, P. (2017). Development of Circadian Sleep Regulation in the Rat: A Longitudinal Study Under Constant Conditions. *Sleep*, *40*(3). https://doi.org/10.1093/SLEEP/ZSW077

Freeman, R., Durso-DeCruz, E., & Emir, B. (2008). Efficacy, safety, and tolerability of pregabalin treatment for painful diabetic peripheral neuropathy: Findings from seven randomized, controlled trials across a range of doses. *Diabetes Care*, *31*(7), 1448–1454.

https://doi.org/10.2337/dc07-2105

Furlan, A. D., Sandoval, J. A., Mailis-Gagnon, A., & Tunks, E. (2006). Opioids for chronic noncancer pain: a meta-analysis of effectiveness and side effects. *CMAJ*, *174*(11), 1589–1594. https://doi.org/10.1503/CMAJ.051528

Furman, B. L. (2021). Streptozotocin-Induced Diabetic Models in Mice and Rats. *Current Protocols*, *1*(4), 1–21. https://doi.org/10.1002/cpz1.78

Gajdošík, A., Gajdošíková, A., Štefek, M., Navarová, J., & Hozová, R. (1999). Streptozotocin-Induced Experimental Diabetes in Male Wistar Rats. *Gen Physiol Biophys*, *18*, 54–62.

Gammaitoni, A. R., Alvarez, N. A., & Galer, B. S. (2003). Safety and tolerability of the lidocaine patch 5%, a targeted peripheral analgesic: A review of the literature. *Journal of Clinical Pharmacology*, *43*(2), 111–117. https://doi.org/10.1177/0091270002239817

Ganguly, S., Panetta, J. C., Roberts, J. K., & Schuetz, E. G. (2018). Ketamine pharmacokinetics and pharmacodynamics are altered by P-glycoprotein and breast cancer resistance protein efflux transporters in mice. *Drug Metabolism and Disposition*, *46*(7), 1014–1022. https://doi.org/10.1124/DMD.117.078360/-/DC1

Gao, Y. J., Ren, W. H., Zhang, Y. Q., & Zhao, Z. Q. (2004). Contributions of the anterior cingulate cortex and amygdala to pain- and fear-conditioned place avoidance in rats. *Pain*, *110*(1–2), 343–353. https://doi.org/10.1016/j.pain.2004.04.030

Gao, Z., Wei, H., Chen, Z., Jalava, N., Koivisto, A., & Pertovaara, A. (2019). Ongoing pain in streptozotocin model of diabetes in the rat: correlation with cutaneous cheminociception. *Journal of Physiology and Pharmacology : An Official Journal of the Polish Physiological Society*, *70*(6), 969–978. https://doi.org/10.26402/jpp.2019.6.14

Gerke, M. B., Duggan, A. W., Xu, L., & Siddall, P. J. (2003). Thalamic neuronal activity in rats with mechanical allodynia following contusive spinal cord injury. *Neuroscience*, *117*(3), 715–722. https://doi.org/10.1016/S0306-4522(02)00961-2

Ghasemi, A., & Jeddi, S. (2023). Streptozotocin as a tool for induction of rat models of diabetes: a practical guide. *EXCLI Journal*, *22*, 274. https://doi.org/10.17179/EXCLI2022-5720

Gilbert, J. R., & Zarate, C. A. (2020). Electrophysiological Biomarkers of Antidepressant Response to Ketamine in Treatment-Resistant Depression: Gamma Power and Long-Term Potentiation. *Pharmacology, Biochemistry, and Behavior*, *189*, 172856. https://doi.org/10.1016/J.PBB.2020.172856

Gillespie, K. M. (2006). Type 1 diabetes: pathogenesis and prevention. *CMAJ*, *175*(2), 165–170. https://doi.org/10.1503/CMAJ.060244

Gilron, I., Baron, R., & Jensen, T. (2015). Neuropathic pain: Principles of diagnosis and treatment. *Mayo Clinic Proceedings*, *90*(4), 532–545. https://doi.org/10.1016/j.mayocp.2015.01.018

Gilron, I., & Dickenson, A. H. (2014). Emerging drugs for neuropathic pain. *Expert Opinion on Emerging Drugs*, *19*(3), 329–341. https://doi.org/10.1517/14728214.2014.915025

Gouin, O., L'Herondelle, K., Lebonvallet, N., Le Gall-Ianotto, C., Sakka, M., Buhé, V., Plée-Gautier, E., Carré, J. L., Lefeuvre, L., Misery, L., & Le Garrec, R. (2017). TRPV1 and TRPA1 in cutaneous neurogenic and chronic inflammation: pro-inflammatory response induced by their activation and their sensitization. *Protein and Cell*, *8*(9), 644–661. https://doi.org/10.1007/s13238-017-0395-5

Gould, S. A., Doods, H., Lamla, T., & Pekcec, A. (2016). Pharmacological characterization of

intraplantar Complete Freund's Adjuvant-induced burrowing deficits. *Behavioural Brain Research*, *301*, 142–151. https://doi.org/10.1016/J.BBR.2015.12.019

Gregory, N. (2013). An overview of animal models of pain: disease models and outcome measures. *Bone*, *23*(1), 1–7. https://doi.org/10.1038/jid.2014.371

Grieger, N., Schwabedal, J. T. C., Wendel, S., Ritze, Y., & Bialonski, S. (2021). Automated scoring of pre-REM sleep in mice with deep learning. *Scientific Reports 2021 11:1*, *11*(1), 1–14. https://doi.org/10.1038/s41598-021-91286-0

Guidozzi, F. (2015). Gender differences in sleep in older men and women. *Climacteric, 18*(5), 715–721. https://doi.org/10.3109/13697137.2015.1042451

Guimarães Pereira, J. E., Pereira, L. F. G., Linhares, R. M., Bersot, C. D. A., Aslanidis, T., & Ashmawi, H. A. (2022). Efficacy and Safety of Ketamine in the Treatment of Neuropathic Pain: A Systematic Review and Meta-Analysis of Randomized Controlled Trials. *Journal of Pain Research*, *15*(April), 1011–1037. https://doi.org/10.2147/JPR.S358070

Guntel, M., Huzmeli, E. D., & Melek, I. (2021). Patients With Neuropathic Pain Have Poor Sleep Quality. *Journal of Nervous & Mental Disease*, *209*(7), 505–509. https://doi.org/10.1097/NMD.0000000000001325

Guo, X. xuan, Wang, Y., Wang, K., Ji, B. ping, & Zhou, F. (2018). Stability of a type 2 diabetes rat model induced by high-fat diet feeding with low-dose streptozotocin injection. *Journal of Zhejiang University: Science B*, *19*(7), 559–569. https://doi.org/10.1631/jzus.B1700254

Gustafsson, H., & Sandin, J. (2009). Oral pregabalin reverses cold allodynia in two distinct models of peripheral neuropathic pain. *European Journal of Pharmacology*, *605*(1–3), 103–108. https://doi.org/10.1016/J.EJPHAR.2009.01.014

Habib, S. L. (2018). Kidney atrophy vs hypertrophy in diabetes: which cells are involved? *Cell Cycle*, *17*(14), 1683–1687. https://doi.org/10.1080/15384101.2018.1496744

Haider, S., Ahmed, S., Tabassum, S., Memon, Z., Ikram, M., & Haleem, D. J. (2013). Streptozotocin-induced insulin deficiency leads to development of behavioral deficits in rats. *Acta Neurologica Belgica*, *113*(1), 35–41. https://doi.org/10.1007/s13760-012-0121-2

Hains, B. C., & Waxman, S. G. (2007). Sodium channel expression and the molecular pathophysiology of pain after SCI. In *Progress in Brain Research* (Vol. 161, pp. 195–203). Elsevier. https://doi.org/10.1016/S0079-6123(06)61013-3

Hamzeh, H., Gaudillère, A., Sabido, O., Tchou, I., Lambert, C., Schmitt, D., Genin, C., & Misery, L. (2000). Expression of PGP9.5 on Langerhans' cells and their precursors. *Acta Dermato-Venereologica*, *80*(1), 14–16. https://doi.org/10.1080/000155500750012423

Haroutounian, S., Nikolajsen, L., Bendtsen, T. F., Finnerup, N. B., Kristensen, A. D., Hasselstrøm, J. B., & Jensen, T. S. (2014). Primary afferent input critical for maintaining spontaneous pain in peripheral neuropathy. *Pain*, *155*(7), 1272–1279. https://doi.org/10.1016/j.pain.2014.03.022

Hassan, M. A., Fraser, M., Conway, B. A., Allan, D. B., & Vuckovic, A. (2015). The mechanism of neurofeedback training for treatment of central neuropathic pain in paraplegia: A pilot study. *BMC Neurology*, *15*(1), 200. https://doi.org/10.1186/s12883-015-0445-7

Heinzel, J., Längle, G., Oberhauser, V., Hausner, T., Kolbenschlag, J., Prahm, C., Grillari, J., & Hercher, D. (2020). Use of the CatWalk gait analysis system to assess functional recovery in rodent models of peripheral nerve injury – a systematic review. *Journal of Neuroscience Methods*, *345*, 108889. https://doi.org/10.1016/J.JNEUMETH.2020.108889

Hendricks, P. S., Thorne, C. B., Clark, C. B., Coombs, D. W., & Johnson, M. W. (2015). Classic psychedelic use is associated with reduced psychological distress and suicidality in the United States adult population. *Http://Dx.Doi.Org/10.1177/0269881114565653*, *29*(3), 280–288. https://doi.org/10.1177/0269881114565653

Ho, A., Lee, S. J., Drew, V. J., Jung, J., Kang, J., Kim, T., & Cheong, C. (2024). Sleep disturbance correlated with severity of neuropathic pain in sciatic nerve crush injury model. *Journal of Sleep Research*. https://doi.org/10.1111/JSR.14137

Holden, J. E., Jeong, Y., & Forrest, J. M. (2005). The endogenous opioid system and clinical pain management. *AACN Clinical Issues*, *16*(3), 291–301. https://doi.org/10.1097/00044067-200507000-00003

Hu, X., Liu, Y., Wu, J., Liu, Y., Liu, W., Chen, J., & Yang, F. (2020). Inhibition of P2X7R in the amygdala ameliorates symptoms of neuropathic pain after spared nerve injury in rats. *Brain, Behavior, and Immunity*, *88*(April), 507–514. https://doi.org/10.1016/j.bbi.2020.04.030

Hubrecht, R. C., & Carter, E. (2019). The 3Rs and Humane Experimental Technique: Implementing Change. *Animals : An Open Access Journal from MDPI*, *9*(10). https://doi.org/10.3390/ANI9100754

Huerta, M., Cisneros, E., Alique, M., & Roza, C. (2024). Strategies for measuring non-evoked pain in preclinical models of neuropathic pain: Systematic review. *Neuroscience and Biobehavioral Reviews*, *163*, 105761. https://doi.org/10.1016/j.neubiorev.2024.105761

Inglis, J. J., McNamee, K. E., Chia, S. L., Essex, D., Feldmann, M., Williams, R. O., Hunt, S. P., & Vincent, T. (2008). Regulation of pain sensitivity in experimental osteoarthritis by the endogenous peripheral opioid system. *Arthritis and Rheumatism*, *58*(10), 3110–3119. https://doi.org/10.1002/art.23870

Inglis, J. J., Notley, C. A., Essex, D., Wilson, A. W., Feldmann, M., Anand, P., & Williams, R. (2007). Collagen-induced arthritis as a model of hyperalgesia: Functional and cellular analysis of the analgesic actions of tumor necrosis factor blockade. *Arthritis and Rheumatism*, *56*(12), 4015–4023. https://doi.org/10.1002/art.23063

Iwata, K., Kamo, H., Ogawa, A., Tsuboi, Y., Noma, N., Mitsuhashi, Y., Taira, M., Koshikawa, N., & Kitagawa, J. (2005). Anterior cingulate cortical neuronal activity during perception of noxious thermal stimuli in monkeys. *Journal of Neurophysiology*, *94*(3), 1980–1991. https://doi.org/10.1152/jn.00190.2005

Jackson, S. J., Andrews, N., Ball, D., Bellantuono, I., Gray, J., Hachoumi, L., Holmes, A., Latcham, J., Petrie, A., Potter, P., Rice, A., Ritchie, A., Stewart, M., Strepka, C., Yeoman, M., & Chapman, K. (2017). Does age matter? The impact of rodent age on study outcomes. *Laboratory Animals*, *51*(2), 160–169. https://doi.org/10.1177/0023677216653984

Jaggi, A. S., Jain, V., & Singh, N. (2011). Animal models of neuropathic pain. *Fundamental and Clinical Pharmacology*, *25*(1), 1–28. https://doi.org/10.1111/j.1472-8206.2009.00801.x

Jensen, M. P., Castarlenas, E., Tomé-Pires, C., de la Vega, R., Sánchez-Rodríguez, E., & Miró, J. (2015). The Number of Ratings Needed for Valid Pain Assessment in Clinical Trials: Replication and Extension. *Pain Medicine*, *16*(9), 1764–1772. https://doi.org/10.1111/pme.12823

Jensen, M. P., Hakimian, S., Sherlin, L. H., & Fregni, F. (2008). New Insights Into Neuromodulatory Approaches for the Treatment of Pain. *Journal of Pain*, *9*(3), 193–199. https://doi.org/10.1016/j.jpain.2007.11.003

Jensen, M. P., Sherlin, L. H., Gertz, K. J., Braden, A. L., Kupper, A. E., Gianas, A., Howe, J. D., & Hakimian, S. (2013). Brain EEG activity correlates of chronic pain in persons with spinal cord injury: Clinical implications. *Spinal Cord*, *51*(1), 55–58. https://doi.org/10.1038/sc.2012.84

Jensen, T. S., Baron, R., Haanpää, M., Kalso, E., Loeser, J. D., Rice, A. S. C., & Treede, R.-D. D. (2011). A new definition of neuropathic pain. *Pain*, *152*(10), 2204–2205. https://doi.org/10.1016/j.pain.2011.06.017

Jensen, T. S., & Finnerup, N. B. (2014). Allodynia and hyperalgesia in neuropathic pain: Clinical manifestations and mechanisms. *The Lancet Neurology*, *13*(9), 924–935. https://doi.org/10.1016/S1474-4422(14)70102-4

Jin, Q. Q., Wu, G. Q., Peng, W. W., Xia, X. L., Hu, L., & Iannetti, G. D. (2018). Somatotopic representation of second pain in the primary somatosensory cortex of humans and rodents. *Journal of Neuroscience*, *38*(24), 5538–5550. https://doi.org/10.1523/JNEUROSCI.3654-17.2018

Jirkof, P. (2014). Burrowing and nest building behavior as indicators of well-being in mice. *Journal of Neuroscience Methods*, *234*, 139–146. https://doi.org/10.1016/j.jneumeth.2014.02.001

Jirkof, P., Leucht, K., Cesarovic, N., Caj, M., Nicholls, F., Rogler, G., Arras, M., & Hausmann, M. (2013). Burrowing is a sensitive behavioural assay for monitoring general wellbeing during dextran sulfate sodium colitis in laboratory mice. *Laboratory Animals*, *47*(4), 274–283. https://doi.org/10.1177/0023677213493409

Johnson, P. D., & Besselsen, D. G. (2002). Practical aspects of experimental design in animal research. *ILAR Journal, 43*, 202–206. https://doi.org/10.1093/ilar.43.4.202

Johnston, I. N., Tan, M., Cao, J., Matsos, A., Forrest, D. R. L., Si, E., Fardell, J. E., & Hutchinson, M. R. (2017). Ibudilast reduces oxaliplatin-induced tactile allodynia and cognitive impairments in rats. *Behavioural Brain Research*, *334*, 109–118. https://doi.org/10.1016/j.bbr.2017.07.021

Kaluve, A. M., Le, J. T., & Graham, B. M. (2022). Female rodents are not more variable than male rodents: A meta-analysis of preclinical studies of fear and anxiety. *Neuroscience and Biobehavioral Reviews, 143*, 104962. https://doi.org/10.1016/j.neubiorev.2022.104962

Kamata, Y., Kambe, T., Chiba, T., Yamamoto, K., Kawakami, K., Abe, K., & Taguchi, K. (2020). Paclitaxel Induces Upregulation of Transient Receptor Potential Vanilloid 1 Expression in the Rat Spinal Cord. *International Journal of Molecular Sciences 2020, Vol. 21, Page 4341*, *21*(12), 4341. https://doi.org/10.3390/IJMS21124341

Kambiz, S., van Neck, J. W., Cosgun, S. G., van Velzen, M. H. N., Janssen, J. A. M. J. L., Avazverdi, N., Hovius, S. E. R., & Walbeehm, E. T. (2015). An Early Diagnostic Tool for Diabetic Peripheral Neuropathy in Rats. *PLOS ONE*, *10*(5), e0126892. https://doi.org/10.1371/journal.pone.0126892

Kantor, S., Lanigan, M., Giggins, L., Lione, L., Magomedova, L., de Lannoy, I., Upton, N., & Duxon, M. (2023). Ketamine supresses REM sleep and markedly increases EEG gamma oscillations in the Wistar Kyoto rat model of treatment-resistant depression. *Behavioural Brain Research*, *449*, 114473. https://doi.org/10.1016/J.BBR.2023.114473

Karatan, B., Akşam, E., Erden, E., & Demirseren, M. E. (2019). Effects of adipose derived stromal vascular fraction on diabetic neuropathy: an experimental study. *Journal of Plastic Surgery and Hand Surgery*, *53*(6), 335–340. https://doi.org/10.1080/2000656X.2019.1632205

Kato, H., Miyazaki, M., Takeuchi, M., Tsukuura, H., Sugishita, M., Noda, Y., & Yamada, K. (2015). A retrospective study to identify risk factors for somnolence and dizziness in patients treated

with pregabalin. *Journal of Pharmaceutical Health Care and Sciences*, *1*(1). https://doi.org/10.1186/S40780-015-0022-7

Kim, B., Kim, Y. Y., Nguyen, P. T. T., Nam, H., & Suh, J. G. (2020). Sex differences in glucose metabolism of streptozotocin-induced diabetes inbred mice (C57BL/6J). *Applied Biological Chemistry, 63*(1). https://doi.org/10.1186/s13765-020-00547-5

Kim, J. Y., Abdi, S., Huh, B., & Kim, K. H. (2021). Mirogabalin: Could it be the next generation gabapentin or pregabalin? *Korean Journal of Pain*, *34*(1), 4–18. https://doi.org/10.3344/KJP.2021.34.1.4

Kim, W., Chung, Y., Choi, S., Min, B. Il, & Kim, S. K. (2017). Duloxetine protects against oxaliplatin-induced neuropathic pain and spinal neuron hyperexcitability in rodents. *International Journal of Molecular Sciences*, *18*(12). https://doi.org/10.3390/ijms18122626

King, A., & Bowe, J. (2016). Animal models for diabetes: Understanding the pathogenesis and finding new treatments. *Biochemical Pharmacology*, *99*, 1–10. https://doi.org/10.1016/j.bcp.2015.08.108

Kline IV, R. H., & Wiley, R. G. (2008). Spinal μ-Opioid Receptor-Expressing Dorsal Horn Neurons: Role in Nociception and Morphine Antinociception. *Journal of Neuroscience*, *28*(4), 904–913. https://doi.org/10.1523/JNEUROSCI.4452-07.2008

Knopp, K. L., Stenfors, C., Baastrup, C., Bannon, A. W., Calvo, M., Caspani, O., Currie, G., & Treede, R. D. (2015). Experimental design and reporting standards for improving the internal validity of pre-clinical studies in the field of pain: Consensus of the IMI-Europain consortium. *Scandinavian Journal of Pain,* 7(1), 58–70. https://doi.org/10.1016/j.sjpain.2015.01.006

Kolbman, N., Liu, T., Guzzo, P., Gilligan, J., Mashour, G. A., Vanini, G., & Pal, D. (2023). Intravenous psilocybin attenuates mechanical hypersensitivity in a rat model of chronic pain. *R1282 Current Biology*, *33*, 1263–1283. https://doi.org/10.1016/j

Kontinen, V. K., Ahnaou, A., Drinkenburg, W. H. I. M., & Meert, T. F. (2003). Sleep and EEG patterns in the chronic constriction injury model of neuropathic pain. *Physiology and Behavior*, *78*(2), 241–246. https://doi.org/10.1016/S0031-9384(02)00966-6

Koseli, E., Buzzi, B., Choi, E., Honaker, T., González-Maeso, J., Youkin, J., Manetti, D., Romanelli, M. N., Arias, H. R., & Damaj, M. I. (2023). Effect Of Hallucinogenic And Non-Hallucinogenic Psychedelic Analogs On Chronic Neuropathic Pain In Mice. *The Journal of Pain*, *24*(4), 6–7. https://doi.org/10.1016/J.JPAIN.2023.02.034

Kou, Z. Z., Li, C. Y., Hu, J. C., Yin, J. Bin, Zhang, D. L., Liao, Y. H., Wu, Z. Y., Ding, T., Qu, J., Li, H., & Li, Y. Q. (2014). Alterations in the neural circuits from peripheral afferents to the spinal cord: possible implications for diabetic polyneuropathy in streptozotocin-induced type 1 diabetic rats. *Frontiers in Neural Circuits*, *8*(JAN). https://doi.org/10.3389/FNCIR.2014.00006

Kourbanova, K., Alexandre, C., & Latremoliere, A. (2022). Effect of sleep loss on pain—New conceptual and mechanistic avenues. *Frontiers in Neuroscience*, *16*, 1009902. https://doi.org/10.3389/FNINS.2022.1009902/BIBTEX

Koyama, S., LeBlanc, B. W., Smith, K. A., Roach, C., Levitt, J., Edhi, M. M., Michishita, M., Komatsu, T., Mashita, O., Tanikawa, A., Yoshikawa, S., & Saab, C. Y. (2018). An Electroencephalography Bioassay for Preclinical Testing of Analgesic Efficacy. *Scientific Reports*, *8*(1), 1–10. https://doi.org/10.1038/s41598-018-34594-2

Koyama, S., Xia, J., Leblanc, B. W., Gu, J. W., & Saab, C. Y. (2018). Sub-paresthesia spinal cord

stimulation reverses thermal hyperalgesia and modulates low frequency EEG in a rat model of neuropathic pain. *Scientific Reports*, *8*(1), 1–7. https://doi.org/10.1038/s41598-018-25420-w

Kremer, M., Salvat, E., Muller, A., Yalcin, I., & Barrot, M. (2016). Antidepressants and gabapentinoids in neuropathic pain: Mechanistic insights. *Neuroscience*, *338*, 183–206. https://doi.org/10.1016/j.neuroscience.2016.06.057

Krupina, N. A., Churyukanov, M. V., Kukushkin, M. L., & Yakhno, N. N. (2020). Central Neuropathic Pain and Profiles of Quantitative Electroencephalography in Multiple Sclerosis Patients. *Frontiers in Neurology*, *10*(January), 1–14. https://doi.org/10.3389/fneur.2019.01380

Kulkarni, B., Bentley, D. E., Elliott, R., Youell, P., Watson, A., Derbyshire, S. W. G., Frackowiak, R. S. J., Friston, K. J., & Jones, A. K. P. (2005). Attention to pain localization and unpleasantness discriminates the functions of the medial and lateral pain systems. *European Journal of Neuroscience*, *21*(11), 3133–3142. https://doi.org/10.1111/j.1460-9568.2005.04098.x

Kumar, N., Laferriere, A., Yu, J. S. C., Leavitt, A., & Coderre, T. J. (2010). Evidence that pregabalin reduces neuropathic pain by inhibiting the spinal release of glutamate. *Journal of Neurochemistry*, *113*(2), 552–561. https://doi.org/10.1111/j.1471-4159.2010.06625.x

Kundermann, B., Spernal, J., Huber, M. T., Krieg, J. C., & Lautenbacher, S. (2004). Sleep deprivation affects thermal pain thresholds but not somatosensory thresholds in healthy volunteers. *Psychosomatic Medicine*, *66*(6), 932–937. https://doi.org/10.1097/01.PSY.0000145912.24553.C0

Kurdi, M. S., Theerth, K. A., & Deva, R. S. (2014). Ketamine: Current applications in anesthesia, pain, and critical care. *Anesthesia, Essays and Researches*, *8*(3), 283. https://doi.org/10.4103/0259-1162.143110

Kwon, M., Altin, M., Duenas, H., & Alev, L. (2014). The Role of Descending Inhibitory Pathways on Chronic Pain Modulation and Clinical Implications. *Pain Practice*, *14*(7), 656–667. https://doi.org/10.1111/PAPR.12145

Labuz, D., Spahn, V., Celik, O., & Machelska, H. (2015). *Opioids and TRPV1 in the peripheral control of neuropathic pain e Defining a target site in the injured nerve*. https://doi.org/10.1016/j.neuropharm.2015.10.003

Lakes, E. H., & Allen, K. D. (2016). Gait analysis methods for rodent models of arthritic disorders: reviews and recommendations. *Osteoarthritis and Cartilage*, *24*(11), 1837–1849. https://doi.org/10.1016/j.joca.2016.03.008

Lalli, P., Chan, A., Garven, A., Midha, N., Chan, C., Brady, S., Block, E., Hu, B., & Toth, C. (2013). Increased gait variability in diabetes mellitus patients with neuropathic pain. *Journal of Diabetes and Its Complications*, *27*(3), 248–254. https://doi.org/10.1016/j.jdiacomp.2012.10.013

Langford, D. J., Crager, S. E., Shehzad, Z., Smith, S. B., Sotocinal, S. G., Levenstadt, J. S., Chanda, M. L., Levitin, D. J., & Mogil, J. S. (2006). Social modulation of pain as evidence for empathy in mice. *Science*, *312*(5782), 1967–1970.

Lanigan, M. T., Burnett, M., Kennard, P., Upton, N., Prichard, S., Fisher, A., & Lione, L. (2020). The effect of a reduced streptozocin dose and social housing on well-being, mechanical hypersensitivity and burrowing behaviour in type 1 diabetes rodents. In *IASP*.

Latremoliere, A., & Woolf, C. J. (2009). Central Sensitization: A Generator of Pain Hypersensitivity by Central Neural Plasticity. *The Journal of Pain*, *10*(9), 895–926. https://doi.org/10.1016/j.jpain.2009.06.012

Lau, W., Dykstra, C., Thevarkunnel, S., Silenieks, L. B. B., de Lannoy, I. A. M. A. M., Lee, D. K. H. K. H., & Higgins, G. A. A. (2013). A back translation of pregabalin and carbamazepine against evoked and non-evoked endpoints in the rat spared nerve injury model of neuropathic pain. *Neuropharmacology*, *73*, 204–215. https://doi.org/10.1016/j.neuropharm.2013.05.023

Lauria, G., Lombardi, R., Borgna, M., Penza, P., Bianchi, R., Savino, C., Canta, A., Nicolini, G., Marmiroli, P., & Cavaletti, G. (2005). Intraepidermal nerve fiber density in rat foot pad: Neuropathologic- neurophysiologic correlation. *Journal of the Peripheral Nervous System*, *10*(2), 202–208. https://doi.org/10.1111/j.1085-9489.2005.0010210.x

Leach, M. C., Klaus, K., Miller, A. L., Scotto di Perrotolo, M., Sotocinal, S. G., & Flecknell, P. A. (2012). The assessment of post-vasectomy pain in mice using behaviour and the Mouse Grimace Scale. *PloS One*, *7*(4). https://doi.org/10.1371/journal.pone.0035656

LeBlanc, B. W., Bowary, P. M., Chao, Y.-C., Lii, T. R., & Saab, C. Y. (2016). Electroencephalographic signatures of pain and analgesia in rats. *PAIN*, *157*(10), 2330–2340. https://doi.org/10.1097/j.pain.0000000000000652

LeBlanc, B. W., Lii, T. R., Huang, J. J., Chao, Y. C., Bowary, P. M., Cross, B. S., Lee, M. S., Vera-Portocarrero, L. P., & Saab, C. Y. (2016). T-type calcium channel blocker Z944 restores cortical synchrony and thalamocortical connectivity in a rat model of neuropathic pain. *Pain*, *157*(1), 255–263. https://doi.org/10.1097/j.pain.0000000000000362

Leblanc, B. W., Lii, T. R., Silverman, A. E., Alleyne, R. T., & Saab, C. Y. (2014). Cortical theta is increased while thalamocortical coherence is decreased in rat models of acute and chronic pain. *Pain*, *155*(4), 773–782. https://doi.org/10.1016/j.pain.2014.01.013

Lee, S. Il, Kim, J. S., Oh, S. H., Park, K. Y., Lee, H. G., & Kim, S. D. (2008). Antihyperglycemic effect of Fomitopsis pinicola extracts in streptozotocin-induced diabetic rats. *Journal of Medicinal Food*, *11*(3), 518–524. https://doi.org/10.1089/jmf.2007.0155

Leemburg, S., Vyazovskiy, V. V., Olcese, U., Bassetti, C. L., Tononi, G., & Cirelli, C. (2010). Sleep homeostasis in the rat is preserved during chronic sleep restriction. *Proceedings of the National Academy of Sciences of the United States of America*, *107*(36), 15939–15944. https://doi.org/10.1073/PNAS.1002570107/SUPPL_FILE/PNAS.201002570SI.PDF

Leiser, S. C., Dunlop, J., Bowlby, M. R., & Devilbiss, D. M. (2011). Aligning strategies for using EEG as a surrogate biomarker: A review of preclinical and clinical research. *Biochemical Pharmacology*, *81*(12), 1408–1421. https://doi.org/10.1016/j.bcp.2010.10.002

Lenzen, S. (2008). The mechanisms of alloxan- and streptozotocin-induced diabetes. *Diabetologia*, *51*(2), 216–226. https://doi.org/10.1007/s00125-007-0886-7

Leung, V. S. Y., Benoit-Biancamano, M. O., & Pang, D. S. J. (2019). Performance of behavioral assays: The Rat Grimace Scale, burrowing activity and a composite behavior score to identify visceral pain in an acute and chronic colitis model. *Pain Reports*, *4*(2), e718. https://doi.org/10.1097/PR9.0000000000000712

Leys, L. J., Chu, K. L., Xu, J., Pai, M., Yang, H. S., Robb, H. M., Jarvis, M. F., Radek, R. J., & McGaraughty, S. (2013). Disturbances in slow-wave sleep are induced by models of bilateral inflammation, neuropathic, and postoperative pain, but not osteoarthritic pain in rats. *Pain*, *154*(7), 1092–1102. https://doi.org/10.1016/j.pain.2013.03.019

Li, C. L., Yu, Y., He, T., Wang, R. R., Geng, K. W., Du, R., Luo, W. J., Wei, N., Wang, X. L., Wang, Y., Yang, Y., Yu, Y. Q., & Chen, J. (2018). Validating rat model of empathy for pain: Effects of pain expressions in social partners. *Frontiers in Behavioral Neuroscience*, *12*, 403250.

https://doi.org/10.3389/FNBEH.2018.00242/BIBTEX

Li, X. H., Miao, H. H., & Zhuo, M. (2019). NMDA Receptor Dependent Long-term Potentiation in Chronic Pain. *Neurochemical Research*, *44*(3), 531–538. https://doi.org/10.1007/S11064-018-2614-8/FIGURES/1

Li, Y., Ge, J., Luo, Y.-J. J., Xu, W., Wang, J., Lazarus, M., Hong, Z.-Y. Y., Qu, W.-M. M., & Huang, Z.-L. L. (2019). High cortical delta power correlates with aggravated allodynia by activating anterior cingulate cortex GABAergic neurons in neuropathic pain mice. In *Pain* (Vol. 161, Issue 2). https://doi.org/10.1097/j.pain.0000000000001725

Light, G. A., Williams, L. E., Minow, F., Sprock, J., Rissling, A., Sharp, R., Swerdlow, N. R., & Braff, D. L. (2010). Electroencephalography (EEG) and Event-Related Potentials (ERP's) with Human Participants. *Current Protocols in Neuroscience / Editorial Board, Jacqueline N. Crawley [et Al.]*, *CHAPTER*(SUPPL. 52), Unit. https://doi.org/10.1002/0471142301.NS0625S52

Lindner, M. D., Bourin, C., Chen, P., McElroy, J. F., Leet, J. E., Hogan, J. B., Stock, D. A., & Machet, F. (2006). Adverse effects of gabapentin and lack of anti-allodynic efficacy of amitriptyline in the streptozotocin model of painful diabetic neuropathy. *Experimental and Clinical Psychopharmacology*, *14*(1), 42–51. https://doi.org/10.1037/1064-1297.14.1.42

Ling, B., Authier, N., Balayssac, D., Eschalier, A., & Coudore, F. (2007). Behavioral and pharmacological description of oxaliplatin-induced painful neuropathy in rat. *Pain*, *128*(3), 225–234. https://doi.org/10.1016/j.pain.2006.09.016

Ling, B., Coudoré-Civiale, M. A., Balayssac, D., Eschalier, A., Coudoré, F., & Authier, N. (2007). Behavioral and immunohistological assessment of painful neuropathy induced by a single oxaliplatin injection in the rat. *Toxicology*, *234*(3), 176–184. https://doi.org/10.1016/J.TOX.2007.02.013

Ling, B., Coudoré, F., Decalonne, L., Eschalier, A., & Authier, N. (2008). Comparative antiallodynic activity of morphine, pregabalin and lidocaine in a rat model of neuropathic pain produced by one oxaliplatin injection. *Neuropharmacology*, *55*(5), 724–728. https://doi.org/10.1016/j.neuropharm.2008.06.007

Ling, H. Q., Chen, Z. H., He, L., Feng, F., Weng, C. G., Cheng, S. J., Rong, L. M., & Xie, P. G. (2022). Comparative Efficacy and Safety of 11 Drugs as Therapies for Adults With Neuropathic Pain After Spinal Cord Injury: A Bayesian Network Analysis Based on 20 Randomized Controlled Trials. *Frontiers in Neurology*, *13*, 818522. https://doi.org/10.3389/FNEUR.2022.818522/BIBTEX

Lione, L. A., Lanigan, M., & Fisher, A. (2023). Animal Models: Practical Use and Considerations. In S. E. Ward & A. Davis (Eds.), *The Handbook of Medicinal Chemistry 2nd edition* (p. 437 - 484). The Royal Society of Chemistry. https://doi.org/10.1039/9781837671076

Liu, S., Guo, Y., Ni, J., Yin, N., Li, C., Pan, X., Ma, R., Wu, J., Li, S., & Li, X. (2022). Chemotherapy-induced functional brain abnormality in colorectal cancer patients: a resting-state functional magnetic resonance imaging study. *Frontiers in Oncology*, *12*, 900855. https://doi.org/10.3389/FONC.2022.900855/BIBTEX

Liu, W., Lv, Y., & Ren, F. (2018). PI3K/Akt Pathway is Required for Spinal Central Sensitization in Neuropathic Pain. *Cellular and Molecular Neurobiology*, *38*(3), 747–755. https://doi.org/10.1007/S10571-017-0541-X/FIGURES/5

Liu, Y., Lin, D., Wu, B., & Zhou, W. (2016). Ketamine abuse potential and use disorder. *Brain Research Bulletin*, *126*, 68–73. https://doi.org/10.1016/J.BRAINRESBULL.2016.05.016

Llinas, R. R., Ribary, U., Jeanmonod, D., Kronberg, E., & Mitra, P. P. (1999). Thalamocortical Dysrhythmia : A neurological and neuropsychiatric syndron characterized by magnetoencephalography. *Proceedings of the National Academy of Sciences of the United States of America*, *96*(26), 15222–15227.

Loeser, J. D. (2011). Pain terms a current list with definitions and notes on usage. *Pain*, *24*, S215–S221. https://doi.org/10.1016/0304-3959(86)90113-2

Long, S., Ding, R., Wang, J., Yu, Y., Lu, J., & Yao, D. (2021). Sleep Quality and Electroencephalogram Delta Power. *Frontiers in Neuroscience*, *15*(December), 803507. https://doi.org/10.3389/fnins.2021.803507

López-Martínez, A. E., Esteve-Zarazaga, R., & Ramírez-Maestre, C. (2008). Perceived Social Support and Coping Responses Are Independent Variables Explaining Pain Adjustment Among Chronic Pain Patients. *Journal of Pain*, *9*(4), 373–379. https://doi.org/10.1016/j.jpain.2007.12.002

Lowe, H., Toyang, N., Steele, B., Valentine, H., Grant, J., Ali, A., Ngwa, W., & Gordon, L. (2021). The Therapeutic Potential of Psilocybin. *Molecules 2021, Vol. 26, Page 2948*, *26*(10), 2948. https://doi.org/10.3390/MOLECULES26102948

Lu, C., Yang, T., Zhao, H., Zhang, M., Meng, F., Fu, H., Xie, Y., & Xu, H. (2016). Insular Cortex is Critical for the Perception, Modulation, and Chronification of Pain. *Neuroscience Bulletin*, *32*(2), 191–201. https://doi.org/10.1007/s12264-016-0016-y

Luippold, G., Bedenik, J., Voigt, A., & Grempler, R. (2016). Short- and Longterm Glycemic Control of Streptozotocin-Induced Diabetic Rats Using Different Insulin Preparations. *PLoS ONE*, *11*(6). https://doi.org/10.1371/JOURNAL.PONE.0156346

Lundt, A., Wormuth, C., Siwek, M. E., Müller, R., Ehninger, D., Henseler, C., Broich, K., Papazoglou, A., & Weiergräber, M. (2016). EEG radiotelemetry in small laboratory rodents: A powerful state-of-the art approach in neuropsychiatric, neurodegenerative, and epilepsy research. *Neural Plasticity*, *2016*, 10–12. https://doi.org/10.1155/2016/8213878

Lv, X., Mao, Y., Cao, S., & Feng, Y. (2023). Animal models of chemotherapy-induced peripheral neuropathy for hematological malignancies: A review. *Ibrain*, *9*(1), 72–89. https://doi.org/10.1002/IBRA.12086

Lyes, M., Yang, K. H., Castellanos, J., & Furnish, T. (2023). Microdosing psilocybin for chronic pain: a case series. *Pain*, *164*(4), 698–702. https://doi.org/10.1097/J.PAIN.0000000000002778

Mahfouz, F. M., Li, T., Joda, M., Harrison, M., Horvath, L. G., Grimison, P., King, T., Marx, G., Goldstein, D., & Park, S. B. (2024). Sleep dysfunction associated with worse chemotherapy-induced peripheral neurotoxicity functional outcomes. *Supportive Care in Cancer*, *32*(1). https://doi.org/10.1007/S00520-023-08245-W

Malcangio, M., & Bowery, N. G. (1996). GABA and its receptors in the spinal cord. *Trends in Pharmacological Sciences*, *17*(12), 457–462. https://doi.org/10.1016/S0165-6147(96)01013-9

Malmberg, A. B., & Yaksh, T. L. (1995). Effect of continuous intrathecal infusion of ω-conopeptides, N-type calcium-channel blockers, on behavior and antinociception in the formalin and hot-plate tests in rats. *Pain*, *60*(1), 83–90. https://doi.org/10.1016/0304-3959(94)00094-U

Marchettini, P., Lacerenza, M., Mauri, E., & Marangoni, C. (2006). Painful Peripheral Neuropathies. *Current Neuropharmacology*, *4*(3), 175. https://doi.org/10.2174/157015906778019536

McGivern, J. G. (2007). Ziconotide: a review of its pharmacology and use in the treatment of pain. *Neuropsychiatric Disease and Treatment*, *3*(1), 69. https://doi.org/10.2147/NEDT.2007.3.1.69

Medeiros, P., Dos Santos, I. R., Júnior, I. M., Palazzo, E., Da Silva, J. A., MacHado, H. R., Ferreira, S. H., Maione, S., Coimbra, N. C., & De Freitas, R. L. (2021). An Adapted Chronic Constriction Injury of the Sciatic Nerve Produces Sensory, Affective, and Cognitive Impairments: A Peripheral Mononeuropathy Model for the Study of Comorbid Neuropsychiatric Disorders Associated with Neuropathic Pain in Rats. *Pain Medicine*, *22*(2), 338–351. https://doi.org/10.1093/PM/PNAA206

Melzack, R., & Wall, P. D. (1965). Pain Mechanisms: A New Theory. *Science*, *150*(3699), 971–979. https://doi.org/10.1126/science.150.3699.971

Merlin, E., Salio, C., & Ferrini, F. (2024). Painful Diabetic Neuropathy: Sex-Specific Mechanisms and Differences from Animal Models to Clinical Outcomes. *Cells, 13*, 2024. https://doi.org/10.3390/cells13232024

Mezzanotte, J. N., Grimm, M., Nolan, T., Worthen-Chaudhari, L., & Lustberg, M. B. (2022). Updates in the treatment of chemotherapy-induced peripheral neuropathy HHS Public Access. *Curr Treat Options Oncol*, *23*(1), 29–42. https://doi.org/10.1007/s11864-021-00926-0

Michels, L., Moazami-Goudarzi, M., & Jeanmonod, D. (2011). Correlations between EEG and clinical outcome in chronic neuropathic pain: surgical effects and treatment resistance. *Brain Imaging and Behavior*, *5*(4), 329–348. https://doi.org/10.1007/s11682-011-9135-2

Miller, R. E., Tran, P. B., Das, R., Ghoreishi-Haack, N., Ren, D., Miller, R. J., & Malfait, A. M. (2012). CCR2 chemokine receptor signaling mediates pain in experimental osteoarthritis. *Proceedings of the National Academy of Sciences of the United States of America*, *109*(50), 20602–20607. https://doi.org/10.1073/pnas.1209294110

Miltenburg, N. C., & Boogerd, W. (2014). Chemotherapy-induced neuropathy: A comprehensive survey. *Cancer Treatment Reviews*, *40*(7), 872–882. https://doi.org/10.1016/J.CTRV.2014.04.004

Minassian, A., Young, J. W., Cope, Z. A., Henry, B. L., Geyer, M. A., & Perry, W. (2016). Amphetamine increases activity but not exploration in humans and mice. *Psychopharmacology*, *233*(2), 225. https://doi.org/10.1007/S00213-015-4098-4

Mitani, O., Masui, K., Tsujimoto, H., Jinbo, K., Watanabe, Y., Ohkura, T., Taya, K., & Ikeda, H. (2008). Histopathological Changes of Streptozotocin-induced Painful Diabetes and Antihyperalgesic Effect of Capsaicin Cream in Rats. In *J Toxicol Pathol* (Vol. 21).

Mogil, J. S. (2015). Social modulation of and by pain in humans and rodents. *Pain*, *156 Suppl*(4), S35–S41. https://doi.org/10.1097/01.J.PAIN.0000460341.62094.77

Mogil, J. S. (2020). Qualitative sex differences in pain processing: emerging evidence of a biased literature. *Nature Reviews Neuroscience, 21*(7), 353–365. https://doi.org/10.1038/s41583-020-0310-6

Mogil, J. S., Graham, A. C., Ritchie, J., Hughes, S. F., Austin, J.-S. S., Schorscher-Petcu, A., Langford, D. J., & Bennett, G. J. (2010). Hypolocomotion, asymmetrically directed behaviors (licking, lifting, flinching, and shaking) and dynamic weight bearing (gait) changes are not measures of neuropathic pain in mice. *Molecular Pain*, *6*(1), 1744-8069-6–34. https://doi.org/10.1186/1744-8069-6-34

Mostafavinia, A., Amini, A., Ghorishi, S. K., Pouriran, R., & Bayat, M. (2016). The effects of dosage and the routes of administrations of streptozotocin and alloxan on induction rate of typel diabetes mellitus and mortality rate in rats. *Laboratory Animal Research, 32*(3), 160–165. https://doi.org/10.5625/lar.2016.32.3.160

Muralidharan, A., Kuo, A., Jacob, M., Lourdesamy, J. S., de Carvalho, L. M. S. P., Nicholson, J. R., Corradini, L., & Smith, M. T. (2016). Comparison of burrowing and stimuli-evoked pain behaviors as end-points in rat models of inflammatory pain and peripheral neuropathic pain. *Frontiers in Behavioral Neuroscience*, *10*(MAY), 1–9. https://doi.org/10.3389/fnbeh.2016.00088

Musk, G. C. (2020). Refinements to Animal Models for Biomedical Research. *Animals : An Open Access Journal from MDPI*, *10*(12), 1–3. https://doi.org/10.3390/ANI10122425

Mussigmann, T., Bardel, B., & Lefaucheur, J.-P. (2022). Resting-state electroencephalography (EEG) biomarkers of chronic neuropathic pain. A systematic review. *NeuroImage*, *258*, 119351. https://doi.org/10.1016/j.neuroimage.2022.119351

Muto, V., & Berthomier, C. (2023). Looking for a balance between visual and automatic sleep scoring. *Npj Digital Medicine 2023 6:1*, *6*(1), 1–3. https://doi.org/10.1038/s41746-023-00915-7

NC3Rs. (n.d.). Retrieved July 27, 2021, from https://www.nc3rs.org.uk/the-3rs

Negus, S. S. (2019). Core outcome measures in preclinical assessment of candidate analgesics. *Pharmacological Reviews*, *71*(2), 225–266. https://doi.org/10.1124/pr.118.017210

Nicholson, B., & Verma, S. (2004). Comorbidities in chronic neuropathic pain. *Pain Medicine*, *5*(SUPPL. 1), S9–S27. https://doi.org/10.1111/J.1526-4637.2004.04019.X/2/PME_4019_F4.JPEG

Nigam, P., & Nigam, A. (2010). BOTULINUM TOXIN. *Indian Journal of Dermatology*, *55*(1), 8. https://doi.org/10.4103/0019-5154.60343

Nokia, M. S., Anderson, M. L., & Shors, T. J. (2012). Chemotherapy disrupts learning, neurogenesis and theta activity in the adult brain. *European Journal of Neuroscience*, *36*(11), 3521–3530. https://doi.org/10.1111/ejn.12007

Nørgaard, S. A., Sand, F. W., Sørensen, D. B., Abelson, K. S. P., & Søndergaard, H. (2018). Softened food reduces weight loss in the streptozotocin-induced male mouse model of diabetic nephropathy. *Laboratory Animals*, *52*(4), 373–383. https://doi.org/10.1177/0023677217747915/ASSET/IMAGES/LARGE/10.1177_0023677217747915-FIG5.JPEG

Nozawa, K., Karasawa, Y., Shidahara, Y., & Ushida, T. (2022). Efficacy of Combination Therapy with Pregabalin in Neuropathic Pain: A Preclinical Study in the Rat L5 Spinal Nerve Ligation Model. *Journal of Pain Research*, *15*, 3469. https://doi.org/10.2147/JPR.S383981

Nutt, D. J., Wilson, S., & Paterson, L. (2008). Sleep disorders as core symptoms of depression. *Dialogues in Clinical Neuroscience*, *10*(3), 329. https://doi.org/10.31887/DCNS.2008.10.3/DNUTT

Obata, H. (2017). Analgesic Mechanisms of Antidepressants for Neuropathic Pain. *International Journal of Molecular Sciences*, *18*(11). https://doi.org/10.3390/IJMS18112483

Ossipov, M. H., Morimura, K., & Porreca, F. (2014). Descending pain modulation and chronification of pain. *Current Opinion in Supportive and Palliative Care*, *8*(2), 143. https://doi.org/10.1097/SPC.0000000000000055

Pabbidi, M. R., & Premkumar, L. S. (2017). Role of Transient Receptor Potential Channels Trpv1 and Trpm8 in Diabetic Peripheral Neuropathy. *Journal of Diabetes and Treatment*, *2017*(4).

Palagini, L., Baglioni, C., Ciapparelli, A., Gemignani, A., & Riemann, D. (2013). REM sleep dysregulation in depression: State of the art. *Sleep Medicine Reviews*, *17*(5), 377–390. https://doi.org/10.1016/J.SMRV.2012.11.001

Park, J. F., & Luo, Z. D. (2010). Calcium channel functions in pain processing. *Channels*, *4*(6), 510. https://doi.org/10.4161/CHAN.4.6.12869

Pasi, R., & Ravi, K. (2022). Type 1 diabetes mellitus in pediatric age group: A rising endemic. *Journal of Family Medicine and Primary Care*, *11*(1), 27. https://doi.org/10.4103/jfmpc.jfmpc_975_21

Percie Du Sert, N., & Rice, A. S. C. C. (2014). Improving the translation of analgesic drugs to the clinic: Animal models of neuropathic pain. *British Journal of Pharmacology*, *171*(12), 2951–2963. https://doi.org/10.1111/bph.12645

Perret, D., & Luo, Z. D. D. (2009). Targeting Voltage-Gated Calcium Channels for Neuropathic Pain Management. *Neurotherapeutics*, *6*(4), 679–692. https://doi.org/10.1016/j.nurt.2009.07.006

Pitzer, C., Kuner, R., & Tappe-Theodor, A. (2016). Voluntary and evoked behavioral correlates in neuropathic pain states under different social housing conditions. *Molecular Pain*, *12*, 174480691665663. https://doi.org/10.1177/1744806916656635

Pope, J. E., Deer, T. R., Amirdelfan, K., McRoberts, W. P., & Azeem, N. (2017). The Pharmacology of Spinal Opioids and Ziconotide for the Treatment of Non-Cancer Pain. *Current Neuropharmacology*, *15*(2), 206. https://doi.org/10.2174/1570159X14666160210142339

BNF | NICE. (n.d.). Retrieved April 7, 2024, from https://bnf.nice.org.uk/drugs/pregabalin/

Prendergast, B. J., Onishi, K. G., & Zucker, I. (2014). Female mice liberated for inclusion in neuroscience and biomedical research. *Neuroscience and Biobehavioral Reviews, 40*, 1–5. https://doi.org/10.1016/j.neubiorev.2014.01.001

Prichep, L. S., John, E. R., Howard, B., Merkin, H., & Hiesiger, E. M. (2011). Evaluation of the Pain Matrix Using EEG Source Localization: A Feasibility Study. *Pain Medicine*, *12*(8), 1241–1248. https://doi.org/10.1111/j.1526-4637.2011.01191.x

Prinsloo, S., Novy, D., Driver, L., Lyle, R., Ramondetta, L., Eng, C., Lopez, G., Li, Y., & Cohen, L. (2018). The Long-Term Impact of Neurofeedback on Symptom Burden and Interference in Patients With Chronic Chemotherapy-Induced Neuropathy: Analysis of a Randomized Controlled Trial. *Journal of Pain and Symptom Management*, *55*(5), 1276–1285. https://doi.org/10.1016/j.jpainsymman.2018.01.010

Prinsloo, S., Novy, D., Driver, L., Lyle, R., Ramondetta, L., Eng, C., McQuade, J., Lopez, G., & Cohen, L. (2017). Randomized Controlled Trial of Neurofeedback on Chemotherapy-Induced Peripheral Neuropathy: A Pilot Study. *Cancer*, *123*(11), 1989. https://doi.org/10.1002/CNCR.30649

Quintão, N. L. M., Santin, J. R., Stoeberl, L. C., Corrêa, T. P., Melato, J., & Costa, R. (2019). Pharmacological Treatment of Chemotherapy-Induced Neuropathic Pain: PPARγ Agonists as a Promising Tool. *Frontiers in Neuroscience*, *13*(AUG). https://doi.org/10.3389/FNINS.2019.00907

Rakieten, N., Rakieten, M, L., & Nadkarni, M. R. (1963). Studies on the diabetogenic action of streptozotocin (NSC-37917). *Cancer Chemotherapy Reports. Part 1*, *29*, 91–98.

Raskin, J., Pritchett, Y. L., Wang, F., D'Souza, D. N., Waninger, A. L., Iyengar, S., & Wernicke, J. F. (2005). A double-blind, randomized multicenter trial comparing duloxetine with placebo in the management of diabetic peripheral neuropathic pain. *Pain Medicine*, *6*(5), 346–356. https://doi.org/10.1111/j.1526-4637.2005.00061.x

Rayan, A., Agarwal, A., Samanta, A., Severijnen, E., van der Meij, J., & Genzel, L. (2022). Sleep scoring in rodents: Criteria, automatic approaches and outstanding issues. *European Journal of Neuroscience*, *59*(4), 526–553. https://doi.org/10.1111/ejn.15884

Razazian, N., Baziyar, M., Moradian, N., Afshari, D., Bostani, A., & Mahmoodi, M. (2014). Evaluation of the efficacy and safety of pregabalin, venlafaxine, and carbamazepine in patients with painful diabetic peripheral neuropathy: A randomized, double-blind trial. *Neurosciences*, *19*(3), 192–198.

Reddan, M. C., & Wager, T. D. (2018). Modeling Pain Using fMRI: From Regions to Biomarkers. In *Neuroscience Bulletin* (Vol. 34, Issue 1, pp. 208–215). Springer. https://doi.org/10.1007/s12264-017-0150-1

Regnell, S. E., & Lernmark, Å. (2011). Hepatic steatosis in type 1 diabetes. *The Review of Diabetic Studies : RDS*, *8*(4), 454–467. https://doi.org/10.1900/RDS.2011.8.454

Rice, A. S. C., Dworkin, R. H., Finnerup, N. B., Attal, N., Anand, P., Freeman, R., Piaia, A., Callegari, F., Doerr, C., Mondal, S., Narayanan, N., Ecochard, L., Flossbach, Y., & Pandhi, S. (2021). Efficacy and safety of EMA401 in peripheral neuropathic pain: results of 2 randomised, double-blind, phase 2 studies in patients with postherpetic neuralgia and painful diabetic neuropathy. *Pain*, *162*(10), 2578–2589. https://doi.org/10.1097/J.PAIN.0000000000002252

Rice, A. S. C., Finnerup, N. B., Kemp, H. I., Currie, G. L., & Baron, R. (2018). Sensory profiling in animal models of neuropathic pain. *PAIN*, *159*(5), 819–824. https://doi.org/10.1097/j.pain.0000000000001138

Roche, E. F., Menon, A., Gill, D., & Hoey, H. (2005). Clinical presentation of type 1 diabetes. *Pediatric Diabetes*, *6*(2), 75–78. https://doi.org/10.1111/J.1399-543X.2005.00110.X

Rosenberger, D. C., Blechschmidt, V., Timmerman, H., Wolff, A., & Treede, R.-D. (2020). Challenges of neuropathic pain: focus on diabetic neuropathy. *Journal of Neural Transmission*, *127*(4), 589–624. https://doi.org/10.1007/s00702-020-02145-7

Rosenstock, J., Tuchman, M., LaMoreaux, L., & Sharma, U. (2004). Pregabalin for the treatment of painful diabetic peripheral neuropathy: a double-blind, placebo-controlled trial. *Pain*, *110*(3), 628–638. https://doi.org/10.1016/j.pain.2004.05.001

Rosner, H., Rubin, L., & Kestenbaum, A. (1996). Gabapentin Adjunctive Therapy in Neuropathic Pain States. *The Clinical Journal of Pain*, *12*(1), 56–58. https://doi.org/10.1097/00002508-199603000-00010

Rossato, M. F., Rigo, F. K., Oliveira, S. M., Guerra, G. P., Silva, C. R., Cunha, T. M., Gomez, M. V., Ferreira, J., & Trevisan, G. (2018). Participation of transient receptor potential vanilloid 1 in paclitaxel-induced acute visceral and peripheral nociception in rodents. *European Journal of Pharmacology*, *828*(March), 42–51. https://doi.org/10.1016/j.ejphar.2018.03.033

Russell, W. M. S., & Burch, R. L. (1959). *The Principles of Humane Experimental Technique*. Methuen & Co Ltd.

Rutten, K., Gould, S. A., Bryden, L., Doods, H., Christoph, T., & Pekcec, A. (2018). Standard analgesics reverse burrowing deficits in a rat CCI model of neuropathic pain, but not in models of type 1 and type 2 diabetes-induced neuropathic pain. *Behavioural Brain Research*, *350*(May), 129–138. https://doi.org/10.1016/j.bbr.2018.04.049

Saadane, A., Lessieur, E. M., Du, Y., Liu, H., & Kern, T. S. (2020). Successful induction of diabetes in mice demonstrates no gender difference in development of early diabetic retinopathy. *PLoS ONE, 15.* https://doi.org/10.1371/journal.pone.0238727

Sachau, J., Sendel, M., Péchard, M., Schnabel, K., Schmieg, I., Medkour, T., Ecochard, L., Woischnik, M., Liedgens, H., Pogatzki-Zahn, E., Baron, R., & Bouhassira, D. (2023). Patient Reported

Outcome Measures in Chronic Neuropathic Pain Clinical Trials – A Systematic Literature Review. *Journal of Pain*, *24*(1), 38–54. https://doi.org/10.1016/j.jpain.2022.09.003

Sadler, K. E., Mogil, J. S., & Stucky, C. L. (2022). Innovations and advances in modelling and measuring pain inanimals. *Nature Reviews. Neuroscience*, *23*(2), 70. https://doi.org/10.1038/S41583-021-00536-7

Saif, M. W., & Reardon, J. (2005). Management of oxaliplatin-induced peripheral neuropathy. *Therapeutics and Clinical Risk Management*, *1*(4), 249–258.

Sandkühler, J., Ju¨, J., Sandku¨hler, J., & Sandku¨hler, S. (2009). Models and Mechanisms of Hyperalgesia and Allodynia. *Physiological Reviews*, *89*(2), 707–758. https://doi.org/10.1152/physrev.00025.2008

Sanei, S., & Chambers, J. A. (2007). *Conventional Electrode Positioning*. *2007*.

Sarnthein, J., & Jeanmonod, D. (2008). High thalamocortical theta coherence in patients with neurogenic pain. *NeuroImage*, *39*(4), 1910–1917. https://doi.org/10.1016/j.neuroimage.2007.10.019

Sarnthein, J., Stern, J., Aufenberg, C., Rousson, V., & Jeanmonod, D. (2005). Increased EEG power and slowed dominant frequency in patients with neurogenic pain. *Brain*, *129*(1), 55–64. https://doi.org/10.1093/brain/awh631

Sawynok, J. (2014). Topical analgesics for neuropathic pain: Preclinical exploration, clinical validation, future development. *European Journal of Pain (United Kingdom)*, *18*(4), 465–481. https://doi.org/10.1002/J.1532-2149.2013.00400.X/SUPPINFO

Sazgar, M., & Young, M. G. (2019). Overview of EEG, Electrode Placement, and Montages. In *Absolute Epilepsy and EEG Rotation Review* (pp. 117–125). Springer International Publishing. https://doi.org/10.1007/978-3-030-03511-2_5

Scholz, J., Broom, D. C., Youn, D. H., Mills, C. D., Kohno, T., Suter, M. R., Moore, K. A., Decosterd, I., Coggeshall, R. E., & Woolf, C. J. (2005). Blocking Caspase Activity Prevents Transsynaptic Neuronal Apoptosis and the Loss of Inhibition in Lamina II of the Dorsal Horn after Peripheral Nerve Injury. *The Journal of Neuroscience*, *25*(32), 7317. https://doi.org/10.1523/JNEUROSCI.1526-05.2005

Schulman, J. J., Ramirez, R. R., Zonenshayn, M., Ribary, U., & Llinas, R. (2005). Thalamocortical dysrhythmia syndrome: MEG imaging of neuropathic pain. *Thalamus and Related Systems*, *3*(1), 33–39. https://doi.org/10.1017/S1472928805000063

Schütz, S. G., & Robinson-Papp, J. (2013). HIV-related neuropathy: current perspectives. *HIV/AIDS (Auckland, N.Z.)*, *5*, 243. https://doi.org/10.2147/HIV.S36674

Sevak, R. J., Koek, W., Daws, L. C., Owens, W. A., Galli, A., & France, C. P. (2008). Behavioral effects of amphetamine in streptozotocin-treated rats. *Eur J Pharmacol*, *581*(2), 105–112. https://doi.org/10.1016/j.ejphar.2007.11.047

Shaikh, A. S., & Somani, R. S. (2010). Animal models and biomarkers of neuropathy in diabetic rodents. *Indian Journal of Pharmacology*, *42*(3), 129–134. https://doi.org/10.4103/0253-7613.66833

Shamsaldeen, Y. A., Lione, L. A., & Benham, C. D. (2020). Dysregulation of TRPV4, eNOS and caveolin-1 contribute to endothelial dysfunction in the streptozotocin rat model of diabetes. *European Journal of Pharmacology*, *888*(May), 173441. https://doi.org/10.1016/j.ejphar.2020.173441

Shepherd, A. J., Cloud, M. E., Cao, Y. Q., & Mohapatra, D. P. (2018). Deficits in burrowing behaviors

are associated with mouse models of neuropathic but not inflammatory pain or migraine. *Frontiers in Behavioral Neuroscience*, *12*. https://doi.org/10.3389/fnbeh.2018.00124

Shore, R., Dobson, K., Thomson, N., Barnim, N., Bergman, H., Rideout, K., Mckeown, S., Olmstead, M. C., Goldie, C., Dumont, E., Dobson, K., & Olmstead, M. (2024). Behavioural Investigations of Psilocybin in Animals 1962-2021: A Scoping Review. *BioRxiv*, 2024.01.04.574146. https://doi.org/10.1101/2024.01.04.574146

Siegel, R. L., Miller, K. D., Fedewa, S. A., Dennis, ;, Ahnen, J., Reinier, ;, Meester, G. S., Barzi, A., & Jemal, A. (2017). Colorectal cancer statistics, 2017. *CA: A Cancer Journal for Clinicians*, *67*(3), 177–193. https://doi.org/10.3322/CAAC.21395

Simis, M., Pacheco-Barrios, K., Uygur-Kucukseymen, E., Castelo-Branco, L., Battistella, L. R., & Fregni, F. (2022). Specific Electroencephalographic Signatures for Pain and Descending Pain Inhibitory System in Spinal Cord Injury. *Pain Medicine*, *23*(5), 955–964. https://doi.org/10.1093/PM/PNAB124

Simons, L. E., Moulton, E. A., Linnman, C., Carpino, E., Becerra, L., & Borsook, D. (2014). The human amygdala and pain: Evidence from neuroimaging. *Human Brain Mapping*, *35*(2), 527–538. https://doi.org/10.1002/hbm.22199

Sindrup, S. H., Otto, M., Finnerup, N. B., & Jensen, T. S. (2005). Antidepressants in the Treatment of Neuropathic Pain. *Basic & Clinical Pharmacology & Toxicology*, *96*(6), 399–409. https://doi.org/10.1111/J.1742-7843.2005.PTO_96696601.X

Sivanesan, E., Maher, D. P., Raja, S. N., Linderoth, B., & Guan, Y. (2019). Supraspinal Mechanisms of Spinal Cord Stimulation for Modulation of Pain: Five Decades of Research and Prospects for the Future. *Anesthesiology*, *130*(4), 651–665. https://doi.org/10.1097/ALN.0000000000002353

Smith, M. L., Hostetler, C. M., Heinricher, M. M., & Ryabinin, A. E. (2016). Social transfer of pain in mice. *Science Advances*, *2*(10). https://doi.org/10.1126/SCIADV.1600855/SUPPL_FILE/1600855_SM.PDF

Soliman, N., Kersebaum, D., Lawn, T., Sachau, J., Sendel, M., & Vollert, J. (2023). Improving neuropathic pain treatment – by rigorous stratification from bench to bedside. *Journal of Neurochemistry, 00*, 1–16. https://doi.org/10.1111/JNC.15798

Staff, N. P., Grisold, A., Grisold, W., & Windebank, A. J. (2017). Chemotherapy-induced peripheral neuropathy: A current review. *Annals of Neurology*, *81*(6), 772–781. https://doi.org/10.1002/ana.24951

Starr, C. J., Sawaki, L., Wittenberg, G. F., Burdette, J. H., Oshiro, Y., Quevedo, A. S., & Coghill, R. C. (2009). Roles of the insular cortex in the modulation of pain: Insights from brain lesions. *Journal of Neuroscience*, *29*(9), 2684–2694. https://doi.org/10.1523/JNEUROSCI.5173-08.2009

Steel, L. C. E., Tam, S. K. E., Brown, L. A., Foster, R. G., & Peirson, S. N. (2024). Light sampling behaviour regulates circadian entrainment in mice. *BMC Biology, 22*. https://doi.org/10.1186/s12915-024-01995-x

Stern, J., Jeanmonod, D., & Sarnthein, J. (2006). Persistent EEG overactivation in the cortical pain matrix of neurogenic pain patients. *NeuroImage*, *31*(2), 721–731. https://doi.org/10.1016/j.neuroimage.2005.12.042

Sufianov, A. A., Shapkin, A. G., Sufianova, G. Z., Elishev, V. G., Barashin, D. A., Berdichevskii, V. B., & Churkin, S. V. (2014). Functional and Metabolic Changes in the Brain in Neuropathic Pain Syndrome against the Background of Chronic Epidural Electrostimulation of the Spinal Cord.

Bulletin of Experimental Biology and Medicine, *157*(4), 462–465. https://doi.org/10.1007/s10517-014-2591-0

Sullivan, E. M., Timi, P., Hong, L. E., & O'Donnell, P. (2015). Reverse translation of clinical electrophysiological biomarkers in behaving rodents under acute and chronic NMDA receptor antagonism. *Neuropsychopharmacology*, *40*(3), 719–727. https://doi.org/10.1038/npp.2014.228

Summa, K. C., Jiang, P., González-Rodríguez, P., Huang, X., Lin, X., Vitaterna, M. H., Dan, Y., Surmeier, D. J., & Turek, F. W. (2024). Disrupted sleep-wake regulation in the MCI-Park mouse model of Parkinson's disease. *Npj Parkinson's Disease 2024 10:1*, *10*(1), 1–9. https://doi.org/10.1038/s41531-024-00670-w

Takatsu-Coleman, A. L., Patti, C. L., Zanin, K. A., Zager, A., Carvalho, R. C., Borçoi, A. R., Ceccon, L. M. B., Berro, L. F., Tufik, S., Andersen, M. L., & Frussa-Filho, R. (2013). Short-term social isolation induces depressive-like behaviour and reinstates the retrieval of an aversive task: mood-congruent memory in male mice? *Journal of Psychiatry & Neuroscience : JPN*, *38*(4), 259–268. https://doi.org/10.1503/JPN.120050

Takeshita, E., Ishibashi, K., Koda, K., Oda, N., Yoshimatsu, K., Sato, Y., Oya, M., Yamaguchi, S., Nakajima, H., Momma, T., Maekawa, H., Tsubaki, M., Yamada, T., Kobayashi, M., Tanakaya, K., & Ishida, H. (2021). The updated five-year overall survival and long-term oxaliplatin-related neurotoxicity assessment of the FACOS study. *Surgery Today*, *51*(8), 1309–1319. https://doi.org/10.1007/S00595-021-02230-8/METRICS

Tan, E. C. T. H., Bahrami, S., Kozlov, A. V., Kurvers, H. A. J. M., Ter Laak, H. J., Nohl, H., Redl, H., & Goris, R. J. A. (2009). The Oxidative Response in the Chronic Constriction Injury Model of Neuropathic Pain. *Journal of Surgical Research*, *152*(1), 84–88. https://doi.org/10.1016/J.JSS.2008.03.035

Taneja, A., Della Pasqua, O., & Danhof, M. (2017). Challenges in translational drug research in neuropathic and inflammatory pain: the prerequisites for a new paradigm. *European Journal of Clinical Pharmacology*, *73*(10), 1219. https://doi.org/10.1007/S00228-017-2301-8

Tappe-Theodor, A., King, T., & Morgan, M. M. (2019). Pros and Cons of Clinically Relevant Methods to Assess Pain in Rodents. *Neuroscience and Biobehavioral Reviews*, *100*(December 2018), 335–343. https://doi.org/10.1016/j.neubiorev.2019.03.009

Targher, G., Mantovani, A., Pichiri, I., Mingolla, L., Cavalieri, V., Mantovani, W., Pancheri, S., Trombetta, M., Zoppini, G., Choncho, M., Byrne, C. D., & Bonora, E. (2014). Nonalcoholic fatty liver disease is independently associated with an increased incidence of chronic kidney disease in patients with type 1 diabetes. *Diabetes Care*, *37*(6), 1729–1736. https://doi.org/10.2337/DC13-2704

Taylor, C. P., Vartanian, M. G., Po-Wai, Y., Bigge, C., Suman-Chauhan, N., & Hill, D. R. (1993). Potent and stereospecific anticonvulsant activity of 3-isobutyl GABA relates to in vitro binding at a novel site labeled by tritiated gabapentin. *Epilepsy Research*, *14*(1), 11–15. https://doi.org/10.1016/0920-1211(93)90070-N

Tesfaye, S., Boulton, A. J. M., & Dickenson, A. H. (2013). Mechanisms and management of diabetic painful distal symmetrical polyneuropathy. *Diabetes Care*, *36*(9), 2456–2465. https://doi.org/10.2337/dc12-1964

Thomas, C. W., Blanco-Duque, C., Bréant, B. J., Goodwin, G. M., Sharp, T., Bannerman, D. M., & Vyazovskiy, V. V. (2022). Psilocin acutely alters sleep-wake architecture and cortical brain activity in laboratory mice. *Translational Psychiatry 2022 12:1*, *12*(1), 1–13.

https://doi.org/10.1038/s41398-022-01846-9

Thomas, L., & Juanes, F. (1996). The importance of statistical power analysis: an example fromAnimal Behaviour. *Animal Behaviour*, *52*(4), 856–859. https://doi.org/10.1006/anbe.1996.0232

Tilley, D. M., Vallejo, R., Kelley, C. A., Benyamin, R., & Cedeño, D. L. (2015). A continuous spinal cord stimulation model attenuates pain-related behavior in vivo following induction of a peripheral nerve injury. *Neuromodulation*, *18*(3), 171–176. https://doi.org/10.1111/ner.12280

Timmermann, L., Ploner, M., Haucke, K., Schmitz, F., Baltissen, R., & Schnitzler, A. (2001). Differential coding of pain intensity in the human primary and secondary somatosensory cortex. *Journal of Neurophysiology*, *86*(3), 1499–1503. https://doi.org/10.1152/jn.2001.86.3.1499

Timotius, I. K., Roelofs, R. F., Richmond-Hacham, B., Noldus, L. P. J. J., von Hörsten, S., & Bikovski, L. (2023). CatWalk XT gait parameters: a review of reported parameters in pre-clinical studies of multiple central nervous system and peripheral nervous system disease models. *Frontiers in Behavioral Neuroscience*, *17*. https://doi.org/10.3389/FNBEH.2023.1147784/FULL

Tofthagen, C., Donovan, K. A., Morgan, M. A., Shibata, D., & Yeh, Y. (2013). Oxaliplatin-induced peripheral neuropathy's effects on health-related quality of life of colorectal cancer survivors. *Supportive Care in Cancer*, *21*(12), 3307–3313. https://doi.org/10.1007/s00520-013-1905-5

Tokunaga, S., Takeda, Y., Shinomiya, K., Yamamoto, W., Utsu, Y., Toide, K., & Kamei, C. (2007). Changes of Sleep Patterns in Rats with Chronic Constriction Injury under Aversive Conditions. *Biological and Pharmaceutical Bulletin*, *30*(11), 2088–2090. https://doi.org/10.1248/BPB.30.2088

Tominaga, M., & Tominaga, T. (2005). Structure and function of TRPV1. *Pflugers Archiv : European Journal of Physiology*, *451*(1), 143–150. https://doi.org/10.1007/S00424-005-1457-8

Torta, R., Ieraci, V., & Zizzi, F. (2017). A Review of the Emotional Aspects of Neuropathic Pain: From Comorbidity to Co-Pathogenesis. *Pain and Therapy*, *6*.

Urban, R., Scherrer, G., Goulding, E. H., Tecott, L. H., & Basbaum, A. I. (2011). Behavioral indices of ongoing pain are largely unchanged in male mice with tissue or nerve injury-induced mechanical hypersensitivity. *Pain*, *152*(5), 990–1000. https://doi.org/10.1016/j.pain.2010.12.003

van der Wal, S., Cornelissen, L., Behet, M., Vaneker, M., Steegers, M., & Vissers, K. (2015). Behavior of neuropathic pain in mice following chronic constriction injury comparing silk and catgut ligatures. *SpringerPlus*, *4*(1). https://doi.org/10.1186/S40064-015-1009-4

van Hecke, O., Austin, S. K., Khan, R. A., Smith, B. H., & Torrance, N. (2014). Neuropathic pain in the general population: A systematic review of epidemiological studies. *Pain*, *155*(4), 654–662. https://doi.org/10.1016/j.pain.2013.11.013

Vanneste, S., Song, J.-J. J., & De Ridder, D. (2018). Thalamocortical dysrhythmia detected by machine learning. *Nature Communications*, *9*(1), 1103. https://doi.org/10.1038/s41467-018-02820-0

Velasco, R., Alemany, M., Villagrán, M., & Argyriou, A. A. (2021). Predictive Biomarkers of Oxaliplatin-Induced Peripheral Neurotoxicity. *Journal of Personalized Medicine*, *11*(7). https://doi.org/10.3390/JPM11070669

Velzen, M. van, Dahan, J. D. C., van Dorp, E. L. A., Mogil, J. S., Hooijmans, C. R., & Dahan, A. (2021). Efficacy of ketamine in relieving neuropathic pain: a systematic review and meta-analysis of animal studies. *Pain*, *162*(9), 2320–2330. https://doi.org/10.1097/j.pain.0000000000002231

Vieira, W. F., Malange, K. F., de Magalhães, S. F., dos Santos, G. G., de Oliveira, A. L. R., da Cruz-Höfling, M. A., & Parada, C. A. (2020). Gait analysis correlates mechanical hyperalgesia in a model of streptozotocin-induced diabetic neuropathy: A CatWalk dynamic motor function study. *Neuroscience Letters*, *736*(May), 135253. https://doi.org/10.1016/j.neulet.2020.135253

Vieira, W. F., Malange, K. F., de Magalhães, S. F., Lemes, J. B. P., dos Santos, G. G., Nishijima, C. M., de Oliveira, A. L. R., da Cruz-Höfling, M. A., Tambeli, C. H., & Parada, C. A. (2022). Anti-hyperalgesic effects of photobiomodulation therapy (904 nm) on streptozotocin-induced diabetic neuropathy imply MAPK pathway and calcium dynamics modulation. *Scientific Reports 2022 12:1*, *12*(1), 1–18. https://doi.org/10.1038/s41598-022-19947-2

Vinik, A. I., Perrot, S., Vinik, E. J., Pazdera, L., Jacobs, H., Stoker, M., Long, S. K., Snijder, R. J., van der Stoep, M., Ortega, E., & Katz, N. (2016). Capsaicin 8% patch repeat treatment plus standard of care (SOC) versus SOC alone in painful diabetic peripheral neuropathy: A randomised, 52-week, open-label, safety study. *BMC Neurology*, *16*(1), 251. https://doi.org/10.1186/s12883-016-0752-7

Viswanath, O., Urits, I., Jones, M. R., Peck, J. M., Kochanski, J., Hasegawa, M., Anyama, B., & Kaye, A. D. (2019). Membrane Stabilizer Medications in the Treatment of Chronic Neuropathic Pain: a Comprehensive Review. *Current Pain and Headache Reports*, *23*(6), 1–9. https://doi.org/10.1007/S11916-019-0774-0/METRICS

Vollenweider, F. X., & Preller, K. H. (2020). Psychedelic drugs: neurobiology and potential for treatment of psychiatric disorders. *Nature Reviews Neuroscience 2020 21:11*, *21*(11), 611–624. https://doi.org/10.1038/s41583-020-0367-2

von Hehn, C. A., Baron, R., & Woolf, C. J. (2012). Deconstructing the Neuropathic Pain Phenotype to Reveal Neural Mechanisms. *Neuron*, *73*(4), 638–652. https://doi.org/10.1016/j.neuron.2012.02.008

Vorwerk, J., Aydin, Ü., Wolters, C. H., & Butson, C. R. (2019). Influence of head tissue conductivity uncertainties on EEG dipole reconstruction. *Frontiers in Neuroscience*, *13*(JUN), 1–17. https://doi.org/10.3389/fnins.2019.00531

Voute, M., Riant, T., Amodéo, J. M., André, G., Barmaki, M., Collard, O., Colomb, C., Créac'h, C., Deleens, R., Delorme, C., de Montgazon, G., Dixneuf, V., Dy, L., Gaillard, J., Gov, C., Kieffer, X., Lanteri-Minet, M., Le Borgne, J. M., Le Caër, F., … Pickering, G. (2022). Ketamine in chronic pain: A Delphi survey. *European Journal of Pain (London, England)*, *26*(4), 873–887. https://doi.org/10.1002/EJP.1914

Vrinten, D. H., & Hamers, F. F. T. (2003). "CatWalk" automated quantitative gait analysis as a novel method to assess mechanical allodynia in the rat; a comparison with von Frey testing. *Pain*, *102*(1–2), 203–209. https://doi.org/10.1016/s0304-3959(02)00382-2

Vučković, A., Altaleb, M. K. H., Fraser, M., McGeady, C., & Purcell, M. (2019). EEG correlates of self-managed neurofeedback treatment of central neuropathic pain in chronic spinal cord injury. *Frontiers in Neuroscience*, *13*(JUL), 1–18. https://doi.org/10.3389/fnins.2019.00762

Vučković, A., Gallardo, V. J. F., Jarjees, M., Fraser, M., & Purcell, M. (2018). Prediction of central neuropathic pain in spinal cord injury based on EEG classifier. *Clinical Neurophysiology*, *129*(8), 1605–1617. https://doi.org/10.1016/j.clinph.2018.04.750

Vučković, A., Jajrees, M., Purcell, M., Berry, H., & Fraser, M. (2018). Electroencephalographic Predictors of Neuropathic Pain in Subacute Spinal Cord Injury. *Journal of Pain*, *19*(11), 1256.e1-1256.e17. https://doi.org/10.1016/j.jpain.2018.04.011

Vyazovskiy, V. V., Achermann, P., & Tobler, I. (2007). Sleep homeostasis in the rat in the light and dark period. *Brain Research Bulletin*, *74*(1–3), 37–44. https://doi.org/10.1016/J.BRAINRESBULL.2007.05.001

Vyazovskiy, Vladyslav V., & Delogu, A. (2014). NREM and REM sleep: Complementary roles in recovery after wakefulness. *Neuroscientist*, *20*(3), 203–219. https://doi.org/10.1177/1073858413518152

Wan, F. P., Bai, Y., Kou, Z. Z., Zhang, T., Li, H., Wang, Y. Y., & Li, Y. Q. (2017). Endomorphin-2 inhibition of substance P signaling within lamina I of the spinal cord is impaired in diabetic neuropathic pain rats. *Frontiers in Molecular Neuroscience*, *9*, 167. https://doi.org/10.3389/FNMOL.2016.00167/BIBTEX

Wang-Fischer, Y., & Garyantes, T. (2018). Improving the Reliability and Utility of Streptozotocin-Induced Rat Diabetic Model. *Journal of Diabetes Research*, *2018*. https://doi.org/10.1155/2018/8054073

Warren, G., Osborn, M., Tsantoulas, C., David-Pereira, A., Cohn, D., Duffy, P., Ruston, L., Johnson, C., Bradshaw, H., Kaczocha, M., Ojima, I., Yates, A., & O'Sullivan, S. E. (2024). Discovery and Preclinical Evaluation of a Novel Inhibitor of FABP5, ART26.12, Effective in Oxaliplatin-Induced Peripheral Neuropathy. *Journal of Pain*, *25*(7), 104470. https://doi.org/10.1016/j.jpain.2024.01.335

Watson, A., Power, A., Brown, C., El-Deredy, W., & Jones, A. (2012). Placebo analgesia: cognitive influences on therapeutic outcome. *Arthritis Research & Therapy*, *14*(3), 206. https://doi.org/10.1186/ar3783

Weber, F. D., Supp, G. G., Klinzing, J. G., Mölle, M., Engel, A. K., & Born, J. (2021). Coupling of gamma band activity to sleep spindle oscillations – a combined EEG/MEG study. *NeuroImage*, *224*, 117452. https://doi.org/10.1016/J.NEUROIMAGE.2020.117452

Widerstrom-Noga, E. G., Felipe-Cuervo, E., & Yezierski, R. P. (2001). Chronic pain after spinal injury: Interference with sleep and daily activities. *Archives of Physical Medicine and Rehabilitation*, *82*(11), 1571–1577. https://doi.org/10.1053/apmr.2001.26068

Wilson, F. J., Leiser, S. C., Ivarsson, M., Christensen, S. R., & Bastlund, J. F. (2014). Can pharmaco-electroencephalography help improve survival of central nervous system drugs in early clinical development? *Drug Discovery Today*, *19*(3), 282–288. https://doi.org/10.1016/j.drudis.2013.08.001

Wilson, S., & Argyropoulos, S. (2005). Antidepressants and Sleep. *Drugs*, *65*(7), 927–947. https://doi.org/10.2165/00003495-200565070-00003

Woolf, C. J., & Thompson, S. W. N. (1991). The induction and maintenance of central sensitization is dependent on N-methyl-D-aspartic acid receptor activation; implications for the treatment of post-injury pain hypersensitivity states. *Pain*, *44*(3), 293–299. https://doi.org/10.1016/0304-3959(91)90100-C

Wydenkeller, S., Maurizio, S., Dietz, V., & Halder, P. (2009). Neuropathic pain in spinal cord injury: Significance of clinical and electrophysiological measures. *European Journal of Neuroscience*, *30*(1), 91–99. https://doi.org/10.1111/j.1460-9568.2009.06801.x

Xi, C., He, L., Huang, Z., Zhang, J., Zou, K., Guo, Q., & Huang, C. (2023). Combined metabolomics and transcriptomics analysis of rats under neuropathic pain and pain-related depression. *Frontiers in Pharmacology*, *14*. https://doi.org/10.3389/FPHAR.2023.1320419

Xiao, R., Shida-Tokeshi, J., Vanderbilt, D. L., & Smith, B. A. (2018). Electroencephalography power

and coherence changes with age and motor skill development across the first half year of life. *PLoS ONE*, *13*(1). https://doi.org/10.1371/JOURNAL.PONE.0190276

Xiao, W. H., Zheng, H., & Bennett, G. J. (2012). Characterization of oxaliplatin-induced chronic painful peripheral neuropathy in the rat and comparison with the neuropathy induced by paclitaxel. *Neuroscience*, *203*, 194–206. https://doi.org/10.1016/j.neuroscience.2011.12.023

Xie, W., Strong, J. A., & Zhang, J. M. (2015). Local knockdown of the NaV1.6 sodium channel reduces pain behaviors, sensory neuron excitability, and sympathetic sprouting in rat models of neuropathic pain. *Neuroscience*, *291*, 317. https://doi.org/10.1016/J.NEUROSCIENCE.2015.02.010

Yam, M. F., Loh, Y. C., Tan, C. S., Adam, S. K., Manan, N. A., & Basir, R. (2018). General pathways of pain sensation and the major neurotransmitters involved in pain regulation. *International Journal of Molecular Sciences, 19*(8). https://doi.org/10.3390/ijms19082164

Yamamoto, H., Shimoshige, Y., Yamaji, T., Murai, N., Aoki, T., & Matsuoka, N. (2009). Pharmacological characterization of standard analgesics on mechanical allodynia in streptozotocin-induced diabetic rats. *Neuropharmacology*, *57*(4), 403–408. https://doi.org/10.1016/J.NEUROPHARM.2009.06.037

Yamamoto, K., Tsuboi, M., Kambe, T., Abe, K., Nakatani, Y., Kawakami, K., Utsunomiya, I., & Taguchi, K. (2016). Oxaliplatin administration increases expression of the voltage-dependent calcium channel α2δ-1 subunit in the rat spinal cord. *Journal of Pharmacological Sciences*, *130*(2), 117–122. https://doi.org/10.1016/J.JPHS.2016.01.006

Yamamoto, S., Ono, H., Kume, K., & Ohsawa, M. (2016). Oxaliplatin treatment changes the function of sensory nerves in rats. *Journal of Pharmacological Sciences*, *130*(4), 189–193. https://doi.org/10.1016/J.JPHS.2015.12.004

Yi, Y., Li, L., Song, F., Li, P., Chen, M., Ni, S., Zhang, H., Zhou, H., Zeng, S., & Jiang, H. (2021). L-tetrahydropalmatine reduces oxaliplatin accumulation in the dorsal root ganglion and mitochondria through selectively inhibiting the transporter-mediated uptake thereby attenuates peripheral neurotoxicity. *Toxicology*, *459*, 152853. https://doi.org/10.1016/J.TOX.2021.152853

Younger, J., McCue, R., & Mackey, S. (2009). Pain outcomes: A brief review of instruments and techniques. *Current Pain and Headache Reports*, *13*(1), 39–43. https://doi.org/10.1007/s11916-009-0009-x

Zafar, M., & Naeem-ul-Hassan Naqvi, S. (2010). Effects of STZ-Induced Diabetes on the Relative Weights of Kidney, Liver and Pancreas in Albino Rats: A Comparative Study. *International Journal of Morphology*, *28*(1). https://doi.org/10.4067/S0717-95022010000100019

Zajączkowska, R., Kocot-Kępska, M., Leppert, W., Wrzosek, A., Mika, J., & Wordliczek, J. (2019). Mechanisms of Chemotherapy-Induced Peripheral Neuropathy. *International Journal of Molecular Sciences*, *20*(6), 1451. https://doi.org/10.3390/ijms20061451

Zhang, X. Y., Barakat, A., Diaz-Delcastillo, M., Vollert, J., Sena, E. S., Heegaard, A. M., Rice, A. S. C., & Soliman, N. (2022). Systematic review and meta-analysis of studies in which burrowing behaviour was assessed in rodent models of disease-associated persistent pain. *Pain*, *163*(11), 2076–2102. https://doi.org/10.1097/J.PAIN.0000000000002632

Zhou, R., Wang, J., Qi, W., Liu, F.-Y., Yi, M., Guo, H., & Wan, Y. (2018). Elevated Resting State Gamma Oscillatory Activities in Electroencephalogram of Patients With Post-herpetic Neuralgia. *Frontiers in Neuroscience*, *12*(October), 1–11. https://doi.org/10.3389/fnins.2018.00750

Zhu, M., & Huang, H. (2023). The Underlying Mechanisms of Sleep Deprivation Exacerbating Neuropathic Pain. *Nature and Science of Sleep*, *15*, 579. https://doi.org/10.2147/NSS.S414174

Ziff, S., Stern, B., Lewis, G., Majeed, M., & Gorantla, V. R. (2022). Analysis of Psilocybin-Assisted Therapy in Medicine: A Narrative Review. *Cureus*, *14*(2). https://doi.org/10.7759/CUREUS.21944

Zubieta, J. K., Bueller, J. A., Jackson, L. R., Scott, D. J., Xu, Y., Koeppe, R. A., Nichols, T. E., & Stohler, C. S. (2005). Placebo effects mediated by endogenous opioid activity on μ-opioid receptors. *Journal of Neuroscience*, *25*(34), 7754–7762. https://doi.org/10.1523/JNEUROSCI.0439-05.2005